

Performance Analysis of Slope-Compensated Current Controlled Universal PV Battery Charger for Electric Vehicle Applications

Proceedings of International Conference on Power Electronics and Renewable Energy Systems pp 407-415 | Cite as

- S. Ramprasath (1) Email author (ramprasath-eee@saranathan.ac.in)
- R. Abarna (1)
- G. Anjuka (1)
- K. Deva Priya (1)
- S. Iswarya (1)
- C. Krishnakumar (1)

1. Saranathan College of Engineering, , Trichy, India

Conference paper

First Online: 22 November 2021

- 74 Downloads

Part of the [Lecture Notes in Electrical Engineering](#) book series (LNEE, volume 795)

Abstract

The main purpose of the proposed system is to design a low-cost universal PV battery charger for electric vehicle application. The proposed system is integrated with a slope-compensated current controller which controls the charging current that corresponds to maximum power point of the PV module. As an interface converter, the proposed system consists of a buck converter to control the flow of the charging current and to find out the reference current I_{ref} from the PV array at MPP. The battery control circuit is implemented by measuring the state of charge (SOC) of the battery, and an LCD display has been used to monitor the battery parameters. This proposed system acts as a smart and efficient PV battery charger for e-vehicles.

Keywords

Electric vehicle Battery charger State of charge Slope compensated

This is a preview of subscription content, [log in](#) to check access.

References

1. Biswas S, Huang L, Vaidya V, Ravichandran K, Mohan N, Dhople SV (2016) Universal current-mode control schemes to charge Li-Ion batteries under DC/PV source. In: IEEE transactions on circuits and systems I: regular papers, Sept. 2016, vol 63(9), pp 15311542.
<https://doi.org/10.1109/TCSI.2016.2571218>
(<https://doi.org/10.1109/TCSI.2016.2571218>)
2. Singh HK, Kumar N (2020) Current controlled charging scheme for off board electric vehicle batteries from solar PV array. In: 2020 7th International conference on signal processing and integrated networks (SPIN), Noida, India, pp 935–940. <https://doi.org/10.1109/SPIN48934.2020.9071160>
(<https://doi.org/10.1109/SPIN48934.2020.9071160>)
3. Maity A, Patra A, Yamamura N, Knight J (2011) Design of a 20 MHz DC-DC buck converter with 84 percent efficiency for portable applications. In: 2011 24th international conference on VLSI design, Chennai, India, pp 316–321.
<https://doi.org/10.1109/VLSID.2011.37>
(<https://doi.org/10.1109/VLSID.2011.37>)
4. Achai bou N, Haddadi M, Malek A (2012) Modeling of lead acid batteries in PV systems. Energy Proc 18:538–544. ISSN 1876–6102.
<https://doi.org/10.1016/j.egypro.2012.05.065>
(<https://doi.org/10.1016/j.egypro.2012.05.065>)
5. Sant'Ana WC et al (2019) Implementation of automatic battery charging temperature compensation on a peak-shaving energy storage equipment. In: 2019 IEEE 15th Brazilian power electronics conference and 5th IEEE Southern power electronics conference (COBEP/SPEC), Santos, Brazil, pp 1–7.
<https://doi.org/10.1109/COBEP/SPEC44138.2019.9065670>
(<https://doi.org/10.1109/COBEP/SPEC44138.2019.9065670>)
6. Kondrath N, Kazimierzczuk MK (2013) Slope compensation and relative stability of peak current-mode controlled PWM dc-dc converters in CCM. In: 2013 IEEE 56th international midwest symposium on circuits and systems (MWSCAS), Columbus, OH, USA, pp 477–480. <https://doi.org/10.1109/MWSCAS.2013.6674689R>
(<https://doi.org/10.1109/MWSCAS.2013.6674689R>)
7. Sivakumar R, Ramprasath S, Babu PR (2015) Efficiency and power packing density improvement for DC-DC boost converter by soft switching techniques. In: 2015 International conference on circuits, power and computing technologies [ICCPCT-2015], Nagercoil, India, pp 1–7.
<https://doi.org/10.1109/ICCPCT.2015.7159504>
(<https://doi.org/10.1109/ICCPCT.2015.7159504>)
8. Wiesner, Diez R, Perilla G (2013) Design and implementation of a buck converter with MPPT for battery charge from solar module. In: 2013 Workshop on power electronics and power quality applications (PEPQA), Bogota, pp 1–6.
<https://doi.org/10.1109/PEPQA.2013.6614938>
(<https://doi.org/10.1109/PEPQA.2013.6614938>)
9. Zhong J, Liu S (2011) Design of slope compensation circuit in peak-current controlled mode converters. In: 2011 International conference on electric information and control engineering, ICEICE 2011—Proceedings. IEEE, pp 1310–1313. <https://doi.org/10.1109/ICEICE.2011.5778040>
(<https://doi.org/10.1109/ICEICE.2011.5778040>)

10. Hu Y, Wei Y, Wang J, Sun M (2016) Design of slope compensation for a high-efficiency high-current DC-DC converter. In: Proceedings 13th IEEE international conference solid-state integration circuit technology (ICSICT), October 2016, pp 1306–1308
[Google Scholar](https://scholar.google.com/scholar?q=Hu%20Y%2C%20Wei%20Y%2C%20Wang%20J%2C%20Sun%20M%20%282016%29%20Design%20of%20slope%20compensation%20for%20a%20high-efficiency%20high-current%20DC-DC%20converter.%20In%3A%20Proceedings%2013th%20IEEE%20international%20conference%20solid-state%20integration%20circuit%20technology%20%28ICSICT%29%2C%20October%202016%2C%20pp%201306%E2%80%931308) (<https://scholar.google.com/scholar?q=Hu%20Y%2C%20Wei%20Y%2C%20Wang%20J%2C%20Sun%20M%20%282016%29%20Design%20of%20slope%20compensation%20for%20a%20high-efficiency%20high-current%20DC-DC%20converter.%20In%3A%20Proceedings%2013th%20IEEE%20international%20conference%20solid-state%20integration%20circuit%20technology%20%28ICSICT%29%2C%20October%202016%2C%20pp%201306%E2%80%931308>)
11. Matwankar CS, Alam A (2019) Solar powered closed-loop current controlled DC-DC buck converter for battery charging application. In: 2019 International conference on vision towards emerging trends in communication and networking (ViTECoN), Vellore, India, pp 1–5.
<https://doi.org/10.1109/ViTECoN.2019.8899645>
 (<https://doi.org/10.1109/ViTECoN.2019.8899645>)
12. Radianto D, Dousoky GM, Shoyama M (2015) Design and implementation of fast PWM boost converter based on low cost microcontroller for photovoltaic systems. IECON 2015–41st annual conference of the IEEE industrial electronics society, Yokohama, Japan, pp 002324–002328.
<https://doi.org/10.1109/IECON.2015.7392449>
 (<https://doi.org/10.1109/IECON.2015.7392449>)

Copyright information

© The Author(s), under exclusive license to Springer Nature Singapore Pte Ltd. 2022

About this paper

Cite this paper as:

Ramprasath S., Abarna R., Anjuka G., Deva Priya K., Iswarya S., Krishnakumar C. (2022) Performance Analysis of Slope-Compensated Current Controlled Universal PV Battery Charger for Electric Vehicle Applications. In: Subramani C., Vijayakumar K., Dakyo B., Dash S.S. (eds) Proceedings of International Conference on Power Electronics and Renewable Energy Systems. Lecture Notes in Electrical Engineering, vol 795. Springer, Singapore. https://doi.org/10.1007/978-981-16-4943-1_38

- First Online 22 November 2021
- DOI https://doi.org/10.1007/978-981-16-4943-1_38
- Publisher Name Springer, Singapore
- Print ISBN 978-981-16-4942-4
- Online ISBN 978-981-16-4943-1
- eBook Packages [Energy](#), [Energy \(RO\)](#)
- [Reprints and Permissions](#)

Personalised recommendations

SPRINGER NATURE

© 2020 Springer Nature Switzerland AG. Part of Springer Nature.

Not logged in Not affiliated 106.203.16.158

Solid State Technology

[Home](#) [Current](#) [Aims and Scope](#) [For Authors ▾](#) [Archives](#) [Ethics & Policies](#) [About ▾](#)

[Home](#) / [Archives](#) / [Vol. 64 No. 1 \(2021\)](#) / [Articles](#)

IMPLEMENTATION OF P & O ALGORITHM FOR MULTI LEVEL CASCADED-BOOST CONVERTER

Reka.J, Vijayalakshmi.S, Marimuthu.M, Paranthagan.B, Vijay.R, Venugopal.R

Abstract

Maximum power point (MPP) monitoring is an unavoidable feature of a solar (PV) array energy conversion system. Thus an attempt is made to implement the new multi-level cascaded boost converter for maximum power point tracking. MPPT plays a vital role in Photo Voltaic power system as they provides the maximum power output for PV System for different weather conditions and thereby gives improved array efficiency. The goal is accomplished here by implementing the Perturb & Observe MPPT algorithm, which also provides high voltage gain by the use of the proposed converter circuit. The MATLAB/SIMULINK is used for Testing and Implementing the required objective. The algorithms are implemented in m-file of MATLAB.

 PDF

Issue

[Vol. 64 No. 1 \(2021\)](#)

Section

Articles

A Novel Isolated DC-DC Multi-Level Flyback Converter for Multi-Level Inverter Application

Venugopal R

Department of Electrical and
Electronics Engineering
Saranathan College of Engineering
Trichy, India
venugopalramadoss@gmail.com

Dr. Vijayalakshimi S

Department of Electrical and
Electronics Engineering
Saranathan College of Engineering
Trichy, India
bksvijji@gmail.com

Marimuthu M

Department of Electrical and
Electronics Engineering
Saranathan College of Engineering
Trichy, India
marimuthueephd@gmail.com

Chandra Kishore M

Department of Electrical and
Electronics Engineering
Saranathan College of Engineering
Trichy, India
chandra.083.ck@gmail.com

Mohammed Rifat Z

Department of Electrical and
Electronics Engineering
Saranathan College of Engineering
Trichy, India
rifatzahir@gmail.com

Niresh Shankar P

Department of Electrical and
Electronics Engineering
Saranathan College of Engineering
Trichy, India
niresshine@gmail.com

Abstract --- The main theme of this paper is to present a high voltage gain dc-dc boost converter using flyback and multilevel concept. The proposed converter focuses on multilevel outputs with voltage multiplier cell. The input of the general dc-dc converters is either PV array or battery or fuel cell. The circuit is composed of diodes and capacitors which acts as voltage multiplier and also as a rectifier. The implemented multilevel flyback converter can be connected to an H-bridge forming a multilevel inverter. With the help of a single driven semiconductor switch namely MOSFET, the designed converter can produce a high voltage gain in continuous conduction mode. The proposed multilevel flyback converter has been simulated and verified with theoretical values. The results have been demonstrated in the report.

Keywords --- Flyback Converter - Multilevel Flyback - Voltage Multiplier (VM).

I. INTRODUCTION

Intergovernmental Panel on Climate Change, regularly access the latest climate science reports for every country which is established in 1988. The earth's average temperature is rising at an unprecedented rate, causing rapid warming and climate changes in the contrary of fossil fuels like coal and petrol. Since 1973, various acts like Air act which aims to control the levels of air pollution through measures of National Ambient Air Quality Standards (NAAQS) and Motor vehicles Act (1988) is aimed to address the vehicular traffic and transportation of hazardous wastes. In order to reduce consumption of fossil fuels, solar cars comes into picture. Hybrid Solar vehicles and Commercial Solar Vehicles are replacing the conventional auto Mobiles. The Solar Vehicles requires a wide range dc input voltages for its operation so the demand for DC-DC Converters are in the rise. Isolated converter which has high voltage is combined with VM cell is implemented in this paper.

The flyback converter is a power supply topology that uses mutually coupled inductor or transformer to store energy. The flyback converters are similar to the booster converters in architecture and performance. However, the primary winding of the transformer replaces inductor while

the secondary provides the output. In the flyback configuration, the primary and secondary windings of transformer are utilized as two separate inductors. The basic flyback converter uses a relatively small number of components. A switching device chops the input DC voltage and the energy in the primary is transferred to the secondary through the switching transformer. A diode in the secondary rectifies the voltage while the capacitor boosts and removes the ripple.

A voltage multiplier is an electrical circuit with combination of capacitor and diode that converts AC electrical power from a lower voltage to a higher DC voltage. Voltage multiplier cells are very much similar to rectifier. Usage in electrical and electronic application such as in microwave ovens, strong electric field coils for cathode-ray tubes, electrostatic and high voltage test equipment, etc. The DC output voltage of a rectifier is limited to the peak value of its sinusoidal input voltage. While combining multiple diodes and capacitors as VM cells, we can effectively multiply the DC output voltage for some odd or even multiples.

II. DESIGN AND OPERATION OF MULTILEVEL FLYBACK CONVERTER

The overall block diagram for the need of high gain converter is shown in fig 1. The ultimatum of the proposed converter is to design a multilevel flyback converter using voltage multiplier cells. This interlinking of flyback and VM makes it possible to develop any number of levels of output just by adding combinations of diodes and capacitors. The main topology is to terminate the limitation of output.

The circuit is going to be operated in continuous conduction mode. Hence an inductor which act as a filter is connected parallel in the primary side of transformer. The inductor is used to limit high input voltage. A single semiconductor switch N-channel MOSFET has been used to control the pwm. Arduino micro controller has been used to provide gate pulse to the MOSFET. The switching frequency implemented is 50 kHz. The converter can operate in extremely high frequencies and so smaller value of inductor is enough. The circuit diagram has been shown in fig 2.

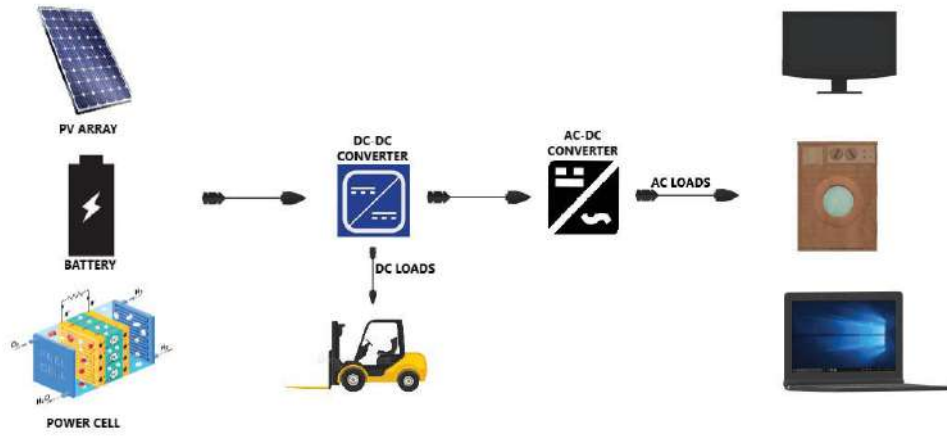


Fig. 1. Generalized Block Diagram of Multilevel flyback converter

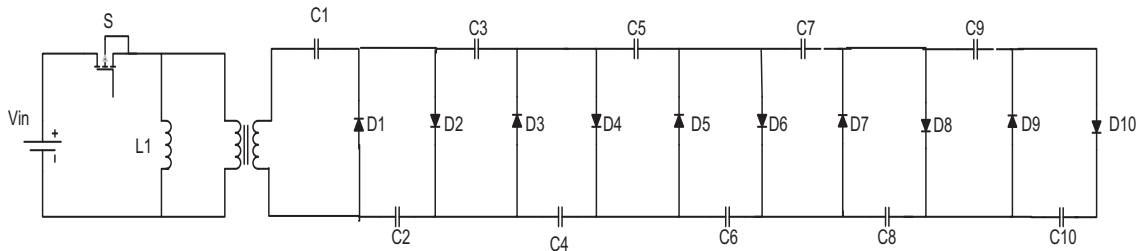


Fig. 2. Circuit diagram of non-isolated Five Level Multilevel Flyback Converter

The dc component of the source current i_g is

$$I_g = (i_g) = D(I) + D'(O) \quad (1)$$

The value of the capacitor can be determined by

$$C = (1-d) / 2RfC$$

The required Inductance L , (2)

$$L = \{(V_0 + \Delta V)(1-D)T\} / (2 * I_o) \quad (3)$$

The proposed converter works under ten modes of operation based on the switching of MOSFET. When MOSFET switch is closed the current flows in counter-clockwise direction in the primary side of the transformer. When MOSFET switch is off, the current flows in clockwise direction. Similarly the switching in the secondary side of transformer is explained next.

A. Mode1: Switch is Closed

When the switch is ON, the odd numbered diodes (D1, D3, D5, D7 and D9) are in closed condition whereas the even numbered diodes (D2, D4, D6, D8 and D10) are in open condition and the supply flows through the primary side to the secondary side. Thus the current flows in clockwise direction through the Capacitor C1 and it gets charged. So the voltage across Capacitor C1 will be twice the input Voltage V_{in} . It is illustrated in fig 2a.

B. Mode2: Switch is Open

When the switch is OFF, the odd numbered diodes (D1, D3, D5, D7 and D9) are in open condition whereas the even

numbered diodes (D2, D4, D6, D8 and D10) are in closed condition. The current flows in clockwise direction through the Capacitor C1 and Capacitor C2. Due to the flow of current these capacitors get charged. Hence the voltage across Capacitor C2 will be twice the amount of voltage across Capacitor C1. As shown in fig 2b.

C. Mode3: Switch is Closed

During this mode, the negative half cycle, diode D3 is forward biased. Now voltage during this negative half cycle reaches peak value. The direction of voltage is C2, D3, C3, and C1. Therefore the current flows through capacitor C3 making it charged. Represented in fig 2c.

D. Mode4: Switch is Open

In this mode of operation, during the positive half cycle, diode D4 is forward biased. The current flow is C1, C3, D4, C4 and C2. Therefore the voltage across the capacitor C4 will be twice the voltage across capacitor C3. The output of in this stage $2V_m$. As shown in fig 2d.

E. Mode 5: Switch is Closed

During this mode, the negative half cycle the current begins to flow through source C2, C4 through D5 conduct C5, C3, C1. Thus the current flows are in counter clockwise direction through the Capacitor C5 and it gets charged as shown in fig 2e.

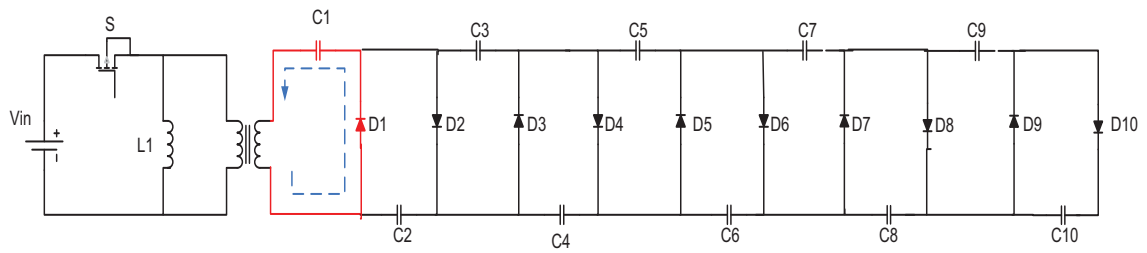


Fig 2 (a)

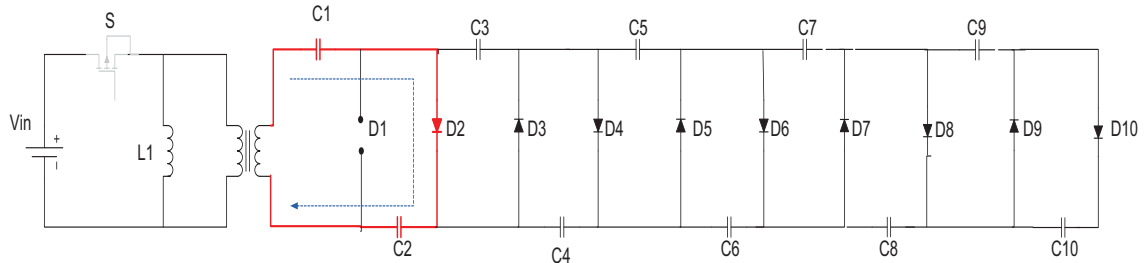


Fig 2 (b)

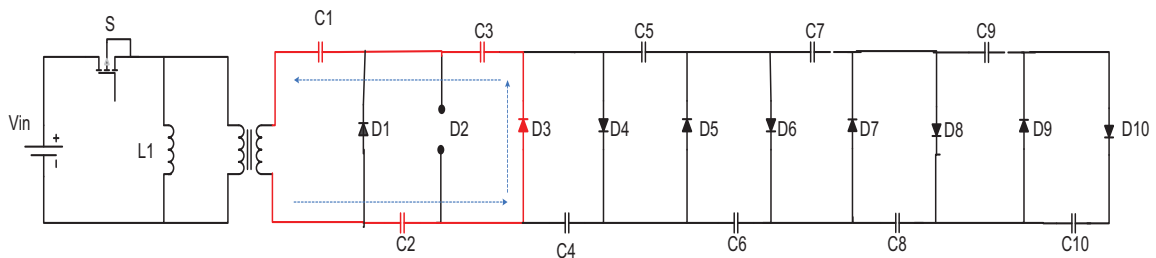


Fig 2 (c)

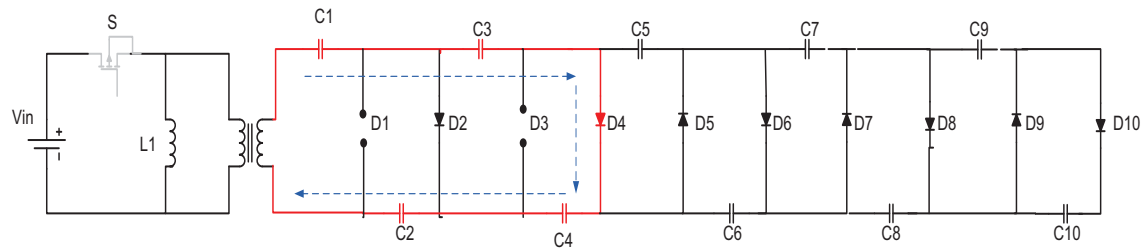


Fig 2 (d)

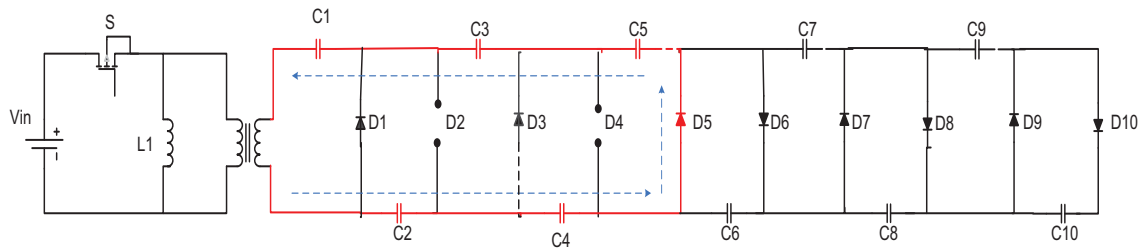


Fig 2 (e)

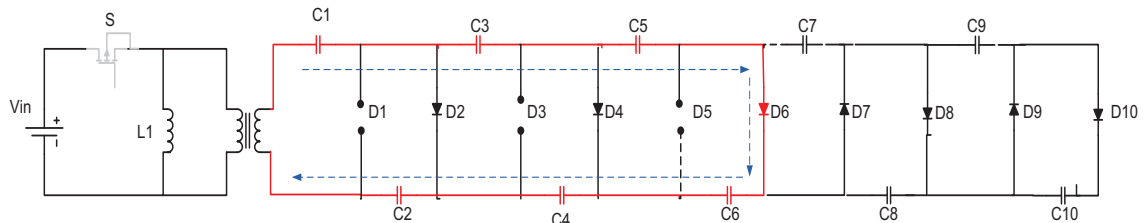


Fig 2 (f)

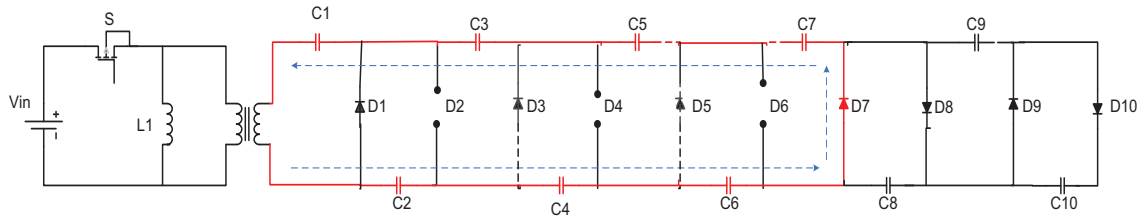


Fig 2 (g)

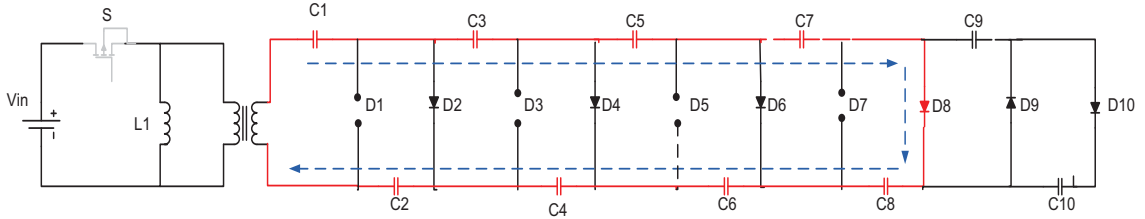


Fig 2 (h)

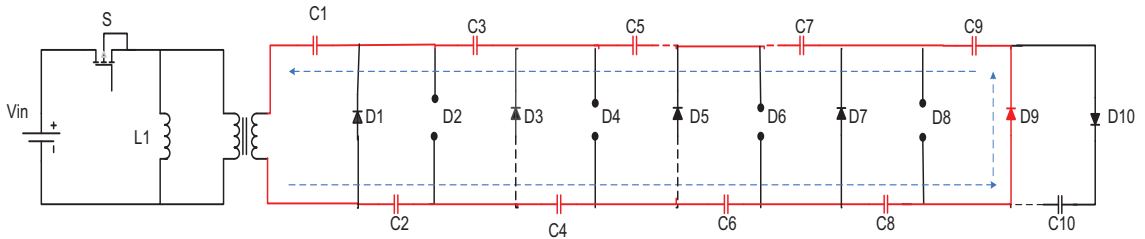


Fig 2 (i)

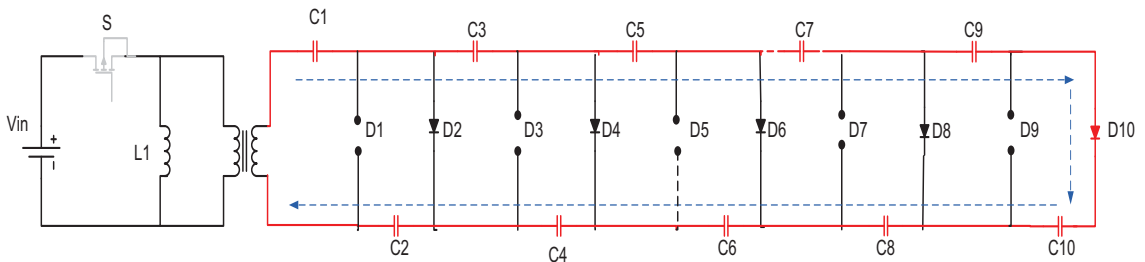


Fig 2 (j)

F. Mode 6: Switch is Open

In this mode of operation, the current flow is positive half cycle C1, C3, C5, C6, C4 and C2 with the help of diode D6 illustrated in fig 2f. Therefore the voltage across the capacitor C6 will be twice the voltage across capacitor C5. The output of in this stage is $3V_m$.

G. Mode 7: Switch is Closed

The switch is ON condition in this mode, the current flowing through the Capacitor C2, C4, C6, C7, C5, C3, and C1 through diode D7. It is presented in fig 2g.

H. Mode 8: Switch is Open

In this mode the switch is in OFF condition, the odd numbered diodes (D1, D3, D5, D7 and D9) are in open condition whereas the even numbered diodes (D2, D4, D6 and D8) are in closed condition. The current flows in clockwise direction through the Capacitor C1 to Capacitor C8 with the help of diode D8. Due to the flow of current these capacitors get charged. Hence the voltage across Capacitor C8 will be twice the amount of voltage across Capacitor C7. This the 4th level in this stage we get $4V_m$. Diagram is present in fig 2h.

I. Mode 9: Switch is Closed

In mode nine of operation, the current flows Capacitor C1 to C9 through diode D9. Hence the voltage will be twice than capacitor C8. As shown in fig 2i.

J. Mode 10: Switch is Open

Here the voltage across the last capacitor C10 will be twice than capacitor C9. The charged capacitors will be C1 to C10. I.e. all the capacitors will be conducting proved in fig 2j. Therefore the total voltage will be twenty times the input voltage.

III. SIMULATION RESULT:

A sole simulation for the proposed Multilevel Flyback converter has been administered using MATLAB/Simulink. The output voltage of the converter varies according to the load provided to the converter- fig 3a, 3b. The converter primarily works as a flyback converter but when a voltage multiplier cell connected in series with the flyback circuit based on the number of VM cells the output voltage gets multiplied. And so the voltage across each level of VM cells has been noted through simulation. The voltage across each level is 47.5v, 95v, 142v, 190v, 237v which is shown in fig 3. Since the voltage multipliers are combination of capacitors and diodes, a rectifier circuit is not necessary.

From simulation it is determined that the voltage across MOSFET switch is only 25V. Hence the percentage of voltage stress on the MOSFET is only 10% of the maximum

output voltage. Therefore a higher rating of MOSFET is not required to drive the proposed converter circuit.

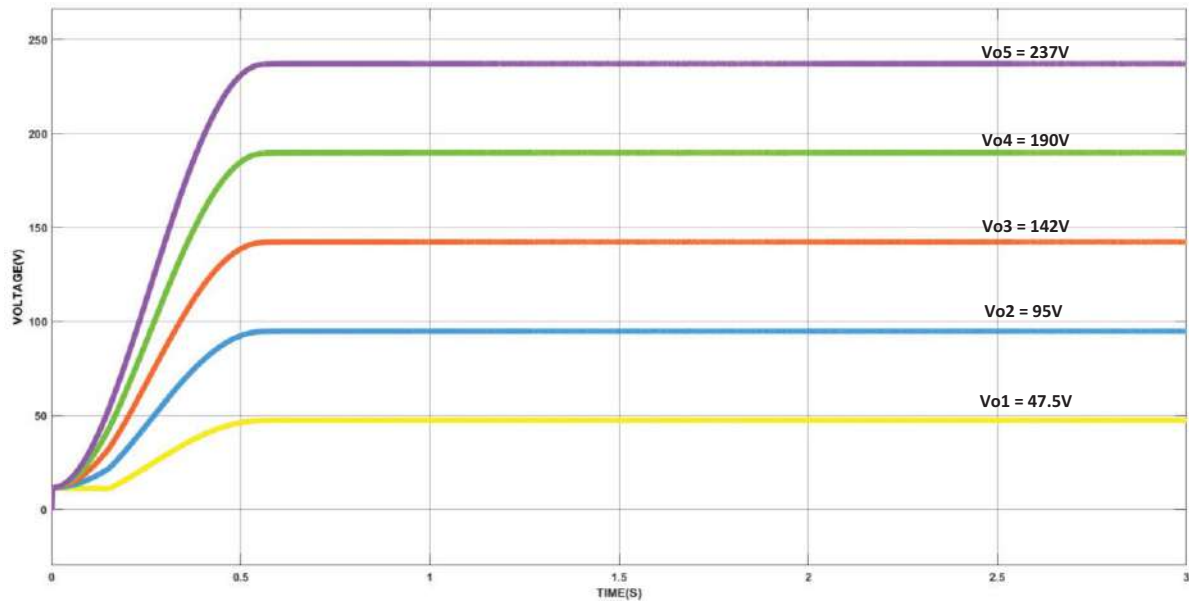


Fig 3a Output waveform for the proposed Multilevel Flyback Converter without Load

IV. SALIENT FEATURES OF PROPOSED CONVERTER WITH EXISTING CONVERTER

A foster simulation has been conducted to analyse and compare the performance of the proposed multilevel flyback converter to the existing converters by calculating various factors.

A. Voltage gain

It has been originated that the design has an output voltage of 237V for an input voltage of 12V which has a

voltage gain ratio of 19.33% while boosted. The extensive boost in voltage has been achieved with a duty ratio of 50%. Hence proving the high gain in voltage.

B. No. of Switches

The proposed converter has only one switch which is more than enough to drive the entire circuit. In the design the switch works at a switching frequency of 50 kHz. The converter which are compared in reference have many switches which leads to switching losses.

Features	Ref [4]	Ref [2]	Ref [7]	Proposed
Input voltage V_{in}	15	24	60	12
Output voltage V_0	200	380	1100	237
Duty Ratio	0.62	0.56	0.55	0.5
Voltage gain M	13.33	15.83	18.33	19.8
Power Handling Capacity	0.87	0.56	3	0.2
Gain Factor	CI & super	CI, Diod Capacitc	Interleaved Lift Capacitor CI & VMC	Voltage Multiplier Cells
No. of switches	1	2	3	1
No. of Diodes	4	4	10	10
Capacitors	4	5	8	10
Total No. of components	10	13	24	25

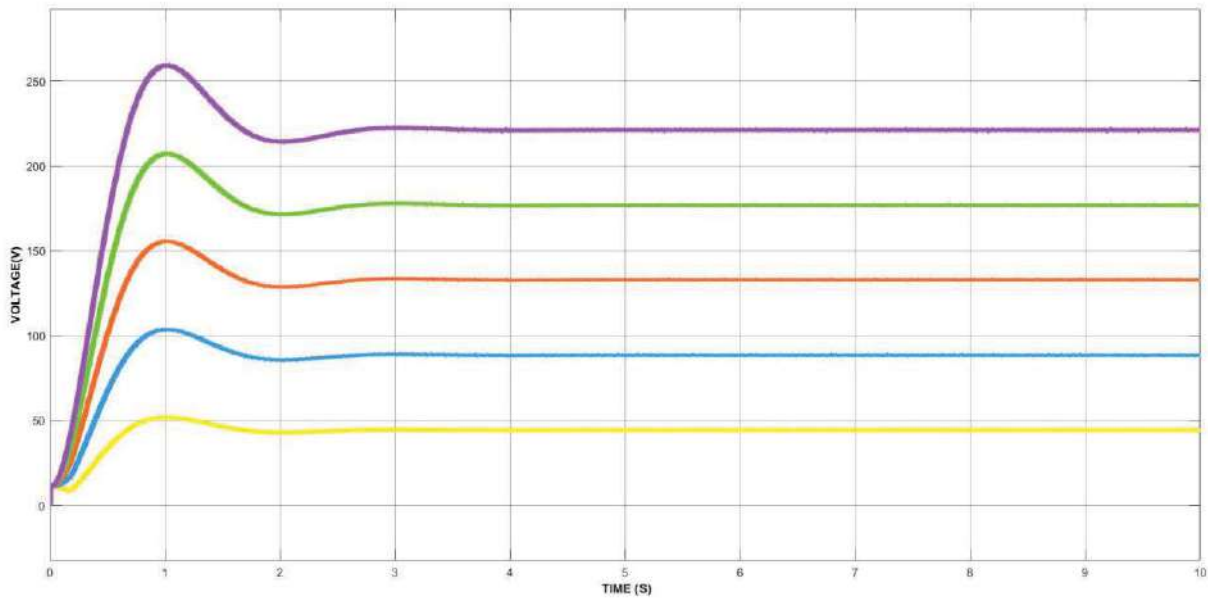


Fig 3b Output waveform for the proposed Multilevel Flyback Converter with Load

V. MULTILEVEL INVERTER APPLICATION ON MULTILEVEL FLYBACK CONVERTER

The proposed multilevel converter is then connected multilevel inverter circuit to produce an AC output. From the outputs of converter which acts as input to inverter, the H-bridge inverter generates an output of 11 level AC voltage

with a switching frequency of 50 kHz. The generated output voltages are +42v, +86v, +131v, +175v, +220v, 0, -42v, -86v, -131v, -175v, -220v. The drop in the output voltage is due to the inverter load. Therefore providing an output voltage with an efficiency of 94.5%. The circuit and simulation are shown in fig 6a & 6b.

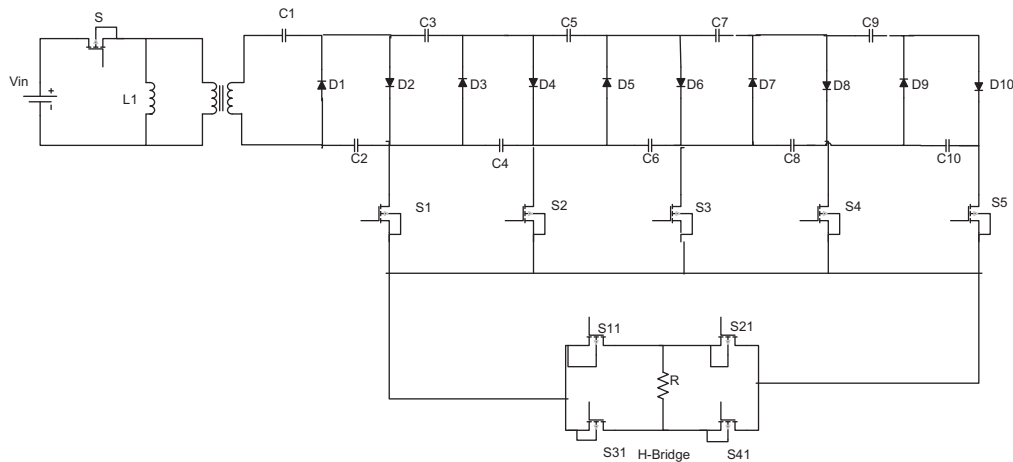


Fig 6a Circuit diagram for Multilevel Inverter from Multilevel Flyback

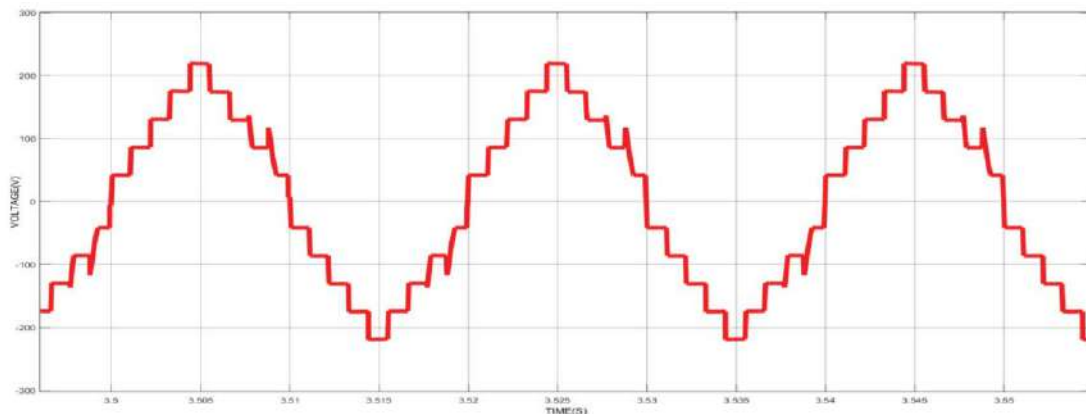


Fig 6b Output waveform for the proposed MLI circuit

VI. CONCLUSION

A simplified and idealized multilevel flyback converter with high voltage gain of 237v with 12v input has been designed. The voltage multiplier can be added any number of levels without detracting the primary circuit. The switching element used in this converter is MOSFET which has high rating and high switching speed. The proposed converter has been profitably simulated using MATLAB. The fly back approach is a viable contender under several applications, especially attractive when multiple dc outputs and input isolation are required. Active filters are included to avoid excessive voltage. The design has been implemented in continuous conduction mode, which has merits in good performance of the converter and its control scheme in steady state operation as well as during transient operation. Based on the any number of voltage multipliers can be added or removed, suitable for switching power supplies accommodating a wide input range. Hence the proposed converter is most promising choice for high voltage supplies of both AC and DC machines like TV, Monitor CRTs, copiers and cell phone and mobile device chargers, standby power supplies for computers, vehicle electronics, electric cars, etc. The proposal can also have any sort of supplies like PV array, fuel cells, battery, etc.

REFERENCES

- [1] G. Wu, X. Ruan, and Z. Ye, "High step-up DC-DC converter based on switched capacitor and coupled inductor," *IEEE Trans. Ind. Electron.*, vol. 65, no. 7, Jul. 2017.
- [2] Sizkoohi HM, Milimonfared J, Taheri M, Salehi S (2015) High step-up soft-switched dual-boost coupled-inductor-based converter integrating multipurpose coupled inductors with capacitordiode stages. *IET Power Electron* 8(9):1786–1797
- [3] B. Zhu, L. Ren, and X. Wu, "Kind of high step-up DC/DC converter using a novel voltage multiplier cell," *IET Power Electron.*, vol. 10, no. 1, Jan. 2017.
- [4] Bahrami H, Iman-Eini H, Kazemi B, Taheri A (2015) Modified step-up boost converter with coupled-inductor and super-lift techniques. *IET power Electron* 8(6):898–905
- [5] Ponzio, G.M., Capponi, G.,Scalia, P., & Boscaino, V.(2009). An improved Flyback converter. 2009 6th International Conference on Electrical Engineering/Electronics, Computer, Telecommunications and InformationTechnology.doi:10.1109/ecticon.2009.5137015.
- [6] Khan, I., Singh, B., Sharma, T., & Srikakolapu, J. (2014). Simulation of fly back converter for continuous and discontinuous mode of operation. 2014 IEEE International Conference on MOOC, Innovation and Technology in Education (MITE). doi:10.1109/mite.2014.7020245
- [7] Revathi BS, Mahalingam P (2018) Hybrid modular converter for DC microgrids. *IET Power Electron* 11(5):856–865
- [8] M. Maalandish, S. H. Hosseini, and T. Jalilzadeh, "High step-up DC/DC converter using switch-capacitor techniques and lower losses for renewable energy applications," *IET Power Electron.*, vol. 11, no. 10, Aug. 2018, doi: 10.1049/iet-pe.2017.0752.
- [9] Axelrod B, Beck Y, Berkovich Y (2015) High step-up DC–DC converter based on the switched-coupled-inductor boost converter and diode-capacitor multiplier: steady state and dynamics. *IET Power Electron* 8(8):1420–1428.
- [10] R Venugopal, D Mohan, S Manikandan - International Journal of Computer Applications, 2013Single Stage High Frequency LC Resonant Inverter

Design and Implementation of Proportional Resonant Controller for Power Inverters

C.Pearline Kamalini¹, Dr.M.V.Suganyadevi², Bharathi Freetha K³,
Madhu shree S⁴

¹ AssistatProfessor, pearline-eee@saranathan.ac.in

² Associate Professor, suganyadevi-eee@saranathan.ac.in

^{3,4} UG students, ms.s.madhushree@gmail.com

Department of EEE, Saranathan College of Engineering, Trichy

ABSTRACT.

This paper provides a design procedure of single-phase inverter with LC filter and the inverter load current is regulated by Proportional-resonant controller. The Proportional-resonant controller provides an effective control of single-phase inverter suitable for various Distributed Generation systems i.e grid connected and stand-alone systems. The performance study is based on frequency response and the model is simulated in MATLAB/SIMULINK environment which provides better stability, improved load current regulation with low THD value prescribed in the IEEE standards. The prototype model is also fabricated with Atmega328 processor and performance are satisfied.

Keywords: PV inverter, LC filter, PR controller, APF,THD.

Date of Submission: 10-07-2021

Date of Acceptance: 26-07-2021

I. INTRODUCTION

Inverter is one of the main power conditioning devices in the integration of renewable energy, other distributed energy sources. Voltage source converter is the basic component in power quality improvement to filter out the harmonics i.e Active Power filters and Facts devices. The power conversion from DC to AC with good power quality is from an Inverter. As a consequence, power converters for renewable energy sources are becoming increasingly common. It's vital to produce clean and green energy. It is important to sustain the inverter output and the proposed system is designed with an LC filter to filter out high frequency components. [1] The various control techniques to control the PV inverters to provide high quality of output current and voltage connected to a linear or

non-linear load are hysteresis current controller, Predictive Current controller, Proportional Integral (PI) controller and Proportional Resonant (PR) controller [2]. The effect of harmonics such as power losses, decay of quality power reduces the equipment life and failure of components. In a grid-connected application, for example, the power converter must follow many typical grid parameters, including voltage, current, frequency, harmonics, power factor, and flicker.

Based on literature the hysteresis controller is simple, unconditional stability and good accuracy with comprehensive band harmonic spectrum. The predictive controller force the measured current to track the reference current. The famous conventional controller PI controller produces steady state error while tracking the sinusoidal reference due to dynamic integral term[3]. The proposed PR controller provides zero steady state error, high gain in wide range of frequency response with fast tracking of specified references and with low value of %THD. The block diagram of single-phase inverter with PR controller is shown in Fig:1.

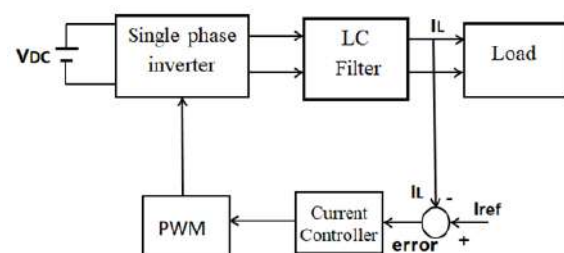


Fig.1 Closed loop Block diagram of single-phase inverter

II. DESIGN PROCEDURE OF THE SYSTEM

From Fig:1 the system input is 400V DC and it is converted to 230V AC by a single phase inverter circuit. DC components are filtered out by LC filter and the ripple free signal is fed to the load. The filter output is maintained by developing a closed loop system with a current controller. The controller compares the actual load current and the reference current and the error signal is modulated [10] with the help of proposed PR controller. From the PR controller output unipolar PWM pulses are generated to trigger the power semiconductor switches of the inverter. The step by step design procedure of each block is as follows:

Step 1: Design of single-phase Inverter

The design parameters of 2KW, 230V, 50Hz single-phase inverter is charted in Table:1. Four IGBT switches with a switching frequency of 10KHz.

Table:1 Design parameters of the proposed model

Description	Parameters	Values
Input DC Voltage	V_{in}	400V
Output AC Voltage	V_o	230V
Supply Frequency	f_o	50Hz
Output Power	P_o	2KW
Switching Frequency	F_s	10KHz
Voltage THD	THD _v in %	<5%
Ripple Current	I_{rp} in %	<20%

Step 2: Design of LC filter

a) Inductor L:

The voltage across the inductor is given by eq.1 and the potential difference between the inductor is defined by eq.2 and shown in Fig.2. Inductor ripple current is calculated by using eq.3 [7] and the maximum ripple current is derived by differentiating ΔI_{pp} with respect to time and equate it to zero, the obtained result is eq.4.

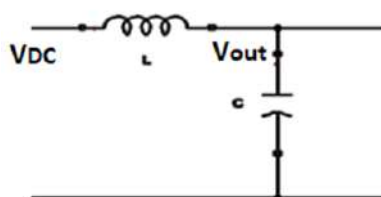


Fig.2 LC filter

$$V = Li \frac{di}{dt} \quad (1)$$

$$V_{dc} - V_{out} = Li \frac{\Delta I_{pp}}{DT_s} \quad (2)$$

$$\Delta I_{pp} = \frac{DT_s(V_{dc} - V_{out})}{L_i} \quad (3)$$

$$\Delta I_{pp} = \frac{V_{dc} * T_s}{4 * L_i} \quad (4)$$

The duty cycle is calculated by eq.5 where m_a is the modulation Index and output voltage is calculated as per eq.6 and eq.7. Inductor current is calculated as per eq.9.

$$D(\omega t) = m_a * \sin(\omega t) \quad (5)$$

$$V_o = V_{dc} * D \quad (6)$$

$$V_o = V_{dc} * m_a * \sin(\omega t) \quad (7)$$

$$L_i = \frac{V_{dc}}{4 * f_{sw} * \Delta I_{pp \max}} \quad (8)$$

Therefore by substituting the values in eq.8

$$L_i = \frac{400}{4 * 10000 * 8.7 * \sqrt{2} * 0.2} \quad (9)$$

$$L_i = 4.06 \text{mH} \quad (10)$$

$$I_{out} = \frac{KW}{V_{out}} = \frac{2000}{230} = 8.7 \text{A} \quad (11)$$

From the above design the value of inductor is calculated as 4.06mH shown in eq.9 and the current through the inductor is 8.7A given in eq.11.

b) Capacitor C:

The cut-off frequency is calculated using eq.10 and it is 10% of switching frequency as shown eq.11. The capacitor value is found out using eq.12, the values are substituted in eq.13 and as per the design the value of capacitor is calculated as 6.23 μF .

$$F_c = \frac{1}{2\pi\sqrt{LC}} \quad (10)$$

$$F_c \leq \frac{f_{sw}}{10} \quad (11)$$

$$C = \left(\frac{10}{2\pi f_{sw}} \right)^2 * \left(\frac{1}{L_i} \right) \quad (12)$$

$$C = \left(\frac{10}{2 * \pi * 10000} \right)^2 * \left(\frac{1}{4.06 * 10^{-3}} \right) \quad (13)$$

$$C = 6.23 \mu\text{F}$$

Step 3: Design of PR controller:

The general block diagram of PR controller is shown in Fig:3 The ideal and non-ideal PR controller in s-domain is represented in eq.14 and eq.15 respectively. The ideal PR controller suffers from stability problem and sudden phase shift and these are eliminated by non-ideal PR controller [3].

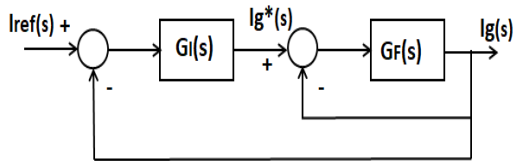


Fig.3 Block diagram of non-ideal PR controller

where K_p = Proportional Gain
 K_i = Integral Gain
 $\omega_0 = 2\pi f_0$ = Resonant frequency
 ω_c = Cut-off frequency

The performance of system dynamic can be improved by proper tuning of gain .By including the harmonic compensator the selected harmonics i.e lower order harmonics are eliminated.

a) Voltage controller:

The voltage controller is designed by considering the Controller time constant as $200\mu s$, filter capacitance of $6.23\mu F$ and Capacitor ESR = $0.0042\ \Omega$. The proportiona

gain value is estimated as 0.003115 given by eq.15

$$K_p = \frac{\text{Capacitance}}{\text{Time Constant}} \quad (15)$$

$$K_p = 0.03115 \quad (16)$$

b) Current Controller:

For current controller design, let us consider the controller time constant as $150\mu s$, filter Inductor as $4.06mH$ and Inductor series resistance as

a) Resonant gain K_r :

The general transfer function of resonant gain is given by eq.18

$$G_n = \frac{K_r \omega_n}{\omega_n^2 - \omega^2} \quad (18)$$

Where $\omega_n = \frac{1}{\sqrt{LC}}$ and $\omega = 2\pi * f$,

let the value of G_n is 0.1 and K_r for voltage controller is 100

$$\frac{\omega^2}{K_r} = \frac{2 * \pi * 50^2}{100} \quad (19)$$

$$\frac{\omega^2}{K_r} = 986.83 \quad (20)$$

Let K_r for current controller is 400

$$\frac{\omega^2}{K_r} = \frac{2 * \pi * 50^2}{400} \quad (21)$$

$$\frac{\omega^2}{K_r} = 246.7$$

Thus the inverter, filter and controller parameters are calculated as per the specifications.

III. SIMULATION AND RESULT

The single-phase inverter with PR controller is modeled and simulated as per the design calculation. The inverter power switches are triggered by unipolar PWM pulses generated by the PR controller block. The system is demonstrated in MATLAB Simulink as per the proposed design shown in Fig.4. and the various

system parameters are observed as shown below. The Unipolar PWM pulses are generated to operate the four switches i.e SW1, SW2, SW3 and SW4 by comparing the actual inverter output voltage and reference voltage shown in Fig.5.

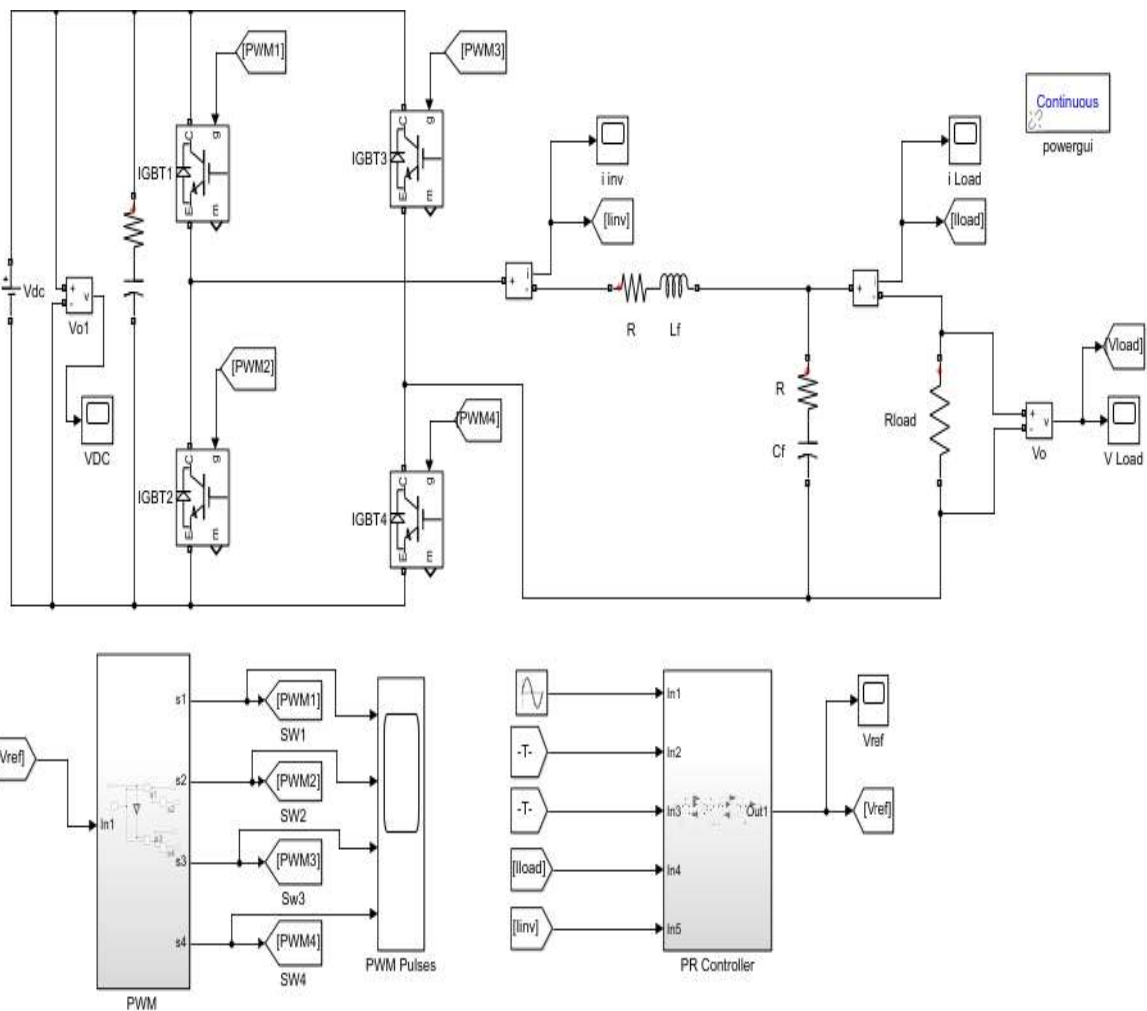


Fig:4 simulation model of power inverter with PR controller

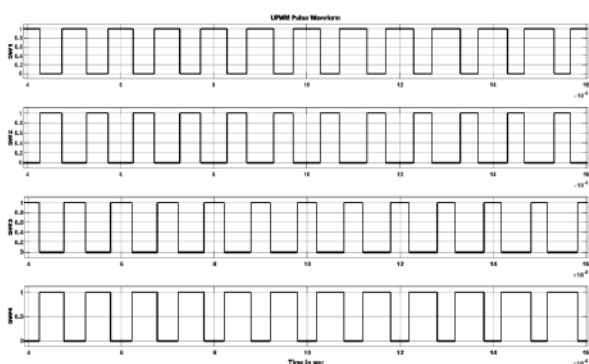


Fig.5. UPWM pulse of inverter

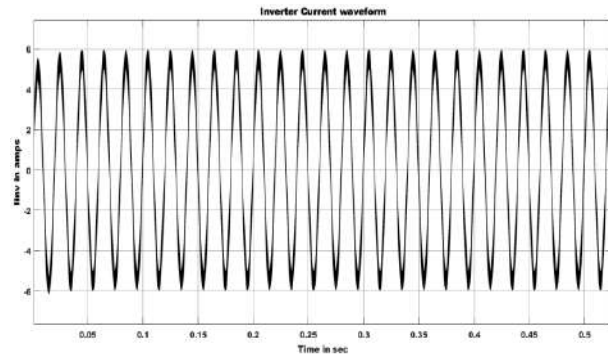


Fig.6. Inverter current waveform of inverter

The inverter current waveform and the load current waveform as per design are traced as shown in Fig.6 and Fig.7 respectively.

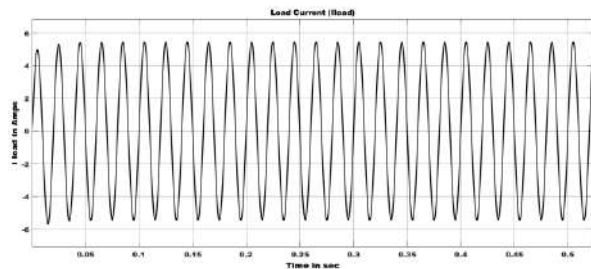


Fig.7 Load current waveform of inverter

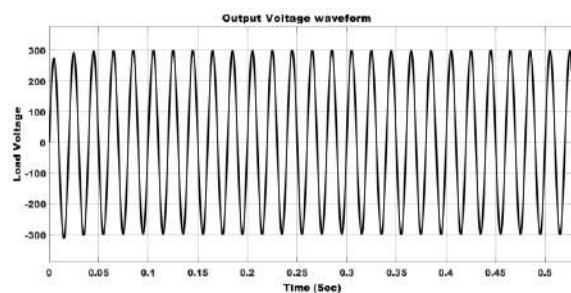


Fig.8. Output Voltage waveform of Inverter

The output voltage is witnessed across the load resistance as shown in Fig.8. By proper design of PR controller the specified output load voltage of 230V is maintained for variation input and as well as variation in load. The input, output waveforms are traced for $V_{DC} = 400V$ & $380V$ as shown below in Fig.9 and Fig.10.

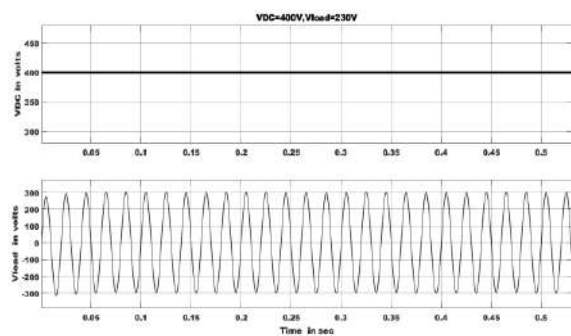


Fig.9. Output Voltage waveform of Inverter $V_{DC} = 400V$

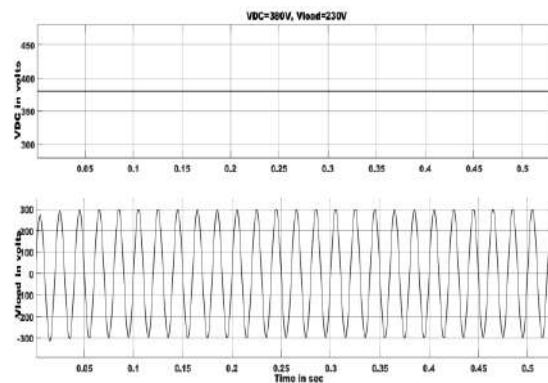


Fig.10. Output Voltage waveform of Inverter $V_{DC} = 380V$

The Fig:11 shows the Frequency spectrum of load voltage for the rated supply frequency 50HZ is 300 and the Total Harmonic Distortion is very much reduced to

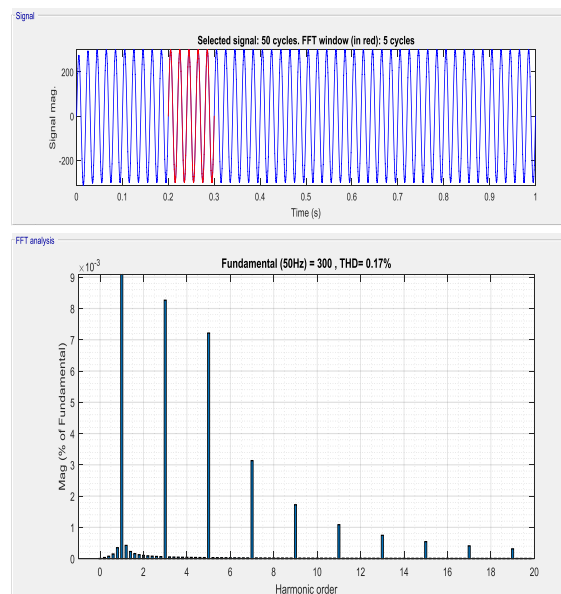


Fig.11. Frequency Spectrum of load voltage

0.17% compared to the conventional PI controller [4][5].

IV. EXPERIMENTAL RESULTS



Fig:12 Prototype model of single phase inverter with arduino-ATMEGA 328 based PR controller

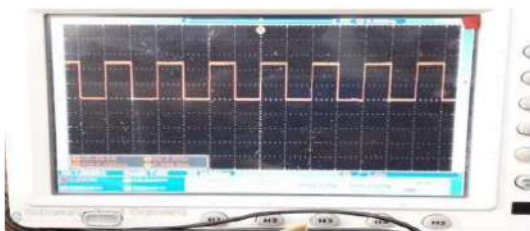


Fig:13 UPWM pulse waveform

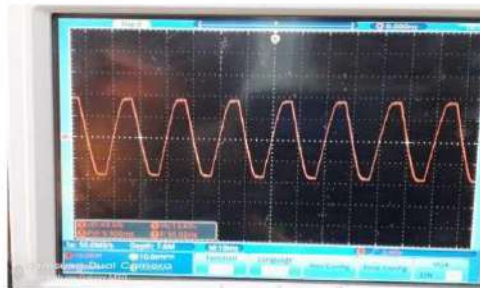


Fig 14: Output Voltage Waveform of Inverter with PR controller

The Fig:12 shows the experimental prototype model of single phase inverter with arduino based PR controller. In the experimental setup the PR controller is implemented using Arduino IDE with ATMEGA-328 microcontroller with to generate the pulse signal to the power inverter switches. Fig:13 and Fig:14 shows the UPWM pulse waveform and Inverter output voltage for load variations measured from experimental setup. The performance is verified using the design values and it is satisfied.

V. CONCLUSION

Thus the single-phase inverter is designed and implemented with proportional-Resonant controller. The performance of inverter is improved compared with the PI controller. The designed

inverter topology is suitable for a PV based generation with grid connected system and stand-alone applications. This Power inverter with PR controller design is suitable for Active Power Filter to mitigation of harmonics generated by a non-linear load. It is concluded that from FFT analysis of load voltage, the THD value is 0.17%. This shows the performance of PR controller is better than the PI controller[6]-[8]. Based on the design procedure the experimental set is fabricated and the triggering pulses are generated using ATega328 and the performance is satisfied.

REFERENCES:

- [1]. I.Abdel-Qawee, et al., "Closed-loop control of single phase selective harmonic elimination PWM inverter using proportional-resonant controller," in Modelling, Identification & Control (ICMIC), 2013 8 Proceedings of International Conference on, 2013, pp. 169-174.
- [2]. D. Zammit , Staines ,C.S.,and Apap ,M . "Comparison between PI and PR Current Controllers in Grid Connected PV Inverters," International Journal of Electrical, Electronic Science and Engineering, vol. 8, 2014.
- [3]. Sushil Silwal and Masoud Karimi-Ghartemani "On the Design of Proportional Resonant Controllers for Single-Phase Grid-Connected Inverters" 12th IEEE International Conference on Control & Automation (ICCA) Kathmandu, Nepal, June 1-3, 2016
- [4]. M. Muthazhagi and N. S. Kumar, "Comparison of controllers for power quality improvement employing shunt active filter," in Computing Electronics and Electrical Technologies (ICCEET), 2012 International Conference on. IEEE, 2012, pp. 248–253.
- [5]. C.Pearline Kamalini, Dr.M.V.Suganyadevi, "Mitigation of harmonics using PI Controller and Fuzzy logic Controller based shunt Active Power Filter" in the proceedings of National Conference on Recent Advances in ON-Board Ship Automation (RAOBSA-2019)" ISBN: 978-93-85434-75-4
- [6]. A. Chatterjee and K. B. Mohanty, "Development of Stationary Frame PR Current Controller for Performance Improvement of Grid Tied PV Inverters," IEEE, 2014.
- [7]. A. Akhavan, H. Reza Mohammadi, and J. M. Guerrero, "Modeling and design of a multivariable control system for multi-paralleled grid-connected inverters with LCL filter," Int. J. Electr. Power Energy Syst., vol. 94, pp. 354–362, 2018.
- [8]. D. Zammit, c. s. Staines, and M. Apap,

- “Comparison between PI And PR Current Controllers in Grid Connected PV Inverters,”*Int. Sch. Sci. Res. Innov.*, vol. 8, no. 2, pp. 221226,2014.
- [9]. H. Zhou, C. Tong, M. Mao, and C. Gao, “Development of Single-phase Photovoltaic Grid-connected Inverter Basedon DSP Control,” *IEEE*, pp. 650-653, 2010.
- [10]. Gandham Krishna Kanth,T Lova Lakshmi,M Gopichand Naik ,”Modelling of PR Controller For A Grid Connected Single Phase Inverter” *International Journal of Engineering Development and Research* Volume 5, Issue 4 | ISSN: 2321-9939.

C.Pearline Kamalini, et. al. “Design and Implementation of Proportional Resonant Controller for Power Inverters.” *International Journal of Engineering Research and Applications (IJERA)*, vol.11 (7), 2021, pp 25-31.

Improved STATCOM Control to Improve Transient Stability of Power of a Power System using PSO technique

DR.M.V.Suganyadevi

*Department of Electrical and Electronics Engineering
Saranathan College of Engineering
Trichy, India*

Sankari S

*Department of Electrical and Electronics Engineering
Saranathan College of Engineering
Trichy, India*

Preethi V

*Department of Electrical and Electronics Engineering
Saranathan College of Engineering
Trichy, India*

Srijah R

*Department of Electrical and Electronics Engineering
Saranathan College of Engineering
Trichy, India*

Abstract-In recent year, photovoltaic is widely used in diverse application. The photovoltaic is a device which converts solar energy into a DC electrical energy. The wind farm produces a ac source by integrating these two renewable energy causes a voltage dip in grid side to overcome this problem we introduces a facts devices. FACTS devices boost power network performance by rerouting facility flow on transmission lines so that thermal limits aren't surpassed, all while meeting grid stakeholders' contractual obligations and increasing system load ability. FACTS devices work in the steady state by providing or consuming reactive electricity, increasing or decreasing voltage, and regulating transmission line or phase series impedance. The benefits of FACTS devices, on the other hand, are based on their form, size, number, and position within the transmission. Particle swarm optimization is one of several heuristic or analytical methods for locating the best locations for given FACTS devices within the power grid (PSO).This paper shows the transient stability of a power system and it is achieved by using a particle swarm algorithm, which was one of the fast simple, fast converging technique. The above mentioned topology is analyzed using MATLAB/ SIMULINK platform and the result is acquired for an inter machine's stability.

Keywords: *Multi-machine-DFIG -Facts device-Solar-STATCOM*

I. INTRODUCTION

Considerable attempts have been made to blend renewable energy in order to satisfy demand, onto grid for long-term and stable generation of electricity. Taking into account the complementary wind and solar energy features, the expansion of the current wind farm with photovoltaic panels will greatly reduce the fluctuations in power generation and increase the operating economy [1]. The primary goal of this paper is really to discuss the use of solar power plants, wind turbines, and synchronous machines concurrently inside the grid of the facility. In this scenario, the intermittent interaction of renewable solar and wind also may threaten grid accuracy and performance. Wind turbines based on double-powered induction generators (DFIG) use small-scale, limited-voltage controlled converters. The low over current withstand capability of DFIG-based wind turbines makes them highly susceptible to grid faults. Modern double fed induction generator systems commonly implement rotor circuit protections to safeguard the rotor side converter (RSC) during fault conditions. Because of insecurity and

uncertainty of operating conditions, integrating wind turbines into power systems creates a replacement issue. Crowbar safety at the rotor circuit is often used in modern DFIG systems to safeguard the rotor side converter (RSC) during fault conditions. Because of instability and volatility inherent in operating conditions, integrating wind turbines into power systems introduces a replacement complex case. Doubly-fed induction generators (DFIGs) are preferred for wind energy generation options implemented in to the power systems because of real and reactive powers can be controlled independently and at varying speeds.. Due to the rapid loss of internal magnetization relative to the missing voltage, the DFIG device is highly dangerous on voltage instability caused by power fluctuations. Voltage dips cause the turbine to over speed and thus its safe operation. In a DFIG turbine, the generator stator is linked directly to the power system, while the generator rotor is linked back -to- back protected gate bipolar transistor pulse width modulator converters via an intermediary dc link capacitor. Grid demands are provided in relation to them, in which case technical specifications such as low voltage ride-through (LVRT) and reactive capability of injecting electricity should receive much more attention [2-5]. Because of lower Photo voltaic cell prices and advancements in power electronics technology, perforation would skyrocket. Due to lower PV cell prices and advancements in power electronics technology, penetration would skyrocket. Unintentional islanding operation of grid connected Photovoltaic systems could cause far more serious grid problems than that of the initial event, such as power outages and voltage flickers. As a result, some European countries changed their grid codes for voltage systems in order to address possible issues. The proportion of total installed power capacity dedicated to wind power is rising globally at the moment. Because of its advantages, Double fed induction generator is the most extensively utilized wind turbine generator at the moment (WTs) [9-12]. Improved stability and protection, as well as a more energy efficient transmission .FACTS devices increase the performance of power networks by redistributing power flow in such a way that the transmission lines that the thermal thresholds aren't being exceeded by meeting contractual obligations grid-related specifications stakeholders and framework extension capacity to load .The numerically efficient control approach for Flexible AC Transmission System presented here is expected. (Because of the MPC horizons being so short) and robust (in the face of complication) Mechanisms of separation).FACTS devices function in the steady state by providing or receiving energy. Absorbing and rising reactive capacity or lowering the voltage and regulating it transmission impedance in sequence lines or angle step. The development of stability of a system is investigated in this paper PV and wind turbines are used to fuel the grid.

II. Wind farm

The wind farm is made up of DFIG, a wind turbine with a drive train system, rotor side converter, grid side converter, DC-link capacitor, pitch controller, coupling transformer, and protection system.The Double fed induction Generator wind turbine is also an induction-type generator, comprising windings on a stator lined up to the three-phase system with field winding feeding via a three-phase back-to-back insulated-gate bipolar transistor (IGBT)-based on the pulse width modulation (PWM) converter.

III. DFIG

The turbine rotor that removes K.E. from wind may be difficult aerodynamic device .The word "aerodynamic torque" refers to turbine is given a torque input:

Equation (1) shows that the input torque of the turbine (1)

$$T_{ae} = \frac{\rho}{2\omega_m} A_{wt} c_p(\lambda, \theta) \omega_w^3 \quad (1)$$

ρ - Air density, ω - rotor speed, A_{wt} -swept field, c_p -pitch angle and λ - speed ratio.The turbine-mounted drivetrain converts aerodynamic torque T_{ae} in two stages. The drivetrain is traditionally considered as two lumped weights, the weight of the turbine and the weight of the generator, that are bound together by a shaft to certain values of harmonics and friction coefficients.. The weight of the turbine comprises lumped inertia of turbine, part of the gearbox, therefore, the low speed shaft and engine weight include the weight of the generator, the high-

speed shaft beside the disc brake, and therefore the remaining component of the gearbox. The dynamics of the shaft are also expressed as [20]

$$\dot{\omega}_m = \frac{1}{2H_m} [T_{ae} - K_s \gamma - D_m \omega_m] \quad (2)$$

$$\dot{\omega}_G = \frac{1}{2H_G} [K_s \gamma - T_e - D_G \omega_G] \quad (3)$$

$$\dot{\gamma} = 2\pi f \left(\omega_m - \frac{1}{N_g} \omega_G \right) \quad (4)$$

H - constant of inertia, K_s - torsion tension, Δ - torsion angle, D - torsion damping, T_e 's - electric torque, f - frequency of the grid, and N_g -proportion of the gear. The facility is collected by the induction generator from a stiff high speed shaft.

The relation between the mechanical torque (T_m) and the degree of torsion is expressed as.

$$T_m = K_s \gamma \quad (5)$$

$$\dot{s} = \frac{1}{2H_G} [T_e - T_m] \quad (6)$$

$$\dot{E}'_{qr} = \frac{1}{T'_o} [E'_{qr} - (X - X') i_{ds}] - s \omega_s E'_{dr} - \omega_s v'_{dr} \quad (7)$$

$$\dot{E}'_{dr} = \frac{1}{T'_o} [E'_{dr} + (X - X') i_{qs}] + s \omega_s E'_{qr} + \omega_s v'_{qr} \quad (8)$$

$$v_{ds} = R_s i_{ds} - X'_{qs} + E'_{dr} \quad (9)$$

$$v_{qs} = R_s i_{qs} + X'_{qs} + E'_{qr} \quad (10)$$

$$v_t = \sqrt{v_{ds}^2 + v_{qs}^2} \quad (11)$$

$$X' = X_s + X_m X_r (X_m + X_r) \quad (12)$$

$$X = X_s + X_m \quad (13)$$

$$T'_o = \frac{L_r + L_m}{R_r} \quad (14)$$

$$T_e = E_{dr} i_{ds} + E_{qr} i_{qs} \quad (15)$$

$$v'_{dr} = \frac{v_{dr} X_m}{(X_m + X_r)} \quad (16)$$

$$v'_{qr} = \frac{v_{qr} X_m}{(X_m + X_r)} \quad (17)$$

Where (12) (13) (14) (15) (16) (17) E' - transient voltage, X' - transient reactance, X - open circuit of rotor reactance, T_e - electromagnetic torque in (6)–(17). The voltage of a dc link are frequently written as

$$C v_{dc} \dot{v}_{dc} = -\frac{v_{dc}^2}{R_{loss}} - P_r(t) - P_g(t) \quad (18)$$

$$P_r = v_{rd} i_{rd} + v_{rq} i_{rq} \quad (19)$$

Where C is the dc capacitance, V_{dc} is the voltage of capacitor, $P_r(t)$ - input rotor power, and $P_g(t)$ - GSC's instantaneous output power. Chowdhury[12] have P_r and P_g .

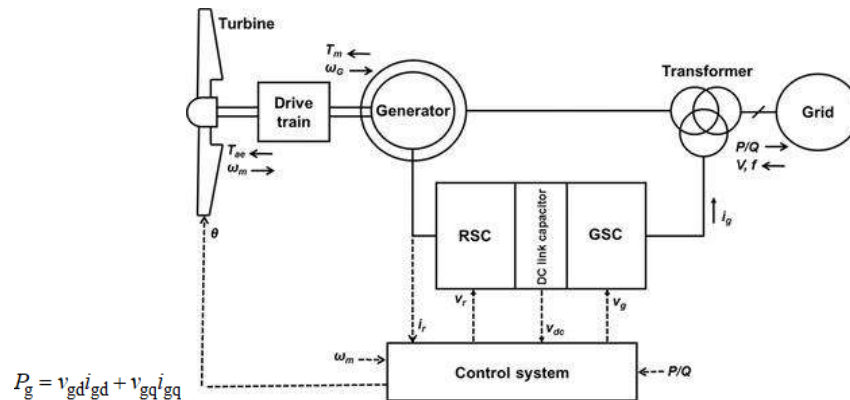


Fig.1. Block diagram of DFIG

IV. Functional block of a typical PV system

The role is fed by the general PV method. Solar PV is a technology that converts light energy into electricity. A DC link voltage is normally used to regulate the gridside converter. A three-phase PV inverter is easier to synchronous than asingle-phase PV inverter, so the PV system's life span is typically longer.

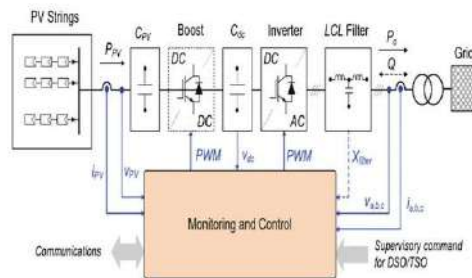


Fig.2. Control function block of a PV system

This block diagram shows that the PV array produces the DC source which is boost with the help of boost converter. The boost converter boost the voltage produced by the PV array. The dc source is passed inverter via C_{dc} . The inverter converts the DC into AC. LCL filter is used to reduce the harmonics and amplifies the output. Now the ac source is entered into the grid.

V. PV CELL

The PV cell is the most important component of the PV organization of electrical wonder. The daylight subordinates cells for the increase in proper current, high force, and probable difference. In everyday uses, an

energy single cell is comparable to a diode with the crossing point scheduled by the semiconductor material. When the light is absorbed by the electrical phenomenon, influence at the point of crossing, it automatically provides the streams. The PV module MATLAB model was constructed to take into account the effect of temperature and isolation on the exhibition of the PV module.

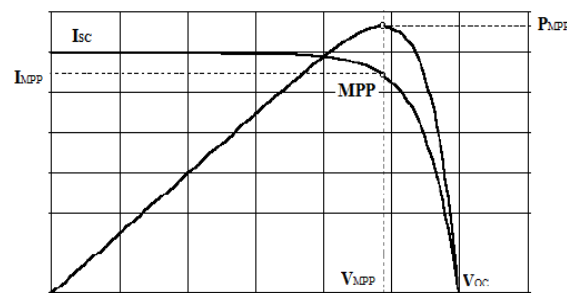


Fig.3. I-V and P-V Curve of PV Cell

Parameter	Specification
(V_{oc})	22.2 V
(I_{sc})	1.73A
(P)	30W
Voltage MPP (V_{mp})	18.85V
Current MPP (I_{mp})	1.673A
Current temp-coefficient	-0.123A/K
Voltage temp-coefficient	0.0032V/K

TABLE 1 PANELS SPECIFICATIONS

VI. FACTS DEVICES

FACTS devices increase the performance of power networks by rerouting facility flow on transmission lines. Lines in such way that the thermal energy is not lost Limits aren't breached, and completing contractual obligations stakeholders in the grid and increasing the load ability of the machine [3]. FACTS devices function in the steady state by providing or consuming reactive power, respectively. Growing or decreasing voltage, as well as regulating the series impedance Lines of transmission or process [4]. The benefits of FACTS devices, on the other hand, are based on their form, size, number, and position within the system. [5] transmission. There are many approaches to finding the best solution, including heuristic and empirical methods for the specified locations THE FACTS devices that are part of the power grid, such as Tabu [6–10], genetic algorithm (GA) Simulated quest (TS) [11, 12]. Particle swarming (PS) [12], annealing (SA) [13–15] Optimization (PSO) in addition [16–] Evolutionary algorithm (EA) [19]. Transmission lines are often moved to the limits of their thermal capacity, if not beyond, in order to achieve maximum performance to meet the increased demand for electricity as a result of the rapid rise in demand the unanticipated power shifts. As a result, transmit power and noise have improved across the power system. As a result line voltages and bus voltages must be preserved. One is to hold load in predetermined limits. It is the difficult tasks in support of the engineers who work on facility systems. Regulation of reactive node compensation will change the voltage profile and would be the main point of versatile AC transmission (FACTS) technology. FACTS controllers are still used in transmission and they use power not only to enhance the system reliability however, to increase load capability of a system. Because of current flow via the wires is the function of the all sides have a voltage, as well as impedance of the process of connecting, thus the reduction of the power losses at either the static and dynamic position of the grid. With the help of the FACTS controllers, the power flow of reactive power, and hence active power loss within the lines are shortened by a wide margin by

introducing a difference in phase between sending and receiving end buses linked by a route.

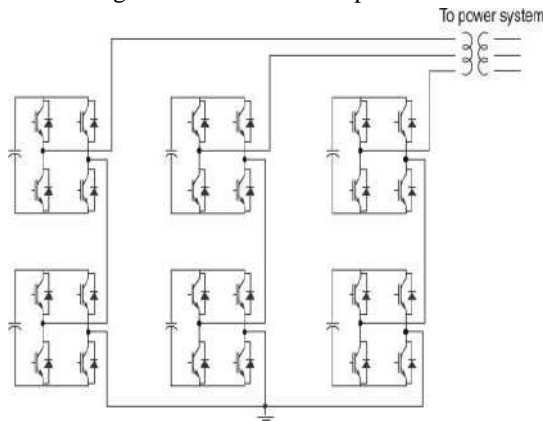


Fig.4. Schematic and functional block of FACTS Devices

VII. STATCOM

STATCOM is a synchronous compensator. STATCOM is a one of the member of the facts family. It is a shunt connected power electronics converter based FACTS devices. STATCOM is otherwise known as static synchronous condenser. STATCOM devices are used in AC transmission line. It is used to provide a voltage stability control and reactive power control in a transmission line .It is used to improve the stability of the power system a transmission line.

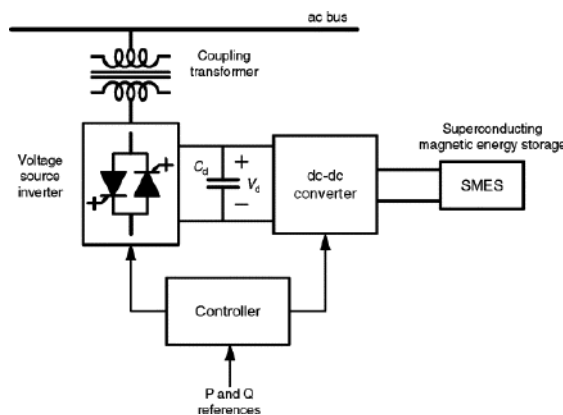


Fig.5. Schematic block of STATCOM

The STATCOM circuit consist of a converter coupled with a Ac transmission line. The rectifier converts the AC source into DC source. The DC source enters into the STATCOM circuit converts the dc into AC with low reactive power and increases the voltage stability. Thus the AC source enters into the distributed load via the transmission line.

VIII. ALGORITHM

Kennedy, Eberhart , and Shi acknowledged PSO for simulating individual interaction as an expressionistic depiction of the evolutionary process moving inside a bird flock or fish school fashion. When comparing different computational methods available in literature, PSO is regarded as a computational method that defines the problem and improves the problem through an iterative process in order to generate a convergence rate with quality in mind. The suspension system planning problem is converted into a nonlinear optimization problem with an inter optimization process. To find optimal parameters, the current technique uses particle swarm optimization (PSO) algorithms. It is proposed that the PSO-based PSS be used to enhance the alignment of PSS parameters in order to increase optimizing synthesis and thus the speed of converge. The Particle swarm algorithm [12] has the

potential to useful formulaic algorithm for dealing with combined optimization problems. Theoretically, the Particle swarm algorithm is shown to convergence to the best solution [13].

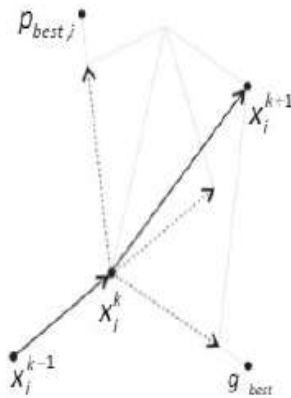


Fig.6.Movement of particle during optimization iterative process

Furthermore, the Particle swarm algorithm is strong, which means that the final solution efficiency is not too dependent on the initial solution choice. Another advantage of the Optimization algorithms is its sophistication. The PSSs architecture (PSOPSS) is formulated as an inter optimization problem that is solved using the Particle swarm optimization. The objects in the Particle swarm Optimization method are a collection of simple entities that are located within the search space of a problem or function and determine the target function at its current position.

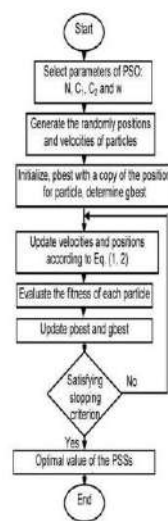


Fig .7 .Flowchart of PSO

IX. BLOCK DIAGRAM

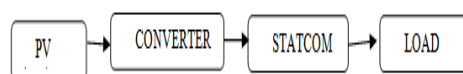


Fig.8. block diagram of solar system (open loop)

The above block diagram shows that the PV array produces the dc voltage. The dc voltage enters into the STATCOM circuit the STATCOM circuit consist of the converter coupled with the transmission line .The converter converts the dc source into ac source .Now the ac source is applied into the load.

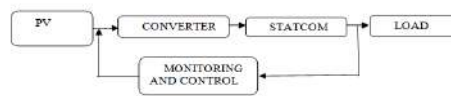


Fig.9. block diagram of solar system (closed loop)

The above block diagram shows that the PV array produces the dc voltage .The dc voltage enters into the STATCOM circuit the STATCOM circuit consist of the converter coupled with the transmission line .The converter converts the dc source into ac source. In this stage the STATCOM controlled by using particle swarm algorithm, which will reduces the reactive power.

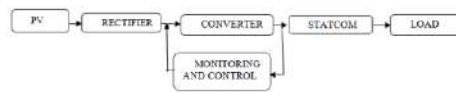


Fig 10. Block diagram of wind system

The above block diagram shows that the wind farm is connected with the rectifier. The wind farm produces the ac source. The rectifier converts the ac source into ac source. The STATCOM circuit is controlled by using particle swarm algorithm, which reduces the reactive power

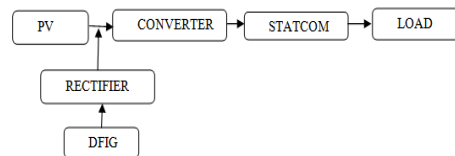


Fig.11. block diagram of multi-machine (open loop)

The above block diagram shows that integration of PV system and wind farms .The array produces the dc voltage as the output . The wind farm is coupled with the rectifier, the rectifier covers the ac –dc. The dc source entered into the STATCOM. The STATCOM which converts the dc –ac .The required ac source is used for the load source.

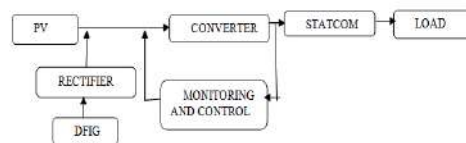


Fig.12. block diagram of multi-machine (closed loop)

The above block diagram shows that integration of PV system and wind farms .The array produces the dc voltage as the output. The wind farm is coupled with the rectifier, the rectifier covers the ac –dc. The dc source entered into the STATCOM. The STATCOM which converts the dc –ac. The STATCOM is controlled with the help of particle swarm optimization to increase the stability and reduce the reactive power. The required ac source is used for the load source.

X SIMULATED PERFORMANCE OF PROPOSED SYSTEM

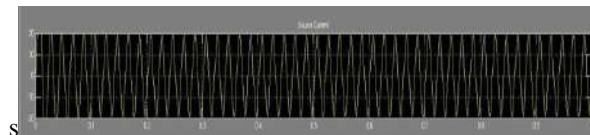
TABLE 2 DESIGN PARAMETERS OF PROPOSED SYSTEM

Parameter	Value
Inductor L1	0.4mH
Inductor L2	0.4mh
Capacitor C1	2.2nF
Capacitor C2	2.2nF
Resistance	100ohm

Table 3 INPUT SPECIFICATION FOR A PROPOSED SYSTEM

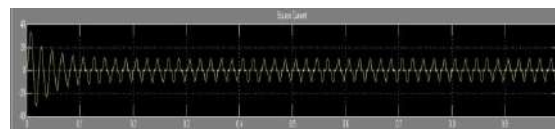
Parameter	Value
Input Voltage(Vs)	230V
Power	30 W
Source current (Is)	20A
RL	5ohms,30mh
Switching frequency	50Hz

A.Source VI and Rectifier pulse



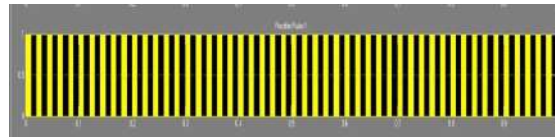
Fig(13) source voltage of the multi-machine system

Fig (13) shows that the source voltage, In this graph the time scale is represented by the X axis as well as the voltage scale is represented by the Y axis, which is represented as V_{sc} . The source voltage is obtained from the wind farm.



Fig(14) source current of the multi-machine system

Fig (14) shows that the source current, In this graph the time scale is represented by the X axis as well as the current scale is represented by the Y axis which is represented as I_{sc} .



Fig(15) Rectifier of the multi-machine system

Fig (15) shows that the rectifier Pulse. The rectified output pulse is obtained from AC source. The rectifier is used to convert AC source into DC source.

A.Open- Loop:

This simulation diagram shows that open-loop of a multi-machine. The ac source V_s denotes the output of the wind system and the dc source V_{dc} denotes the output of the solar system by integrating these two to improve the system's transient stability. The rectifier is used to ac into dc The rectifier circuit consist of a IGBT The dc source is produced by the solar system. Now the dc source is injected into the STATCOM circuit. The STATCOM circuit consist of a MOSFET-s1,s2,s3,s4,s5,s6.The STATCOM circuit is coupled with a transmission line .we had used resistor as load .By this process we enhance the transient stability of a system and also decreases reactive power.

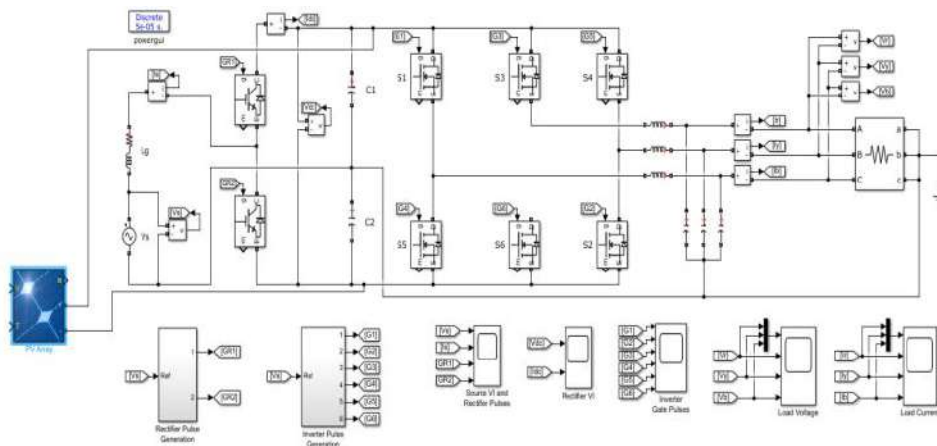
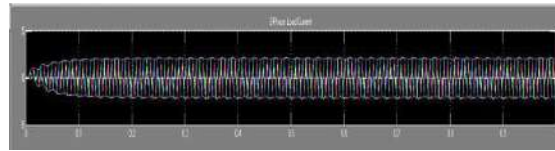


Fig.16. The Simulink model of the open loop system using MATLAB/Simulink

This simulation diagram shows that open-loop of a multi-machine. The ac source V_s denotes the output of the wind system and the dc source V_{dc} denotes the output of the solar system by integrating these two to improve the system's transient stability. The rectifier is used to ac into dc. The rectifier circuit consist of a IGBT The dc source is produced by the solar system. Now the dc source is injected into the STATCOM circuit. The STATCOM circuit consist of a MOSFET-s1,s2,s3,s4,s5,s6. The STATCOM circuit is coupled with a transmission line .we had used resistor as load .By this process we enhance the transient stability of a system and also decreases reactive power.

SINULATION RESULT OF A MULTI-MACHINE (open loop):



16.a .Load current :

Fig 16.a1.3 phase load current of the multi-machine system (open loop)

Fig 16.a1.shows that the 3 phase load current. The X-axis in this graph represents time, and the Y axis represents the load current of a multi-machine system in open loop.

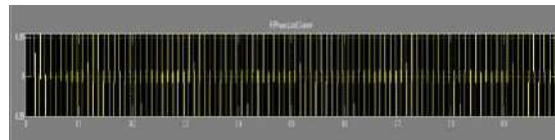


Fig16.a2. R phase load current of the multi-machine system (open loop)

Fig 16.a2.shows that the load current in R phase. The X-axis in this graph represents time, and the Y-axis represents the load current of a multi-machine system in open loop.

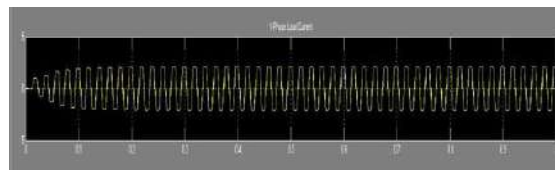


Fig16.a3. Y phase load current of the multi-machine system (open loop)

Fig 16.a3.shows that the load current in Y phase. In this graph the X-axis represents the time and the Y-axis represents the load current of a multi-machine system in open loop condition.

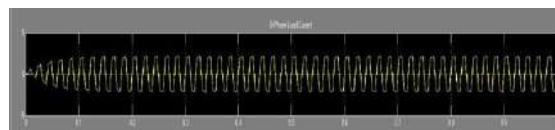


Fig16.a4. B phase load current of the multi-machine system (open loop)

Fig 16.a5. Shows that the load current in the B phase. The X-axis in this graph represents time, and the Y-axis represents the load current of a multi-machine system in open loop.

16.b. Voltage

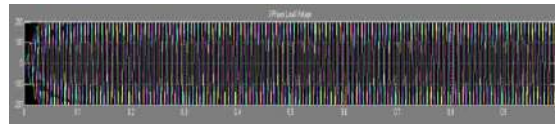


Fig16.b1. 3 phase load current of the multi-machine system (open loop)

Fig 16.b1. shows that 3phase load voltage in R,Y and B phase .In this graph the X axis represents the time and Y axis represents the load voltage of the multi-machine system (open loop)

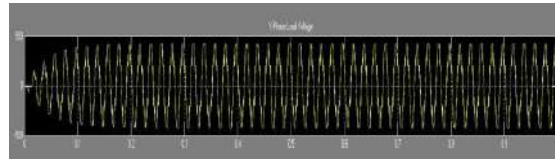


Fig 16.b3. Y phase load current of the multi-machine system (open loop)

Fig 16.b3. shows that the load voltage in the Y phase The X axis in this graph represents time, and the Y axis represents the load voltage of the multi-machine system (open loop)

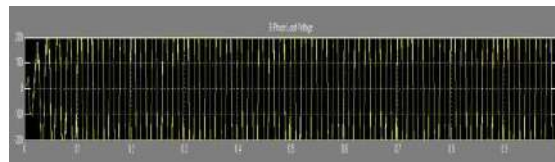
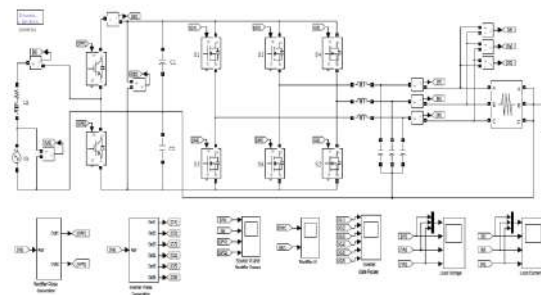


Fig16.b4.B phase load current of the multi-machine system (open loop)

Fig 16.b4.shows that the load voltage in the B phase The X axis in this graph represents time, and the Y axis represents the load voltage of the multi-machine system (open loop)

C. ClosedLoop:



: Fig.17. The Simulink model of the closed loop of a multi-machine system using MATLAB/Simulink

This simulation diagram shows that closed-loop of a multi-machine. The ac source V_s denotes the output of the wind system and the dc source V_{dc} denotes the output of the solar system by integrating these two to improve the system's transient stability. The rectifier is used to ac into dc .The rectifier circuit consist of a IGBT The dc source is produced by the solar system. Now the dc source is injected into the STATCOM circuit. The STATCOM circuit consist of a MOSFET-s1,s2,s3,s4,s5,s6.The STATCOM circuit is coupled with a transmission line .we had used resistor as load .By this process we enhance the transient stability of a system and also reduces the reactive power. When compared to open loop system the closed loop system reduces the harmonics .We used PI controller with the help of PSO technique.

SIMULATION RESULT OF MULTI-MACHINE (Closed loop):

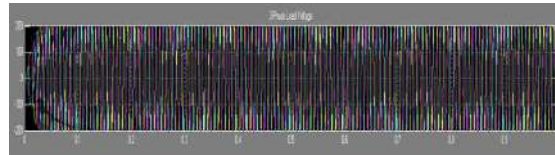


Fig17.a1. 3 phase load voltage of the multi-machine system (closedloop)

Fig 17.a1. Shows the 3phase load voltage curve .When compared to open loop the harmonics will be reduced in the closed loop .In this graph the X axis represents the time and Y axis represents the voltage of a multi-machine system(closed system)

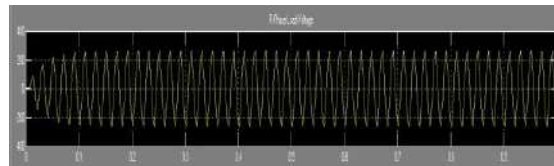


Fig 17.a2.R phase load voltage of the multi-machine system (closed loop)

Fig 17.a2. Shows the R phase load voltage curve .When compared to open loop the harmonics will be reduced in the closed loop .In this graph the X axis represents the time and Y axis represents the voltage of a multi-machine system (closed system)

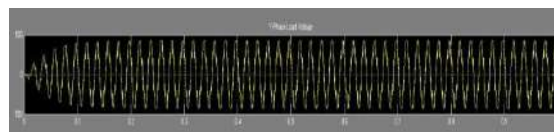


Fig17.a3.Y phase load voltage of the multi-machine system (closed loop)

Fig17.a3. shows the Y phase load voltage curve .When compared to open loop the harmonics will be reduced in the closed loop .In this graph the X axis represents the time and Y axis represents the voltage of a multi-machine system (closed system)

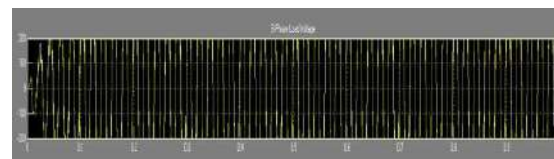


Fig17.a4.B phase load voltage of the multi-machine system (closed loop)

Fig 17.a4.shows the B phase load voltage curve. When compared to open loop the harmonics will be reduced in the closed loop .In this graph the X axis represents the time and Y axis represents the voltage of a multi-machine system(closed system)

B Current

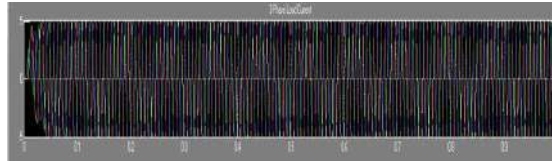


Fig 17.b1.phase load current of the multi-machine system (closed loop)

Fig 17.b1. Shows the 3 phase load current curve .When compared to open loop the harmonics will be reduced in the closed loop .In this graph the X axis represents the time and Y axis represents the current of a multi-machine system(closed system)



Fig17.b2. R phase load current of the multi-machine system (closed loop)

Fig 17.b2.shows the R phase load current curve .When compared to open loop the harmonics will be reduced in the closed loop .In this graph the X axis represents the time and Y axis represents the current of a multi-machine system(closed system)

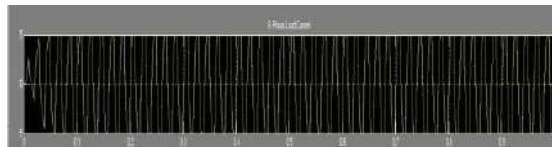


Fig17.b3 B phase load current of the multi-machine system (closed loop)

Fig 17.b3shows the B phase load current curve . When compared to open loop the harmonics will be reduced in the closed loop .In this graph the X axis represents the time and Y axis represents the current of a multi-machine system(closed system)

XI CONCLUSION:

Thus the improved STATCOM control architecture to increase a power system's transient stability through the use of particle swarm optimization (PSO) using MATLAB\ Simulink modal. While integrating the renewable energy, which creates voltage dip and causes the over voltage and affects the transient stability of a transmission line to overcome this problem we uses one of the FACTS devices as STATCOM.

XII REFERENCE

1. Y. Cao, Y. Zhang, and X. Shi : PV with a high probability of success Wind farm expansion capacity planning based on data from NASA IEEE Transactions on Keep the electricity flowing (1291–300. 2017;8(March):1291–300).
2. A. Jalilian and S. B. Naderi : Use DC to improve the low voltage ride-through of a DFIG-based wind turbine a fault of the switchable resistive kind limiter of new Energy Electrification (86(March):104–19 in Syst).
3. MA Chowdhury and AH Sayem : To boost low-voltage ride-through capability, a robust active disturbance rejection controller was designed. wind induction generator with two feeds agribusiness Renew Power Generation is an initiative of the Institute of Electrical and Electronics Engineers(IET).(9(November):961–9. 2015;9(November):961–9).

4. Abdou A, Abu-Siada A : Impact of VSC faults on complex output and low voltage travel.Electricity is produced by DFIG.(2015;65(February):334–47)
5. Long T, Shao S, Abdi E : Asymmetrical low-voltage ride through of brushless doubly fed motors.wind turbine induction generators generation of electricity IEEE Transactions on 2013;28(June):502-11.
6. Wang L, Quang-Son V. A. Movahedi and colleagues : Stability improvement of a multi-machine power system.Systems for Electrical Power and Energy a large-scale hybrid wind-photovoltaic farm powered by a supercomputer capacitor is a type of capacitor. IEEE Transactions on Industrial Applications(521–68 in September 2017)
7. He Haibo, Tang Y : Adaptive dynamic monitoring of a wind farm's power system stability programmable IEEE Transactions on Smart Grid, (vol. 6, no. 1, January 2015, pp. 166–77).
8. SR Samantaray: In a versatile AC transmissions-based transmission line, fault zone detection and classification are achieved using decision trees. IET Transmission Distribution Generator (3(May):425–36, 2009).
9. Y. Lei, A. Mullane, G. Lightbody, and R. Yacamini : IEEE Transmission Energy Conversation., 2006, 21, pp. 257–264, 'Modeling of the wind turbine with a doubly fed induction generator for grid integration studies'.
- 10.1109/TEC.2005.847958 (<https://doi.org/10.1109/TEC.2005>)



e-ISSN: 2278-8875
p-ISSN: 2320-3765

International Journal of Advanced Research in Electrical, Electronics and Instrumentation Engineering

Volume 10, Issue 6, June 2021

ISSN INTERNATIONAL
STANDARD
SERIAL
NUMBER
INDIA

Impact Factor: 7.282

☎ 9940 572 462

☑ 6381 907 438

✉ ijareeie@gmail.com

@ www.ijareeie.com



Design and Development of Floor Cleaner Robot (Automatic and Manual Mode)

Mr.S.Ram Prasath, P.Keerthiga, K.Pavithra, S.Yamuna

Assistant Professor, Dept. of EEE, Saranathan College of Engineering, Trichy, Tamilnadu, India

Final Year UG Students, Dept. of EEE, Saranathan College of Engineering, Trichy, Tamilnadu, India

ABSTRACT: In the present-day scenario all the members of family are busy with their work and are not getting proper time to clean the house. The cleaning robot helps to clean the floor. This is done by simply pressing a switch and the robot does the work. This also cuts down the labour used in factories for cleaning floor. Above being the case, motivated for the design and development of an automatic cleaning robot that does all the cleaning work with a simple press of a button. This robot can be controlled manually with the help of a mobile Bluetooth. The main motto of the project is to make this affordable and suitable for the Indian users and factories. The development of the robot starts with the design of a simple and most effective chassis for the robot which is a very important part as it has to carry all the weight on the robot. The electronics part where, the type of motor and its specification that should be used to run the bot, the sensors to be used, the microcontroller, the motor drivers, The wheels and other electronic components to be used on the robot are decided. Further, the assembling of the components will be done and finally testing and calibrating the device. A robot which is capable of efficient dust cleaning of the floor of a given room is the main aim of the robot. It is aimed to make the robot economic and feasible for the economic class society. The target time of operation of the robot is one hour. The developed robot will be useful for the household application and industries. This helps to keep the workspace and house clean without the physical labor. Also, the device will clean the room with a single switch of button.

KEYWORDS: Floor cleaner, automatic cleaning, motor drivers, Bluetooth.

I. INTRODUCTION

In recent years, robotic cleaners have taken major attention in robotics research due to their effectiveness in assisting humans in floor cleaning applications at homes, hotels, restaurants, offices, hospitals, workshops, warehouses and universities etc. Basically, robotic cleaners are distinguished on their cleaning expertise like floor mopping, dry vacuum cleaning etc. Some products are based on simple obstacle avoidance using infrared sensors while some utilize laser mapping technique. Each cleaning and operating mechanism of robotic floor cleaners has its own advantages and disadvantages. For example, robots utilizing laser mapping are relatively faster, less time consuming and energy efficient but costly, while obstacle avoidance-based robots are relatively time consuming and less energy efficient due to random cleaning but less costly. Countries like Pakistan are way back in manufacturing robotic cleaners. Importing them from abroad increases their costs. The main objective of this work is to provide a substantial solution to the problem of manufacturing robotic cleaner utilizing local resources while keeping it low costs.

II. LITERATURE REVIEW

Recently there is surge of innovative cleaner robots in the market. All these robots are based on the technical analysis of research work published in some of the papers described below. Manreet Kaur and Preeti Abrol, in the paper “Design and development of floor cleaning robot” have made the cleaning using automatic and manual modes. They have used RF modules for wireless communication between remote and robot having range of 50m. In the automatic mode, robot controls all operations itself and changes the lane in case of hurdle detection and moves back. In the manual mode keypad is used to perform the expected task and to operate the robot. The drawback in this model is that it does not have the feature of self-charging. Systematic cleaning was an important feature and modifications to the environment to support the navigation of the robot. Many more systems were proposed and among that is the system proposed by J.Y. Sung, R. E. Grinter and H. I. Christensen in “Housewives domestic robot technology international journal of social robotics”. In this paper a new type of home intelligent cleaner adopted the ultrasonic and IR sensor array which had the function of real time environment perception is introduced and the cleaner is driven by step motor has the ability of autonomous working by itself and the functions of automatic detection and obstacle avoidance. This paper adopts grid scan algorithm placed on electric map, realize floor coverage task and designs synthesis detection



system based on sensor array finding method technology according to algorithm characteristics. However this system did not support wet detection and it only performed dry cleaning. Therefore we are proposing a system to overcome the drawbacks of the existing system.

III.HARDWARE USED

- a) Arduino UNO
- b) Ultrasonic, IR sensor
- c) Motor driver
- d) Suction unit (Vacuum, Scrubber)

IV.BLOCK DIAGRAM

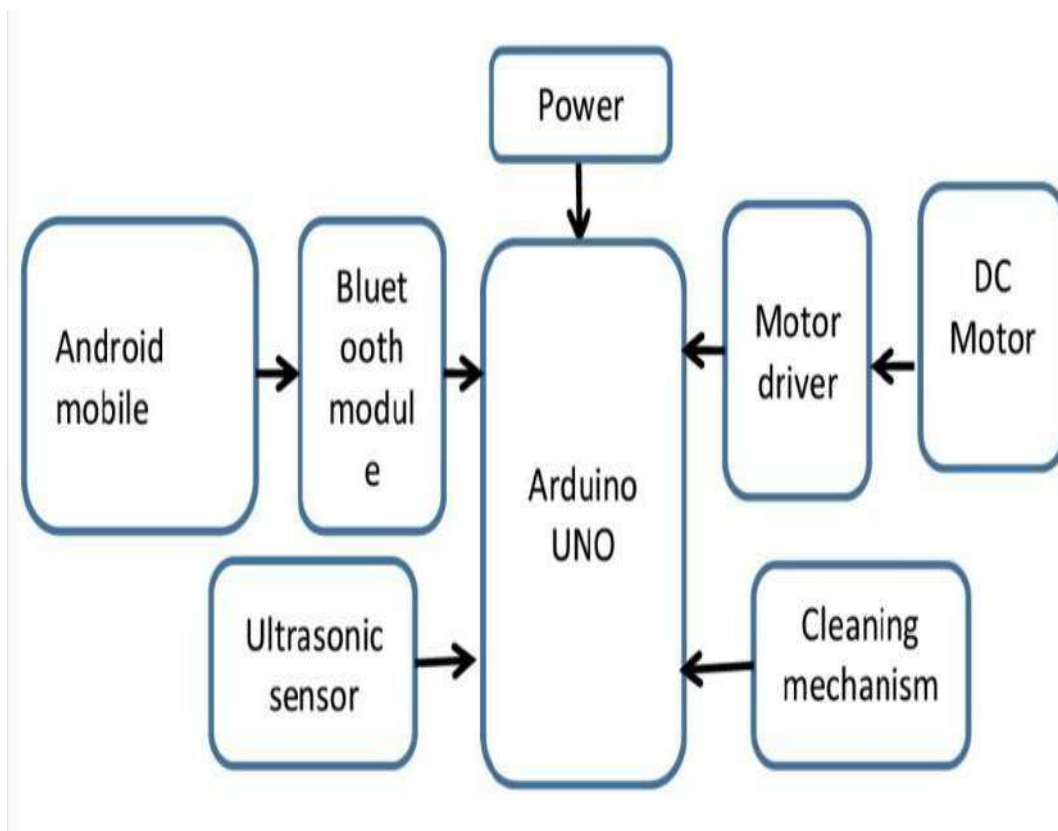


Fig.1 Block Diagram

V. WORKING

For the aimed feature of application, the robot will be provided with sweeping and vacuuming the floor simultaneously. As soon as a obstacle is detected the robot stops and moves reverse and then checks whether to move left or right . This application is done with help of us sensor . The robot is fitted with rotating brushes parallel to the cleaning surface and rotating in opposite directions such that the dust in the way is collected and fed to the vacuum mouth which is just behind the rotating brushes. Robot moves till it is switched off . Once the user needs it to be manual then he can switch it on so that he or she can control it via mobile phone with android mobile app “ Arduino Bluetooth RC car.



VI. FLOW CHART

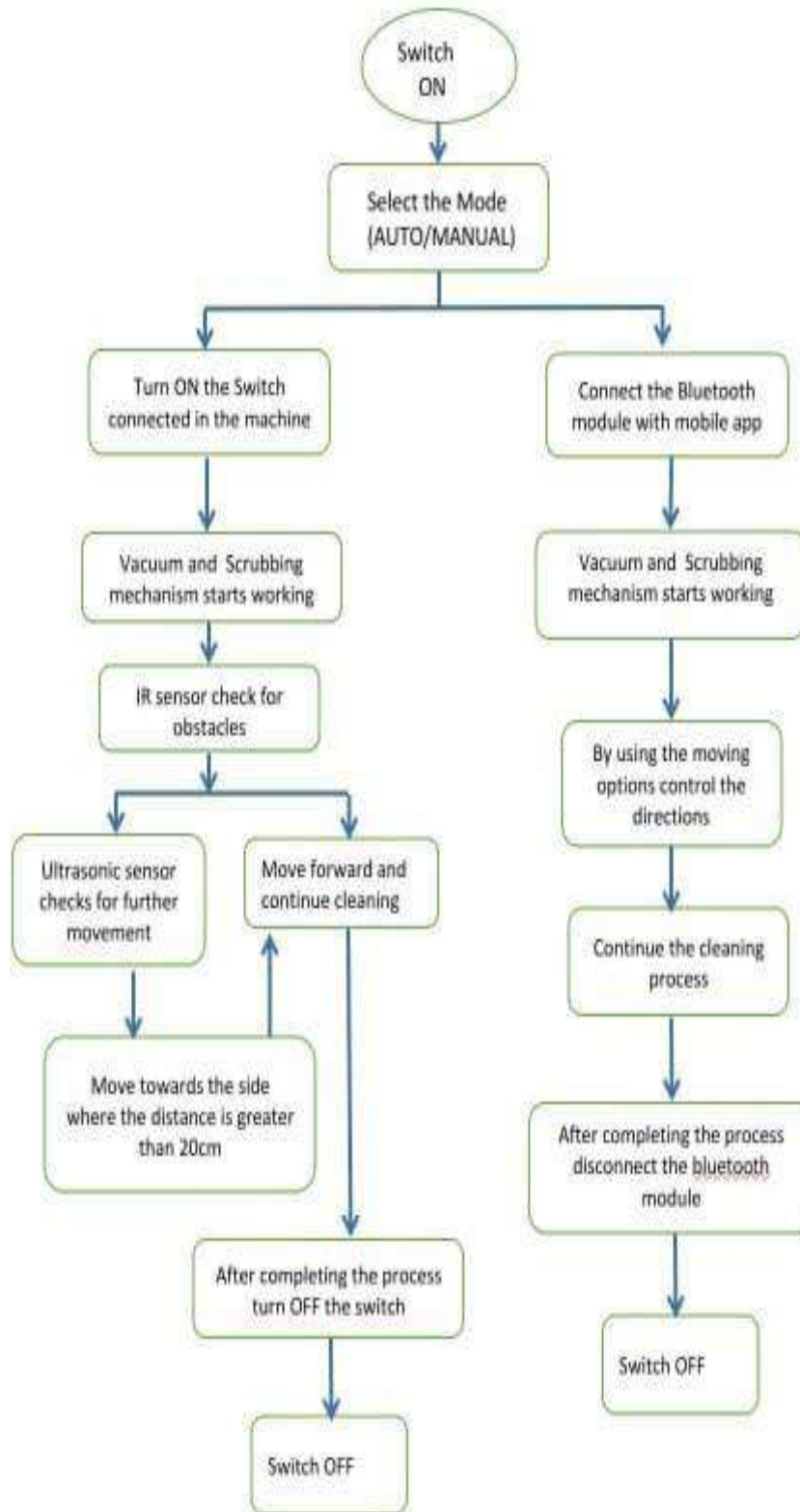


Fig.2 Flow chart of working



VII. PROJECT PICTURE



Fig.3 Hardware kit left side view

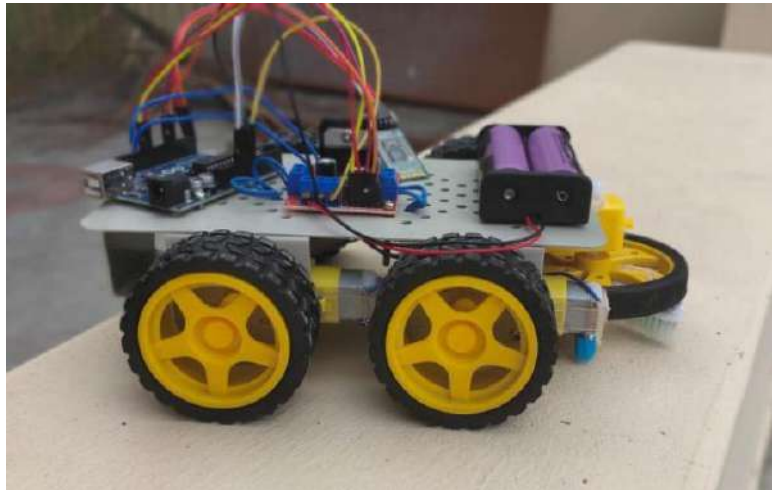


Fig.4 Hardware kit Right side view

VIII. ADVANTAGES

1. It reduces human energy and efforts. People in cities have irregular and long working times. In such a situation a person will always find ways of saving time.
2. Helping physically disable person is also advantage of this project. Automatic mode of this robot helps physical disable person.
3. We can use this robot in Automatic and Manual mode also. Easy mounting and easy to operate. Due to that, it is user friendly.

XI. APPLICATIONS

1. Main purpose of this project is Cleaning.
2. We can save our time by using this robot.
3. Able to go under furniture and around corners

X. CONCLUSION

This research facilitates efficient floor cleaning. Since in project the floor cleaner is incorporated with different devices like DC motor(s), ultrasonic sensors etc., so it will be easy to handle it also saves time and will work automatically for cleaning purpose at homes and offices. With simple algorithm and program, the cleaner will be able to cover large floor areas as well as find its way into and out of small corners. As the cleaner traverses the room, the sweeper installed in it



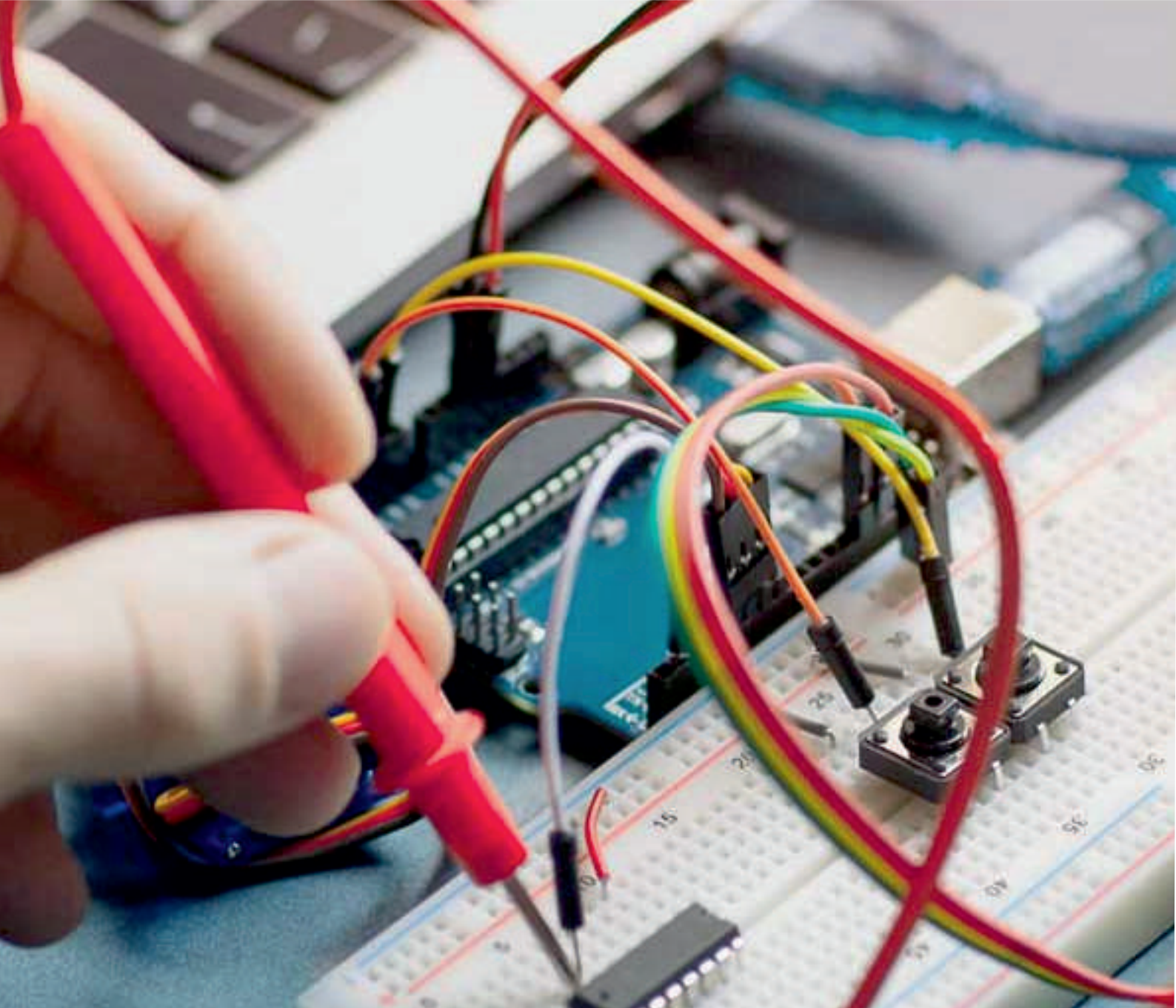
will manage to pick up a significant amount of dirt. Manual Sweeping might not be that effective as it will not be picking up everything in as it is not in sight but using the automatic floor cleaner it can be done easily

XI. ACKNOWLEDGEMENT

We would like to express our deepest gratitude to our Head of Department Dr. C Krishna Kumar for providing us the opportunity to build this project. We heartily thank our project guide Mr. Ramprasath for his valuable guidance and constant support throughout the project.

REFERENCES

- [1] IEEE Standard for User Interface Elements in Power Control of Electronic Devices employed in Office/Consumer Environments, IEEE Standard 1621,2004(R2009).
- [2] Irobot.com, 'iRobot Corporation: We Are the Robot Company', 2015. [Online]. Available: <http://www.irobot.com/>.
- [3] Neato, 'Neato Robotics | Smartest, Most Powerful, Best Robot Vacuum', 2015. [Online]. Available: <http://www.neatorobotics.com/>.
- [4] Dyson.com, 'Latest Dyson Vacuum Cleaner Technology | Dyson.com', 2015. [Online]. Available: <http://www.dyson.com/vacuum-cleaners.aspx>.
- [5] Dyson 360 Eye robot, 'Dyson 360 Eye robot', 2015. [Online]. Available: <https://www.dyson360eye.com/>.
- [6] Buck, 'The Best Robot Vacuums of 2015 | Top Ten Reviews', TopTenREVIEWS, 2014. [Online]. Available: <http://robot-vacuumreview.toptenreviews.com/>.
- [7] Harvey Koselka, Bret A. Wallach, David Gollaher, "Autonomous floor mopping apparatus," U.S. Patent 6741054 B2, May 25, 2004.
- [8] Joseph L. Jones, Newton E. Mack, David M. Nugent, Paul E. Sandin, "Autonomous floor-cleaning robot," U.S. Patent 6883201 B2, April 6, 2005.
- [9] Andrew Ziegler, Duane Gilbert, Christopher John Morse, Scott Pratt, Paul Sandin, Nancy Dussault, Andrew Jones, "Autonomous surface cleaning robot for wet and dry cleaning," U.S. Patent 7389156 B2, June 17, 2008.
- [10] Shih-Che HUNG, Yao-Shih Leng, "Cleaning robot and control method thereof," U.S. Patent 20130231819 A1, September 5, 2013.
- [11] Andrew Ziegler, Christopher John Morse, Duane L. Gilbert, Jr., Andrew Jones, "Autonomous surface cleaning robot for dry cleaning," U.S. Patent 8782848 B2, July 22, 2014.
- [12] Michael Dooley, James Philip Case, and Nikolai Romanov, "System and method for autonomous mopping of a floor surface," U.S. Patent 8 892 251 B1, November 18, 2014



INNO  **SPACE**
SJIF Scientific Journal Impact Factor
Impact Factor: 7.282



ISSN INTERNATIONAL
STANDARD
SERIAL
NUMBER
INDIA



International Journal of Advanced Research

in Electrical, Electronics and Instrumentation Engineering

 **9940 572 462**  **6381 907 438**  **ijareeie@gmail.com**



www.ijareeie.com

Scan to save the contact details

Improving Efficiency and Power Loss Minimization in Landsman DC-DC Converter using Particle Swarm Optimization Technique (PSO)

Danila Shirly.A.R
Assistant Professor

Electrical and Electronics Engineering
Saranathan College of Engineering
Trichy, India
ardanilashirly@gmail.com

Sudhilaya M
UG Scholar

Electrical and Electronics Engineering
Saranathan College of Engineering
Trichy, India
sudhimathesh307@gmail.com

Priyadharshini Y
UG Scholar

Electrical and Electronics Engineering
Saranathan College of Engineering
Trichy, India
priyadharshiniyoga0506@gmail.com

Shamni J
UG Scholar

Electrical and Electronics Engineering
Saranathan College of Engineering
Trichy, India
shamnipra23@gmail.com

Poorani J
UG Scholar

Electrical and Electronics Engineering
Saranathan College of Engineering
Trichy, India
poorani.siva1209@gmail.com

Abstract—This paper predominantly focuses on the design and implementation of efficient Landsman DC-DC converter with power loss minimization using Particle Swarm Optimization (PSO) a hybrid soft computing technique. The various controller design parameters are optimised in an iterative way using PSO algorithm and the comparative results are presented. The landsman converter work as buck-boost converter to deals with the power factor correction, constant output voltage and reduced harmonic distortions. The Landsman converter is operated in Continuous Conduction Mode so as to reduce current and voltage stress on the components of the device. The static and dynamic behaviour of the proposed system is analysed and the simulation results are obtained for the PSO controller. The Particle Swarm Optimization is mainly contributed in this paper for its easy implementation and its computational efficiency and fast convergence when compared with mathematical algorithm. This topology is simulated in MATLAB/Simulink platform and the result is presented.

Keywords—Landsman Converter, Particle Swarm Optimization, Power loss minimization, Continuous Conduction Mode, Efficiency.

I. INTRODUCTION

Boost converters are the most primarily focused switching mode power supplies used as the output voltage produced will be greater than its corresponding input voltage. It is widely implemented in solar power applications for its better dynamic response. Landsman converter is an advanced DC-DC converter to perform power factor correction, constant output voltage and reduced harmonic distortion and also capable of achieving DC voltage control in single stage utilizing just a single control technique. The landsman converter makes use of only few passive components when compared with other converters like Zeta, CUK, SEPIC [2]. It does not require any special input ripple filter as in the case of canonical switching cell (CSC) converter and LUO converter. The input inductor used in the proposed Landsman converter is relatively small when compared with other buck-boost converters like CUK converter. The Landsman converter's best attributes are as follows, it acts as the DC-DC boost converter to produce smooth transient response, better dynamic output voltage,

less ripple content and fast settling time are to name a few. Hence to achieve best transient response and good dynamic voltage closed loop current or voltage controller is considered [4]. Landsman converter is used in applications such as to track maximum power from PV array in addition to boosting the voltage gain. It uses less active and passive components .It is also capable of performing buck and boost operation but delivers a non-inverted output. It is preferred to operate the Landsman converter always in continuous conduction mode (CCM) in order to reduce stress in its power semiconductor devices and its components [7]. Among various DC-DC converters, Landsman converter meets the desired performance for power loss minimization. The particle swarm optimization (PSO) is a computational method that identifies the problem and optimizes the solution by iteration process so as to develop a candidate solution with concern given to the quality. It solves the problem by dubbed particles which move according its position and its velocity. It is usually anticipated to move the swarm position towards the best solution available. PSO is a stylized computation method form of representing the organism's movement in a fish school or bird flock model. The algorithm was deduced to perform optimization and finding the solution for the identified problem. Due to PSO advantages, it finds its application very suitable for research and in solving real life problems related to evolutionary computing, optimization and many other fields. In simple terms, it can be said that PSO is associated with artificial life particularly to concepts of swarming and simulation of social behaviours. Here, PSO is adopted for its easy implementation and its computational efficiency to minimise the power loss. This algorithm is preferred much due to its admirable features like, less adjusting parameters, fast convergence speed, can be applied broadly in various fields. By using the closed loop mechanism the simulation results of output current, output voltage and output power has been obtained. The PSO algorithm is adopted to evolve the internal parameter of processing layer. The main applications of PSO are applied in training of neural networks, optimization of electric power distribution networks, structural optimization, and biochemistry process and system identification in biomechanics. The Landsman converter delivers output voltage with less ripple content, high

efficiency and good voltage regulation, hence this converter is preferred widely when compared to other DC-DC converters.

II. DESIGN OF LANDSMAN CONVERTER

The Landsman converter is designed to operate in continuous conduction mode (CCM) so that the current and voltage stress on the power semiconductor device is reduced [1], [3]. The circuit diagram of Landsman DC-DC Converter is shown in Fig. 1 and its operation can be analyzed by considering two modes as shown and the corresponding modes of operation waveform are generated.

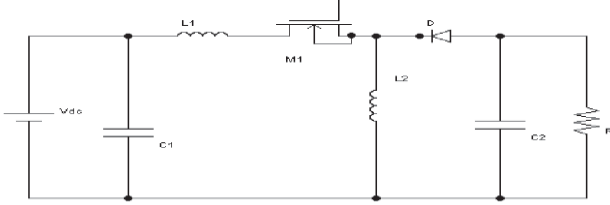


Fig. 1. Circuit Diagram of Landsman Converter

A. Mode 1- when switch is ON

When the switch is in ON condition, \$V_{C1}\$, the voltage across intermediate capacitor \$C_1\$ reverse biases the diode, resulting in the circuit diagram as shown in Fig 2. The inductor current \$I_L\$ flows through the closed switch and as \$V_{C1}\$ is larger than the output voltage \$V_o\$, \$C_1\$ discharges through the switch, transferring its energy to the inductor \$L\$ and the output. As a result, \$V_{C1}\$ decreases and \$I_L\$ increases which is depicted in Fig. 4. The input supplies energy to the input inductor \$L_1\$.

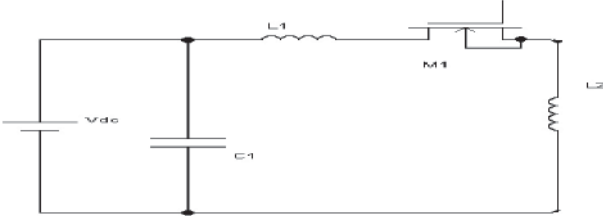


Fig. 2. Mode I operation of Landsman Converter

B. Mode 2- when switch is OFF

When the switch is in OFF condition, the diode conducts as it is now forward biased, resulting in a circuit diagram as depicted in Fig. 3. The inductor current \$I_L\$ now flows through the diode and the energy stored in Mode I is transferred to output through the diode. Alternatively, \$C_1\$ is getting charged through the diode by energy received from both the input and \$L_1\$. As a result of it, \$V_{C1}\$ increases and \$I_L\$ decreases which is shown in Fig. 4 of Mode II.

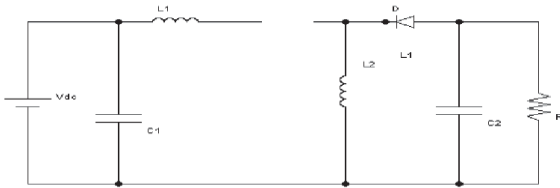


Fig. 3. Mode II operation of Landsman Converter

C. Input Ripple Inductor Current

The ripple content present in the input current, flows through \$L_1\$, it (\$I_{L1}\$) can be calculated by considering the waveform as shown in Fig. 4. For CCM operation, let us assume that the entire ripple component in \$L_1\$ current flows through \$C_1\$. The shaded area indicated in the waveform of Fig. 4 of \$V_{C1}\$ represents an additional flux [6].

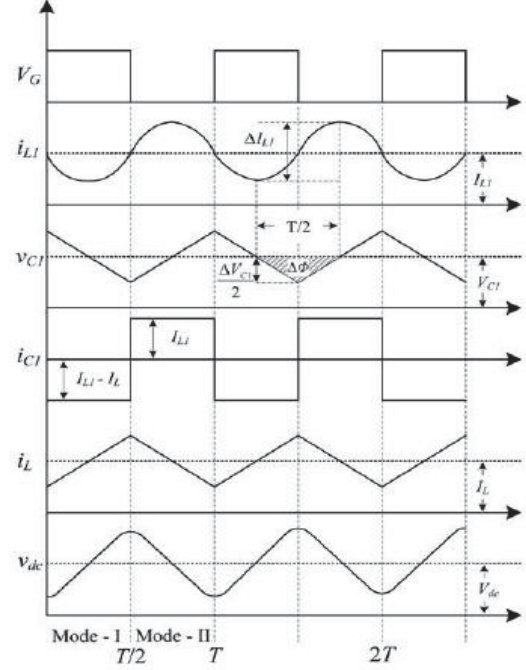


Fig. 4. Waveforms of Landsman Converter

Thus, the peak to peak current ripple flowing through \$L_1\$ can be written as

$$\Delta I_{L1} = \frac{\Delta \Phi}{L_1} = \frac{1}{L_1} \frac{1}{2} \frac{\Delta V_{C1} T}{2} \quad (1)$$

In Mode II operation, the current through \$C_1\$ is represented as

$$i_{C1} = I_{L1} = C_1 \frac{\Delta V_{C1}}{(1-D)T} \quad (2)$$

where, \$D\$ is represented as the duty cycle ratio and \$T\$ is represented as the switching time period. The voltage ripple content in \$V_{C1}\$ is assessed from eqn (2) in the following manner,

$$\Delta V_{C1} = \frac{I_{L1}}{C_1} (1-D)T \quad (3)$$

Therefore, substituting \$\Delta V_{C1}\$ from eqn (3) into eqn(1) gives

$$\Delta I_{L1} = \frac{1}{L_1} \frac{1}{2} \frac{I_{L1}}{2C_1} (1-D)T \frac{T}{2} \quad (4)$$

Or

$$\Delta I_{L1} = \frac{1}{8L_1 C_1} \frac{I_{L1} (1-D)}{f_{sw}^2} \quad (5)$$

The above can be normalized as,

$$\frac{\Delta I_{L1}}{I_{L1}} = \frac{1}{8L_1 C_1} \frac{(1-D)}{f_{sw}^2} \quad (6)$$

where, $f_{sw} = 1/T$ is the switching frequency. From the input-output relationship, it is evident that

$$I_{L1} = \frac{D}{1-D} I_{dc} \quad (7)$$

where, I_{DC} is the output current of Landsman converter.

Consequently, substituting I_{L1} from eqn (7) into eqn (5) and rearranging the order of terms, we derive

$$L_1 = \frac{D I_{dc}}{8 f_{sw}^2 C_1 \Delta I_{L1}} \quad (8)$$

TABLE I. DESIGN SPECIFICATIONS OF LANDSMAN CONVERTER

Parameter	Equations	Preliminary data	Value
Duty cycle	$\frac{V_{out}}{V_s + V_{out}}$	$V_s=18V$ $V_{out}=32V$	0.64
$C_1=C_2$	$\frac{D \times I}{f \times \Delta V_{c1}}$	$D=0.64$ $f=20KHz$ $\Delta V_{c1}= 20\%$ of V_{c1} $\Delta V_{c1}= 0.01$	512 μ F
L_1	$\frac{D \times I}{8f^2 \times \Delta I_{L1} \times C_1}$	$C_1=512\mu F$ $\Delta I_{L1} =0.048$	0.015mH
L_2	$\frac{D \times V_{out}}{f \times \Delta I_{L2}}$	$D=0.64$ $\Delta I_{L2}=0.0279$	0.036H

III. POWER LOSSES IN PROPOSED SYSTEM

The main objective is to improve efficiency which can be done by minimization of losses present in the proposed Landsman converter. The reason for improving the efficiency is to provide a better regulated power system whose stability gets distorted due to the inclusion of power semiconductor devices. The power losses in the proposed converter are due to switching losses, capacitor and inductor losses. Here in this section capacitor and inductor losses constraint are considered and their losses are minimized with the usage of PSO. The power losses in a Landsman converter comprise of two losses namely active and passive losses. Hence, the converter efficiency can be deduced as follows.

$$\eta = \frac{P_{out}}{P_{out} + P_{losses}}$$

where, P_{out} and P_{losses} represents the power output and the power losses respectively.

$$P_{losses} = P_{Ind} + P_C$$

where, P_{Ind} represents the inductors loss and P_C represents the capacitor loss.

A. Inductor Losses:

The losses that occur in L1 and L2 are taken into consideration by considering its physical parameters like OD, ID and H which are the outside diameter, inside diameter and height respectively. The core diagram is shown in Fig. 5.

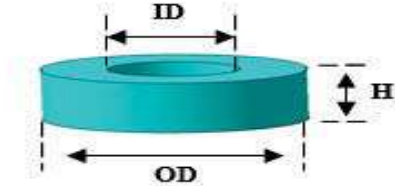


Fig. 5. Inductor Core

The losses that occur in inductor comprises of core loss and copper loss. The factors that influence the core loss of inductor are switching frequency f_{sw} and magnetic induction B. The inductor core loss can be evaluated using the following Steinmetz equation [5].

$$P_{core} = 6.11 \cdot 10^{-18} \cdot B^{2.7} \cdot f_{sw}^{2.04} \quad (9)$$

While calculating copper losses, the factors that influence it are the following parameters such as size of the window, number of copper wire turns, and size of the wire. The inductor copper loss in the copper winding can be evaluated using the following equation.

$$P_{cu} = R_{DC,1} \cdot I_{L1,rms}^2 + R_{DC,2} \cdot I_{L2,rms}^2 \quad (10)$$

Where, $R_{DC,1}$, $R_{DC,2}$, $I_{L1,rms}$ and $I_{L2,rms}$ represents the DC resistances of inductor L1 & L2 and the rms currents in the inductors L1 & L2 respectively.

The DC resistances $R_{DC,1}$ and $R_{DC,2}$ can be evaluated using the following expression.

$$R_{DC,1} = \frac{\rho \cdot N1 \cdot MLT}{S_{cu}} \quad (11)$$

$$R_{DC,2} = \frac{\rho \cdot N2 \cdot MLT}{S_{cu}} \quad (12)$$

where, ρ represents the resistivity of the copper, $N1$ and $N2$ are the numbers of turns, S_{cu} represents the cross section area of the winding wire and MLT is the Mean Length Turn of the inductor core.

$$MLT = 2 \cdot (H+2 \cdot r) + 2 \cdot ((OD-ID)/2 + 2 \cdot r) \quad (13)$$

where, r represents the radius of the copper wire.

The rms currents in the inductors can be found using the expression mentioned below.

$$I_{L1,rms} = \frac{d \cdot I_{out}}{1-d} \quad (14)$$

$$I_{L2,rms} = I_{out} \quad (15)$$

The total power loss in the inductors is deduced as the expression mentioned below

$$P_{Ind} = P_{core,L1} + P_{cu,L1} + P_{core,L2} + P_{cu,L2} \quad (16)$$

where, $P_{core,L1}$, $P_{cu,L1}$, $P_{core,L2}$, $P_{cu,L2}$ represent the core and the copper losses in both inductors L1 and L2 respectively.

B. Capacitor losses:

Capacitor is selected based on the following primary factors like rms current, the maximum voltage and the equivalent series resistances (ESR). The capacitors losses can be found using the following equation.

$$P_C = ESR1 \cdot I_{C1,rms}^2 + ESR2 \cdot I_{C2,rms}^2 \quad (17)$$

where, ESR1, ESR2, $I_{C1,rms}$, $I_{C2,rms}$ represent the equivalent series resistance and the rms current in the C_1 and C_2 respectively.

$$I_{C1,rms} = I_{out} \sqrt{d/(1-d)} \quad (18)$$

$$I_{C2,rms} = I_{out} \sqrt{d/(1-d)} \quad (19)$$

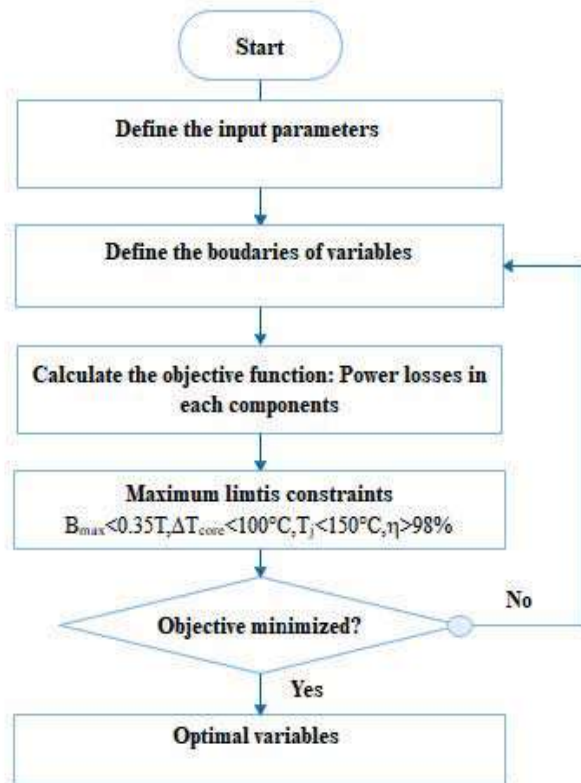


Fig. 6. Flowchart of optimization iterative process

IV. PARTICLE SWARM OPTIMIZATION (PSO)

PSO was accredited by Kennedy, Eberhart and Shi for simulating social behaviour as a demonstration in stylized form for the organism's movement in a bird flock or fish school fashion[8],[9]. While comparing various computational methods present in literature, PSO is considered as a computational method that identifies the problem and optimizes the solution by iteration process so as to develop a candidate solution with concern given to the quality. The foremost benefits of PSO algorithm are simplicity, robustness, easy to implement, computational efficiency, and fast convergence when compared to other computing techniques.

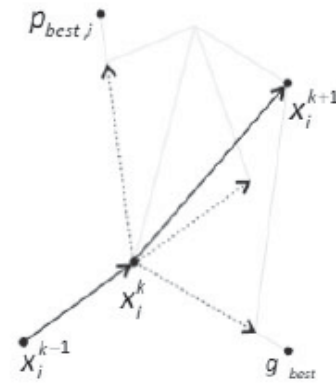


Fig. 7. Movement of particle during optimization iterative process

V. SIMULATED PERFORMANCE OF PROPOSED SYSTEM

The performance of Landsman converter was analysed in the previous section. In this section, the converter operation with and without PSO control technique was analysed. The results are studied and visualized using MATLAB software. The mathematical modeling of the converter expresses the converter's dynamic performance and compares the efficiency for a particular voltage.

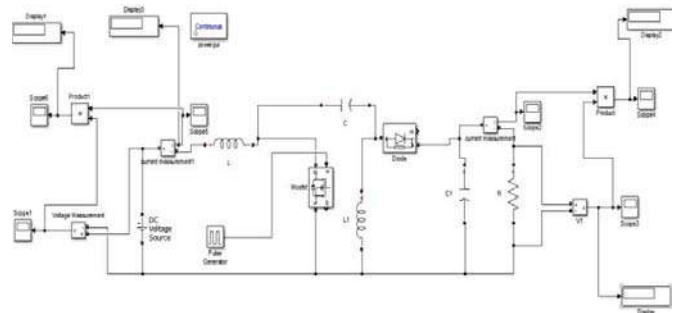


Fig. 8. The Simulink model of the landsman converter open loop using MATLAB/Simulink

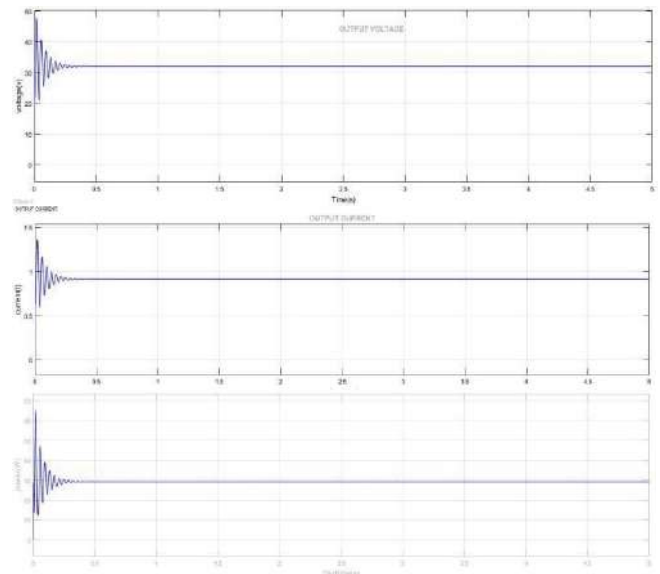


Fig. 9. The output waveform of the open loop landsman converter

Here the DC voltage source is used as input source for Landsman converter. The inductors and capacitors are used as per the calculated values. The above simulation is simulated using the designed values. On simulating this we obtain an output power of 27.8W and efficiency of nearly 92.69% with switching frequency of 20 KHz.

The output voltage, current and power are 31.6V, 0.88 A and 27.8W respectively. Its efficiency is 92.69%.

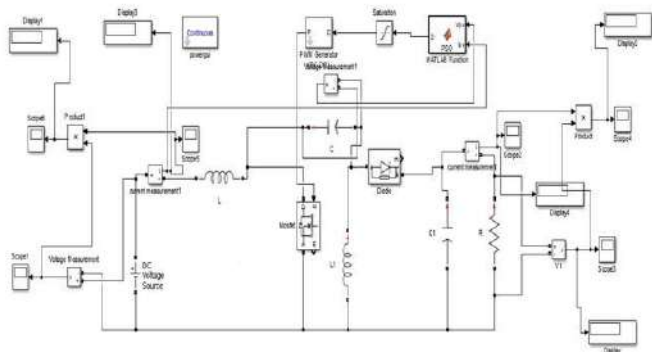


Fig. 10. The Simulink model of the landsman converter with PSO closed loop using MATLAB/Simulink

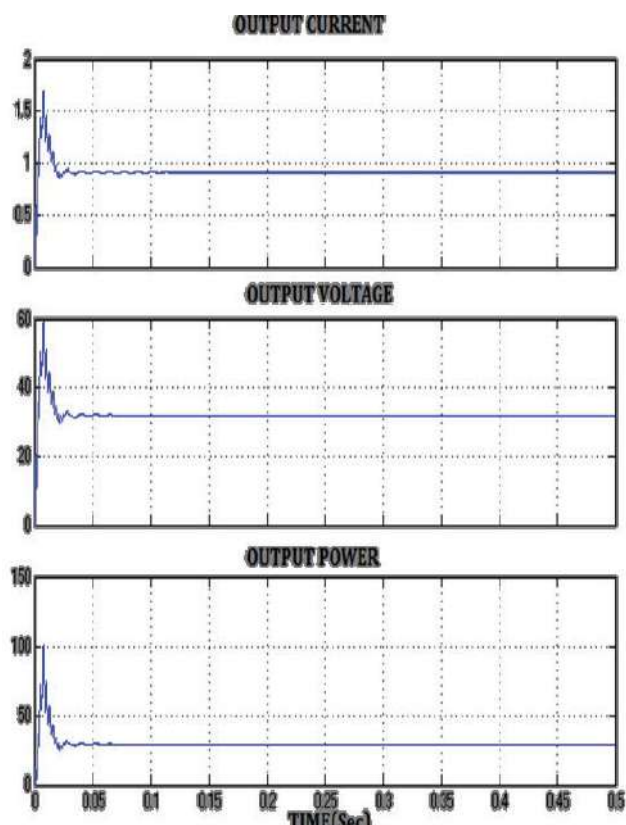


Fig. 11. . The output waveform of the closed loop landsman converter

The output voltage, current and power are 32V, 0.92 A and 29.44W respectively. Its efficiency is 98.13%. The following table compares the input, output, settling time and efficiency of Landsman converter for with and without PSO control technique used.

TABLE II. PERFORMANCE COMPARISON OF LANDSMAN CONVERTER

Converter	Input (V)	Input (A)	Output (V)	Output (A)	Settling time (sec)	η (%)
Landsman without PSO	18	1.6	31.6	0.88	0.3 sec	92.69
Landsman with PSO	18	1.6	32	0.92	0.05 sec	98.13

VI. CONCLUSION

The main objective of this paper is to improve the efficiency of landsman converter. The efficiency of landsman converter is improved by implementing the hybrid soft computing technique namely Particle Swarm Optimization (PSO). The losses present in the proposed converter is given as the input to PSO and the output is taken as a duty cycle for the converter. Finally, the landsman converter efficiency in open loop is 92.69% by implementing PSO the efficiency is improved to 98.13%. Here, an optimization process of fast convergence, easy to implement is utilized with only one objective to attain which to reach the maximum efficiency achievable in current power system scenario with the help of particle swarm optimization technique (PSO). In the proposed system, parameters such as inductor and capacitor losses of the Landsman DC-DC Converter are considered and the value is optimized with the usage of PSO. The results establish the criteria that the PSO algorithm is most suited for improving the efficiency by minimizing the power losses present in Landsman DC-DC converter.

REFERENCES

- [1] Power factor improvement in modified Bridgeless landsman converter fed EV Battery charger; Article in IEEE transactions on Vehicular technology PP(99):1-1*February 2019; RadhaKushwaha; Bhim singh.
- [2] V.Suganya, A.R.Danila Shirly, "Solar Powered Battery charger using Sliding Mode Controller", International Journal of Engineering Science and Computing (IJESC), pp. 3012-3018, Vol. 6, Issue. 3, March 2016.
- [3] Praveen kumar singh; Vashibist; kamal Al-haddad; Ambrish Chandra; BLDC motor drive based on Bridgeless landsman PFC converter with Single sensor and Reduced stress on power devices ; IEEE transactions on Industry applications (volume :54,Issue:1,Jan-feb.2018).
- [4] A.R.Danila Shirly, Srinath.G, Sidharth Prasad, Vignesh.S, Viswnathan.M, "Design and Hardware Implementation of Modified SEPIC Converter based ANFIS Controller", TEST Engineering & Management, pp. 26768-26776, Vol. 83, June 2020, ISSN: 0193-4120.
- [5] L.Bachouch, L.Bouslimi and L.E.Amraoui, Power losses minimization in the SEPIC DC-DC converter using particle swarm optimization technique(PSO)," 2019 19th International conference on sciences and techniques of automatic control and computer engineering (STA), Sousse, Tunisia, 2019, pp.388-393.
- [6] Khadlic Ali khan lecturer Bridgeless landsman converter based BDLC motor drive using IFOC department of electronics and communication engineering ,Mettu university Ethipoia
- [7] Vivek Agarwal, C. Sreekumar. A Control Algorithm for Voltage regulation in DC-DC Boost Converter. IEEE Transactions on Electronics. 2008; 55(6).

- [8] A. H. Ahmad N. S. Sultana. Hybrid Fuzzy Logic Based A Particle Swarm Optimization Controller Design for ZETA Converter.
- [9] J.Kennedy and R. Eberhart, "Particle Swarm Optimization",
- [10] Proceedings of IEEE International Conference on Neural Networks (ICNN'95), Vol. IV, pp.1942-1948, Perth, Australia, 1996 .



Institutional Sign In

All



ADVANCED SEARCH

Conferences > 2021 2nd International Confer... ?

Simulated Design and Implementation of Solar based Water Pumping System

Publisher: IEEE

Cite This

PDF

Vijay Ravindran ; RamPrakash Ponraj ; R PRAVEEN ; K Praveenkumar ; P Ravichandr... All Authors



Alerts

Manage Content Alerts

Add to Citation Alerts

More Like This

Grid interfaced solar PV based water pumping using brushless DC motor drive 2016 IEEE International Conference on Power Electronics, Drives and Energy Systems (PEDES) Published: 2016

Solar Photovoltaic based Brushless DC Motor Driven Water Pumping System using PSO-MPPT Algorithm 2019 54th International Universities Power Engineering Conference (UPEC) Published: 2019

Show More

Abstract

Document Sections

- I. Introduction
- II. Related Works
- III. Operation Involved In Solar Photo Voltaic Cells
- IV. Design and Operation of Boost Converter:
- V. Calculation of Duty Cycle:

Show Full Outline



Download PDF

Abstract:The efficiency of solar PV systems is influenced by external factors such as solar irradiance and temperature. Because of the low cost and environmentally friendly design... **View more**

Metadata

Abstract: The efficiency of solar PV systems is influenced by external factors such as solar irradiance and temperature. Because of the low cost and environmentally friendly design, Photovoltaic (PV) based water pumping systems are viable alternative to conventional water pumps which are powered by electricity or diesel. Hence these systems are perfect for those areas that do not have connections to the power grid. As a consequence, in this article; we will look at how solar energy is transformed into electrical energy using a boost converter. The boost converter is used when the output voltage from a solar panel is inadequate to power a motor. A MATLAB/Simulink-based designs of a solar-powered pumping system with a DC Motor were performed in this study.

Published in: 2021 2nd International Conference for Emerging Technology (INCET)

Date of Conference: 21-23 May 2021 **INSPEC Accession Number:** 20712796

Date Added to IEEE Xplore: 22 June 2021

DOI: 10.1109/INCET51464.2021.9456131

Authors

Figures

References

Citations

☰ Contents

I. Introduction

Solar photovoltaic systems are a good substitute for electricity and diesel-driven water pumps because they are pollution-free. Although it generates power directly from natural sources, it faces some challenges because its efficiency is dependent on external operating conditions such as irradiance, temperature, shading, and so on. As the cost of diesel increases in daily life, transitioning to renewable energy sources such as solar, wind, and thermal energy and the vast quantities of power can be generated. Since irradiance (the power per unit area obtained from the sun) is so important for solar panel performance, it's important to choose the right values for the right time, and the temperature range should be about 25° Celsius. The next important factor that might influence the performance of the panel is shading. Shade is something that blocks that flow in typical solar panel strings. If a tree or a chimney casts shade on even one of the panels in the string, the output of the entire string will so reduced to practically zero for the duration of the shadow. However, if there is a separate, un-shaded series, it will continue to generate power as usual. But we can avoid shading in many number of ways, this is the first and most obvious move in ensuring that your system is not adversely affected by partial shading. When deciding whether or not to install solar panels, it's crucial to consider all times of day and seasons of the year. Using a variety of mapping tools, a solar system installer should be able to tell you whether shading would be issue. Solar system owners should also keep an eye out for nearby trees that might grow tall enough to cause shading problems in the future. Trees have plenty of time to grow throughout the solar system's lifetime, which is estimated to be 25 years or more. In order to get the required voltage to power the motor, a normal DC to DC boost converter is designed. The boost converter is a non-isolated step-up DC-DC converter with high switching voltage tension and low static gain that has been widely used in the literature.. This paper is structured as follows; Section 1 describes how a solar photovoltaic array operates and contrasts its advantages and disadvantages. Section 2 describes the proposed boost converter's configuration and operation, as well as the selected parameters. Section 3 describes the analysis and results for the DC motor as well as the proposed converter. The proposed solar water pump's efficiency merits are discussed in Section 5 of the paper and it ends here. Fig. 1.

Block diagram of solar water pumping system.

Authors	▼
Figures	▼
References	▼
Citations	▼
Keywords	▼



Institutional Sign In

All



ADVANCED SEARCH

Conferences > 2021 2nd International Confer... ?

A Hybrid Multilevel Inverter for Electric Vehicle Applications

Publisher: IEEE

Cite This



S Vijayalakshmi ; M Marimuthu ; R Venugopal ; M Suryaprakash ; V Shyaam prasath ; ... All Authors



Alerts

Manage Content Alerts

Add to Citation Alerts

More Like This

Modeling of the Operation of an Asynchronous Electric Drive of an Electric Vehicle in Slip Modes
2020 IEEE Problems of Automated Electrodrive. Theory and Practice (PAEP)
Published: 2020

Modeling The Dynamic Processes of The Electric Drive of Electric Vehicle While Wheels are Slipping
2020 IEEE Problems of Automated Electrodrive. Theory and Practice (PAEP)
Published: 2020

Show More

Abstract



Downl

PDF

Document Sections

I. Introduction

II. Working Principle

III. Simulation Circuit and Results Discussion

IV. Comparison of 7-Level Inverter Topology

V. Hardware Implementation

Show Full Outline

Abstract:Multi-level inverters have become popular for very large power applications in recent years. Various topologies and thresholds for utility and drive applications have been published in present literature. This paper is ke... **View more**

Metadata

Abstract: Multi-level inverters have become popular for very large power applications in recent years. Various topologies and thresholds for utility and drive applications have been published in present literature. This paper is ke... to the study of a seven-level multi-level inverter based induction machine drive Topological assembly and working principles of a multi-level inverter are used in a number of industrial applications. The viability of the projected method is confirmed by MatLAB/Simulink computer simulations. This seven-level multilevel inverter topology consists of 7 switches used for drive applications.

Published in: 2021 2nd International Conference for Emerging Technology (INCET)

Authors

Figures

References

Keywords

Date of Conference: 21-23 May 2021 **INSPEC Accession Number:** 20867089

Date Added to IEEE Xplore: 22 June 2021

DOI: 10.1109/INCET51464.2021.9456364

ISBN Information:

Publisher: IEEE

Contents

I. Introduction

Inverter is a device which converts fixed DC into AC voltage. Mainly inverter can be classified into many levels but switches and levels may vary in every topology. However, the design and manufacturing of multilevel inverter are cheap for high power application. In this multilevel inverter consists of IGBT and MOSFET switches and also a DC source. A load will be connected to the inverter. The inverter is mainly used in high application such as metro train, lifts etc. This inverter has a voltage of 36V. Then the value of input voltage depends upon the application. For example, some may require very high voltage (i.e 1000V) some may require low voltage (i.e 12V). The output will be seen in a sinusoidal waveform. Its waveforms are based on sine, square or PWM. And also it can produce changed sine wave and clean sine wave.

Authors



Figures



References



Keywords



Metrics



IEEE Personal Account

CHANGE
USERNAME/PASSWORD

Purchase Details

PAYMENT OPTIONS
VIEW PURCHASED
DOCUMENTS

Profile Information

COMMUNICATIONS
PREFERENCES
PROFESSION AND
EDUCATION
TECHNICAL INTERESTS

Need Help?

US & CANADA: +1 800 678
4333
WORLDWIDE: +1 732 981
0060
CONTACT & SUPPORT

Follow



[About IEEE Xplore](#) | [Contact Us](#) | [Help](#) | [Accessibility](#) | [Terms of Use](#) | [Nondiscrimination Policy](#) | [IEEE Ethics Reporting](#) | [Sitemap](#) | [Privacy & Opting Out of Cookies](#)

A not-for-profit organization, IEEE is the world's largest technical professional organization dedicated to advancing technology for the benefit of humanity.

© Copyright 2022 IEEE - All rights reserved.

IEEE Account

» Change Username/Password
» Update Address

Purchase Details

» Payment Options
» Order History
» View Purchased Documents

Profile Information

» Communications Preferences
» Profession and Education
» Technical Interests

Need Help?

» **US & Canada:** +1 800 678 4333
» **Worldwide:** +1 732 981 0060
» Contact & Support



Institutional Sign In

All



ADVANCED SEARCH

Conferences > 2021 2nd International Confer... ?

Dynamic Performance Enhancement of Modified Sepic Converter

Publisher: IEEE

Cite This

PDF

Vijay Ravindran ; RamPrakash Ponraj ; S Syed Zameerbasha ; N Santhosh Kanna ; S ... All Authors



Alerts

Manage Content Alerts

Add to Citation Alerts

More Like This

Discussions on control loop design in average current mode control [PWM DC/DC power converters]
Conference Record of the 2000 IEEE Industry Applications Conference. Thirty-Fifth IAS Annual Meeting and World Conference on Industrial Applications of Electrical Energy (Cat. No.00CH37129)
Published: 2000

Saturable reactor assisted soft-switching full-bridge DC-DC power converters
IEE Proceedings B - Electric Power Applications
Published: 1991

Show More

Abstract



Downl

PDF

Document Sections

- I. Introduction
- II. Related Works
- III. Boost Converter and Sepic
- IV. Modified Sepic Converter
- V. Working Principle:

Show Full Outline

Authors

Figures

References

Citations

Keywords

Metrics

Abstract: This paper introduced a non-isolated DC-DC boost converter with high voltage gain and low switching voltage stress for any level of input and output voltage applications.... **View more**

Metadata

Abstract:

This paper introduced a non-isolated DC-DC boost converter with high voltage gain and low switching voltage stress for any level of input and output voltage applications. The high boost converter is designed with the concept of Single Ended Primary Inductor Converter called as modified SEPIC converter. Normal Boost and SEPIC converters were assessed and compared to the updated SEPIC converter for their efficiency. For the modified converter, a 15 V input voltage and a 170 V output voltage with 100 W output power are suitable. Moreover, for switching the converter uses lower input current and displays low voltage stress. In general, the high-gain SEPIC DC-DC converters would have a high ripple value, which would make the output voltage unstable. But in our modified SEPIC converter, the output voltage and current are steady DC values without any ripples. The study of time reaction indicates that the suggested converter settles faster than the other comparable converter at steady state voltage and current.

Published in: 2021 2nd International Conference for Emerging Technology (INCET)

Date of Conference: 21-23 May 2021 **INSPEC Accession Number:**

More Like This

Date Added to IEEE Xplore: 22 June 2021
DOI: 10.1109/INCET51464.2021.9456403
Publisher: IEEE
Conference Location: Belagavi, India

Contents

I. Introduction

Consumption of electricity has now increased and demand is now raising a lot. The generation of energy from traditional sources, such as coal and oil, leads to a rise in the global greenhouse effect and environmental pollution problems. A big barrier to industrial development has been the lack of power generation and pollution issues. The use of electricity from non-conventional sources is crucial as its use does not generate emissions and sources are inexhaustible. Due to its efficiency, eco-friendliness, low maintenance and low operating cost, photovoltaic (PV) is one of the most outstanding renewable energy resources in the universe.

Authors	▼
Figures	▼
References	▼
Citations	▼
Keywords	▼
Metrics	▼

IEEE Personal Account

CHANGE USERNAME/PASSWORD

Purchase Details

PAYMENT OPTIONS
VIEW PURCHASED DOCUMENTS

Profile Information

COMMUNICATIONS PREFERENCES
PROFESSION AND EDUCATION
TECHNICAL INTERESTS

Need Help?

US & CANADA: +1 800 678 4333
WORLDWIDE: +1 732 981 0060
CONTACT & SUPPORT

Follow



[About IEEE Xplore](#) | [Contact Us](#) | [Help](#) | [Accessibility](#) | [Terms of Use](#) | [Nondiscrimination Policy](#) | [IEEE Ethics Reporting](#) | [Sitemap](#) | [Privacy & Opting Out of Cookies](#)

A not-for-profit organization, IEEE is the world's largest technical professional organization dedicated to advancing technology for the benefit of humanity.

© Copyright 2022 IEEE - All rights reserved.

IEEE Account

» Change Username/Password
» Update Address

Purchase Details

» Payment Options
» Order History
» View Purchased Documents

Profile Information

» Communications Preferences
» Profession and Education
» Technical Interests

Need Help?

» **US & Canada:** +1 800 678 4333
» **Worldwide:** +1 732 981 0060
» Contact & Support

Analysis of PV Panel based Bidirectional Converter for Electric Vehicle

Vijayalakshmi S
Department of EEE

Saranathan college of Engineering,
Trichy, India
bksviji@gmail.com

Shivabalan N
Department of EEE

Saranathan college of Engineering,
Trichy, India
shivabalan1999@gmail.com

Thayananth.T
Department of EEE

Saranathan college of Engineering,
Trichy, India

Marimuthu M
Department of EEE

Saranathan college of Engineering,
Trichy, India
marimuthueephd@gmail.com

Shathishkumar VK
Department of EEE

Saranathan college of Engineering,
Trichy, India
shathishgokul@gmail.com

Venugopal. R
Department of EEE

Saranathan college of Engineering,
Trichy, India
venugopal-eee@saranathan.ac.in

Pravinraj T
Department of EEE

Saranathan college of Engineering,
Trichy, India
pravinprince1122@gmail.com

Abstract: This paper present an analysis of PV panel based Bidirectional converter for Electric vehicle charging. This system consists of solar cell battery, bidirectional dc -dc converter. A Battery is provided for supply power to dc motor during no sunlight condition. The bidirectional dc-dc converter is working in both charging and discharging the battery and can manage the flow of power in both the direction and hence excess energy from the PV panel can be stored in battery. Under the influence of varying irradiance and varying load conditions, the MPPT controller extracts full power from the PV module. Evaluation and analysis of model output was carried out via MatLAB/Simulink.

Keywords: PV panel, Bidirectional Converter, battery, Maximum Power Point Tracking (MPPT).

I. INTRODUCTION:

Solar energy is becoming the most difficult source of energy. In fact, solar energy is used in many domestic & industrial or commercial applications. In order to minimise Co2 emissions, solar energy is a crucial source.. On our country, ICE (Internal combustion Engines) are a major source of pollution, hence Electric vehicles become the promising solution. Renewable energy sources such as solar power are superior to charging plug-in electric vehicles for many purposes that take environmental and cost factors into account. In India, mostly IC engines where used for the transportation. The Indian government is promoting more and more electric vehicles to be promoted in order to minimise air pollution and climate change and raise fossil fuel prices (EV). The Indian government has set an aim to speed up the adoption of electric vehicles to minimise pollution and many other benefits, such as high torque and easy speed regulation. However, all IC engines have to be replaced by an energy storage battery with the help of suitable converter.

In [1], the authors suggest a second-life Li-ion battery AC charging station, combining solar PV and wind energy. This station is connected to a grid that, depending on the utilisation, allows the export or import of electricity. A control strategy of a multi-port, grid-connected, direct DC

PV charging station was proposed by the authors in [2], [4], the energy source here can be either PV panels or AC grid, the flow of energy from AC grid is bidirectional, so it is possible to inject PV energy into AC grid. Many converters are used for these two topologies, which reduce performance .A charging strategy to reduce energy costs is proposed in[5] and charging time is split into intervals to minimise the peak usage of a fleet of EVs during the day. In this case, the charging station is linked to the grid; in addition, the topology was not given. The impact of fast charging EVs on the AC grid was studied in[8]: DC fast charging is the charging station in[8], and only the grid is used as a source of electricity. Four possible designs are suggested for a solar EV charger and compared in[9], these configurations are also linked to the grid, two possible options for the AC grid interconnection: AC interconnection or DC interconnection. Via the use of multiple DC-DC and DC-AC converters, performance is reduced.

Our proposed PV fed bidirectional converter for EV vehicle is illustrated in Figure 1. This block diagram consists of PV panel, bidirectional converter, battery, and E-bike. The power from PV panel is irregular in nature, so when solar power generation is higher than the demand of the load, then the surplus energy is served to the battery station via bidirectional converter. The lack of power demand is supplied by the station battery via the converter at any moment when the load demand goes beyond instantaneous solar power generation. When the absence of solar power, the battery power is transferred to the load through bidirectional converter. This study can be done for 1KW Solar charging station to charge electric bikes. In our method, due to its simplicity and less computational requirements, the P&O algorithm was used to implement MPPT. Also, for the algorithm to operate, no previous knowledge of the PV system is required. The sun has been playing numerous roles in humane existence.

A. Maximum Power Point Tracking (MPPT)

Maximum Power Point Tracking, or MPPT, is a charge controller algorithm that extracts the maximum available

power from a PV module under certain conditions. Maximum power point refers to the voltage at which a PV module will produce the most power (or peak power voltage). Solar radiation, ambient temperature, and solar cell temperature all affect maximum strength.

In this paper, a charge controller with MPPT capability is proposed to extract full power from the PV column. The indirect and direct techniques are the two broad types of MPPT techniques.

B. DC-DC converters

DC-DC converters are commonly used to efficiently generate a regulated voltage from a source that may or may not be well managed to a variable load. DC-DC converters are high-frequency power conversion circuits that smooth out switching noise into controlled DC voltages using high-frequency switching and inductors, transformers, and capacitors. And when the input voltages and output currents change, closed feedback loops retain a constant voltage output. They are usually much more effective and smaller than linear regulators, with 90% performance. Non-isolated and isolated DC-DC converters are available. Whether or not the input ground is connected to the output ground determines isolation.

A simple DC-DC converter takes current and converts it to an AC square wave signal by passing it through a switching element. The wave is then passed through another filter, which converts it to a DC signal with the appropriate voltage.

C. Non-isolated converter

When the voltage change is minimal, non-isolated converters are used. In this circuit, the input and output terminals share a common ground. The various types of converters in this category are listed below. The downside is that it is unable to provide protection against high electrical voltages and produces more noise.

D. Step down buck converter

To produce a lower voltage than the input, a step-down circuit is used. It's also known as a buck. The polarities in the output are identical to those in the input. A buck converter, also known as a step down voltage regulator, is a system that already exists. Since it's a DC-DC converter, it completes the job with the aid of a few transistor switches and an inductor.

E. Step-up (boost) converter

To produce a higher voltage than the input voltage, a step-up circuit is used. It's known as a boost. The polarities are identical to those found in the input. One of the most basic types of switch mode converter is the boost converter. It takes an input voltage and improves or raises it, as the name implies. An inductor, a semiconductor switch, a diode, and a capacitor are the only components.

F. Isolated converters

The input and output terminals of these converters are separated. They have a very high isolation voltage. They

have the ability to filter out noise and interference. As a result, they are able to generate a cleaner DC source.

G. Fly back converter

This converter functions similarly to the non-isolating category's buck-boost converter. The difference is that instead of an inductor, it stores energy in a transformer.

H. Bidirectional Converter

Bi-directional dc-dc converters have recently been extensively researched and developed for a variety of applications, including battery charger dischargers, electric cars, and UPS systems.

Electric energy flows between the engine and the battery in battery fed electric vehicles (BFEVs). The vehicle can be powered solely by batteries or other forms of electrical energy to achieve zero emissions. This can be used to provide desired power flow control in Hybrid Electric Vehicles (HEVs) with a battery as an energy storage feature.

Energy storage systems in hybrid electric vehicles serve as catalysts to provide an energy boost. However, its use has been limited due to its high initial cost and short driving range at BFEVS. The traction systems in Hybrid Electric vehicles depend heavily on bidirectional dc-dc converters. Its implementation in a Bi-directional dc-dc converter fed de motor drive for electric vehicles (EVs) allows for appropriate control of both motoring and regenerative braking operations, as well as a major increase in the drive system's overall performance.

I. Solar panel selection

A photovoltaic (PV) module is referred to as a solar panel. A PV module is an installation-ready assembly of photovoltaic cells assembled in a system. Photovoltaic cells produce direct current electricity using sunlight as a source of energy. A PV Panel is a set of PV modules, and an Array is a collection of Panels.

Solar panel selection is influenced by the battery, inverter, and charge controller. For example, if we choose a 12V PV panel, we must also use a 12V battery. A 24V battery can be used with a 24V solar panel. A key point to remember is that while a 24V battery is not currently available on the market, you can make one by connecting two 12V batteries in sequence.

In this , section 2 consists of proposed circuit, section 3 contains simulation circuit and results discussion are carried out in section 4, finally section 5 consists of conclusion.

The figure 1 clearly represents the usage of bi-directional converter which is connected to a battery and vice versa to a load. It can operate in the boost mode when the output power is greater than the load power. It operates in buck mode when output power is lesser than the load power during the night time. No irradiation occurs, so the S1 switch switches off, so the S3 turn ON battery side boost circuit works, so that the battery receives power from the load. In that way, the bidirectional converter functioned, so that the load can receive the power from both PV panel and the battery.

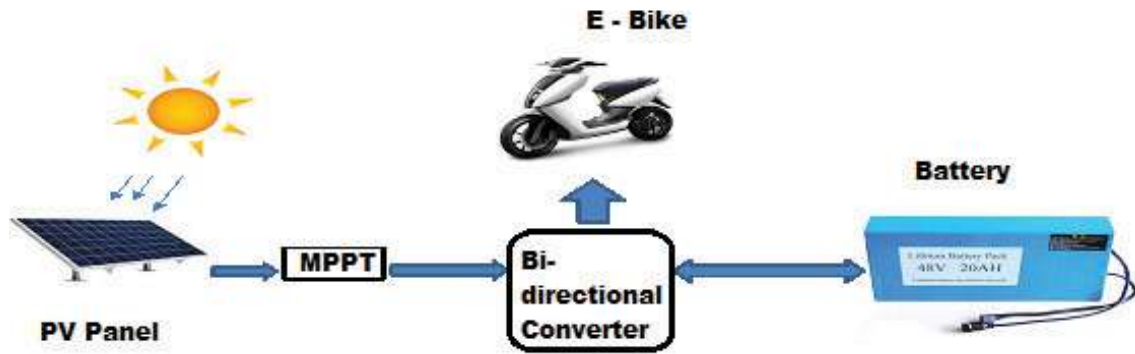


Fig. 1. PV fed bidirectional converter for E-vehicle block diagram

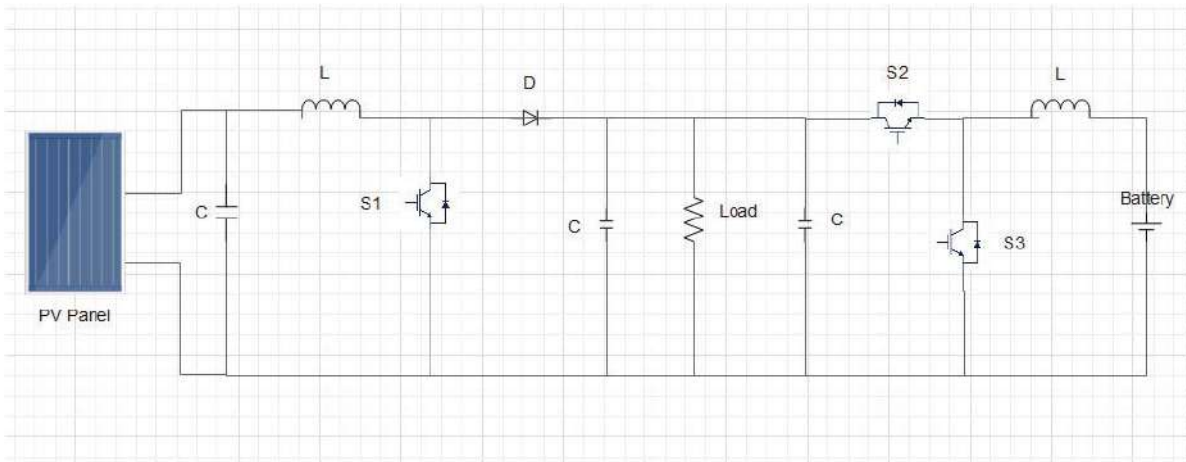


Fig. 2. PV fed bidirectional converter for E-Vehicle circuit

II. CIRCUIT DIAGRAM:

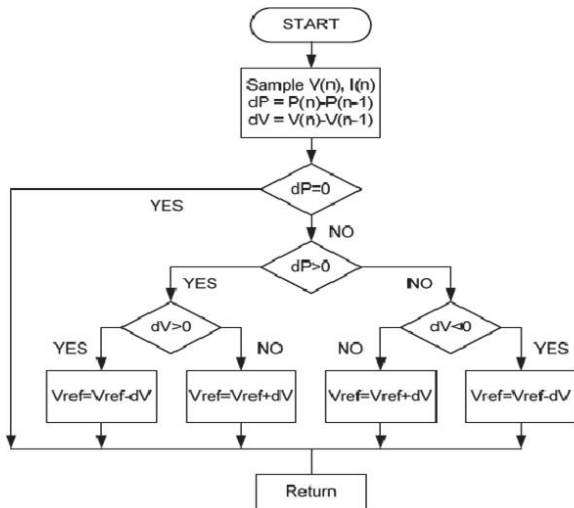


Fig. 3. P & O Algorithm

Figure 2 shows the proposed circuit for PV fed bidirectional converter for E-Vehicle. In this Figure 2, The left side of the load, PV panel – C – L – S1-D – C constitutes boost circuit. Right side of the load, C – S2 – L – battery behaves as the buck converter and the battery – L – S3 – S2 – C – Load function as battery side boost circuit. Whenever the irradiance occurs, the PV panel generates the supply voltage. The switch S1 turns ON and the boosted voltage fed to the load, as well as S2 turn ON and the buck voltage which charge the battery. The maximum output of the PV

panel is derived from the load by connecting the MPPT controller to the PV panel. To extract maximum power from the panel, the Perturb & Observe (P & O) algorithm is used in the MPPT. The P & O algorithm is explained through flow chart is given in Figure 3.

III. SIMULINK MODEL OF A PV PANEL BASED BIDIRECTIONAL CONVERTER FOR EV CHARGING

MATLAB is a programming environment tailored to engineers and scientists. The MATLAB language, a matrix-based language that allows the most natural expression of computational mathematics, is at the heart of MATLAB. One can do the following with MATLAB:

- Conduct data analysis • Create algorithms • Develop models and applications:
- Conduct data analysis • Create algorithms • Develop models and applications

The following block diagram was designed by MATLAB/SIMULINK with the help of the circuit diagram. As a preliminary step, we have analysed the Bidirectional converter with the help of this block diagram to find the drawback so that we can design the effective one.

Figure 4 shows the Simulation circuit for PV panel powered Bidirectional Converter for E-Vehicle using MatLAB/Simulink. The circuit consists of a PV panel, an MPPT (P & O) control circuit, and all simulated battery charging control circuits. The simulation output is depicted in Figure 5 and Figure 6.

There is no generation of input supply in PV When no irradiance, reference voltage is around 48V. When no input generation, State of charge decreases to 44.98% because battery is delivering supply to the load. When no input generation, battery current is around 18A, battery in discharge condition When no input generation, battery voltage is 25.6V in discharge condition When no input generation, PV panel output power is zero When no input generation, output voltage to load is around 48V.

When no input generation, output voltage to load is around 48V. PV input power generation is higher because irradiation is higher and it provides the input to the load and the battery charges the same thing. PV Panel power is around 900 irradiances; State of charge is in increase because the battery is in charging condition. Battery is in charge mode, battery voltage is around 26V. Battery current is negative because the battery is charging condition. Output voltage to load is maintain constant 48V using bidirectional converter are depicted in Figure 6.

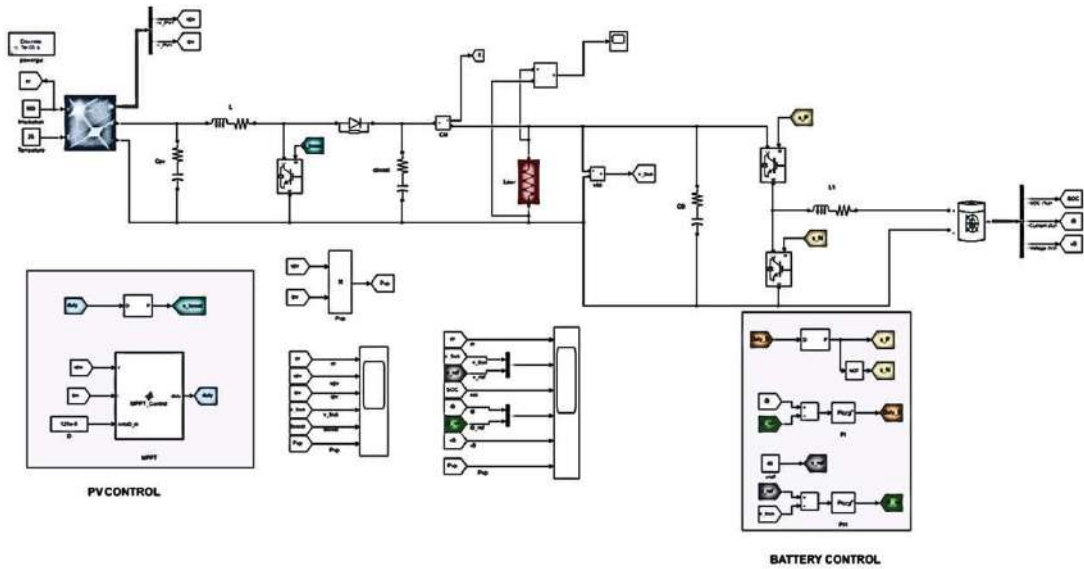
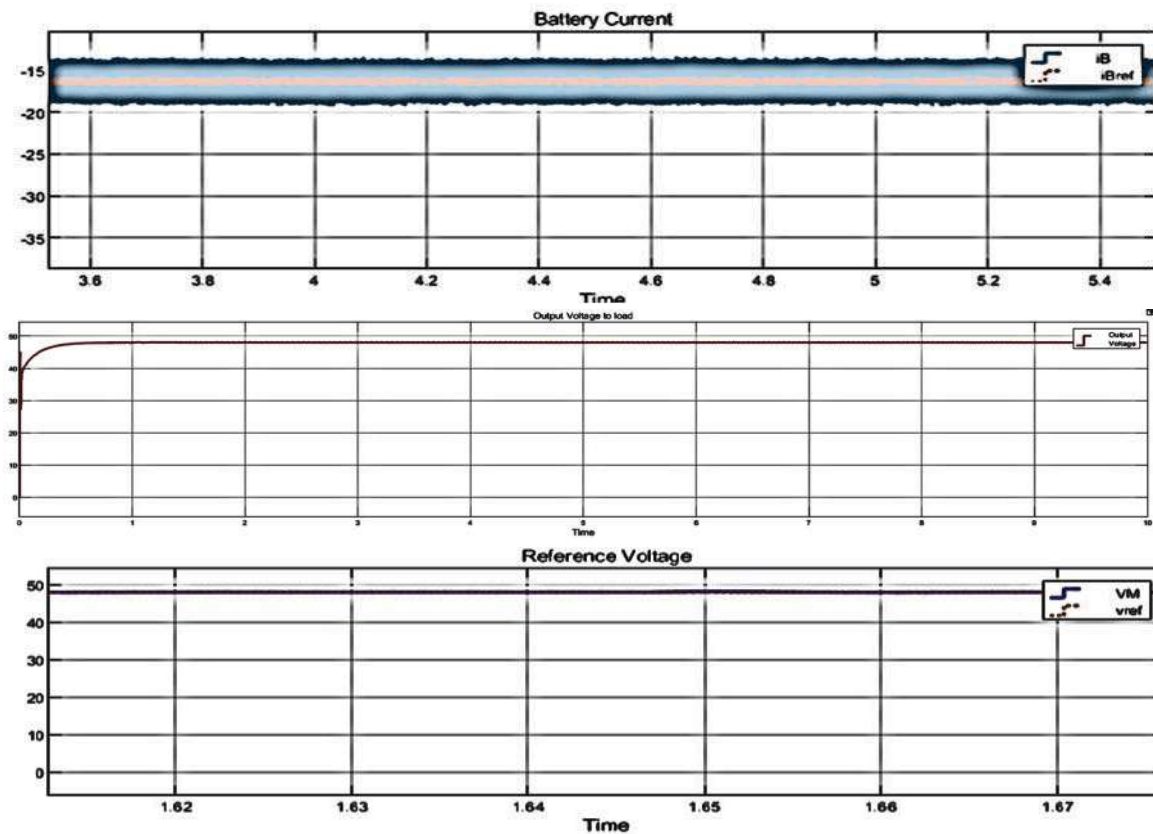


Fig. 4. Simulation circuit for PV fed bidirectional converter for E-Vehicle

IV. SIMULATION RESULT DISCUSSION:



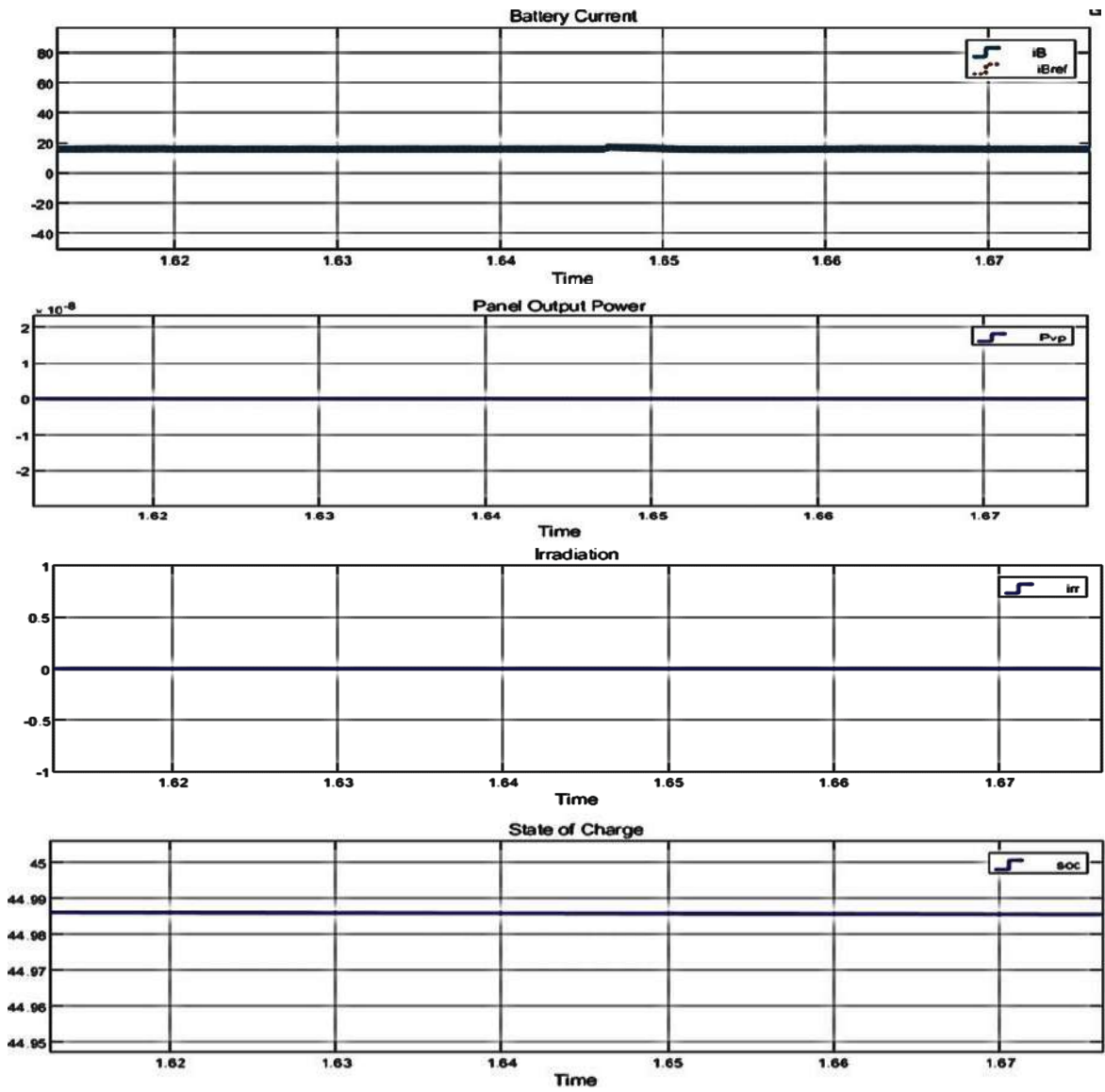
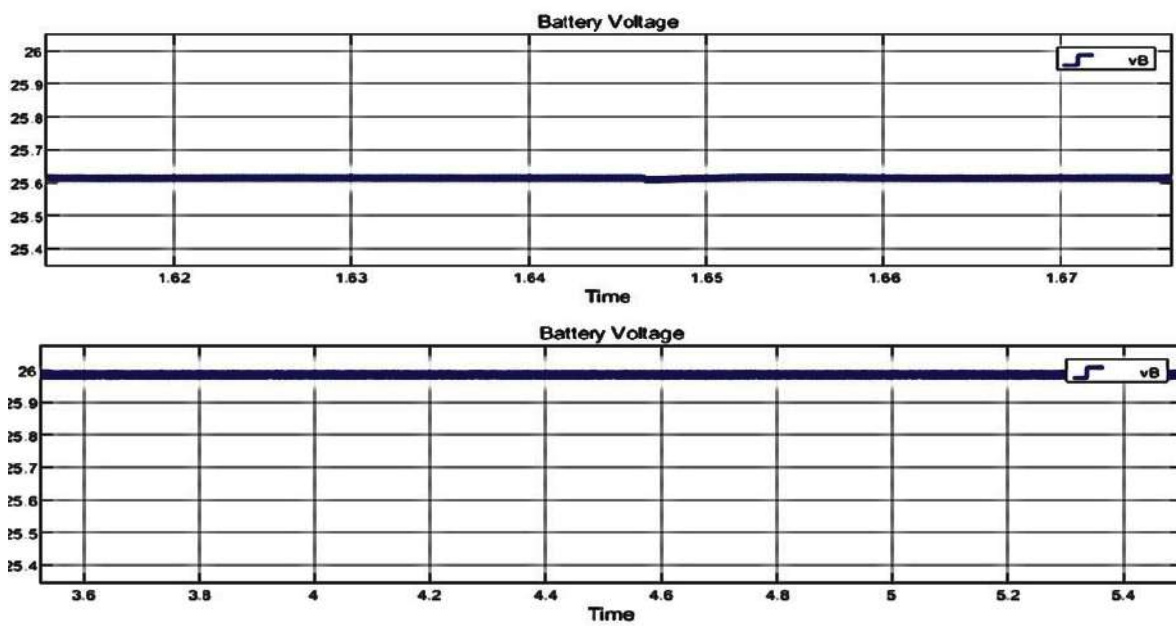


Fig. 5. Battery response during PV panel under zero irradiance condition



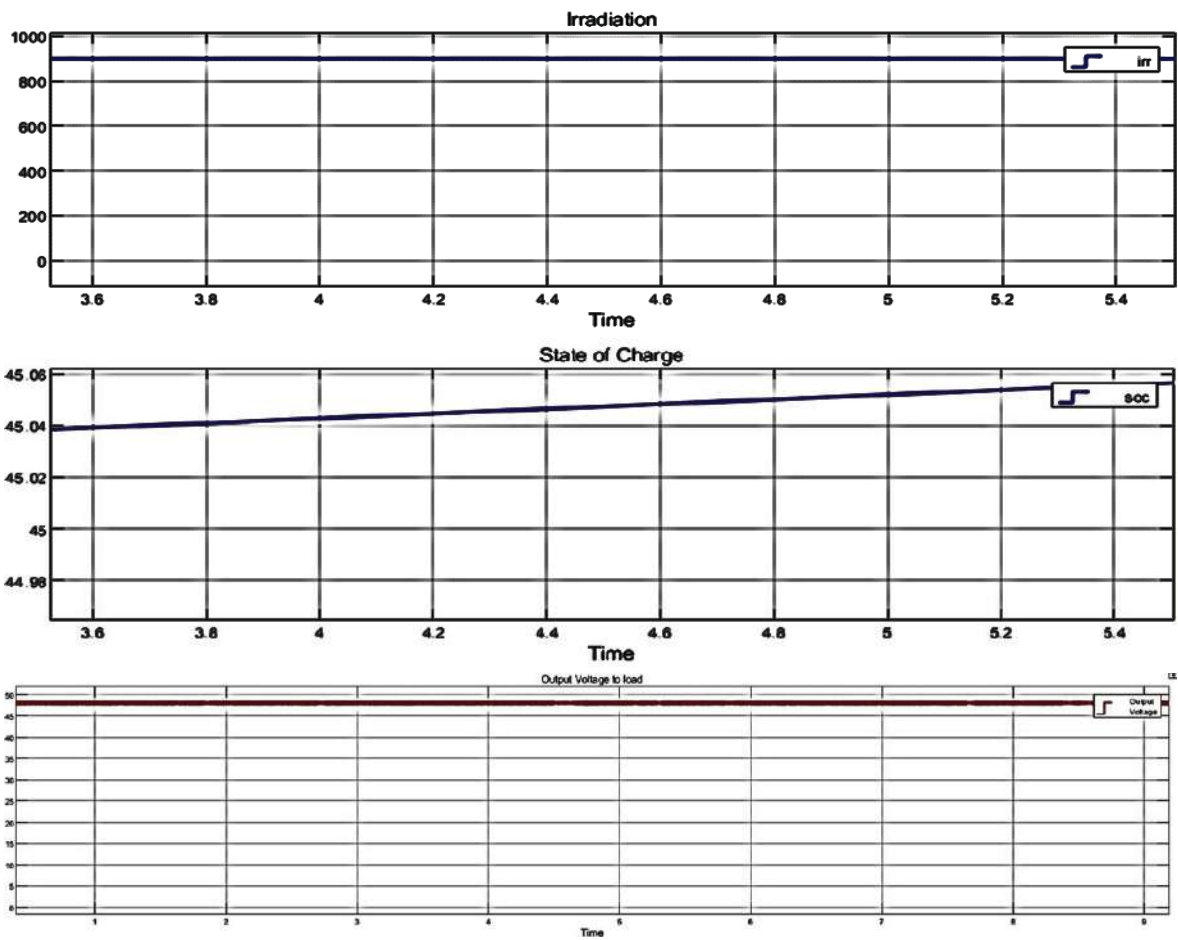


Fig. 6. Battery response during PV panel under 900 irradiance condition

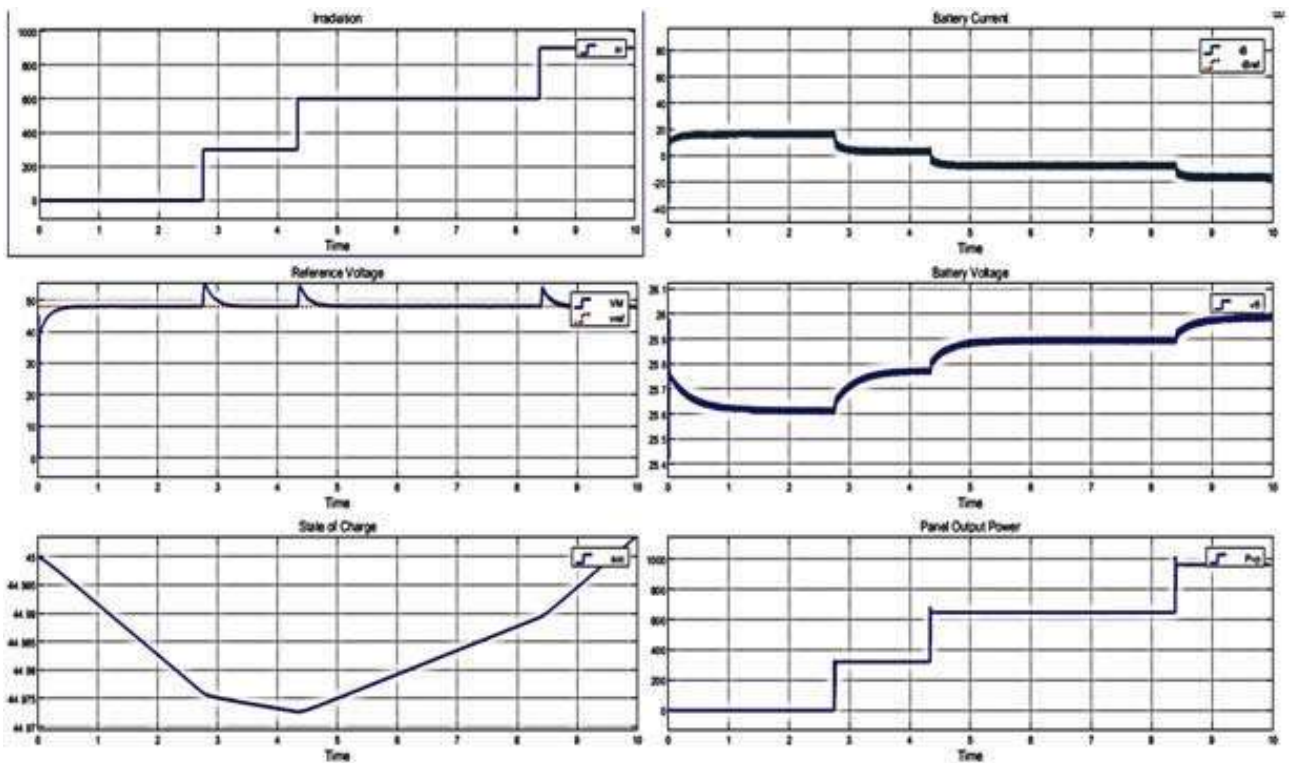


Fig. 7. Output results for various irradiance condition

V. RESULT DISCUSSION

Figure 7 shows the various irradiance condition in the PV panel whose related panel output power, state of charge in the battery, battery current, and battery voltage. The increasing irradiance increase the state of charge, battery voltage are also shown in Figure 7. From the simulation result one can understand that the proper operation of bidirectional converter, how it charge the battery during irradiance condition and discharge the battery to the load under no irradiance condition.

VI. CONCLUSION:

The DC Motor using PV panel and Battery is implemented in MatLAB/Simulink and its effectiveness is tested under different solar power generation and battery power requirement. It is found that at a certain radiance and temperature, the power supplied by the solar panel depends on the load across it.

REFERENCES

- [1] A. Hamidi, L. et. al "EV Charging Station Integrating Renewable Energy and Second - Life Battery,"2013 Int. Conf. Renew. Energy Res. Appl., no. October, pp. 20--23, 2013.J. Clerk Maxwell, A Treatise on Electricity and Magnetism, 3rd ed., vol. 2. Oxford: Clarendon, 1892 ,pp. 68-73.
- [2] C. Hamilton et.al "System architecture of a modular direct-DC PV charging station for plug-in electric vehicles, "IECON Proc. (Industrial Electron. Conj, pp. 2516-2520, 20 10.K. Elissa, "Title of paper if known,"tmpublish ed.
- [3] K. Bao, "Battery Charge and Discharge Control for Energy Management in EV and Utility Integration," 2012.
- [4] G. Gamboa, et. al, "Control Strategy of a Multi-Port, Grid Connected, Direct-DC PV Charging Station for Plug-in Electric Vehicles "EGGE congress and expo. pp. 1173-1177, 20 10.
- [5] C. E.A. Ines, "Charging Strategies to Minimize the Energy Cost for an Electric Vehicle Fleet, " pp. 1-7, 2014.
- [6] S. Y. Park, et.al "A universal battery charging algorithm for Ni Cd, Ni-MH, SLA, and Li-Ion for wide range voltage in portable applications,"PESC Rec. - IEEE Annu. Power Electron. Spec.Conj, pp. 4689694, 2008.
- [7] Moroccan Agency for Solar Energie Home Moroccan solar plan-Sunshine map, 02 June 20 15.
- [8] J. Y. Yong, et.al "Modeling of electric vehicle fast charging station and impact on network voltage," 2013 IEEE Conf. Clean Energy Technol., pp. 399 04,2013.
- [9] G. R. C. Mouli, et.al, "Comparison of System Architecture and Converter Topology for a Solar Powered Electric Vehicle Charging Station,"pp. 1908-1915, 2015.
- [10] S. Vijayaakshmi, T. Sree Renga Raja, "Time domain based digital PWM controller for DC-DC converter, Automatika, Vol. 55, No. 4, 2014, pp. 434-445.

Non-isolated Multilevel Zeta Converter for MLI Application

Proceedings of International Conference on Power Electronics and Renewable Energy Systems pp 21-30 | Cite as

- Marikannu Marimuthu (1)
- Subramanian Vijayalakshmi (1)
- B. Paranthagan (2)
- R. Venugopal (3)
- S. Srinithi (4)
- B. Yuvaraj (5)
- R. Soundarajan (5)
- S. K. Vasantha Kumar (5)

1. Department of Electrical and Electronics Engineering, Saranathan College of Engineering, , Trichy, India
2. Associate Professor, Department of Electrical and Electronics Engineering, Saranathan College of Engineering, , Trichy, India
3. Assistant Professor, Department of Electrical and Electronics Engineering, Saranathan College of Engineering, , Trichy, India
4. PG Scholar, Department of Electrical and Electronics Engineering, Saranathan College of Engineering, , Trichy, India
5. UG Student, Department of Electrical and Electronics Engineering, Saranathan College of Engineering, , Trichy, India

Conference paper

First Online: 22 November 2021

- 72 Downloads

Part of the [Lecture Notes in Electrical Engineering](#) book series (LNEE, volume 795)

Abstract

A new multilevel zeta converter which converts fixed DC voltage to multilevel DC output voltage is discussed in this paper. Proposed converter has stable voltage feedback capacity and produces high gain output voltages with less input current. Voltage supplied by the PV panel or the fuel cell is at an output of a low voltage. These output voltages can be interfaced with standalone (or) grid connected inverter system by employing the proposed converter. By using a single transistor with the multilevel capacitor geometric structure, the proposed converter is able to generate an output voltage that is much higher and has ripple free output current with a higher step-up conversion ratio. It allows for operation at much higher frequencies for a much longer

period of time. Additionally, it does not require for the electrical transformer for high gain. The output of the zeta converter generates four output level voltages which are simulated and verified with theoretical results.

Keywords

Zeta converter High voltage gain Multilevel voltages Multilevel Inverter
Self-balancing capacitor

This is a preview of subscription content, [log in](#) to check access.

References

1. Gaurav P, Dhote VP, Modak. Study and analysis of zeta converter fed by solar photovoltaic system using PID controller
[Google Scholar](#) (<https://scholar.google.com/scholar?q=Gaurav%20P%2C%20Dhote%20VP%2C%20Modak.%20Study%20and%20analysis%20of%20zeta%20converter%20fed%20by%20solar%20photovoltaic%20system%20using%20PID%20controller>)
2. Manikandan K, Sivabalan A, Sundar R, Sury P. A study of landsman, sepic and zeta converter by particle swarm optimization technique. 978-1-7281-5197-7/20/\$31.00 ©2020 IEEE
[Google Scholar](#) (<https://scholar.google.com/scholar?q=Manikandan%20K%2C%20Sivabalan%20A%2C%20Sundar%20R%2C%20Sury%20P.%20A%20study%20of%20landsman%2C%20sepic%20and%20zeta%20converter%20by%20particle%20swarm%20optimization%20technique.%20978-1-7281-5197-7%2F20%2F%2431.00%20%2C%20A92020%20IEEE>)
3. Suresh P, Kirubakaran D (2018) Novel zeta converter with multi level inverter connected to grid. In: IJEECS, vol 11, no 3, September 2018, pp 814–820
[Google Scholar](#) (<https://scholar.google.com/scholar?q=Suresh%20P%2C%20Kirubakaran%20D%20%282018%29%20Novel%20zeta%20converter%20with%20multi%20level%20inverter%20connected%20to%20grid.%20In%3A%20IJEECS%2C%20vol%2011%2C%20no%203%2C%20September%202018%2C%20pp%20814%2E2%80%93820>)
4. Falin J (2010) Designing DC/DC converters based on ZETA topology. Analog Appl J
[Google Scholar](#) (<https://scholar.google.com/scholar?q=Falin%20J%20%282010%29%20Designing%20DC%2FDC%20converters%20based%20on%20ZETA%20topology.%20Analog%20Appl%20J>)
5. Marimuthu M, Vijayalakshmi S, Shenbagalakshmi R (2020) A novel non-isolated single switch multilevel cascaded DC-DC boost converter for multilevel inverter application. J Electrical Eng Technol. The Korean Institute of Electrical Engineers 2020
[Google Scholar](#) (<https://scholar.google.com/scholar?q=Marimuthu%20M%2C%20Vijayalakshmi%20S%2C%20Shenbagalakshmi%20R%20%282020%29%20A%20novel%20non-isolated%20single%20switch%20multilevel%20cascaded%20DC-DC%20boost%20converter%20for%20multilevel%20inverter%20application.%20J%20Electrical%20Eng%20Technol.%20The%20Korean%20Institute%20of%20Electrical%20Engineers%202020>)

Password based circuit breaker operation for the safety of lineman during maintenance work

- Sakthi Raja V, Rakesh K.K, Pravin kumar N, Saravanan S,
Dr.M.V.Suganyadevi

Department of Electrical and Electronics Engineering, Saranathan College of Engineering, Trichy

ABSTRACT

Nowadays, accidental death of lineman is a commonly occurring tragedy. so, it is compulsory for us to guarantee the safety of linemen by adapting a new method of operation. A new system should be adapted to regulate and manage the control panel which consists of all the electrical components and circuit breakers. These accidents are on the rise throughout the country, main reason being miscommunication between the maintenance workers and sub-station workers. The planned system gives a solution for this problem and reduces the risk for linemen. The control to activating/ deactivating the control panel is in the hands of the linemen only. In this new method of operation, a "Passcode or Password" is needed to access the control panel and further to operate the circuit breaker (ON/OFF). An encrypted Passcode/Password is sent from the substation to the circuit breaker operators (linemen), for the purpose of executing maintenance works. The password is registered and forwarded to the lineman's mobile and also to the management panel by the help of GSM module. The received passcode/password is typed in through the matrix keyboard which acts as the input device and also it is interfaced to the microcontroller present inside the panel. The password entered by the lineman is compared with the encrypted passcode received from the substation through the GSM module. Only when both the passwords match, the lineman will be able to access the control panel and to operate the circuit breaker, so he can proceed to do the repair works and maintenance works. If any third party enters a wrong password, he/she will not be able to access or operate the control panel and hence the system will be completely secured.

Keywords: Security, lineman, password, control panel

Date of Submission: 21-04-2021

Date of Acceptance: 06-05-2021

I. INTRODUCTION

In present times, casualties of line-workers due to accidents occurring during maintenance works is on the rise. Until now, to execute maintenance works, Line clearance method is used to shut down the electrical line in which the work is to be done. There are lots of short-comings to this method, like accidental charging of the line due to mistake of the operators at station, which can lead to serious injuries, and in some unfortunate cases, even deaths of line-workers. The employment of microcontrollers can be a solution to this issue. The employment of communication networks will increase the potency of the pilotless devices. This new method with the help of GSM module, reduces the risk of physical contact with the high voltage electrical lines, and enables us to control the circuit breakers automatically. so, we decided to implement GSM based circuit to control the operation of the electrical lines.

A circuit breaker is a protective device which acts as a switch designed to safeguard an

electrical circuit from damage caused by short circuit. When operated manually there is a chance of fatal accidents occurring to the line-workers such as linemen and occurrence of these accidents are steadily increasing during the electric line repair due to the lack of communication and coordination between the maintenance staff and the electric substation staff [1]. Circuit breakers are an important necessity for an electrical system as they play a vital role in protecting the electrical components. And their malfunctioning can cause damage to the electrical equipment and could result in unstable operating conditions. When doing repair works on electrical lines there is a probability of miscommunication between the linemen and substation workers. This miscommunication could result in an accident and result in the death of the line-workers.

There are many major disadvantages to the existing system of Circuit Breaker operation, for example: During maintenance or repair works, the entire line is turned off which is a major

inconvenience for the consumers, and sometimes, miscommunication between line-workers and substation workers may result in fatal accidents.

So as a solution to this outdated method of operation and to increase the safety of the linemen, we propose a new system of operation which doesn't require manual operation of the Circuit breaker. Here's how our system will work; The Passcode entered by the lineman will be displayed in the LCD display. This passcode will be compared with the password which was received through the GSM module. Our system uses a microcontroller which is embedded in Arduino. If a particular line needs repair or maintenance, the substation workers will send an encrypted password to the lineman and also to the Arduino through the GSM module. The lineman will then enter the received passcode in the keypad present in the panel. This Passcode will be compared with the password in the Arduino. If both these passwords match, the control panel door will be opened. A relay gives the control signal to the panel and the circuit breaker for the required operation. As soon as the repair work is done, lineman should enter the same passcode to switch ON the circuit breaker, and hence the electrical line will be active again. Hence, the

control of the circuit breakers and the ability to access the control panel will be in the hands of linemen and substation workers only[3].

In this proposed method, there are numerous advantages, starting from increase in the safety of Linemen, User friendly operation of main line, the proposed system is easy to install and operate, this method of operation is very Cost-effective, and most importantly it is easy to maintain and repair.

The primary objectives of our system is to decrease the physical work required while switching ON/OFF the CB's, and also to increase the safety of Line-men during maintenance works.

II. METHODOLOGY:

- We referred all the previous researches done in this domain.
- Literature review on Operations of Arduino based protection.
- Searched about a different type of controlling circuit systems, Relays and other components.
- Designed the block diagram
- Designed a Model Circuit with all the components.

III. BLOCK DIAGRAM

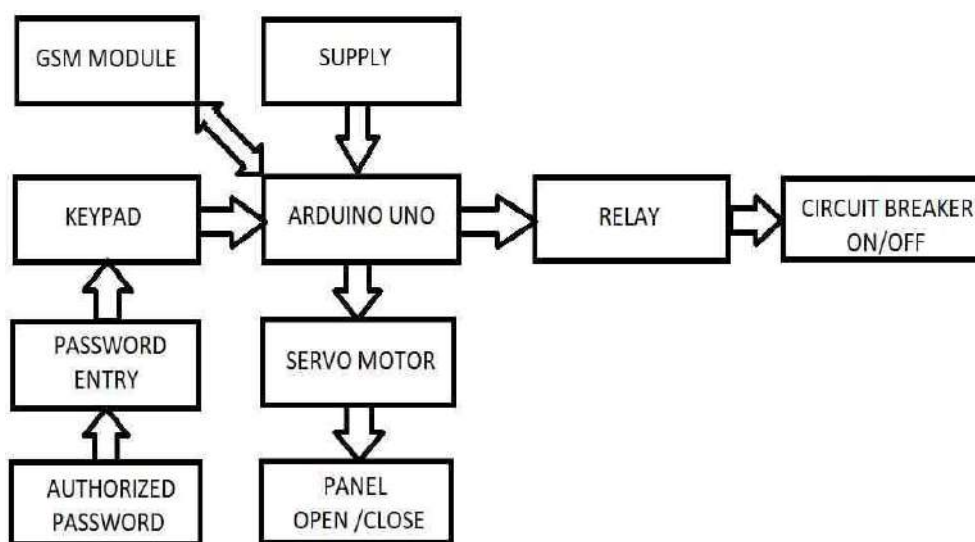


Fig 1

IV. COMPONENTS

- Matrix keypad
- GSM module
- Arduino
- Relay
- LCD
- Servo motor

Component specification

Component Name	Type	Operating Voltage/Current	Quantity
Matrix Keypad	4X4	50mA(max)	1
GSM module	SIM900A	5V	1
Arduino	UNO R3	5V	1
Relay	SPDT	5V	1
LCD	16X2	5V	1
Servomotor	SG90	5V	1
Connecting wires			As required

4.1 Matrix keypad:

The matrix keypad acts as the input device. It has 12(3x3) or 16(4x4) keys in total, which means that it has unique value for each key and hence the password can be entered through this. The entered password or the button clicked will be displayed in the LCD.



Fig 2

4.2 GSM module:

A GSM module is a wireless modem that operates as a wireless network. The key difference between the dial-up modem and GSM modem is that the dial-up modem transmits and receives data through a telephone line cables whereas a wireless modem transmits and receives data through radio waves signal. In order of the radio waves, it requires a SIM card for this to operate. The Global System for Mobile Communication is used for sending and receiving information to the Arduino interfaced with it and to the control room. Generally, it acts as the mobile phone which can communicate with the other mobiles when it is interfaced with the Arduino.



Fig 3

4.3 Arduino ATMEGA 328:

Arduino board comprises of various microprocessors where ATMEGA 328 is the microprocessor used here. It is a low power CMOS which gives highly efficient performance with 8-bit microcontroller based on AVR enhanced RISC architecture. AT stands for ATMEL, MEGA which represents Frequency in Megahertz. Here 328 represents 32Kbyte Flash Memory. It consists of 14 digital pins where it can be act as both input and output in which 6 can be used as PWM outputs. The Arduino can be programmed to do a specific task based on different projects. Simply is acts as the heart of the system.

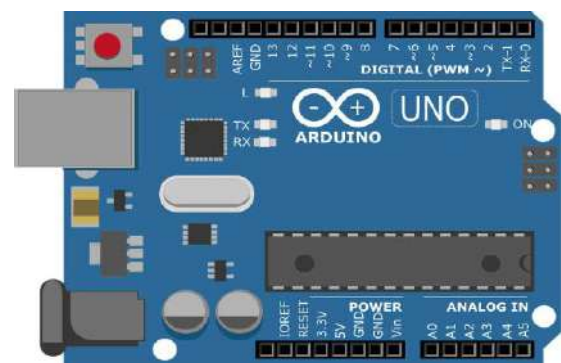


Fig 4

Features

- High-performance.
- Low-power Consumption.
- Fully Static Operation.
- 32Kbytes Flash program memory

4.4 Relay:

A circuit used to switch on and off a light bulb or any other load connected to main supply. It works on the principle of electromagnetic operation where magnetic field is created to operate the lever to control the flow of current in specific direction to turn on/off the load. Here the load given is LED to specify the on/off conditions of relay.



Fig 5

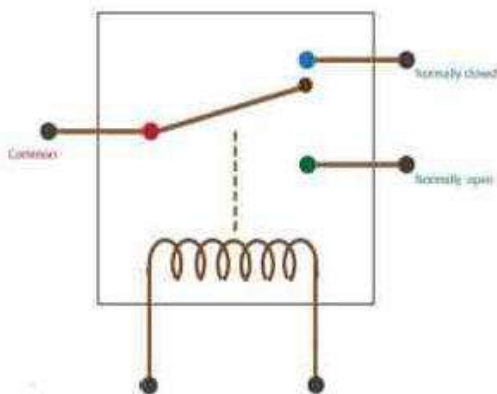


Fig 6

4.6 Servo Motor:

There are different types of motor among which, the servo motor is named for its great precision. Commonly servo motor can rotate with perfect position because it consists of a control circuit that provides feedback on the current position of the motor shaft allows it to rotate with great precision and accuracy.



Fig 8

4.5 LCD:

Liquid crystal display (LCD) is also called as flat panel display which works on the principle of blocking light. It is used for displaying numeric and alphanumeric characters in dot matrix and segmental way. The entered password will be processed by the Arduino and will be displayed by the LCD. It consists of 16 rows and 2 columns to display the numeric and alphanumeric contents



Fig 7

V. CIRCUIT DIAGRAM

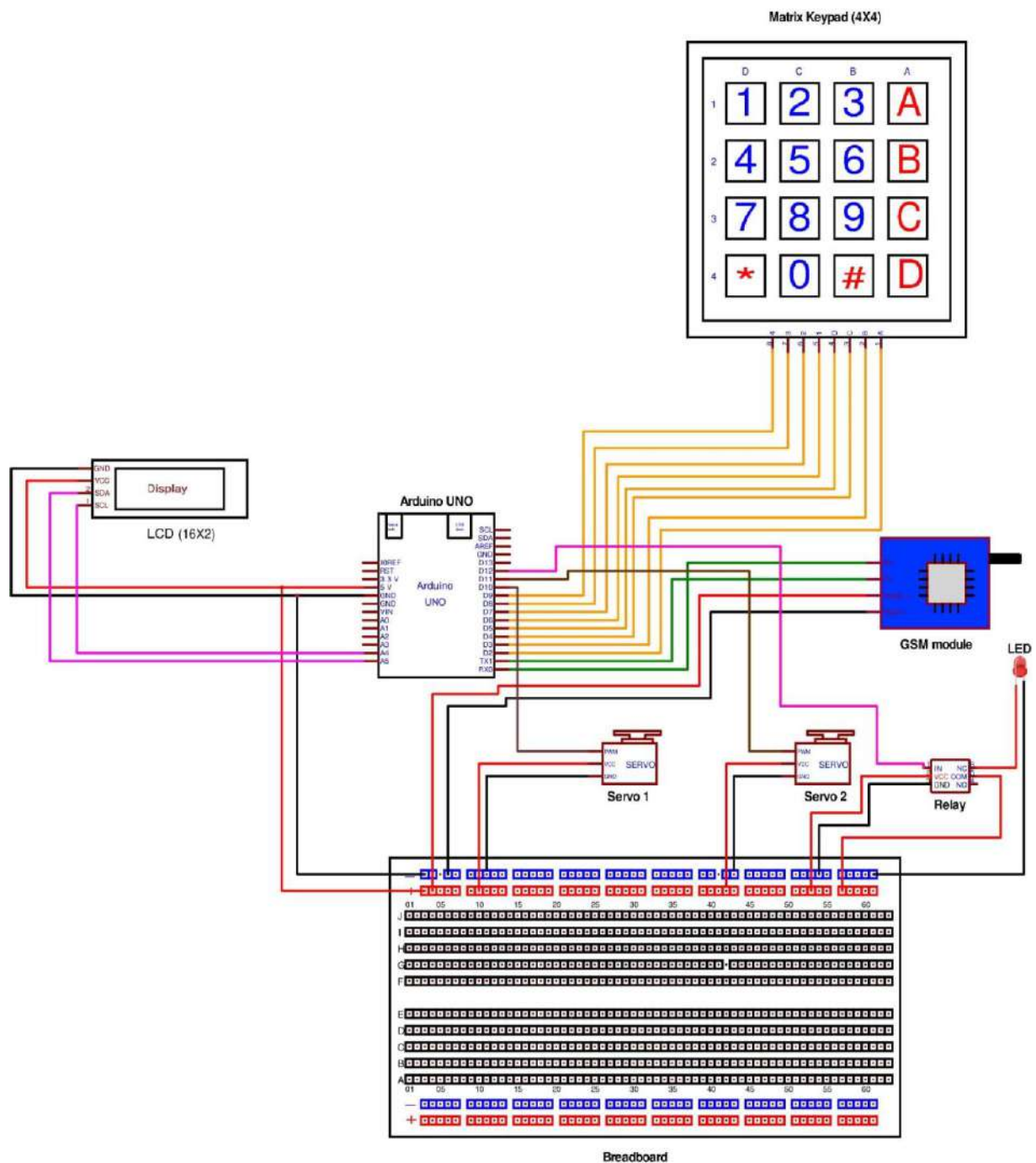


Fig 9

VI. WORKING

1. The secure Password must be sent to the Arduino through GSM module by the substation worker.
2. The Password must be entered in the Matrix Keypad by the lineman.
3. The passcode entered by the lineman is compared with the password given by substation worker.
4. If both the passwords match, the control panel and the relay are opened.
5. If the passwords do not match, "incorrect password" message is displayed.

VII. OUTCOME

- The proposed model will perform switching of CB's with minimal manual work.
- The proposed model will significantly improve safety of Line-men.
- The proposed model will make operation of CB's easy, efficient and encrypted.

VIII. CONCLUSION

This proposed system ensures safety of lineman. As there is no physical contact between the lineman and the line, the life of the lineman is on no risk. It can work immediately once the password is given. The password to operate can be changed simultaneously and system can be operated efficiently with the changed password. No intruder can access the breaker once the password is changed successfully. It gives no option of password hacking and hence effective in providing safety to the working staff. It is cost-effective and can be easily installed.

REFERENCE

- [1]. Abdallah, Fahad EltoumAlebaid, et al. *Password Based Circuit Breaker with GSM Module*. Diss. Sudan University of Science and Technology, 2018.
- [2]. Kumar, Jay, et al. "Password Based Circuit Breaker." *International Journal of Recent ResearchAspects* 1 (2016): 80-88.
- [3]. Nair, Athira P., et al. "Electric Line Man Safety System with OTP Based Circuit Breaker." *IJRET: International Journal of Research in Engineering and Technology eISSN* (2015):2319-1163
- [5]. Raza, MD Wasiq, and Amit Naitam. "ELECTRIC LINEMAN PROTECTION USING USER CHANGEABLE PASSWORD BASED CIRCUIT BREAKER." *International Journal of ResearchInScience & Engineering* 3 (2017).
- [6]. Redekar, Abhijeet, et al. "Electric Lineman Protection Using Keypad AndGsm Based CircuitBreaker." (2018).
- [7]. Manivannan, S., et al. "Design Implementation and Evaluation of Password Protected Circuit Breaker for Reliable Power System Protection and Maintenance." *Advances in Materials Research*. Springer, Singapore, 2021. 933-942
- [8]. Antony, Santhi Mary A., and D. Ramya. "Password Based Circuit Breaker Using GSM Modem." *RESEARCH JOURNAL OF PHARMACEUTICAL BIOLOGICAL AND CHEMICAL SCIENCES* 8.2 (2017): 1472-1477.
- [9]. P.A.Y. Prabhakar, P.S.K. Oza, N.Shrivastava&P.Srivastava. "Password Based Door Lock System", *Int. Journal of Science and Technology*. Pp. 1154-1157, 2013
- [10]. M.G. Hudedmani, N.Ummannavar, M.D.Mudaliyar, C. Sooji, &M.Bogar. "Password Based Distribution Panel and Circuit Breaker Operation for the safety of Linemen during Maintenance Work," *Adv. J. Grad. Res.*, vol.1, no.1, pp. 35-39, 2017
- [11]. Sebin J Olickal, "Electric line man safety system with one time password-based circuit breaker"
- [12]. IJRET, vol. 04 Special Issue: 03 Apr-2015
- [13]. Narendra Khandelwal, TanujManglani, Ganpat Singh, Amit Kumar, Dilip Khatri, "Automated load distribution with password protected circuit breakers" *International Journal of Recent Research and Review*, vol. VIII, Issue 1, March 2015.
- [14]. [12]K.B.V.S.R.Subrahmanyam, "Electric lineman protection using user changeable password based circuit breaker" *IJCESR*, vol. 2, ISSUE-5, 2015.
- [15]. Michael faxa, "Application of disconnecting circuit breakers, p.11" Retrieved 9 July 2012.
- [16]. Viral P. Solanki, Ajit J. Parmar, Nikul S. Limbachiya, Rakesh Koringa, and Shivangi Patel, "Arduino Based Protection System for Wireman," *Int. J. Electr. Electron. Res.*, vol. 3, no. 1, pp. 76– 79,2015.
- [17]. GAUTAMYASH PAL; "password-based circuit breaker with gsm module", *international journal of advance research, ideas and innovations in technologydr. A.p.jabdul kalamuniversity*, issn 2454-132x ,2017
- [18]. MR. TARUN NARUKA and others, "password-based circuit breaker", *imperial journal of interdisciplinary research ijr*, issn 2454-1362, vol-3, issue-4, 2017.

Password based circuit breaker operation for the safety of lineman during maintenance work

- Sakthi Raja V, Rakesh K.K, Pravin kumar N, Saravanan S,
Dr.M.V.Suganyadevi

Department of Electrical and Electronics Engineering, Saranathan College of Engineering, Trichy

ABSTRACT

Nowadays, accidental death of lineman is a commonly occurring tragedy. so, it is compulsory for us to guarantee the safety of linemen by adapting a new method of operation. A new system should be adapted to regulate and manage the control panel which consists of all the electrical components and circuit breakers. These accidents are on the rise throughout the country, main reason being miscommunication between the maintenance workers and sub-station workers. The planned system gives a solution for this problem and reduces the risk for linemen. The control to activating/ deactivating the control panel is in the hands of the linemen only. In this new method of operation, a "Passcode or Password" is needed to access the control panel and further to operate the circuit breaker (ON/OFF). An encrypted Passcode/Password is sent from the substation to the circuit breaker operators (linemen), for the purpose of executing maintenance works. The password is registered and forwarded to the lineman's mobile and also to the management panel by the help of GSM module. The received passcode/password is typed in through the matrix keyboard which acts as the input device and also it is interfaced to the microcontroller present inside the panel. The password entered by the lineman is compared with the encrypted passcode received from the substation through the GSM module. Only when both the passwords match, the lineman will be able to access the control panel and to operate the circuit breaker, so he can proceed to do the repair works and maintenance works. If any third party enters a wrong password, he/she will not be able to access or operate the control panel and hence the system will be completely secured.

Keywords: Security, lineman, password, control panel

Date of Submission: 21-04-2021

Date of Acceptance: 06-05-2021

I. INTRODUCTION

In present times, casualties of line-workers due to accidents occurring during maintenance works is on the rise. Until now, to execute maintenance works, Line clearance method is used to shut down the electrical line in which the work is to be done. There are lots of short-comings to this method, like accidental charging of the line due to mistake of the operators at station, which can lead to serious injuries, and in some unfortunate cases, even deaths of line-workers. The employment of microcontrollers can be a solution to this issue. The employment of communication networks will increase the potency of the pilotless devices. This new method with the help of GSM module, reduces the risk of physical contact with the high voltage electrical lines, and enables us to control the circuit breakers automatically. so, we decided to implement GSM based circuit to control the operation of the electrical lines.

A circuit breaker is a protective device which acts as a switch designed to safeguard an

electrical circuit from damage caused by short circuit. When operated manually there is a chance of fatal accidents occurring to the line-workers such as linemen and occurrence of these accidents are steadily increasing during the electric line repair due to the lack of communication and coordination between the maintenance staff and the electric substation staff [1]. Circuit breakers are an important necessity for an electrical system as they play a vital role in protecting the electrical components. And their malfunctioning can cause damage to the electrical equipment and could result in unstable operating conditions. When doing repair works on electrical lines there is a probability of miscommunication between the linemen and substation workers. This miscommunication could result in an accident and result in the death of the line-workers.

There are many major disadvantages to the existing system of Circuit Breaker operation, for example: During maintenance or repair works, the entire line is turned off which is a major

inconvenience for the consumers, and sometimes, miscommunication between line-workers and substation workers may result in fatal accidents.

So as a solution to this outdated method of operation and to increase the safety of the linemen, we propose a new system of operation which doesn't require manual operation of the Circuit breaker. Here's how our system will work; The Passcode entered by the lineman will be displayed in the LCD display. This passcode will be compared with the password which was received through the GSM module. Our system uses a microcontroller which is embedded in Arduino. If a particular line needs repair or maintenance, the substation workers will send an encrypted password to the lineman and also to the Arduino through the GSM module. The lineman will then enter the received passcode in the keypad present in the panel. This Passcode will be compared with the password in the Arduino. If both these passwords match, the control panel door will be opened. A relay gives the control signal to the panel and the circuit breaker for the required operation. As soon as the repair work is done, lineman should enter the same passcode to switch ON the circuit breaker, and hence the electrical line will be active again. Hence, the

control of the circuit breakers and the ability to access the control panel will be in the hands of linemen and substation workers only[3].

In this proposed method, there are numerous advantages, starting from increase in the safety of Linemen, User friendly operation of main line, the proposed system is easy to install and operate, this method of operation is very Cost-effective, and most importantly it is easy to maintain and repair.

The primary objectives of our system is to decrease the physical work required while switching ON/OFF the CB's, and also to increase the safety of Line-men during maintenance works.

II. METHODOLOGY:

- We referred all the previous researches done in this domain.
- Literature review on Operations of Arduino based protection.
- Searched about a different type of controlling circuit systems, Relays and other components.
- Designed the block diagram
- Designed a Model Circuit with all the components.

III. BLOCK DIAGRAM

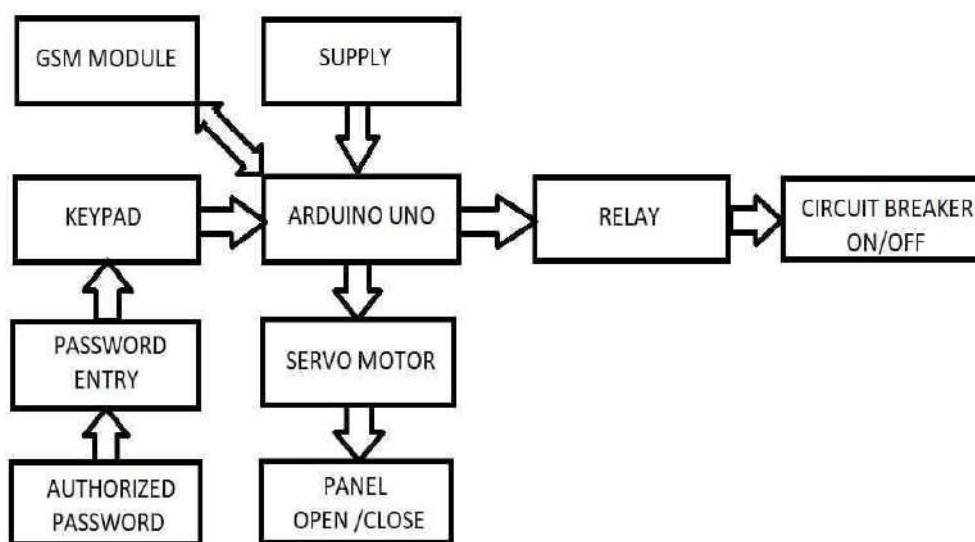


Fig 1

IV. COMPONENTS

- Matrix keypad
- GSM module
- Arduino
- Relay
- LCD
- Servo motor

Component specification

Component Name	Type	Operating Voltage/Current	Quantity
Matrix Keypad	4X4	50mA(max)	1
GSM module	SIM900A	5V	1
Arduino	UNO R3	5V	1
Relay	SPDT	5V	1
LCD	16X2	5V	1
Servomotor	SG90	5V	1
Connecting wires			As required

4.1 Matrix keypad:

The matrix keypad acts as the input device. It has 12(3x3) or 16(4x4) keys in total, which means that it has unique value for each key and hence the password can be entered through this. The entered password or the button clicked will be displayed in the LCD.



Fig 2

4.2 GSM module:

A GSM module is a wireless modem that operates as a wireless network. The key difference between the dial-up modem and GSM modem is that the dial-up modem transmits and receives data through a telephone line cables whereas a wireless modem transmits and receives data through radio waves signal. In order of the radio waves, it requires a SIM card for this to operate. The Global System for Mobile Communication is used for sending and receiving information to the Arduino interfaced with it and to the control room. Generally, it acts as the mobile phone which can communicate with the other mobiles when it is interfaced with the Arduino.



Fig 3

4.3 Arduino ATMEGA 328:

Arduino board comprises of various microprocessors where ATMEGA 328 is the microprocessor used here. It is a low power CMOS which gives highly efficient performance with 8-bit microcontroller based on AVR enhanced RISC architecture. AT stands for ATMEL, MEGA which represents Frequency in Megahertz. Here 328 represents 32Kbyte Flash Memory. It consists of 14 digital pins where it can be act as both input and output in which 6 can be used as PWM outputs. The Arduino can be programmed to do a specific task based on different projects. Simply is acts as the heart of the system.

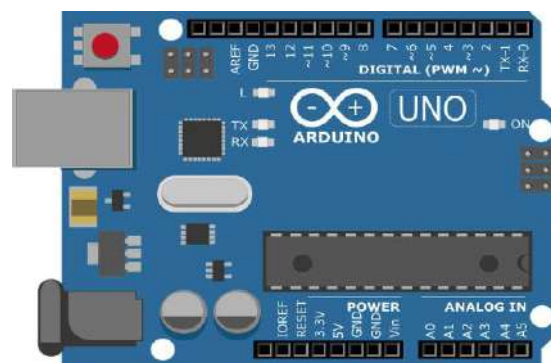


Fig 4

Features

- High-performance.
- Low-power Consumption.
- Fully Static Operation.
- 32Kbytes Flash program memory

4.4 Relay:

A circuit used to switch on and off a light bulb or any other load connected to main supply. It works on the principle of electromagnetic operation where magnetic field is created to operate the lever to control the flow of current in specific direction to turn on/off the load. Here the load given is LED to specify the on/off conditions of relay.



Fig 5

4.6 Servo Motor:

There are different types of motor among which, the servo motor is named for its great precision. Commonly servo motor can rotate with perfect position because it consists of a control circuit that provides feedback on the current position of the motor shaft allows it to rotate with great precision and accuracy.



Fig 8

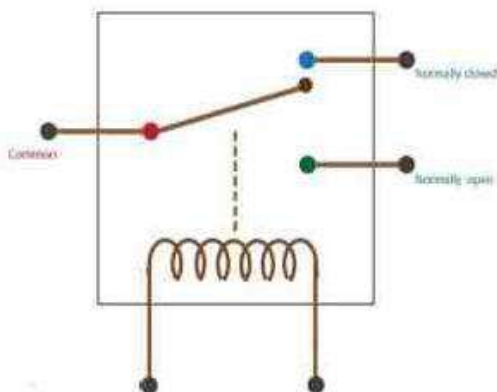


Fig 6

4.5 LCD:

Liquid crystal display(LCD) is also called as flat panel display which works on the principle of blocking light. It is used for displaying numeric and alphanumeric characters in dot matrix and segmental way. The entered password will be processed by the Arduino and will displayed by the LCD. It consists of 16 rows and 2 columns to display the numeric and alphanumeric contents

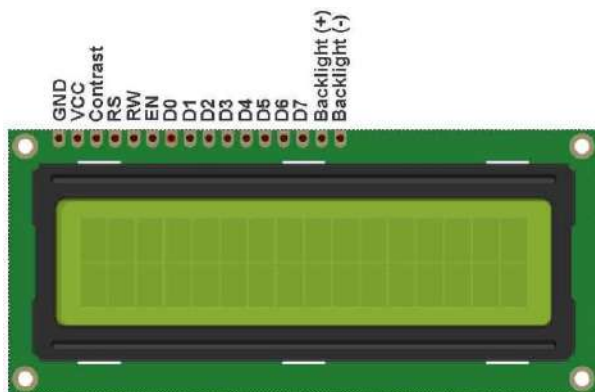


Fig 7

V. CIRCUIT DIAGRAM

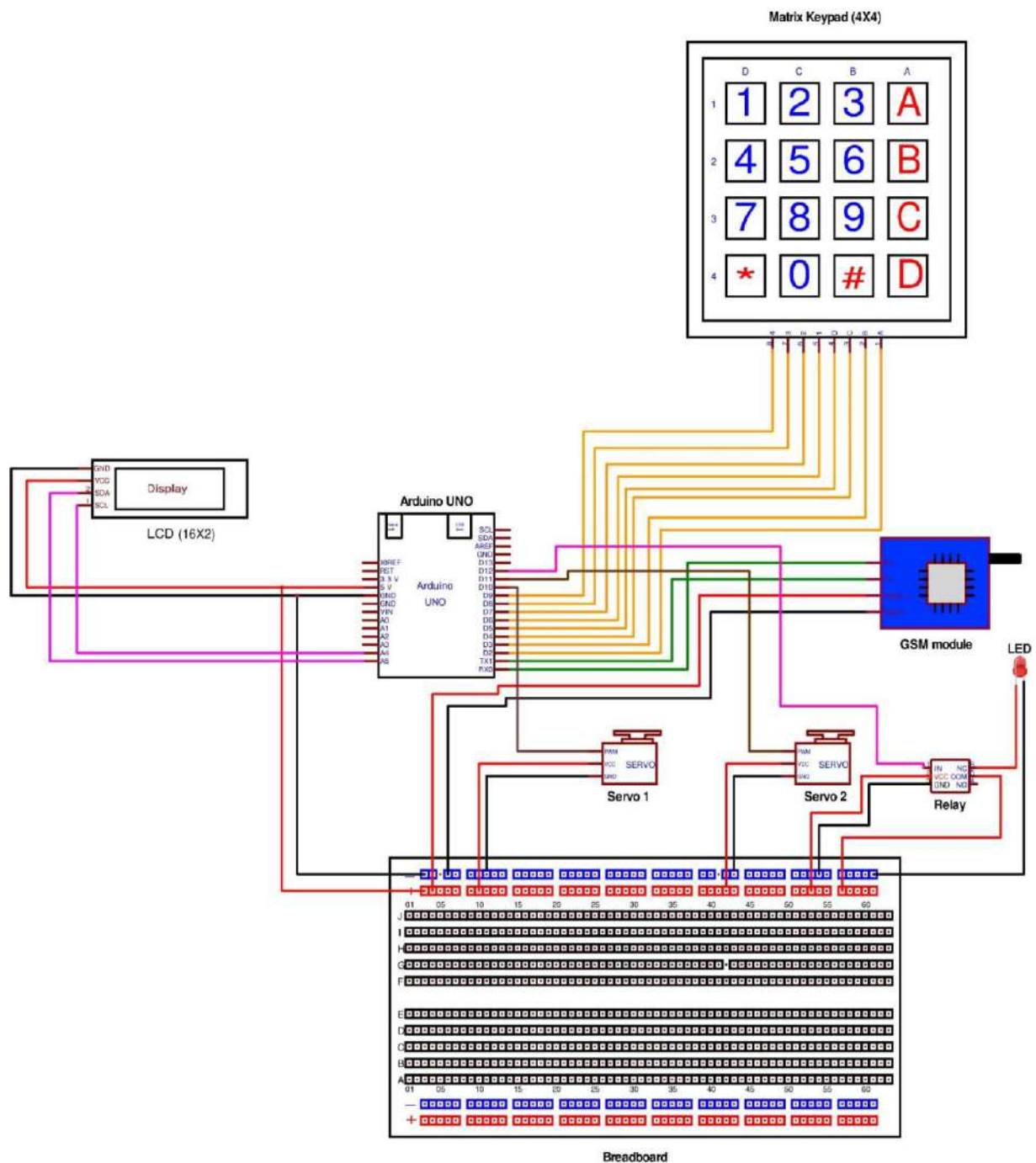


Fig 9

VI. WORKING

1. The secure Password must be sent to the Arduino through GSM module by the substation worker.
2. The Password must be entered in the Matrix Keypad by the lineman.
3. The passcode entered by the lineman is compared with the password given by substation worker.
4. If both the passwords match, the control panel and the relay are opened.
5. If the passwords do not match, "incorrect password" message is displayed.

VII. OUTCOME

- The proposed model will perform switching of CB's with minimal manual work.
- The proposed model will significantly improve safety of Line-men.
- The proposed model will make operation of CB's easy, efficient and encrypted.

VIII. CONCLUSION

This proposed system ensures safety of lineman. As there is no physical contact between the lineman and the line, the life of the lineman is on no risk. It can work immediately once the password is given. The password to operate can be changed simultaneously and system can be operated efficiently with the changed password. No intruder can access the breaker once the password is changed successfully. It gives no option of password hacking and hence effective in providing safety to the working staff. It is cost-effective and can be easily installed.

REFERENCE

- [1]. Abdallah, Fahad EltoumAlebaid, et al. *Password Based Circuit Breaker with GSM Module*. Diss. Sudan University of Science and Technology, 2018.
- [2]. Kumar, Jay, et al. "Password Based Circuit Breaker." *International Journal of Recent ResearchAspects* 1 (2016): 80-88.
- [3]. Nair, Athira P., et al. "Electric Line Man Safety System with OTP Based Circuit Breaker." *IJRET: International Journal of Research in Engineering and Technology eISSN* (2015):2319-1163
- [5]. Raza, MD Wasiq, and Amit Naitam. "ELECTRIC LINEMAN PROTECTION USING USER CHANGEABLE PASSWORD BASED CIRCUIT BREAKER." *International Journal of ResearchInScience & Engineering* 3 (2017).
- [6]. Redekar, Abhijeet, et al. "Electric Lineman Protection Using Keypad AndGsm Based CircuitBreaker." (2018).
- [7]. Manivannan, S., et al. "Design Implementation and Evaluation of Password Protected Circuit Breaker for Reliable Power System Protection and Maintenance." *Advances in Materials Research*. Springer, Singapore, 2021. 933-942
- [8]. Antony, Santhi Mary A., and D. Ramya. "Password Based Circuit Breaker Using GSM Modem." *RESEARCH JOURNAL OF PHARMACEUTICAL BIOLOGICAL AND CHEMICAL SCIENCES* 8.2 (2017): 1472-1477.
- [9]. P.A.Y. Prabhakar, P.S.K. Oza, N.Shrivastava&P.Srivastava. "Password Based Door Lock System", *Int. Journal of Science and Technology*. Pp. 1154-1157, 2013
- [10]. M.G. Hudedmani, N.Ummannavar, M.D.Mudaliyar, C. Sooji, &M.Bogar. "Password Based Distribution Panel and Circuit Breaker Operation for the safety of Linemen during Maintenance Work," *Adv. J. Grad. Res.*, vol.1, no.1, pp. 35-39, 2017
- [11]. Sebin J Olickal, "Electric line man safety system with one time password-based circuit breaker"
- [12]. IJRET, vol. 04 Special Issue: 03 Apr-2015
- [13]. Narendra Khandelwal, TanujManglani, Ganpat Singh, Amit Kumar, Dilip Khatri, "Automated load distribution with password protected circuit breakers" *International Journal of Recent Research and Review*, vol. VIII, Issue 1, March 2015.
- [14]. [12]K.B.V.S.R.Subrahmanyam, "Electric lineman protection using user changeable password based circuit breaker" *IJCESR*, vol. 2, ISSUE-5, 2015.
- [15]. Michael faxa, "Application of disconnecting circuit breakers, p.11" Retrieved 9 July 2012.
- [16]. Viral P. Solanki, Ajit J. Parmar, Nikul S. Limbachiya, Rakesh Koringa, and Shivangi Patel, "Arduino Based Protection System for Wireman," *Int. J. Electr. Electron. Res.*, vol. 3, no. 1, pp. 76– 79,2015.
- [17]. GAUTAMYASH PAL; "password-based circuit breaker with gsm module", *international journal of advance research, ideas and innovations in technologydr. A.p.jabdul kalamuniversity*, issn 2454-132x ,2017
- [18]. MR. TARUN NARUKA and others, "password-based circuit breaker", *imperial journal of interdisciplinary research ijr*, issn 2454-1362, vol-3, issue-4, 2017.

A Novel IUPQC for Multi-Feeder Systems Using Multilevel Converters With Grid Integration of Hybrid Renewable Energy System

NOORUL AMEEN S, PASHITH H, PRAHATHISH B, VAIKUNTH B, DR. M.V.SUGANYADEVI

Saranathan College of Engineering, Trichy

ABSTRACT:

Multi-Microgrid (MMG) is a combination of two or more microgrids (MGs), based on renewable energy sources, integrated at a common point of coupling. However, due to the fluctuating resources and also with different variable loads, it is difficult to maintain a balance between sources and loads, which consequently leads to power quality problems such as voltage and current distortions. In this regard, a novel multi-function device like Interline Unified Power Quality Conditioner (IUPQC) is proposed to mitigate these power quality issues. IUPQC consists of series and shunt active power filter (APF) linked through a common DC link capacitor. However, unlike Unified Power Quality Conditioner (UPQC), in IUPQC, the APFs are individually connected to two independent distribution feeders. The shunt APF mitigates current imperfections of feeder 1 and regulates the DC voltage of the DC link capacitor whereas the series APF mitigates voltage imperfections of feeder. This paper presents the incorporation of IUPQC between two MGs (feeders) in MMG, and design of its controller to compensate and minimize the voltage and current harmonics due to the source and load disturbances

Keywords: Power Factor, Power quality Conditioner, Capacitors

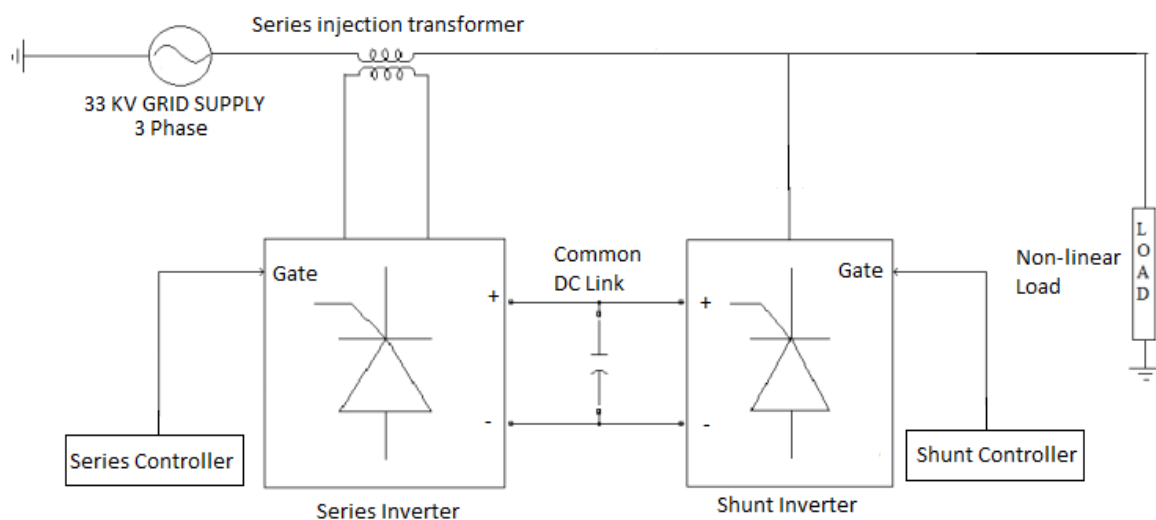
INTRODUCTION

The energy is neither be created nor destroyed but it can be converted from one form to another. The generation of an electrical energy is nothing but the conversion of various other forms of energy into an electrical energy. The electrical power is generated in bulk at the generating stations which are also called power stations. The generated electrical energy is demanded by the consumers. This causes due to power losses and power quality problems in the transmission lines FACTS device is introduced to reduce such problems. Microgrid leads to effective distribution in rural area all distribution includes effective power processor to control and monitor the power exchange between the grid. When such processor get fully exploited it leads to high power quality problems and power consumption by developing narrow band communication and local control algorithm full microgrid is exploited with marginal investment. This study deals with experimental verification of inter line Power Flow Controller. Interline Power Flow Controller (IPFC) is a Concept of Flexible AC Transmission System (FACTS) controller with the unique capability for series compensation with the unique capability of power flow management among multi-line of a substation. In low-voltage residential micro-grids, where number and type of DERs and loads is unpredictable and may vary during daytime, cooperative operation can be achieved by simple cross-communication among neighbor EPPs, without centralized supervisor or additional control units. During disturbances, the generation and corresponding loads can separate from the distribution system to isolate the microgrid's load from the disturbance (providing UPS services) without harming the transmission grid's integrity. The system also shows the possibility to achieve auxiliary functions such as voltage unbalance correction and harmonic current compensation. The DGs are properly controlled to autonomously compensate for voltage unbalance while sharing the compensation effort and also active and reactive powers. The control system of the DGs mainly consists of active and reactive power droop controllers, a virtual impedance loop,

voltage and current controllers, and an unbalance compensator. A special task force of the IEEE PES Renewable Technologies Subcommittee is a review of hybrid renewable/alternative energy (RE/AE) power generation systems focusing on energy sustainability. The major among them are the discontinuity and variation in power, high generation cost, complex-design of generation and control-schemes. So, in order to meet the world-wide increasing demand of renewable energy conversion systems, an urgent need of some sustainable source or scheme for continuous and constant power generation at low cost is deeply observed. To solve the condition of unstable power, a hybrid backup supply system is proposed in this work. Interfacing the DC microgrid with current-fed full-bridge isolated DC-DC converter, the fuel cell can provide stable backup power for the grid. Most of the research on Hybrid Power Systems (HPS) is to provide an economical and sustainable power to the rural electrification. This paper focuses on the design of an HPS for the building which is a part of the urban electrification. The concept of a capacitor-less static synchronous compensator (STATCOM) that uses a matrix converter (MC) and model predictive control (MPC) to compensate lagging power factor (p.f.) loads using inductors instead of electrolytic capacitors (e-caps) for energy storage. Distribution Static Compensator (DSTATCOM) is proposed for load compensation using photovoltaic (PV) array and Permanent Magnet Synchronous Generator (PMSG) based wind turbine for dc generation; forming hybrid renewable energy sources based dc-link voltage source inverter (VSI).

The objective is to increase the electrical power which is affected by harmonic contamination, non linear load, voltage and current flickering due to arc and to increase the TSD Total Harmonic Distordation in Power System for Literature review on the Power factor correction and Total harmonic Distordation. We referred all the previous research done in the domain designed the block diagram and simulated the block diagram with references values

BLOCK DIAGRAM:



Grid Supply: An electrical grid, electric grid or power grid, is an interconnected network for delivering electricity from producers to consumers

Series Injection Transformer: This type of transformer without secondary is for injecting a variable voltage into a current loop formed by the cable and accessories under test. It can be designed with opening frame to facilitate the installation of the secondary cable.

Shunt Inverter: It compensates current harmonics by injecting equal-but-opposite harmonic compensating current. It operates as a current source injecting the harmonic components generated by the load but phase shifted by 180deg

Series Inverter: It acts as a controlled voltage source and can compensate all voltage-related problems such as voltage harmonics, voltage sags & swells, voltage flicker etc.

DC Link: The DC that is fed into the inverter is called the DC link. As the name implies, the two sources are linked together with a filter capacitor

Series Controller : It controls the series inverter which has inverter and controller in series connection

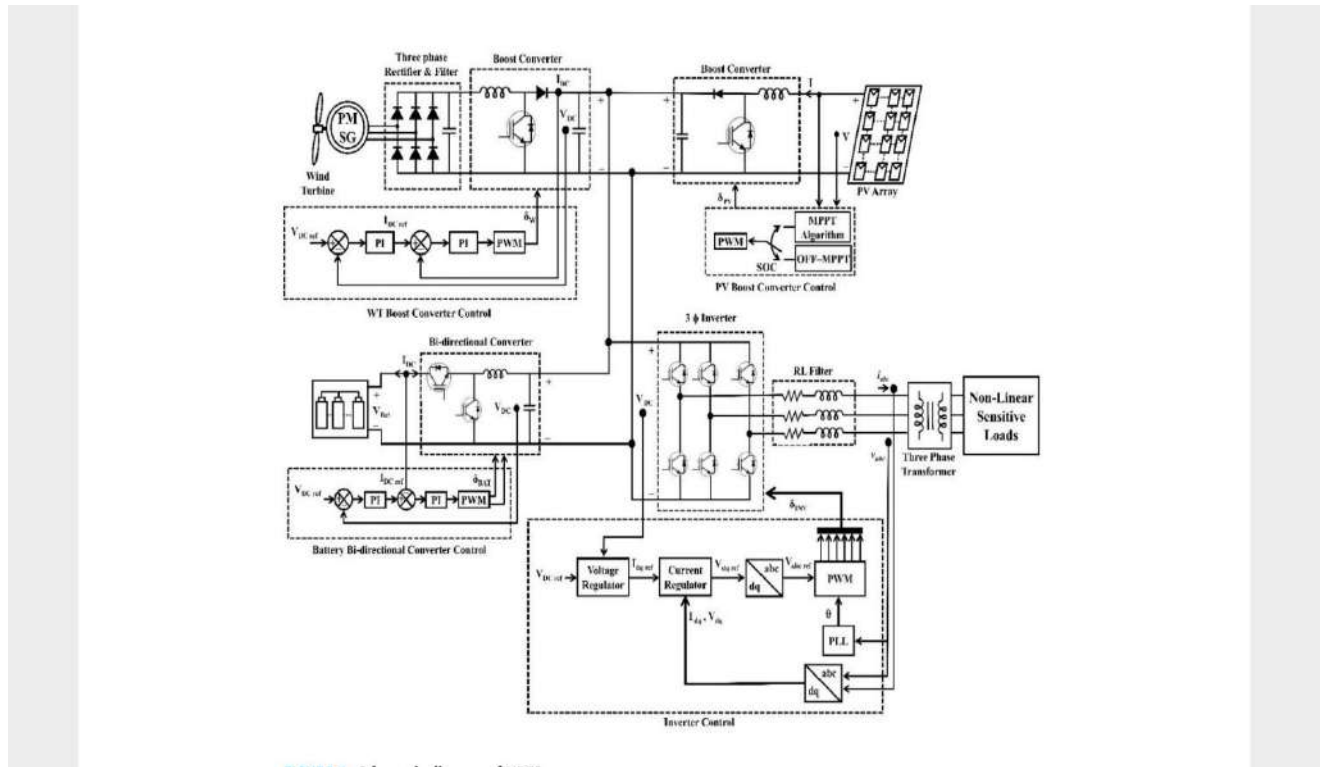
Shunt Controller : It controls the Shunt inverter which has inverter and controller in parallel connection

Load: It draws in currents in abrupt short pulses.

COMPONENTS SPECIFICATION:

DESCRIPTION	QUNATITY
PV array (300KW)	1
Wind Turbine	1
Battery	1
RL filter	1
Voltage Regulator (400W)	1
Current Regulator (300W)	1
Connecting wires	1
Wires	1

CIRCUIT DIAGRAM:

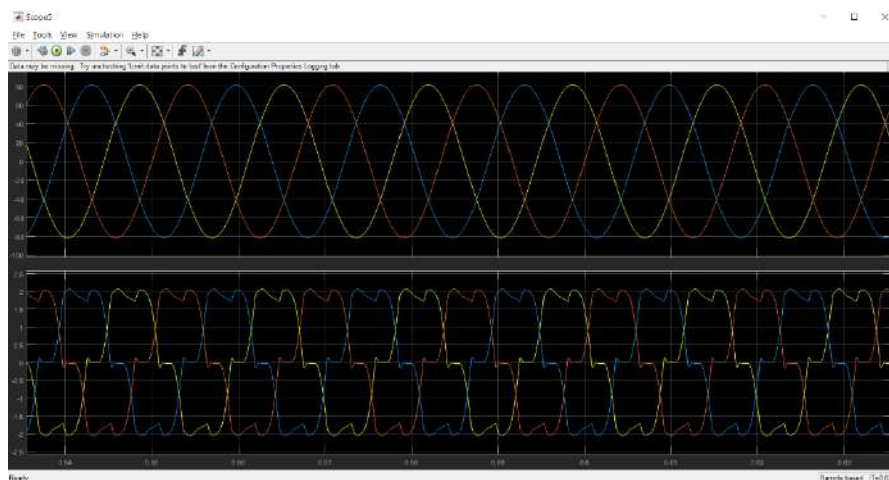


OPERATION:

The Unified Power Quality Conditioner (UPQC) combines the Shunt Active Power Filter with the Series Active Power Filter, sharing the same DC Link, in order to compensate both voltages and currents, so that the load voltages become sinusoidal and at nominal value, and the source currents become sinusoidal and in phase with the source voltage

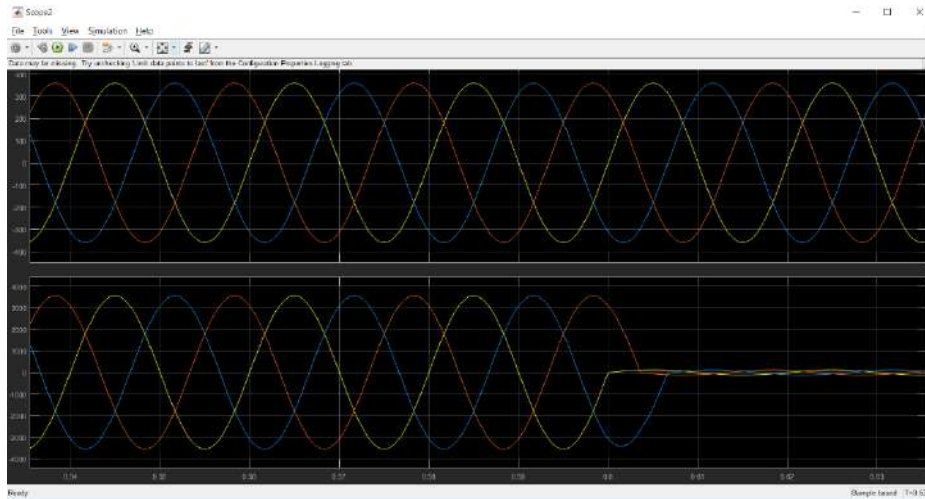
SIMULATION RESULT:

1. Voltage and current



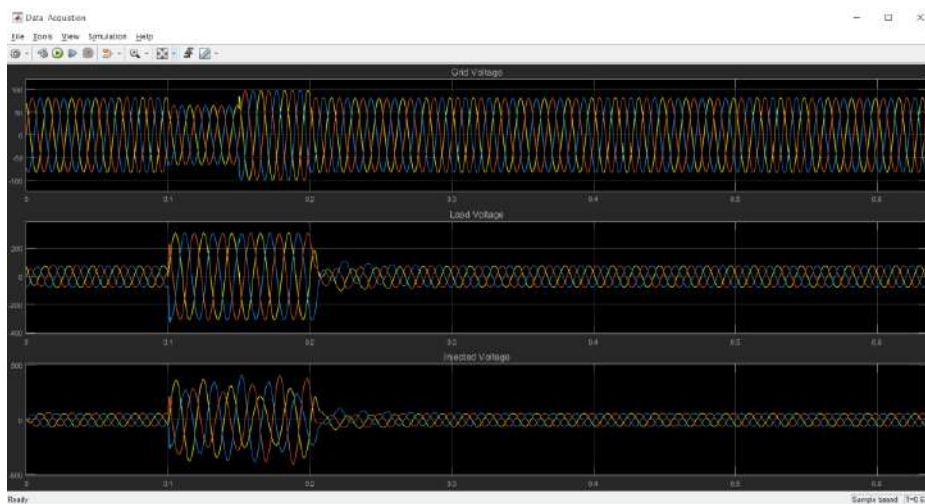
The above diagram represents the voltage and the current are in 180 deg respective with each other and there is no harmonic distortion

2. Wind system voltage and current



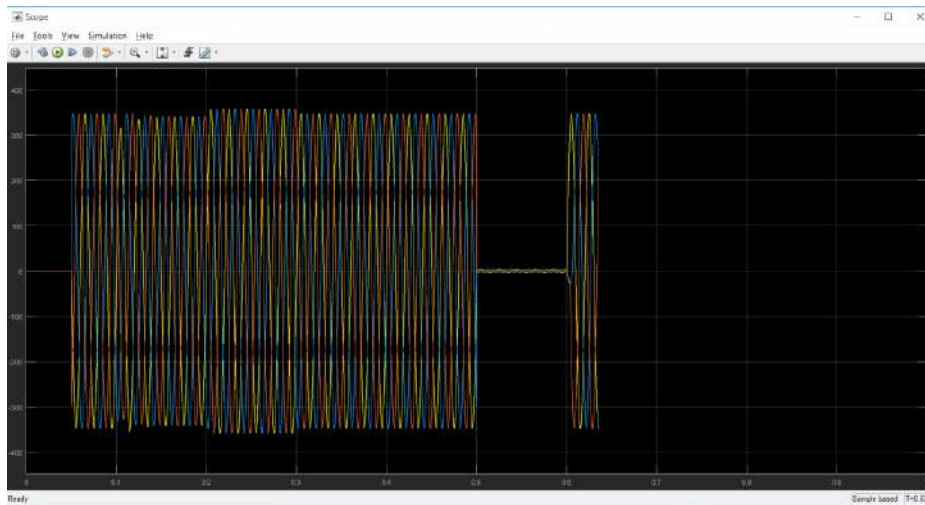
The above diagram represents the output wave form of wind system

3. Sag and swell condition



The above diagram represents the Sag and swell condition in the grid voltage which occurs due to non linear load for the time period 0.1 to 0.5 secs and 0.1 to 0.2 secs

4. Fault voltage and current condition



The above diagram represents the Sag and swell condition occurred in the grid voltage is rectified by IUPQC Interlined Unified Power Quality Conditioner and hence the output voltage is rectified from 0.1 to 0.2 secs

CONCLUSION:

In the simulation study, MATLAB Simulink environment is used to simulate the model of IPQC connected to a 3 phase system. The modeling of IPQC and analysis of power systems embedded with IPQC has been presented, which is capable of solving large power networks very reliably with the IPQC. The investigations related to the variation of control parameters and performance of the IPQC on power quality results are carried out. Simulation results show the effectiveness of IPQC to reduce the harmonics. IPQC system is proposed to reduce the power quality problem arising in multiline. Subsystems along with IPQC and measurement block are carried out. Voltage unbalances in multiline also reduced by means of measurement block.

REFERENCE:

1. A. Toward, P. Conditioners, and S. E. Savings, "High-performance MCUs Boost the Efficiency of Photovoltaic Power Generators and Power Conditioners," 2010.
2. A. Mokhtarpour, M. Bathae, and H. A. Shayanfar, "Power Quality Compensation in Smart Grids with a Single Phase UPQC-DG."
3. M. Malla, N. Pradhan, N. B. Araya, T. A. Adamu, A. Petterteig, S. Scientist, J. Are, W. Suul, and T. M. Undeland, "Power Quality Control in Smart Distribution Grids using Power Electronic Converters Power Electronics for Renewable Energy."
4. M. M. a. Chaudhari, "Three-phase Series Active Power Filter as Power Quality Conditioner," 2012 IEEE Int. Conf. Power Electron. Drives Energy Syst., pp. 1–6, Dec. 2012.
5. G. J. S. M. Sandeep and S. Rasoolahammed, "Importance of Active Filters for Improvement of Power Quality," vol. 4, 2013.
6. "Improving power quality in microgrid by means of using power quality conditioner Devices", 2014

7. G. Irusapparajan and S. Rama Reddy “Experimental Results of Interline Power Flow Controller Systems| Research Journal of Applied Sciences”, Engineering and Technology 3(7): 612-616, 2011
8. Paolo Tenti, Alessandro Costabeber, Paolo Mattavelli, and Daniela Trombetti “Distribution Loss Minimization by Token Ring Control of Power Electronic Interfaces in Residential Microgrids”, IEEE transactions on industrial electronics, vol. 59, no. 10, october 2012
9. Robert H. Lasseter, Paolo Piagi University of Wisconsin-Madison “Microgrid: A Conceptual Solution”, PESC’04 Aachen, Germany 20-25 June 2004
10. Fei Wang, Jorge L. Duarte, and Marcel A. M. Hendrix, “Grid-Interfacing Converter Systems With Enhanced Voltage Quality for Microgrid Application—Concept and Implementation”, IEEE transactions on power electronics, vol. 26, no. 12, december 2011
11. Mehdi Savaghebi, Alireza Jalilian, Juan C. Vasquez and Josep M. Guerrero, “Autonomous Voltage Unbalance Compensation in an Islanded Droop Controlled Microgrid” IEEE transactions on industrial electronics, vol. 60, no. 4, april 2013

A Simplified Beginner's Guidelines for Design and Fabrication of Prototype Electrical Vehicle

Proceedings of International Conference on Power Electronics and Renewable Energy Systems pp 271-281 | Cite as

- P. Ramesh Babu (1)
- P. Vigneshwar (1)
- R. Udaya Simha (1)
- S. Tanweer Ahamed (1)
- S. Vengatesh (1)
- V. Vijay (1)

1. Saranathan College of Engineering, , Trichy, India

Conference paper

First Online: 22 November 2021

- 75 Downloads

Part of the [Lecture Notes in Electrical Engineering](#) book series (LNEE, volume 795)

Abstract

The aim of this paper is to build a prototype electric vehicle out of structural materials. It is influential in the development of a modern, safe, and environmentally sustainable mode of public mobility. The objective of its design is to create a lightweight, compact three-wheeled electric vehicle frame. The design phase entails the creation of a 3D model, a practical prototype, and frame refinement using CAD software and the material parameters. The electrical and mechanical study is performed, the results recorded 125 km per charge, and the weight of the vehicle is 180 kg. The top speed is 40kmph along with >80% efficiency of the BLDC hub motor.

Keywords

Electric vehicle Lithium-ion battery BLDC hub motor Suspension Steering
This is a preview of subscription content, [log in](#) to check access.

Notes

Acknowledgements

The authors would like to express their gratitude to the National Solar Vehicle Challenge (NSVC) and the Saur Urja Vehicle Challenge (SUVVC) for validating our prototype electric vehicle through competition in India. And we'd like to thank our college for supporting us to work in various aspects, as well as fabricate the completed prototype vehicle.

- 2nd Runner-up in NATIONAL SOLAR VEHICLE CHALLENGE 2019
- Runner-up in SAUR URJA VEHICLE CHALLENGE 2020.

References

1. Nabil T, El-Naghi BE, Saeed M, Kamal A, Gharib E, Mohsen M, Ahmed I (2019) Design and fabrication of prototype battery electric three wheeled vehicles. *J Asian Electr Veh* 17(2):1823–1834
CrossRef (<https://doi.org/10.4130/jaev.17.1823>)
Google Scholar (http://scholar.google.com/scholar_lookup?title=Design%20and%20fabrication%20of%20prototype%20battery%20electric%20three%20wheeled%20vehicles&author=T.%20Nabil&author=BE.%20El-Naghi&author=M.%20Saeed&author=A.%20Kamal&author=E.%20Gharib&author=M.%20Mohsen&author=I.%20Ahmed&journal=J%20Asian%20Electr%20Veh&volume=17&issue=2&pages=1823-1834&publication_year=2019)
2. Casalino G, Moradi M, Moghadam MK, Khorram A, Perulli P (2019) Experimental and numerical study of AISI 4130 steel surface hardening by pulsed Nd: YAG laser. *Materials* 12(19):3136
CrossRef (<https://doi.org/10.3390/ma12193136>)
Google Scholar (http://scholar.google.com/scholar_lookup?title=Experimental%20and%20numerical%20study%20of%20AISI%204130%20steel%20surface%20hardening%20by%20pulsed%20Nd%3A%20YAG%20laser&author=G.%20Casalino&author=M.%20Moradi&author=MK.%20Moghadam&author=A.%20Khorram&author=P.%20Perulli&journal=Materials&volume=12&issue=19&pages=3136&publication_year=2019)
3. Wilhelm E, Bornatico R, Widmer R, Rodgers L, Soh GS (2012) Electric vehicle parameter identification. *World Electr Veh J* 5(4):1090–1099
CrossRef (<https://doi.org/10.3390/wevj5041090>)
Google Scholar (http://scholar.google.com/scholar_lookup?title=Electric%20vehicle%20parameter%20identification&author=E.%20Wilhelm&author=R.%20Bornatico&author=R.%20Widmer&author=L.%20Rodgers&author=GS.%20Soh&journal=World%20Electr%20Veh%20J&volume=5&issue=4&pages=1090-1099&publication_year=2012)
4. Paterson J, Ramsay M (1993) Electric vehicle braking by fuzzy logic control. In: Conference record of the 1993 IEEE industry applications conference twenty-eighth IAS annual meeting. IEEE, pp 2200–2204
Google Scholar (<https://scholar.google.com/scholar?q=Paterson%20J%2C%20Ramsay%20M%20%281993%29%20Electric%20vehicle%20braking%20by%20fuzzy%20logic%20control.%20In%3A%20Conference%20record%20of%20the%201993%20IEEE%20industry%20applications%20conference%20twenty-eighth%20IAS%20annual%20meeting.%20IEEE%2C%20pp%202200%E2%80%932204>)

Design And Implementation Of PV Based Standalone Air Cooler

Paranthagan B¹, Aadimaathavan K², Hariharan K³, Kalaiyarasan N⁴, Karthikeyan N⁵

¹Associate Professor, Dept. of EEE, Saranathan College of Engineering, Trichy, Tamilnadu, India

²Final year student, Dept of EEE, Saranathan college of Engineering, Trichy, Tamilnadu, India

³Final year student, Dept of EEE, Saranathan college of Engineering, Trichy, Tamilnadu, India

⁴ Final year student, Dept of EEE, Saranathan college of Engineering, Trichy, Tamilnadu, India

⁵Final year student, Dept of EEE, Saranathan college of Engineering, Trichy, Tamilnadu,

Abstract

This paper is about designing and developing of PV based Air cooler without the access of grid system. It is mainly used for industrial and working areas where we can reduce the power usage. Air blower is coupled with PMDC motor and speed is controlled with Arduino UNO controller which is cost efficient and simple in programming. DC-DC buck converter is placed between PV panel and PMDC motor for step down of input voltage from PV panel. The performance of the proposed system is simulated in MATLAB/ Simulink environment and the result are validated.

Keywords: PV based air cooler, DC/DC Buck power converter; PMDC motor; MATLAB/Simulink.

Article Info

Volume 83

Page Number: 11076 - 11081

Publication Issue:

May - June 2020

Article History

Article Received: 19 November 2019

Revised: 27 January 2020

Accepted: 24 February 2020

Publication: 19 May 2020

I. INTRODUCTION

Due to rapid increase in population rate, energy consumption is rapidly increasing and at the same time fossil fuels are depleting enormously, thus result in requirement of alternative resource. This paved the way for available renewable resource in which solar is available in abundance and it can be effectively harvested to fulfil the requirement.

Though the initial cost is more, energy can easily be acquired compared to grid power system. In recent years, the usage of solar energy is increased due to the development of technology among industries and awareness among the people. Considering the environment condition several researches have been undergoing which is based on renewable energy in which majority of the project is based on the photovoltaic cell.

Even though several researches have been carried out on PV array combining DC-DC converter and motor drives only less work has been carried out on home application.

The application of PMDC is relatively high, efficient and easy control when compared to single phase ac motor. Controlling of PMDC motor is easier than controlling BLDC motor.

This paper is organized as follow. Section II gives the detailed account of Solar air cooler system. Section III describes the design procedure of individual components of solar air cooler and finally IV provides the conclusion of the paper.

II. Standalone Air cooler configuration

The solar air cooler consists of PV panel, PMDC motor coupled to fan, DC-DC buck converter, driver circuit which is controlled by Arduino. Power from the PV panel is given to the buck converter and the driver circuit is connected to the fifth pin and ground pin of the Arduino and then output of the driver is connected to the gate and source of the buck converter, this converter is used for step down of voltage from PV panel and here optocoupler is used in driver circuit for providing gate signal to the buck converter finally the output of buck converter is given to the PMDC motor which is coupled to the fan blower and by varying the duty cycle the speed of the motor can be adjusted.

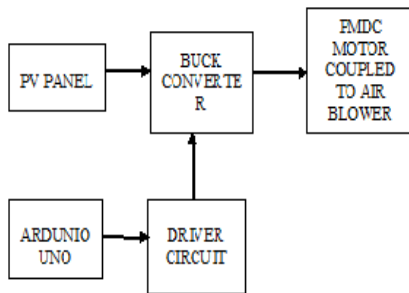


Fig 1 Block diagram of the air cooler system

III. Layout of Solar air cooler system

For efficient development of air cooler system, design and development of each component is required. The design of each component such as the buck converter, PMDC motor driving the air blower are described as follows

A. Sizing of PV array

A PV array of peak power capacity of 200W is used which is higher than required by the motor so that system performance is not affected by the losses associated with the motor and the converter. The standard insolation of 1000W/m² are estimated for all parameter of the PV array. A PV module manufactured by Bosch solar energy c-Si M60-225-16 is used with Maximum Power Point of 225W, Voltage at Maximum Power Point of 28.3V and current at Maximum Power Point of 7.95A is considered for required capacity

$$\text{Current at MMP, } I_{mpp} = i_{pv} = p_{pv}/v_{pv} = 4A$$

Numbers of modules connected in series are as,
 $N_s = V_{mpp}/V_m = 7.9V$

Number of modules connected in parallel are as, $N_p = I_{mpp}/I_m = 1$

B. Design of DC-DC buck converter

Buck converter is a switch mode DC-DC electronic converter in which output voltage will be transformed to level less than the input voltage it is also called step down converter. The name step down converter comes from the fact that analogous to step down transformer that is input voltage is stepped down to level less than input voltage. By Law of conservation of energy, the input power has to be equal to the output power. The circuit consists of an inductor, a capacitor, a diode and a switch. In which inductor in the input circuit resists sudden variation in input current. When the switch is ON the inductor stores the charges in the form of magnetic energy and discharges it when it is closed. The capacitor in the output circuit is assumed large enough that time constant RC circuit in the output stage is high. The large time constant output voltage this circuit can be operated in two modes based on OFF and ON states of switch.

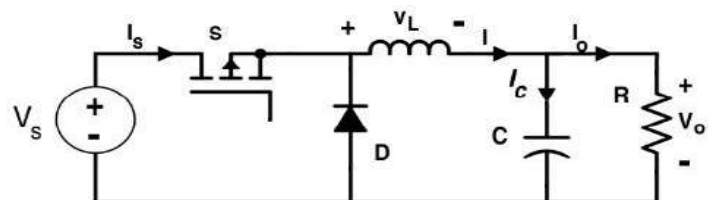


Fig. 2 Diagram of Buck converter

TABLE-1: Data sheet of the PV panel

MODEL PARAMETER	VALUE
Input voltage	22.8V
Power	132W
Output voltage	12V
Switching frequency	8KHz
Inductor	$1.071 \times 10^{-3} \text{H}$
Capacitor	$2.1484 \times 10^{-4} \text{H}$

$$L = V * (T / \Delta I_L)$$

$$= 1.0719 * 10^{-3} \text{H} \quad (7)$$

The capacitor value is

$$C = \Delta I_L / (8 * f * V_c)$$

$$V_c = 2\% \text{ of } V_o = 0.2 \text{V}$$

$$C = 2.1484 * 10^{-4} \text{H} \quad (8)$$

MODE I

when is switch is in ON state so the diode is reverse biased so that it is open circuited condition and in this state inductor is charged by V_{in} . Voltage and Current when switch is ON state

$$V_L = L \, dI_L / dt \quad (1)$$

$$\Delta I_{LON} = (V_i - V_o) / L \quad (2)$$

MODE II

Here the switch is in off state the diode is forward biased and now the inductor discharges through the diode and capacitor C

Voltage and Current when switch is OFF state

$$V_L = L \, dI_L / dt \quad (3)$$

$$\Delta I_{LOFF} = - (V_o / L) \, t_{off} \quad (4)$$

The duty cycle of buck converter is given by

$$D = V_o / V_{in} = 0.4240 \quad (5)$$

The inductor current of buck converter is given by $\Delta I_L = 30\%$ of I_L load

$$= (30/100) * 11 = 3.3 \text{A} \quad (6)$$

The inductor value is

TABLE-2: Design parameters of Buck converter

PARAMETER	VALUE
Peak Power	225 W _P
Open circuit voltage (V_{oc})	36V
Short circuit current (I_{sc})	8.7A
Voltage at maximum power (V_{mp})	28.3V
Current at maximum power (I_{mp})	7.95A

C.Design of Driver circuit

Driver circuit consists of optocoupler, three resistor and an input, output port. Optocoupler (TLP250) is an electronics component that transfer electrical signals between two isolated circuits by using lights. It also prevents high voltage from affecting the system receiving the signals. It is used for driving gate terminal of power switches. The major difference from other MOSFET driver is that its input is independent of output. It consists of GaAlAs (Gallium-aluminum-Arsenide) light emitting diode and the outside gets a driver signals through an integrated photodetector. The main feature is

electrical isolation between low and high-power circuits and it is available as an 8 pin DIP package.

D.Design of PMDC motor

PMDC motor is designing to drive the blower, the rating of the motor is 132W. it acts as a load and to which supply is given through PV which acts a input source it is interfaced through buck converter. It is cost efficient and required less maintenanceand it is more efficient compare to single phase induction motor and more over by using PMDC motor the inverter stage can be avoided

E.Design of blower fan

The blower fan is based on the load torque -speed characteristics. These characteristics exhibits similar torque speed relation which is given by

$$T_x = K_x \omega_x^2$$

T_x - blower fan load torque

ω - rotor mechanical speed (rad / sec)

value of K_x can be obtained using

$$K_x = p_x / \omega_x^3$$

F.Arduino UNO board

The Arduino is an open source microcontroller board based on has 8-bit ATmega328P controller. Is consists of crystal oscillator, voltage regulator series communication etc. and it is consisting of analog a digital pin in which it has 14 digital input/output pins and 6 analog pins a total of 20 pin. It is used instead of PID controller because it is less cost, versatile and easily programmable and its biggest advantage is that it can be connected to the pc through USB cable so that power supply to the Arduino and the computer. It provided with a voltage of 7 to 20 volts

IV. Result and Discussion

The buck converter part of the proposed scheme has been the simulated in MATLAB/SIMULINK environment and schematic of the proposed system is shown in figure 3.

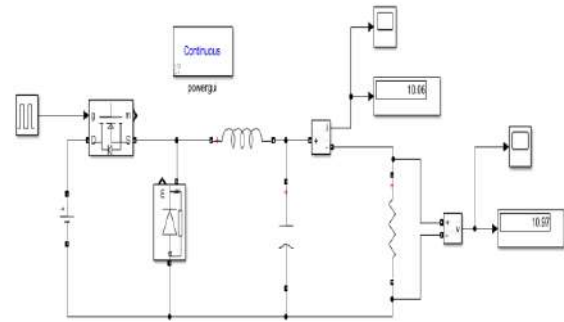


Fig .3 simulation of buck converter

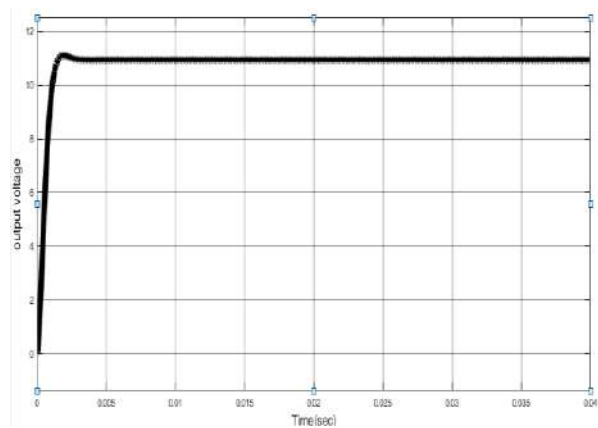


Fig .4 output voltage of buck converter

In fig 4, buck converter output voltage of magnitude 12 V is shown. Output voltage settles at 12V with slight peak overshoot. In fig 5, load current of magnitude 10A is shown

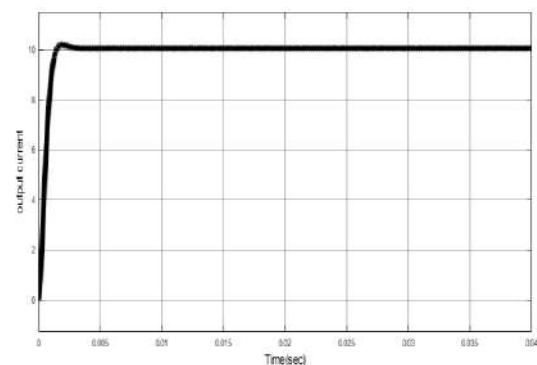


Fig. 5 output current of buck converter

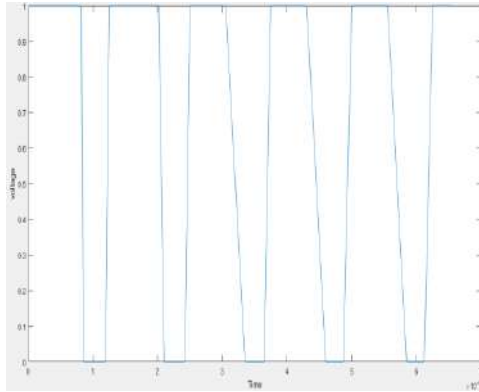


Fig 6. Pulse generator of buck converter

In fig 6, pulses of frequency 7.81KHz generated from Arduino microcontroller is shown. The pulses with duty cycle of 68% is given to the MOSFET of the buck converter

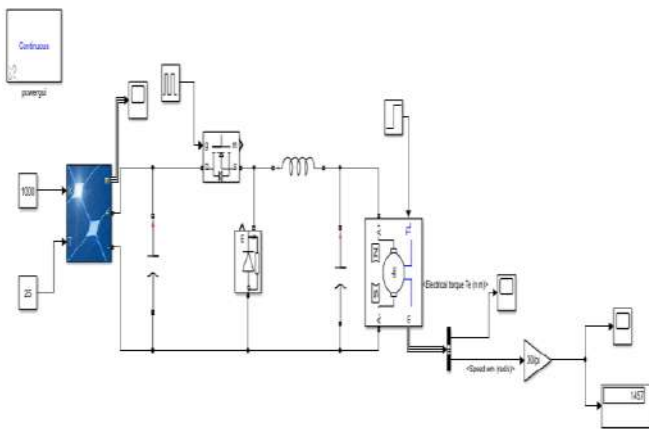


Fig .7 simulation circuit of proposed system

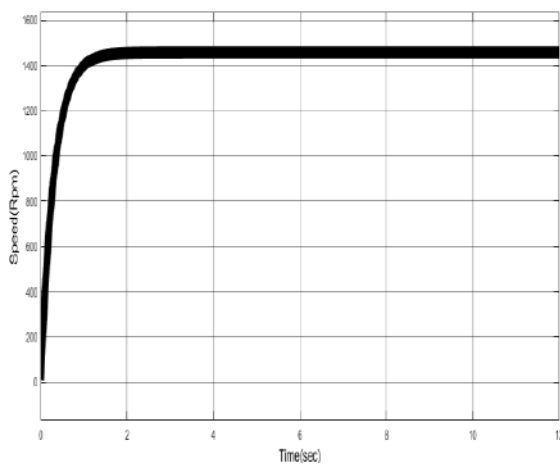


Fig .9 output speed of PMDC motor with PV source

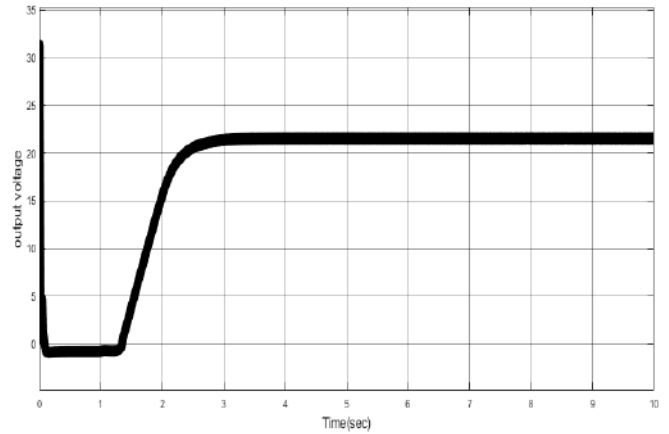


Fig 10. Output Voltage of PMDC motor using solar array

The circuit model of the proposed system is shown in fig 7. As per data sheet of the solar panel, solar panel voltage is around 21V as shown in fig 9 and current is around 5.5A as shown in fig 10 for duty cycle value of 68% of the buck converter.

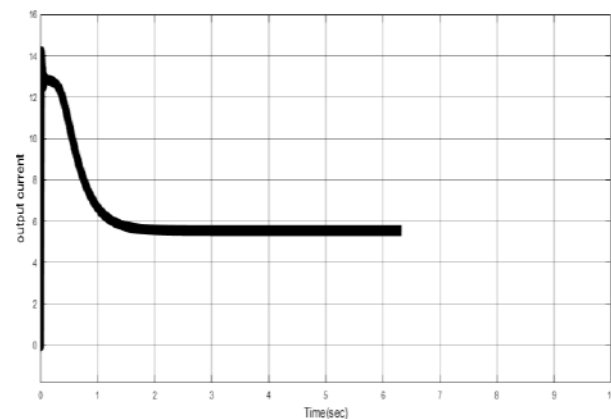


Fig 11. Output Current of PMDC motor using solar array

CONCLUSION

The proposed system has been simulated in the MATLAB/Simulink environment and the results have been presented. In commercial air cooler systems, single phase induction motors are still used whose efficiency is very poor. Since the proposed system uses PMDC motor for driving the air blower, efficiency of the overall system is greatly enhanced.

Also, unlike the BLDC motor-based air cooler system, the proposed system does not require inverter stage and controlling of the PMDC motor-based system is rather easy. In addition to this, cost of PMDC motor is less than BLDC motor.

REFERENCE

- [1] Deepak Pullaguram, Sukumar Mishra “Standalone BLDC Solar Air Cooler with MPPT Tracking for Improved Efficiency”, 2016.
- [2] Angalaeswari.S, Amit Kumar, Divyanshu Kumar, Shubham Bhadoriya “Speed Control Magnet (PM)DC Motor Using Arduino And LabVIEW”, 2016
- [3] J. Linares-Flores and H. Sira-Ramirez “DC motor velocity control through a DC-to-DC Power Converter” Centro de Investigacion y de Estudios Avanzados del I.P.N Avenida IPN, No.2508, Dec 2004
- [4] Lewis NS, Crabtree G. “Basic research needs for Solar energy utilization: report of the basic energy sciences workshop on Solar energy utilization”, April 18-21, 2005
- [5] Pillai, Unnai. “Drives of cost reduction in Solar photovoltaic. Energy Economics 50 (2015): 286-293.
- [6] W.V. Jones, “Motor Selection Made Easy: Choosing the Right Motor for Centrifugal Pump Application”, in IEEE Transaction on Industrial Application Magazine, vol.19, no.6 pp.36-45, Nov-Dec.2013
- [7] B. Singh and R. Kumar, “Simple brushless DC motor drive for Solar photovoltaic array fed water pumping system,” in *IET power Electronics*, vol. 9, no. 7, pp.1487-1495, 6 8 2016
- [8] R. Kumar and B. Singh, “BLDC Motor-Driven Solar PV Array-Fed Water Pumping System Employing Zeta Converter,” in *IEEE International Symposium on Industrial Electronics*, Gdansk, 2011, pp.613-618.
- [9] R. RamaKumar, H.J Allison and W.L Huges, “Solar Energy Conversion And Storage System For The Future,” in *IEEE Transaction on power Apparatus and System*, vol. PAS-94, no.6 November /December 1975
- [10] T.Esram and P.L Chapman, “Comparison of Photovoltaic Array Maximum Power Point Tracking Techniques ,” in IEEE Transcation.

**International Research Journal of Management
Science & Technology**
ISSN 2250 – 1959(Online)
2348 – 9367 (Print)

An Internationally Indexed Peer Reviewed & Refereed Journal



**Shri Param Hans Education &
Research Foundation Trust**

www.IRJMST.com
www.SPHERT.org

Published by iSaRa Solutions

LOW COST POWER QUALITY ANALYSER WITH DATA LOGGING

Ramprasath.S¹, Booma.G², Dharshini.R³, Joicy.J⁴, Nandhini.T⁵

Assistant professor¹, UG student ^{2,3,4,5}, Saranathan college of Engineering, Trichy-12.

ramprasath-eee@saranathan.ac.in, booma249@gmail.com, dharshiniraj26@gmail.com, joicyjohnson1998@gmail.com,
rosynandhini1999@gmail.com

ABSTRACT- In this prototype, an automated smart remote metering system, low cost power quality analyser (LCPQA) is fabricated to measure true root mean square value of voltage, current and Power factor for small scale industries. The measurement system is an ARDUINO UNO based master-slave wireless technology that incorporates smart monitoring via Android mobile application. This wireless technology requires ESP8266 wifi module for transmitting and receiving data. The hardware model of the smart metering system senses voltage and current by graphical method to find true RMS values and calculates parameters like power, power factor and energy. Remotexy open source android application act as a front end for remote monitoring and it helps to generate embedded code for data manipulation. As of now the data can be monitored within the wifi range. Further development is to collect data all over the world using cloud technology.

Key words – LCPQA, Remotexy, ESP8266.

I. INTRODUCTION

In the power grid of the future, sensors and transducers will play an important role to monitor energy in real time. The analyzer can provide remote power monitoring and data storage capability, so as to take decisions in real time. This proposed LCPQ analyzer is provided with data logging facility and [1], [2] remote monitoring of the electrical parameters.

The term smart digital device implies a time-sampled system. An analog-to-digital converter (ADC) samples current and voltage from transducers' output at a high frequency. The digital processor translates real-world waveforms to binary words which can be manipulated by software to measure electrical parameters. The ADC's resolution and speed influence the duplication quality of continuous time signals, also affects the microprocessor bandwidth required for calculations. Analog value once converted to a digital signal, the voltage and current waveforms can be manipulated by software code to extract any necessary information for smart electrical systems. The main function of controllers is to collect data samples at regular intervals and the sample time determines the operating speed of the LVPQA.

Noise sensitive equipment and machine that needs stable flow of energy have become a standard. Because of that, power quality concern has increased and the consumers are looking for the best option in the market of electrical energy. Any power problem manifested in voltage, current or frequency deviations result in failure of customer equipment. The power quality meter available in market is capable of measuring all power quality parameters such as phase currents, voltages, real, reactive and apparent power, power factor etc. The cost of that power quality analyzer is very high. So we framed our goal to develop cost effective and better efficiency device. A smart wireless monitoring system [3] for measuring voltage, current and power is designed and implemented. It monitors single phase electrical parameters using an Arduino microcontroller

to read the true RMS voltage and true RMS current from sensors and then send the measured data to mobile applications using ESP8266 wifi module. The smart monitoring system Arduino UNO [5] basic board is interfaced with ESP8266 wifi module to collect and monitor data within the wifi range. The voltage sensing is done using LEM LV25-p Hall voltage sensor which has inherent galvanic separation between the primary circuit and secondary circuit which is capable of measuring up to 500V AC. Current is sensed using ACS712 Hall Effect-Based Linear Current Sensor with 2.1 KV RMS Voltage Isolation. Remotexy [6] android mobile application software is used to interface smart phone with Arduino controller using wifi to monitor the electrical parameters. The complete block diagram of smart wireless monitoring system is shown in figure 1.1.

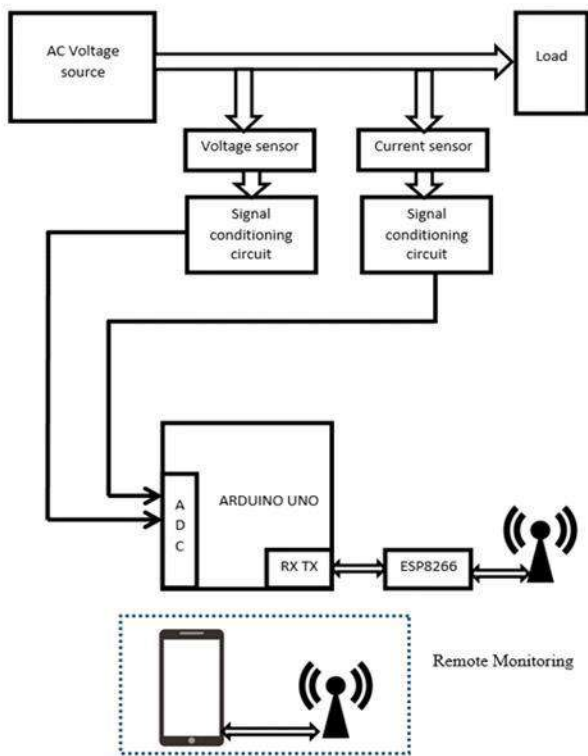


Figure 1.1 Overall Block Diagram

The prototype model is designed to measure 230V AC, 50Hz supply capable of delivering 1KW of power to the load. The voltage and current is sensed and fed to the signal conditioning circuit for amplification and to shift the negative cycle of ac voltage from sensor. The microcontroller performs the calculations using the developed algorithms to monitor different electrical parameters.

II. METHODOLOGY

A. Equations For Electric Power Measurement

Voltage and current signals have **harmonic components**, which distort the sinewave signal. Dividing the peak value by the square root of 2 will not provide correct value, because the signal is no longer a pure sinusoid. For non-sinusoidal signal we need to use graphical method to find true RMS value.

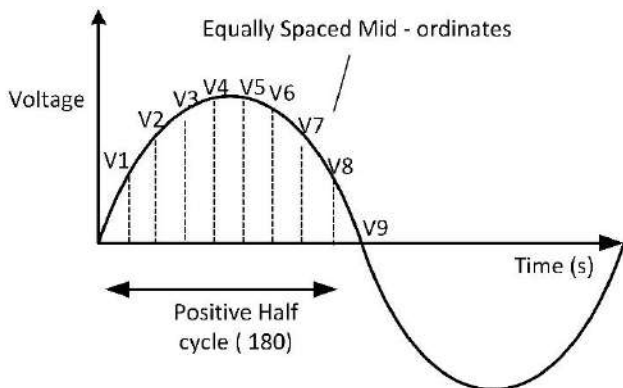


Fig 2.1 Positive Cycle Waveform to Collect Periodic Samples

The RMS value is the square root of the mean of the square of the mid-ordinates of the voltage waveform.

$$V_{rms} = \sqrt{\frac{\text{sum of mid - ordinates (Voltage)}^2}{\text{number of mid - ordinates}}} \quad (1)$$

For 12 periodic samples of a half cycle, the true RMS value is

$$V_{rms} = \sqrt{\frac{(V_1^2 + V_2^2 + V_3^2 + V_4^2 + V_5^2 \dots \dots + V_{12}^2)}{12}} \quad (2)$$

Similarly for current measurement,

$$I_{rms} = \sqrt{\frac{(I_1^2 + I_2^2 + I_3^2 + I_4^2 + I_5^2 \dots \dots + I_{12}^2)}{12}} \quad (3)$$

Active power is the time average of periodic instantaneous power.

$$p = \frac{1}{T} \int_{t_0}^{t_0+T} v(t)i(t)dt \quad (4)$$

Apparent power is the product of rms voltage and current

$$S = V_{rms} I_{rms} \quad (5)$$

Power factor is the ratio of active power to apparent power

$$pf = \frac{P}{S} \quad (6)$$

B. Voltage Sensor Module design

The LEM LV 25-P Hall Effect transducer is selected for the voltage sensing.

Table 2.1: Hall Sensor specification

Description	Value
Primary nominal R.M.S current	I _{PN} =10mA
Primary current	I _p -Range = 0 TO ±14mA
Supply voltage	V _c = ±15V DC
Measuring resistance	R _m –must be in the range (30ohm to 190 ohm)

Fig 2.2 shows the schematic circuit for designing voltage sensor for 230V, 5A, AC supply.

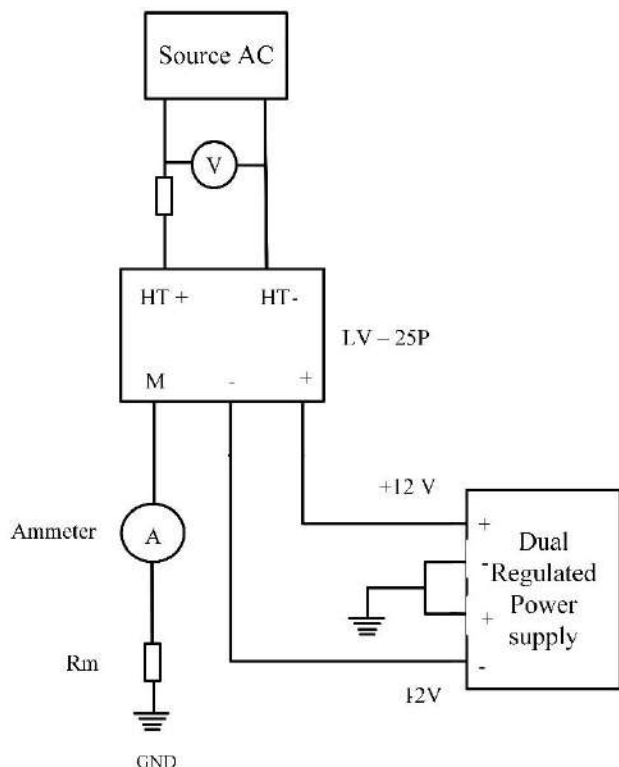


Figure 2.2: Voltage sensor Schematic

The maximum primary current I_{pn} is 10mA

$$R1 = \frac{\text{Measuring voltage}}{10\text{mA}}$$

For 220 V AC,

$$R1 = \frac{220 \text{ V dc}}{10\text{mA}} = 22\text{K ohm}$$

Maximum secondary current I_{SN} is 25mA

($K_N - 2500:1000$)

R_m value is

- From datasheet, R_m must be in the range (30 ohm – 190 ohm)
- The analog input to controller must be an integer, ranges from (1V to 5V) DC. Here for this example we choose 4 Vdc, so we have to choose R_m value according to it.

$$\begin{aligned} V &= IR \\ 4\text{V} &= 25\text{mA} \times R_m \\ R_m &= 160 \text{ ohm.} \end{aligned}$$

C. Current sensor module design

ACS712 current sensor senses the current from the system and generates the signal proportional to the detected current either in the form of analog voltage or digital output. This sensor uses indirect sensing method to calculate the current. It is provided in a SOIC8 package. Applied current flowing through a copper conduction path generates a magnetic field which is sensed by the integrated Hall IC and converted into a proportional voltage. It has 100mV/amp sensitivity.

Table 2.2: ACS712 Specification

Description	Value
Supply voltage	5V
Sensitivity (±5, ±20, ±30)A	(66,100,185) mV/A

Current consumption	10mA
Temperature	-40°C to +85°C

D. Overall Schematic

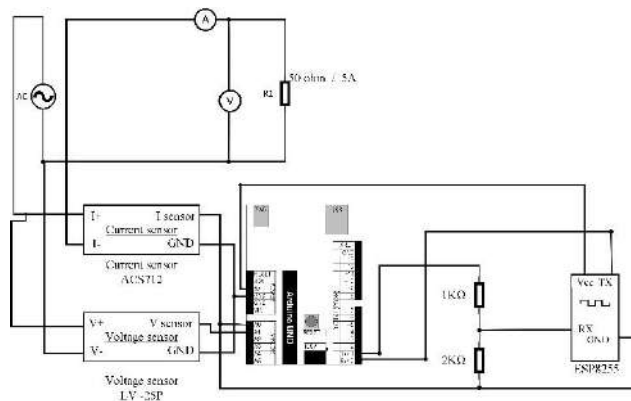


Figure 2.3: Schematic diagram of the smart monitoring system

Fig 2.3 shows schematic diagram of complete wiring circuit for smart wireless system. The ESP8255 supply voltage is 3.3V, but the Tx pins output level is 5V hence to reduce the voltage level to 3.3V a potential divider is used.

III. SOFTWARE DEVELOPMENT

A. Voltage Measurement

To measure the true RMS voltage it is necessary to collect samples at regular intervals and the square root of the mean of the square of the mid-ordinates of the voltage waveform gives the exact value. Arduino Uno board accept positive 5V as input to ADC. It has 10 bit ADC resolution, $2^{10} = 1024$ decimal value we get for a 5v as input.

Pin A1 is assigned for voltage sensor.

Algorithm:

- Step1: `voltage_a[i]=analogRead(A2); // read the value`
Read the values from A0 analog pin.
Create an array `voltage_a[i]` and store the periodic samples (100 samples)
- Step2: `voltage_a[i]= map(voltage_a[i], 0, 1024, 0, 326); //mapping the measured value`
The measured value is mapped for peak rms value 326.
- Step3: `cumulative_v += sq(voltage_a[i]); //square the value after sum the square value`
Cumulative Addition of all the mid-ordinate squared value
- Step4: `V_rms = (sqrt((cumulative_v/100))); // average and square root the cumulative value`

The true RMS value is obtained by taking square root of cumulative values.

B. Current Measurement

Analog pin A0 is preferred for analog current value from ACS712 sensor.

Algorithm:

- Step1: `current_a[i]=(analogRead(A0)-506); // read the analog value`

The sensor give a 2.5 V as output when no current flows, so we subtract analog value by 506 equivalent to 2.5V.

Step2: $current_a[i] = (current_a[i] * vpp) / 0.1 // 20A$
sensitivity is 100.

Step3: The current value is calibrate with vpp. ($vpp = (5/1024) = 0.0048828125$) the multiple value is divided into 0.1 because the current sensor sensitivity is 100mV/Amp

Step3: $cumulative_i += sq(current_a[i]) //$ square the value after sum the square value.

Step4: cumulative Addition of all the mid-ordinate squared value
 $I_rms = (sqrt(cumulative_i / 100));$

The true RMS value is obtained by taking square root of cumulative values.

C. Flow chart

Fig3.1 shows the flow chart to calculate the true rms value for voltage and current. For proposed LCPQA we prefer to take 100 samples for each half cycle. By software manipulation we can calculate power, power factor, harmonics and voltage sag from the rms voltage and current measured.

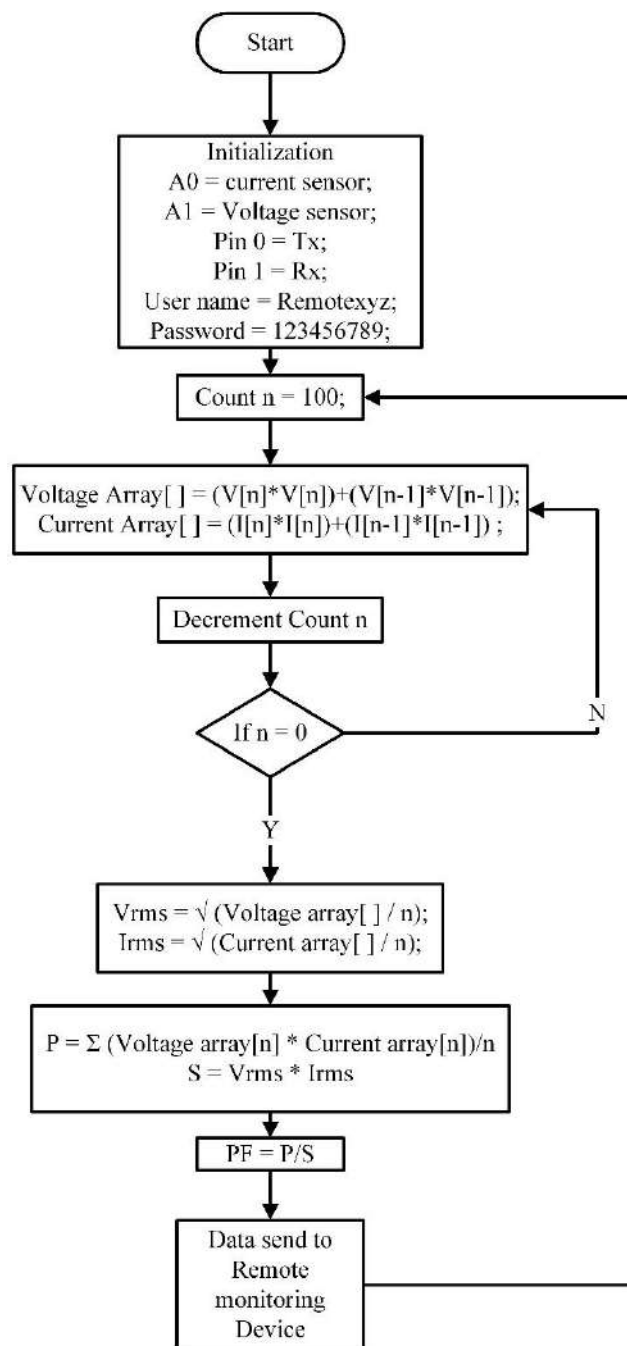


Figure 3.1: Flow chart

D. Power Measurement

The total power = $V_{rms} * I_{rms}$ and then the real power is $V(i) * I(i)$. The real power and reactive power are divided get the power factor.

$$S_{total_power} = V_{rms} * I_{rms};$$

$$Pf = p_{real} / S_{total_power};$$

E. Wifi Module Interface

The smart monitoring system uses ESP8266 wifi module for data transfer from ARDUINO to smart phone using remotexy application software. RemoteXY is an open source code generating application and uses a mobile graphical user interface

for Arduino controller boards. Fig 3.2 shows the schematic to interface ESP8255 module.

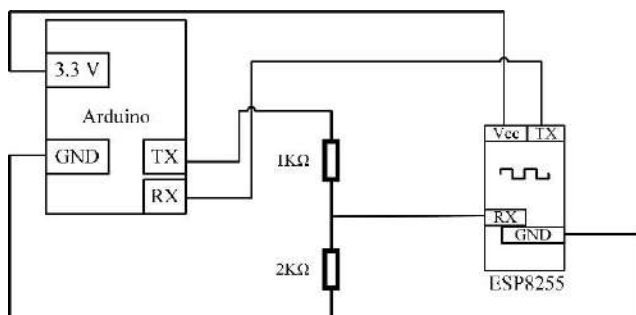


Figure 3.2: Wifi Module Interface

The mobile application remotexy includes an editor window where mobile graphical interface elements are interfaced with Arduino processor to display the electrical parameters. The element window contains control elements, indication elements and decorative elements which the user can make use of this to create front end for remote monitoring. The property window provides hardware configuration and generates code for the specified devices used. Mobile application which allows us to connect to the controller and control it via graphical interface. RemoteXY allows user to develop any graphical management interface, using the control, display and decoration elements. User have to install remotexy application in their smart phone, which can be downloaded from play store. The user can connect the mobile to the Arduino processor using wifi setup. Fig3.3 shows the functional block diagram for interfacing mobile with Arduino. The user have to create a profile in remotexy to save the projects, which can be accessed from any place. Fig 3.4 shows the frontend of LCPQA using remotexy editor with 4 indicating elements, to measure the rms voltage, current, power and power factor.

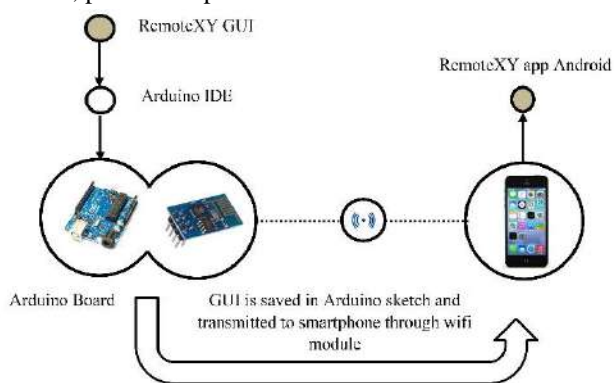


Figure 3.3: Functional block diagram for remotexy

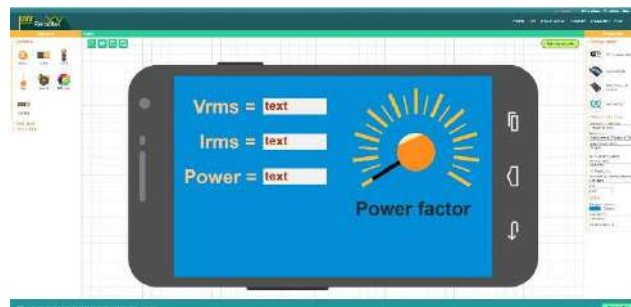


Figure 3.4: frontend of LCPQA

IV. RESULT

The results obtained from the monitoring system is compared with analog test meters and the values are tabulated below.

Table 4.1 Experimental Results

S.No	Smart meter		Analog meters	
	Vrms(V)	Irms(A)	Vrms(V)	Irms(A)
1	20	0.40	18	0.36
2	40	0.80	36	0.72
3	60	1.20	58	1.16
4	80	1.60	76	1.52
5	100	2.00	95	1.9
6	120	2.40	118	2.36
7	140	2.80	136	2.72
8	160	3.20	157	3.14
9	180	3.60	178	3.56
10	200	4.00	196	3.92
11	220	4.40	218	4.36

Fig4.1. shows the mobile screen which acts as frontend display unit for LCPQA. It contains four indicator elements to display Vrms, Irms, power and power factor.

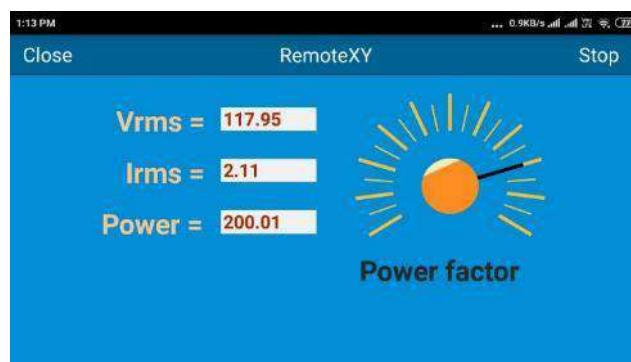


Figure 4.1 Graphical Interface

A. Hardware setup

Fig 4.2 shows the complete hardware prototype for LCPQA, comprises of sensing module, controller module, wireless module and power supply module. A connecting port is provided to connect the prototype to a single phase system of 1000W capacity. Fig 4.2 shows the measured parameters seen remotely in the smart phone within wifi range.

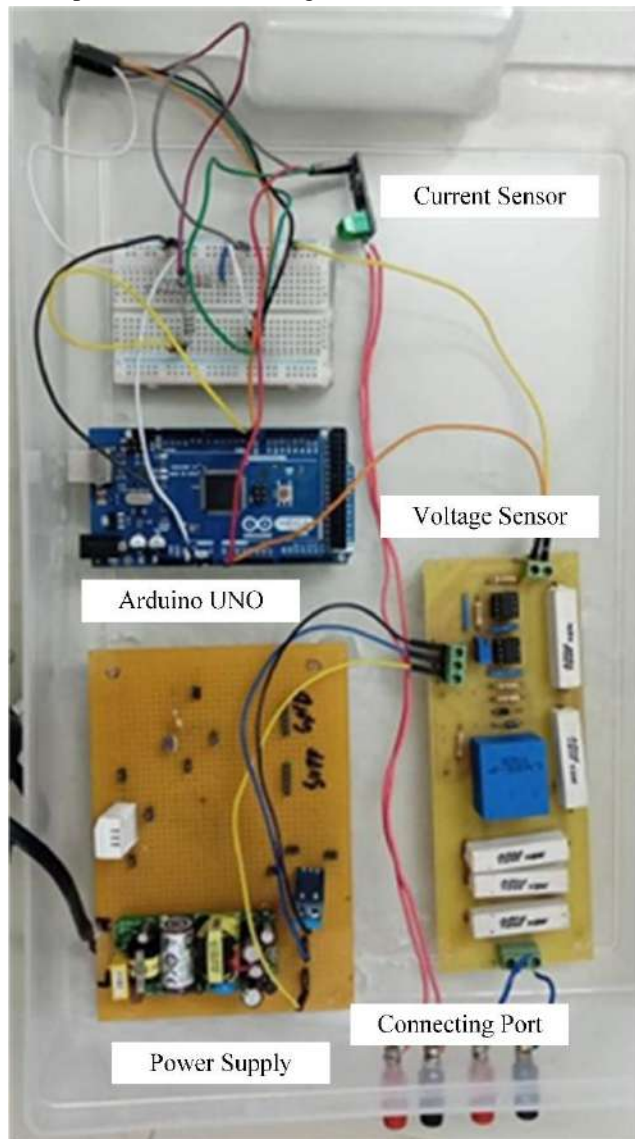


Figure 4.2 Hardware

V. CONCLUSION

The fabricated prototype of LCPQA is a good option for the measurement of electrical parameters. They have the capacity to store data and communicate with different electronic systems. The advance of electronic device technology contributes to the

simplicity in the design and accuracy during measurements. However, this work has presented the prototype of a digital electric power meter using an ARDUINO microcontroller. The prototype does not use very sophisticated electronic components, besides low cost, which leads to an economic design as a result. Another characteristic of the design is that the meter can send data to mobile application to monitor the electrical parameters.

VI. REFERENCE

[1] Q. Sun, H. Li, Z. Ma, C. Wang, J. Campillo, Q. Zhang, F. Wallin, J. Guo, "A Comprehensive Review of Smart Meters in Intelligent Energy Networks", *IEEE Internet of Things Journal*, vol. 3, no. 4, pp. 464-479, 2015.

[2] J. Zheng, D. W. Gao, L. Lin, "Smart meters in smart grid: An overview", *Proc. IEEE Green Technol. Conf.*, pp. 57-64, Apr. 2013.

[3] X. Hao et al., "Smart meter deployment optimization for efficient electrical appliance state monitoring", *Proc. IEEE 3rd Int. Conf. Smart Grid Commun. (SmartGridComm)*, pp. 25-30, Nov. 2012.

[4] A. Di Nisio, T. Di Noia, C. G. C. Carducci, M. Spadavecchia, "High dynamic range power consumption measurement in microcontroller-based applications", *IEEE Trans. Instrum. Meas.*, vol. 65, no. 9, pp. 1968-1976, Sep. 2016.

[5] Arduino.cc. (2019). *Arduino - Home*. [online] Available at: <https://www.arduino.cc/> [Accessed 2 Jul. 2019].

[6] Remotexy.com. (2019). *Remote control Arduino - RemoteXY*. [online] Available at: <http://remotexy.com/en/editor/> [Accessed 2 Jul. 2019].



EARN YOUR MBA

WWW.IIMPS.IN



Accreditation & Ranking



UGC / NCTE Approved.

INFO@IIMPS.IN

☎ 011-41005174

R
S
E
A
R
C
H
G
A
T
E
W
A
Y

STOP PLAGIARISM



Arogyam Ayurveda
Holistic Healing through herbs



A
R
O
G
Y
A
M
O
N
L
I
N
E

PARIVARTAN PSYCHOLOGY CENTER



COLOR PSYCHOLOGY : HOW COLOR AFFECT YOUR CHILD



- BLUE** Calms your Child's Mind & Body
- YELLOW** Promotes Concentration, Stimulates the Memory
- PINK** Evokes Empathy, makes your Child Calm
- RED** Excites and energizes your Child's body
- GREEN** Improves Reading speed and Comprehension

www.parivartan4u.com



Confuse about your children's future?



Shri Param Hans Education & Research Foundation Trust
www.SPHERT.org

भारतीय भाषा, शिक्षा, साहित्य एवं शोध

ISSN 2321 – 9726

WWW.BHARTIYASHODH.COM



**INTERNATIONAL RESEARCH JOURNAL OF
MANAGEMENT SCIENCE & TECHNOLOGY**

ISSN – 2250 – 1959 (O) 2348 – 9367 (P)

WWW.IRJMST.COM



**INTERNATIONAL RESEARCH JOURNAL OF
COMMERCE, ARTS AND SCIENCE**

ISSN 2319 – 9202

WWW.CASIRJ.COM



**INTERNATIONAL RESEARCH JOURNAL OF
MANAGEMENT SOCIOLOGY & HUMANITIES**

ISSN 2277 – 9809 (O) 2348 - 9359 (P)

WWW.IRJMSSH.COM



**INTERNATIONAL RESEARCH JOURNAL OF SCIENCE
ENGINEERING AND TECHNOLOGY**

ISSN 2454-3195 (online)

WWW.RJSET.COM



**INTEGRATED RESEARCH JOURNAL OF
MANAGEMENT, SCIENCE AND INNOVATION**

ISSN 2582-5445

WWW.IRJMSSI.COM



DYNAMIC COMPENSATION OF REACTIVE POWER: COMPARITIVE ANALYSIS OF POWER FACTOR CORRECTION TECHNIQUES

A.R.Danila Shirly^{1*}, K.Vijayaragavan², R.Vishnu Chander³, M.Santhosh⁴,
M. Praveen Kumar⁵,

¹Assistant Professor, Department of Electrical and Electronics Engineering, Saranathan College Of Engineering,
Tamil Nadu, India,

^{2,3,4,5}UG Scholar, Department of Electrical and Electronics Engineering, Saranathan College Of Engineering, Tamil
Nadu, India,

*Corresponding Author: ardanilashirly@gmail.com

ABSTRACT

This study explores the various power factor correction techniques used in industrial loads and a new topology is proposed to automatically improve the power factor by injecting the reactive power generated by the capacitor bank connected with a load. It consists of a relay which detects the value of $\cos \phi$ and compares with a set point value based on Tamil Nadu Electricity Regulatory Commission, if the measured value goes below the set point value it will readily inject the generated reactive power without human intervention. At present the automatic power factor improvement is gaining prominence owing to the superiority of it over the fixed capacitor bank in compensating the reactive power with different loading condition. The main aim of this proposed device is to compensate the reactive power near the load side rather than disturbing the entire power system. This paper describes the various methods for compensating the reactive power and concludes the best method for reactive power compensation of industrial loads.

Keywords: APFC Relay, Dynamic compensation, Reactive power compensation, STATCOM, Static VAR compensator, Synchronous Condensers, TANGEDCO.

1. Introduction

Power factor is defined as the cosine of phase difference between the voltage and current for a given load system. In an Electrical technology, possible loads are a) Resistive load b) Inductive load c) Capacitive load. For a resistive load there is no concern about the power factor since the voltage and current are in-phase with each other. But for other two loads, power factor plays a major role i.e. lagging power factor for inductive load and leading power factor for capacitive load. The words lagging and leading are defined by the voltage and current relation for a particular load. Lagging means the current lags the voltage by an angle ideally 90° and similar case for leading condition in which current leads the voltage by an angle ideally 90° . As noted for inductive load the load current lags the voltage by an angle which is called phase angle (ϕ) and the cosine of that phase angle (ϕ) is called power factor. In other terms, it is defined as the ratio of real power (kW) utilized by the load to the apparent power (kVA) flowing in the circuit. The other power term is called Reactive power, or kVAr. Reactive power is not really a power, but

represents the product of volts and amperes that are in out-of-phase with each other. It represents the part of electrical energy that is required to form and sustain the fields of electrostatic force and magnetism which are needed by the alternating current devices. Compensating the reactive power is one of the tedious processes performed in the power system. Generally, the capacitive load will generate the reactive power and the inductive load will consume the reactive power.

In industry most of the loads used are inductive load which consume reactive power. Therefore, the installed capacitor bank will generate the required reactive power to compensate the demanded load reactive power. Hence the current drawn from the power system is minimized, reducing the power losses and improving the efficiency of the load system. It can be proved by taking a small example; [1]. Consider a machine having a full load rated capacity of 1000A at 500V.

$$\text{Rating of the alternator} = 500 \text{ kVA}$$

If the alternator is operating at unity power factor,

$$\text{Load supplied} = 500 \times 1 = 500 \text{ kW}$$

If the power factor is 0.6,

$$\text{Load supplied} = 500 \times 0.6 = 300 \text{ kW}$$

Although the machine is fully loaded, i.e. developing its maximum current and voltage yet when the PF is 0.6, it is supplying only 60% of its full load capacity. So in order to supply 500 kW at 0.6 PF the machine must be overloaded and conductors must be made of much larger cross-section area to withstand the overload current. Hence for a given power, lower the PF the larger must be the size of the machines and larger must be the size of the conductors of transmission; or in other words, the greater will be the cost of the system.

1.1. Advantages of Reactive Power Compensation

In the above discussion we have seen that if the load system works at low power factor which will increase the cost per unit. Thus it is always advantageous for the both consumers as well as supplier to work at higher improved power factor. Usually suppliers induce the people to work at improved power factor by adopting a two part tariff charging the consumer on his maximum demand in kW as well as the number of units consumed by the consumer.

The maximum demand of the consumer is measured with a maximum demand meter installed at consumer premises the reading of which is taken annually. If the consumers will try to work at low power factor, for the same power it will draw more current or is kVA demand is increased for which customer have to pay extra penalty[2]. This is how the consumer is discouraged to have low power factors. The tariff consideration for low power factor usage in

Tamil Nadu is specified in table 1.

Table 1

Compensation charges issued by TANGEDCO (Tamil Nadu Generation and Distribution Corporation Limited) that will be levied for low power factor utilization by consumers

Power Factor Range	Low Power Factor Surcharge
Below 0.90 and up to 0.85	One per cent of the current consumption charges for every reduction of 0.01 in power factor from 0.90
90 Below 0.85 to 0.75	One and half per cent of the current consumption charges for every reduction of 0.01 in power factor from 0.90
Below 0.75	Two per cent of the current consumption charges for every reduction of 0.01 in power factor from 0.90

The following is the advantages of the improved power factor:

- The efficiency of load system is increased.
- The regulation of the lines is improved.
- The overall cost per unit decreased.

1.2. Methods of Reactive Power Compensation

- Series compensation.
- Shunt compensation.
- Static VAR compensator.
- STATCOM.
- Synchronous condenser.

1.2.1. Series Compensation

When a compensating device is connected in series with the transmission line is called series compensation as depicted in Fig 1. It can be connected anywhere in the line.

There are two modes of compensation based the type of load demand.

- Capacitive mode.
- Inductive mode.

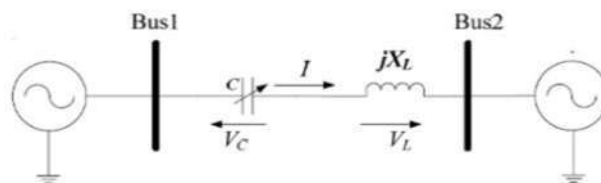


Fig 1. Transmission Line with Series Compensation

1.2.2. Shunt compensation

When a compensating device is connected in parallel with the transmission line is called shunt

compensation as shown in Fig 2. It can be connected only at the middle of the line [8].

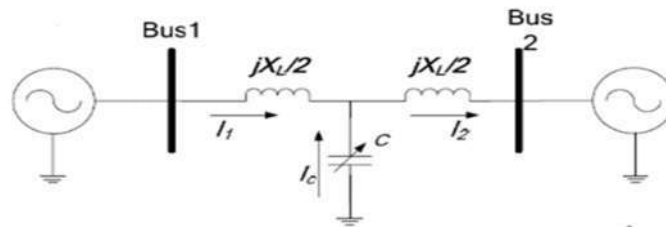


Fig 2. Transmission Line with Shunt Compensation

1.2.3. Static VAR Compensator

It is an electrical device which provides reactive power on transmission network. Static refers that there is no moving parts in its operation [3]. SVC is an automatically designed device for impedance matching, to bring the system closer to the unity power factor [7]. If the load is leading, the SVC will use reactor usually in the form of (TCR) Thyristor controlled reactors to consume VAR from the system thereby lowering the system voltage. In case of inductive load lagging, the SVC will use capacitor in the form of switched capacitor banks as shown in Fig 3.

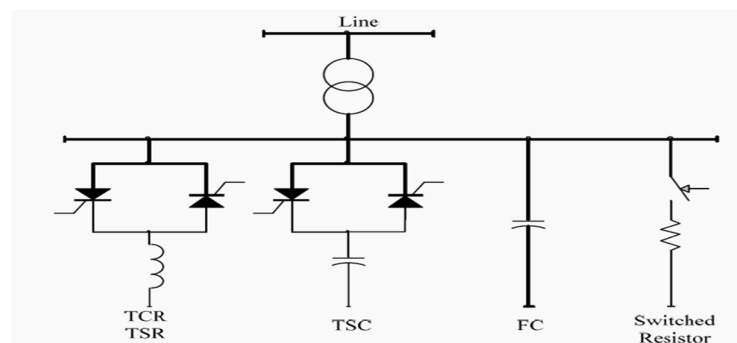


Fig 3. Static VAR Compensator

Advantages

- Reliable.
- Faster operations.
- Smooth and flexible operations with the help of thyristors.

1.2.4. STATCOM (Static Synchronous Compensator)

It is a device which uses Synchronous Voltage Source (SVS) for generating or absorbing reactive power. A SVS is made using a voltage source converter which is driven by a dc storage capacitor and the SVS is connected to the ac system bus through an interface transformer.

The transformer steps the system voltage down such that the voltage rating of SVS switches are within specified limit [6].

The STATCOM consist of following units:

- Power converter.
- Coupling reactor or step up transformer.
- Controller.

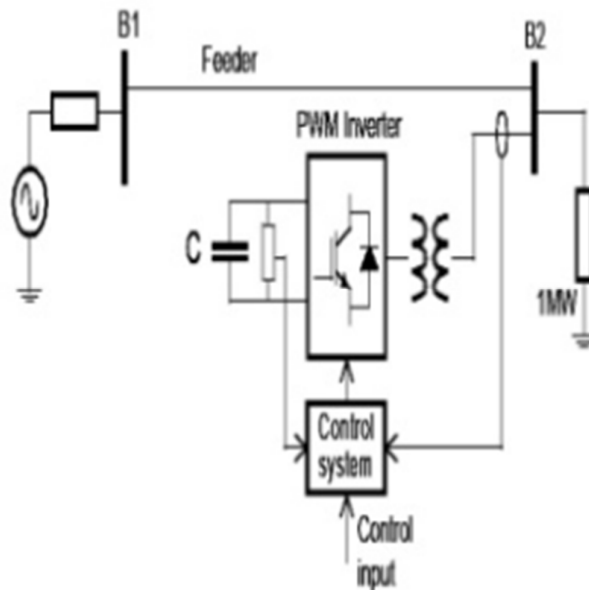


Fig 4. STATCOM unit

1.2.5. Synchronous Condensers

A synchronous condenser is a synchronous machine that produces reactive power which leads real power by 90 degrees in phase. It is a synchronous motor, whose shaft is not linked to anything but spins freely without load. Its duty is not to convert electric power to mechanical power or vice versa, but to regulate situations on the electric power transmission grid. Its field is regulated by a voltage regulator to increase or decrease the reactive power as needed to modify the grids voltage, or to enhance power factor. Before the use of power electronics devices, synchronous condenser is used for reactive power compensation.

Merits

The quantity of reactive power from a synchronous condenser can be steadily regulated.

Demerits

- Considerable foundation is required at work place due to large size.
- Right automatic exciter circuit is needed for reactive power control.
- Starting and protective gadgets are required.
- It cannot be adjusted fast enough to balance fast load changes.
- High initial and maintenance cost.

2. Dynamic Compensation of Reactive Power for Three Phase Induction Motor

The overall block diagram of dynamic compensation of reactive power [9] for three phase induction motor is shown in Fig 5.

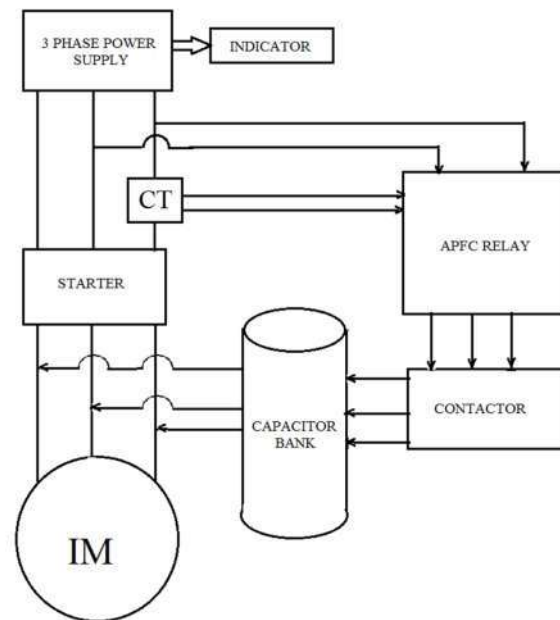


Fig 5. Block Diagram

2.1. APFC RELAY

The automatic power factor correction relay is shortly known as APFC Relay. The APFC Relay introduces most effective power factor correction. APFC is an automatic control panel [4] which is used to improve the power factor wherever required by switching ON and OFF the required capacitor. That can be done in both the ways in automatic or by manual. The APFC have reliable capacitor bank, microprocessor – controllers, harmonic filters and other components. The APFC Relay is basically classified as two, four, six, eight stages. It is an inbuilt programmable relay. The program can be done by giving three phase power supply to the APFC Relay. The APFC Panel are most widely used in industries because in industries most of the loads are inductive in nature which results in lagging power factor that is why there are more losses and wastage which result in high electricity bill. Hence by using APFC panel the capacitor is added in it. In this method 6 stage APFC Relay is employed.

2.2. Circuit Diagram of Dynamic Compensation

Power supply is given to the three phase induction motor through the stator, current transformer is employed to sense the input current, if it exceeds the supply it will be tripped off by MCB and if it deviates from the pre-set value, the signal will send to the APFC relay. After that the relay makes the contactor to incorporate the capacitor bank. The value of capacitance to get into the

the capacitor bank gets departed. Only at the starting of induction motor, the compensation is required. Whenever there is a sudden reduction of power factor, the relay senses and the capacitor bank will be conducted. The circuit is depicted in Fig 6.

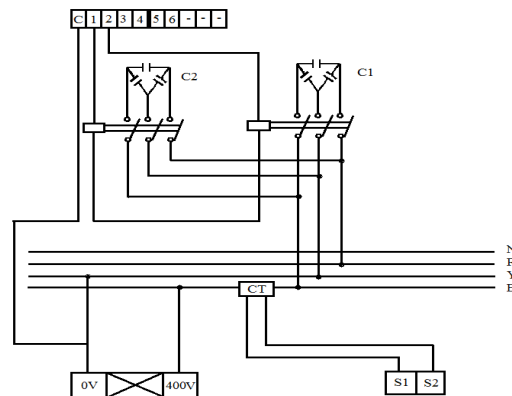


Fig 6. Circuit Diagram of Dynamic Compensation

Power supply is given to the three phase induction motor through the stator, current transformer is employed to sense the input current, if it exceeds the supply it will be tripped off by MCB and if it deviates from the pre-set value, the signal will send to the APFC relay. After that the relay makes the contactor to incorporate the capacitor bank. The value of capacitance to get into the action depends on the level of reduction in the power factor. Once the power factor is corrected, the capacitor bank gets departed. Only at the starting of induction motor, the compensation is required. Whenever there is a sudden reduction of power factor, the relay senses and the capacitor bank will be conducted.

2.2. Programming of APFC Relay

2.2.1. Numerical Programming

There are two types of program in APFC Relay. They are

- Manual mode
- Automatic Mode

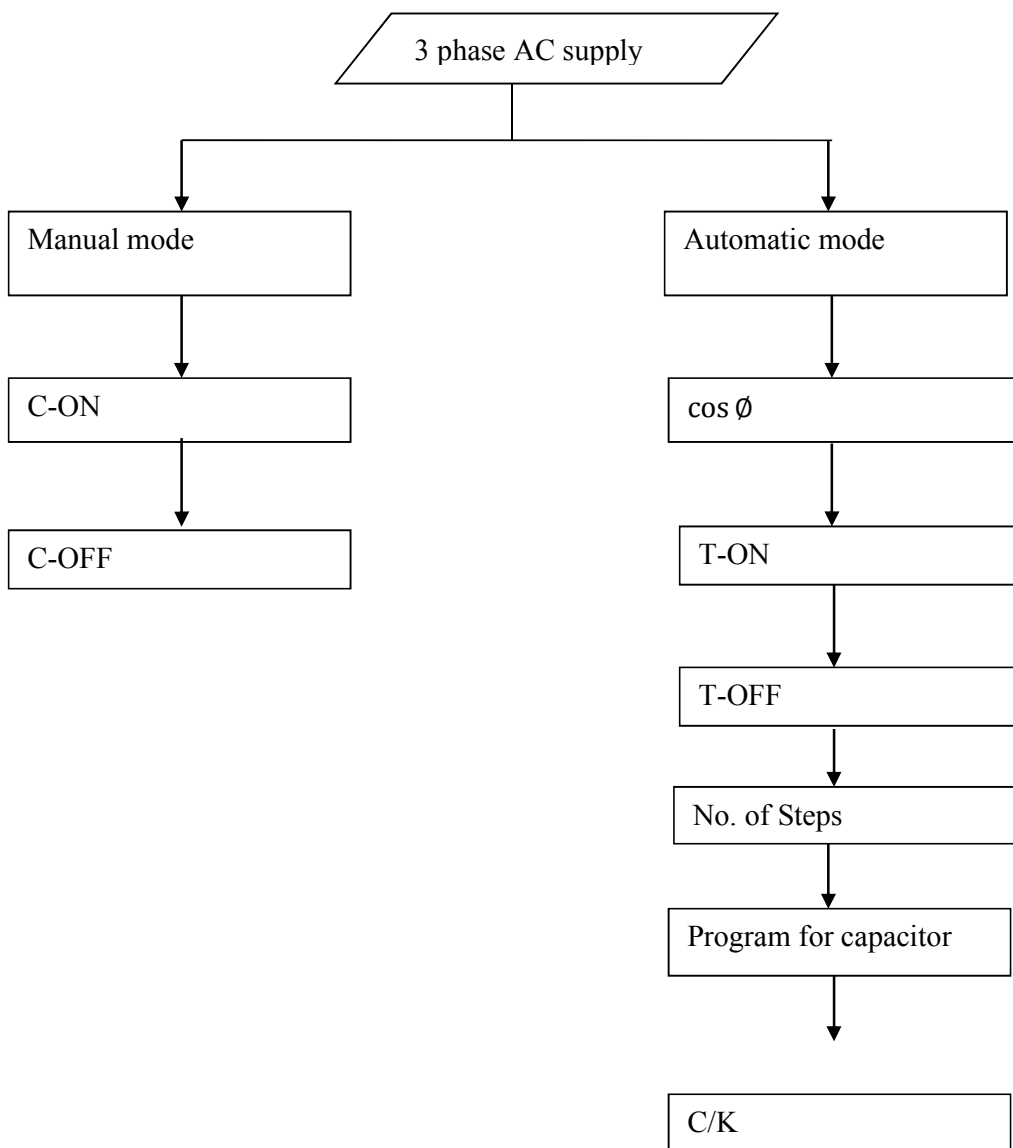
In Manual mode the injection of capacitance is done by manual or manpower. It is an old technique in power factor correction and it is not accuracy.

The next method is, Automatic mode it follows the following methods they are,

- Select the Automatic mode. And set the $\cos\phi$. It is a target or assumed power factor.
- Next step is to set the Response delay .It should be in sec at maximum 10 sec.
- The function of the Response delay time taken to inject the capacitor.
- Next step is to set the Reconnection. It should be in sec at minimum 50 sec.

- The function of reconnection delay time taken is to cut off the capacitor.
- Next step is to set the Number of steps. It means number of step used in the APFC relay example (1, 2, 3, 4, 5, 6 stages).
- Next step is to set the Program type. It is generally common in all system. That program is (PS1).
- Next step is to set the C/k it is all most common in all program, it is all most 0.5.
- Next step is to set the CT value. It is 5.

2.2.2. Programming Flow Chart



3. Result and Discussions

Introducing the dynamic compensator with the three phase induction motor load the readings were taken and tabulated. Fig 7 shows the hardware implementation of dynamic compensation and table 2 & 3 shows the power factor reading with and without the proposed model.



Fig 7. Hardware Implementation

Table 2
Without Project Model

Line Current (I _L in A)	Line Voltage (V _L in V)	Speed N (rpm)	Wattmeter Readings (Watts)				Spring Balance (kg)		Input Power P _i (Watts)	Torque (Nm)	Output Power P _o (Watts)	% η	% slip	Power Factor	
			W1		W2		Input Power P _i (Watts)	S1							S2
			Observed	Actual	Observed	Actual									
3.3	404	1452	150	1200	30	240	1440	2	9	1440	7.966	1219.6	84.7	2.53	0.624

Table 3

With Project Model

Line Current (I _L in A)	Line Voltage (V _L in V)	Speed N (rpm)	Wattmeter Readings (Watts)				Spring Balance (kg)		Input Power P _i (Watts)	Torque (Nm)	Output Power P _o (Watts)	% η	% slip	Power Factor	
			W1		W2		Input Power P _i (Watts)	S1							S2
			Observed	Actual	Observed	Actual									
3.3	404	1452	225	1800	33	264	2064	2	9	1440	7.966	1219.6	84.7	2.53	0.893

Here MF (Multiplication Factor) is 8.

The formulas used for getting the values are as follows:

$$\text{Torque, } T = (S_1 - S_2) * (r + \frac{t}{2}) * 9.81 \text{ Nm} \quad (1)$$

$$\text{Output Power, } P_o = \frac{2\pi NT}{60} \text{ W} \quad (2)$$

$$\text{Input Power, } P_i = (W_1 + W_2) \text{ W} \quad (3)$$

$$\% \text{ Efficiency, } \eta = \frac{P_o}{P_i} * 100 \quad (4)$$

$$\% \text{ Slip, } S = \frac{(N_s - N)}{N_s} * 100 \quad (5)$$

$$N_s = \frac{120 * f}{p} \text{ rpm} \quad (6)$$

Where f – supply frequency in Hz

P – Number of poles

$$\text{Power factor} = \frac{(W_1 + W_2)}{(\sqrt{3} \cdot V_L \cdot I_L)} \quad (7)$$

From the above table it is proved that the power factor has been improved by injecting the power in the input side with the help of capacitor bank connected through APFC Relay.

4. Conclusion

The proposed model helps in correcting the power factor automatically or through manual control. It can be concluded that the model can also be used in several applications in industries, domestic and power systems. On observing all aspects of power factor it is clear that it is the most notable part for the industrial loads as well as for the domestic consumers. The problems with power factor are not a constant rather than it is varying with respect to the load. In an induction motor during the no load condition the current drawn is high and in addition during that stage the power factor is low in the range of 0.5-0.6. Hence during that stage itself designed device will inject the reactive power generated by the capacitor so that compensating the low power factor and improve it to near unity [5]. Manual process is a tedious process since it is a short time problem which cannot be compensated by manual switching; therefore automatic sensing and switching of capacitor to inject the required reactive power to the load system rather than disturbing the power system. The main application is that the industry is free from the power losses hence it avoids low power factor penalty charges. On installing a suitable sized automatic switching power capacitors into the circuit, the power factor is improved and the values becomes nearer to unity, thus minimizing the line losses and improving the efficiency of the load systems.

REFERENCES

- [1] Dr.S.L.Uppal, “ Electric Power” - Text Book.
- [2] Ravi Dhameliya, Kaushik Domadiya, Pratik Miyani,Hiren Savaliya, Pratik Jariwala “Automatic Power Factor Control Using Arduino Uno”, SJIF-Journal 2017.

- [3] Arun Pundir, Gagan Deep Yadav, “Comparison Of Different Types Of Compensating Devices In Power System”, IRJET Nov-2016.
- [4] Anuja Vijay Patil, Pooja Balkrishna Dhuri, Prachi Prakash Kushe, Pratibha Ashok Mondkar, Suraj Acharekar “Minimizing Penalty In Industrial Power Consumption By Using Apfc Unit” IEEE-Conference 2019.
- [5] Kabir Yasin, Mohsin Yusuf And Khan Mohammad, “Automatic Power Factor Correction And Energy Monitoring System” IEEE 2017.
- [6] Pourya Sarvghadi, Ali Yazdian, Reza Ghazi, “Increasing Redundancy and Cost Reduction to Improve Power Factor and Reduce Harmonic Using Parallel Connection of D-STATCOMs”, EPDC 2018.
- [7] Ajay Lohate, Mandar Chaudhari, “Thyristor Binary Compensator Strategy for Reactive Power Compensation and PF Improvement using Static VAR Compensator”, 2018 International Conference on Recent Innovations in Electrical, Electronics & Communication Engineering (ICRIEECE).
- [8] Adrian Pana, Flavius Dan Surianu, Alexandru Baloi, ” MATLAB simulation applied to study the mechanism of load balancing by unbalanced capacitive shunt compensation in a three-phase three-wire network”, 2011 IEEE EUROCON - International Conference on Computer as a Tool.
- [9] A. Rajabi, H. Monsef, “Valuation of dynamic reactive power based on probability aspects of power system”, 2017 42nd International Universities Power Engineering Conference.

JOURNAL OF REMOTE SENSING GIS & TECHNOLOGY

[HOME](#) [ABOUT](#) [LOGIN](#) [REGISTER](#) [CATEGORIES](#) [SEARCH](#)
[CURRENT](#) [ARCHIVES](#) [ANNOUNCEMENTS](#)

[Home](#) > [Vol 6, No 3 \(2020\)](#) > [Vijayalakshmi](#)

 [Open Access](#)  [Subscription Access](#)

ISLAND MICRO-GRID HEALTH TRACKER SHOES

S. Vijayalakshmi, M. Marimuthu, S. K. Lakshmi, S. Megadharshini Megadharshini, K. Narmada Devi

ABSTRACT

This paper presents an automated wearable technology that is being incorporated into an essential daily accessory, a shoe. This ensures round the clock monitoring of health and activity. Since being self-powered, accuracy and compatibility are the key features of the paper. Harvesting parasitic mechanical as well as thermal energy makes the shoe an island Pico grid that can function effectively.

FULL TEXT:

 [PDF](#)

REFERENCES

Emaus A, Degerstrøm J, Wilsgaard T, Hansen

BH, Dieli- Conwright CM, Furberg AS, Pettersen SA, Andersen LB, Eggen AE, Bernstein L, Thune I. (2010), Does a variation in self-reported physical activity Reflect variation in objectively measured physical activity, resting heart rate, and physical fitness? Results from the Tromso study, Scand J Public Health, DOI: 10.1177/1403494810378919.

World Health Organization (2017), Global Strategy on Diet, Physical Activity, and Health, WHO, Available at: <http://www.who.int/dietphysicalactivity/pa/en> website.

Finkelstein EA, Haaland BA, Bilger M, Sahasranaman A, Sloan RA, Nang EE, Evenson K. R. (2016), Effectiveness of activity trackers with and without incentives to increase physical activity (TRIPPA): a randomized controlled trial, Lancet Diabetes Endocrinol, DOI: 10.1016/S2213-8587(16)30284-4.

Jakicic JM, Davis KK, Rogers RJ, King WC, Marcus MD, Helsel D, Rickman AD, Wahed AS, Belle SH (2016), Effect of wearable technology combined with lifestyle intervention on long-term weight loss: the IDEA randomized clinical trial, J Am Med Assoc, DOI: 10.1001/jama.2016.12858.

Susana Carneiro, Joana Silva, Bruno Aguiar, Tiago Rocha, Ines Sousa, Tiago Montanha and Jose Ribeiro (2015), "Accelerometer- Based Methods for Energy Expenditure using the Smartphone, 2015 IEEE International Symposium on Medical Measurements and Applications (MeMeA) Proceedings, DOI: 10.1109/MeMeA.2015.7145190.

Meethu Malu, Leah Findlater (2016), "Toward Accessible Health and Fitness Tracking for People with Mobility

[OPEN JOURNAL
SYSTEMS](#)

[Journal Help](#)

USER

Username

Password

Remember me

SUBSCRIPTION

[Login to verify
subscription](#)

NOTIFICATIONS

[View](#)
[Subscribe](#)

**JOURNAL
CONTENT**

Search

Search Scope

All

Browse

[By Issue](#)
[By Author](#)
[By Title](#)
[Other Journals](#)
[Categories](#)

FONT SIZE

INFORMATION

[For Readers](#)
[For Authors](#)
[For Librarians](#)

Impairments” PervasiveHealth '16, Available at: <https://dl.acm.org/doi/10.5555/3021319.3021344>.

Joana Silva, Diana Gomes, Francisco Nunes, Dinis Moreira, José Alves, Ana Pereira, Inés Sousa (2018), “Position-independent Physical Activity Monitoring: Development and Comparison with Market Devices” IEEE 2019, DOI: 10.1109/MeMeA.2019.8802140.

Matthew George Pateman (2015), “The design and aesthetics of wearable activity trackers”, Semantic Scholar, Available at: <https://www.semanticscholar.org/paper/The-design-and-aesthetics-of-wearable-activity-Pateman/ff8c8aa9faea38b7d04558629ad6bfd0ba6eed14>.

Bhaskar N. Patel, Satish G. Prajapati, Dr. Kamaljit I. Lakhtaria (2012), “Efficient Classification of Data Using Decision Tree” Bonfring International Journal of Data Mining, Vol. 2, No. 1, Available at: <http://journal.bonfring.org/abstract.php?id=2&archiveid=4>.

REFBACKS

- There are currently no rebacks.
-

USING SOFT COMPUTING TECHNIQUES THE MEASUREMENT OF VOLTAGE STABILITY OF THE POWER SYSTEM

Dr. M. V. Suganyadevi

Associate Professor, Department of Electrical and Electronics Engineering,
Saranathan College of Engineering, Trichy- 12, India

Perumal Raja. S, Pradeep. P, M. Vasanth, M. Viswanathan

UG Scholar, Department of Electrical and Electronics Engineering,
Saranathan College of Engineering, Trichy- 12, India

ABSTRACT

In this paper we propose measurement based voltage stability using different soft computing technique for estimating the output data of the voltage stability margin. In the conventional method of monitoring of the voltage stability limits of the power system through different lines to busses consumes more time to get the desired values for the analysis. In this method we use some of the optimization techniques such as Support Vector Regression (SVR), Artificial Neural network (ANN) to obtain more specific results in a limited time frame. We use IEEE 30-bus system for testing.

Keywords: Voltage stability assessment, PSAT, CPF, ANN, ANFIS, SVR, Voltage stability limits

Cite this Article: Dr. M. V. Suganyadevi, Perumal Raja. S, Pradeep. P, M. Vasanth and M. Viswanathan, Using Soft Computing Techniques the Measurement of Voltage Stability of the Power System, *International Journal of Electrical Engineering & Technology*, 11(3), 2020, pp. 32-39.

<http://iaeme.com/Home/issue/IJEET?Volume=11&Issue=3>

1. INTRODUCTION

Electric power system has become more complex and larger. Power system components operate very much closer to their stability limits, with the small security margin. In case of occurrence of any type of fault or disturbance in generator, transmission line, transformer can lead to voltage instability [1]. These changes of the operating limit of the electrical parameter increases such that they cannot be controlled by corrective devices used in control system parameter. When power quality problems occurring in a system causing decrease in voltage level of the system or sag, gradual increase or swell that occurs in the system under heavily loaded system. Some well-known example of voltage instability accidents such as German, Sweden, Belgium, Japan, USA [2] [3].

The problem of voltage stability in the power system is due to the increased loading of power system components causing drop in voltage from their unity per unit values. The paper done by some new indices for voltage stability margin are introduced and demonstrated using continuation load flow in IEEE 30 Bus along with new voltage stability indices are proposed [4]. The usage of voltage stability indices helps to rectify these problems where the change of the parameter involved are indicated by the values ranging from zero to one if the system is stable state.

In 2012 the paper on Determination of Voltage Stability in Distribution Network Using ANN Technique that simplifies the voltage stability level that are indicated by voltage stability indices using two stages of switching process which includes local and global searches for achieving required network configuration using Artificial Neural Network (ANN) on 11 kV radial distribution network with 52 buses to achieve the best voltage stable condition of the system [5]

Voltage stability margin are done to by Kernel Extreme Learning Machine (KELM) which takes in account of different operative conditions for three different type of customers (residential commercial and industrial) using IEEE 39 bus power system where the performance of different soft computing technique such as support vector machine (SVM) and an Artificial Neural Network (ANN) approach with which the proposed [6].

The voltage stability margin calculation is done using network reduction algorithms for estimation of accuracy in a multi area system using Artificial Neural network with the help of IEEE 14 and 118 Test bus systems [7]

The application of ANN for stability assessment of voltage in IEEE 57 Bus System with the help of Matlab Environment to overcome the difficulties faced in Static and Dynamic Security Assessment in Power System [8]

In the recent past, and support vector regression (SVR) developed from support vector machine (SVM), an artificial intelligence (AI) that is based on the superior structural risk minimization (SRM) principle which provides a lot of advantages over the traditional techniques ANN ANFIS technique for providing advantages like unique, global and optimal solution [9].

In 2020 the Voltage collapse point) proposed a prominence with the voltage stability parameters as dependent variable and loading at consumer for both constant loads as well as voltage dependent loads as independent variable as introducing the term collapse point. This paper also deals with the Load modeling considering optimal power flow [10]

2. VOLTAGE STABILITY INDICES

The necessity of the Voltage Stability Indices is to find out the voltage stability margin point in the locus of the loading in the continuous power flow curve where loading above the critical which the system stability is collapsed. The different parameters of VSI that shows the margin of stability are discussed. Voltage stability.

2.1. Line Voltage Stability Indices

2.1.1. Line stability index

This index derived by M.Moghavemmi ET [11] proposes that the whole range of stability parameters could be stated with the help of Thevenin equivalent model representing the equivalent source and reactance of the whole power system where the equivalent value of voltage quadratic equation between zeros to one for the system to be stable.

The Line stability index is defined as

The Line stability index is defined as

$$L_{mn} = \frac{4xQ_j}{[V_j \sin(\theta - \delta)]^2} \quad (1)$$

$V_i V_j$ - Voltage on sending and receiving busses

$P_i Q_i$ -Active and reactive power on the sending buses

$P_j Q_j$ -Active and reactive power on the receiving buses

$S_i S_j$ -Apparent power on the sending and receiving busses

$\delta_i - \delta_j = \delta$ -Angular difference between the sending and receiving end busses.

Where, Until the stability indices remain less than unity the system is said to be in state of equilibrium and when the values becomes greater than the margin of stability the system is in the state of instability.

2.1.2. Line Stability Factor [LQP]

A. Mohamed et al [12] proposed these indices based on single line. LQP can be calculated based on both real and reactive power. It is defined as,

$$LQP = 4 \left[\frac{X}{V_i^2} \right] \left[\frac{X}{V_i^2} P_i^2 + Q_j \right] \quad (2)$$

Where P_i and Q_i values that are calculated from nominal load flow calculation along with maximum real and wattles power that can be transmitted through the system

2.1.3. Fast Voltage Stability Index

The FVSI indices proposed by I.Musirin et al [13] the calculates the margin ability up to which the loading of the receiving end till the system needs to be stable which can be determined how the value of indices are closer to unity values. As the parameter varies inversely to the square of generator voltage, the parameter changes very fast. Hence knowns as Fast Voltage Stability Index.

If the value is much lesser than unity the system stability can be ensured for a large range of voltage loading.

$$FVSI = \frac{4Z^2 Q_j}{V_i^2 X} \quad (3)$$

2.1.4. Voltage collapse Proximity Index [VCPI]

The voltage collapse Proximity index referred as VCPI was proposed by M.Moghavvemi et al [14] states that the stability of the transmission line of the system can be indicated on the concept of steady state stability limits of power transmission over the line of consideration

Where P_i and Q_i values that are calculated from nominal load flow calculation along with maximum real and wattles power that can be transmitted through the system

$$VCPI_{(1)} = \frac{P_j}{P_{j(max)}} \quad (4)$$

$$VCPI_{(2)} = \frac{Q_j}{Q_{j(max)}} \quad (5)$$

2.1.5. On Line Voltage stability Index [LVSI]

Online voltage stability index is stated in the way to establish the link between line real and reactive power and the bus voltage can be transmitted. The value of indices varies from zero to unity from no load to full load

$$LVSI = -\frac{4P_j r}{[V_i \cos(\theta - \delta)]^2} \leq 1.0 \quad (6)$$

3. SUPPORT VECTOR REGRESSION (SVR)

Support Vector Machine (SVM) is based on statistical learning theory and structural risk minimization. It is effectively computation technique due to this performance in solving classification and regression problem. Support Vector Regression (SVR) is the regression version of SVM which has widespread form of application. SVR is used to evaluate voltage stability of power system in flexible Ac transmission system was introduces by Suganyadevi and Babulal [12].

Support Vector Regression (SVR), the extended version of SVM was initilly suggested by Vapnik. It has become a paramount computational tool due to its effective application in regression and prediction problems.

4. TEST SYSTEM AND ANALYSIS TOOLS

4.1. Test System

The Simulation model of IEEE 30 bus system which contains 6 generator bus bars, 24 load bus bars, 47 transmission lines. A bus in a power system is defined as the vertical line at which the several components of the power system like generators, loads, and feeders are connected. The buses in a power system are associated with four quantities. These quantities are the magnitude of the voltage, the phase angle of the voltage, active or true power and the reactive power. The effort to do this study is to find out the possibility of voltage falling out of step by comparing the different parameters with the standard prescribed to withstand voltage stability. They produced with the help of stability in parameters in PSAT with the help of which the values are compared. This were done as offline part. In online part we use Artificial Neural Network (ANN), Adaptive Neuro fuzzy Interference system (ANFIS), Support Vector Regression (SVR) were done to estimate voltage stability. The Offline inputs were given to online program modules computes better result of margin of stability with lesser computational time.

4.2. Power System Analysis Toolbar (PSAT)

Dr. Federico Milano developed free and open-source software tool for power system analysis and modelling, namely Power System Analysis Toolbox (PSAT) for Mat lab and GNU/Octave. PSAT is a MATLAB based package. It runs on the commonest operating system. Power system analysis tollbar were used to quickly solve the nonlinear load flow problem and calculate short circuit current. It can perform several power systems analyses such as Continuation power flow (CPF), Optimal, power flow (OPF), Small signal stability analysis, Time domain simulation. In order to perform accurate and complete power system analysis, PSAT supports a variety of static and dynamic models. Dynamic model includes the non-conventional synchronous machines and controls. It creates bridge between the mat lab and other specialized software package. We are using the MATLAB R-2013a version to determine the voltage stability by using the IEEE-30 bus.

5. RESULT AND DISCUSSION

In this project MATLAB R2013 is used to predict the various voltage stability indices for both online and offline methods. The MATLAB was installed and the result was observed in the HP. laptop that as Windows 10 Education OS, 8GB RAM, INTEL i5 8th gen processor with 1.80 GHz speed and 1TB internal storage drive.

There are two methods online and offline method are used to find the voltage stability. In IEEE 30 bus system there having 24 load bus and 6 generator bus bars. In the offline method the real , reactive and both real and reactive values are changed separately in the 26th bus to find the particular Continuous Power Flow (CPF) value in that total 1000 values are obtained V, λ, δ, P, Q .

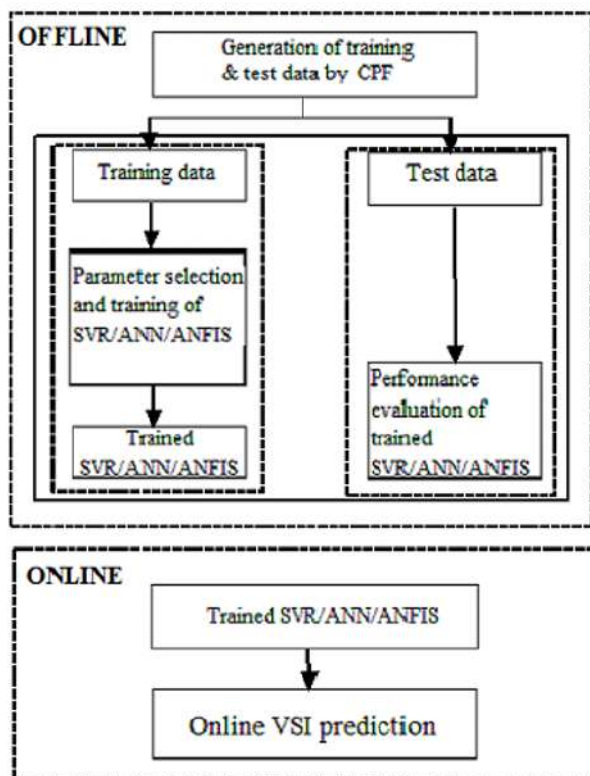


Figure 1 Flow chart of loadability margin estimation

Table 1 Real Load Increased: Lines Indices

Loading (p.u)	line	L_{mn}	FVSI	LVSI	LQP	VCPI _(P)	VCPI _(Q)
P	1	1.2329	0.8434	0.0928	0.8546	0.8012	0.8012
	5	2.4989	1.3963	0.9865	1.3904	0.7835	0.7835
	39	0.2099	0.1604	0.7639	0.1321	0.6022	0.6022
	31	0.3109	0.2938	0.524	0.2079	0.3933	0.3933
	32	0.4166	0.4082	0.9996	0.3972	0.5698	0.5698

The offline method obtained 1000 values that contains V, λ, δ, P, Q . In V, δ, P, Q the 1st 600 data are taken as input training data and other 400 are taken as testing output data. In λ the 1st 600 data are taken as training output data and other 400 data are taken as output data. The 600 training input data of V, δ, P, Q and training output data of λ are given to the ANN, ANFIS and SVR given as input data. The output data of the ANN ANFIS and SVR are compared with the remaining 400 data of the λ that certain output values are compared with the remaining 400 data of the λ . In this process the error lies between $10^{-3} - 10^{-5}$ when comparing the output of the online and offline method. The obtained error compared with the ANN ANFIS and SVR. This process concluded that the SVR having minimum error and less process time when compared to the others.

Table 2 Various Load Increased scenario Vs Lines Indices

Loading (p.u)	line	L _{mn}	FVSI	LVSI	LQP	VCPI _(P)	VCPI _(Q)
Q	1	1.2539	0.8542	0.0919	0.865	0.811	0.811
	5	2.5042	1.3973	0.9812	1.3911	0.7794	0.7794
	32	0.4223	0.4113	0.9855	0.401	0.5742	0.5742
	38	0.1831	0.1152	0.5276	0.0852	0.4645	0.4645
	39	0.2269	0.1697	0.7964	0.1427	0.6373	0.6373
P&Q	1	1.2948	0.8749	0.0924	0.8849	0.8306	0.8306
	5	2.6276	1.4392	0.9792	1.4319	0.7906	0.7906
	38	0.1751	0.1127	0.5262	0.0834	0.4542	0.4542
	39	0.2153	0.1634	0.7744	0.1347	0.6134	0.6134
	32	0.4276	0.4185	1.021	0.408	0.5842	0.5842

The Table 4 & 5 shows the training Time and for various C in the ϵ -SVR with RBF Kernel for IEEE 30 bus test system. The capacitance value are should varies according to value that as less to the training time that as to near to the 1 are preferred. Fig 6 represent the Testing MSE and Gamma values for various C in the ϵ -SVR with RBF Kernel for IEEE 30 bus test system as same as the minimum value are taken. Fig.7 shows the Comparison of ϵ -SVR, ν -SVR and ANN with CPF for IEEE 30 test bus system the minimum value are compared with the final output

Table 5 Estimating load ability margin in terms of MSE and time for two types of SVR with different c, γ values of poly kernel type for IEEE 30 bus type

SVR Types	C=1			C=10			C=100			C=1000		
	γ	Time	MSE	γ	Time	MSE	Γ	Time	MSE	γ	Time	MSE
ν -SVR	0.1	8.5169	1.8618	0.1	37.81471	3.19794	0.1	134.838	4.36155	0.1	53.2295	5.5594
	0.2	15.161	2.1176	0.2	139.7339	5.49493	0.2	166.355	5.80031	0.2	420.425	14.218
	0.5	29.951	2.6992	0.5	95.38272	9.77581	0.5	247.571	21.3361	0.5	257.390	19.726
	0.8	56.769	3.2977	0.8	168.1091	10.1435	0.8	238.821	50.9331	0.8	311.414	66.082
ϵ -SVR	0.1	0.1133	1.2682	0.1	18.122101	1.23445	0.1	19.15214	1.25479	0.1	45.976	3.1022
	0.2	0.2655	1.2919	0.2	22.895304	1.46322	0.2	29.993	4.8953	0.2	56.709	10.41
	0.5	0.7083	1.4446	0.5	54.342372	1.8136	0.5	100.6473	2.00475	0.5	134.98	12.098
	0.8	2.9350	1.5668	0.8	83.95402	1.83973	0.8	127.468	2.99824	0.8	187.33	13.671

Table 6 Comparison results of ANFIS, ϵ -SVR and ANN

Bus System	Parameters	ANFIS	ϵ -SVR	ANN
IEEE 30	Training Data	28800	28800	28800
	Testing Data	7200	7200	7200
	Computational Time	1.4509	0.9737	2.306
	Training Average Error	0.0098	0.00732	0.0183
	Testing Average Error	0.015	0.0026	0.018

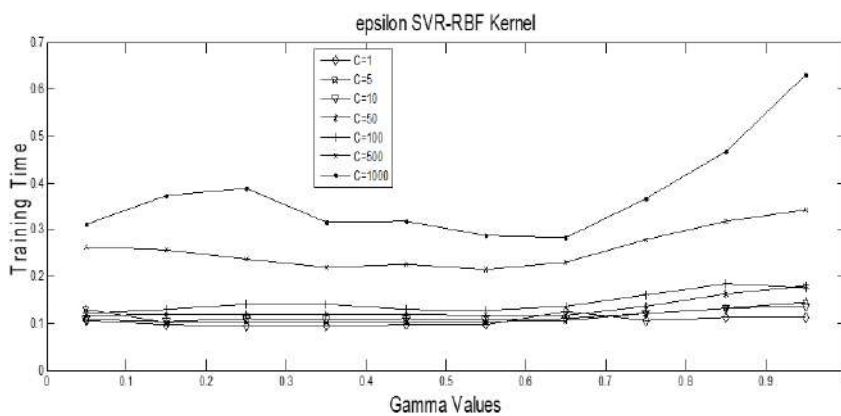


Figure 2 Training Time and Gamma values for various C in the ϵ -SVR with RBF Kernel for IEEE 30 bus test system

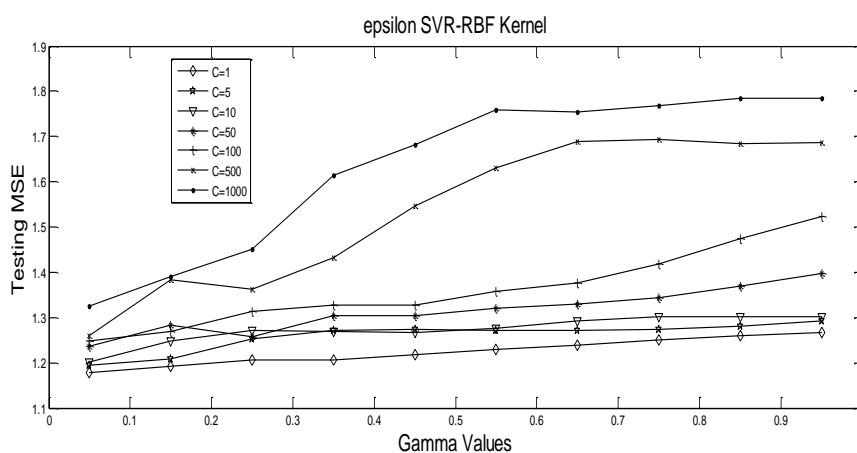


Figure 3 Testing MSE and Gamma values for various C in the ϵ -SVR with RBF Kernel for IEEE 30 bus test system

6. CONCLUSION

The estimation of voltage stability limits of a power system is not a simple process. It is a complicated task which takes a huge amount of time. The traditional method has their own disadvantages mainly of being very time consuming and accuracy. When compared to the traditional method the soft computing technique significant improvement in error $10^{-3} - 10^{-5}$ and the duration.

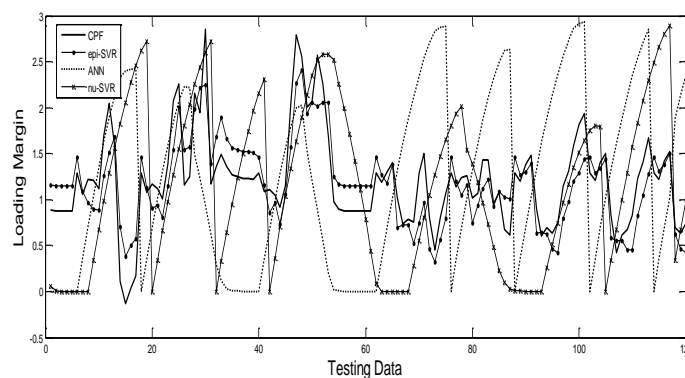


Figure 4 Comparison of ϵ -SVR, v-SVR & ANN with CPF for IEEE 30 test bus system

REFERENCES

- [1] IEEE Task Force on Blackout Experience, Mitigation, and Role of New Technologies, Blackout Experiences and Lessons, Best Practices for System Dynamic Performance, and the Role of New Technologies, IEEE, Technical Report. Special Publication 07TP190 (2007)
- [2] P. Kundur "Power System Stability and Control" Mc Graw Hill, New York, 1994. Tools and Industry Experience", IEEE Committee Vol. IEEE/PES 93TH0358-2-PWR 19
- [3] Neerugattu, et.all "New criteria for voltage stability evaluation in interconnected power system." In Nat. Power Syst. Conf. 2012.
- [4] Kayal, Partha, Sayonsom Chanda, and C. K. Chanda. "Determination of Voltage Stability in Distribution Network Using ANN Technique." International Journal on Electrical Engineering and Informatics 4, no. 2 (2012): 347.
- [5] Villa-Acevedo, W.M., López-Lezama, J.M. and Colomé, D.G., 2020. Voltage Stability Margin Index Estimation Using a Hybrid Kernel Extreme Learning Machine Approach. *Energies*, 13(4), p.857.
- [6] Ashraf, et.all 2017. Voltage stability monitoring of power systems using reduced network and artificial neural network. *International Journal of Electrical Power & Energy Systems*, 87, pp.43-51
- [7] Tiwary, S.K. and Pal, J., 2017, October. ANN application for voltage security assessment of a large test bus system: A case study on IEEE 57 bus system. In 2017 6th International Conference on Computer Applications in Electrical Engineering-Recent Advances (CERA) (pp. 332-334). IEEE.
- [8] Sanchez, Z.G., et all, 2020. Voltage Collapse point evaluation considering the load dependence in a power system stability problem. *International Journal of Electrical & Computer Engineering* (2088-8708)10.
- [9] M.Moghavvemi, F.M.Omar "Technique for Contingency Monitoring and Voltage Collapse Prediction" IEEE Proceeding on Generation, Transmission and Distribution, Vol. 145, N6, pp. 634-640 November 1998
- [10] Suganyadevia, M. V., and C. K. Babulalb. "Estimating of loadability margin of a power system by comparing Voltage Stability Indices." In 2009 International Conference on Control, Automation, Communication and Energy Conservation, pp. 1-4. IEEE, 2009.
- [11] I.Musirin, T.K.A.Rahman "Novel Fast Voltage Stability Index (FVSI) for Voltage Stability Analysis in Power Transmission System" 2002 Student Conference on Research and Development Proceedings, Shah Alam, Malasia, July 2002.
- [12] Suganyadevi, M. V., et.all "Support vector regression model for the prediction of loadability margin of a power system." *Applied Soft Computing* 24, 2014, 304-315
- [13] B. Suresh Kumar, Enhancement of Voltage Stability Using Static Synchronous Series Compensator (SSSC) With Pi Controller-Lllg Fault, *International Journal of Advanced Research in Engineering and Technology (IJARET)*, Volume 4, Issue 5, July – August (2013), pp. 164-175.
- [14] Mrs. K. Sree Latha and Dr. M. Vijaya Kumar, FLC Based Statcom For A DFIG Driven Wind Turbine to Enhance Voltage Stability, *International Journal of Electrical Engineering & Technology (IJEET)*, Volume 6, Issue 6, June (2015), Pp. 35-43.
- [15] Ibrahim A. Murdas and Riyad A. Alalwany, Wireless on Line Solution to Voltage Stability Problem of Electrical Power System Using Field Programmable Gate Array (FPGA) Circuit, *International Journal of Advanced Research in Engineering and Technology (IJARET)*, Volume 5, Issue 2, February (2014), pp. 109-120.
- [16] Vasily Germanovich Chirkin, Nikolay Anatolyevich Khripach, Dmitry Anatolyevich Petrichenko and Boris Arkadyevich Papkin, A Review of Battery-Supercapacitor Hybrid Energy Storage System Schemes for Power Systems Applications, *International Journal of Mechanical Engineering and Technology* 8(10), 2017, pp. 699–707.

Modified Multi Input Multilevel DC-DC Boost Converter for Hybrid Energy Systems



Ram Prakash Ponraj, Devadharshini Ganeshprabhu, Haripriya Balaji, Hemadharshini Ganesan, Keerthana Dhanabalan

Abstract: DC-DC converters are playing an important role in designing of Electric Vehicles, integration of solar cells and other DC applications. Contemporary high power applications use multilevel converters that have multi stage outputs for integrating low voltage sources. Conventional DC-DC converters use single source and have complex structure while using for Hybrid Energy Systems. This paper proposes a multi-input, multi-output DC-DC converter to produce constant output voltage at different input voltage conditions. This topology is best suitable for hybrid power systems where the output voltage is variable due to environmental conditions. It reduces the requirement of magnetic components in the circuit and also reduces the switching losses. The proposed topology has two parts namely multi-input boost converter and level-balancing circuit. Boost converter increases the input voltage and Level Balancing Circuit produce Multi output. Equal values of capacitors are used in Level Balancing Circuit to ensure the constant output voltage at all output stages. The operating modes of each part are given and the design parameters of each part are calculated. Performance of the proposed topology is verified using MATLAB/Simulink simulation which shows the correctness of the analytical approach. Hardware is also presented to evaluate the simulation results.

Keywords : DC-DC converter, Multi input Multi output (MIMO), PWM technique, wide-input range, level-balancing, hybrid energy systems.

I. INTRODUCTION

Availability of fossil fuels depleted and the price increases over the years. Increasing demand thrive the studies on alternate energy sources. Renewable energy sources are found to be the right alternate for the fossil fuels and available

abundant in nature. New methodologies have been introduced over the past years to increase the stake of the renewable energy sources and also to meet the increasing power demand. Inverters and Converters were widely used however choppers had less attention in power conversion in spite of used virtually in all power conversion processes [1]. At the present time, due to Electric Vehicles and of various advantages like low harmonics and low EMI DC-dc converters are gathering attention and the use of DC-DC converters are burgeoning [2].

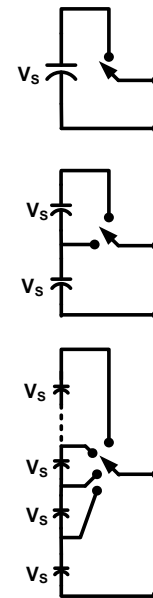


Fig.1. Basic DC-DC conversion system

Choppers also use less magnetic components that decrease the complexity of the circuit and overall manufacturing cost [3]. But the DC-DC converters have more voltage balancing problems compared to converters and inverters [4]. Most of the renewable energy sources are not being used throughout the year and their utilization is limited. By using multiple sources; normally renewable energy sources, hybrid power systems increase the reliability and utilization of renewable energy sources [5].

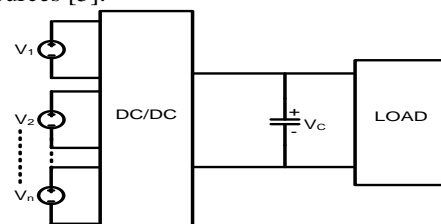


Fig.2. DC-DC converter system with multiple sources

Revised Manuscript Received on April 12, 2020.

* Correspondence Author

Ram Prakash Ponraj*, is currently working as Assistant Professor in Department of Electrical and Electronics Engineering in Saranathan College of Engineering, Tiruchirapalli, India. PH-+919487676423. E-mail: gprsahara@gmail.com

Devadharshini Ganeshprabhu, is currently pursuing her Bachelor degree in Electrical and Electronics Engineering in Saranathan College of Engineering, Tiruchirapalli, India.

Haripriya Balaji, is currently pursuing her Bachelor degree in Electrical and Electronics Engineering in Saranathan College of Engineering, Tiruchirapalli, India.

Hemadharshini Ganesan, is currently pursuing her Bachelor degree in Electrical and Electronics Engineering in Saranathan College of Engineering, Tiruchirapalli, India.

Keerthana Dhanabalan, is currently pursuing her Bachelor degree in Electrical and Electronics Engineering in Saranathan College of Engineering, Tiruchirapalli, India.

© The Authors. Published by Blue Eyes Intelligence Engineering and Sciences Publication (BEIESP). This is an open access article under the CC BY-NC-ND license (<http://creativecommons.org/licenses/by-nc-nd/4.0/>)

Contemporary applications like Electric Vehicle also require multiple DC voltages and uses Multiple Input and Multiple Output (MIMO) choppers [6]. Basic multiple input DC converter structure is given in Fig.1 and Fig.2. In these structures, output voltage is the sum of all input voltages [7]. These type of converters used in Distributed generations and high voltage applications due to their simple structure, less volume, less switches and magnetic components [8]. These converters are categorized in to three major categories such as magnetic, Electrical and Electromagnetic type [9]. Earlier days the inputs are connected in parallel to develop a multi-input DC-DC converter. Modern topologies use many configurations to create multiple inputs [10,11]. These topologies use high energy rating capacitors to reduce stress on components and inductor, ripple in the input current and to achieve high effective switching frequency [12,13]. To reduce the effect of capacitors and inductors in increasing the input and output voltages, many inputs are connected in series through semiconductor switches. Output voltage of these converters is the sum of input voltages and these converter reduce the effect of magnetic components in the circuit also [14,15]. The important contemporary applications of these converters are Electric Vehicle for torque ripple reduction [16,17] and Multi-level Inverter circuits [18]. From the manuscripts cited above, this article proposes a novel DC-DC converter topology with multiple inputs and multiple outputs. A General structure of the proposed topology also presented. Performance of the converter is verified using simulation and Hardware implementation.

II. BASIC MODULES

The Basic module of Multi-input DC converter is presented in Fig.2. It uses ‘n’ number of sources in which each source connected in series with a switch. If the switch is ‘ON’ then the sources is connected with the circuit. If the switch is ‘OFF’ then the source is not connected in the circuit and bypassed using a diode connected in parallel.

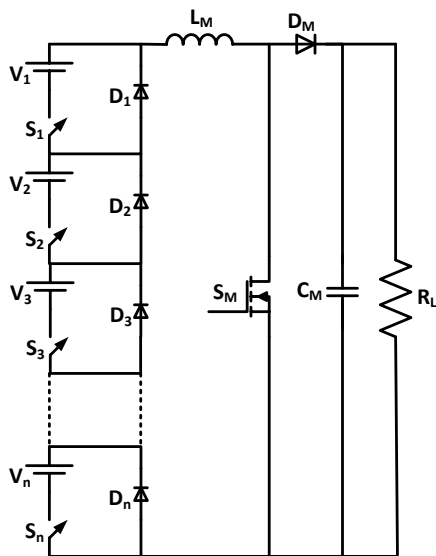


Fig.3. General structure of Multi input DC-DC Converter System

The double input structure derived from Fig.3, is given in Fig.4. It uses two sources connected in series with the switches. Each module is connected with a bypass diode to bypass the current when the source is not connected. The

inputs are connected with a normal boost converter comprising of an Inductor L_M , Switch S_M and capacitor C_M . Entire setup is connected with a load R_L .

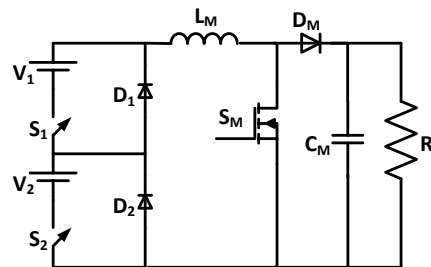


Fig.4 Double input boost converter topology

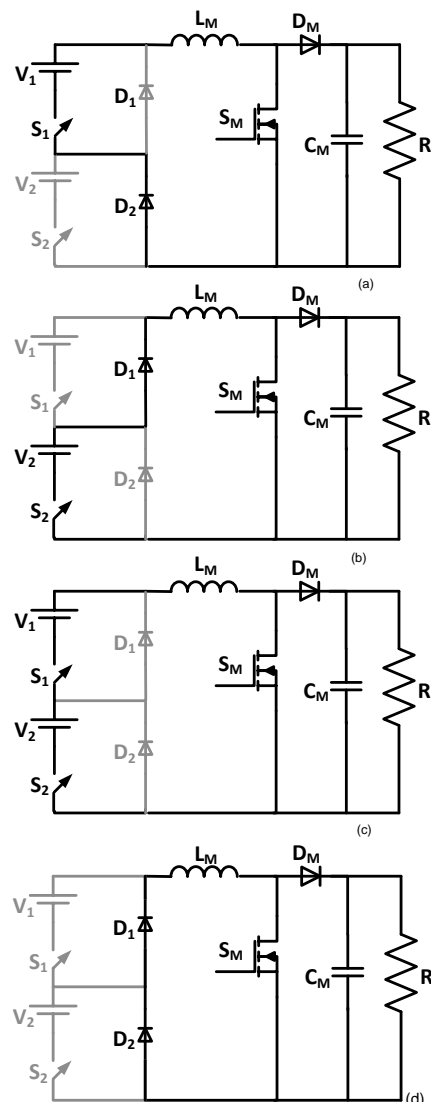


Fig.5. operation of boost converter when a) S_1 ON b) S_2 ON c) both S_1 and S_2 ON d) Both inputs are OFF

Fig.5.a shows the operation of the topology when V_1 alone is supplying power to the Load. The load voltage is described by the switching angle of S_M and input V_1 alone. V_2 is in OFF condition and it is bypassed through the diode D_2 .

Fig.5.b shows the operation of the topology when V_2 alone is supplying power to the Load. The load voltage is described by the switching angle of S_M and input V_2 alone. V_1 is in OFF condition and it is bypassed through the diode D_1 .

Fig.5.c shows the operation of the topology when both V_1 and V_2 are supplying power to the Load. Now the load voltage is described by the switching angle of S_M and sum of inputs V_1 and V_2 . No bypass diodes are conducting at this mode.

Fig.5.d shows the operation of the topology when both inputs are OFF. Now, Inductor L_M starts discharging through the load R_L or through the Switch S_M and the loop closed through the bypass diodes D_1 and D_2 .

A. Design of Basic Module

The duty cycle of the boost converter used in the system is calculated for the output voltage V_o and the maximum input voltage of $n \cdot V_s$ as,

$$\text{Duty cycle } D = 1 - \frac{n \cdot V_s}{V_o} \tag{1}$$

$$\text{Output Voltage } V_o = \frac{n \cdot V_s}{(1-D)} \tag{2}$$

Where n is the number of input sources. The minimum value of inductance L_{LOW} and Capacitance C_{LOW} are,

$$L_{LOW} = \frac{D(1-D)^2 R_L}{2f} \tag{3}$$

$$C_{LOW} = \frac{D}{R_L \cdot A_r \cdot f} \tag{4}$$

The ripple voltage with respect to the output voltage is taken as,

$$A_{ripple} = \left(\frac{\Delta V_o}{V_o} \right) \tag{5}$$

The determined value of load current and the change in load current value is given by,

$$I_{L,high} = \frac{n \cdot V_s}{(1-D)R_L} \tag{6}$$

$$\frac{\Delta I_L}{2} = \frac{V_s D T}{2L_M} \tag{7}$$

Where, V_s – source voltage, f – switching frequency and R_L – Load impedance. Ripple Voltage A_{ripple} is considered as 0.5% of the output voltage

III. PROPOSED CONVERTER MODULE

The proposed DC converter is shown in Fig.6. It consists of a multi input boost converter and a level balancing circuit. Multi input boost converter was already discussed in previous chapter. The level balancing circuit consists of two diodes D_1, D_2 , a voltage balancing capacitor C_A and a voltage level shifting capacitor C_1 .

The overall load of the proposed network includes the resistance of Load R_L , Internal Resistance of each switch R_{SW} and the internal Resistance of each diode R_{diode} at forward bias condition.

$$R_{L,max} = R_L + 2 \cdot R_{SW} + 3 \cdot R_{diode} \tag{8}$$

Since the internal resistance of the switches and diode is negligible, then (8) would be restated as

$$R_{L,max} = R_L \tag{9}$$

The Voltage across each capacitor is equal to the input voltage V_{DC} . So the overall output voltage across the capacitor C_M is,

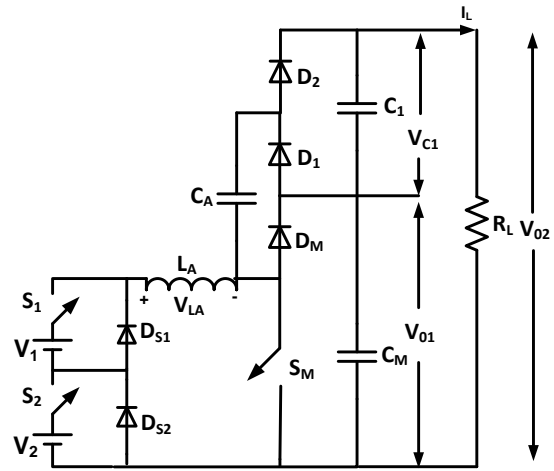
$$V_{o1} = \frac{2V_s}{(1-D)} \tag{10}$$

Since the input voltage of the self-balancing circuit is the output of the boost converter, then the output voltage of the level-balancing circuit is,

$$V_{o2} = V_{C1} = 2 \cdot V_{o1} = \frac{4V_s}{(1-D)} \tag{11}$$

The load current I_L is calculated for the proposed inverter from (2) – (6) and is given by,

$$I_{L,high} = \frac{4 \cdot V_s}{(1-D)R_L} \tag{12}$$



MULTI INPUT BOOST CONVERTER LEVEL BALANCING CIRCUIT
Fig.6. Proposed DC/DC Boost Multi-level Converter circuit

Various operating modes of proposed DC-DC converter is given in Fig.7. It shows the output and input voltages at various conditions. It also shows the output current and inductor current at various time periods.

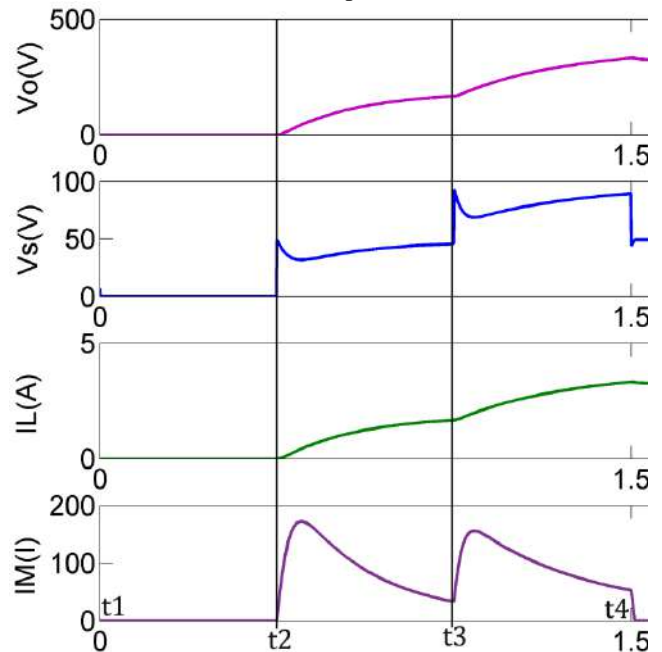


Fig.7. Circuit parameters at various operating modes

At operating mode 1 ($t_1 - t_2$): Both inputs are OFF which is shown in Fig.8(a). The magnetic components are discharging through the diodes D_{S1} and D_{S2} . The input voltage is $V_s = 0$ and the output of boost converter is also zero. Take the inductor is charged at a value of I_{M1} .

At operating mode 2 ($t_2 - t_3$): Shown if Fig.8(b) at which any of the two inputs V_1 and V_2 is ON and the input voltage is $V_s = V_1$ or V_2 . Output voltage of the boost converter is described from (10) and is given by,

$$V_{o1} = \frac{V_s}{(1-D)} \tag{13}$$

Capacitors C_1 and C_2 start charging and the output voltage start increasing. Inductor also starts charging, take initial value of inductor current as I_{M1} and the new value of inductor current I_{M2} at time t_3 is,

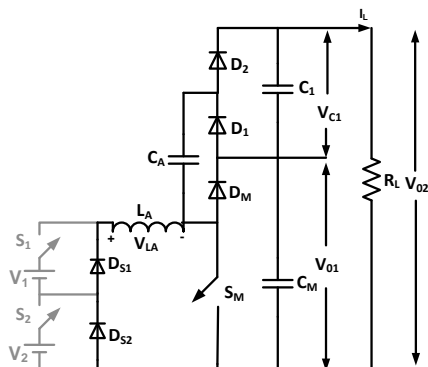


Fig.8(a) Operating mode-1 of proposed topology

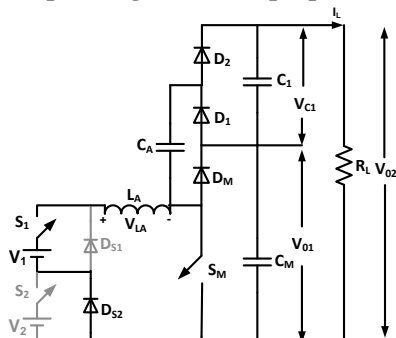


Fig.8(b) Operating mode-2 of proposed topology

$$I_{M2} = I_{M1} + \frac{1}{L} \int_{t_2}^{t_3} V_{LA} dt = I_{M2} + \frac{1}{L} V_{LA}(t_3 - t_2) \quad (14)$$

Since $V_{LA} = V_S = V_1 = V_2$,

$$I_{M2} = I_{M1} + \frac{V_S}{L} (t_3 - t_2) = I_{M1} + \frac{V_1}{L} (t_3 - t_2) \quad (15)$$

At operating mode 3 ($t_3 - t_4$): Both inputs are ON and the input voltage is $2V_S = V_1 + V_2$ and the topology at this operating mode is shown in Fig.8(c). Output of boost converter is described the duty cycle of the Switch S_M and the value is given by (10). Take initial value of inductor current as I_{M1} and the new value of inductor current I_{M2} at time t_2 is,

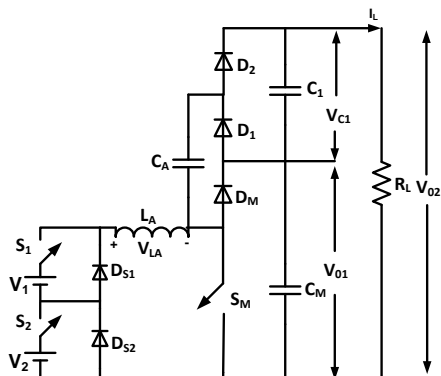


Fig.8(c) Operating mode-3 of proposed topology

$$I_{M3} = I_{M2} + \frac{1}{L} \int_{t_3}^{t_4} V_{LA} dt = I_{M2} + \frac{1}{L} V_{LA}(t_4 - t_3) \quad (16)$$

Since $V_{LA} = V_1 + V_2 = 2V_S$,

$$I_{M3} = I_{M2} + \frac{2V_S}{L} (t_4 - t_3) = I_{M2} + \frac{2V_1}{L} (t_4 - t_3) \quad (17)$$

Overall output voltage across load R_L is given by (11) and the load current is given by (12).

By comparing multiple input multiple output (MIMO) topologies presented in [19-21] and [15], it states that proposed topology requires less number of magnetic components and switches. Table 1 summarizes the comparison of proposed topology and conventional topologies in view of inductor and switch requirement.

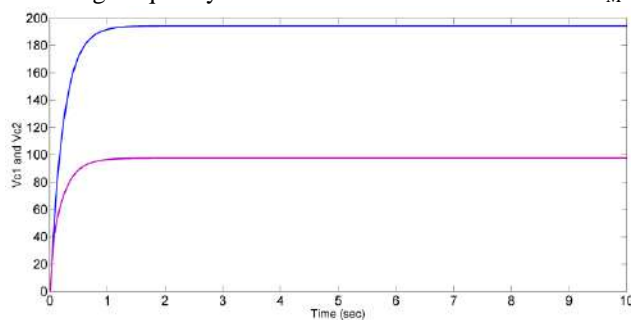
Table.1. comparison of topologies with component requirement

	$N_{DC \text{ SOURCES}}$	$N_{INDUCTORS}$	$N_{SWITCHES}$
Proposed topology	n	1	n+1
Topology in [19]	n	1	m
Topology in [20]	m	1	n+m
Topology in [21]	m	m	m^2
Topology in [15]	n	1	n+1

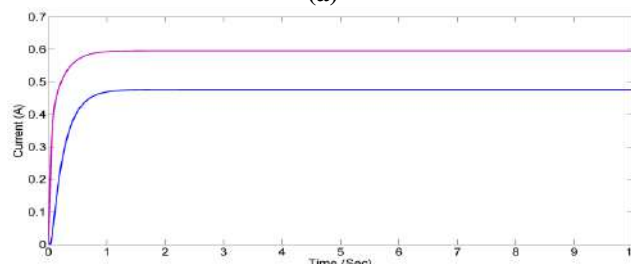
Topology [21] requires ‘m’ number of inductors for multi-stage output which increases complexity of the circuit. Proposed topology requires less number of switches compared to [19] and [20]. This decreases cost, volume and deriver requirement. Topology [15] requires same number of components but it requires asymmetric input voltages to get multi-stage output.

IV. SIMULATION AND HARDWARE RESULTS

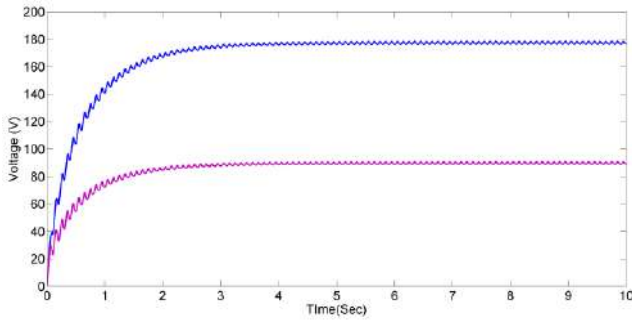
Performance of the proposed topology is evaluated with the Simulation and Hardware. Simulation has been carried out using Matlab/Simulink R2014a and the results are presented in Fig.9. Simulation was carried out for an input voltage of 50V. The load values of 50Ω and 25Ω are considered for full load and half load conditions respectively. The inductor value has been chosen as 8mH and the capacitor values at both the stages are made equal at a value of 89μF. Switching frequency of 10kHz is chosen for the switch S_M .



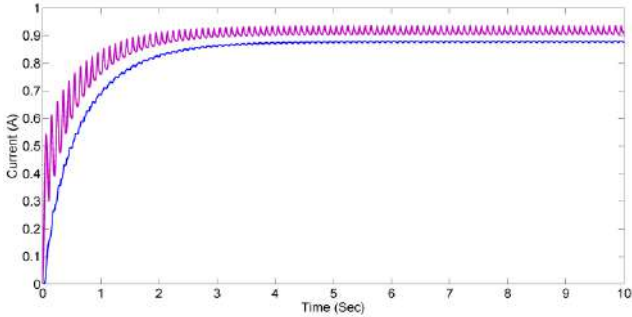
(a)



(b)



(c)



(d)

Fig.9. a)- d) Output Voltage and Current waveforms at different load conditions

Fig.9.a describes the output voltage V_{02} which is around 192 V for an input of 50V. Voltage across C_M (V_{01}) is 96 V which is exactly half of the load voltage. Fig.8.b. shows the load current I_L and current due to voltage V_{01} at half load conditions. It shows the load current of 0.6A and current of 0.45A due to voltage V_{01} at half load is used across it. Fig.8.c shows the output voltage V_{02} of 165V and capacitor Voltage V_{01} of 82V at half load condition (25Ω). Fig.8.d shows the current values at half load condition.

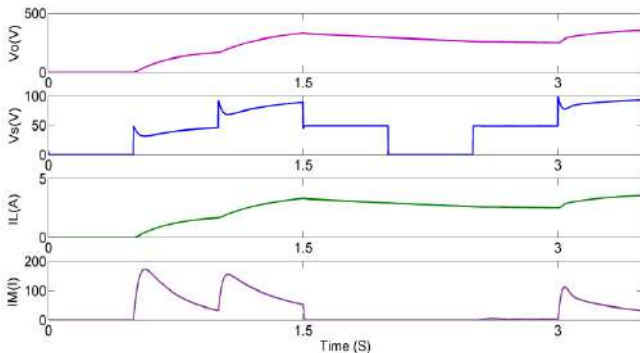


Fig.10 Performance parameters of proposed topology at various inputs

Simulation diagrams clearly describe that the output voltage V_{02} is twice as the capacitor voltage V_{01} as stated in (10) and (11). Fig.10 shows the performance parameters of proposed topology at different input conditions. Output voltage V_0 is decrease slightly when input increases from V_S of 50V to $2V_S$ of 100V. There is a sudden change in the output voltage due to charging and discharging of capacitors.

Inductor starts charging with change in input voltage and starts discharging. Load current decrease slightly when the input changes to zero. From the load current values, it is clearly known that the topology working in continuous conduction mode.

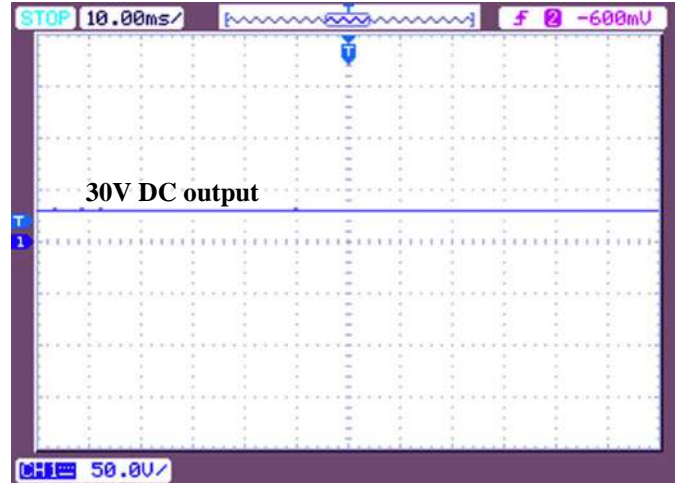


Fig.11. Output voltage of Proposed DC-DC converter

To evaluate the simulation results, hardware prototype has been developed and the output voltage is shown in Fig.11. An output voltage of 30V is achieved for an input of 6V. Hardware use IRF840 Mosfet as switch. IC8951 is used to generate the gate pulses of Switches for switches S_1 and S_2 . A PWM pulse of 10 KHz is given to switch S_M . The parameters used in prototype are given in table 2.

Table.2. Parameters used in Hardware Prototype

Load	25Ω
Switch	IRF840
Controller	IC8951
Switching Frequency	10 kHz
Input Voltage	6 V (both inputs)
Output Voltage	30 V

Fig.12 shows the input waveforms and output voltage waveform. Inputs are given alternatively and it shows no decrement or change in the output voltage. The output voltage is maintained as constant at 30V for the alternating inputs of 6V. From the simulation and experimental results, it is clearly shown that the the topology can produce constant output voltages for variable input voltages.

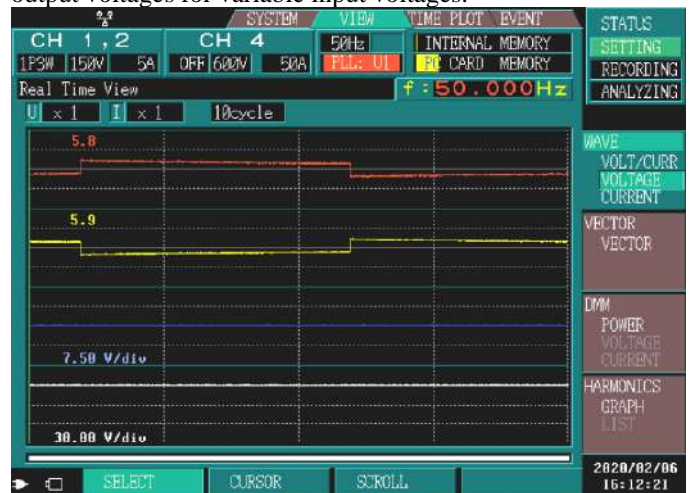


Fig.12. Input and output waveforms

V. CONCLUSION

A novel multi-input and multi-output (MIMO) DC-DC converter was presented in this paper. The generalized structure and a dual input dual output topology also presented. This topology is suitable for hybrid power system uses renewable energy sources with variable output. Performance of the topology was discussed with analytical approach. This topology requires less number of inductor and switches to reduce the cost, volume and driver requirements. A detailed comparison with other topologies was also given. with Performance of the topology was verified using simulation and hardware prototype. The output was maintained constant with variable input voltages. By using closed loop control and MPPT techniques, the proposed topology can also be used for the hybrid systems with unequal input voltages.

REFERENCES

- Hu, R., Zeng, J., Liu, J. and Yang, J., ‘Double-input DC-DC converter for applications with wide-input-voltage-ranges’, *Journal of Power Electronics*, 18(6), 2018, pp.1619-1626.
- Fang Zheng Peng, ‘A generalized multilevel inverter topology with self voltage balancing’, *IEEE Transactions on Industry Applications*, Volume 37, Issue 2, March-April 2001 pp.611 - 618
- Shen, M., Peng, F.Z. and Tolbert, L.M., ‘Multilevel DC-DC power conversion system with multiple DC sources’, *IEEE Transactions on Power Electronics*, 23(1), 2008, pp.420-426.
- Zhang, Fan, Fang Z. Peng, and Zhaoming Qian. ‘Study of the multilevel converters in DC-DC applications.’ 2004 IEEE 35th Annual Power Electronics Specialists Conference (IEEE Cat. No. 04CH37551), IEEE, vol. 2, 2004, pp. 1702-1706.
- Nahavandi, A., Hagh, M.T., Sharifian, M.B.B. and Danyali, S., ‘A nonisolated multiinput multioutput DC-DC boost converter for electric vehicle applications’, *IEEE Transactions on Power Electronics*, 30(4), 2004, pp.1818-1835.
- Dobbs, B.G. and Chapman, P.L., ‘A multiple-input DC-DC converter topology’, *IEEE Power Electronics Letters*, 1(1), 2003, pp.6-9.
- Shen, Miaosen, Fang Z. Peng, and Leon M. Tolbert. ‘Multi-level dc/dc power conversion system with multiple dc sources.’ 2007 IEEE Power Electronics Specialists Conference, IEEE, 2007, pp. 2008-2014..
- Rosas-Caro, Julio C., Juan M. Ramirez, and Pedro Martín García-Vite. ‘Novel DC-DC multilevel boost converter.’ *IEEE Power Electronics Specialists Conference*, IEEE, 2008, pp. 2146-2151.
- Khosrogorji, S., Ahmadian, M., Torkaman, H. and Soori, S., ‘Multi-input DC/DC converters in connection with distributed generation units—A review’, *Renewable and Sustainable Energy Reviews*, 66, 2016, pp.360-379.
- Forouzesh, M., Siwakoti, Y.P., Gorji, S.A., Blaabjerg, F. and Lehman, B., ‘Step-up DC-DC converters: a comprehensive review of voltage-boosting techniques, topologies, and applications’, *IEEE Transactions on Power Electronics*, 32(12), 2017, pp.9143-9178.
- Chen, J., Wang, C., Li, J., Jiang, C. and Duan, C., ‘An Input-Parallel-Output-Series Multilevel Boost Converter With a Uniform Voltage-Balance Control Strategy’, *IEEE Journal of Emerging and Selected Topics in Power Electronics*, 7(4), 2019, pp.2147-2157.
- Liao, Z., Lei, Y. and Pilawa-Podgurski, R.C. ‘Analysis and design of a high power density flying-capacitor multilevel boost converter for high step-up conversion’, *IEEE Transactions on Power Electronics*, 34(5), 2018, pp.4087-4099.
- Bhaskar, M.S., Meraj, M., Iqbal, A. and Padmanaban, S., ‘Nonisolated Symmetrical Interleaved Multilevel Boost Converter With Reduction in Voltage Rating of Capacitors for High-Voltage Microgrid Applications’, 2019, *IEEE Transactions on Industry Applications*, 55(6), pp.7410-7424.
- Rosas-Caro, J.C., Ramirez, J.M., Peng, F.Z. and Valderrabano, A., ‘A DC-DC multilevel boost converter’, *IET Power Electronics*, 3(1), 2010, pp.129-137.
- Babaei, E. and Abbasi, O., ‘Structure for multi-input multi-output dc-dc boost converter’, 2016, *IET Power Electronics*, 9(1), pp.9-19.
- Rezayi, S., Iman-Eini, H., Hamzeh, M., Bacha, S. and Farzamkia, S., ‘Dual-output DC/DC boost converter for bipolar DC microgrids’, *IET Renewable Power Generation*, 13(8), 2019, pp.1402-1410.

- Sundaramurthy, R, Sigamani, Titus, ‘FITF-PDM: Unified controller design for non-isolated bidirectional DC-DC converter’, *International Transaction Electrical Energy Syst.*, Vol.28, No.3, 2018.
- M.Nandhini Gayathri, et.al., ‘Performance Evaluation of Modified Cascaded Multilevel Inverter’, *Journal of Applied Sciences*, 14,15, 2014, pp. 1750-1756.
- Keyhani, H., Toliyat, H.A.: ‘A ZVS single-inductor multi-input multi-output dc-dc converter with the step up/down capability’. *Proc ECCE*, Denver, USA, 2013, pp. 5546-5552
- Behjati, H., Davoudi, A.: ‘Single-stage multi-port DC-DC converter topology’, *IET Power Electron.*, 2013, 6, (2), pp. 392-403
- Jafari, M., Hunter, G., Zhu, J.: ‘A new topology of multi-input multi-output buck-boost DC-DC converter for microgrid applications’. *Proc. Power and Energy (PECon)*, Kota Kinabalu, Malaysia, 2012, pp. 286-291.

AUTHORS PROFILE



Ram Prakash Ponraj is currently working as Assistant Professor in Department of Electrical and Electronics Engineering in Saranathan College of Engineering, Tiruchirapalli, India. He is having more than ten years of teaching experience. He is the Life member of ISTE and MIE.



Devadharshini Ganeshprabhu is currently pursuing her Bachelor degree in Electrical and Electronics Engineering in Saranathan College of Engineering, Tiruchirapalli, India.



Haripriya Balaji is currently pursuing her Bachelor degree in Electrical and Electronics Engineering in Saranathan College of Engineering, Tiruchirapalli, India.



Hemadharshini Ganesan is currently pursuing her Bachelor degree in Electrical and Electronics Engineering in Saranathan College of Engineering, Tiruchirapalli, India.



Keerthana Dhanabalan is currently pursuing her Bachelor degree in Electrical and Electronics Engineering in Saranathan College of Engineering, Tiruchirapalli, India

Design and Implementation of Cloud based Digital Energy Meter using ESP8266

P. Ramesh Babu, A. Pradeep, P. Rajendra Prasath, R. Rishikesh kumar, J. Sharvin

Abstract: Increasing cost in energy sector demands for structured use of energy. It is vital to understand the rate of energy consumption during specific period utilizing Energy Meters. Energy consumption can be measured using a traditional energy meter; however, their use is restricted in inaccessible areas or in occasion of poor visibility resulting in limited functionality. Also, the main drawback is that a person has to take readings area by area from every house and institute make it time consuming. We propose a Cloud based Wireless Energy Meter [1] which can send data via wireless communication (cloud computing) to a PC or mobile phones in the form of E-mails or mobile application notification or through web page; where surveillance and analysis of the data will be made. This computational system can be used to measure energy quantities of transformers and high voltage towers at remote locations, industries, domestic area, and institutions.

Keywords: Arduino, Current sensor, Energy meter, IOT, Node MCU, Voltage sensor.

I. INTRODUCTION

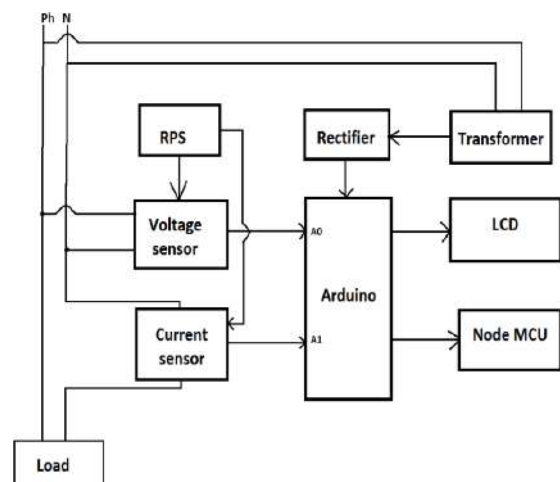
In recent days tracking of the electricity usage in traditional Energy meter is impossible and also analysis of data on the periodic basis is also complex. The consumer is facing severe problem like receiving the pay bill which is already paid, sometimes paying extra charges due to error while taking energy reading [2] and it is impossible to measure in inaccessible area. To overcome this problem and also to keep tracking, currently developed "Design and Implementation of Cloud based Digital Energy meter using ESP8266" this is addressable for both consumer and the electricity board. The paper mainly deals with the embedded system of hardware and software enabled system on the basis of cloud computing with Node MCU module as source of Wi-Fi access. With the help of Node MCU the data can accessed through both mobile application and Web page. The usage notification can be sent in the form of E-mail and application notification. This system will read the monthly energy usage of a consumer automatically and send the information to Electricity board. This can be achieved through Wi-Fi Module and Arduino that can continuously monitor the

electricity usage with cloud storage. This can be displayed on web page and E-mail on customer request.

II. OBJECTIVES

The main objectives of using IOT based Wireless Energy Meter is to save energy and also in this modern appliance we can send the data using wireless communication where the monitoring and analyzing of data will be made much easier. In this device data, can be stored and retrieved whenever the data is required. This project can be used in remote locations and this has more advantages than traditional energy meter.

III. BLOCK DIAGRAM



IV. METHODOLOGY

Here, we describe a Wireless Digital Energy meter using Arduino and ESP8266 NODE MCU [3] which can monitor the energy usage in real time and can send Emails of electricity bill to any location at a single touch point. MQTT Dashboard Android App can be used to monitor our Energy usage. Cloud Based Digital Wireless Energy Meter can be used to monitor using from anywhere in the world and also triggers an alert Email when the Electricity consumption is high.

Revised Manuscript Received on March 30, 2020.

P. Ramesh Babu, Electrical and Electronics Engineering, Saranathan College of Engineering, Trichy, India. Email:ramnira@gmail.com

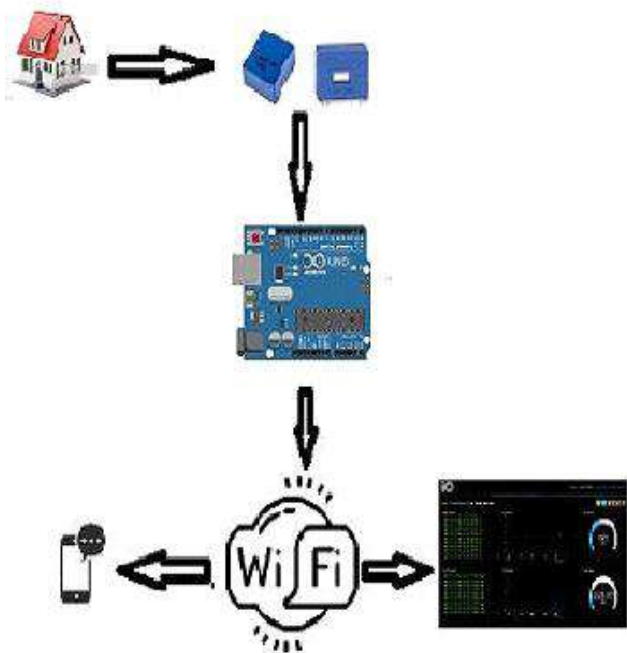
A. Pradeep, Electrical and Electronics Engineering, Saranathan College of Engineering, Trichy, India. Email: pradeepaakash7@gmail.com

P. Rajendra Prasath, Electrical and Electronics Engineering, Saranathan College of Engineering, Trichy, India. Email: rajendraprasath8199@gmail.com

R. Rishikesh kumar, Electrical and Electronics Engineering, Saranathan College of Engineering, Trichy, India. Email: rishi.ranjith1988@gmail.com

J.Sharvin, Electrical and Electronics Engineering, Saranathan College of Engineering, Trichy, India. Email: jayasharvin@gmail.com

V. ARCHITECTURAL DIAGRAM



VI. ENERGY METER AND SENSORS

A. Digital Energy meter

The quantity of electrical energy used by the consumers can be measured by energy meter. Electricity board is responsible for installing the energy meter at consumers' location to calculate the electricity consumption. By measuring the V and I, the instrument will calculate the power value (V*I). This value of power is calculated over a time period, which is used to find energy consumed over that time period.

B. Current Sensor

Current sensor is a sensing unit which can measure a physical phenomenon and compute the values. A current sensor (closed loop current transducer) is a device which identifies the current in the system, using the Hall Effect method. By completely filling the primary hole with a single bar, best dynamic performances can be achieved. The ideal model to accomplish efficient magnetic coupling is by running the primary winding over the top edge of the equipment.

C. Hall Effect Sensor

For high frequency measurements, Hall Effect is the ideal sensing technology. The Hall element is created using a thin sheet of conductive material with output connections perpendicular to the direction of current flow. Upon application of a magnetic field, a proportional output voltage response can be obtained. Thus, obtained voltage output is very small (μV) and can be converted to useful voltage levels using additional electronics. Finally, Hall Effect Sensor is formed, when the Hall element is combined with the associated electronics.

D. Voltage Sensor

Voltage division method is widely used for voltage sensing with the help of voltage sensor LEM LV-25P [5].The obtained value is in the form of Analog value which will be converted by specific calculation.

VII. CONVERSION FORMULA

A. Formula For Voltage Conversion

```
float volSen = readvoltage(A1); // voltage sensor reading, LEM connected to A1
Vout Voltage(mV) = (volSen/ Vconv )*Ioffset; // Calibration as per multimeter values
```

B. Formula For Current Conversion

```
float curSen = readvoltage(A0);
//current sensor reading, LEM connected to A0
//Calibration as per multimeter values float Voffset;
curSen = curSen + 3ffset;
float amps = curSen*Iconv;
//calibration may vary as per conditions
```

VIII. TABULATIONS

Table-I: Parameters and symbols used

Parameters	Symbol	Value
Input voltage	Vin	220V
Output voltage	readvoltage	220-260V
Offset current	Voffset	As per multimeter
Offset voltage	Ioffset	As per multimeter
Input current	Iin	10A
Read current	curSen	5-10A
Vconversion	Vconv	204.8
Iconversion	Iconv	48(Calibration Value)

Table-II: Current value with no load

Table-III: Current value with R-load

Analog value(mv)	Current through wire(A)
1.11	0.43
1.12	0.54

Table-IV: Voltage value with no load

Analog value(mv)	Current through wire(A)
1.75	1.10
1.77	1.11

Table-V: Voltage value with R-load

Analog value(mv)	VOLTAGE through wire
4.7	265
4.9	250

Analog value(mv)	VOLTAGE through wire
4.8	265
4.7	250

IX. WAVEFORMS

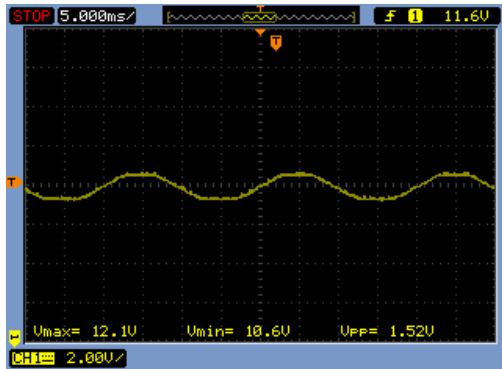


Fig.1 Output waveform of Voltage wave

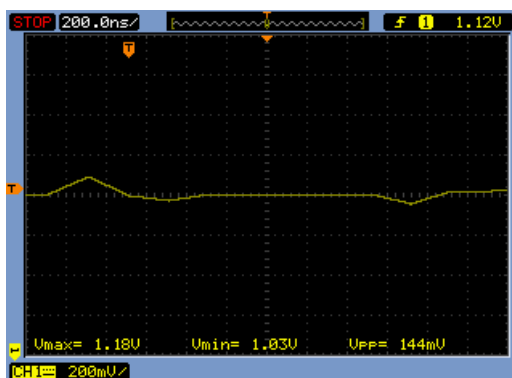


Fig.2 Output waveform of Current wave

X. HARDWARE AND SOFTWARE SETUP

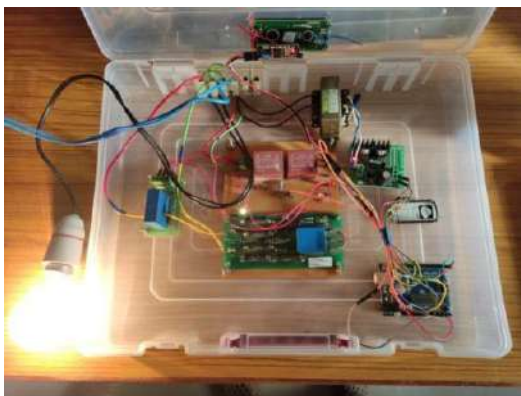


Fig.3 Hardware Prototype



Fig.4 IOT Dashboard result

XI. ARDUINO AND NODE MCU

A. Arduino Uno

Arduino board is the vital component of our system. Entire system functionality depends on this controller. Arduino [8] responds to the 5v given by RPS source, thus, calculating the power consumed as well as the cost. The data is constantly stored on cloud, which is accessible to the user at any time. The system can be programmed to reacts like message sending, receiving, retrieve data.

B. Node Mcu (Esp8266)

Wi-Fi means Wireless Fidelity. Wi-Fi acts as source for IoT [4]. Thus, using Wi-Fi the consumer can view the bill; he can modulate or control the energy meter. Time to time the data can be programed to be displayed on mobile application as well as website. Consumer also has accessibility to the Arduino board and the meter with help of Node MCU as source.

Features

- Integrated 10-bit ADC
- Integrated low power 32-bit MCU
- Integrated PLL and power administration units
- Sustained antenna multiplicity
- Support Smart Link Function for both Android and iOS devices
- Wi-Fi 2.4 GHz, support WPA/WPA2
- SDIO 2.0, (H) SPI, UART, I2C, I2S, IR Remote Control, PWM, GPIO
- Profound current < 5uA
- Reserve power consumption of < 1.0mW (DTIM3)
- awaken and transmit packets in < 2ms
- -40°C ~ 125°C, wide operating temperature range
- +20 dBm output power in 802.11b mode

C. Internet Of Things

An organized unit of computing devices, digital and mechanical machines, animals, people or objects with unique identifiers (UIDs) is called Internet of Things (IoT)[8]. IoT has potential to transfer data, without human-to-computer or human- to-human interaction, over a network.

XII. CONCLUSION

The proposed system emphasized an inexpensive and reliable Cloud Based Digital Energy Meter. With the proposed energy meter; measurement as well as wireless transmission of data are attainable through E-mail and Application notification at single touch point is possible. Enables even comparison and monitoring are made simple with the data received from the Node MCU. Above described system will be cost effective with reduced time consumption compared to traditional energy meter. Future work may include reduction of harmonics distortion, correction of power factor, compact design in sensors; reduction in size; improve data security, Artificial intelligence platform will be proposed.

(India).

REFERENCES

1. Shahrara, R. (2011). *Design and Implementation of a Microcontroller Based Wireless Energy Meter* (Doctoral dissertation, Eastern Mediterranean University (EMU)).
2. Bharath, P., Ananth, N., Vijetha, S., & Prakash, K. J. (2008, November). Wireless automated digital energy meter. In *2008 IEEE International Conference on Sustainable Energy Technologies* (pp. 564-567). IEEE.
3. Barman, B. K., Yadav, S. N., Kumar, S., & Gope,(2018, June). IOT based smart energy meter for efficient energy utilization in smart grid. (ICEPE) (pp. 1-5). IEEE
4. Somayya Madakam, R Ramaswamy, Siddharth Tripathi, "Internet of things (iot): A literature review", *Journal of Computer and Communications*, vol. 3, no. 05, pp. 164, 2015.
5. Oancea, C. D., & Dinu, C. (2015, May). LEM transducers interface for voltage and current monitoring. In *2015 9th International Symposium on Advanced Topics in Electrical Engineering (ATEE)* (pp. 949-952). IEEE.
6. Roy Efficient Power Consumption. Available at SSRN 3493056.Chowdhury, A., Saha, B., Sarkar, G., Choudhary, J., Sahana, S., & Singh, D. (2019). IoT Based Energy Meter Towards
7. Wang, Ming, et al. "An IoT-based appliance control system for smart homes." 2013 fourth international conference on intelligent control and information processing (ICICIP). IEEE, 2013.
8. Hiwale AP, Gaikwad DS, Dongare AA, Mhatre PC. Iot Based Smart Energy Monitoring. *International Research Journal of Engineering and Technology (IRJET)*. 2018 Mar;5(03).



J. Sharvin pursuing B.E degree in Electrical and Electronics Engineering from Saranathan College of Engineering, Trichy, Tamil Nadu, India in 2016-2020. His interest includes embedded system, Internet of Things, power electronics, and attended several workshops, participated in India International Science Festival (IISF)-2018, participated in National solar vehicle challenge in 2019, participated Texas instruments quarter finals 2018 & 2019, participated in regional convention of Viswakarma awards 2019, President of EEE association, department co-ordinator in e-magazine and member of The Institution of Engineers [IEI] (India).

AUTHORS PROFILE



P. Ramesh Babu received the M.E degree from Saranathan College of Engineering, Trichy in 2011 and B.Tech degree from Sastra University, Trichy in 2006. He is currently pursuing Ph.D degree in Anna University, Chennai and working as Assistant Professor in the department of EEE in Saranathan College of Engineering, Trichy. He has 13 years of experience in teaching. He has published papers in International conferences and Journals. His research

interest includes Power Electronics and Drives, Electrical Machines, Solar energy conversion systems.



A. Pradeep pursuing B.E degree in Electrical and Electronics Engineering from Saranathan College of Engineering, Trichy, Tamil Nadu, India in 2016-2020. His interest includes power system, power electronics, and attended several workshops, participated in India International Science Festival (IISF)-2018, participated in National Solar Vehicle Challenge in 2019, participated in Texas instruments quarter finals 2018 & 2019, participated in regional convention of Viswakarma awards 2019, completed LabVIEW course and member of The Institution of Engineers [IEI] (India).



P. Rajendra Prasath pursuing B.E degree in Electrical and Electronics Engineering from Saranathan College of Engineering, Trichy, Tamil Nadu, India in 2016- 2020. His interest includes Internet of Things, power electronics, machines and attend several workshops, participated Texas instruments quarter finals 2018 & 2019, participated in regional convention of Viswakarma awards 2019 and member of The Institution of Engineers [IEI] (India).



R. Rishikesh kumar pursuing B.E degree in Electrical and Electronics Engineering from Saranathan College of Engineering, Trichy, Tamil Nadu, India in 2016-2020. His interest includes embedded system, Internet of Things, solid state drives and attended several workshops, participated Texas instruments quarter finals 2018 & 2019, participated in regional convention of Viswakarma awards 2019, member of EEE association and member of The Institution of Engineers [IEI]



The Prediction and Prevention of Varicose vein using Raspberry pi

Dr. S.Vijayalakshmi M.E., Ph.D

Associate Professor

Department of Electrical and Electronics Engineering

Saranathan College of Engineering

Trichy, Tamilnadu, India

Arulraja K

Department of

Electrical and Electronics Engineering

Saranathan College of Engineering

Trichy, Tamilnadu, India

Ganeshkumar V

Department of

Electrical and Electronics Engineering

Saranathan College of Engineering

Trichy, Tamilnadu, India

Guhan R

Department of

Electrical and Electronics Engineering

Saranathan College of Engineering

Trichy, Tamilnadu, India

Gokulnath A J

Department of

Electrical and Electronics Engineering

Saranathan College of Engineering

Trichy, Tamilnadu, India

Abstract—The habit of idleness is becoming common these days. In this technological era people are becoming lazy. This leads to physical inactivity. It causes reduced blood flow in our body. Therefore, the vascular epithelial cell undergoes inflammation which is called as varicose vein. Mostly it affects our lower extremities, but it can be anywhere in the body. When varicose veins clot, the condition is called superficial thrombophlebitis and it is usually very painful. Based on the survey the collected data is used to form predefined dataset. The predefined dataset acts like threshold value. The positional data of a person is analysed using various sensors. The data to be analysed are standing, bending of knee and movement with respect to time. The acquired positional data is processed in Raspberry pi using Artificial Intelligence (AI). It is a non-invasive diagnostic & therapeutic solution for varicose vein using thermal & vibration therapy.

Keywords— lower extremities, vascular epithelial cell, varicose vein, thrombophlebitis, Artificial Intelligence, non-invasive.

I. INTRODUCTION

Varicose veins are larger and swollen veins that appear on the legs and the feet. It happens when the blood flow is interrupted regularly. The veins need treatment for health issues, but if swelling, aching, and painful legs result, if there is discomfort. Treatments available for varicose veins are surgery, ligation and stripping, sclera therapy, radio frequency ablation, endogenous laser treatment, Trans illuminated phlebectomy. The veins have one-way valves so the blood can travel only in one direction.

If the walls of the vein become stretched and less flexible (elastic) then the valves may get weaker. A weakened valve can allow the blood to leak backward and eventually flow in the opposite direction. When this occurs, blood can accumulate in the vein(s), which become enlarged and swollen veins. This can happen because of pregnancy, age, constipation, tumour, or overweight and obesity.

Nearly 50% of the population in the age of 40 has some smaller form of varicose veins. Generally 10% and 20% adults have significant varicose veins, and 0.5% has superficial varicose veins with chronic venous and ulceration. In India over 10 million people were affected in a year. The Edinburgh Venous study (EVS) published examined over 1500 adults in UK, showed that 39.7% of men and 32.2% of women had a dilated tortuous trunk of the long or short saphenous vein and their first or second order branches. The No of varicose vein cases in India is increasing exponentially and it become clear that venous thrombosis, varicose veins, and venous diseases are as problematic here as all over the world.

A prospective study was conducted in CG hospital and Bapuji hospital attached to JJM Medical College, Davangere from June 2009 to May 2011. A total of 40 cases were included in the study duration. All patients who presented to the outpatient department with signs and symptoms of primary varicose veins were interviewed. The incidence of varicose veins was seen most commonly in male

when compared to female in this study. The family history of varicose veins was seen in only 12.5% of the subjects. In this study patients presented with different symptoms, out of which the dilated veins was most common of 37 (92.5%) patients followed by the aching pain 22 patients [55%].

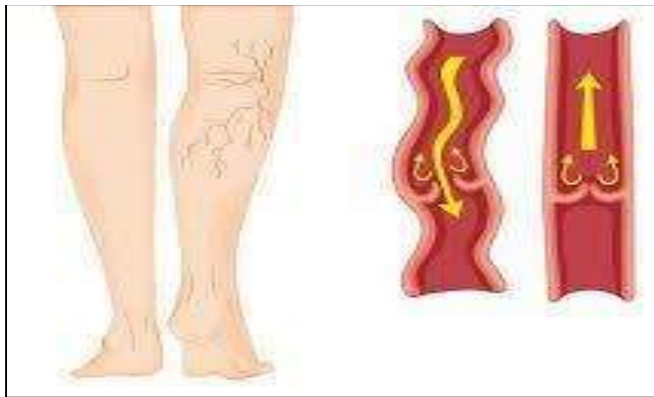


Fig.1 Varicose vein

When the vein is affected, the blood flows in a backward direction. It makes the blood deoxygenated and the colour of blood is changed.

II. LITERATURE REVIEW

Yapei Zhao analyses the algorithm based upon the vascular endothelial cell in amnation images and multi-scale deep learning, called MSDCNN. Ruizong zhu¹, Huipingniu they obtained the images of vascular endothelial cells in patients with varicose veins of the lower extremities and normal subjects & convolutional layers extract multi-scale features of vascular endothelial cell images. The MFM activation function is used to introduce a competitive mechanism that extracts more features that are compact and reduces network layer parameters. The network uses a 3×3 convolution kernel to improve the network feature extraction capability and use the 1×1 convolution kernel for dimensionality reduction to further streamline network parameters[6].

The mechanical parameters of the human vein are often measured and the uniaxial test is conducted under various temperature conditions in the proposed system of Alexander Vasilyevich Gavrilenko [2].

Parth rana suggests the machine learning process for the prediction of obesity disease in the modern era. This is due to the growing lifestyle because of the irregular biological pattern [5]. Prof G.D Parmar using the IR image processing technique to find the varicose vein with the computer software module and modified IR webcam [3]. Navdeepsinh V. Limbad 's proposed system says the detection of vein pattern using the IR sensitive Webcam, this system is also a non-invasive system[5]. Ultrasound (US) is the main modality for examination of venous disease. Color Doppler and occasionally spectral Doppler US (SDUS) are used for evaluation of the venous flow. Thor Bechsgaard proposed this system, the main base is chronic venous, which creates the varicose veins, by using ultrasound the chronic venous are eliminated [4]. H. Clarke's proposed system mainly deals with the elasticity of the vein while origin of the disease. The elastic modulus test was determined with normal veins and varicose veins[7]. Machine learning based obesity & varicose prediction. Pick the most suitable algorithm with the best

accuracy through ROC, Confusion Matrix, Calibration Plot and test it with various sampling schemes [1].

III. EXISTING IDEA

The varicose vein is determined using various methods like infrared image processing, scanning, physical examination. You need an ultrasound test to find if the veins are normal or if they have any blood clots in the lower part. In this non-invasive test, the technician runs a transducer against the skin over the area of the body to be examined. The Purpose of the transducer is to send the images to the monitor to examine. The image processing is used for the analysis of the vein with the help of deep learning algorithms.

SURGERY

Surgery is one of the traditional treatments for these cases. This surgery is based on typing and pulling away of smaller branch of veins. But these causes severe pain to the patient and takes long time to recover.

SCLEROTHERAPY

This method is based on injecting the medicines to the veins, and make them to shrink it. The complications of these therapy includes allergies, burning, stinging at injection sites, skin ulcerations and inflammation. It may cause strokes due to over dose of sclerosant.

ENDOVASCULAR LASER THERAPY

This method uses the laser to destroy the varicose veins. It generally takes 30-35 mins for procedure and recovery easily and fastly. Endovascular laser therapy changes in color. After that it requires the patients to wear pressure stockings.

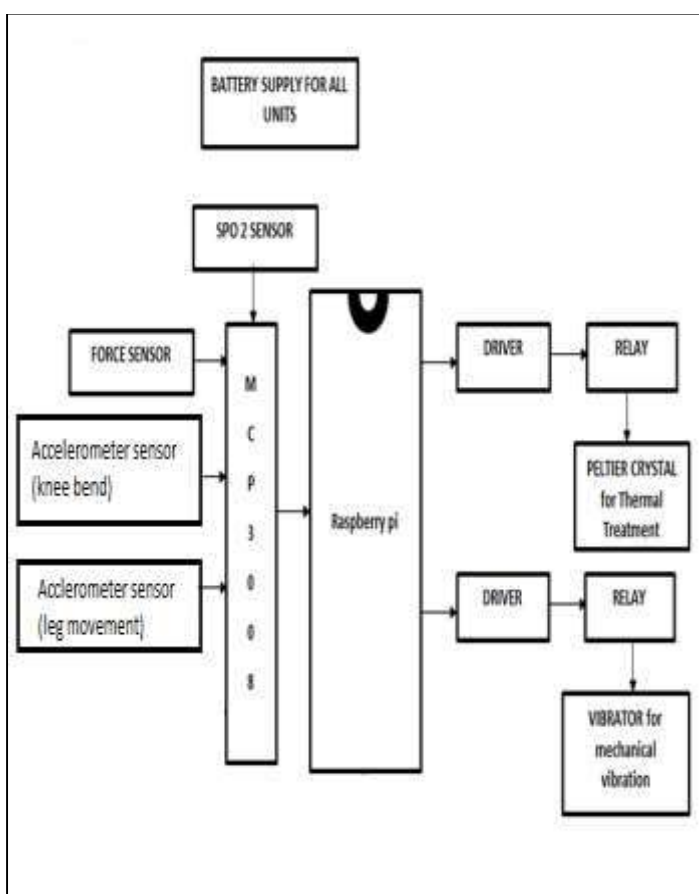
IV. NEED FOR VEIN DETECTION

For providing medical and drug support to the patients, intravenous supplements are given by doctors after thorough medical inspection. If any vein diseases occur for example deep vein thrombosis and varicose veins, bruises on skin, treatment and medical support for these diseases is highly recommended for easy recovery. Skin scarring may also occur in terms of any accidental damage to the vein. So the skin appears deterred which causes the skin to appear in whitish colour or darker. The identification of these veins become tough. In this process blood is given to the person intravenously. Blood donation, kidney dialysis also requires good vein detection. In case of children and infants vein detection may be especially difficult and requiring to puncture the veins with a needle is very frightful and agonizing. Also in case of some age old people require numerous blood tests or medicinal injections and an efficient puncture would decrease the extra bruise and enhance the victims comfort.

V. BLOCK DIAGRAM

The block diagram of the proposed system consists of a resistance based analogue sensor, two motion detecting sensors and a sensor for monitoring blood oxygen. The analogue sensors used are force sensor, accelerometers and a SPO2 sensor. The force sensor is used to determine the force given by the person. The force values keep on varying for different positions of the leg. When the entire force is applied

by the person. There are two accelerometers, one is used to determine the motion of the person. Another accelerometer is used to determine the bending of the knee. This is obtained from the axis values that change with respect to the person. The analog values from the sensors are converted into digital values as the Raspberry pi module processes only digital values. The analog sensors are interfaced to the Raspberry pi using an analog to digital converter (ADC – MCP3008). The ADC is an eight channel module. The analogue input from the person is fed to the Raspberry pi to check the status of the person's leg. This data is processed in the Raspberry pi module and compares the current data with the previous data. The driver circuit which connects to the raspberry pi is used to activate the peltier module and vibration motor. This non-invasive solution is obtained using a four channel relay circuit which is a driver circuit. The switch consists of a driver module ULN2003 which is basically a transistor.



VI. PROPOSED IDEA

The determination of the disease is done using non-invasive diagnostic techniques with the help of sensors. These values are obtained with respect to time.

The sensors used are flex sensor, force sensor and accelerometer. The flex sensor gives bending of the knee as the blood circulation gets reduced when the knee is in a bending position. When the leg is in an idle position for the long time then the voltage value will be constant for a given period of time. The force gives the state of the leg (i.e. standing or walking). If the person is standing then, the force given by the person is determined. This is to determine the pressure given to the veins in the lower extremities. Accelerometer is also a sensor used to determine the state of the leg, especially for walking. When the accelerometer value varies it means the person is walking. With these analog inputs the positional and physical parameters of the leg are obtained.

Non-invasive methods of treatment do not require a catheter or anything that is required for the operation. It takes very less time for the procedure and recovery also occurs at a very high rate. In this wearable socks, we are using SPO₂, force sensor, accelerometer sensor, flex sensor & tilt sensor to monitors the blood flow, pressure and long time standing which reduces blood regulation inside body leads to varicose vein. These sensors values are fed to raspberry pi which is diagnoses early based artificial intelligence. Some therapies which are based on the use of heat or other energy can be applied to tissues of the body which occur in numerous therapeutics results. It achieves a required treatment effect, reaching a temperature of the tissue at least reaches 45°C to 50°C. Low cost wearable device based sock therapy, we are using the peltier crystal & vibration to treat the varicose vein non-invasively and to increase blood flow inside veins. In this thermoelectric therapy there are two ways of treatment, one by thermal and mechanical.

VII. HARDWARE



FORCE SENSOR

This force sensitive resistor with a round of having a 0.5" diameter sensing area is known as Force Sensing Resistor. The FSR varying the resistance depending upon the pressure is being applied to the scan area of the sensor. The harder the force makes the lower resistance. When no pressure is applied to the FSR its resistance have larger than 1MΩ. This sensor senses the force anywhere in the range of 100g-10kg.

Two pins extend from the bottom of the sensor with 0.1" pitch making it bread board friendly. There is a peel-and-stick rubber backing on the other side of the sensing area to mount the FSR. These sensors have simple setup and having great sensing pressure, but it is less accurate. It may not want to use it as a scale. This force sensor is placed under the heel to know the person's various movements like standing, walking, continuous standing, and continuous sitting. The dataset is taken for decision making operation. Dataset is made based on the values taken from the sensors output.

The dataset may vary for different person. So for the every individual a new dataset need to be created.

ACCELEROMETER

The ADXL337 is a low power, small, thin complete 3-axis accelerometer having signal conditioned voltage outputs. The product measuring range acceleration with minimum full-scale range of ±3 g, also measures the static acceleration of gravity in tilt sensing applications, as well as dynamic acceleration resulting from motion, shock, or vibration. The user can selects the bandwidth of the accelerometer using the CX, CY, and CZ capacitors at the

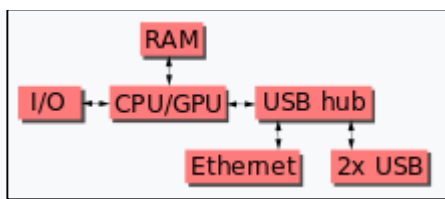
XOUT, YOUT, and ZOUT pins. Bandwidths are selected to suit the application, with a range of 0.5 Hz to 1600 Hz for X and Y axes, and a range of 0.5 Hz to 550 Hz for the Z axis. The ADXL337 is available in small and low profile. This sensor is a three axis sensor giving values of X, Y and Z axes. In this non-invasive therapeutic treatment two accelerometer is used. One is fitted just above the knee bend and the one is placed in the calf. These two will help to find the person is standing or walking or sitting. If he is standing means then he is continuously standing or continuously walking is identified.

SpO2

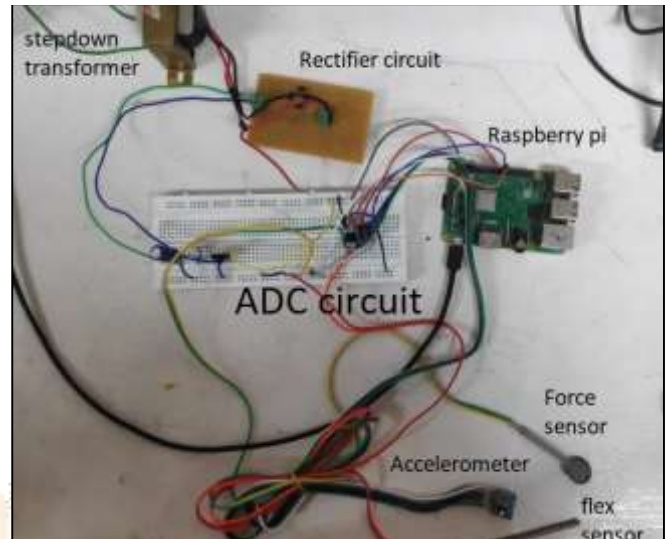
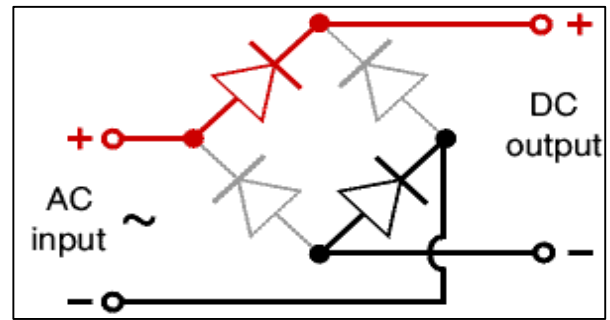
The SpO2 (peripheral capillary oxygen saturation) sensor uses two emitting LED's one in the red region and the other in the infrared region of the spectrum. The reflected light of each one of these LED's is absorbed by a photodiode that converts this current into a digital value that is sent via SPI. This sensor can be used to estimate the oxygen saturation level on the blood with +/- 2% accuracy compared to a medical sensor.

RASPBERRY PI

The Raspberry Pi hardware has several versions that feature the variations in memory capacity and various peripheral-device support.



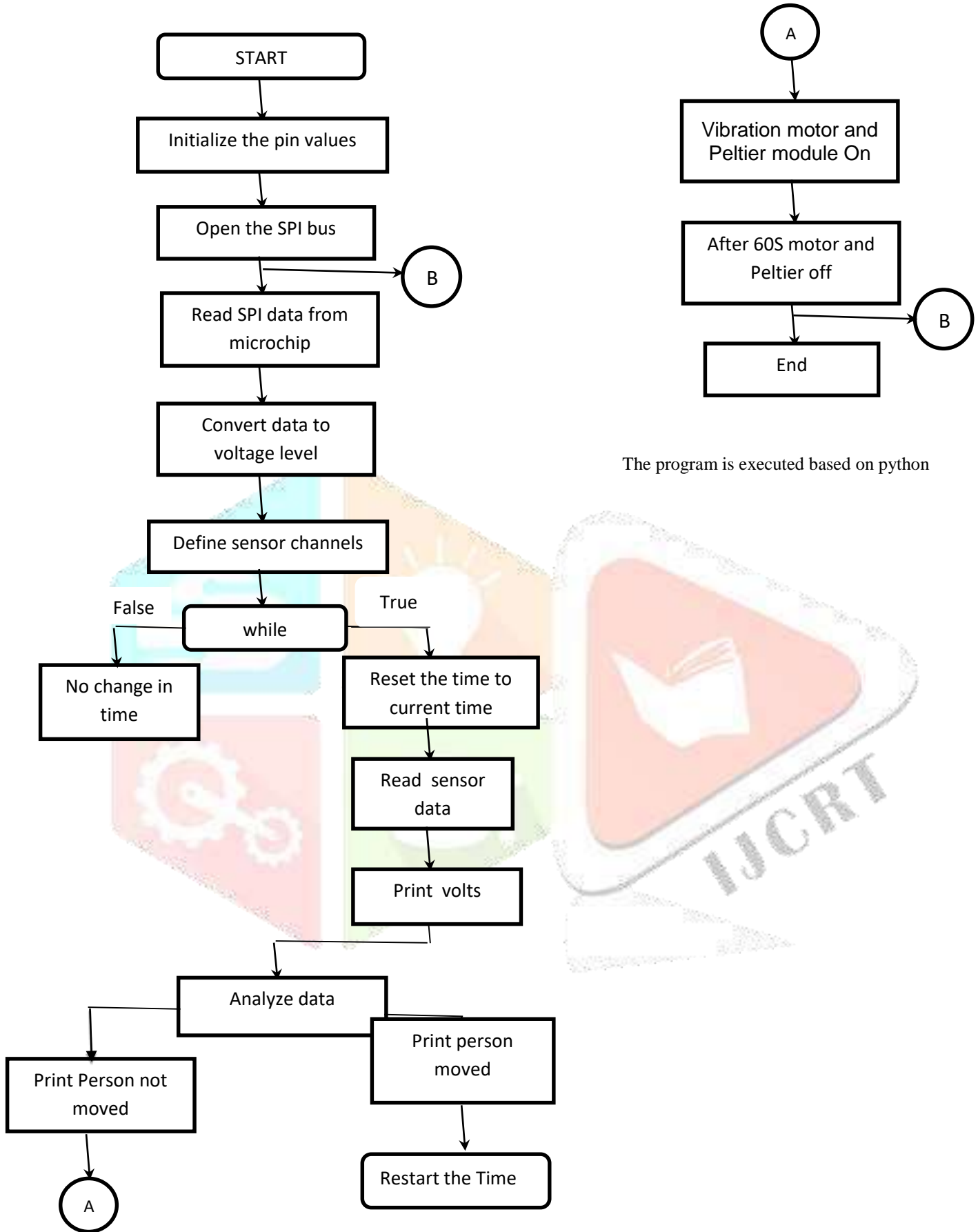
This block diagram describes Model B and B+; Model A, A+, and the Pi Zero is similar, but lacks the Ethernet and USB hub components. The Ethernet adapter is internally connected to an additional USB port. In Model A, A+, and the Pi Zero, the USB port is connected directly to the system on a chip (SoC). On the Pi 1 Model B+ and later models the USB/Ethernet chip contains a five-port USB hub, of which four ports are available, while the Pi 1 Model B only provides two. On the Pi Zero, the USB port is also connected directly to the SoC, but it uses a micro USB (OTG) port. Unlike all other Pi models, the 40 pin GPIO connector is omitted on the Pi Zero with solderable through holes only in the pin locations. The raspberry pi acts as a processor and stores the data temporarily in it. The Raspbian operating system controls the whole processor. There are several versions of Raspbian including Raspbian Buster and Raspbian Stretch. The movement of the person is detected and activate the respective Peltier module and vibration motor.



BRIDGE RECTIFIER

A bridge rectifier can be made using four individual diodes. 1.4V is used in the bridge rectifier because each diode uses 0.7V. Bridge rectifier are rated by the maximum current they can pass and maximum reverse voltage they can withstand.

VIII. FLOWCHART



The program is executed based on python

IX. CONCLUSION

The ultimate aim of this project has been to provide the early prediction of varicose veins and to prevent the lower part of the veins from the disease. The blood flow is the main problem that leads to reversal and blocking of blood vessels. This paper analyzes the output data from the respective sensors and compares these values using raspberry pi. This project has conquered these problems within its implementation. After consulting some doctor suggestions we conclude and use some basic data to predict the disease. The blood flow can be regularly monitored by the respective sensor. In prevention process the peltier module which activates by the relay driver circuit and simultaneously it changes heat and cold state for the regular blood flow. The vibration motor has been connected from the relay circuit and activates if the flow interrupt and also we verify the performance of the sensor circuits like flux, accelerometer, tilt, spo2. The raspberry pi is the 32 bit 900mhz cortex A7 processor used for the communication between the analog and digital parts of the circuit. By the help of these processor the output result can be viewed through the generic computers when the sensors are pressured. The processor acts as a CPU the datas are stored in the RAM respectively.

The future work of these projects is to make them compatible to the person in need to reduce the weight. Circuits like ADC, relay driver, raspberry pi are compactly arranged in simple packages.

X. REFERENCES

1. Deepika Princess D., Mohan Jagannath and Biju ShalvinY.J, "Ultrasound Therapy for Varicose Vein", International Research Journal of MedicalSciences, Vol.1(10), November(2013), no.1, 22-25.
2. Gennady Victorovich Savrasov, Nikita Vladimirovich Belikov, Alexander Vasilyevich Gavrilenko, Irina VitalyevnaKhaydukova, Anna SergeevnaBorde, Irina Alexandrovna Seliverstova, AnastasiyaDmitrievnaSolntseva "Comparison of Mechanical Parameters of the Great Saphenous Vein under Various Test Conditions", IEEE AACCESS(2019), no.2, 44-47.
3. G.D.Parmar, NavdeepsinghV.Limbada "Vein Pattern Detection System Using Cost Effective Modified IR Sensitive Webcam", International Journal For Technoligical Research, Volume 1,issue 9, May-2014, no.3.
4. ManamMansoor, Sravani S.N, Sumbul Zahra Naqvi, Imran Badshah, "Real Time Low Cost Infrared Vein Imaging System" International conference on signal processing and pattern, IEEE 2013, no.4.
5. Naomi Christianne Pereira, Jessica D'souza, Parth Rana, SupriyaSolaskar "OBESITY RELATED DISEASE PREDICTION FROM HEALTHCARE COMMUNITIES USING MACHINE LEARNING", IEEE – 45670, July 6-8, 2019, no.5.
6. Ruizong Zhu , HuipingNiu , Ningning Yin , Tianjiao Wu, Yapei Zhao"Analysis of Varicose Veins of Lower Extremities Based on Vascular Endothelial Cell Inflammation Images and Multi-Scale Deep Learning", IEE ACCESS. 2019.2954708, Vol. 7, December 16, 2019, no.6.
7. S. Prasantamrongsiri "3D finite element analysis of varicose vein therapy by using microwave ablation" Biomedical Engineering international conference ,2012, no.7.
8. Thor Bechsgaard, Kristoffer Lindskov Hansen, Andreas Hjelm Brandt, Simon Holbek "Blood Flow Velocity in the Popliteal Vein using Transverse Oscillation Ultrasound ", Proc of SPIE Vol.9790 979003-1, no.8.

ADVANCED ENERGY METER BASED ON INTERNET OF THINGS

Dr.M.V.Suganyadevi*, **P.Priyadharshani¹**, **S.Selvashanthini²**, **S.Suruthi³**, **M.Swarnasri⁴**

^{1,2,3,4} UG Student, Department of EEE & Saranathan College of Engineering, Trichy, India

* Associate Professor, Department of EEE & Saranathan College of Engineering, Trichy, India,
suganyadevi-eee@saranathan.ac.in

Abstract - Today the world is developed with lots and lots of technology in all the aspects. As the people survive in this technological world they are very much dependent on the electrical and electronic equipments for their day today life. And, day by day the population growth is also drastically increasing. These both issues make the usage of power more. As the usage of power is more the electricity reading is complex which may causes human errors while notifying the readings. Due to this the energy crisis and energy theft occurs. To eradicate these problems an advanced energy meter using internet of things (IoT) is implemented. The features of this energy meter are whenever the over voltage arises the indication is provided in the form of alarm to the respective consumers so as to limit the usage of power. This provides the day today power reading that is voltage and current used by the consumers in regular time intervals. And this device provides the electricity theft indication .Additional feature is that, if the consumer who has not paid the electricity payment the disconnection of the service is done and the service is resumed in case when the payment is done from the utility side. This paper deals with these entire concepts which are mentioned above in a detailed manner. The main concept of advanced energy meter is that it is a low cost and effective energy meter than a normal energy meter which provides the over voltage indication, the consumed power in a regular intervals, indication of electricity theft to the respective consumers by using a microcontroller and a Wi-Fi module along with IoT.

Key Words: Internet of Things, Advanced energy meter, microcontroller, Wi-Fi module

I. INTRODUCTION

Today the world is developed with multiple technologies one such is wireless technology. This is helpful in automatic devices and reduces the human work with the help of microcontrollers. This is implemented in the advanced energy meter.

In case of existing energy meter requires human power to note down the data and for calculating the power. And calculation of reading sometimes gives error data due to human error while calculating.

As the users are increased day by day this creates problem in maintaining and regulating the system periodically. And the operator has to do calculation and billing manually for each and every consumer. If the consumer is not in their residence when the operator comes to take reading it becomes difficult situation for the operator. These all makes hectic situation for operator. And also it is a time consuming process.

And there comes a difficult situation for an operator even during weather condition is bad and during natural calamities. And if the energy is theft the consumers are not notified about that problem. But the billing becomes expensive without using more power.

These issues are limited in wireless technology. This does not need any human intervention like operators. In case of wired system there is a need a regular maintenance as there is lot of connection and also cost high.

In case of wireless technology the maintenance is easy and it is convenient for users. In the proposed system wireless technology based of Internet of Things (IoT) is done.

Internet of Things sends message to consumer and also monitors the energy consumption. It reduces human intervention. Using IoT the data is transferred to cloud. Clouds are used as single organization and also as public cloud. Here Thingspeak cloud is used for displaying the data such as current and voltage regularly and also instantly. This implemented system has features like overvoltage indication, energy theft indication and also the readings are updated to consumer in regular intervals.

II. EXISTING SYSTEM

In the conventional energy meter there is possibility of human error due manual calculation reading. And the process of calculating the reading is a time consuming process. Over voltage is a critical issue in the electrical system which damages the equipment. But this issue is not notified by the consumers as they do not get any indications based on that.

In the existing system, no such arrangements like overvoltage indication. The usage of power is more by humans nowadays due to high demand. And the billing also increased due to that. They do not get any notifications about the usage of power per day in the existing system.

And also if the energy is theft from the concerned users, they didn't know about the issue and billing becomes expensive but they might consume the power less. This is also an important problem in the existing system.

In the existing system the GSM module is used which transmits the data to the consumers. But this causes interference to the electronic gadgets and creates various problems in the system.

In the normal energy meter there is no special feature to control the over voltage issue which would decrease the life of the equipment.

So these problems raised in the existing energy meter are rectified in the proposed system which provides the over voltage indication, the reading are updated in regular intervals and also provides energy theft indication.

III. PROPOSED SYSTEM

3.1 OVER VOLTAGE INDICATION

If the consumers, consumes more power than the tolerance limit the overvoltage occurs. To limit this issue the over voltage indication is provided. Here single phase AC is stepped down using step down transformer. Hence stepped down values of voltage and current are measured using current and power transformer. If the over voltage occurs the values are sent to microcontroller PIC16F877A. Then these values are sent to IoT module ESP8266 and the overvoltage indication is provided by LCD display. Then the control of overvoltage is done by the regulator which interrupts the work and corrects up the voltage and again the corrected values are sent to the microcontroller and these values are passed to IoT module. Through the IoT module the balanced voltage message is displayed by LCD.

3.2 UPDATING OF ENERGY METER READING

To make the consumer to know about how much power is consumed this updating of energy meter reading is done. Here power transformer is connected .And the values of voltage and current are sensed by microcontroller.

The sensed values are passed to the IoT module which provides information to the consumer that how much power they are consumed through LCD display. The readings are updated to the consumers at regular time intervals.

3.3 ENERGY THEFT INDICATION

In conventional energy meter if the energy is theft the concern consumer doesn't know about it. To create awareness about the energy theft to the consumer in the advanced energy meter the energy theft indication is implemented. In this if the energy is theft the microcontroller collects the data and controls. Then the data is passed to the IoT module. This is then passed to consumers through LCD display.

IV. BLOCK DIAGRAM

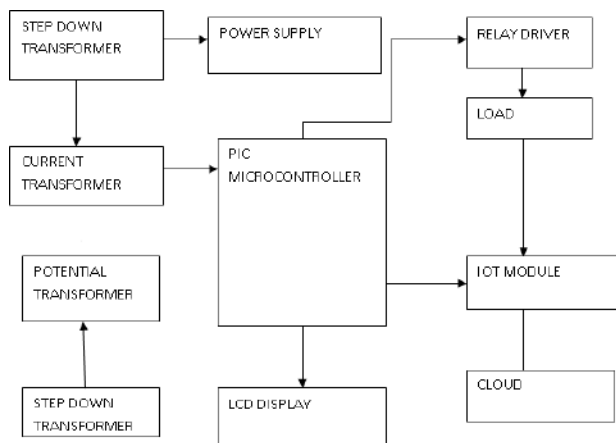


Fig - 1: Block diagram of advanced energy meter

In this block we are using two step down transformers, a current transformer, a potential transformer. The power supply is given to a step down transformer. Here single phase AC is stepped down using step down transformer. Hence stepped down values of voltage and current are measured using current and power transformer. If the over voltage occurs the values are sent to microcontroller. Then the message is sent to concern consumer as an alert by wi-fi module using cloud. And also the updation of energy meter reading is done in regular interval of time. And if the energy is theft the indication is provided to concern consumer.

V. OUTPUTS OF ADVANCED ENERGY METER

5.1 OVER VOLTAGE INDICATION

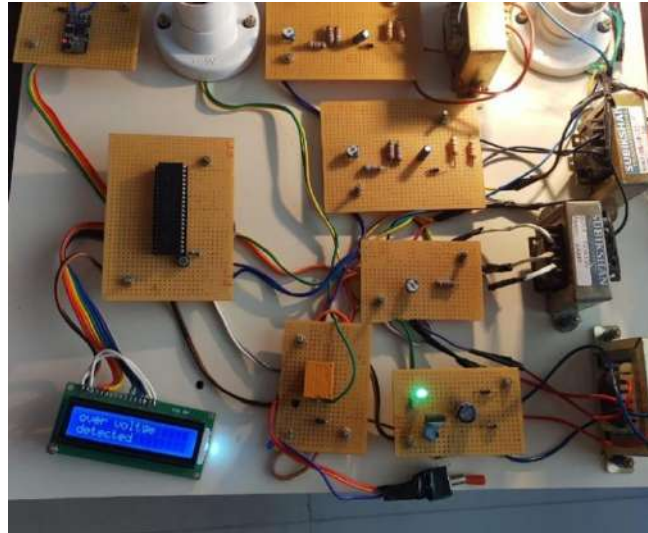


Fig - 2: Over Voltage Indication

Here, the over voltage is indicated in a LCD display. This indication is passed to a concern consumer by a wi-fi module. The data is controlled using microcontroller.

5.2 OVER VOLTAGE BALANCED INDICATION

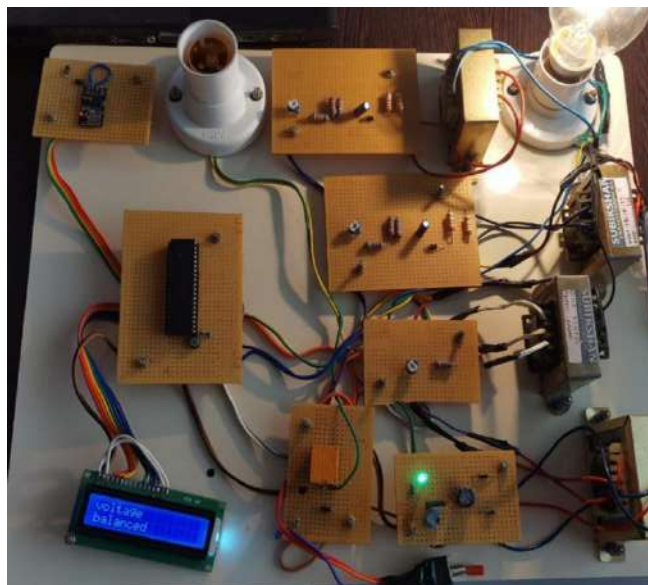


Fig - 3: Over voltage Balanced Indication

If the over voltage occurs the will also be balanced. The control of the power is done using microcontroller. And the indication is provided in LCD display.

5.3 UPDATING OF ENERGY METER READING



Fig - 4: Updating of Energy Meter Reading

Here, the readings of current and voltages are taken using the current and potential transformer respectively at regular intervals. And the data is passed to controlled as well as displayed in LCD. Then the data is passed to consumers using wi-fi module.

VI. CONCLUSIONS

The electricity demand of consumers rapidly increases day by day. This causes increasing power theft. It is also equally important to protect the expensive equipment from overvoltage. To track the usage of power consumption there should be some kind of warning to control the usage. This project deals with these three problems mentioned above. Consumers can check the power consumption status whenever required. Regarding the theft of power, the consumers will be given an alert message through the IoT to the concerned consumer also it provides over-voltage indication and correct the overvoltage and protect the equipment. The advantage of advanced energy meter is that electricity can be cut off to the specific consumer from the utility side this greatly excludes the need for manpower.

REFERENCES

- [1] Darshan, I. N., & Radhakrishna, K. A. (2015). IoT Based Electricity Energy Meter Reading, Theft Detection and Disconnection using PLC modem and Power optimization. *International Journal of Advanced Research in Electrical, Electronics and Instrumentation Engineering*, 4(7), 6482-649
- [2] Jain, A., & Bagree, M. (2011). A prepaid meter using mobile communication. *International Journal of Engineering Research & Technology (IJERT)*, 160-166.

- [3] Mohamed Mufassirin, M. M., & Hanees, A. L. (2018). Cost Effective Wireless Network Based Automated Energy Meter Monitoring System for Sri Lanka Perspective. *International Journal of Information Technology and Computer Science(IJTCS)*, 68-75.
- [4] Mohamed Mufassirin, M. M., Hanees, A. L., & Shafana, M. S. (2016). Energy theft detection and controlling system model using wireless communication media. *5th Annual Science Research Sessions - 2016* (pp. 123-130). Sammanthurai: Faculty of Applied Sciences, South Eastern University of Sri Lanka
- [5] Mufassirin, M., & Hanees, A. L. (2014). GSM based Automated Energy Meter Reading for Electricity Bill Processing. *4th Annual Science Research Session (ASRS) - 2014* (p. 13). Sammanthurai: Faculty of Applied Sciences, South Eastern University of Sri Lanka
- [6] Pooja, D. T., & Kulkarni, S. B. (2016). IoT Based Energy Meter Reading. International Muhammed, A. A., & Hanees, A. L. (2018). IOT Based Waste Collection Monitoring System Using Smart Phones. *8th International Symposium - 2018*. South Eastern University of Sri Lanka. "In Press"News, V. L. (2014, July 18). Electricity theft on the rise. Retrieved from VivaLanka
- [7] Ashna.k and Sudhish N George,"GSM Based Automatic Energy Meter Reading System with Instant Billing" This project was supported and financed by National Institute of Technology, Calicut, IEEE 2013.
- [8] Champ Prapasawad, Kittitach pornprasitpol, Wanchalermpona, "Development of an automatic meter reading system based on Zigbee pro smart energy profileIEEE802.15.4standard", *International Conference on Electronic Devices and Solid State Circuit (EDSSC)*.
- [9] R.B Hiware, P.Bhaskar, Uttam Bombale, Nilesh Kumar, "Advance Low Cost Electricity Billing System using GSM" Hiware et al.,*International Journal of Advanced Engineering Technology E-ISSN 0976-3945*.
- [10] A. Abdollahi, M. Dehghani, and N. Zamanzadeh , "SMS- sbased reconfigurable automatic meter reading system," *IEEE International Conference on Control Applications (CCA 2007)*, Oct, 2007, pp. 1103 – 1107.
- [11] O.Homa Kesav and B. Abdul Rahim, "Automated Wireless Meter Reading System for Monitoring and Controlling Power Consumption" *International Journal of Recent Technology and Engineering Volume-1, Issue- 2, June 2012*
- [12] Tariq Jamil,"Design and Implementation of a wireless Automatic Meter Reading System" *Proceeding of the World Congress on Engineering 2008 Vol 1 WCE 2008 ,London, U.K*

PROCEEDINGS OF AICTE SPONSORED



Two-day International e-Conference

On

**Cutting Edge Technologies in Electrical,
Communication, Embedded System and Soft
Computing Techniques (ICECES'20)**

(5th& 6th November 2020)

Organized by



*Department of Electrical and Electronics
Engineering*

(Accredited by NBA) &

*Department of Electronics and Communication
Engineering*

(Accredited by NBA)

SARANATHAN COLLEGE OF ENGINEERING

Venkateswara Nagar, Panjappur,

Tiruchirappalli – 620012, Tamilnadu, India

PROCEEDINGS OF AICTE SPONSORED



Two-day International e-Conference

On

**Cutting Edge Technologies in Electrical,
Communication, Embedded System and Soft
Computing Techniques (ICECES-20)**

(5th & 6th November'2020)

Organized by



*Department of Electrical and Electronics
Engineering &*

(Accredited by NBA)

*Department of Electronics and Communication
Engineering*

(Accredited by NBA)

SARANATHAN COLLEGE OF ENGINEERING

Venkateswara Nagar, Panjappur,

Tiruchirappalli - 620012



Shri. S. Ravindran
Secretary

I am given to understand that the Departments of ECE and EEE are jointly organizing an International e- Conference titled “Cutting Edge Technologies in Electrical, Communication Embedded System and Soft Computing Techniques” and that it is being organized on 5th and 6th of November 2020. Post Covid the focus of the Government is likely to be on their slogan - “Be Vocal, Buy Local”. In light of this the organization of such an e-conference assumes enormous importance. As “buying local” increases the need for manufacturing will also exponentially increase. Newer and better methods of manufacturing of products that meet international quality expectations will have to be found. That would mean innovations have to happen in the fields of Electrical and Electronic Engineering coupled with soft computing techniques.

The necessary raw materials by way of men, materials and money are all available. What needs to be done is, addition of another essential raw material in the form of management to create the right environment for innovation. Given the right environment, the young minds of India WILL come up with socially relevant optimal usage of technology.

It is very gratifying to be briefed that quite a few researchers from different premier institutes across the globe have contributed their papers to this conference. An open and objective brainstorming on those papers would surely result in development of disruptive technological solutions.

I take this opportunity to welcome all the participants to this e-conference and to wish the participants, organizers and committee members all success in their endeavor.

All the best! May God Bless you all!



Prof. Dr. Y. Venkataramani
Dean (R&D)

I am pleased to offer my felicitations to the organisers of the e-conference for having conducted with great success, the first e-conference in Saranathan College of Engineering. The conference provided a forum for researchers, in various areas, to highlight their research work and also understand the work being done by other researchers. I am sure, the interaction among the delegates, will lead to lot of new collaborative projects. My congratulations to the EEE and ECE departments for the meticulous planning and conduct of the Conference



Prof. Dr. D. Valavan
Principal

I'm glad to know that an International e- Conference titled “Cutting Edge Technologies in Electrical, Communication and Soft Computing Techniques” is being jointly organized on 5th and 6th of November 2020 by the Departments of ECE and EEE. The theme of the Conference is very appropriate to the current times. With the focus on local manufacturing under “Atmanirbharta Abhiyan” any discussion on research and innovation in any field has assumed immense importance – in the fields of Electrical and Electronics Engineering more so.

"Change is a certainty and Innovation is the best way to address that change"

Innovation is learning to do tasks differently but more efficiently. Since it is essentially doing a task it will have to be only hands-on. Given the right challenging ambience, young minds will come up with new and disruptive technological ideas. This platform must serve that purpose and create the right challenging ambience. Any research or innovation can be termed successful ONLY when that innovation brings about social betterment.

I'm glad to know the researchers from different premier institutes across the globe have contributed their papers to this conference. I hope those papers would generate objective interactions that would result in disruptive technological solutions.

I welcome all the participants to this e-conference. Wishing the organizers and committee members Godspeed! Have a great e-conference!!



Prof. Dr. C. Krishna Kumar

HoD / EEE

Convener

I am extremely glad to present the proceedings of the International e-Conference on Cutting Edge Technologies in Electrical, Communication, Embedded systems and Soft Computing Techniques (ICECES '2020) held on 5th& 6th November, 2020. This conference is an accomplishment of the Electrical and Electronics Engineering department& Electronics and Communication Engineering department of Saranathan College of Engineering, Trichy. The conference is organised with the support of All India Council for Technical Education, and diligent efforts from the faculty members and students. The objective of this conference is to bring together research scholars, scientists, engineers, and students to exchange and share their new ideas and research findings about all aspects of main themes and tracks. After the rigorous peer-review process, the submitted papers were selected on the basis of novelty, importance, and clarity for the purpose of the conference. I extend my sincere thanks to all those who have contributed to the success of ICECES '2020, especially all the authors and the participants who responded to our call for papers.

I congratulate the Conference Technical Programme Committee Members for their efforts and dedication, who made this event possible.



Prof. Dr. M. Santhi
HoD / ECE
Convener

It is my great pleasure to welcome you all to our 1st AICTE Sponsored International e-Conference on Cutting Edge Technologies in Electrical, Communication, Embedded Systems and Soft Computing Techniques (ICECES'20), held during 5th and 6th of November, 2020 in Saranathan College of Engineering, Tiruchirappalli. The objective of this e-Conference is to bring all the researchers, Academicians, industrialists and students at one platform, and also to inculcate the research culture among the entire fraternity of Education in the country.

I hope that this conference would certainly induce innovative ideas among the participants, paving way for new inventions and technologies in Electrical, Communication, Embedded Systems and Soft Computing Techniques and related fields. We received 150 papers out of which 143 papers were selected for presentation. I would like to thank AICTE and our management for providing financial support to organize this conference.

I am grateful to our Honorable Secretary Shri. S. Ravindran, for his constant support and encouragement to conduct such a prestigious conference in our college. I thank our respected Principal Dr. D. Valavan for his motivation and support to organize this conference. My sincere gratitude goes to our respected Dean R&D Dr. Y. Venkataramani for his fullest guidance towards this conference. Special thanks to the Keynote Speakers, Dr. Seok-Bum Ko, Professor, University of Saskatchewan, Saskatoon, Canada and, Dr. Y. Venkataramani, Dean (R&D) of our college for sharing their knowledge on current research topics. I would like to thank our vibrant faculty members for their un-tired efforts for the successful conduct of this conference. I hope the deliberations from various distinguished speakers and the paper presentations will benefit the participants to update their knowledge.

I extend my best wishes for great success of the conference.

Keynote Speaker



Prof. Dr. Seokbum Ko

University of Saskatchewan, Canada

Seokbum Ko is currently a Professor at the Department of Electrical and Computer Engineering and the Division of Biomedical Engineering, University of Saskatchewan, Canada. He got his PhD degree from the University of Rhode Island, USA in 2002.

His research interests include computer architecture/arithmetic, efficient hardware implementation of compute-intensive applications, deep learning processor architecture and biomedical engineering.

He is a senior member of IEEE circuits and systems society and associate editors of IEEE TCAS I and IEEE Access.

Keynote Speaker



Prof. Dr. Y. Venkataramani

Dean (R&D), Saranathan College of Engineering

Dr.Y.Venkataramani obtained his B.Tech & M.Tech degree from I.I.T Chennai. He was awarded Ph.D. by I.I.T. Kanpur. He has rich academic experience. He served as a faculty for 34 years and later headed the Dept of Electrical Engineering at NIT, Calicut He served as Principal of Saranathan College of Engineering, Trichy from 2001 to 2009 and from 2011 to 2013.

He has authored a book titled “Linear Integrated circuits and applications”. He has guided more than 15 research scholars in various domains. Eight of our staff members have completed their Ph.D. under his able guidance. He has presented many papers in International conferences and refereed Journals.

He has been invited to give key note address in various International conferences and FDPs. In many NITs, he has delivered guest lecturers. At present he is serving as Dean (R & D) in our institution. His areas of interest include Computer Networks, Signal Processing and Network security.

Saranathan College of Engineering, Trichy -12
AICTE Sponsored two-day International e-conference (ICECES'20)
Schedule

Date	Time	Track 1	Track 2	Track 3
Day – 1 5th Nov'20	10.00 AM – 10.45 AM	Keynote Address by Prof. Dr.Seok-Bum Ko, Professor, University of Saskatchewan, Canada		
	10.45 AM – 11.00 AM	Break		
	11.00 AM – 2.00 PM (Session – 1)	Judges : Dr.A. Nazar Ali, Associate Professor/EEE, Rajalakshmi Engineering College, Chennai, TN Prof. C. Pearline kamalini, Assistant Professor/EEE, Saranathan College of Engineering, Trichy, TN Prof.R. Vijay, Assistant Prof/EEE, Saranathan College of Engineering, Trichy, TN	Judges : Dr.J.Manikandan, Professor, Crucible of Research and Innovation (CORI), PES University, Bangalore, KA Dr.V.Mohan, Associate Professor /ECE, Saranathan College of Engineering, Trichy, TN Dr.M.BarithaBegum, Assistant Professor, Saranathan College of Engineering, Trichy, TN	Judges : Dr.L.Saikala Associate Professor/Civil NIT, Trichy, TN Dr.G. Dhanalakshmi, Prof & Head/Civil Saranathan College of Engineering, Trichy, TN Mr.A.Anandraj, Assistant Professor/Civil Saranathan College of Engineering, Trichy, TN
	1.00PM – 4.00 PM (Session – 2)	Judges : Dr.K.Dhayalini, Professor & Head/EEE, K.Ramakrishna College of Engineering, Trichy, TN Prof. B.Paranthagan, Associate Professor/EEE, Saranathan College of Engineering, Trichy, TN Prof.P.Ramesh babu, Assistant Professor/EEE, Saranathan College of Engineering, Trichy, TN	Judges : Dr.K.Swaminathan, Head-FPGA Design Team, Jiva sciences Pvt Ltd, Bangalore, Karnataka. Dr.M.Santhi, Professor & HOD/ECE, Saranathan College of Engineering, Trichy, TN Dr.S.A. Arunmozhi, Associate Professor / ECE, Saranathan College of Engineering, Trichy, TN	--

Date	Time	Track 1	Track 2	Track 3
Day – 2 6th Nov'20	10.00 AM – 10.45 AM	Keynote Address by Prof.Dr.Y.Venkataramani, Dean (R&D), Saranathan College of Engineering, Trichy, Tamilnadu		
	10.45 AM – 11.00 AM	Break		
	11.00 AM – 2.00 PM (Session – 1)	Judges : Dr.G.Kannan, Associate Professor/ECE, B.S.Abdur Rahman Crescent Institute of Science & Technology, Chennai, TN Prof.S.Ramprasath, Assistant Prof/EEE, Saranathan College of Engineering, Trichy, TN Prof.R.Venugopal, Assistant Professor/EEE, Saranathan College of Engineering, Trichy, TN	Judges : Dr.M.Maheswari, Professor & Head/ECE, K.Ramakrishna College of Engineering, Trichy, TN Dr.C.Vennila, Professor /ECE, Saranathan College of Engineering, Trichy, TN Dr.M.Padmaa, Prof/ECE, Saranathan College of Engineering, Trichy, TN	Judges : Dr. Jasmine Beulah Gnanadurai, Professor, Kristu Jayanthi College Bangalore Dr.V.Punitha Associate Professor/CES Saranathan College of Engineering, TN Dr.R.Senthamil selvi Assistant Prof/CES, Saranathan College of Engineering, TN
	1.00 PM – 4.00 PM (Session – 2)	Judges : Dr.R.Shenbagalakshmi, Professor/EEE, SKN Sinhgad Institute of Technology & Science, Lonavala, MH Dr.S.Vijayalakshmi, Associate Professor/EEE, Saranathan College of Engineering, Trichy, TN Prof.M.Marimuthu, Assistant Professor/EEE, Saranathan College of Engineering, Trichy, TN	Judges : Dr.R.Rajeswari, Professor/ECE, Rajalakshmi Institute of Technology, Chennai, TN Dr.S.Rajeswari, Associate Professor / ECE, Saranathan College of engineering, Trichy, TN Dr.P.Shanmugapriya, Associate Professor /ECE, Saranathan College of engineering, Trichy, TN	

Index

Sl.No	Paper Title and Author Name	Page No.
1.	Design of Multistage Cascaded DC-DC Boost Converter <i>Ayisha Banu.A.P, Marimuthu.M</i>	1
2.	Wireless Battery Monitoring System with Live Tracking for an E-Vehicle <i>Devi sri.J, Indhu.R, Kowsalya.S, Madhumita.S, S.Ramprasath</i>	1
3.	The Determination and Curing of Varicose Vein using Raspberry Pi <i>Dr. S.Vijayalakshmi, Arulraja K, Ganeshkumar V, Guhan R, Gokulnath A J</i>	2
4.	Design and Development of Three Level Converter <i>J. Anitha, M. Monica, Dr.S.Vijayalakshmi</i>	3
5.	Design and Implementation of Cloud Based Digital Energy Meter using ESP866 <i>P. Ramesh Babu, A.Pradeep, P. Rajendra prasath, R. Rishikesh kumar, J.Sharvin</i>	3
6.	Design and Simulation of Solar Powered MPPT Control for AC Off Grid <i>S Kiruthiga, P Ramesh Babu</i>	4
7.	Interleaved Topology Based Proficient Buck-Boost Converter <i>A.Srimathi, Dr.S.Vijayalakshmi</i>	4
8.	Smart Monitoring to be incorporated in Existing Public Toilets – Intelligent Toilets <i>Mohamed Ameenullah H, Dilip R, Gayathri N</i>	5
9.	Wireless Power Transfer for Charging Electric Vehicle using Solar <i>S.Shree Haarrini, R. Satheesh, A. Sophiya Josephine, B. Subashree, R. Sundhara Lakshmi</i>	5
10.	Low Cost Digital Control Strategy for Four Quadrant Operation of PMDC Motor <i>K.Subhiksha, N. Suganya, R. Swetha, S. Therasa mettilda</i>	6
11.	Design of Modified SEPIC Converter based ANFIS Controller for Power Factor Correction <i>A.R Danila Shirly, Srinath.G, Sidharth Prasad, Vignesh.S, Viswnathan.M</i>	6
12.	Dynamic Compensation of Reactive Power by Power Factor Improvement for Three Phase Induction Motor <i>A.R.Danila Shirly, M. Praveen Kumar, M.Santhosh, K.Vijayaragavan, R.Vishnuchander</i>	7
13.	Self-Powered Activity Tracker <i>Dr. S. Vijayalakshmi Lakshmi Sk, Megadharshini S, Narmatha Devi K</i>	8

14.	Equal Load Sharing using PWM Circulation Scheme for Three Phase Cross Switched MLI <i>Dr.C. Krishnakumar, Atchaya.S, Becca.R, Bhuvaneswari.S, Meenatchi.V</i>	8
15.	Centered Sourced Multilevel Boost Converter <i>V.Abhirami, P.Harshini, M.Keerthana, S.Keerthimalini, M.Marimuthu</i>	9
16.	Design and Implementation of Integrated Water System Management Using IOT <i>Gayathri N, Aravindh V, Mohamed Nasrullah N, Chandramohan P, Eswar M</i>	9
17.	AGC of Multi Area Multi Source Electric Power System with Differential Evolution Algorithm Based PID Controller under Deregulated Environment <i>B. Prakash Ayyappan, Dr. R. Kanimozhi</i>	10
18.	Accelerometer Gesture Controlled Robot using Arduino <i>Dr.S. Vijayalakshmi, B.Dhanraj, K.Irshath Ali, S.Karthick, T.Mohamed Faizal</i>	10
19.	IOT Based Smart Vehicle Over-Speed Accident Detection and Rescue System <i>Dhurga Devi.A, Kanimozhi.SA, Madhuranthagi.T, Vijay R</i>	11
20.	A Survey on Prediction of Health Insurance Frauds Using Machine Learning <i>Saravanan Parthasarathy, Arun Raj, Lakshminarayanan, Selvaprabu Jeganathan</i>	11
21.	Internet of Things Based Advanced Energy Meter <i>P.Priyadharshani, S.Selvashanthini, S.Suruthi, M.Swarnasri, Dr.M.V.Suganyadevi</i>	12
22.	Implementation of Solar Stove Using Solar Power <i>Nethra.M, Pragatheeswari.G, Shahanaz Mariyam.M, Yuvasri.M, Marimuthu. M</i>	13
23.	Implementation of P&O Algorithm for Multi Cascaded-Boost Converter <i>Reka.J, M.Marimuthu</i>	13
24.	Analysis of Different Approaches for Dynamic Power Dissipation in Digital Circuit <i>Dr. Lokesh C, Channakka Lakkannavar, Dr. Rekha K. R., B V Manjula</i>	14
25.	Elimination of Voltage Sag and Harmonics in Inverter of Distributed Power Generation System <i>Santhosh R, Siddharthan M A, Shyam Antoni S, Sudharson N A</i>	14
26.	Security and Self Defence System for Women Using Raspberry Pi <i>Mohamed Suhail, Shanmugarajeshwaran, Chandrasekar, R.Sridhar</i>	15

27.	Step-Down DC-DC Converter with Continuous Output Current Using Coupled-Inductors <i>G.Sriram, Parthasarathy, S.Vignesh, A.Tamizhazhagan, R.Sridhar</i>	15
28.	An Optimized Detection Classifier Model for Multiple Power Quality Disturbances <i>B. Devi Vighneshwari, Jayakumar N, Nisha C.Rani</i>	16
29.	Analysis of Classification Models to Predict the Post Graduate Admissions <i>Selvaprabu Jeganathan, Arun Raj Lakshminarayanan, Saravanan Parthasarathy, K. Martin Sagayam</i>	17
30.	A Direct Pulse Width Modulation Strategy for Three Phase Cross Switched MLI <i>Dr.C.Krishnakumar, Dr.S.Thamizharasan, S. Atchaya</i>	18
31.	Design and Development Of SEPIC Converter Fed BLDC Motor Driver For Photovoltaic Application <i>Dr. M. V. Suganyadevi, L. Ajay, T. Ananth, N. Balaji, K. Mathavan</i>	18
32.	Design and Implementation of Standalone PV Based Air Cooler <i>Hariharan.K, Aadhi mathavan.K, Kalaiyarasan.R, Karthikeyan.K Paranthagan.B</i>	19
33.	Transformerless Inverter Topology for Single Phase Application with Elimination of Leakage Current <i>Dr.K.Rajkumar, R.Manikandan, T.Nidhish, N.Sethulakshmanan, M.Prasanth</i>	19
34.	Design of Knowledge Based Agriculture and Energy Management System <i>G. Ramaprabha, R. Satheesh, G. Saranya, Sathya Uma, S.Sivapriya</i>	20
35.	Bridgeless Buck Rectifier for Led Applications <i>C Pearline Kamalini, R V Nirubhanjali, S Soundharya, J S Suruthi, S Valliammai</i>	20
36.	Design and Fabrication of Power Electronic Interface for Fixing and Removal of Bearing and Coupling in Mechanical System Using Induction Heating <i>A.E. Manish, B. Antony Rozario Gnanaraj, S. Ganesan, Dr. S. Vijayalakshmi</i>	21
37.	Design and Implementation of Central Source Multilevel Boost Converter with Fuzzy Logic Controller <i>M. Gomathi, M. Marimuthu</i>	21
38.	Implementation of Fuzzy System on Intelligent Soot Blowing Designing for Thermal Power Plant Modernization <i>S.Sambhu Prasad, Subodh Panda, D.Sirisha</i>	22
39.	Modified Single Source Multi Level Inverter for Hybrid Energy Systems	23

	<i>P.Ramprakash, G.Devadharshini, B.Haripriya, G.V.Hemadharshini, D.Keerthana</i>	
40.	Worst Case Analysis for Synchronous Buck Converter Based on Extreme Value Algorithm <i>Dr. M. Shyamalagowri, V. V. Nijil</i>	23
41.	Using Soft Computing Techniques Measurement of Voltage Stability of The Power System <i>M.V.Suganyadevi, Perumal Raja.S, Pradeep.P, M.Vasanth, M.Viswanathan</i>	24
42.	A High Gain Multilevel DC-DC Zeta Converter for High Voltage Application <i>S.Srinithi, M.Marimuthu, Dr.S.Vijayalakshmi</i>	24
43.	Regenerative Control of Electric Two-Wheeler Using Supercapacitor <i>L.Pradeepa, X.PrecillaPoorani, DR.K.Rajkumar,S.Vijayalakshmi</i>	25
44.	Automated Epileptic Seizure Detection Using Whale Optimization Based Random Forest Classifier <i>A. Phraeson Gini, Dr. M P Flower Queen</i>	25
45.	Low Cost Power Quality Analyser with Data Logging <i>Ramprasath.S, Booma.G, Dharshini.R, Joicy.J, Nandhini.T</i>	26
46.	Hybrid Energy Source Based Three Level DC-DC Converter for Electrical Vehicles <i>Shenbagalakshmi</i>	26
47.	Linear Codes Do Not Achieve the Capacity of Asymmetric Three-Input Discrete Memoryless Channels <i>R N Krishnakumar</i>	27
48.	Microcontroller Based Sinusoidal PWM Smart Inverter <i>R. Balasubramanian, Rohit Mallya, Prabhakaran.S, Vignesh.S, Sachin.S</i>	27
49.	Single Phase Multilevel Inverter Based on A Novel Switching Scheme Using Buck Converter <i>¹Sudharsan.N, ²Paranthagan.B</i>	28
50.	Design and Implementation of Oil Sludge Cleaning Rover <i>Balasubramanian R, Dinesh Kumar R, Kumaran R</i>	28
51.	Active Bridges Based Bidirectional DC-DC Converter for Solar PV Application <i>Dr.M.V.Suganyadevi, S.Kamalakannan, C.Pearline Kamalini</i>	29
52.	A Bi-Structural Converter Based Four Quadrant Operation of Permanent Magnet BLDC Motor <i>S.Rajalakshmi</i>	29

53.	Design and Analysis of a Novel Multilevel Inverter for Isolated Load Application <i>C.Keerthika, S.RamPrasath</i>	30
54.	Power Capability Enhancement with TCSC-UPFC Combined Using Social Group Optimization <i>Sunil Kumar A.V, Dr.R Prakash, Dr.Shivakumar aradhya R S,Mahesh Lamsal</i>	31
55.	Algorithmic Skeleton for Coupled Numerical Analysis of Switched Reluctance Motor Using Soft Magnetic Composite Iron Powder <i>K.Vijayakumar, C. Shanmugasundram, A. Joseph Basanth, R. Karthikeyan</i>	31
56.	Iot Based Digital Notice Board <i>V. Vinodhini, Gowthami.G, Ramya.S, Ridha Preen.C, Udhaya.S</i>	32
57.	A Contemplate of High Level Data Flow in Reversible Logic Gates <i>Kirankumar Manivannan, Dr. M. Santhi</i>	32
58.	A Study of Data Security in Fog Computing <i>N. Shanmugapriya, P. Arul</i>	33
59.	Using Blockchain Based Security For E-Health Data Access Management <i>S Renuka, P Arul</i>	34
60.	Automatic Vehicle Accident Detection and Rescue System <i>Reshma Radhakrishnan, Livin Anto Nelliserry, Muralikrishnan O, Rojan Thambi, Dr.Parvathy M</i>	34
61.	Fpga Implementation of Enhanced Speed Systolic Array Multiplier Using Pipelining Approach for Matrix Multiplication <i>S.Subathradevi, M. Deepika Eswari, M. Keerthana, S. Mahalakshmi</i>	36
62.	Smart Agriculture with Macronutrient Fertilizer's <i>D. Rasi, R. Sowndharya, S. Sudha, M. Pooja</i>	36
63.	Insect Classification Based on Improved Squeeze-And-Excitation Network <i>Divya Balasubramaniam, Dr. M. Santhi</i>	37
64.	Enhanced Performance of Image Steganography Using Hash Code in Quantum-Dot Cellular Automata <i>M. Jeyalakshmi, Dr. M. Santhi</i>	37
65.	Auto Intensity Control of Street Light with Pollution Sensor <i>Indirani M, Prarthana.M, Sonia.R Suriya.R, Showmiya.K</i>	38
66.	Iot Based Automatic Facial Detection <i>S.Athistalakshmi</i>	39
67.	Enhancement of An Adaptive Automated Warehouse Using Concussion Free Routing Algorithm	39

	<i>S. Janani, B. Savithri, K. Swetha, S. Swetha, K. Vasantha</i>	
68.	Structure Subject Model Based Visual Investigation System for Railroad Maintenance <i>M. Desika, S. Kavitha, S. Kaviya, R. Dhaunya, K. Nagarajan, G. Prathiba</i>	40
69.	Secure Communication with QKDP In WSN Using Reversible Logic Gates <i>Mrs. V. Sathya, Mr. Kirankumar Manivannan, Dr. V. Vani, Dr. Sridhar Chandrasekaran</i>	41
70.	Fpga Implementation of High Speed-Low Power Two Different Parallel Prefix Adder (Carry Tree Adder) For DSP Applications <i>Ananda.M, Malarvizhi.M, Ramya.K, Subthradevi.S</i>	41
71.	Smart Drainage Worker Safety System <i>Roshini T, Shanmuga Priya R, Vaishali A, Valantina Nivetha V, C. Vennila</i>	42
72.	Trash Cleaning Robot <i>S.Merlin, K.Shivani, S.Sandhiya, P.Keerthani, Dr. S.A.Arunmozhi</i>	43
73.	High Performance Montgomery Multiplier Using High Speed Adders for RSA Cryptosystems <i>Sruthi P, Subbhapriya.A, Hariprasath S</i>	43
74.	Hand Gesture Recognition Based on CNN <i>S.Melvin Nehemiah, H.Mohamed Faize, Z.Mohamed Aashik, V.Periyannan, Dr.M.Baritha Begum</i>	44
75.	Analysis of High Gain in Windmill Shaped Ultra-Wideband Array Antenna for Mobile Application <i>S. A. Arunmozhi, V. Benita Esther Jemmima</i>	45
76.	Wireless Food Ordering System with Maglev Based Food Service <i>Manishankar.K, Saravana Kumaran.B, Saren Kumar.B.P, Sunil Kumar M, .M.Anthuwan Lydia</i>	45
77.	Traffic Sign Recognition and Detection for Land Vehicle <i>VR.Durgasri Swethaa, R.Elakkiya, Dr.M.Santhi</i>	46
78.	IOT Based Recycle IC System <i>Priyadharshini K, Ruckmani S, Silambarasi E, Ms. Eindhumathy J</i>	47
79.	Human Action Recognition <i>Swarnaa R, SwathyPriya B, Vinubala M, Mohan V</i>	47
80.	Dysarthric Speech Enhancement Using Empirical Mode Decomposition <i>P. Shanmugapriya, P. Surya</i>	48
81.	Agricultural Skid Steering Robot Designed for Leaf Disease Detection Using Image Processing <i>Subiksha S V, Saranya P, Pavithra V, Shalini P, Shamim Banu A</i>	48

82.	To Improve Secrecy Throughput of Primary Pair in Cognitive Radio Networks <i>S.Veeralakshmi , C.Vennila</i>	49
83.	Diagnosis and Treatment Methods for Vegetable Leaf Disease Classification Using Support Vector Machine Algorithm <i>M. Santhi, T. Ragavi</i>	50
84.	Smart Helmet and Vehicle System <i>L.Aarathi, A.Abarna ,M.Abinaya, K.Malaisamy</i>	51
85.	Automatic Cough Detection Using Deep Neural Network <i>A. Sharan jasmine, Dr.V. Mohan</i>	51
86.	Recognition of Plant Leaf Diseases <i>Elakeyaa P V, Keerthana A, Bharathi P, Ezhilmani S, V. Mohan</i>	52
87.	Analysis of Retinal Images Using Textural Classifier <i>S.Hariprasath, R. Sathya</i>	53
88.	Design of Stay on Alert System for Women Safety <i>Dr.Padmaa M, Mohsina G, Pavithra P, Preetha B</i>	53
89.	Forest Fire Detection Using Deep Learning Algorithm <i>G.Sivakannu, R.Kishorekumar, M.Sureshkumar, C.Venkatesh</i>	54
90.	Gesture Controlled Bomb Disposal Robot <i>V.Ramya,P.Anushiya, K. Deepika ,J. Irene Naveena</i>	55
91.	Gain Enhanced Miniaturized Microstrip Wearable Dual-Band Antenna Design <i>Salai Gayathri M, Dr.S.A.Arunmozhi</i>	56
92.	Analysis of Epilepsy in Women with A Statistical Approach <i>Maalathy G, Dr Mohan V</i>	56
93.	Medical Tag Based on Telemetry System to Monitor CVD's Patient in A Localized Crowd Area <i>A.Shamim Banu, T.Mahesh, R.Selvakumar, A.Mohammed jawith, P.Hariprasath</i>	57
94.	Military Quadcopter <i>K.Malaisamy, A.Kesavan , P.Mohanraj, R.Vigneshwaran</i>	57
95.	IOT Based Patient Monitoring System <i>Dr.S.Rajeswari, R. Ganesh, V. Karundeva</i>	58
96.	Energy Based Void-Avoidable Opportunistic Routing for Under Water Sensor Network <i>S. Rajeswari, R. Yogasheeba</i>	59
97.	Voice Assisted Bill Reading System for Visually Impaired Persons	59

	<i>Dr.M.Baritha Begum, P.Anusiyaa, N.Archana, M.Claudius Grace</i>	
98.	Eavesdropping Aware Routing and Spectrum/Code Allocation in CDMA Based Eons Using DASS <i>M. Padmaa, J. Vinitha</i>	60
99.	Design of Circular Microstrip Patch Antenna For 5G Applications <i>Priyadarshini. G, Priya Dharshini. R, Ronikha Rajam. V, Sangeetha. S, V. Koushick</i>	61
100.	Improving Performance of Multiuser Full Duplex Device to Device Communication Underlaying Cellular Networks <i>Dr. M. Baritha begum, K.Sharmila</i>	61
101.	Efficient Decision Support System for Agriculture Using IOT <i>Maglin Fathima.V, Prathiba.R, Santhya.S, Varshini.R</i>	62
102.	Intelligent Traffic Light Control Using Image Processing (Road-Fi) <i>M. Santhi, P. Catherine Joyce S. Deepika, R. Akilandeshwari, M. Dhanvarshini</i>	62
103.	Detection of Parkinson Disease Through Speech Recognition <i>Shanmuga Priya P, Saranya G, Swetha K, Bavathareni SA, Padmavathi M</i>	63
104.	Epilepsy Alert System <i>Dinakaran G ,Ananthkrishnan P, Joshua Tribhuvandev Bennet ,Sivagamasundhari P</i>	64
105.	An Energy Efficient Programmable Controller for Personalized Biomedical Applications <i>Keerthana R, Adhilakshmi K N M, Esther Nisha K, Iswarya R, Vaishanavi R</i>	64
106.	“UGY” -The Defense Bot <i>Jerald Joel M, Joseph Leyans Brighton B, Hari Krishnan V.S, Haris T.S, Shanmuga Priya P</i>	65
107.	Angel Guardian <i>B. Nivedhaa, M.Kanishka, N.Jananie, V.Hebeya, Dr.C.Vennila,</i>	66
108.	Automated Classification of Wastes and Real-Time Monitoring Using IOT <i>Akshaya B, Gayathri R, Hamshavardni G, Mahendran M</i>	66
109.	Authenticated Ration Distribution System Using RFID <i>Aadhithya P, Devi Priya K, Divya Prabha M, Kavitha S</i>	67
110.	Trace and Track Food Supply Chain Based on Block Chain and EPICS <i>S.D. Sairam, A. Ashif Ameer, K. Akash,R. Ezhil Valavan, S. Jaya Suriya</i>	67
111.	An IOT Based Staple Food Endowment and Waste Management System for Foster Care Using Arduino And Blockchain <i>M.Janani, R.Gunaseeli, B.Abarna, B.Malarvizhi, V.Dinesh</i>	68

112.	Dual Code Data Shielding Based on Video Steganography <i>Dr.S.A.Arunmozhi, A.Abinaya, S.Anusha, J.Divyadharshini, R.Hemamalini</i>	69
113.	IoT Based Automatic Vacuum Cleaner <i>Srinidhi P B, Lavanya S, Dr.S.Rajeswari</i>	70
114.	Spotting of Unsolicited Messages and Deceptive User Identification on Social Networks <i>R. Senthamilselvi, Aarthi. M, Jusmitha. N, Kavya Priyadharshini. S, Keerthana. B</i>	71
115.	A Blockchain based Confidential Schema for Organized Data in Distributed Servers <i>A. T. Barani Vijaya Kumar, Abirami. V, Aruna. C, Jothika. S, Paven Priah. J P</i>	71
116.	Voice Based Medicine Prescription in Healthcare <i>R. Mohankumar, Anuradha. R, Bavya. P, Brahadambal. S, Deepashree. M</i>	72
117.	A simple statistical analysis approach for security risk management and cyber insurance coverage for cloud services <i>P.L. Rajarajeswari, Harini. R, Jeba Mary. G, Kaleeswari. M, Keerthika. S</i>	72
118.	Driver exhaustion detection based on facial nodal points <i>S. Mohana, Darshna. S, Ishwarya. S, Madhumitha. K, Fouzia</i>	73
119.	Secure document transfer application using Image Steganography and Visual Cryptography <i>R.Thillaikarasi, Alagu. S, Beryl Susanna. B, Bhavadarani. M, Keerthana. S</i>	74
120.	Online Purchase System using Cryptography and Steganography <i>R.Thillaikarasi, Dhivakar. S, Dinesh. T, Kisore. S</i>	74
121.	Automatic Prediction of Lung Cancer using Deep Learning Approach <i>N. Kavitha, Bhuvaneswari. M, Janani. R, Jayashree. S, Kasthuri. B</i>	75
122.	Voicepad, Java Programming by Voice <i>R. Senthamil Selvi, Nandha gopala krishnan. C, Vignesh. K, Sagul Hameed. M, Suhail Yusuff Azees. A</i>	76
123.	Defense Method for DDoS Attack by Detecting IoT Botnet Devices <i>V. Punitha, Raaja Vignesh. C, Naveen. K.S.R, Nirmal. R, Prasanna Kumar. R</i>	76
124.	Enhancing and Evaluating the Privacy of the User in Bitcoin Transaction <i>P L Rajarajeswari, Revathi. A.U, Rajalakshmi. G, Nithyasri. K, Shalini. S</i>	77
125.	Disease Prediction using Machine Learning Techniques <i>V. Punitha, Sri Gopala Krishnan. R, Pragadeesh. P, Prasanna Venkatesh. S, Sriram. S</i>	77
126.	An Approach for Job Recommendation by Exploring Job Portal	78

	<i>S Mohana, Prakash. V, Sanjay. D, Venkatramanan. A.S, Vinoth. M</i>	
127.	NVEDU <i>S. A. Sahaaya Arul Mary, Rohit Raj, Vatsala. R, Thayalan. G.R, Surya Prakash. R</i>	79
128.	Partial Replacement of Cement and Fine Aggregate by Using Bentonite and Waste <i>G.Kannan, S.Viknesh, S.Dinesh, P.Balaji, S.Abdhul Malik</i>	80
129.	Interlocking Cavity Blocks <i>Anbuselvan.A, Vasanth.M, Babu.S, Pradeep Kumar.S, Dhanalakshmi.S</i>	80
130.	A Review Paper on Effect of Self Repairing Mechanism in Concrete Using Biomatic Materials <i>Kesavaraja.C, Yuvatharani.P, Kalpana.A, Abinaya.R, Padmavathi.V</i>	81
131.	Removal of Chromium from Synthetic Wastewater by Using Low Cost Adsorbent <i>C.Nivedhitha, B.Nanthini, R.Preetha, R.Siva Sakthi</i>	82
132.	Experiment Investigation on Concrete with Partial Replacement of Cement By Cow Dung Ash <i>G.Venkatesan, Giridharan.D, Kashim Khan.N, Selva Ganesh.A, Vasanth.A.D</i>	82
133.	Experimental Investigation of Flexural Strength of Reinforced Concrete Beam Incorporating Ultrafine Slag <i>S.Kannan, S.Mohammed Aashik, A.Harish, R.Nihal Yasar, M.Mohamed Thageer</i>	83
134.	Experimental Study of Concrete with Partial Replacement of Cement by Using Lime Stone <i>Kesavaraja.C, Praveen Kumar.P, Surya Prakesh.B, Madhan Kumar.S, Suresh Kumar.M</i>	84
135.	Experimental Study on Concrete with Partial Replacement of Cement By Using Rice Husk Ash <i>G.Venkatesan, S.P.Aravindh, A.S.Ashwin, Balasubramanian, R.R.Barani</i>	84
136.	Evaluation of Road Safety Audit on Existing Highway by Empirical Babkov's Method <i>A.Anadaraj, Sadeesh.P, Saisaravana.PL.M, Satheesh Kumar.S, Vigneshwaran.S</i>	85
137.	An Experimental Study and Investigation of Self Healing Concrete Using Crystalline Admixtures <i>C.Kesavaraja, J.Madhumitha, A.Mufeena, S.Shalini</i>	86
138.	Study on Cracks in Building	86

	<i>Ellakiya Esthar.P, Nivetha.S, Sherly Agnes.A, Vijaya Shanthi.R, Dhanalakshmi.G</i>	
139.	Investigation of Water Aeration Process at Hydraulic Jump in The Venturi-Flume <i>Anandraj.A, Abarna.S, Harshitha.M, Srinivashini.V</i>	87
140.	Effect of Web Pattern Reinforcement in Slab <i>P.Vaishali, S.Ahamed Asfaq, S.M.Ajith Kumar, M.V.Naveen, A.Niranjana</i>	87
141.	Performance Analysis of Flexible Pavement- A Microcosm Study <i>Dr.G.Dhanalakshmi, Akilan.R, Aravindh.A.L, Arun Kumar.M, Kizhore Kumar.R</i>	88
142.	Automated Robotic Electric Vehicle Charging Machine with Digital Payment <i>Akshay Dhanesh, Jibin Thomas, Mohammed Sijah, Tony Tomy, Dr. Divya Nath K</i>	89
143.	Effect of Granite Dust and Aggregate on Strength of Bricks <i>P.Vaishali, S.Keerthiga, M.Neevitha Shivaani, E.Sivagmasundari, R.Viveka</i>	89

OPTICAL CHARACTER RECOGNITION BASED TEXT TO BRAILLE CONVERTER

Aswanth B, Ajith Arumugam A, Mohamed Asif K, Pradeep Kumar M, Tamilarasan T

Department of Electrical and Electronics, Saranathan College of Engineering

Tiruchirappalli-620012, Tamil Nadu, India

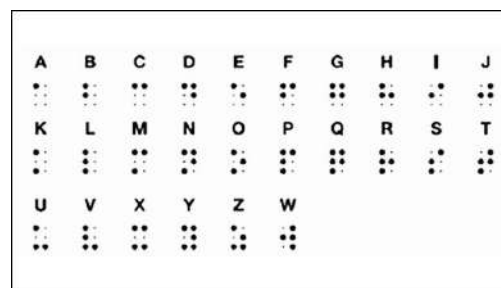
Abstract - This paper is based on a project which facilitates the education of visually impaired people through a device that helps to read text from books by them. Nowadays, visually impaired people uses Braille coded books for reading which are not easily affordable and voluminous in their size. This project is about a compact device which converts normal texts from a book to Braille coded tactile display. The conversion process is performed by Optical Character Recognition (OCR) and it is displayed with the help of servo motors or push pull solenoids. This reduces the printing cost of Braille coded books as well as the space of storage.

I. INTRODUCTION

People with vision impairment have their own techniques to do their daily activities. One of the most difficult activities is to read text or numbers from books, currencies and any other objects. It cannot be done without the help of others or any other specially designed books. In 1824 a Frenchman named Louis Braille developed a tactile writing system called Braille script for visually impaired people. These Braille characters possess rectangular blocks with some raised dots. The arrangement of these dots is in a manner to distinguish each alphabet. In English Braille there are three levels of encoding:

- GRADE I
- GRADE II
- GRADE III

Grade 1



These set of Braille characters is to recognize letters in basic alphabets.

Grade 2

The Grade 2 Braille script is for abbreviations and contractions.

Grade 3

The Grade 3 Braille script is for various non-standardized personal stenography.

This project is based on Grade 1 level of encoding to recognize the basic English alphabets and further it can be developed to recognize numbers, symbols and punctuation marks in the future.

II.HARDWARE DESIGN

The hardware consists of the following components:

- A. Raspberry PI
- B. Input Camera and Push button
- C. Output Tactile display

A. RASPBERRY PI

The raspberry pi is a Credit card sized single board computer. It is powered a Broadcom BCM2837B0, Cortex – A53 64-bit SoC clocked on 1.4 GHz. It has a 1GB LPDDR2 SDRAM . The raspberry pi has extended 40 pin GPIO header. These GPIO pins are used for general purpose and are configurable. The purpose of raspberry pi is to process image and to control the output devices. It is programmed to convert image to text and to provide the output in the form of tactile display.

B. INPUTS

Input devices are used to make the electronic Braille display a user friendly device. It is used to control the flow of the data in the tactile display as per the reader needs. There are several input devices used. They are,

- Push Buttons
- Camera

Push Buttons:

The push buttons are used for capturing image and to control the flow of texts to be displayed in the tactile display.

Camera:

The camera provides the input image with the text to be read by the visually impaired people.

C. OUTPUTS

The output devices are mainly used to actuate the tactile dots in the electronic Braille display. An electromechanical device is used as an output device. Electromechanical Actuator is a device which converts electrical energy into mechanical energy.

I. SERVO MOTOR

A servomotor is a closed loop servo mechanism with a feedback to control its motion and final position. The input to its control is some signal, either analogue or digital, representing the position commanded for the output shaft. The main use of the servo motor in the project is that it is used as

linear actuator by coupling a length shaft on its end and used to project the 3 rows 2 columns tactile dots in the tactile display.

There are several advantages of servo motor. They are,

- A. A servo motor consumes power as it rotates to the commanded position but then the servo motor rests.
- B. If a heavy load is placed on the motor, the driver will increase the current to the motor coil as it attempts to rotate the motor.



II. LINEAR SOLENOID

A Linear Solenoid is an electromagnetic device which provides a push or pulls force when it is electrically powered. It generally consists of an electrical coil wound around tube with a Ferro-magnetic actuator or “plunger” that is free to move IN or OUT of the coils body.

It can be used as an alternative for servo motor to provide the tactile output in the form of Braille codes. But some solenoids may consume more current than a servo motor therefore an external circuit is required for isolation purpose.

Six linear solenoids can be arranged in 3 rows and 2 columns to provide a tactile display.

II. WORKING MECHANISM

IMAGE CAPTURING:

The image from which the text to be read can be from either a book or any object. The image can be captured through a high resolution camera connected to Raspberry Pi. In this project a phone with IP Webcam is used for image capturing. The IP address of the captured image is send to the programming part of the Raspberry Pi and later processed for text extraction.

IMAGE PROCESSING:

The text can be extracted only if the image contains a processed text data with low noise. Therefore it is processed with the help of Open CV installed in Raspberry Pi. The programming is done using Python 2.7 and above. Firstly, the captured image is converted into Grayscale for better clarity of texts.

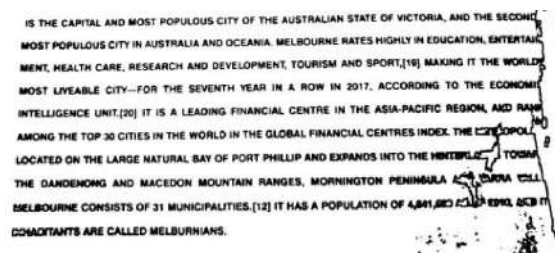
The image captured is processed using various thresholding methods like,

- Adaptive thresholding
- Binary thresholding
- Otsu thresholding

The image is blurred to reduce the background noise in the image.



Fig(a). Captured Image



Fig(b). Threshold Image

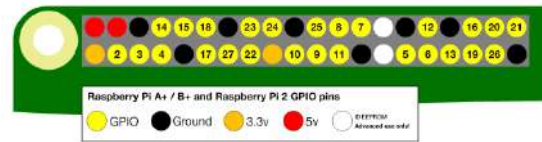
IMAGE TO TEXT CONVERSION:

The text from the processed image is extracted using an OCR engine called Tesseract. It has been installed in the Raspberry Pi and used in the coding for extracting text. The libraries used are:

- Python Image Library
- Pytesseract

TEXT TO TACTILE DISPLAY:

The obtained text is then converted to signals which actuate the respective servo motor to be popped up. Thus out of six servos the respective servo gets actuated for the corresponding alphabet.



POWER SUPPLY:

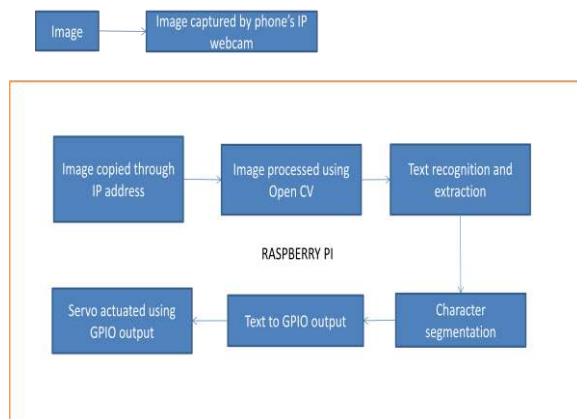
The standard DC power supply for Raspberry Pi is 5V which can be supplied either through the power pin or 5V- GND GPIO pin.

The signals for the Servo Motors are obtained from the GPIO pins of the Raspberry Pi.

The Servo Motor is provided with a external DC supply of 5V.

GPIO SIGNALS:

Letter	Pin No.	Letter	Pin No.
A	ONLY 3	N	3,7,21,19
B	3,5	O	3,7,19
C	3,21	P	3,5,7,21
D	3,21,19	Q	3,5,7,21,19
E	3,19	R	3,5,7,19
F	3,5,21	S	5,7,21
G	3,5,21,19	T	5,7,21,19
H	3,5,19	U	3,7,23
I	5,21	V	3,5,7,23
J	5,21,19	W	21,19,23
K	3,7	X	3,7,21,23
L	3,5,7	Y	3,7,21,19,23
M	3,7,21	Z	3,7,19,23

FUNCTIONAL BLOCK DIAGRAM:**STEP I:**

The text image to be read is captured by using phone's webcam app. The IP address provided by the phone's webcam is linked with Python program in Raspberry Pi. The captured image gets downloaded in the local storage of Raspberry Pi.

STEP II:

The captured image is then converted to Grayscale Image for better processing. Then it is converted to threshold image by Image Processing using Open CV. The thresholded image is blurred to reduce the noise if present in the image.

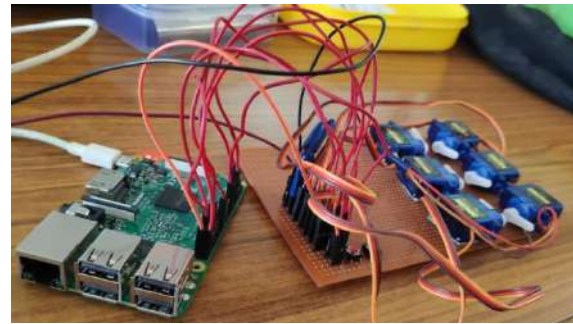
STEP III:

The text from the processed image is extracted using a Optical Character Recognition (OCR) engine called Pytesseract. The characters from the extracted text are segmented by using Python coding.

STEP IV:

Six GPIO pins are assigned in a combination to represent each English alphabet. The segmented character initiates the corresponding GPIO pins to provide signal to the servo motor.

As a result the various combinations of the six servo motors provide the tactile output in the form of Braille codes for the respective character.



This device not only converts image to text but also can be used for reading text from digital document like PDF. The extracted text can also be converted to speech using Text to Speech modules in program.

CONCLUSION:

There are many hurdles in educating visually impaired people. This device eliminates all those hurdles and makes them successful in their carrier. In future this device can be further developed to interface with internet and can be used for object detection, face detection and navigation. Thus the output can be sensed through the tactile display.

REFERENCES:

- [1] Hossain, Shahruk, et al. "Text to Braille Scanner with Ultra Low Cost Refreshable Braille Display." *2018 IEEE Global Humanitarian Technology Conference (GHTC)*. IEEE, 2018.
- [2] Liu, Zhiming, et al. "Finger-eye: A wearable text reading assistive system for the blind and visually impaired." *2016 IEEE International Conference on Real-time Computing and Robotics (RCAR)*. IEEE, 2016.
- [3] Bawdekar, Kaustubh, Ankit Kumar, and Rajkrishna Das. "Text to Braille Converter." *International Journal of Electronics and Communication Engineering and Technology (IJCET) Volume 7: 54-61*.

Implementation of Energy Data Collection and Control over the Low Power Factor Loads Using IoT

Mr Venugopal R¹

Saravanan R², Ragul R³, Sripaul J⁴, Vijayakumar M⁵

U.G. Student, Department of Electrical and Electronics Engineering, Saranathan College of Engineering, Trichy, India^{1,2,3,4}. Assistant Professor, Department Of Electrical and Electronics Engineering, Saranathan College of Engineering, Trichy, India⁵

Abstract - Energy monitoring and conservation hold almost importance in today's world because of the existing difficulties between powers. According to a survey generation and demand, the power generated will get exhausted in the next 20 years. In the current scenario, machines are shut down for a span of 5 days for maintenance work which interrupts the production and also in the profit. Replacing the existing energy auditing with our IoT based Energy Data Collection and Control over Low Power Factor Loads the energy auditing can regularly be done (24*7) and also controls the data and the collected data will be stored in the external storage as well as the cloud storage. This helps in real-time monitoring and also reduces the time, manual work along with cost. The data collected can be stored for further reference which helps to improve the power quality, improve power factor, the efficiency of the machine. The main advantage is that existing energy auditing involves high cost which can be replaced by our project to an acceptable cost and it can easily accessible independent of location.

1. INTRODUCTION

The benefit of the Internet of Things (IoT) and connected nodes has been on a steep incline in recent years. This paper aims to research, build, test and implement a low-cost energy monitoring and control system using IoT devices. Electrical appliances (e.g., air conditioning units and overhead lighting) can be controlled and monitored using IoT technology from any place in the world. A small programmable specialized computing device (e.g., Raspberry Pi) for preliminary testing. This smart node was chosen due to familiarity, and its capabilities, such as general purpose pins and built-in Wi-Fi. The end goal is to observe energy efficiency by monitoring and controlling low factor loads appliances and standard overhead lighting units.

2. METHODOLOGY

This project aim is to provide a Monitoring and Control using IoT which gives innovative services. Energy auditing is one of the major problems faced in today's world. It involves high cost which can be replaced by our project. Our project developed real-time monitoring of load management. It provides two-way communications.

Power quality analyzer is a device used in energy auditing requires a lot of time and manual work which can only be operated by the authorized person. It is a tedious process which can be substituted by our project. The monitoring can be accessed anywhere in the world. The collection of data enables comparison of various data which helps in easy load management.

3. THE INTERNET OF THINGS (IoT) SYSTEM

The hardware aspect of this project requires a variety of components that had to be tested before ordering and implementing into the system. A small programmable specialized computing device, the Raspberry Pi v3, was used for preliminary testing. The Raspberry Pi v3 was chosen due to familiarity and its built-in capabilities for all aspects of the project, including general purpose pins and Wi-Fi capabilities. The Raspberry Pi v3 also had a variety of external attachments for monitoring and control purposes. The electrical relay, an electronic switch that is activated by a current or signal between circuits, used in the preliminary testing was the Spark Fun Beefcake mechanical Control kit which would attach to the

Raspberry Pi v3 directly and become an intermediary for the electrical energy to flow through to the testing devices. The preliminary testing phase of the project, this computational device was changed to the Raspberry Pi Zero Wireless due to its affordability, similar features, and smaller size, as seen in Figure.1 below

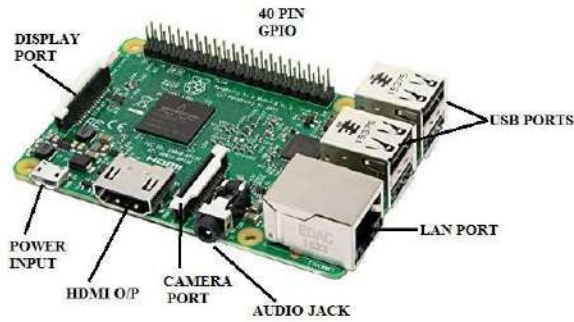


Figure.1
SMART CONTROLLER

The relay was later changed to 25 amp and 60 amp solid state relays due to variance in target appliances. The monitoring aspect involved a Current Transformer (CT) clamp, which uses a magnetic field to measure the current traveling through a wire. The analog signal output from the CT clamp was converted to digital signal by attaching it to a breadboard and then through a Analog-to-Digital-Converter (MCP 3208). Once the hardware development was fully functioning in the testing phase, AC to DC, 5W power converter modules (transformers) were implemented to supply power to the Raspberry Pi via the source from the lighting, or A/C units. The completed preliminary hardware configuration is shown in Figure.2 below

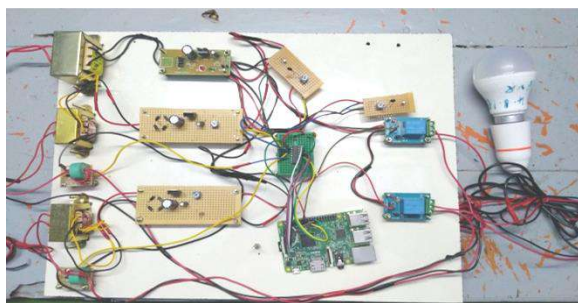


Figure.2
HARDWARE CIRCUIT

The measurements were recorded, and a calibration curve was generated, as shown in Figure.3. The calibration curve formula was implemented within the Python code on the Raspberry Pi for monitoring purposes.

The python code written for the Raspberry Pi also referenced the voltage of the device to be monitored and controlled to generate an energy consumption power rating, seen in formulas (1) and (2)

$$\text{Power} = \text{Current} * \text{Voltage} \text{ (1)}$$

$$\text{Power} = [\text{Calibration Factor} * \text{CT Clamp Reading Offset}] * \text{device_voltage_rating} \text{ (2)}$$

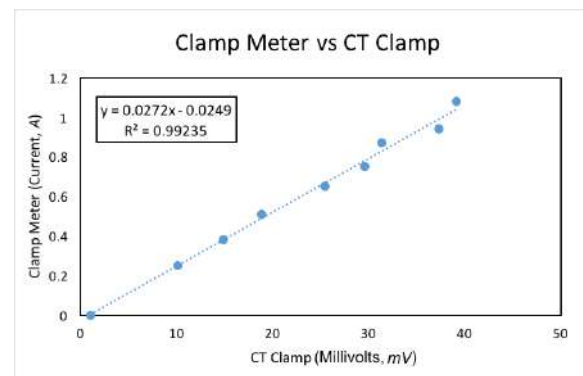


Figure.3
CALIBRATION OF CURRENT TRANSFORMER CLAMPS

Once the data is inserted and stored in the database, it can then be read from the iOS application. Additionally, the iOS application has the functionality of sending data to the database to change a device’s status (e.g., On/Off), which the smart nodes can then interpret and respond in order to satisfy the request.

4. FEASIBILITY

The proposed IoT based energy auditing and controlling is used for real-time monitoring and controlling which gives an added advantage of maximum utilization of energy resources continuously. Easy energy auditing and self healing of the machine is done with better predictability. Timely and accurate report on both sides is calculated independent of location and time. Problems like interruption of production due to

energy auditing, cost hike are eliminated. Various researches are done in this field by Advantech B+B work. No manpower is needed after the installation of this project which can be implemented.

5. INSTALLATION AND DEPLOYMENT

Before the installation began, the specific install locations were assessed on the specified iOS. Information was gathered about the Wi-Fi reliability, A/C unit specifications, equipment/tools and materials necessary for the installation. This process also involved making inquiries for extra hardware components that would be required for the installation to be successful. This inquiry was conveyed to the electrician that worked at the resort about some of the unit specifications and with the IT staff about the networking configuration before proceeding. Prior to the installation, mock wiring schemes were developed in order to fully understand how the various electrical components would be interconnected. The data flow for controlling any specific device can be seen in Figure.4 below.

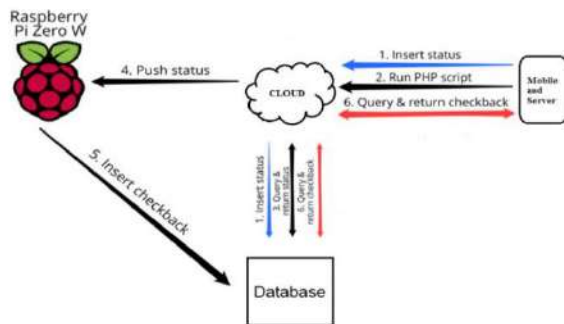


Figure.4
DATA FLOW

The final preliminary installation element that was performed was to verify that the specifications for each A/C unit, previously received from the threshold values are matched to the physical machine specifications. It became apparent that some of the given ratings for the A/C units were not accurately recorded. Installation began with one single unit in order to ensure the procedure could be replicated onto the additional A/C units.

6. MOBILE APP INTERFACE

The iOS mobile application was the primary graphical user interface (GUI) for the product. This interface allowed users to manipulate the power status of electronic devices. The app also allows for hourly data to be interactively displayed on the screen and in various time increments. The data can be viewed per unit and in an increase of hours for the duration of one day, week, or month as shown in Figure.5.

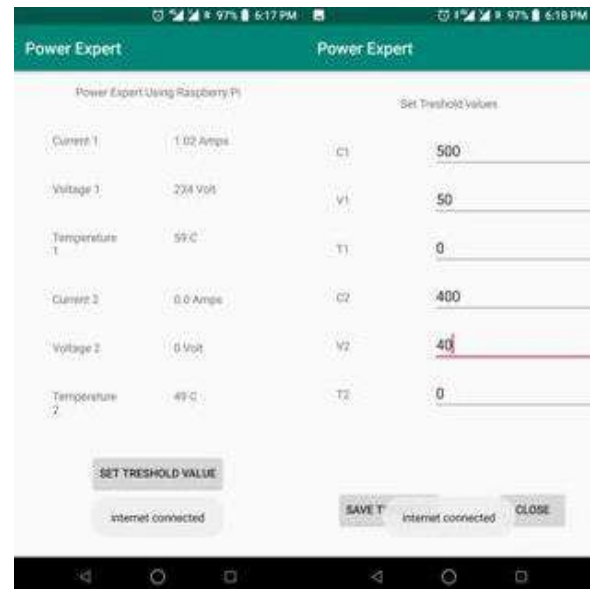


Figure.5
MOBILE APP INTERFACE ON IOS

Additionally, the graphs can be manipulated by touching your fingers to the screen using simple scaling finger gestures. The X-axis is dynamic in the fact that one can zoom in and out to change the X-axis scale. The mobile application has an ‘all control’ button to allow a user to control all components in a specific section. The components were separated by component type (e.g., LPF or lighting) in the application. A server-side scripting language designed for web development was utilized on the server instance (EC2) for the inter-component integration. Various scripts were written and stored in files on the EC2 instance in order to communicate with the database for sending and receiving data.

7. CONCLUSION

In summary, the general design concept and goal of this implementation of energy data collection and control over Low Power Factor Loads using IoT. We mainly concerned to identify the consumption of voltage, current, temperature, of a load at small scale industries and to sought out the problem. The hourly storage and ease of access to energy data accomplished through this project support the concept of energy awareness and conservation. Our product goals include the development of interactive web app/Android functionality for controlling and monitoring applications. Further product includes Wi-Fi improvements to increase responsiveness, such as upgrading to the latest Wi-Fi technologies and increasing the range of Wi-Fi signal on site (i.e., additional access points, repeaters, etc.). Finally, the addition of IoT technology for various other applications such as integrated temperature control and various 'modes' for scheduled operation would create a more versatile product.

8. ACKNOWLEDGEMENT

We really thank our colleague and our guide to overcome the problem facing in small scale industry. Also we thank for our friend who helped us with programming.

9. REFERENCES

1. Wang, Jianhua, et al. "Design of IoT-based energy efficiency management system for building ceramics production line." *Industrial Electronics and Applications (ICIEA)*, 2016 IEEE 11th Conference on. IEEE, 2016.
2. Prof. S.R.Kurkute¹, Gopal Girase², Prashant Patil³ Department of Electronics & Telecommunication, SIEM, Nasik, India
3. Chunchi Gu, Hao Zhang, Qijun Chen College of Electronics and Information, Tongji University, Shanghai, P.R. China guchunchi@126.com zhang_hao@tongji.edu.cn qjchen@tongji.edu.cn
4. A. Zanella, N. Bui, A. Castellani, L. Vangelista and M. Zorzi, "InterBnet of Things for Smart Cities," in *IEEE Internet of Things Journal*, vol. 1, no. 1, pp. 22-32, Feb. 2014.
5. C. h. Lien, Y. w. Bai and M. b. Lin, "Remote-Controllable Power Outlet System for Home Power Management," in *IEEE Transactions on Consumer Electronics*, vol. 53, no. 4, pp. 1634-1641, Nov. 2007.
6. D. M. Han and J. H. Lim, "Design and implementation of smart home energy management systems based on ZigBee," in *IEEE Transactions on Consumer Electronics*, vol. 56, no. 3, pp. 1417-1425, Aug. 2010.
7. Ashna.k, Sudhish N George "GSM Based Automatic Energy Meter Reading System with Instant Billing" *IEEE(2013)*
8. V. V. Rajesh Parvathala, T Venkateswara reddy, N V G Prasad "Arm Based Wireless Energy Meter Reading System ALONG with POWER on/off CIRCUIT" *IJEAT Volume-2, Issue-2, December 2012.*
9. S.Arun,Dr.SidappaNaidu"Design and Implementation of Automatic Meter Reading System Using GSM, ZIGBEE through GPRS" *ijarcsse Volume 2, Issue 5, May 2012.*
10. P.RakeshMalhotra,Dr.R.Seethalakshmi"Automatic Meter Reading and Theft Control System by Using GSM" *IJET Vol 5 No 2 Apr-May 2013.*
11. Shraddha Male, Pallavi Vethekar, Kavita More, Prof. V. K. Bhusari "A Smart Wireless Electronic Energy Meter Reading Using Embedded Technology" *ijera Vol. 4, Issue 1(Version 3), January 2014.*
12. O.HomaKesav, B. Abdul Rahim "Automated wireless meter reading system for monitoring and controlling power consumption" *IJRTE Volume-1, Issue-2, June 2012.*
13. Abhinandan Jain, Dilip Kumar, JyotiKedia "Alcohol Detection and Automatic Drunken Drive Avoiding System" *IJERT Vol. 1 Issue 3, May - 2012.*
14. Masahiro Inoue, Toshiyasu Higuma, Yoshiaki Ito, Noriyuki Kushiro, and Hitoshi Kubota, "Network Architecture for Home Energy Management System," *IEEE Trans. Consumer Electron.*, vol. 49, no. 3, pp. 606-613, Aug. 2003.
15. Rosenthal, Andrew L., Mani, Jeevankumar ;Kachare, Meghraj, "Low cost AC power monitor for residential PV support", *Proceedings of the twenty-ninth IEEE PVSC, May 2002*

Automatic Solar Based Grass Cutter

Saranathan College Of Engineering, Trichy

“Department Of Electrical Engineering”

V. Kavya, R. Meenachi, S. Mahalakshmi
Guided by R. Balasubramanian, Associate Professor

Abstract- This paper is based on survey of identification of classification of solar based grass cutter. The solar grass cutter is a fully automated grass cutting robotic vehicle powered by solar energy that also avoids obstacles and is capable of fully automated grass cutting without the need of any human interaction. The system uses two 6V batteries to power the vehicle movement motors as well as the grass cutter motor. We also use a solar panel to charge the battery so that there is no need of charging it externally. The grass cutter and vehicle motors are interfaced to a microcontroller that controls the working of all the motors. It is also interfaced to an ultrasonic sensor for object detection. The micro-controller moves the vehicle motors in forward direction in case no obstacle is detected. On obstacle detection the obstacle sensor monitors it and the micro-controller thus stops the grass cutter to avoid any damage to the object. Micro-controller then turns the robotic movement as long as it gets clear of the object and then moves the grass cutter in forward direction again.

Keywords - Autonomous Area coverage, Lawn availability, Path planning, Robotic.

INTRODUCTION

Grass cutter machines have become very popular today. Most of the times, grass cutter machines are used for soft grass furnishing. In a time where technology is merging with environmental awareness, consumers are looking for ways to contribute to the relief of their own carbon footprints. Pollution is man-made and can be seen in our own daily lives, more specifically in our own homes. Herein, we propose a model of the automatic grass cutting machine powered through solar energy, (nonrenewable energy). Automatic grass cutting machine is a machine which is going to perform the

grass cutting operation on its own. This model reduces both environment and noise pollution. Our new design for an old and outdated habit will help both customer and the environment. This project of a solar powered automatic grass cutter will relieve the consumer from mowing their own lawns and will reduce both environmental and noise pollution. This design is meant to be an alternate green option to the popular and environmentally hazardous fuel powered lawn mower. Ultimately, the consumer will be doing more for the environment while doing less work in their daily lives. The hope is to keep working on this project until a suitable design can be implemented and then be ultimately placed on the market. Moving the grass cutters with a standard motor powered grass cutters is an inconvenience, and no one takes pleasure in it. Cutting grass cannot be easily accomplished by elderly, younger, grass cutter moving with engine create noise pollution due to the loud engine, and local air pollution due to the combustion in the engine. Also, a motor powered engine requires periodic maintenance such as changing the engine oil. Even though electric solar grasses are environmentally friendly, they too can be an inconvenience. Along with motor powered grass cutter, electric grass cutters are also hazardous and cannot be easily used by all. Also, if the electric grass cutter is corded, mowing could prove to be problematic and dangerous. The prototype will also be will be charged from sun by using solar panels.

Existing System

Now a day's pollution is a major issue for whole world. Pollution is manmade and can be seen in own homes. In case gas powered lawn movers due to the emission of the gases it is responsible for pollution. Also the cost of the fuel is increasing. Hence it is not efficient. The solar powered lawn cutters are introduced. Solar powered lawn mower can be described as the application of solar energy to power

an electric motor which in turn rotates a blade which does the moving of a lawn.

Proposed System

This system uses solar panel to give power to the system and uses the ultrasonic sensor to detect the crop in front of the robot. It is interfaced to an ultrasonic sensor for object detection. The micro-controller moves the vehicle motors in forward direction in case no obstacle is detected. On obstacle detection the obstacle sensor monitors it and the micro-controller thus stops the grass cutter to avoid any damage to the object. It consists of two motors placed front and back of the robot.

METHODOLOGY

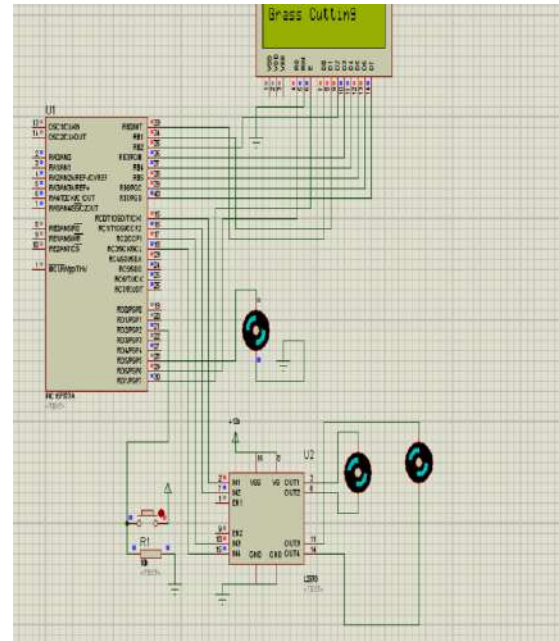
System Architecture and Description:

The grass cutting robot is designed to achieve path planning and obstacle avoidance with the aid of PIC16F877A microcontroller. It is solar energy driven using photovoltaic panel for charging 12 V battery for powering operation of the robot (DC motor for robotic vehicle movement as well as the motor driving the cutting blade). The blade and vehicle movement motors are interconnected to microcontroller that manages the working of the robot.

The research aimed at development of an autonomous solar grass cutting robot that is capable of avoiding obstacle on its way and equally achieve path planning.

The microcontroller directs the vehicle motors in forward motion peradventure no obstacle is detected. Else, the ultrasonic sensor detects any obstacle ahead of it and sends a command to the microcontroller. Depending on the input signal received, the microcontroller redirects the robot to move in an alternate direction by actuating the driving motor thus terminate the rotation of the blade motor so as to avoid any wreck to the contact.

To achieve compatibility of microcontroller and the motors, a driver circuit is used, simulated on Proteus.



System Design:

Obstacle avoidance is the primary requirement of the solar grass cutting robot. The robot is design to navigate in unknown environment by avoiding collisions. A basic algorithm and design is presented which can be further improved depending upon the required applications. The implementation of obstacle avoidance for the solar grass cutting robot involves the writing and compilation of program using MPLAB software. Program written for the obstacle avoidance module was written based on the flowchart. The code for programming the robot is written in C programming language. The code is compiled, debugged and uploaded. Presence of microcontroller to sense the environment through receiving input from sensors. It is also able to control its surrounding through controlling motors.

System Component and Specification

SOFTWARE REQUIREMENT:

- MPLAB IDE
- PROTEUS

S/N	Component	Specification
1	Rechargeable Battery	12v,1.3 amps
2	Microcontroller	40 pin, 8 bit PIC16F877A
3	Solar Panel	12v, 5W
4	Motor IC Driver	L293N H-bridge module
5	Power Supply IC	7805, 7812 regulator IC
6	DC Motor for motion	12v, 100 rpm DC gear motor
7	DC Motor for cutter	12v, 1800 rpm 1 DC gear motor
8	Ultrasonic sensor	HC-SR04 5v, (2cm-500cm) ranging, 0.3 cm resolution
9	Cutting blade	Mild steel,2mm thickness, 4inch diameter

two motors for motion. Ultrasonic Sensor HC-SR04 takes 5v supply from voltage regulator IC which is required for measuring distance and detecting the obstacles. If any obstacles present in the way of robot, it will give command to PIC microcontroller. This signal received by controller and actuates the driving motor in alternate direction.

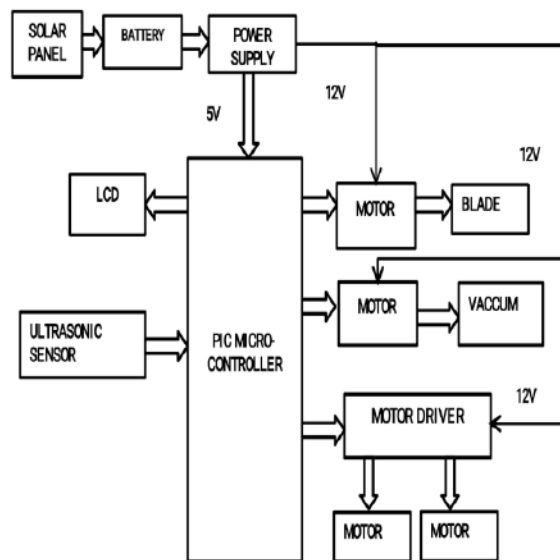
PIC MICROCONTROLLER

Peripheral Interface Controllers (PIC) is one of the advanced microcontrollers developed by microchip technologies. These microcontrollers are widely used in modern electronics applications.

A PIC controller integrates all type of advanced interfacing ports and memory modules. These controllers are more advanced than normal microcontroller like INTEL 8051.

Features OF PIC16F877 are 8 Kbytes of FLASH Program Memory. 368 bytes of data Memory (RAM). 256 bytes of EEPROM Data Memory. 33 inputs or output pins. 20 MHz operating speed (200 ns instruction cycle). High performance RISC CPU. All simple cycle instructions except for program branches which are two cycles.3 timers, 2-16bit CCP, 2-Serial communication modules, 10 bit ADC.

BLOCK DIAGRAM



As we are doing this project mainly focused on solar based system, initially power is taken from the solar panel via 12v battery. For the PIC microcontroller PIC16F877A, 5v is given from the battery after rectification in voltage regulator IC 7812 and 7805. Then, for the motors used for blade and vacuum 12v is supplied separately. 12v supply is given to motor driver IC L293D H-Bridge and its input from PIC microcontroller. This motor driver IC enhances the forward motion of grass cutting robot by controlling

SOLAR PANEL

Rugged 5W 12Vdc photovoltaic solar panel. Sealed to withstand hail, snow and wind. Multicrystalline silicon solar cells in a heavy-duty anodized aluminum frame. High-transparency, low-iron tempered glass. 188 x 195 x 17mm. Junction box with screw or solder terminals are present.

BATTERY SPECIFICATIONS

The rechargeable backup battery provides power to Finger Tec terminals when the primary source of power is unavailable. With the right backup battery, your system won't have to be interrupted during a power failure. 12V,1.5Ah Backup Battery Access Control System: The external Rechargeable Backup Batteries are almost always used in an access control system.

ULTRASONIC SENSOR

The HC-SR04 ultrasonic sensor uses sonar to determine distance to an object. It offers excellent range accuracy and stable readings in an easy-to-use package. Its operation is not affected by sunlight or black material like Sharp rangefinders.

DC MOTOR

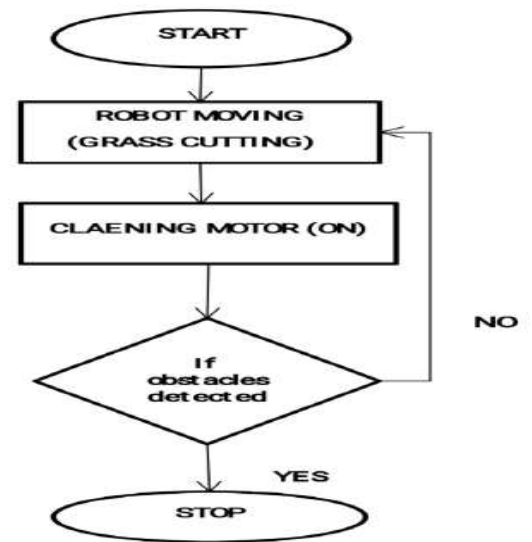
Geared DC motors can be defined as an extension of DC motor which already had its insight details demystified here. A geared DC Motor has a gear assembly attached to the motor. The speed of motor is counted in terms of rotations of the shaft per minute and is termed as RPM. The gear assembly helps in increasing the torque and reducing the speed. Using the correct combination of gears in a gear motor, its speed can be reduced to any desirable figure. This concept where gears reduce the speed of the vehicle but increase its torque is known as gear reduction. This insight will explore all the minor and major details that make the gear head and hence the working of geared DC motor.

L293D –DC MOTOR DRIVER IC

L293D is a popular motor driving IC. It is a 16 pin IC. The IC has 8 pins on both the sides. It has 2 enable pins, 1 V_{SS} pin, 1 V_S pin, 4 ground pins, 4 input pins and 4 output pins. Though not required here, but in case you wish to learn how to [interface L293D with a microcontroller](#)

Algorithm

The implementation of obstacle avoidance for the solar grass cutting robot involves the writing and compilation of program using MPLAB software. Presence of microcontroller to sense the environment through receiving input from sensors. It is also able to control for programming the robot is written using the MPLAB, written in C programming language. The code is compiled, debugged and uploaded to the PIC board after successful compilation.



CONCLUSION

Thus the Solar grass cutter was designed such that the solar plate generates solar energy and utilizing this energy for running the grass cutter motor. Integrating features of all the hardware components used have been developed in it. Presence of every module has been reasoned out and placed carefully, thus contributing to the best working of the unit. Secondly, using highly advanced IC's with the help of growing technology, the project has been successfully implemented. Thus the project has been successfully designed and tested. The solar voltage generated on LCD display unit. This idea can be extended by adding features like give alerting when the battery voltage level goes low below threshold limit. We can add an interfacing of automatic power bank to charge the battery instantly. It can also be extended using driver circuits for controlling intensities, speed levels of the motor. Extensions using Wireless remote controls like RF, zigbee, Wi-Fi networks through which the grass cutter model can be operated from a distance by the user.

REFERENCES

- [1]. IJAEEE, VOLUME1, number 1nor fatimaIssn 2319-1112 / VINI 9-14 IjAEEE

- [2]. Mukherjee, D. Chakrabarti, s., fundamentals of renewable energy systems, new age international publishers, New Delhi, 2005
- [3]. Sharma, p.c., non-conventional power plants, public printing service, New Delhi, 2003
- [4]. Arora, c.p., fundamentals of renewable energy systems new age international limited publishers, New Delhi, 2005
- [5]. Raja, A.K., non conventional power engineering, public printing service, New Delhi., 2007
6. Agarwal M.P., solar energy, S. Chand company ltd, New Delhi.
- [6]. “The Design of Equalizer Windings for Lap-Wound DC Machines”, Alaric Pagel, Member, IEEE, Alan S. Meyer, and Charles F. Landy, Senior Member, IEEE. IEEE TRANSACTIONS ON INDUSTRY APPLICATIONS, VOL. 37, NO. 4, JULY/AUGUST 2001.
- [7]. “Cascaded DC–DC Converter Connection of Photovoltaic Modules”, Geoffrey R. Walker, Member, IEEE, and Paul C. Sernia, IEEE TRANSACTIONS ON POWER ELECTRONICS, VOL. 19, NO. 4, JULY 2004.
- [8]. “Energy Management Based on Frequency Approach for Hybrid Electric Vehicle Applications: Fuel-Cell/Lithium- Battery and Ultra capacitors”, AbdallahTani, MamadouBailoCamara, Member, IEEE, and BrayimaDakyo, Member, IEEE, IEEE TRANSACTIONS ON VEHICULAR TECHNOLOGY, VOL. 61, NO. 8, OCTOBER 2012.
- [9]. “Optimal Design of a 3.5-kV/11-kW DC–DC Converter for Charging Capacitor Banks of Power Modulators”, Gabriel Ortiz, DominikBortis, Student Member, IEEE, Jürgen Biela, Member, IEEE, and Johann W. Kolar, Senior Member, IEEE, IEEE TRANSACTIONS ON PLASMA SCIENCE, VOL. 38, NO. 10, OCTOBER 2010.
- [10]. “DC-DC Power Converters”, Robert W. Erickson Department of Electrical and Computer Engineering University of Colorado Boulder, CO 80309-0425, Article in Wiley Encyclopedia of Electrical and Electronics Engineering.

Power Quality Improvement using Series Active Power Filter

C Pearline Kamalini ¹Abinaya.T, Eazhilarasi.J, Hemadevi.T

¹Assistant

Professor Department of EEE

Saranathan College of Engineering

Abstract— Power quality issues are the major considerations in this modern power system due to the increased usage of power electronic based equipments. This paper describes how to reduce the harmonic distortion and thereby achieving power quality improvement by series active power filter. Harmonic currents in distribution system are increased by larger use of nonlinear loads. A series active power filter is the combination of shunt active power filter with transformer injection with a help of PI controller. Here a MATLAB SIMULINK software is used to simulate and expected results were obtained.

Keywords: Harmonics, THD, Power quality improvement (PQI), Series active power filter (SAPF).

I. INTRODUCTION

Power quality is one of the major issues, in the modern electrical distribution system. The power quality can be analyzed as voltage unbalance, voltage sag and voltage swell, partial or total loss of one or more phases. The voltage unbalance is mainly caused due to uneven distribution of single-phase loads.

The lack of power quality leads to loss of production, damage of equipment or appliances, increased power losses, interference of communication lines and so on. The poor quality of voltage are also affected by the power system equipment and customer equipment's such as overhead and underground cables, transformers and rotating electric machines, protection systems. Traditionally, passive filters have been used for mitigating the distortion due to harmonic current in industrial power sector. But they have many drawbacks such as resonance problem, dependency of their performance on the system impedance, absorption of harmonic current of nonlinear loads, which could lead to further harmonic propagation through the power system.

Active power filters is introduced, to overcome such problem. It has no drawbacks when compared to passive filters. APF inject harmonic voltage or current with appropriate magnitudes and phase angle into the system and cancel harmonics of nonlinear loads.

But it also has some drawbacks such as high initial cost and high power losses due to which their wider applications are limited, especially with high power rating system. The more usage of power electronics based equipments has produced a predominant impact on quality of electric power supply.

Due to the increase in harmonic pollutions in the power system, it has attracted the attention of power electronics and power system engineers to develop dynamic and adjustable solutions to the power quality problems. The unbalanced voltage can be compensated with use of series active filter which regulate the voltage to the desired level.

In this paper, simulation of a single phase series active power filter is used for mitigating harmonics.

II. FILTERS

A filter are circuits which performs signal processing functions, specifically to remove unwanted frequency components from the signal, to enhance wanted ones. Basically two types of filters are used for power quality problems such as Active Power filters and Passive Power filters

1. Passive filter:

The passive filters are used to reduce power quality problems. Moreover, apart from reducing the current harmonics, the passive filters also provide reactive power compensation, thereby, further gaining the system performance. Passive implementations of linear filters are based on combinations of resistors (R), inductors (L) and capacitors (C). These types are collectively known as passive filters, because they do not depend upon an external power supply and they do not contain active components such as transistors.

The most common type of passive filter used is the single tuned passive filter. A single tuned filter, which is a series RLC circuit tuned to a single harmonics frequency provides a low harmonic impedance. Another type of configuration is double tuned filter.

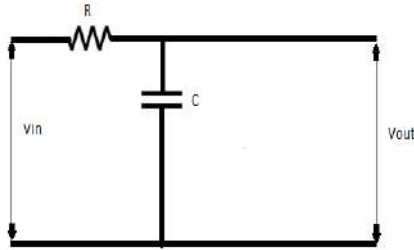


Fig: 1.1 passive filter

2.Active filter:

An active filter is a type of analog circuit implementing an electronic circuit using active components as shown in fig 6. An active filter can have complex poles and zeros without using a bulky or expensive inductor. Active filters contain active components such as op amps, transistors or FET's within their internal design. They draw their power from an external power source and use it to boost or amplify the output signal. It can be easily adjusted over a wide frequency range without alerting the dynamic response. Active filters not be affected by the load as it has low output impedance, and it has high input impedance which prevents the overloading of the source.

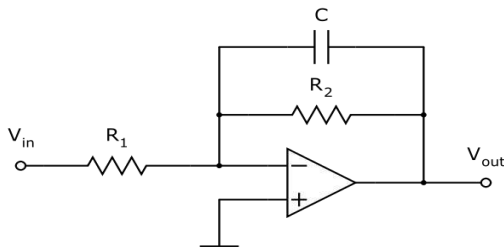


Fig:1.2 active filter

III.HARMONICS ELIMINATION

A harmonic is a signal or wave whose frequency is an integral multiple of the frequency of some reference signal or wave. According to IEEE 519, harmonic voltage distortion on power systems 69 kV and below is 5.0% total harmonic distortion (THD) with each individual harmonic limited to 3.0%.

$$THD_F = \frac{\sqrt{V_2^2 + V_3^2 + V_4^2 + \dots}}{V_1}$$

where V_n is the RMS voltage of the n th harmonic and $n = 1$ is the fundamental frequency.

Harmonic contaminations are due to the

increment of nonlinear loads, such as large thyristor power converters, rectifiers and arc furnaces, has become a serious problem in power systems. These problems are partially solved with the help of LC passive filters. However, this kind of filter cannot solve random variations in the load current waveform. They can also produce series and parallel resonance with source impedance. To solve these problems, series active power filters have been developed which are widely investigated today. These filters work as current sources, connected in series with the nonlinear load, generating the harmonic currents the load requires. In this form, the mains only need to supply the fundamental, avoiding contamination problems along the transmission lines. With an appropriated control strategy, it is also possible to correct harmonic distortions and unbalanced loads.

IV.SERIES ACTIVE POWER FILTER

Series active filter is usually proposed to solve voltage distortions, current distortions and other related issues. They are more competent than shunt compensators as they are able to compensate current issues. A series active filter eliminates the harmonic contents created due to non-linear loads from the output load side. It takes line to neutral voltages and line currents at its input and calculates the compensating voltages which need to be added in series with the distorted load voltage. The advantages of series active filter are – automatic compensation for varying loads, resonance free, does not affect power factor and can be combined with passive filter network.

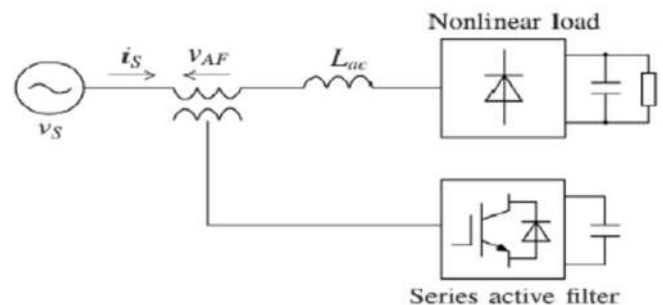


Fig:1.3 series active power filter

Series active power filter injects the voltage component in series with the supply voltage and hence it acts as a controlled voltage source, compensating voltage sag, swells and on the load sides. The main function of series active power filter is to protect the sensitive loads from voltage sag, voltage swell and harmonics. SAPF provides no compensation at fundamental frequency. At harmonic frequency, the SAPF acts as series harmonic compensator, cancelling the effect of equivalent harmonic voltage source and meeting out the harmonic requirement of the load. In other words, the harmonic

source injected in the lines is in phase with the source harmonic current. Thus, it acts as a high valued resistor for the harmonic current from supply side and as a voltage harmonic source for harmonic component of load current, completely providing the need of harmonic current required / produced by the load. This prevents any flow of harmonic current towards source side.

V.CONTROL SCHEME

The aim of series active filters control is to generate signals for switching power devices in accordance with the estimated reference signal. Active filter performances are significantly influenced by the choice of control techniques. For active filter applications can specify a variety of control techniques: linear control, the hysteresis control, digital deadbeat control.

Hysteresis technique assumes instantaneous control between two limits, which require the offset signal, current i_f or voltage u_f , expected to follow the reference signal ($i_{f,ref}$ or $u_{f,ref}$) with some deviation imposed by the choice of hysteresis band width. Control scheme is illustrated by block diagram in Fig. 1.4

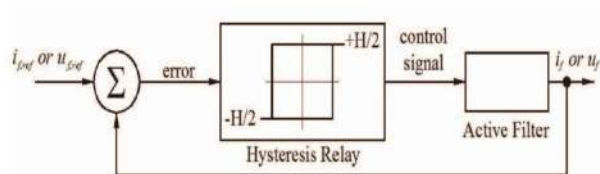


Fig:1.4 Block diagram of hysteresis control technique

This control technique requires a deviation H of a reference signal $i_{f,ref}$ or $u_{f,ref}$, which determine the upper and lower limits of the hysteresis band. Output signals, i_f or u_f , are measured and compared with its reference value $i_{f,ref}$ or $u_{f,ref}$, the resulting error is applied to a controller with a changeover relay. This generates control signals for power switching devices, when the lower

(estimated reference - $H / 2$) or upper (estimated value of reference + $H / 2$) limit are exceeded. As long as the error is in the hysteresis band, power switching devices will not be switched. Switching occurs when the error is outside the hysteresis band. Active filter is controlled so that the peak to peak value of the compensation signal, current or voltage is limited to specified hysteresis band H . The proposed scheme is implemented with hysteresis current controller with fixed band H . To obtain a compensated current i_f with a current ripple as low as possible, the value of H should be small. This will lead to high switching frequencies and increasing the switching losses. Advantages of using the hysteresis current control are excellent dynamic performance and the ability to control the peak to peak value of current ripple in the specified hysteresis band. Implementation of this control technique is simple, which results from the controller structure in Fig. 1.4. However, the hysteresis control has several unsatisfactory features. The main disadvantage is that results in a variable switching frequency. On the other hand, irregular switching may affect the efficiency and reliability of active filter.

VI.SIMULATION ANDMODEL:

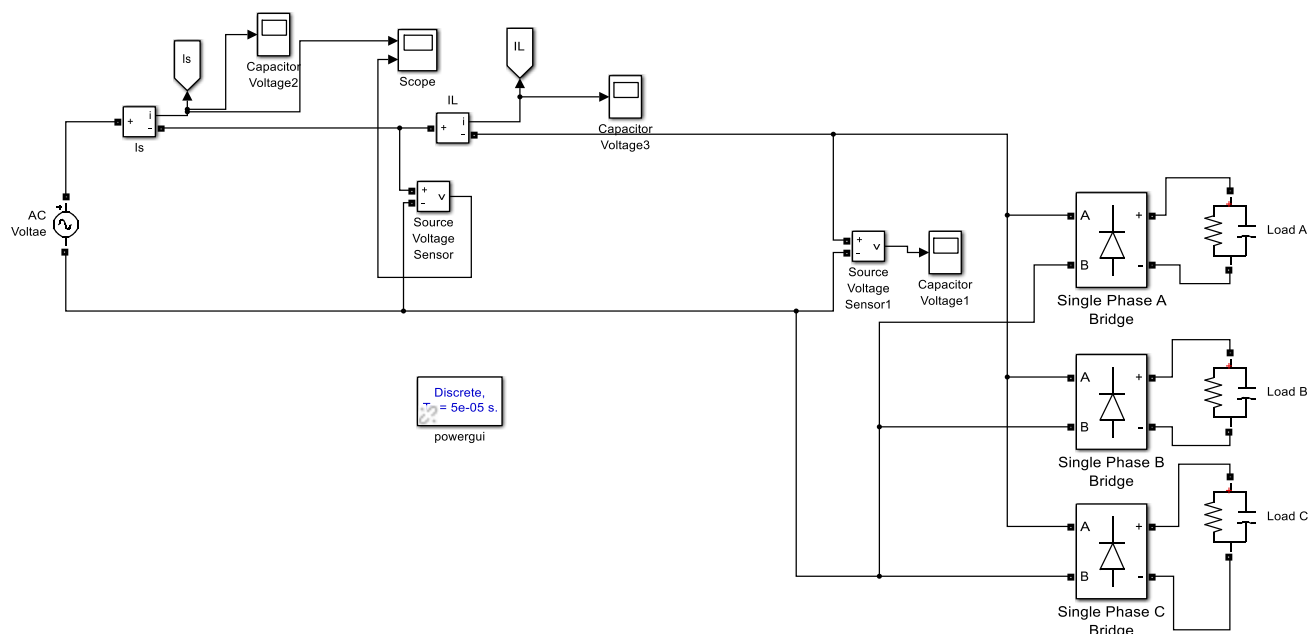


Fig: 1.5 SIMULATION WITHOUT FILTER

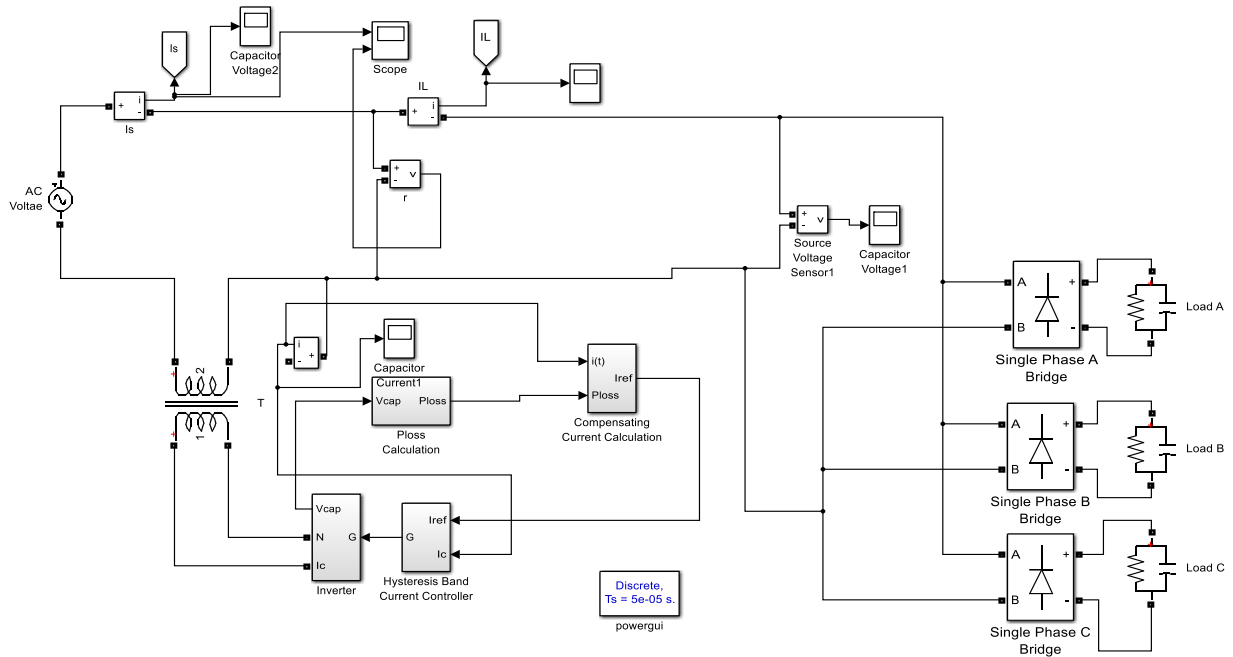


Fig:1.6 simulation with series active filter

Fig 1.5 explains the connection of non-linear load without APF. When this system is connected to supply it creates harmonics in load voltage and load currents due to its non-

VII.SIMULATION RESULTS:

The total system without filter and with series active power filter were simulated and the results were obtained.

1.FFT analysis of load current without APF:

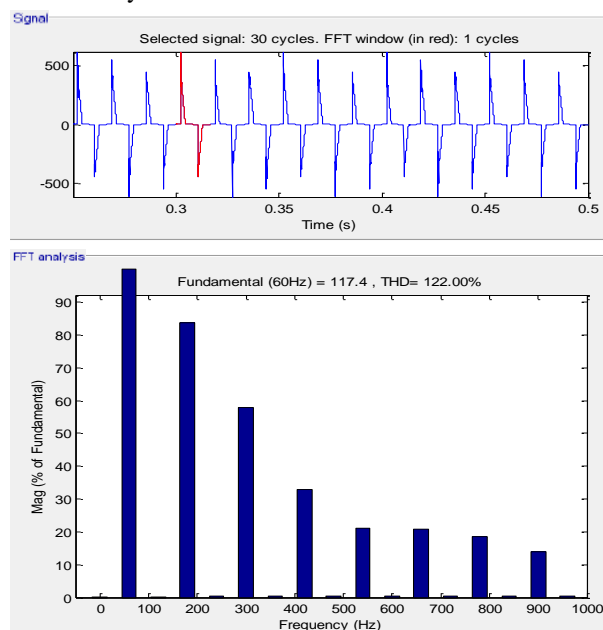


Fig: 1.7 FFT analysis of load current without APF

Fig.1.7 shows a typical non-linear load current output without series APF.After simulation

linear property. The supply voltage is 230V with the fundamental frequency of 50Hz Diode bridge rectifier with RC load act as a non-linear load. corresponding current harmonic spectrum is obtained.Total current harmonic is found to be 122.0% of the fundamental.

2.FFT analysis of load current with APF:

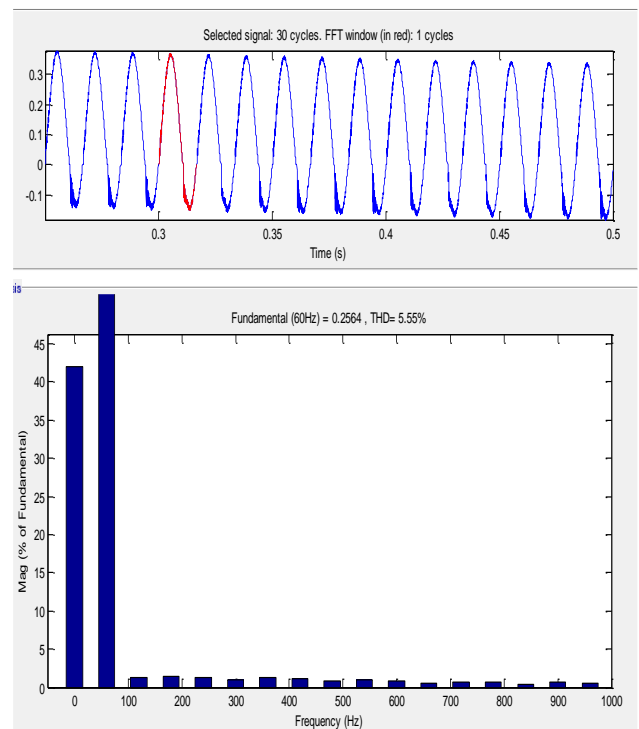


Fig:1.8 FFT analysis of load current with APF

Fig.1.8 shows a typical non-linear load current output with series APF. After simulation corresponding current harmonic spectrum is obtained. Total current harmonic is found to be 5.5% of the fundamental.

3.Results with THD%:

SIMULATED RESULTS CONTAINING TOTAL THD VALUE OF CURRENT WITH AND WITHOUT SERIES ACTIVE POWER FILTER

PARAMETERS	WITHOUT APF(%)	WITH APF(%)
Total THD%	122.00%	5.5%
Third harmonics	82%	3.7%
Fifth harmonics	59%	2.29%
Seventh harmonics	31%	1.3%
Nineth harmonics	19%	0.45%

VIII.CONCLUSION:

In this paper a series active power filter compensation technique is presented. The proposed idea is to reduce current harmonic distortions by SAPF with proper control scheme. This microcontroller based approach is cost, effective and efficient. The fact that the system is not much complex and compensation performance is good and makes it a better choice for robust compensation of voltage distortions due to nonlinear loads. The series active filter can perform better in reduction of THD. The simulation results shows a very good performance of proposed algorithm and it was tested under balanced load supplying to nonlinear load.

IX.REFERENCE:

[1] Peng, F.Z., Akagi, H. and Nabae, A., "A New Approach to Harmonic Compensation in Power Systems", in IEEE Trans. on Industry Applications, vol. 26, no 6, Nov./Dec. 1990, pp. 983-990.
 [2] L.Moran, P.Werlinger, J.Dixon and R.Wallace, "A Series active filter which compensates current harmonics and voltage unbalances simultaneously," Proceeding of the IEEE Conference on power Electronics Specialists, pp.222-227, 1995.
 [3] Design of Series Active Filter for Power Quality Improvement, IEEE, 2014 International conference on Electronics, Communication Computational Engineering.
 [4] B.Singh, K.Al-Haddad, and

A.Chandra, "A review of active power filters for power quality improvement," IEEE Trans.Ind.Electron., vol.45, no.5, pp.960 - 971, Oct 1999. [3].
 [5] M. H J. Bollen, "Understanding Power Quality Problems" in Piscataway, NJ, USA: IEEE Press, 2000. [5] J. Nastran, R. Cajhen, M. Seliger, P. Jereb, "Active power filters for Nonlinear AC loads", IEEE Trans. Power Electron, vol. 9, no. 1, pp. 92-96, 1994.
 [6] Joseph S. Subjak, John S. Mcquilkin, "Harmonics-Causes Effects Measurements and Analysis: An Update", IEEE Trans on Industry Appl, vol. 26, no. 6, pp. 1034-1042, 1990 [7] F. Z. Peng, D. J. Adams, "Harmonics sources and filtering approaches", Proc. Industry Applications conf., vol.1, Oct. 1999.

VULCOPTER

Dr.S.Vijayalakshmi, Ph.D ,
Electrical and Electronics Engineering,
Saranathan College of Engineering,
Trichy- 620 012.
bksviji@gmail.com

Arun Prasath P A
Electrical and Electronics Engineering,
Saranathan College of Engineering,
Trichy- 620 012
prasathanjaan@gmail.com

Cyril Rozario B,
Electrical and Electronics Engineering,
Saranathan College of Engineering,
Trichy- 620 012.
cyrilrozario33@gmail.com

Vignesh V & Kishore Kumar S
Electrical and Electronics Engineering,
Saranathan College of Engineering,
Trichy- 620 012
vignesh.vijay11@gmail.com
kishorekumar1216@gmail.com

I. INTRODUCTION

An UAV Unmanned Aerial Vehicle is considered as a flying mission for different goals. This UAV constrains all host embedded components to grasp over the trained mission in which instructions were fetched into it. This flying platform is considered to be one of the future scope for a development. Here the UAV has a special mission, with the help of the IOT and CLOUD technology and artificial technology which will be a future for all fields. So this project will be useful in aerodynamic field. The UAV is mainly of two types: fixed and multi rotor wing. This is neither of the two types (multi rotor or fixed) which is an ornithopter. The vision of our project is to compete with the foremost firm. Our objective is to monitor, to hunt offender and to prison virtually.

EEE

February 8, 2019

A. Components

Our objective is to monitor, to hunt offender and to prison virtually. The claws of our vulcopter are mainly designed for electrostatic charging and the transmitter 6 Channel 2.4 GHz paves a main advantage for our design as it ranges to 1 km. The thermal sensor, senses a person easily who are far from the point of vision and the long-range OEM camera looks distinct in our operation. MSP-430 is one of the texas instrument and a mixed-signal microcontroller used as it is a low consumption of power. It is given with the USART data which acts virtually outside the drone. In the USART, the transmitter transmits the signal to the reciever and the data recieved will gives the desired output. HC-SR04 is a obstacle detector which can be used to detect the obstacles, the drone going to face. Rather than those components, we use some other components such as electrostatic charge rectifier.

Transceiver 6CH receives the signal from the transmitter for appx. 1km radius with 2.4 GHz. Electronic speed controller (30A) is used to control the current entering the motor based on the load the current consumption may vary.

Motor @ No Load - ESC 5 - 10A

Motor @ Full load - ESC 20-25A

B. Design:

The bird initially tries to take off its speed from initial condition with respect to the four components: Lift, Weight, Drag, Thrust are the main components of vulcopter. These components depends on one another for the resultant force exerted by a bird (ornithopter). The Resultant force is the vector sum of the magnitude of the lift and Thrust. The magnitude of drag and the thrust are in an angle nearer to 180 degree not equal to 180. Likewise Magnitude of lift and the weight resembles the same as that of the drag and the thrust. The direction of the flight depends on the thrust exerted by the body. The mathematical design of magnitude can be calculated with the help of the formula of force. The Thrust resembles as same as that of force, the force is nothing but the rate of change of momentum with respect to time.

$F = mv$ where

F=Force or thrust of the ornithopter

m=Mass of the object

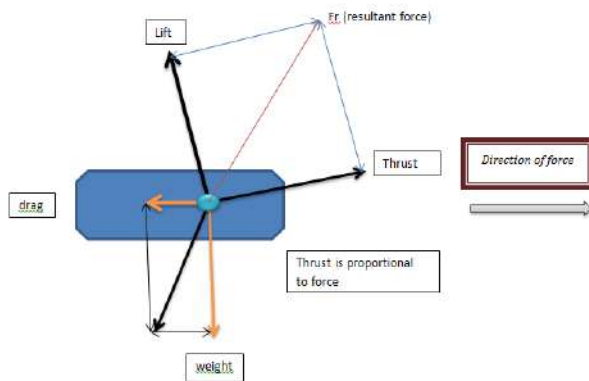
v=Velocity by which the ornithopter moves

So force can be expressed in terms of mass and velocity. The thrust is produced by the engine in which the bird moves in a desired direction. The relationship with the mass and then weight is that , it is directly proportional to each other(weight=mass x acceleration).

The weight of the bird is very less as we use a Hollow Cylindrical Duralumine Aluminium foil to design a bird. As the weight of the ornithopter gets minimum lift power also increases which will not coincide by the straight line with the weight. Then the starting torque will be high which will lift the ornithopter to a desired direction in a desired force. The mathematical model of the ornithopter can be determined by the above equation.

- AGE GROUP -25 and above
- INCOME LEVEL -Rs. 30,000/Month and above
- GEOGRAPHIC AREAS -Military and defense, Agriculture, medical field

Behalf of this some other applications also plays a main role in the ornithopter development. These are tail and wing configuration. The wing is chosen in such a way that should be a fibre such as the PET foil and CFRP(Carbon Fibre Reinforced Polymer). In recent technologies the microbat project reveals the importance of MEMS (Micro Electro Mechanical Sensor) wings which can be used both in UAV (Unmanned Ariel Vehicle) as well as MAV(Micro Air Vehicle). We have used the Delfly II wings since it has the higher efficiency and positioning stiffness and do not have a rounded edge which will provoke the wings efficiency. Now the actuators we have chosen is piezo servo which is made by New Scale. The actuators are mainly used for moving



C. Problem solving

It centres and focuses on Aerodynamic field. The problem I have solved through this design is to monitor, hunt the offender and prison them virtually. This reveals that, normal drone can be easily scanned by the offender and he gets warned, but the ornithopter, camouflages itself from the victim. So this can be used in various fields such as military, medical etc. It has the ability to connect people, understand them and partner with them, as it has innovation and strategies.

It transmits and receives the data simultaneously over long distances. The ornithopter is equipped with first aid kit which can fly above by locating the GPS of that person who is in an emergency (after intimation). This is the big to big deal to solve the catastrophe. For example, flood recovery schemes in Kerala can be made possible. The shape of the vulcopter is a unique feature. The flying mechanism and the shape resembles a vulture. It is designed with the characteristics of an eagle and hence it is presumable to others.

Medical field: Used for Safety Surveillance and for emergency purposes.

Military Field: Flapping wing technology plays a vital role in military applications such as RPAS (Remotely Piloted Aerial Systems) a supervision technology, research and development project. This makes the way for the development and its advancement.

Search and Rescue: Search and rescue of cast away persons. This is equipped with thermal sensor so that, it can easily sense the person who are far from the point of vision. For example flood prevailed in States such as Kerala Karnataka needs the rescue team for sudden relief from flood, for such purposes this plays a vital role in rescue operation

Agricultural field: Used to monitor the crops periodically before harvesting. In draught field the temperature sensor senses weather condition suitable for crops and irrigate the field.

Core Innovation Technology: Charging through the claws finds the uniqueness. Artificial technology. Scanning through thermal sensors. Captures the far away person easily by OEM cameras.

II. TEAM MANAGEMENT:

2.1 Internal Development Team The internal development team will play a role in designing the copter in an efficient way and to enhance the level of strategy to withstand its thrust.

2.2 Maintenance And Service Team This team will pro-voke over the maintenance of copter and check for any update to get a best design.

2.3 Approval And License Team License is the basic necessity for every copters to fly over the sky. This team will take their work.

III. MARKET:

3.1 Market Demand Total Available Market (TAM): UAVs are considered a flying platform and is available in all markets with the stock of market with respect to Visual Line of Sight (VLOS), Extended Visual

Line of Sight (EVLOS), Beyond Line of Sight (BLOS) UAV market in sector is higher in military (70 percent) than commercial (17 percent) appx. (5:1) We may have TAM for our vulcopter to be estimated as 10 million appx. Serviceable Available Market (SAM): The hardware model of the vulcopter will not yield the success in entrepreneur. Service that is used for operating and maintenance will provoke high value. The detailed design of the serviceable available market range for the UAV and the vulcopter is discussed below. The SAM is considered to be the part of TAM so it is estimated as 50 lakhs and hence the SAM is 50 percent of the TAM (for consideration) Serviceable Obtainable Market (SOM): The SOM is the part of the SAM and TAM and considered competitions, trends, demands for the design of the vulcopter. The realistic goal is for selling the vulcopter and if it is estimated as 25 lakhs it is 50 percent of SAM and 25 percent of TAM.

3.2 Customer Segments: System Integrators manufacturers of UAV o Unmanned aerial vehicle operator o Drone pilot o Air force drone pilot o Adults who have trained to drive

IV. COMPREHENSIVE PLAN:

4.1 Acquiring new customer for deal: To acquire new customer, the drone should be well marketable and this is evoked by our marketing team. This is being dealt with the new customers who may be presumed or hobbyist/DIY.

4.2 Key metrics: The key metrics for marketing and business plan will be improved by certain activities - Bug fixes - Reviews/feedback from users - Daily users

4.3 Channels - Drone camps RC - Man and Drone - Flapping micro air vehicle - RC ornithopter

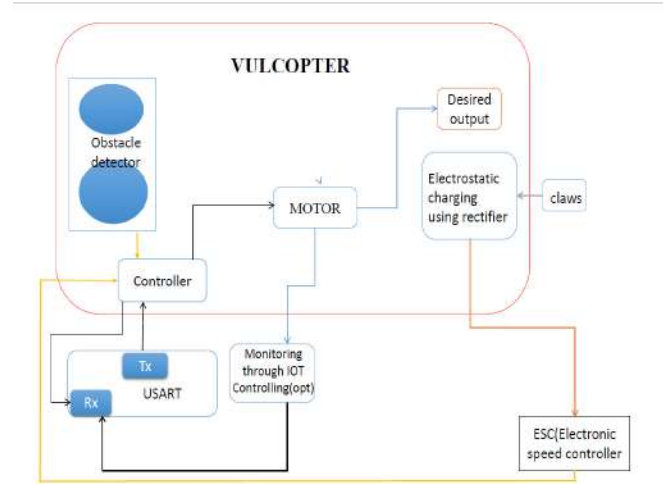
V. FINANCIAL PLAN

The financial plan is based on marketing and design:

5.1 For Marketing:

- UAV Airframe: By Material Type
- UAV Avionics: UAV Propulsion Systems,
- By Component UAV Payloads, By Type UAV Data Links
- UAV Ground Control Stations UAV Launch and Recovery Systems. These are different systems of UAVs where the vulcopter can be marketed with the payload respect to
 - *Monetisation strategy
 - * Start-up cost
 - * Fund Required

5.2 Designing:



Texas products:

MCU : C2000 TM delphino TM 32-bit microcontrollers (<http://www.ti.com/microcontrollers/c2000-real-time-control-mcus/delfino-premium-performance/overview.html>)

Analog to digital: ADS7841E (<http://www.ti.com/product/ADS7841>)

Digital to analog : DAC121S101CIMK/NOPB (<http://www.ti.com/product/DAC121S101>) Rectifier : 2W08M (<http://www.ti.com/tool/TIDA-00858>)

VI. CONCLUSION

In summary, the general design concept and goal of the flapping wing MAV are the major drivers. I am concerned with tail and wing configuration which largely determine the complexity and capabilities of the design. I have shown that at the scale of small flapping wing MAVs, small changes in mass can have a significant impact on the flight time of the flapping wing MAV.

We are looking to make our project a product. So entrepreneur is the main aspect of business and success. Everyone has a desire to start with the new idea. Only a few become successful by creating the idea which helps in solving problems and to market with profit. This is the main vision of every successive entrepreneurship. A young generation looking towards venture behind every entrepreneurship to yield success.

VII. ACKNOWLEDGEMENT

We really thank our colleagues and mechanical peers who helped us to complete this project with determination. Also we like to thank our institution for supporting us.

estimated as 25 lakhs it is 50 percent of SAM and 25 percent of TAM.

3.2 Customer Segments: System Integrators manufacturers of UAV o Unmanned aerial vehicle operator o Drone pilot o Air force drone pilot o Adults who have trained to drive

IV. COMPREHENSIVE PLAN:

4.1 Acquiring new customer for deal: To aquire new customer, the drone should to well marketable and this is evoked by our marketing team. This is being dealt with the new customers who may be presumed or hobbyist/DIY.

4.2 Key metrics: The key metrics for marketing and business plan will be improved by certain activities - Bug fixes - Reviews/feedback from users - Daily users

4.3 Channels - Drone camps RC - Man and Drone - Flapping micro air vehicle - RC ornithopter

V. FINANCIAL PLAN

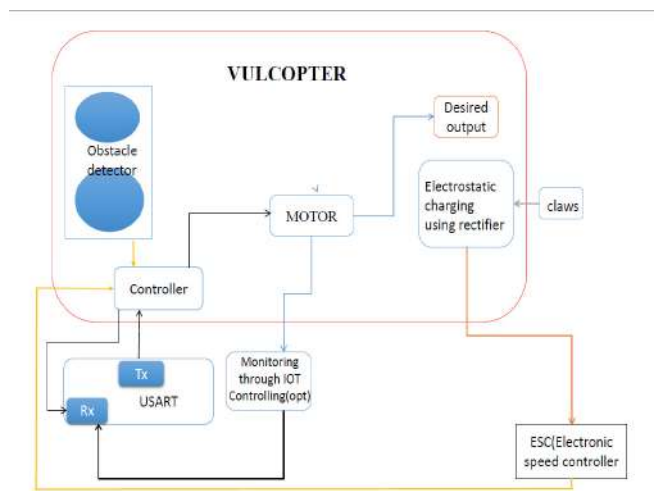
The financial plan is based on marketing and design:

5.1 For Marketing:

UAV Airframe: By Material Type
 UAV Avionics: UAV Propulsion Systems,
 By Component UAV Payloads, By Type UAV Data Links
 UAV Ground Control Stations UAV Launch and Recovery Systems. These are different systems of UAVs where the vulcopter can be marketed with the payload respect to

- *Monetisation strategy
- * Start-up cost
- * Fund Required

5.2 Designing:



Texas products:

MCU : C2000 TM delphino TM 32-bit microcontrollers (<http://www.ti.com/microcontrollers/c2000-real-time-control-mcus/delfino-premium-performance/overview.html>)

Analog to digital: ADS7841E (<http://www.ti.com/product/ADS7841>)

Digital to analog : DAC121S101CIMK/NOBP (<http://www.ti.com/product/DAC121S101>) Rectifier : 2W08M (<http://www.ti.com/tool/TIDA-00858>)

VI. CONCLUSION

In summary, the general design concept and goal of the flapping wing MAV are the major drivers. I am concerned with tail and wing configuration which largely determine the complexity and capabilities of the design. I have shown that at the scale of small flapping wing MAVs, small changes in mass can have a significant impact on the flight time of the flapping wing MAV.

We are looking to make our project a product. So entrepreneur is the main aspect of business and success. Everyone has a desire to start with the new idea. Only a few become successful by creating the idea which helps in solving problems and to market with profit. This is the main vision of every successive entrepreneurship. A young generation looking towards venture behind every entrepreneurship to yield success.

VII. ACKNOWLEDGEMENT

We really thank our colleagues and mechanical peers who helped us to complete this project with determination. Also we like to thank our institution for supporting us.

VIII. REFERENCE

[1] H. Kopka and P. W. Daly, A Guide to LATEX, 3rd ed. Harlow,England: Addison-Wesley, 1999

[2] J.-S. Lee, D.-K. Kim, J.-Y. Lee and J.-H. Han, Experimental evaluation of a flapping-wing aerodynamic model for MAV application, LATEX, 15th SPIE International Symposium Smart Structures/NDE, San Diego, CA, USA, Mar. 2008.

[3] J. D. DeLaurier, An aerodynamic model for flapping-wing flight, LATEX, Aeronautical Journal, Vol.97, No.964, pp. 125-130, 1993.

[4] Y.-S. Shim, C.-H. Kim, Evolving physically simulated flying creatures for efficient cruising, LATEX Artificial Life,-12, No. 4, pp.561-591, 2006.

Implementation of AC Voltage Regulator for Three Phase Induction Motor

Bhavadharini P¹, Haritha R², Vijay R³

Student, Electrical and Electronics, Saranathan College of engineering, Tiruchirapalli, India ¹

Student, Electrical and Electronics, Saranathan College of engineering, Tiruchirapalli, India ²

Professor, Electrical and Electronics, Saranathan College of engineering, Tiruchirapalli, India ³

Abstract: This paper describes a novel method for smooth starting of three phase ac motors. Induction motors are widely used for domestic, industrial and automotive applications. With the advancement in technologies three phase ac motors are having a wide range of applications. Specially designed starters are employed for instantaneous voltage and torque control during starting of three phase ac motors. However, cost effective control over voltage levels during starting is still a far cry. As voltage is directly proportional to speed, we need to control the stator voltage in order to have control over the speed. Thus, our project is all about controlling the stator voltage applied to the motor by phase angle control using TRIACs as a switching device. The semiconductor devices (TRIACs) are triggered by applying a pulse width modulated (PWM) signal to the gate terminal whose width is varied with the help of a potentiometer arrangement. In this way our method serves as a cost effective solution for starting low capacity three phase ac motors.

Keywords: Phase angle control, Pulse width modulation, Starters

I. INTRODUCTION

An electric motor converts electrical energy into mechanical energy which is then used to drive different type of loads. Based on the supply, it may be classified as dc and ac motors. Based on the principle of operation ac motors are further being classified into synchronous motors, single phase or three phase ac motors and other special electric motors. Of all these types three phase ac motors are the most widely used electric motor in industry. They are simple, rugged, robust, low priced, easy to maintain and can be manufactured with characteristics to suit most industrial requirements. Besides, they run at essentially constant speed from no load to full load. Three phase ac motors are further being classified into slip ring and squirrel cage induction motors. Like any electric motor they too carry a stator and rotor winding. Only stator winding is fed from the three phase supply. The rotor winding derives its voltage and power from the externally energized stator winding through electromagnetic induction. The starting of induction motors is followed by inrush currents up to 7-10 times the rated current which in turn influences the starting torque to rise up to three times the running torque. The increased torque results in sudden mechanical stress on the machine which leads to reduction in service life. Thus, starters are employed for smooth starting of the three phase machine.

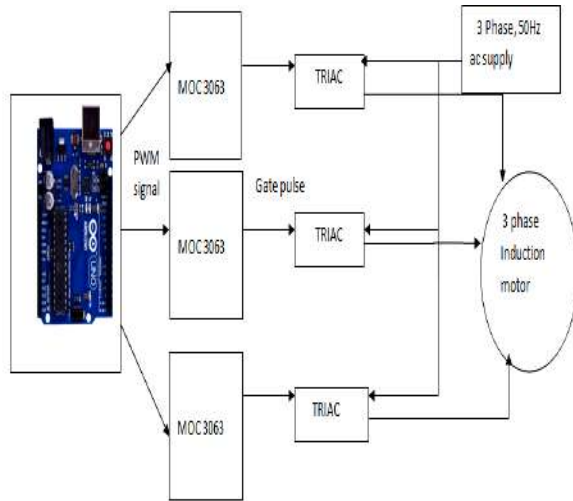
These starters can be mainly classified under two categories electromechanical starters and electronic starters. Electromechanical starters are those that employ external resistance, transformer and contactors giving reduced voltage during starting. Starters like *star delta starter, direct on line starter, autotransformer starter, stator resistance*

starter and rotor resistance starter (applicable only to slip ring induction motor) are some of the conventional electromechanical starters. Electronic starters are those that involve the use of semiconductor switches in their operation like the one used in ac voltage controller type starters and other variable frequency drives. Ac voltage soft starters employing semiconductor switches are widely being used to replace the conventional starters owing to their controlled soft starting capability [2]. The selection of starter depends upon the type and size of the motor. This paper introduces a low cost solid state soft starter for three phase induction motor incorporating a three phase ac voltage regulator using TRIAC as the switching device. Earlier the ac voltage regulator systems were designed with a pair of SCRs connected in antiparallel fashion in each of the phases. But, thyristors may affect the operation of the controller due to its poor commutation characteristics and introduction of low order harmonics [1]. In case of IGBT based soft starters the harmonics produced are of higher order and demands filter design of high values [3].

II. PROPOSED SYSTEM

The proposed system consists of two modules- power circuit module and pulse generation module. The simplified diagram for the proposed system is shown in the figure below. The proposed system is designed such that it is a cost efficient product compared to other systems that are existing now.

A. BLOCK DIAGRAM



The above figure shows the block diagram of the proposed system.

B. System Configuration

The system configuration for the proposed model is shown in the above figure. From the given figure we can infer that the three phases can be controlled independently. The power circuit consists of three triacs T1, T2 and T3 controlling the phases R, Y, B respectively. The triacs are triggered by the gate pulse from the fourth pin of the opto coupler. The optocoupler MOC3063 forms the main element of the power circuit. It has an in built *Infrared emitting diode, Zero crossing detector and TRIAC* arrangement performing the function of triac driver. By giving a simple pulse across the terminals 1(anode) and 2(cathode) the diode connected the terminals get energized and emits infrared light. In our design we have used Arduino to give a pulse width modulated signal to the terminal 1 of the optocoupler through an external resistance. The width of the pulse shall be varied with the help of a potentiometer arrangement. Upon application of this pulse the main terminals 4 and 6 gets closed only during the zero crossing of the supply voltage. Thus, trigger pulse is given to the externally connected Triacs across the three phases. It is the optocoupler that successfully isolates the high voltage side from low voltage side. A series combination of resistor and capacitor connected in parallel to the triac device acts as the snubber circuit for protection against transient conditions.

C. Principle of Operation

In this section the principle of operation of the circuit shall be discussed. The operation of the entire system can be understood by dividing it into power circuit and trigger circuit. The trigger circuit consists of Arduino Uno as the controller board for pulse generation. The controller is powered from a single phase transformer through a combination of rectifier and voltage regulator. The controller is programmed in such a way that it gives a PWM pulse with a phase shift of 60 degree from the initial value of firing angle. For inductive loads the switches in the successive phases should be triggered as α , $\alpha+60$ degree, $\alpha+120$ degree [4].

This phase control strategy may minimize pulsations in torque [2]. The width of the pulse width modulated signal shall be varied by a pot arrangement forming a common control for all the three phases. Thus, the triac circuit is triggered by applying a gate signal through the fourth pin of the optocoupler connected to the respective phases. On the power circuit side of the optocoupler the three phase supply voltage is applied across the main terminal 2 of the triacs. The stator voltage impressed across the motor can be controlled by controlling the firing angle of the triac. The firing angle of the triac circuit can be varied by varying the duty cycle of the pwm signal through a potentiometer arrangement. The pulse width modulated signal and the supply voltage go in synchronization and finally regulated voltage shall be applied across the three phase induction motor during starting. In this way a three phase ac to ac voltage regulator system using triac as a switching device can be used to control the supply voltage and serve as a smooth starter for three phase induction motor.

III WORK DONE

Initially a MATLAB simulation was done with the following machine parameters:

A three phase 415V, 50Hz 0.5Hp induction motor with four poles (P). The machine is found to have the following machine parameters:

$$R_s = 0.433\Omega$$

$$R_r = 0.861\Omega$$

$$L_s = 4\text{mH}$$

$$L_r = 1\text{Mh } L_m = 69.31\text{mH}$$

A. Calculations Involved

$$\begin{aligned} \text{Speed, } \omega_m &= 120(f/p) \\ &= 120 * 50 / 4 \\ &= 50\pi \text{ rad/sec} \end{aligned}$$

$$\begin{aligned} \text{Slip, } S &= (N_s - N) / N_s \\ &= (1500 - 1400) / 1500 \\ &= 0.06 \end{aligned}$$

where,

- f is the supply frequency
- p is the number of poles
- N_s is the synchronous speed
- N is the speed of the rotor

At full load,

$$\begin{aligned} \text{Torque, } T &= \frac{(3/W_{ms}) * (v^2/R_r S)}{((R_s + R_r/S)^2 + (X_s + X_r)^2)} \\ &= \frac{(3/50\pi) * (415^2 * 0.861) / 0.02}{((0.435 + 0.861/0.06)^2 + (4 * 2\pi * 50 * 0.001 + 1 * 2\pi * 50 * 0.001)^2)} \\ &= 74.85 \text{ Nm} \end{aligned}$$

$$\begin{aligned} T_L &= K (1-S)^2 \\ K &= T_L / (1-S)^2 \\ &= 74.855 / (1-0.06)^2 \\ &= 77.94 \end{aligned}$$

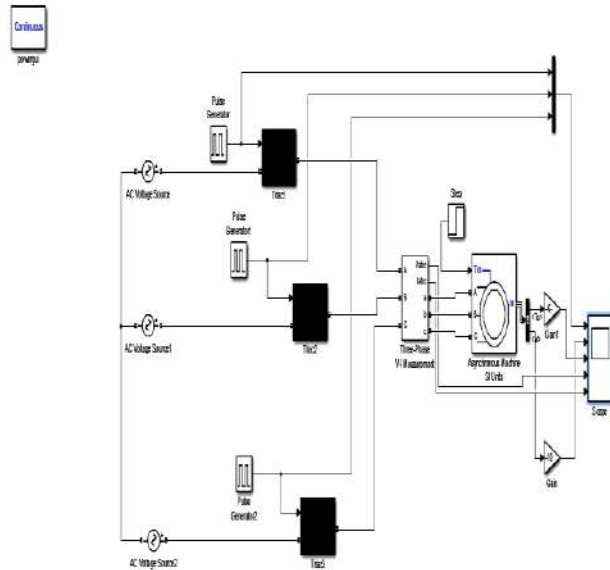
For V,

$$V^2 = \frac{T_L [(R_s + R_r/S)^2 + (X_s + X_r)^2]}{(W_{ms}/3) * (R_r/S)}$$

$$\begin{aligned} T_L &= 77.94 (1-0.06)^2 \\ &= 48.998 \text{ Nm} \end{aligned}$$

Therefore, V = 411.47V

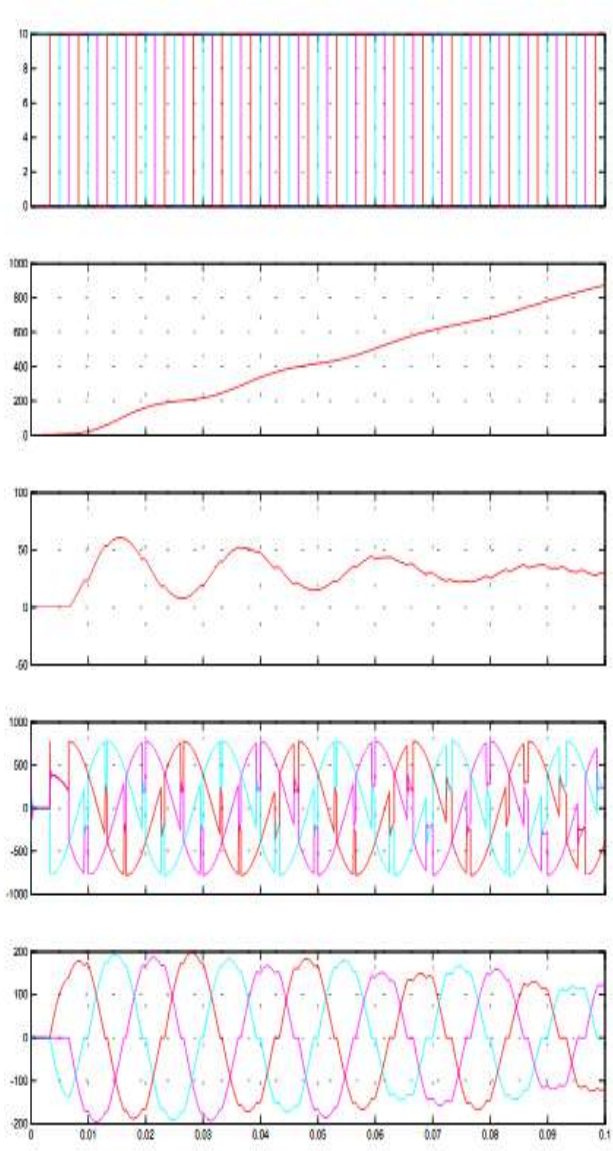
B. Simulation Work



The above figure shows the simulation model for a three phase induction motor constructed on MATLAB. Using a pulse generator block with fifty percent duty cycle the TRIACS connected in the R, Y, B phases of the motor are triggered with a phase angle difference of 60 degree from the instant of firing angle. The reduced three phase voltage applied across the stator is recorded through a three phase V-I measurement block which is then observed through scope block.

Following is the corresponding simulation result of the above MATLAB model. From the simulation results we can conclude that the current conduction is continuous through the motor. This can be achieved by fixing proper firing angles of the triacs of the respective phases. Initially the speed of the motor was less but after a definite amount of time the motor reached the synchronous speed. Torque rises up linearly with time.

- (d) Variation of stator voltage with time
- (e) Variation of stator current with time



From the above waveforms we could observe the following in order:

- (a) Variation of applied pulse with time
- (b) Variation of torque with time
- (c) Variation of speed with time

IV CONCLUSION

A soft starter based on three phase ac voltage regulator was designed and implemented using triac as a switching device. The starter being designed shall be used only for small capacity three phase ac motors (upto 1HP).

Amidst existing soft starters ours serve as a cost effective one because of the simplicity in the choice of components being used. With triac of higher rating followed by appropriate design of snubber circuit the starter can be used for motor of higher rating. It is the snubber circuit that plays a prominent role in the design of starters because with proper design of snubber circuit the initial cogging effects shall be completely minimized thereby increasing the life of the motors.

V REFERENCES

[1] A.M. Eltamaly, A.I. AlolahA and R.M. Hamouda, "Performance Evaluation of Three-Phase Induction Motor under Different AC Voltage Control Strategies Part I" , College of engineering, Saudi Arabia.

[2]Gürkan Zenginobuz, Isik Cadirci, Muammer Ermis, and Cüneyt Barlak , "Performance Optimization of Induction motors during Voltage-Controlled Soft starting" ,IEEE Transactions on energy conversion,Vol.19,No.2,2004.

[3] Ahmed Riyaz, Atif Iqbal, Shaikh Moinoddin, SK.MoinAhmed,Haitham Abu-Rub, "Comparative performance analysis of Thyristor and IGBT based induction Motor soft starters", International Journal of Engineering, Science and Technology Vol. 1, No. 1, 2009, pp. 90-105.

[4] Werner Deleroi, Johan B. Woudstra and Azza A. Fahim," Analysis and application three phase Induction motor voltage controller with improved transient performance", IEEE transactions on industry applications, vol.25.

[5]P.C.Sen, "AC and DC voltage regulator" in Power electronics, Tata McGraw hill education, 2015 edition.

Modified Multi-level Asymmetric Inverter Setup for Renewable Energy applications

U.Aravindhnan

UG Scholar

*Saranathan College of Engineering
Tiruchirappalli, India
uaravind12@gmail.com*

R.Dhineshkumar

UG Scholar

*Saranathan College of Engineering
Tiruchirappalli, India
dhiniraj186@gmail.com*

M.S.Ajay

UG Scholar

*Saranathan College of Engineering
Tiruchirappalli, India
dhiniraj186@gmail.com*

P. Ram Prakash

Asistant Professor,

Electrical and Electronics Engineering

Saranathan College of Engineering

Tiruchirappalli, India

gprsahara@gmail.com

Abstract— It is very challenging to find a direct application for low voltage Renewable Energy systems. This paper proposes a solution for the effective utilization of low power Renewable Energy sources. It also proposes the possibilities of using high voltage and high power loads using low voltage or low power renewable energy systems. The performance of the system has been analyzed using MATLAB/Simulink and the results were verified and compared with Hardware output. This work also concentrates on the utilization of Modified Cascaded Multilevel inverter with reduced switches with an increase in multilevel outputs which inherently reduces the cost and Total Harmonic Distortion.

Keywords— MLI, THD, RAPS, Inverter, Renewable Energy

I. INTRODUCTION

Uninterrupted power supply plays vital role in the development of a country. Population and Industrialization increases the power demand in urban areas and the rural areas far from grid and have low power demand always face difficulties to receive power from the grid[1]. Since the demand for a high-quality power is increased in recent years and to meet the power requirement, in addition to increasing the power generation, it is also essential to improve the power quality and reduce the losses. Standalone PV systems are normally used as Remote area Power Supplies (RAPS) because of their feasibility compared with conventional diesel generators. Research in hybrid systems emerges in recent years to make use of wind power and batteries in rural electrification without grid[2].

Domestic energy applications cannot find large investments because of cost of utilization, political and economic circumstances. Low power renewable energy systems play an important role in domestic applications since the installation cost is very less. Inverters play an important role in transmission, distribution and utilization by improving the power quality[3]. In recent times, the new inverter concepts are used to solve the problems in industries where medium voltage and high power are required. Cascaded Multilevel inverters are highly capable of handling more power in the output side hence they are preferred for larger power industries. In small scale, Microgrids are the better

choices for the small-scale power requirements with improved power quality and reliability. All these applications require a reliable power source either renewable or non-renewable one[4].

Microgrid requires various power sources which definitely includes renewable energy sources. It is very challenging and cost inefficient to install the medium power renewable energy source for a microgrid or for domestic applications. Also the design and installation of filter also costs more. By adding the renewable energy systems in a stepped manner, the required output for the domestic load will be achieved[5].

Cascaded multilevel inverter is the other type has multiple input voltage sources and the output voltage levels are based on the sources. This type of inverter is called as the true inverter because the output voltage is derived from the various input voltage sources and useful for the renewable energy source applications [6-9]. In this paper, concept of cascaded multilevel inverter has been taken and the drawbacks of the inverter are considered. The nine-level asymmetric cascaded inverter is shown in fig.1 for which the output voltage levels have the following relationship with the number of input DC sources[10-14].

Let N is the number of separate DC sources used, then the Number of voltage levels = $2N+3$, and the number of switches = $4N$.

The main drawback of this inverter is the number of switches used in each level is high compared to other inverters. To reduce this count, a new type of multilevel inverter has been used.

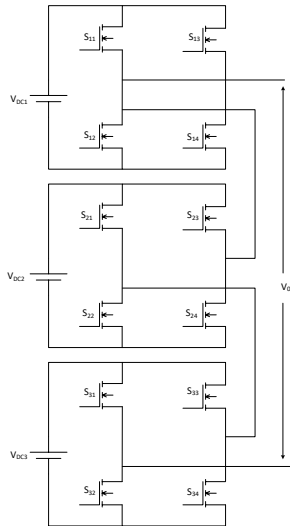


Fig.1.Cascaded nine-level Inverter

II. PROPOSED TOPOLOGY

Modified nine-level inverter with single H-Bridge that shown in fig.2 requires fewer switches compared to the conventional nine-level inverter. The modified inverter for which the output voltage levels have the following relationship with the number of input DC sources.

Let N is the number of independent Renewable energy sources (DC input) used,

Then the number of voltage levels = $2N+3$

The number of switches = $N+4$.

Number of diodes = N.

If $V_{DC1} = V_{DC2} = +V_{dc}$ and $V_{DC3} = +2V_{dc}$ then the overall output changes from $+4V_{dc}$ to $-4V_{dc}$.

For a nine-level inverter, only 7 switches and 3 diodes are required compared to 12 switches of the conventional nine-level inverter.

Table.1.Switching sequence of nine-level inverter

Duration	ON Switches	ON Diodes	Voltage Levels
Positive Half Cycle (S ₁₁ & S ₄₁ ON)	-	-	0
	S ₁	D ₁	+ V _{DC}
	S ₁ , S ₂	D ₂	+2 V _{DC}
	S ₁ , S ₂ , S ₃	-	+4 V _{DC}
Negative Half Cycle (S ₂₁ & S ₃₁ ON)	-	D ₁ , D ₂ , D ₃	0
	S ₁	D ₂ , D ₃	-V _{DC}
	S ₁ , S ₂	D ₃	-2 V _{DC}
	S ₁ , S ₃	D ₂	-3 V _{DC}
S ₁ , S ₂ , S ₃	-	-4 V _{DC}	

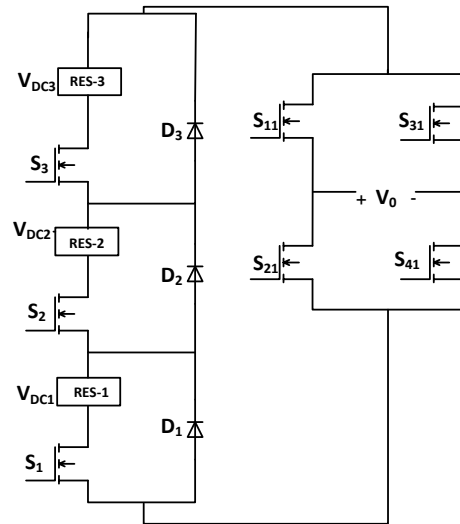
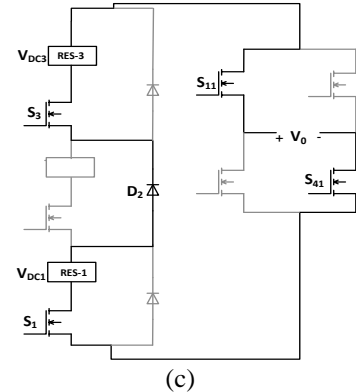
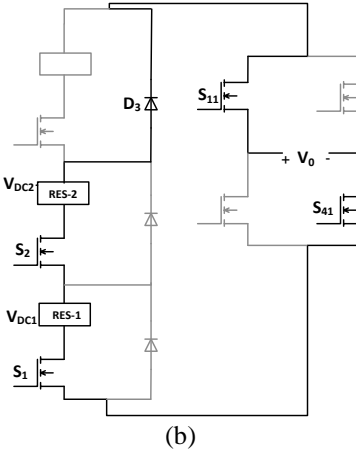
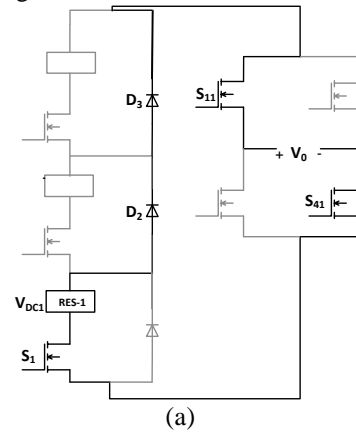


Fig.2. Modified nine-level Inverter



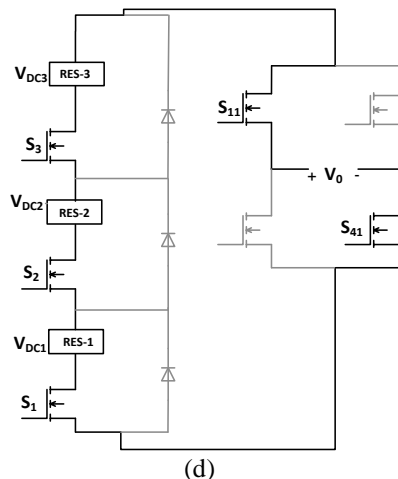


Fig.3. Operating modes of Proposed Topology

The losses due to switching are also reduced. This type of inverter consists of a conversion unit with a switching device connected in series with a Voltage source and a diode is connected in parallel with this structure. The number of conversion units is equal to the count of output levels. For a nine-level inverter, four conversion units are cascaded and connected to an H-Bridge. By triggering S_1 , V_{DC1} is obtained at the output which is equal to V_{dc} . Similarly, by triggering S_1 and S_2 , The input voltages V_{DC3} and V_{DC4} equal to $+2V_{dc}$ can be obtained at the output. The maximum output of $+4V_{dc}$ level will be obtained by turning on all the four switches $S_1, S_2, S_3,$ and S_4 . The switching sequence of the nine-level inverter is given in table.1. and the output waveform is shown Fig.5.

The output levels are unidirectional. By using H-Bridge the output is converted into bidirectional. The output waveform of the H-Bridge contains nine levels as depicted in fig.5. At positive half cycle, Switches S_{11} and S_{41} are on and during negative half cycle S_{21} and S_{31} are on in the H-Bridge.

III. PWM TOPOLOGIES

A. MCPWM Technique

In the Multiple carrier PWM (MCPWM) method, for a m level inverter, (m-1) carrier signals with same frequency f_c and Amplitude A_c are compared with a reference sinusoidal waveform of amplitude A_r and frequency f_r . The frequency of the reference signal determines the frequency of the output waveform.

In MCPWM technique, the amplitude modulation index M_a and the frequency modulation index M_f are defined as

$$M_a = \frac{2A_r}{(m - 1)A_c} \tag{1}$$

$$M_f = \frac{f_c}{f_r} \tag{2}$$

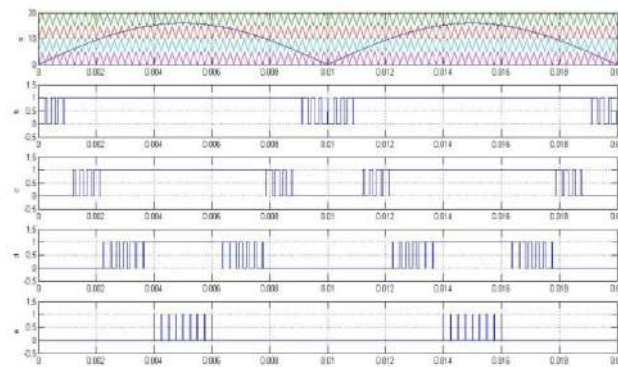


Fig.4. Generation of switching waveforms using MCPWM technique

B. MTPWM Technique

In this scheme, a single triangular carrier and multiple trapezoid [1] modulating signals are used. The intersections between the trapezoid signals and carrier signal define the switching instants of the PWM [4] [5] pulse. These signals can then be used to drive the actual gating signals for the power devices in the inverter module.

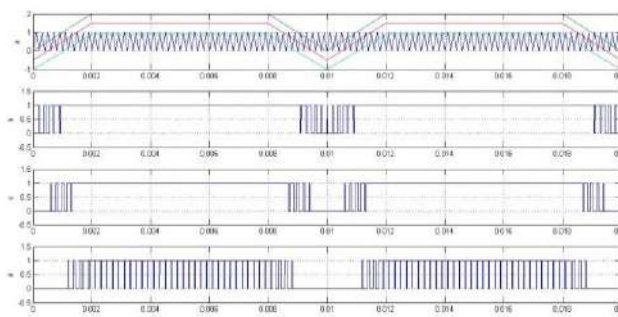


Fig.5. Generation of switching waveforms using MTPWM technique

IV. SIMULATION RESULTS

The simulation model of multilevel inverter has been developed using SIMULINK of MATLAB. Pulse generation scheme for the two methods are shown in fig.6 and fig.7.

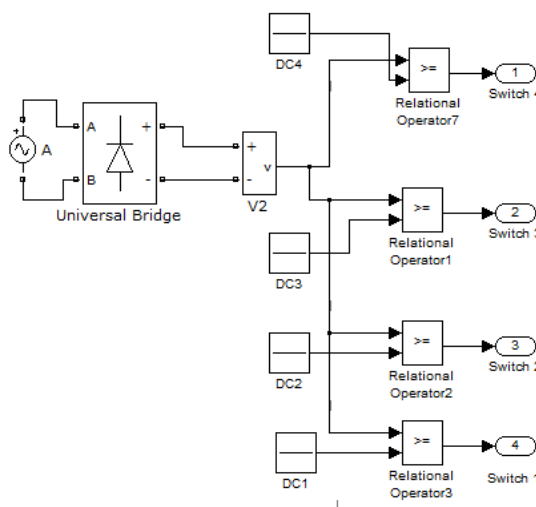


Fig.6. Pulse generation scheme using Single PWM Technique

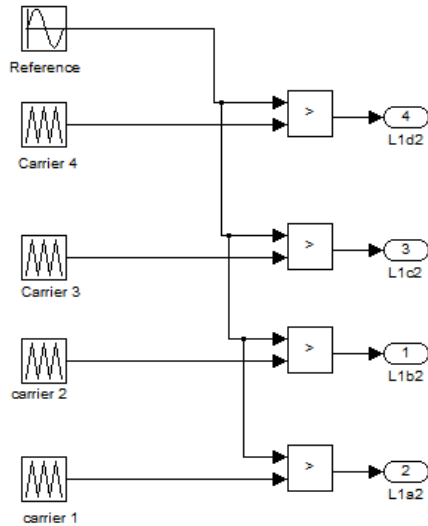


Fig.7. Pulse generation scheme using MCPWM Technique

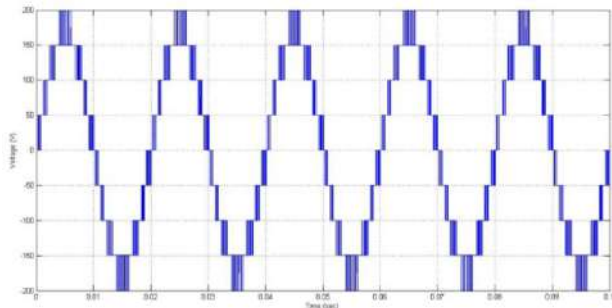


Fig.8. output voltage waveform of MCPWM MLI

Fig.8 shows the output voltage waveform of the proposed nine level topology and it clearly depicts that the output is a nearly sinusoidal waveform. Fig.9 depicts the output current waveform for an RL load of 100Ω and 15mH respectively. The current is smooth and the absence of switching transients also states that the harmonic content of the waveform is less.

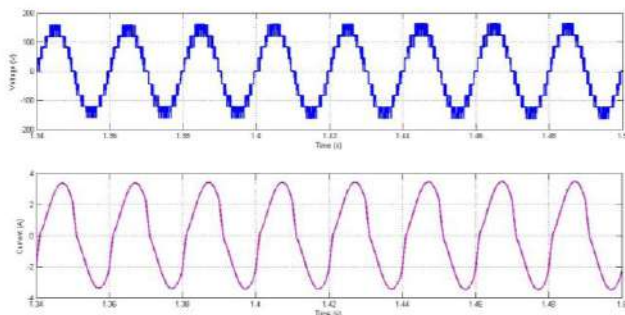


Fig.8. output voltage waveform of MCPWM MLI

V. HARDWARE RESULTS

To prove the simulation results, the hardware of the Single H-Bridge inverter shown in fig.07 has been implemented.. PIC16F has been used for the switching pulse generation. The IRF640 MOSFET is used as switch. The performance of the inverter has been analysed with MTPWM and MCPWM techniques and the result is given in fig.11.



Fig.10. Hardware implementation of single H Bridge MLI

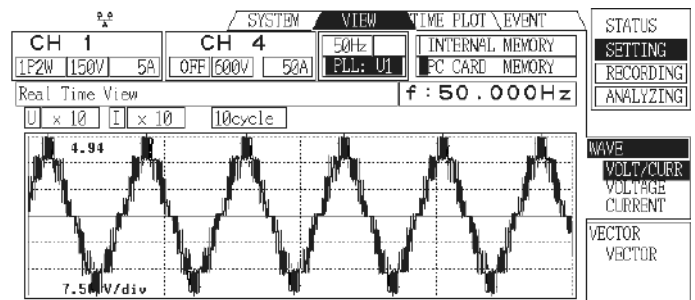


Fig.11. Output voltage waveform of SHB MLI with MCPWM

VI. CONCLUSION

The modified multilevel inverter with reduced number of switches for remote area power applications have been presented in this paper.. Moreover by using two pulse generation techniques, the performance of the single H-Bridge topology has been analysed. Though the MCPWM method reduces the complexity in the pulse generation circuit and MCPWM technique reduces the total harmonic distortion on the circuit. In this technique the power factor has also improved. Hence, the Single H-Bridge inverter with MCPWM method is suitable because of the number of switches and THD and suitable for remote area applications.

REFERENCES

- [1] Tamer Khatib and Wilfried Elmenreich, Optimum Availability of Standalone Photovoltaic Power Systems for Remote Housing Electrification, International Journal of Photoenergy, Volume 2014,pp.1-5.
- [2] A R Syarifah,et.al., Design of Hybrid Power System for Remote Area, The 2nd Annual Applied Science and Engineering Conference (AASEC 2017), 2017
- [3] Lippong Tan, et.al, A comparative case study of remote area power supply systems using photovoltaic-battery vs thermoelectric-battery configuration, 1st International Conference on Energy and Power, ICEP2016, 14-16 December 2016.
- [4] Saif Ur Rehman,et.al., Feasibility study of hybrid energy system for off-grid rural electrification in southern Pakistan, Energy Exploration & Exploitation, 2016, Vol. 34(3), pp.468-482.
- [5] Bojian Jiang and M. Tariq Iqbal, Dynamic Modeling and Simulation of an Isolated Hybrid Power System in a Rural Area of China, Hindawi Journal of Solar Energy, Volume 2018,pp.1-13

- [6] E.Babaei, et.al., Symmetric and asymmetric multilevel inverter topologies with reduced switching devices, journal of electric power system research, 2012, pp.122-130.
- [7] Babaei.E, Optimal topologies for cascaded sub-multilevel converters, Journal of Power Electronics, 10(3), 2010, pp-251-261.
- [8] J. Rodriguez, L.G. Franquelo, S. Kouro, J.I. Leon, R.C. Portillo, M.A.M. Prats, M.A. Perez, Multilevel inverters: an enabling technology for high power applications, Proc. IEEE 97 (11) (2009) 1786–1817.
- [9] C. Feng, J. Liang, V.G. Agelidis, Modified phaseshifted PWM control for flying capacitor multilevel inverters, IEEE Trans. Power Electron. 22 (1) (2007) 178–185.
- [10] Miao Chang-xina, Shi Li-pinga, Wang Tai-xua, Cui Cheng-bao, 2009. Flying capacitor multilevel inverters with novel PWM method, Procedia Earth and Planetary Science, pp 554–1560.
- [11] BusquetsMonge.S, Alepuz.S, Bordonau.J, Peracaula.J, 2008. Voltage balancing control of diode-clamped multilevel converters with passive front ends, IEEE Trans.Ind.Electron., Vol.23, No.4, pp 1751-1758.
- [12] Ebrahimi.J, Babaei.E, Gharehpetian.G.B, 2010. A new multilevel converter topology with reduced number of power electronic components, IEEE Transaction on Industrial Electronics, 59(2), pp.655-667.
- [13] Manjrekar.M.D, Steimer.P and Lipo.T.A, 2000. Hybrid Multilevel Power Conversion System: A Competitive Solution for High Power Applications, IEEE Trans on Industry Applications, Vol.36, No.3, pp. 834-841.
- [14] Murugesan.M, Sivaranjani.S, Asokkumar.G, 2011. Seven Level Modified Cascaded Inverter for Induction Motor Drive Applications, Journal of Information Engineering and Applications, Vol.1, No.1.

Voltage Lift technique based Interleaved boost converter

Z. Mohammed Faisal
 EEE Department
 Saranathan College of Engineering
 Trichy
 faisalz8499@gmail.com

T. Avinash
 EEE Department
 Saranathan College of Engineering
 Trichy
 avinashjai17@gmail.com

E. Ajith
 EEE Department
 Saranathan College of Engineering
 Trichy

S. Muthukumar
 EEE Department
 Saranathan College of Engineering
 Trichy
 muthuvenkat1998@gmail.com

Abstract – *An interleaved dc-dc boost converter is used in this paper. The proposed converter resembles a two-phase interleaved boost converter on its input side while having a voltage multiplier on its output side. This converter offers continuous input current which makes it more appealing for the integration of renewable sources like solar panels to a 330-V dc bus. Furthermore, the voltage multiplier used offers low voltage ratings for capacitors which potentially leads to size reduction. The converter design and component selection has been discussed in detail. A hardware prototype of the proposed converter with $V_{in}=24V$ and $V_{out}=330V$ has been developed to validate the analytical results.*

Keywords—Voltage lift circuit, interleaved boost converter.

I. INTRODUCTION

Distribution systems at 330-V dc have been gaining popularity as they offer better efficiency, higher reliability at an improved power quality, and low cost compared to ac distribution systems. They offer a simpler integration of renewable energy and energy storage systems. Currently, telecom centres, data centres, commercial buildings, residential buildings, and micro grids are among the emerging examples of dc distribution systems. One of the challenges facing such systems is the power electronic converters for integrating renewable sources into the 330-V dc bus. A typical voltage range for solar panels is between 20V dc to 40V dc. Stepping up these voltages to 330-V dc using classic boost and buck-boost converters requires high duty ratios which results in high component stress and lower efficiency. Therefore, a typical choice would be using two cascaded converters; which results in inefficient operation, reduced reliability, increased size, and stability issues. Isolated topologies like flyback, forward, half-bridge, full-bridge, and push-pull converters have discontinuous input currents and hence would require large input capacitors. The second order hybrid boosting converter proposed, offers relatively low voltage gain in comparison to its voltage multiplier component count. It also has a very large input current ripple in proportion to its average. High step-up

converters using single-inductor-energy-storage-cell-based switched capacitors do not offer voltage gains high enough to boost a 24V input to 330V at a reasonable switching duty cycle. The multiple-inductor-energy-storage-cell-based switched capacitor based high voltage converters offer a relatively low voltage gain in proportion to its component count. The switched-capacitor-based active-network converter proposed in has a discontinuous input current ripple due to the series and parallel connection of the inductors in its two modes of operation. The transformer-less high-gain boost converter proposed in offers continuous input current but the switches experience a high voltage stress – more than $2/3^{rd}$ of its output voltage.

Interleaved boost converters using coupled inductors and high frequency transformers have been proposed for the integration of solar panels to 330V dc bus. In such converters, the design of high frequency transformers and coupled inductors is complicated as the leakage inductance increases when higher voltage gains are intended. As a result, the converter switches experience large voltage spikes and therefore would require clamping circuitry to reduce the voltage stress on the switches. These clamping circuits have a negative effect on the converter voltage gains. A family of non-isolated high-voltage-gain dc-dc converters that makes use of VM cells has been proposed. The voltage rating of each VM cell capacitor is twice that of its previous VM cell. Also, the inductors (L_1 , L_2) and switches (S_1 , S_2) experience different current stresses whenever even number of VM cells is used.

A high-voltage-gain dc-dc converter using voltage multiplier circuit is introduced in this paper. This converter is capable of stepping up voltages as low as 24V to 330V. The proposed converter offers continuous input current and low voltage stress ($1/4^{th}$ of its output voltage) on its switches. This converter can draw power from a single source or two independent sources while having continuous input currents, which makes it suitable for applications like solar panels. Compared to the topology presented in [19], the proposed converter requires lower voltage rating capacitors for its VM circuit and also one less diode. The inductors and switches experience identical current stresses making the component selection process for the converter simpler.

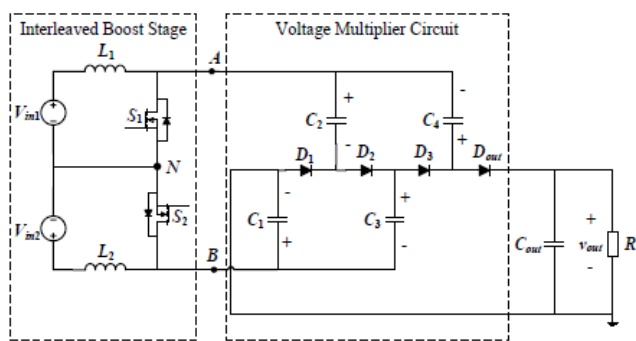


Fig 1. Proposed high voltage dc – dc converter

In section II, voltage multiplier circuit has been discussed. Section III introduces modes of operations. The voltage gain of the proposed converter has been derived in section IV. Section V analyses the component stress and provides supporting simulation results. Section VI discusses the experimental results obtained using the hardware prototype. A comparative analysis of the proposed converter and the high-voltage-gain converter shown has been discussed in section VII. Finally, section VIII concludes the paper.

II. VOLTAGE MULTIPLIER CIRCUIT

The voltage multiplier circuit offers a boosted dc output voltage by charging and discharging its capacitors. The input voltage is a modified square wave voltage. The voltages of the capacitors double at each stage as one traverses from the input side capacitor C_1 to the load side capacitor C_4 . For an output voltage of $V_{out} = 330V$, the voltages of capacitors C_1, C_2, C_3 , and C_4 are 80V, 160V, 240V, and 320V respectively.

For the same output voltage, the voltages of all the capacitors in the voltage multiplier circuit are smaller than the voltage of capacitor C_2 . For an output voltage of $V_{out} = 330V$, the voltages of capacitors C_1, C_2, C_3 , and C_4 are only 150V, 50V, 50V, and 150V, respectively. Therefore the volume of the capacitors used in the voltage multiplier circuit is potentially less.

III. TOPOLOGIES AND MODES OF OPERATION

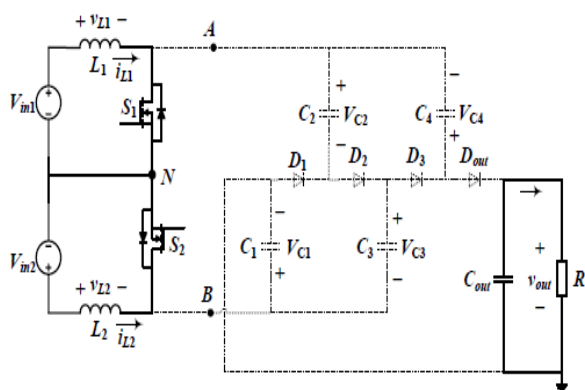


Fig 2. Proposed converter operation in Mode 1

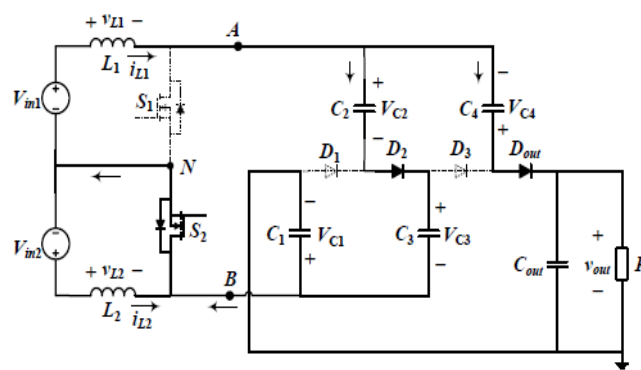


Fig 3. Proposed converter operation in Mode 2

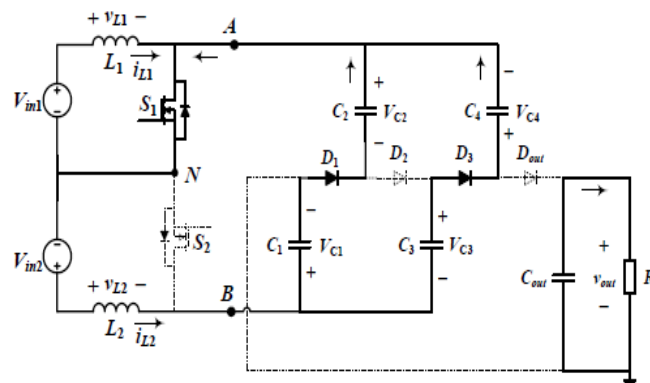


Fig 4. Proposed converter operation in Mode 3

The proposed converter provides a high voltage gain using the modified voltage multiplier circuit (see Fig. 3). On a closer look, it can be seen that the converter is made up of two stages. The first stage is a two-phase interleaved boost converter which outputs an MSW voltage between its output terminals A and B. The second stage is the voltage multiplier circuit that boosts the MSW voltage (V_{AB}) to provide a higher dc output voltage. For the proposed converter to operate normally, both switches S_1 and S_2 must have an overlap time where both are ON and also one of the switches must be ON at any point of time.

A. Mode I

In this mode, both switches S_1 and S_2 of the two-phase interleaved boost converter are ON. Input sources V_{in1} and V_{in2} charge inductors L_1 and L_2 respectively. Inductor currents i_{L1} and i_{L2} both increase linearly. All the diodes of the voltage multiplier circuit are reverse-biased and hence OFF. The voltages of the multiplier capacitors remain same and the output diode D_{out} is reverse biased. Therefore, the load is supplied by the output capacitor.

B. Mode II

In this mode, switch S_1 is OFF and switch S_2 is ON. Diodes D_1 and D_3 are OFF as they are reverse biased while diodes D_2 and D_{out} are ON as they are forward biased. A part of inductor current i_{L1} flows through capacitors C_2 and C_3 and thereby charging them. The remaining current flows through the capacitors C_4 and C_1 discharging them to charge the output capacitor C_{out} and supply the load.

C. Mode III

In this mode switch S_1 is ON and switch S_2 is OFF. Diodes D_1 and D_3 are ON as they are forward biased while

diodes D_2 and D_{out} are OFF as they are reverse biased. Inductor current i_{L2} flows through diode-capacitor voltage multiplier cell capacitors $C_1, C_2, C_3,$ and C_4 . Capacitors C_1 and C_4 are charged while discharging capacitors C_2 and C_3 . In this mode, the output capacitor supplies the load.

IV. VOLTAGE GAIN OF THE CONVERTER

In the proposed converter, the input power is transferred to the output by charging and discharging the voltage multiplier circuit capacitors. For an ideal converter, the voltage gain of the converter can be derived as described below. For inductors L_1 and L_2 , the average voltage across the inductors according to volt-second balance can be written as

Assuming capacitors C_2 and C_3 are identical, the voltage across them would be equal and can be written as

$$V_{C2} = V_{C3} = \frac{1}{2} \times \frac{V_{in1}}{(1-d_1)}$$

By substituting, one can derive capacitor voltages V_{C1} and V_{C4} to be

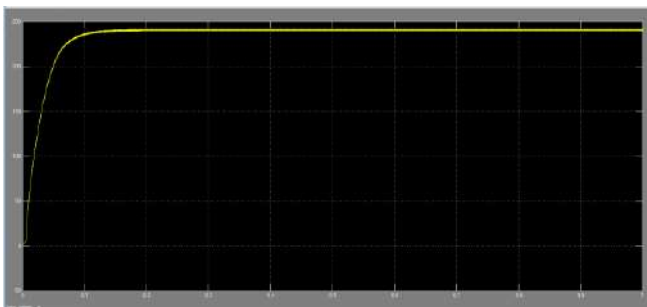
$$V_{C1} = V_{C4} = \frac{1}{2} \times \frac{V_{in1}}{(1-d_1)} + \frac{V_{in2}}{(1-d_2)}$$

Finally, the output voltage is derived by substituting, which yields

$$V_{out} = \frac{2 \times V_{in1}}{(1-d_1)} + \frac{2 \times V_{in2}}{(1-d_2)}$$

A. COMPONENT STRESS AND SIMULATION

This section discusses the voltage and current stresses observed by different components and also provide simulation waveforms during steady-state operation of the proposed converter. The discussions in this section are based on the topology, i.e., using a single voltage source to power the converter while operating both switches S_1 and S_2 of the two-phase interleaved boost stage at a fixed duty cycle d . A simulation model of the proposed converter has been built in MATLAB. The parameters used in the simulation are given.



B. Inductor

The inductor currents in both phases of the interleaved boost stages are similar. The average inductor currents can be calculated. The rms value of the inductor currents used in the calculation of inductor copper losses can be calculated.

The inductance required for a current ripple of ΔI_L is given by

$$L_1 = L_2 = L = \frac{V_{in} \times d}{\Delta I_L \times f_{sw}}$$

From the above equations, it is observed that both the inductors carry same amount of current and require same inductance for an assumed current ripple. Therefore, a similar inductor can be used for both L_1 and L_2 . Moreover as the rms currents of inductors L_1 and L_2 are equal, minimal conduction losses can be achieved in the inductors compared to other similar converters having different values of currents flowing through their boost stage inductors. The inductor current and voltage waveforms obtained from MATLAB simulation are shown. At 200W of output power, both the inductors carry a current of 5A with a ripple of 1.6A

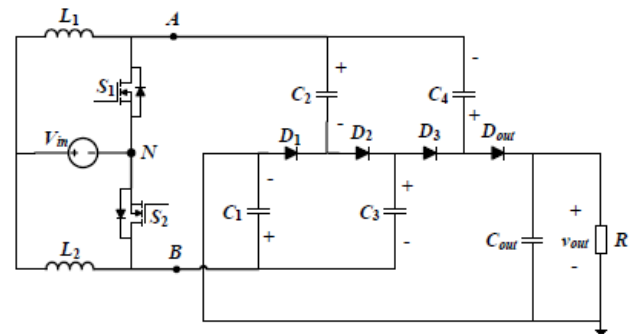


Fig 5. Proposed converter with Single source

B. Input Current

The input source is connected to an interleaved two-phase boost stage. Since it is a boost converter on the input side, the input current is continuous. As the two phases of the interleaved boost are 180 degrees out of phase from each other, the input current ripple is even smaller. This greatly reduces the size of the input filter capacitor required for the converter. The input current waveform of the proposed converter operating at 200W is shown. It can be seen that the ripple of the input current is about 1.2A even though inductor currents i_{L1} and i_{L2} have a ripple of 1.6A each. The reason for this smaller input current ripple is both the boost switches being operated 180 degrees out of phase from each other.

C. Switches

The maximum voltage observed across the switches in the proposed converter is equal to the output of its boost stage. This is a small number compared to the high output voltage of the proposed converter. The switch blocking voltages can be calculated. As current in both the inductors is

the same, the current stress on both switches is same as well. The average current in the switches can be calculated.

$$V_{S1} = V_{S2} = \frac{V_{in}}{(1-d)}$$

$$I_{S1,avg} = I_{S2,avg} = \frac{2 \times I_{out}}{(1-d)}$$

Switches S_1 and S_2 have the same current and voltage stress as can be seen in the simulation waveforms. Since the converter in simulation is operating at 90% switching duty cycle with a 24V input.

D. Diodes

The diodes experience two times higher blocking voltages compared to the switches as it depends on the voltages of the voltage multiplier circuit capacitors. In this topology, all the diodes experience the same blocking voltage which can be calculated using. The average current in the diode can be calculated. Since all the diodes experience same maximum voltage stress, similar diodes can be used for all of them.

$$V_{D1} = V_{D2} = V_{D3} = V_{Dout} = \frac{2 \times V_{in}}{(1-d)}$$

$$I_{D1,avg} = I_{D2,avg} = I_{D3,avg} = I_{Dout,avg} = I_{out}$$

The voltage and current waveforms of diodes D_1 , D_2 , D_3 , and D_{out} in the proposed converter are shown. For the converter operating at 90% switching duty cycle and 24V input. The diodes conduct either only during mode II or mode III of the converter operation. All the diodes carry an average current of 0.5A which is equal to the output current. Only diode D_{out} initially conducts in order to charge the output capacitor and bring in a balance in the voltage. Once the voltage loops are balanced, then the current flowing through the diodes is dependent on the impedance of the capacitors.

VI. EXPERIMENTAL RESULTS

COMPONENT	NAME	RATING
Inductor	L1, L2	2.5 mH
MOSFET	S1, S2	55V, 49A
Diode	D1,D2,D3, Dout	250V, 40A

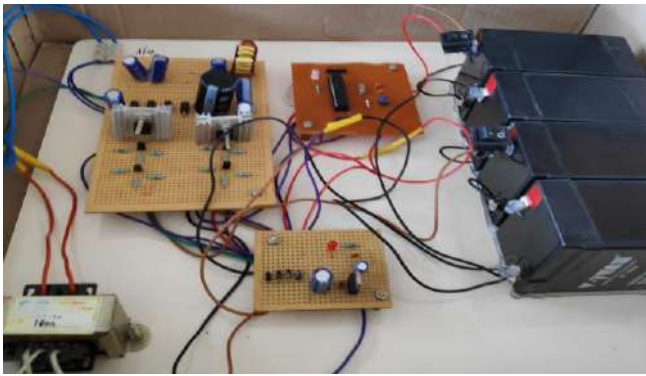
Capacitor	C1,C2,C3, C4	10uF , 450V
Output Capacitor	Cout	400V, 150uF

A hardware prototype of the proposed converter was built to test and validate the proposed converter operation. The specifications of the components used for building the hardware prototype are given in Table III. The power rating of the converter is 400W with an input voltage of 24V and an output voltage of 330V. The proposed converter is tested at a switching frequency of 15 kHz.

A theoretical loss analysis is performed using the ratings of the selected components of the hardware prototype. The converter is assumed to operate at 200W of output power. The calculated losses include conduction losses in inductors L_1 and L_2 , conduction and switching losses in switches S_1 and S_2 , conduction and reverse recovery losses in diodes, and conduction losses in the ESR of the capacitors. The conduction losses in the inductors are calculated as

It is observed that the major percent of losses occur in the diodes which are about 56%. As there are 4 diodes in the converter, each diode has a loss of about 14%. As the diode losses increase, its junction temperature rises and decreases the forward voltage drop across it. This decrease in forward voltage drop reduces the power loss and helps in preventing a further increase in junction temperature which can lead to diode failure. In the worst case scenario, the losses in the selected diode were estimated to be within its power dissipation limits.

Around 24% and 17% of the losses occur among the inductors and switches, respectively. The conduction losses in the inductors can be reduced by selecting an inductor with lower value of DCR (DC Resistance). The selected switches have similar conduction and switching losses. The losses in the capacitors are very small as the ESR of the film capacitors used is in the order of few milliohms and the rms currents are around 1A. The theoretical efficiency of the proposed converter at 200W was around 96.8%. A 400W prototype was built and tested to validate the analytical results. An efficiency of 93.76% was observed at 200W of output power. The difference in the calculated and experimental efficiency can be accounted for the core losses in the inductors that were not considered in the calculated efficiency and the approximate approach to calculating component losses. The efficiency of the prototype over a wide range of output power is shown. A maximum efficiency of 94.16% was achieved at a power rating of 150W.



VII. PROPOSED CONVERTER VS. HIGH-VOLTAGE-GAIN CONVERTERS USING BOOST STAGE AND VOLTAGE MULTIPLIER CIRCUITS

In this section, the proposed converter is compared to the non-isolated boost converter. A comparison is made between the proposed converter and converters that have been discussed earlier in this paper. The comparison is based on the voltage gain of the converters along with the voltage stress on their components. To have a fair comparison, the voltage stress on its components has been normalized with respect to their output voltages. The comparison is summarized in Table IV. The proposed converter offers higher voltage gain, has lower voltage stress on its switches and diodes in comparison to all other converters. The major advantage with the proposed converter is the significantly smaller voltage ratings for its capacitors in comparison to other converters. This greatly contributes to cost and size reduction of the proposed converter.

The proposed converter is also compared to a high-voltage-gain converter using voltage multiplier that is very similar in structure and operation. The comparison of these two converters is shown in Table V. The high-voltage-gain converter using voltage multiplier cells will be referred to as reference converter in the following sections of the paper. Both converters mainly differ in terms of their component stresses. The converters are being compared in terms of component stress and size while both offer a voltage gain of 24, i.e., a 24V input is stepped up to 330V on the output side. Here in this comparison, both converters are sourced from a single source despite the fact that they could be powered from two independent sources.

Both converters achieve a high voltage gain by charging and discharging of the voltage multiplier capacitors. They offer continuous input current which can be owed to the two-phase interleaved boost topology on the input side. The proposed converter is symmetric, i.e., both the interleaved boost phases on the input side experience same voltage and current stresses. Also, some of the capacitors in the voltage multiplier circuit have similar voltage stress. This simplifies the effort and time during component selection of the system design. The switches in the proposed converter have a higher duty ratio as the proposed converter offers slightly lower gain. This leads to a slightly higher voltage stress across the switches compared to the reference topology.

The major difference in the converters being compared is in their voltage multiplier circuits. Apart from the output

capacitor, both the reference converter and proposed converter have four voltage multiplier capacitors. Capacitors C1, C4 have a voltage stress of 150V and C2, C3 have a voltage stress of 50V.

The proposed converter has a smaller size compared to the reference topology due to its voltage multiplier circuit capacitors. Ideally, this can be demonstrated by looking at the total energy of the voltage multiplier capacitors which can be calculated as follows.

It can be seen that the capacitors of the proposed converter hold only 50% of the energy compared to the reference converter. A more practical way to compare the converter size is by looking at the volume of selected voltage multiplier capacitors available in the market. It was observed that the proposed converter had 44% smaller volume of voltage multiplier capacitors compared to the reference converter. Therefore the size of the proposed converter is smaller compared to the reference converter.

The proposed converter has one less diode compared to the reference converter. All the diodes experience the same reverse blocking voltage of 200V which is slightly higher than that of the diodes in the reference converter. This is because of the slightly higher duty ratio of the proposed converter compared to the reference converter. As the output ratings are the same, the output capacitors of both the converters are the same.

VIII. CONCLUSION

In this paper, interleaved boost converter is introduced that can offer a voltage gain of 24, i.e., to step up a 24V input to 330V output. The proposed converter is based on a two-phase interleaved boost and the voltage multiplier circuit. This makes the converter well suited for renewable applications like solar. The proposed converter is symmetric, i.e., the semiconductor components experience same voltage and current stresses which therefore reduces the effort and time spent in the component selection during the system design. The proposed converter has smaller voltage multiplier capacitors compared to a reference converter based on voltage multiplier cells; hence it is smaller in size. The converter finds its application in integration of individual solar panels onto the 330V distribution bus in dc buildings and micro grids.

REFERENCES

- [1] V. A. K. Prabhala, B. P. Baddipadiga, and M. Ferdowsi, "DC distribution systems - An overview," in *Renewable Energy Research and Application (ICRERA), 2014 International Conference on*, 2014, pp. 307-312.
- [2] G. AlLee and W. Tschudi, "Edison Redux: 380 Vdc Brings Reliability and Efficiency to Sustainable Data Centers," *Power and Energy Magazine, IEEE*, vol. 10, pp. 50-59, 2012.
- [3] V. Sithimolada and P. W. Sauer, "Facility-level DC vs. typical ac distribution for data centers: A comparative reliability study," in *TENCON 2010 - 2010 IEEE Region 10 Conference*, 2010, pp. 2102-2107.

[4] S. M. Lisy, B. J. Sonnenberg, and J. Dolan, "Case study of deployment of 400V DC power with 400V/-48VDC conversion," in *Telecommunications Energy Conference (INTELEC), 2014 IEEE 36th International*, 2014, pp. 1-6.

[5] A. Fukui, T. Takeda, K. Hirose, and M. Yamasaki, "HVDC power distribution systems for telecom sites and data centers," in *Power Electronics Conference (IPEC), 2010 International*, 2010, pp. 874-880.

[6] D. J. Becker and B. J. Sonnenberg, "DC microgrids in buildings and data centers," in *Telecommunications Energy Conference (INTELEC), 2011 IEEE 33rd International*, 2011, pp. 1-7.

[7] E. Rodriguez-Diaz, M. Savaghebi, J. C. Vasquez, and J. M. Guerrero, "An overview of low voltage DC distribution systems for residential applications," in *Consumer Electronics - Berlin (ICCE-Berlin), 2015 IEEE 5th International Conference on*, 2015, pp. 318-322.

APPLICATION OF SWARM ROBOTICS IN UNDERGROUND MINE MONITORING SYSTEM

Aathreya S, Karthikhaini K, Keerthana V, Krishnapriya V, Mr Paranthagan B

Department of Electrical and Electronics Engineering

Saranathan College of Engineering, Panjapur, Trichy, Tamil Nadu, India

ABSTRACT:

In the current era, India is in the niche in becoming one of the developed countries in the world in terms of economic development. Thereby the energy requirement of the country would increase exponentially. In countries like India, coal is one of the major sources for raw material supply for power production. But the major issue in coal mining is the lives of human beings involved are endangered. A measure to help reduce the fatality rate necessitates the need for a system that serves the purpose of monitoring optimum survival conditions underground. In this regard out of all the developing technologies, the application of swarm robotics in underground mine monitoring rules out many of the disadvantages oriented with the current monitoring scheme.

Keywords – swarm, underground mine, monitoring, cloud storage

INTRODUCTION:

Swarm robotics hasn't confined its application in the process of Miniaturization, it sweeps the need for human assistants in the field of automation.

Mining Industry in our country is a major economic activity which contributes significantly to the Economy of India. The major drawback of Mining is the lack of monitoring parameters which leads to environmental disturbances .The solution is the

APPLICATION OF SWARM BOTS IN MINING which paves the way for monitoring the mining atmosphere with the mining parameters. With proper surveillance the disturbances to be created is well foreseen in advance.

Environmental inconvenience includes labour related health problems which leads to risk in worker's life, increased labour work .

The major objectives in Swarm robotics which includes the accessibility of inaccessible areas by the bots enhances the monitoring alongwith warning signal when the sensors go beyond threshold value.

COAL MINE TOPOLOGY:

When mining is considered, the most important feature to be taken in account is the temperature, concentration of gases, seismic instability. The major accidents occur in the mining when the gases like Methane and CO exceeds in its concentration above its nominal value. Explosion ,being a major issue in the coal mines takes place when fine particles of coal dust come into contact with source of heat. The maximum temperature ever recorded in the deepest mines is 140 deg Farenheit .When the temperature exceeds ,the methane gas in contact with air and with the source of heat ,may result in explosions.

The carbon-monoxide comes the next being flammable gas and explosive with air in concentration between 12.5 and 74%. It is

considered toxic as it blocks the hemoglobin in blood to carry oxygen from lungs to muscles. In case of landslides, it is necessary to note the sensitivity.

Hence it is a must to keep in note the record of the gas concentrations, temperature and the vibration. Thus the gas sensor, temperature sensor and vibration sensor is used to record the observations.

METHODOLOGY:

The main bot is responsible for the overall coordination of surveillance. The values obtained from the sensors is given to the cloud to store the values and in case if the values exceeds the optimum conditions the system detects an alert signal.

The robot is initially sent inside the mining area and the eminent conditions are continuously noted. In case of obstacle detected, based on the distance output from the Ultrasonic sensor, the bot's position is determined to move forward or backward followed by turning right or left. Emission of gases like methane and Co is the main cause of fire accidents in the area. For the purpose of prevention of the fire accidents, MQ sensor is used for detection of gases. Extreme heat owns the risk of fire too. Hence temperature sensor is used for the temperature detection. The vibrations in case of landslide are also accounted and values correspondingly noted. The overall surveillance thus involves the sensors output along with the movement of the robot.

MOTOR SELECTION

Let,

the torque required to drive the motor be represented as T

the voltage be represented as V

the current be represented as I

and power be represented as P

$$T = (9.5488 * P(\text{kW})) / \text{speed}(\text{rpm})$$

$$V = 12 \text{ V}$$

$$I = 60 \text{ mA (No-load current)}$$

$$I = 300 \text{ mA (Full load current)}$$

POWER CALCULATION:

$$P = V * I$$

$$= 12 * (300 / 1000)$$

$$P = 3.6 \text{ kW}$$

$$P = V * I = 12 * (60 / 1000)$$

$$P = 0.72 \text{ kW}$$

TORQUE CALCULATION:

$$T = (9.5488 * 3.6) / 300$$

$$T = 0.11 \text{ Nm}$$

$$T = (9.5488 * 0.72) / 300$$

$$T = 0.03 \text{ Nm}$$

COMPONENT SELECTION

- ULTRASONIC SENSOR
- GAS SENSOR
- VIBRATION SENSOR
- TEMPERATURE SENSOR
- DC MOTOR
- RASPBERRY PI

ULTRASONIC SENSOR:

Ultrasonic sensor is ideated to measure the distance in which the robot propagates, feeding and instructing the motor to go any other way in any case of obstacle detection nearby that could possibly cause robot crash. The ultrasonic sensor emits the short and high frequency signal. These propagate in the air at the velocity of sound. When an electrical pulse of high voltage is applied to the ultrasonic transducer, it vibrates across a specific spectrum of frequencies and generates a burst of sound waves. It calculates the time taken between sound waves and echo. Thus with the time taken the distance of the objects is measured. When this measured distance is less than the preset safe

distance, the robot is directed to measure the distance either sides with the help of a servo motor forming its neck and moves in the safer side.

GAS SENSOR:

Deep inside an underground mining area there are many potential gases that cause threat to human lives. When the proportion of these gases exceeds a certain value in the air mixture, it becomes potent to take away breath. So if the increase in the proportion of these gases in the mixture could possibly be detected and an alarm is generated, the miners could escape to a safer region and many lives could be saved. The basic working of Gas sensors is the detection of gas sensitivities. There are various gas sensors depending on the gases to be perceived, MQ_x wherein x denotes the number for the detection of particular gases. They are called as Chemresistors and detection is based on the change of resistance of the particular material when gas comes in contact with that sensing material. The gas detection is based on the concentration in terms of ppm.

VIBRATION SENSOR:

The natural hazard that causes the most fatality inside the underground mines is landslide that is caused due to the instability of the rock bed. So here the necessity of a vibration sensor is to detect the seismic instability at the niche and provide a warning signal both inside the miner for the workers and to the control room for the personnel. The basic principle lies in the fact that the sensor consists of a coil spring in which if an object hits the sensor, because of the shear stress produced, the spring and the metal comes in contact and potential difference is created. The output is corresponding to the voltage produced. The vibrations are measured in voltage corresponding to the potential difference. When

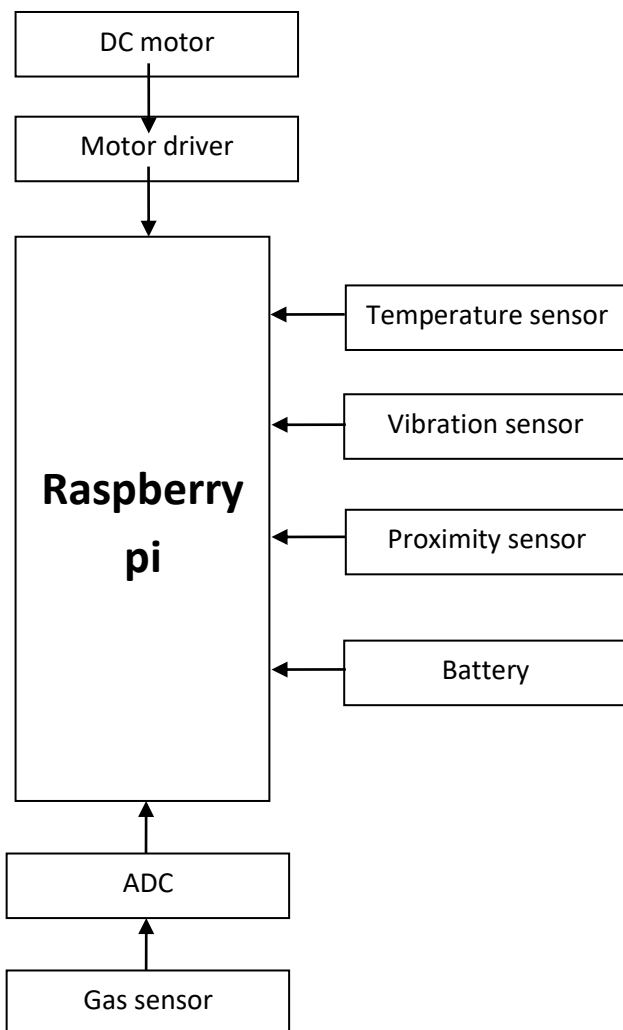
these vibrations are suspected to exceed the safest known level a warning signal will be produced.

TEMPERATURE SENSOR:

Temperature sensor is a transducer that produces electrical actuating quantity in response to temperature variations in the surroundings. The sensor consists of a diode which when the surrounding heat varies, it gives a proportional voltage output. The sensor consists of a material which measures temperature with change in resistance. It gives output voltage linearly proportional to centigrade (Celsius). A warning signal will be provided when the temperature rise exceeds the threshold value of temperature. The maximum operating depth of the miners so far recorded is 2.4 km to 3.9 km. The maximum recorded temperature of the deepest mine is 60°C. The tolerable temperature for human survival in the underground mines is 35°C. If this nominal temperature is exceeded inside the underground mine a warning signal will be provided so that the miners will get time lapse to escape to the safer region.

COMMUNICATION PROTOCOL:

Wireless fidelity is one type of wireless technology allowing local area network to operate without cables and wires. Using this technology telecommunication is made possible between the swarm robots. All the swarm robots will be connected to a host through Wi-Fi. All the information and data that is output by the swarm robots is fed to the cloud. The Wi-Fi used here is host to client connection. Raspberry pi has an inbuilt 802.11n standard Wi-Fi module. The range of the Wi-Fi used is 225 feet to 825 feet i.e. 68 meters to 250 meters.

BLOCK DIAGRAM**CONCLUSION:**

While India progresses towards becoming global super power the care and concern towards the safety of the workers of primary cadre is getting compensated. In an order to reap the benefit of India's advancement in electrical and electronics, the idea of application of swarm robotics in underground mine monitoring system would advocate the effort in the safety concerns of the workers. This could be way more enhanced and productive if the development goes hand in hand with the concern for the workers. Though there are many prevailing underground mine monitoring systems contemporarily, the application of swarm robotics is expected to be comparatively more

efficient and productive. Thus by not only augmenting the development in the regard of economy, swarm robotics in underground mine monitoring system also helps in the well being of the miners and elates the employer-employee relationship.

ACKNOWLEDGEMENT:

1. Saranathan College of Engineering
2. Dr.C.KrishnaKumar, Head – EEE, Saranathan College of Engineering

REFERENCE:

1. Robots, insects and swarm intelligence by Amanda J. C. Sharkey
2. Design of Monitoring System for Coal Mine Safety Based on Wireless Sensor Network by Yu Li-min ; Li Anqi ; Sun Zheng ; Li Hui
3. Automatic Monitoring System for Coal Mine Safety Based on Wireless Network by Jing Jiang Song, Yingli Zhu, Fuzhou Dong
4. <https://www.hindawi.com/journals/isrn/2013/6081>
5. http://www.swarmanoid.org/publications_byyear.php
6. <https://youtu.be/IbKY-n71XCE>
7. <https://im-mining.com/2018/01/04/anglo-sees-future-swarms-underground-modular-mining-robots-operating-deep-mines/>
8. <https://www.youtube.com/playlist?list=PLSsYUxE6dRP3xgjAmXxdk9ZLUTQmOMqGc>
9. <https://github.com/>
10. <https://www.w3schools.com/PYTHON/default.asp>

FUZZY LOGIC CONTROLLER USING SHUNT ACTIVE POWER FILTER FOR POWER QUALITY IMPROVEMENT

C.Pearline Kamalini¹, S.Divya², V.Karthika², P.Kiruthika²

¹ Assistant Professor Department of EEE

² UG Schloar Department of EEE

Saranathan College of Engineering

Trichy

ABSTRACT:

This paper represents the study and simulation of fuzzy logic controller using matlab Simulink. The shunt active power filter is used for harmonics and reactive power compensation of non-linear loads. Here, dc capacitor is controlled by using fuzzy control algorithm. In order to produce high power quality by reducing source current total harmonic distortion. By varying the switching frequency, the performance of active filter is determined.

KEYWORDS- shunt active power filter (APF), power quality (PQ), fuzzy logic controller, harmonics, total harmonic distortion (THD).

I. INTRODUCTION:

It comprises of voltage profile, frequency profile, harmonics contain and reliability of power supply.

Power quality refers to the ability of electrical equipment to consume the energy being supplied to it. A number of power quality issues including electrical harmonics, poor power factor, voltage instability and imbalance impact on the efficiency of electrical equipment. This has a number of consequences including:

- Higher energy usage and costs
- Higher maintenance costs
- Equipment instability and failure

Energy management is an important consideration for any business, and it is critical that power quality be assessed as part of any energy management strategy.[1]

The **quality** of electrical **power** is an **important** contributing factor to the development of any country and this can be achieved through continuous **power quality** monitoring which helps detect, record and prevent **power quality** problems.

Power quality problems are: Automatic Resets, Data Errors, Equipment Failure, Circuit Board Failure, Memory Loss, **Power Supply Problems**, UPS Alarms, Software Corruption, and Overheating of electrical distribution systems. This problems due the voltage sag, voltage swell and harmonics only.

In this project we removing the power quality problem HARMONICS, for improving the quality of power. The Power Quality (PQ) problem can be

Detected from one of the following several symptoms depending on the type of issue involved.

- Lamp flicker
- Frequent blackouts
- Sensitive-equipment frequent dropouts
- Voltage to ground in unexpected

- Locations
- Communications interference
- Overheated elements and equipment.

PE are the most important cause of harmonics, interharmonics, notches, and neutral currents. Harmonics are produced by rectifiers, ASDs, soft starters, electronic ballast for discharge lamps, switched-mode power supplies, and HVAC using ASDs [2]

II. FILTERS:

It is a device which processing the function and it specially removes the unwanted signal frequency components.it consists of two types.

1. **Passive filter**
2. **Active filter**

PASSIVE FILTERS:

It is a device (or) processing the function and it is made up of passive components such as resistors, capacitors, and inductor. [3]

ACTIVE FILTERS:

It employs RC network and amplifiers with feedback and it is having more number of advantages, in order to perform elimination of both higher and lower order of harmonics, filter out the harmonics in which significantly below the filter switching frequency.

III. Shunt active power filter:

Shunt Active power filters is the device which generate the same amount of harmonic generated by the load in which **180 degree** phase shifted. So these harmonics are inserted into the line at the point of common coupling the load current harmonics are eliminated and the utility supply becomes sinusoidal. There are basically two types of active filter: **Series active powerfilter andshunt active power filter.**

We using shunt active power filter for removing the harmonic problem improving the power quality in three phase transmission line where non-linear loads are connected.

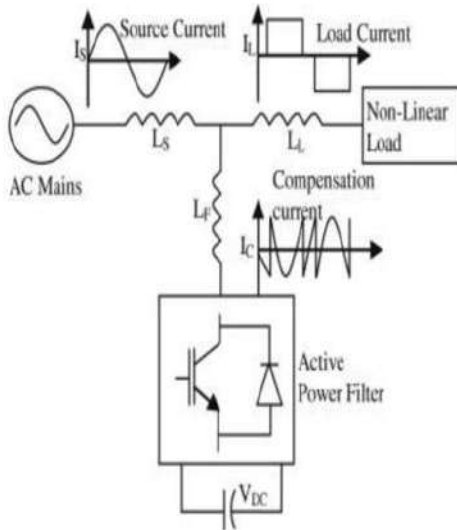
Active power filter:

1. Dominate the harmonics problems
2. It is used as both higher and lower order of harmonic in the power system.

CONDITIONS:

1. When current gets decreased, harmonic is produced.
2. When current gets decreased, voltage fluctuation and distortion are produced.[4]

GENERAL BLOCK DIAGRAM:



SHUNT ACTIVE POWER FILTER GENERAL BLOCK DIAGRAM FIG 1.1

PRINCIPLE FOR SHUNT ACTIVE POWER FILTER:

Let us consider AC mains as a power grid system. **WORKING** The main function of power grid is to be generating the power and distributed to the consumer and that consumer consumes a nonlinear load due to this harmonic problem are created. In transmission line, the reverse harmonics is injected by APF using voltage-controlled device (MOSFET), in order to eliminating the harmonics. This method is known as nullifying method. [4]

IV. HARMONICS:

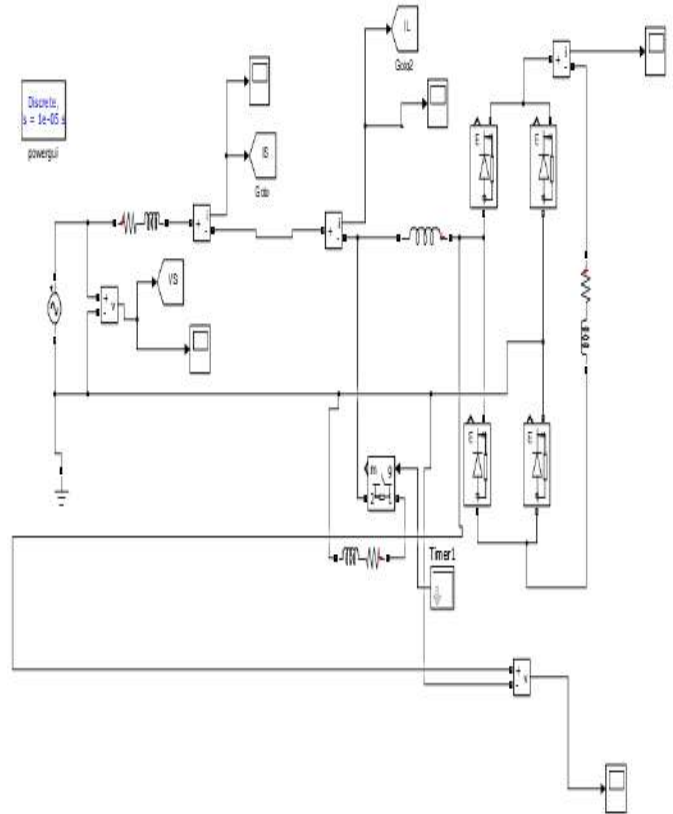
An active harmonic power conditioner/compensator/filter is a device that uses at least one static converter to meet the “harmonic compensation” function. This generic term thus actually covers a wide range of systems, distinguished by The number of converters used and their association mode, their type (voltage source, current source), the global control modes (current or voltage compensation), possible association with passive components (or even passive filters) [3]

It works by blocking the upstream harmonic voltage sources to provide better power to a sensitive load on a troubled power network. However, in practice, this “upstream” technique is of little interest since:

- The “quality” of the energy at the point of common coupling is satisfactory, [1]
- Insertion of an equipment in “shunt” mode is not that easy because of the issues like withstanding short-circuit current,
- It is more useful to look at the actual causes of voltage distortion (harmonic currents) within the network.

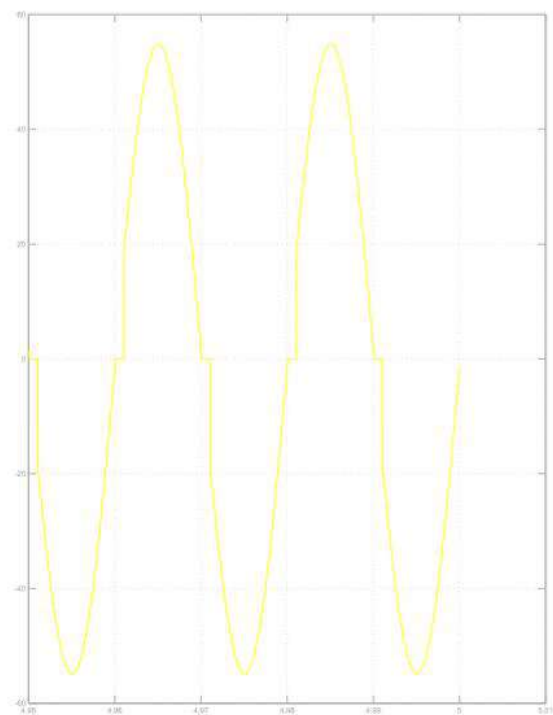
APF is a type of filter that uses either current or voltage source as its major component. They compensate voltage or Current harmonics by injecting the negative of the harmonic signal measured injected signals fed are of same magnitude But in phase opposition with the measured harmonic signals. It is controlled to attract/supply a compensated contemporary From/to the utility, such that it removes reactive and harmonic currents of the non-linear load. Thus, the ensuing general Cutting-edge drawn from the ac mains is sinusoidal. Ideally, the APF wishes to generate just sufficient reactive and Harmonic cutting-edge to compensate the non-linear masses within the line.

I. WITHOUT FILTER:



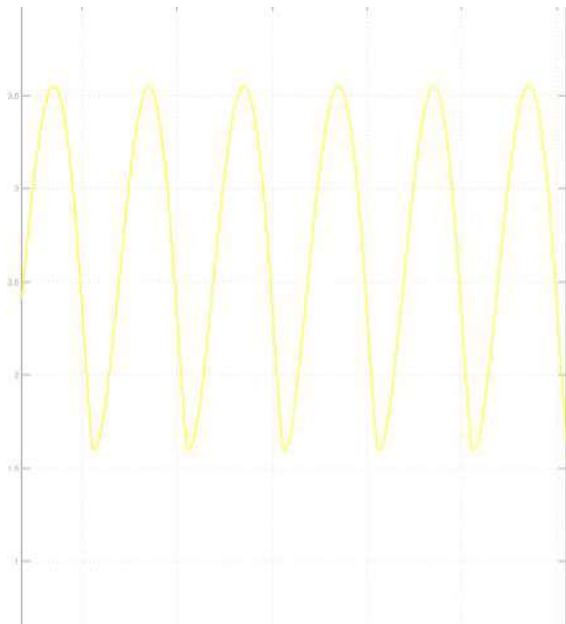
POWER FLOW IN TRANSMISSION LINE WITHOUT FILTER FIG 4.1

OUTPUT OF VOLTAGE:



VOLTAGE WAVEFORM IN WITHOUT FILTER

OUTPUT OF CURRENT:



CURRENT WAVEFORM IN WITHOUT FILTER

PID CONTROLLER:

A proportional–integral–derivative controller (PID controller or three-term controller) is a control loop feedback mechanism widely used in industrial control systems and a variety of other applications requiring continuously modulated control. They are used in most automatic process control applications in industry. PID controllers can be used to regulate flow, temperature, pressure, level, and many other industrial process variables

PID controller combines the advantage of proportional, derivative and integral control action. ... A proportional controller will have the effect of reducing the rise time and will reduce, but never eliminate. If an integrator is added, the control signal is proportional to the integral of error and the integral gain.

We used PID controller for reducing the harmonics problems.

PID CONTROLLER IN SHUNT ACTIVE POWER FILTER IMPLEMENTED:

The error signal is fed to PI controller. The output of PI controller has been considered as peak value of the reference current. It is further multiplied by the unit sine vectors in phase with the source voltages to obtain the reference currents. These reference currents and actual currents are given to a hysteresis based, carrierless PWM current controller to generate switching signals of the PWM converter [2]. The difference of reference current template and actual current decides the operation of switches. To increase current of particular phase, the lower switch of the PWM converter of that particular phase is switched on, while to decrease the current the upper switch of the particular phase is switched on. These switching signals after proper isolation and amplification are given to the switching devices. Due to these switching actions current flows through the filter inductor L_c , to compensate the harmonic current and reactive power of the load, so that only active power drawn from the source.

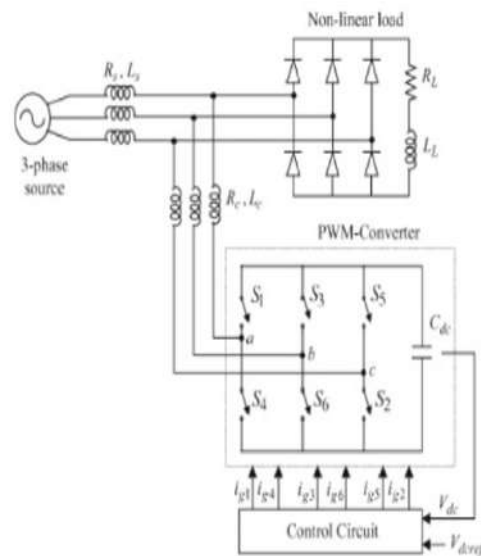
In existing system PID controller based control of shunt active power filter has been implemented. The spectral analysis of the supply current shows the harmonics produced by the load has compensated by the active filter the effect of varying the switching frequency on the performance of the active filter in existing system single tuned filter, damped filter C type, high pass filter has been implemented.

II. FUZZY LOGIC:

Fuzzy logic is a form of many-valued logic in which the truth values of variables may be any real number between 0 and 1 inclusive. It is employed to handle the concept of partial truth, where the truth value may range between completely true and completely false. The term **fuzzy logic** was introduced with the 1965 proposal of fuzzy set theory by Lotfi Zadeh. [4]

Fuzzy logic has been applied to many fields, from control theory to artificial intelligence.

Fig. 4. (1) Shows the block diagram of the implemented fuzzy logic control scheme of a shunt active power filter. Fig.4. (2) shows the schematic diagram of the control algorithm. In order to implement the control algorithm of a shunt active power filter in closed loop, the DC side capacitor voltage is sensed and then compared with a reference value. The obtained error and the change of error signal at the n th sampling instant as inputs for the fuzzy processing. The output of the fuzzy controller after a limit is considered as the amplitude of the reference current I_{MAX} takes care of the active power demand of load and the losses in the system.[5]



FUZZY LOGIC SYSTEM DIAGRAM FOR REMOVING THE HARMONICS

BASIC FUZZY ALGORITHM:

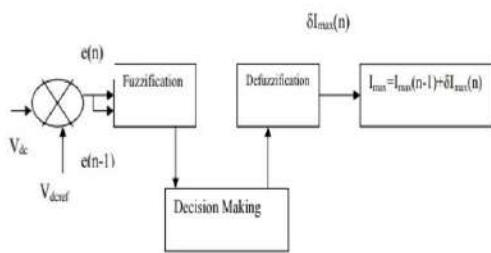
In a fuzzy logic controller, the control action is determined from the evaluation of a set of simple linguistic rules. The development of the rules requires a thorough understanding of the process to be controlled, but it does not require a

mathematical model of the system. The internal structure of the fuzzy controller is shown in Fig.

A fuzzy inference system (or fuzzy system) basically consists of a formulation of the mapping from a given input set to an output set using fuzzy logic. This mapping process provides the basis from which the inference or conclusion can be made.[4]

A fuzzy inference process consists of the following steps:

- Step 1: Fuzzification of input variables Fuzzification Defuzzification $e(n)$ $I_{max}=I_{max}(n-1) + I_{max}(n)$ V_{dc} $e(n-1)$ V_{def} **Decision Making 2**
- Step 2: Application of fuzzy operator (AND, OR, NOT) in the IF (antecedent) part of the rule
- Step 3: Implication from the antecedent to the consequent (THEN part of the rules)
- Step 4: Aggregation of the consequents across the rules
- Step 5: Defuzzification



III. MEMBERSHIP FUNCTION:

The basic properties of Boolean logic are also valid for Fuzzy logic. Once the inputs have been fuzzified, we know the degree to which each part of the antecedent of a rule has been satisfied. Based on the rule, OR(or) AND operation on the fuzzy variables is done. The implication step helps to evaluate the consequent part of a rule. There are a number of implication methods in the literature, out of which Mamdani and TS types are frequently used. Mamdani, proposed this method which is the most commonly used implication method. In this, the output is truncated at the value based on degree of membership to give the fuzzy output. Takagai-Sugeno-Kang method of implication is different from Mamdani in a way that, the output MFs is only constants or have linear relations with the inputs. The result of the implication and aggregation stpes is the fuzzy output which is the union of all the outputs of individual rules that are validated or “fired”. Conversion of this fuzzy output to crisp output is defines as defuzzification. There are many methods of defuzzification out of which Center of Area (COA) and Height method are frequently used. In the COA method (often called the center of gravity method) of defuzzification, the crisp output of particular variable Z is taken to be the geometric center of the output fuzzy value $\mu_{out}(Z)$ area, where this area is formed by taking the union of all contributions of rules whose degree of fulfillment is greater than zero. In height method of defuzzification, the COA method is simplified to consider the height of the each contributing MF at the mid-point of the base. Here in this scheme, the error e and change of error Ce are used as numerical variables from the real system. To convert these numerical variables into linguistic variables, the following seven fuzzy levels or sets are chosen as: NB (negative big), NM (negative medium), NS (negative small), ZE (zero), PS (positive small), PM (positive medium), and PB (positive big) [6]. The fuzzy controller is characterized as follows:

- Seven fuzzy sets for each input and output.

- Triangular membership functions for simplicity.
- Fuzzification using continuous universe of discourse.
- Implication using Mamdani's 'min' operator.
- Defuzzification using the 'height' method[6]

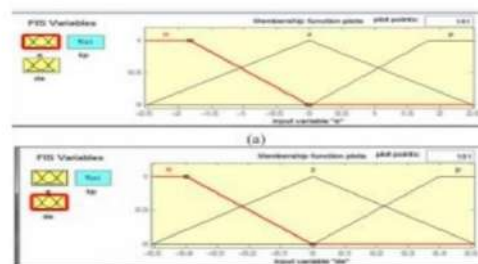
IV. DESIGN OF CONTROL RULES:

The fuzzy control rule design involves defining rules that relate the input variables to the output model properties. As FLC is independent of the system model, the design is mainly based on the intuitive feeling for, and experience of, the process. A new methodology for rule base design based on the general dynamic behavior of the process has been introduced in [18] which is further modified [14]. The input variables of the FLC are the error e and the change of error Ce. The output is the change of the reference current (δI_{max}). The time step response of a stable closed loop system -1 -0.5 -0.2 0 0.2 0.5 1 $\mu\delta I_{max}$ NB NM NS ZE PS PM PB -1 -0.5 -0.25 0 0.25 0.5 1 NB NM NS ZE PS PM PB 27.

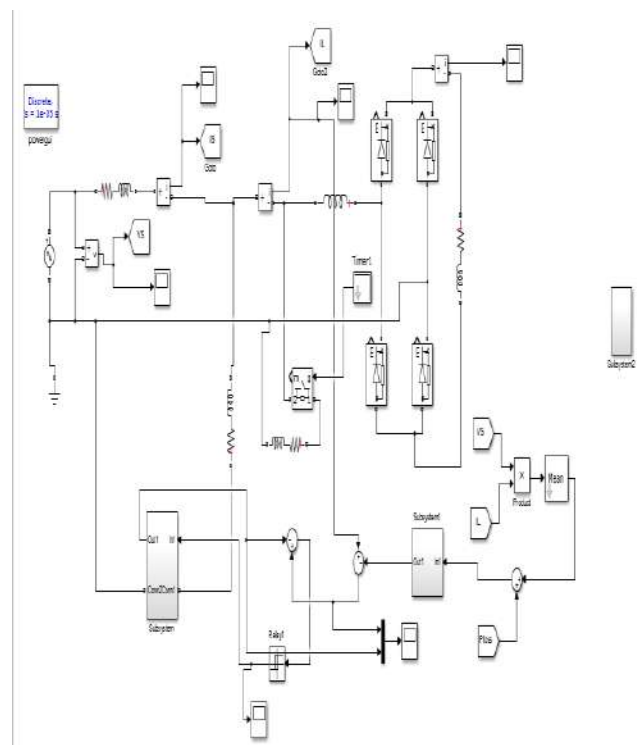
V. CONTROL TABLE:

E	NL	NM	NS	ZE	PS	PM	PL
ΔE	NL	NL	NL	NL	NM	NS	ZE
NL	NL	NL	NL	NL	NM	NS	ZE
NM	NL	NL	NL	NM	NS	ZE	PS
NS	NL	NL	NM	NS	ZE	PS	PM
ZE	NL	NM	NS	ZE	PS	PM	PL
PS	NM	NS	ZE	PS	PM	PL	PL
PM	NS	ZE	PS	PM	PL	PL	PL
PL	NL	NM	NS	ZE	PS	PM	PL

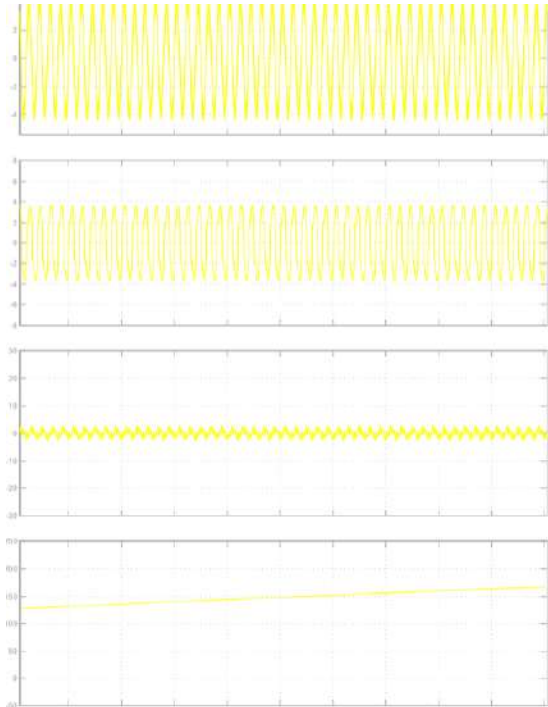
Fuzzy table



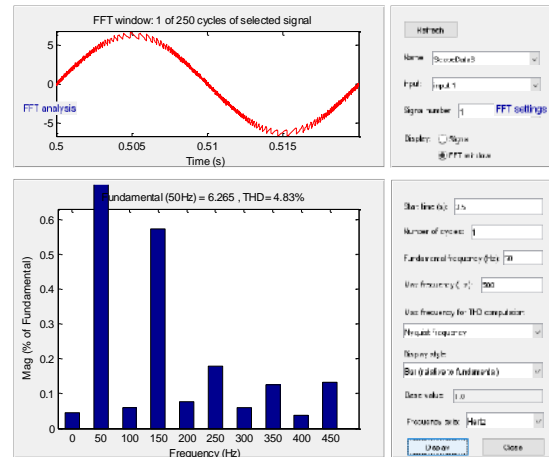
SIMULINK DIAGRAM:



SIMULINK OUTPUT:



HARMONIC DISTORTION:



VI. CONCLUSION:

This paper presents the modelling and simulation of single phase shunt active power filter controlled with fuzzy logic controller. The simulation was performed in MATLAB/SIMULINK. Total harmonic distortion for the load current and source current with and without shunt active power filter. Fuzzy logic controller have shown its capability in mitigating techniques harmonic current and voltage produced by non-linear loads as well as compensating the reactive power of the system.

REFERENCES:

- [1] C. SANKARAN "POWER QUALITY ", Publisher: CRC Press, 2001
- [2] B. Singh, K. Al-Haddad, and A. Chandra, "A review of active filters for power quality Improvement," IEEE Trans. Ind. Electron., vol. 46
- [4] S. K. Jain, P. Agrawal, and H. O. Gupta, "Fuzzy logic controlled shunt active power filter for power quality improvement," Proc. Inst. Elect Eng., Electr. Power Appl., vol. 149, no. 5, 2002.
- [4]H. Ying, "Constructing nonlinear variable gain controllers via the Takagi-Sugeno fuzzy control," IEEE Trans. Fuzzy Syst., vol. 6, no. 2, pp. 226–235, May 1998, pp. 960–971, Oct. 1999
- [6]S. K. Jain, P. Agrawal, and H. O. Gupta, "Fuzzy logic controlled shunt active power filter for power quality improvement," Proc. Inst. Elect Eng., Electr. Power Appl., vol. 149, no. 5, 2002. [12] H. Ying, "Constructing nonlinear variable gain controllers via the Takagi-Sugeno fuzzy control," IEEE Trans. Fuzzy Syst., vol. 6, no. 2, pp. 226–235, May 1998.

H₂O FORECASTING

Boopathinavaneethan.S ^[s], **Barath.R** ^[s], **Bharanidharan M.S** ^[s], **Lakshmi Narayanan.T** ^[s], **Rameshbabu.P** ^[prof]. Department of Electrical & Electronics Engineering, Saranathan College of Engineering, Tiruchirappalli, Tamil Nadu, India

Abstract

It is a real time implementation of water and its resources management system. For better understanding we can take a metro city. More over a metropolitan city is supplied with the fresh water by the Ministry of water resources in India. On having the power system department as a model we can also separate the water resources and distribution departments. The first department will be the resources department which includes lakes, rivers, underground bore wells etc. The second one is the department for purifying the water by some modern treatments such as chlorinating, UV treating etc. The third one will be the distributing one which distributes the water to each and every area in that specified metropolitan city. Now, the sensor which senses the flow and pressure of the water pipe will be fitted to each and every pipe of the above mentioned departments. These sensors will sense the data from the pipes and feeds it into a microcontroller. This microcontroller will feed the data to the clouds. Using the cloud computing system these data will be retrieved and they will be converted in to the graphs. These graphs will show the amount of the water flow in every area and we can monitor it by 24/7.

Introduction

Water, the primary resource for all existing beings in history, war has been erupted for many reason like land ,minerals, oil, wealth and some more. But in recent times the war for the water and water resources has been triggered by some nations. Since the mankind evolved, we have been learning, acquiring, controlling and managing things. We all are doing these things to keep everything in an orderly manner. Once the orderly manner gets unbalanced, that place evidences a war. Water is not an unlimited quantity; it has become a limited edition thing. Since we have only 3% of fresh water we have to manage the resources in an orderly manner to supply the growing population of the world, which has already crossed 650billion.The above said orderly things will play a major role in managing the world's highly populated country India. It

consists of 12 million people. The major hotspots are the capital of each state of the country. Still the country is in its developing era, the states are mainly focusing on their metro-city, the capital of their state. To manage the water resources and to have an effective control and prediction of the water needs of their capital and other cities, this project will play a role as a game changer. Bangalore, the capital of Karnataka state was announced to be the second city running out of its water resources. There have been many disputes in sharing the water resources. For example the river Sindh's dispute between India and Pakistan, the river Brahmaputra's dispute between India and china and even with Bangladesh, the river Cauvery's dispute between the states Karnataka and Tamil Nadu. These disputes were not only due to the insufficiency of water and its resources but also due to the wastage and improper monitoring of the

water resources and its distribution. To monitor and manage the water there must exist a system which must be likely a Xerox of the power system management. By doing so we can even forecast the future water needs and also we can plan the dam, desalination projects in accordance with that forecasted data.

Literature Survey

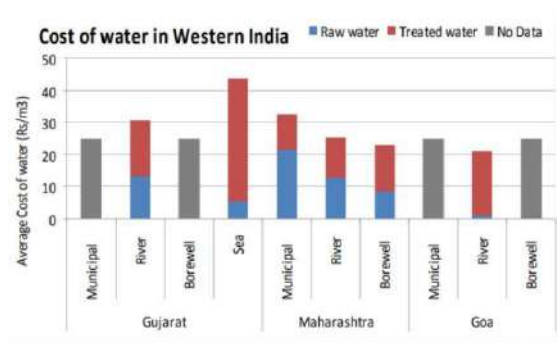
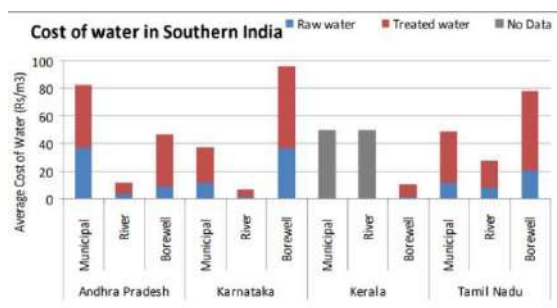
Water Distribution boards of Central and state government are our customers. Everyone can use such system in their home. According to the recent survey there are 248,408,494 registered houses in India. More precisely according to the 2011 survey there 8 metropolitan cities in India which includes Delhi, Mumbai, Chennai, Kolkata etc. Such metropolitan city will have many management issues. by using our product those issues can be easily monitored and solved. The industries which are using water as their raw material can use our product. There are ‘n’ number of industries which is making \$2.65 trillion. Every above said sectors will like to analyze summarize and forecast the water resources. So the will be a huge opening market for our project.

Serviceable Addressable Market (SAM) Identification & Justification:

As per the survey the beverage industries uses approximately 3 litres of water to produce 1 litre of soft drinks. Approximately 300 litres of water have been used per day for their production. Lot of water are wasted during the manufacturing process. The water is not only used for manufacturing but also for the cleaning, removing impurities in the furnace etc. In houses lot of water are wasted in cleaning vehicles and in cooking and cleaning the food items and in gardening etc. By using our product the water is forecasted and can be used in a efficient way.

Internet of Things

Internet of Things (IoT) is defined as the network of physical objects/things - devices, vehicles, buildings embedded with sensor, micro-controller, and network connectivity that enables these objects to collect and exchange data. The IoT can be described as a huge web of embedded objects designed with built-in wireless technologies such that they can be monitored, controlled and linked within the existing Internet infrastructure. Each device has a unique identification and must be able to capture real-time data autonomously. Basic building blocks of IoT consist of sensors, processors, gateways, and applications. It is estimated that by 2020, 50 billion ‘things’ will be connected to the Internet. Wireless technologies such as the Wi-Fi, Bluetooth, ZigBee, RFID, 6LoWPAN (IPv6 Low power Wireless Personal Area Network) allow the device to be connected to the Internet and to each other. The cloud services collect, store and analyze the data collected by the sensors and allow people to take decision accordingly. Mobile data management applications are being increased because of the rapid spread of mobile phones. Smart phones now have become platform both for computing and

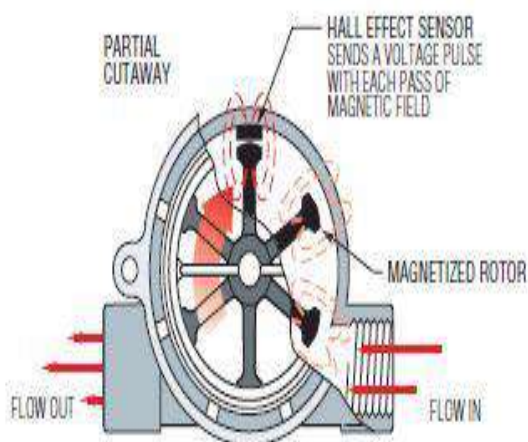


communication. Mobile phones are becoming cheaper, easier to use, and can be used for multiple types of information transmission. The mobile data applications along with sensor technology can improve the efficiency as well as accuracy of the data reporting for water quality monitoring system. Smart phones/tablets having sensors embedded with display and keypad can be connected to the Internet with an IP address (satisfies every requirement of an IoT device). They will serve as the hub/remote control for IoT. In Ubiquitous Network Architecture smart things are part of the Internet; authorized users have access to information; servers act as a sink to collect data from each object. HTTP over Internet. One can create applications like sensor logging, location tracking, and social network of things with status updates with the help of Thing Speak. API of Thing Speak permits processing of numeric data like averaging, median, summing, rounding and time scaling.

Components

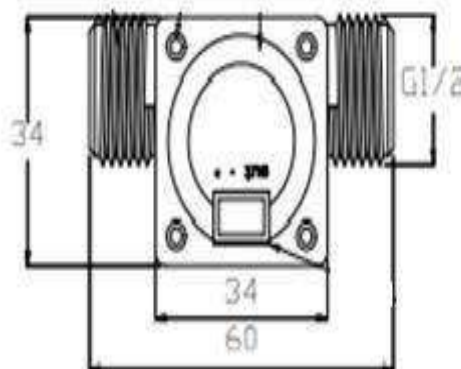
Water Flow Sensor

We are connecting the water flow sensor with the ESP8266 Wi-Fi module. The analog signal of the flow sensor will be converted in to the digital signal with the use of hall sensor which is mounted in the flow sensor.



YF-S201 Hall Effect Water Flow Meter / Sensor:

This sensor sits in line with your water line and contains a pinwheel sensor to measure how much liquid has moved through it. There's an integrated magnetic Hall Effect sensor that outputs an electrical pulse with every revolution. The Hall Effect sensor is sealed from the water pipe and allows the sensor to stay safe and dry.

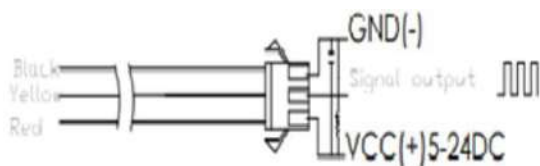


The sensor comes with three wires: red (5-24VDC power), black (ground) and yellow (Hall Effect pulse output). By counting the pulses from the output of the sensor, you can easily calculate water flow. Each pulse is approximately 2.25 milliliters. Note this isn't a precision sensor, and the pulse rate does vary a bit depending on the flow rate, fluid pressure and sensor orientation. It will need careful calibration if better than 10% precision is required. However, it's great for basic measurement tasks!

The pulse signal is a simple square wave so it's quite easy to log and convert into liters per minute using the following formula.

Pulse frequency (Hz) / 7.5 = flow rate in L/min.

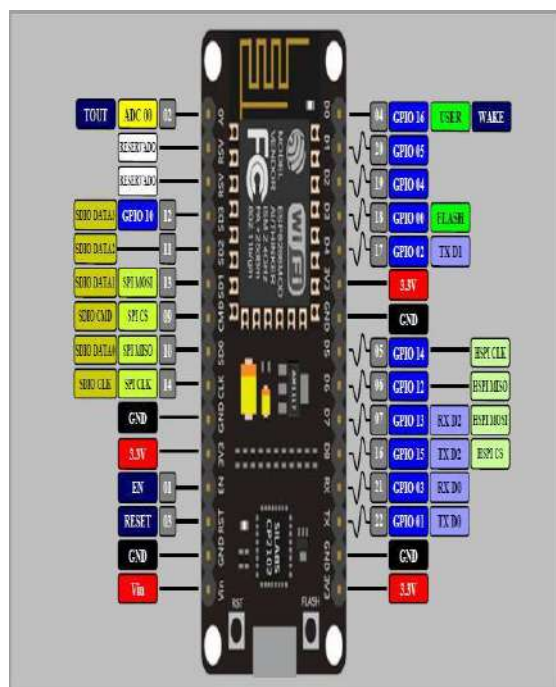
Connection Method



Flow Range: 100L/H-1800H-L/H

Flow (L/H)	Frezq.(HZ)	Erro range
120L/H	16	±10
240L/H	32.5	
360L/H	49.3	
480L/H	65.5	
600L/H	82	
720L/H	90.2	

ESP 8266 Module

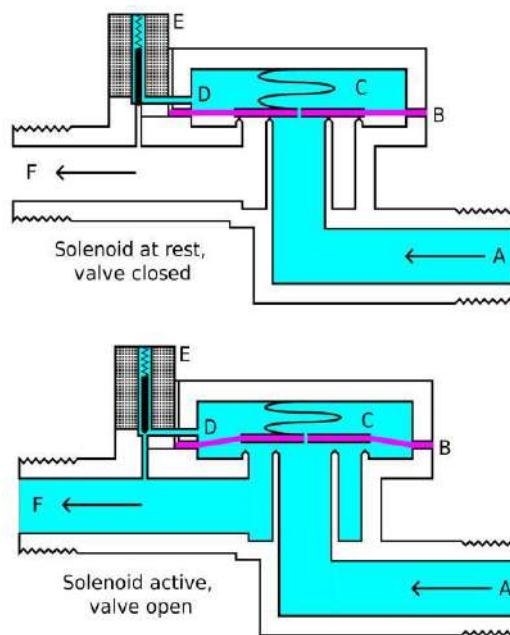


The ESP 8266 is an advanced version of the Arduino, which is specially designed for the IOT projects. Like all the other microcontrollers it is also programmable and once the program has been uploaded, it will not erase until the firing of reset. This can be programmed with Arduino IDE platform.

This one consists of nine digital output pins along with one analog to digital converter. The input voltage for node mcu is 3.3V. It has an inbuilt Wi-Fi Connection option.

The Bolt IOT can also be used in replacement for this node mcu. Even though this node mcu gives us the ease of programming with C++.

Solenoid Valve



The solenoid valve consists of the plunger which is placed inside a winding. The winding is given the supply. Whenever the supply is given, the winding will act as an electromagnet, which will close the valve. This is explained in the above figure.

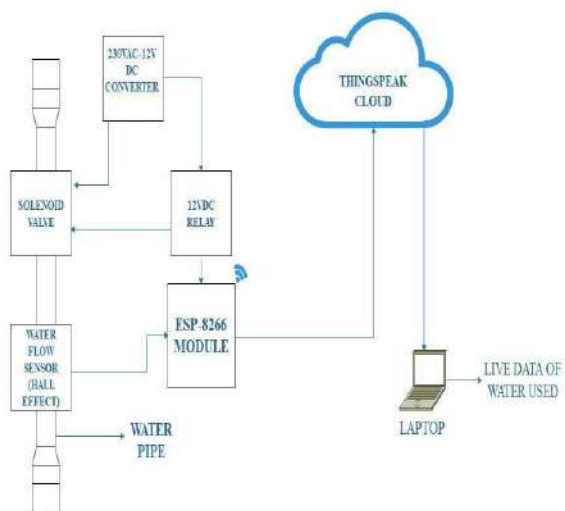
Implementation

The water flow sensor is connected with the node mcu and the solenoid valve is connected to the node mcu via relay module.

The relay module and the solenoid valve will be supplied with a convertor board which gives output of the 12VDC or 24VDC. Since if the radius of the pipe increases the solenoid valve's size.

The flow through the pipe is measured and sent to the private cloud. Later the data from the cloud can be retrieved and saved in the memory. It also enables the live sensing of the data. We have used the Thingspeak cloud to feed and retrieve our live and saved data.

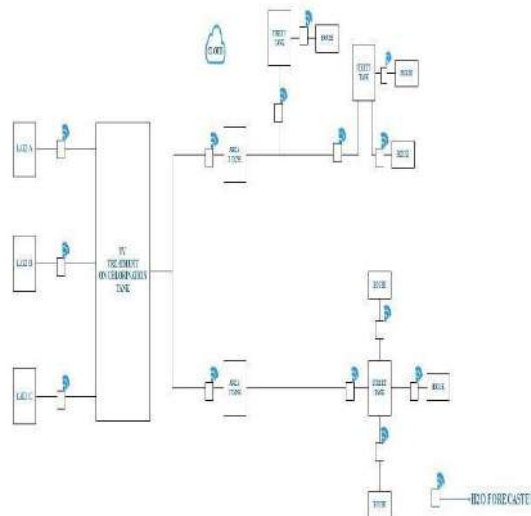
The block diagram of the implementation of our module is shown here and it is named as the h2o forecaster.



Mass Implementation

As said before we can implement and setup a system for a city, water based industry. By doing so we can measure the inlet, outlet, leakage and also we can forecast the water needs of the future.

Here the water supply map of a city which has implemented our idea as example is given.



Conclusion

Over last 3 decades there has been a water management issue which threatens every government. Some of the examples are given. Bengaluru, the capital of Karnataka state was announced to be the second city running out of its water resources in world. There has been many disputes in sharing the water resources. the river Sindh's dispute between India and Pakistan, the river Brahmaputra's dispute between India and china and even with Bangladesh, the river Cauvery's dispute between the states Karnataka and TamilNadu. The water based soft drinks companies are sucking trillion of litres from the land. It's not about the companies, but it is about the management of water with digital equipment, which will leave the future India with more water resources. There has been numerous rallies to conserve water. But they were ended up with no fruit. Once the citizens are given with the precise data of water being wasted, there will be a change in the attitude of our citizens while dealing with water.

Reference Papers

1. G. Gosavi, G. Gawde and G. Gosavi, "Smart water flow monitoring and forecasting system," *2017 2nd IEEE International Conference on Recent Trends in Electronics, Information & Communication Technology (RTEICT)*, Bangalore, 2017, pp. 1218-1222.
2. P. Singh and S. Saikia, "Arduino-based smart irrigation using water flow sensor, soil moisture sensor, temperature sensor and ESP8266 WiFi module," *2016 IEEE Region 10 Humanitarian Technology Conference (R10-HTC)*, Agra, 2016, pp. 1-4.
3. . Awasthi, S. Azeemuddin, S. Purini and M. Annesha, "Flow Sensor IoT Node for Wi-Fi Equipped Apartments and Gated Communities," *2018 IEEE SENSORS*, New Delhi, 2018, pp. 1-4.
4. P. Srivastava, M. Bajaj and A. S. Rana, "Overview of ESP8266 Wi-Fi module based Smart Irrigation System using IOT," *2018 Fourth International Conference on Advances in Electrical, Electronics, Information, Communication and Bio-Informatics (AEEICB)*, Chennai, 2018, pp. 1-5
5. M. S. M. Pakpahan, E. D. Widiyanto and R. Septiana, "Analysis on Batik Water Waste Monitoring System based on LoRa Communication," *2018 5th International Conference on Information Technology, Computer, and Electrical Engineering (ICITACEE)*, Semarang, 2018, pp. 171-175.
6. M. Kumar Jha, R. Kumari Sah, M. S. Rashmitha, R. Sinha, B. Sujatha and K. V. Suma, "Smart Water Monitoring System for Real-Time Water Quality and Usage Monitoring," *2018 International Conference on Inventive Research in Computing Applications (ICIRCA)*, Coimbatore, 2018, pp. 617-621
7. T. Perumal, M. N. Sulaiman and C. Y. Leong, "Internet of Things (IoT) enabled water monitoring system," *2015 IEEE 4th Global Conference on Consumer Electronics (GCCE)*, Osaka, 2015, pp. 86-87.
8. Q. Bin, W. Longshuang, Z. Wenliang, Z. Huiting and W. Xin, "Design and Implement of Real-time Monitoring System of Urban Water Supply," *2013 Third International Conference on Intelligent System Design and Engineering Applications*, Hong Kong, 2013, pp. 536-539.
9. K. Gopavanitha and S. Nagaraju, "A low cost system for real time water quality monitoring and controlling using IoT," *2017 International Conference on Energy, Communication, Data Analytics and Soft Computing (ICECDS)*, Chennai, 2017, pp. 3227-3229.
10. N. Vijayakumar and R. Ramya, "The real time monitoring of water quality in IoT environment," *2015 International Conference on Circuits, Power and Computing Technologies [ICCPCT-2015]*, Nagercoil, 2015, pp. 1-4.

Implementation of MVDC distribution system using quadratic boost converter

PARANTHAGAN.B^[1], AARTHYA^[2], AKHILA B^[3], GAYATHRI N^[4], SRILAXMIE C^[5]
ELECTRICAL AND ELECTRONICS ENGINEERING
SARANATHAN COLLEGE OF ENGINEERING, TRICHY, TAMILNADU, INDIA

Abstract— Due to increasing number of power generation units and load devices operating with direct current (DC) at distribution level, there is a potential benefit of building a DC distribution system. However, there are challenges in implementing a DC distribution system mainly the standardization. The dominance of AC was facilitated by the ease of transforming AC electrical energy to different voltage levels through the AC transformer, needed for efficient transportation over long distances. However, the advances in power electronics nowadays allow for an equally simple transformation of DC voltages. Simulation of buck converter and quadratic boost converter (QBC) for the required DC output value has been executed in MATLAB/SIMULINK environment.

Index Terms—DC distribution, quadratic boost converter, buck converter.

I. INTRODUCTION

In the late 19th century Thomas Edison and George Westinghouse concerned the relative merits of AC and DC distribution system. The first electric power transmission system was made by DC. Despite that it was difficult to transfer power over long distances. Hence the AC system which transfer high voltage obviously using transformers, was selected as standard power system. Since then AC distribution won favour and has entangled with our electrical power system

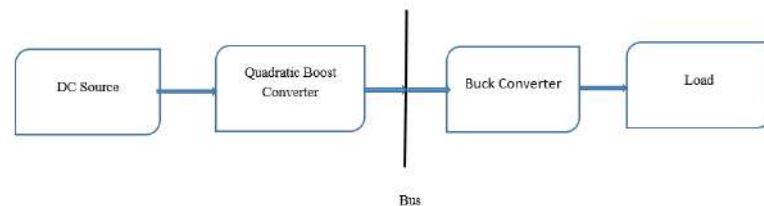
The technology is revamping every day that eventually leads to increased usage of loads. India is running out of energy resources as the peak demand is found to be 11 %^[7]. This motivates the power grid to install renewable energy based generating units. The power delivered by the renewable resources is DC which is converted to AC as the conventional transmission system operates in AC. This AC power is again converted to DC as many home appliances and commercial buildings needs DC power.

In the recent years, due to the advancements in power electronics technology and power semiconductor technology, the limitations in DC distribution system has been gradually overcome^[1]. Thus, making the DC technology appears to emerge again. There are some technical challenges in implementing DC distribution at higher level voltages due to unavailable of DC standarad voltages. Thus, the prototype of DC distribution system at low voltage level has been implemented by using quadratic boost converter and buck converter^[3]. Both the simulation and hardware prototype has been demonstrated. Simulation results of the study shows that

DC system has higher efficiency and reduced losses as compared to traditional AC system.

II. BLOCK DIAGRAM

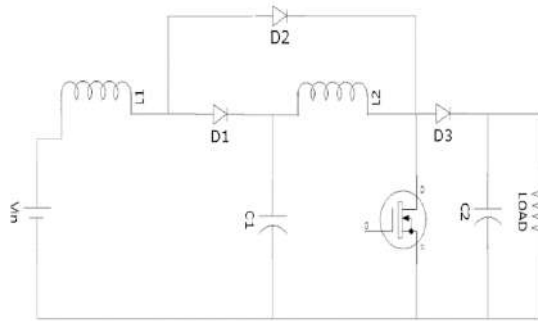
The entire block consists of source, quadratic boost converter, buck converter and a load. The source used is 48V DC source. Quadratic converter is a dc-dc converter which steps up the voltage to 4 to 6 times the input voltage. In this project 48V is stepped up to 300V. The buck converter is a dc-dc converter which steps down the input voltage to a desired value according to the duty cycle specified. The input voltage of the buck converter is 300V which is stepped down to 48V. Any kind of DC load of 100W, 48V can be used. Here lighting load is used.



III. QUADRATIC BOOST CONVERTER

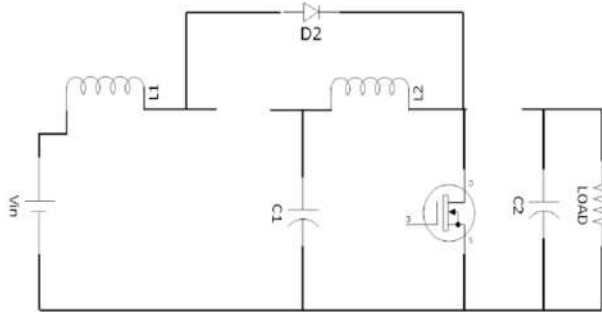
Quadratic boost converter is one of the emerging power electronics converter where the voltage boosts till 4 to 6 times the input voltage, normal boost converter boosts 2 times the input voltage.

The circuit consists of inductors, capacitors, diodes and a switch. The input voltage source can be any kind of DC voltage source. The output voltage is measured across the capacitor C2. There are two modes of operation based on ON and OFF states of switch.



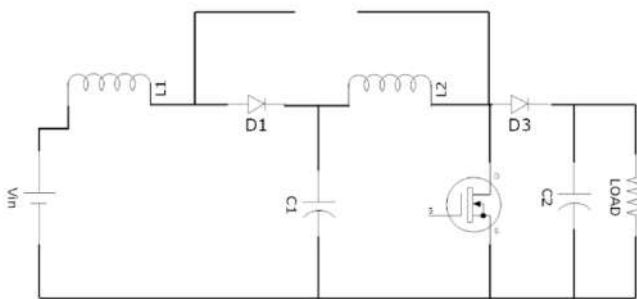
MODE 1

When switch s is turned on D2 is forward biased, whereas D1 and D3 are reverse biased. currents are supplied to L1 and L2 by Vin and C1 respectively.



MODE 2

In this mode D1 and D3 are forward biased, whereas D2 is reverse biased. L1 and L2 are charging C1 and C2 respectively.



QUADRATIC BOOST CONVERTER

The below figure shows the diagram of Quadratic Boost Converter and designed for 48/300 V.

$$D = 1 - ((V_{in}/V_o)^{-1/2})$$

$$= 0.6$$

$$I_{L1avg} = I_o / (1-D)^2$$

$$= 3.125 \text{ A.}$$

$$I_{L2avg} = I_o / (1-D)$$

$$= 1.25 \text{ A}$$

$$I_{L1} = 20\% \text{ of } I_{L1avg}$$

$$= 0.625 \text{ A}$$

$$I_{L2} = 20\% \text{ of } I_{L2avg}$$

$$= 0.25 \text{ A.}$$

$$I_{L1max} = (I_{L1}/2) + I_{L1avg}$$

$$= 3.437 \text{ A.}$$

$$I_{L2max} = (I_{L2}/2) + I_{L1avg}$$

$$= 1.375 \text{ A.}$$

INDUCTANCES VALUES

$$L_1 = (V_{in} * D) / (I_{L1} * f)$$

$$= 5.76 \text{ mH}$$

$$L_2 = (V_{in} * D) / (I_{L2} * f * (1-D))$$

$$= 0.036 \text{ H}$$

CAPACITANCE VALUES

$$C_1 = (I_o * D) / ((1-D) * V_{C1} * f)$$

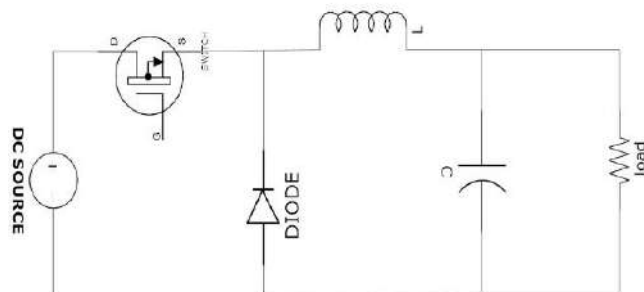
$$= 1.5625 * 10^{-5} \text{ F}$$

$$C_2 = (I_o * D) / (V_{C2} * f)$$

$$= 2.5 * 10^{-6} \text{ F}$$

IV. BUCK CONVERTER

Buck converter is a switch mode DC-DC electronic converter in which output voltage will be transformed to level less than the input voltage .It is also called as step down converter. The name step down converter comes from the fact that analogous to step down transformer the input voltage is stepped down to a level less than input voltage. By law of conservation of energy the input power has to be equal to output power.



Buck converter is the converter in which the inductor in the input circuit resists sudden variation in input current .when the

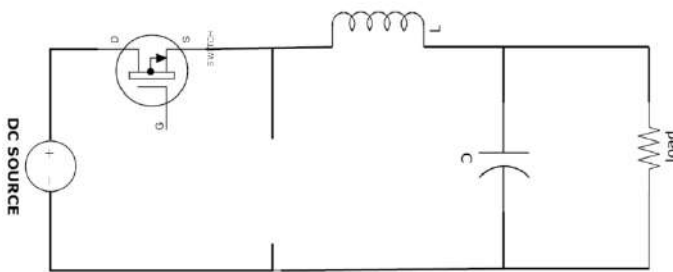
switch is ON the inductor stores energy in the form of magnetic energy and discharges it when the switch is closed. The capacitor in the output circuit is assumed large enough that the time constant of RC circuit in the output stage is high. The large time constant compared to switching period ensures a constant output voltage.

The circuit consists of an inductor, a capacitor, a diode and a switch.

This circuit can be operated in two modes based on ON and OFF states of switch.

MODE 1

When switch is in ON state the diode will be open circuited since it is in reverse biased condition. During this state the inductor gets charged by V_{in} thus closing the circuit through capacitor C.



MODE 2

In this mode the switch is in OFF state the diode will be forward biased. The inductor now discharges through diode and capacitor C.

$$D = V_o / V_{in}$$

$$= 48 / 300$$

$$= 0.16$$

$$I_L = 30\% \text{ of } I_{Load}$$

$$= 0.25 \text{ A.}$$

INDUCTANCE VALUE

$$L = V * (T / I_L)$$

$$(V = V_{in} - V_o)$$

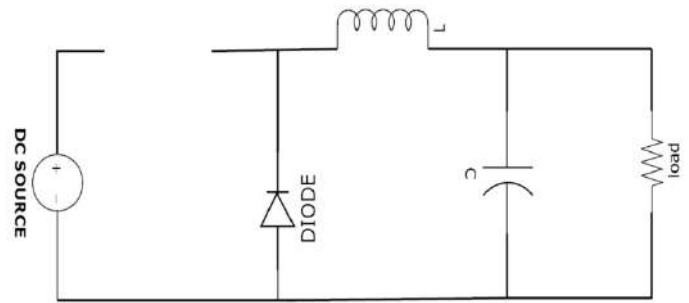
$$= 0.02016 \text{ H.}$$

CAPACITANCE VALUE

$$C = I_L / (8 * f * V_c)$$

$$(V_c = 2\% \text{ of } V_o)$$

$$= 4.069 * 10^{-6} \text{ F}$$



V. SIMULATION

In our project we designed simulation using MATLAB SIMULINK for DC distribution system using Buck Converter and Quadratic Boost Converter and made comparison with AC distribution system. We designed for 1KW system and scale down for 110 W for hardware.

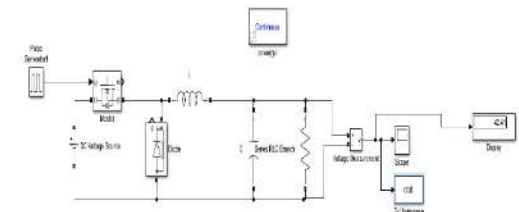


Figure 1: buck converter simulation diagram

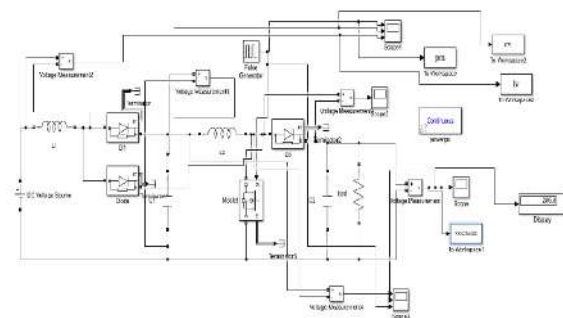


Figure 2: Simulation of Quadratic boost converter

DC DISTRIBUTION SYSTEM

This simulation diagram shows the model of DC distribution system using Quadratic boost converter and buck converter by neglecting the losses in the simulation. Using DC source generating 48 V and boosting to 300 V using Quadratic boost converter and distributed to load side stepped down from 300 V to 48 V using Buck converter. The load considered here is DC loads like LED lamps, computers.

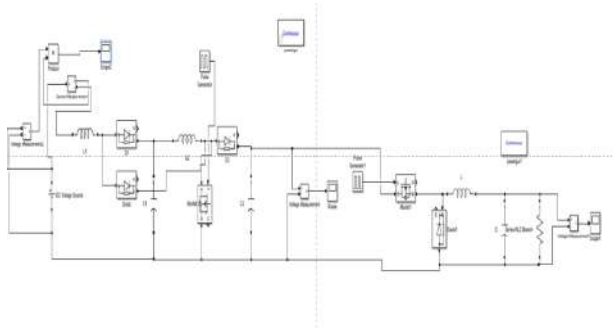


Figure 3: Simulation of DC distribution system

VI.SIMULATION RESULTS AND DISCUSSION

The simulation results shown here for an ideal case (i.e) neglecting losses. For hardware consider the losses and choose the converters for higher efficiency operation. Simulation model shows the efficiency of DC distribution over the AC distribution system.

In Figure 4, at the starting period of time, there are some transients till 0.05 seconds after which it get settled and provide voltage of 270 V.

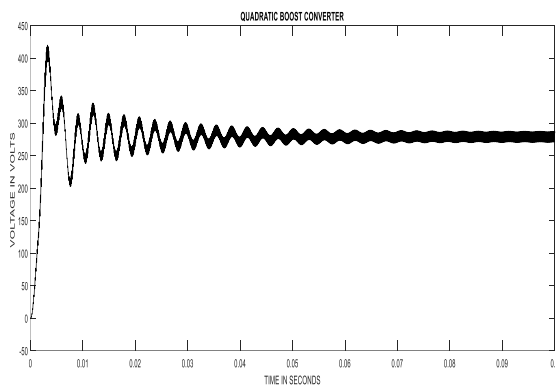


Figure 4:Waveform of quadratic boost converter

In Figure 5, time period of transients is very less and hence provides voltage of 46V at around 0.005s.

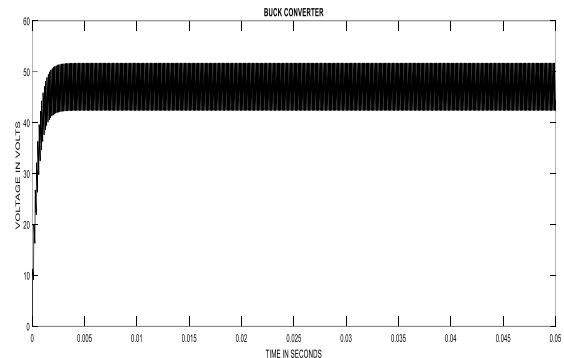


Figure 5: Waveform of buck converter

In Figure 6, due to the interconnection of quadratic boost converter and buck converter the effect of transient in the system is much lesser as compared with quadratic boost converter alone the output gets stabilized in short span of time. This helps the distribution system to feed the load efficiently.

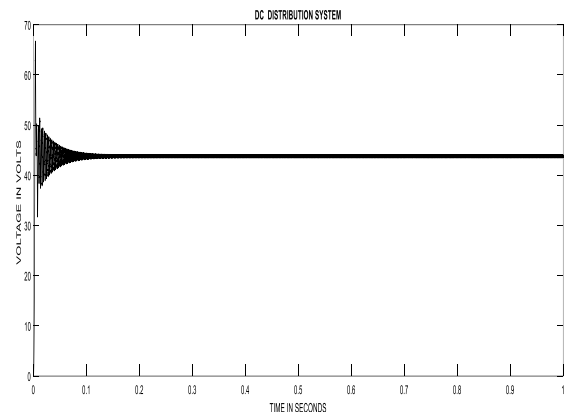


Figure 6:Waveform of DC distribution systems

CONCLUSION

DC is an emerging technique. Due to development of power electronics technology, converters will acts like step up and step down transformer, that will greatly help in distribution system .Developed countries like China, started to implement DC distribution system in a testing model for consumers applications. If certain disadvantages like high cost of DC components , Protection issues are cleared. Surely DC will rule the future electrical systems

REFERENCES

- [1] Toward the Universal DC Distribution System
Laurens Mackay, Nils H. van der Blij, Laura Ramirez-Elizondo & Pavol Bauer, 28 March 2017.
- [2] Coltman, J. W., "The transformer [historical overview]," IEEE, Ind. Appl. Mag., Vol. 8, No. 1, pp. 8–15, January 2002.
- [3] Low Voltage DC Distribution System, Asian Power Electronics Journal, Vol. 8, No. 3, Dec 2014 .
- [4] S. Luo, and I. Batarseh, "A review of Distributed power systems Part 1: DC distributed power system", IEEE Aerosp. Electron. Syst. Mag., vol. 21, no. 6, Jun. 2006, pp. 5-14.
- [5] D. Boroyevich, I. Cvetkovic, D. Dong, R. Burgos, F. Wang, F. C. Lee, "Future electronic power distribution system—a contemplative view", OPTIM' 2010, pp. 1369 – 1380.
- [6] Direct Current Distribution Systems for Residential Areas Powered by Distributed Generation By Faizan Dastgeer
- [7] Performance analysis of power distribution systems with weakly grid connected rural homes in India
R.K. Chauhan a ,*, K. Chauhan b, *Energy and buildings* 307-316, May, 2018.
- [8] K. Garbesi, V. Vossos, and H. Shen, "Catalog of DC appliances and power systems," October 2011.
- [9] Shamsi, P.; Fahimi, B., "Stability Assessment of a DC Distribution Network in a Hybrid Micro-Grid Application," *IEEE Trans. on Smart Grid* , vol.5, no.5, pp.2527,2534, Sept. 2014
- [10] R.J.C. Pinto, S.J.P.S. Mariano, M.D.R.A. Calado, Power quality experimental analysis on rural home grid-connected PV Systems, *Int. J. Photenergy* 2015 (June) (2015) 1–8. <http://dx.doi.org/10.1155/2015/791680> .
- [11] Dong, D.; Cvetkovic, I.; Boroyevich, D.; Zhang, W.; Wang, R.; Mattavelli, P., "Grid-Interface Bidirectional Converter for Residential DC Distribution Systems—Part One: High-Density Two-Stage Topology," *IEEE Trans. on Power Electron.*, vol.28, no.4, pp.1655,1666, April 2013
- [12] B. Morton, I. M. Y. Mareels, "The prospects for dc power distribution in buildings", AUPEC'99.
- [13] H. Pang; E. Lo, B. Pong, "Dc electrical distribution systems in buildings", ICPEA '06, pp. 115-119.
- [14] K. Engelen, J. Dridsen, et al., "Small-scale residential dc distribution systems", 3rd IEEE Benelux Young Researchers Symposium in Electrical Power Engineering, Ghent (2006-4), pp. 1-7.
- [15] F. Dastgeer, A. Kalam, "Evolution of dc distributed power system stability", *International Review of Electrical Engineering*, part B, vol. 5, pp.652-662, April, 2010
- [16] F. Dastgeer, A. Kalam, "Efficiency comparison of DC and AC distribution systems for distributed generation", *Australasian Universities Power Engineering Conference*, pp. 1-5, 2009.

Multiple stage DC-DC Boost Converter for DC Microgrid Applications

M. Marimuthu¹, S. Pavithra Shri², K. Subalakshmi³,
S. Swetha⁴, S. Tharanya⁵

¹ AP/Department of Electrical and Electronics Engineering, Saranathan College of Engineering, Trichy-12

^{2,3,4,5} Department of Electrical and Electronics Engineering, Saranathan College of Engineering, Trichy-12

Abstract— In this paper, a multi-level boost converter is proposed for dc microgrid applications. Considering environmental effects and shortage of fossil fuel, the trend has developed towards the use of more and more renewable energy. For dc grid applications, the output voltage obtained from the renewable sources like photovoltaic arrays is stepped up through the multilevel boost converter. The proposed converter uses basic boost converter combined with diode-capacitor voltage multiplier to get multi level output. MATLAB/SIMULINK is used to demonstrate the performance of the converter.

Keywords— boost converter; multi output; battery; DC loads; photovoltaic; efficiency

I. INTRODUCTION

RENEWABLE energy is fetching more significant and prevalent in distribution systems, which give diverse choices for consumers whether they get power from the main AC grid or in forming a micro source. Mainly to compensate the shortage of fossil fuel and to provide a pollution free environment, renewable sources like fuel cells, PV modules, bio fuels etc., are used. Solar energy is abundantly available and it can be one of the applications of DC microgrid.

A microgrid typically includes various micro sources and loads, which operate when they are either grid-connected or islanded.

The micro source can either be DC or AC. DC micro grid is opting for various renewable energy applications such as PV modules. Considering transmission and distribution losses, the DC Micro grid bus provides low losses comparing to AC grid.

The performance of DC Micro grid system is mainly dependent on the quality of various units combined in a Micro grid system such as Micro sources, power electronic converters and interfaces.

With the growing of distributed generation based on PV systems, and the advent of new sources of distributed generation DC based such as fuel cells, DC-DC converters with high-voltage boost ratios are desirable to use those renewable sources in order to feed multilevel inverters and push the power into the utility for some hundreds of volts.

The main advantage of DC Micro grid is that sources, various loads, and energy storage can be connected through efficient power electronic interfaces.

The increase in demand for step up power conversion requires an optimal boost converter to step up the voltage considerably for various applications.

The Conventional boost converters like interleaved boost converter and cascaded boost converter were used to get the desired high voltage, but it results in low efficiency because of the current ripple and its cost is also high.

The usage of transformers in isolated topologies causes switching losses. Therefore transformer less converter will be an appropriate one for grid connection for better efficiency.

Coupled inductors and switched capacitors can be used to get high voltage gain but it involves complex magnetic elements, for that reason it is not extensively used.

In this paper, a DC-DC multi-level boost converter consists of an usual boost converter combined with voltage multiplier stages.

The topology contains a switch, an inductor, $2N-1$ diodes and $2N-1$ capacitors to get output which is N times the conventional boost converter. The number of levels can be increased by adding two capacitors and two diodes per extra level.

It is proposed to be used as DC link in applications where several controlled voltage levels are wanted with self balancing and unidirectional current flow, such as PV or fuel cell generation systems with multilevel inverters. The major advantages of this topology are:

- (i) continuous input current and
- (ii) a large conversion ratio with low duty cycle and without a transformer.

It can be built in a modular way and more levels can be added without changing the main circuit it provides several self-balanced voltage levels and only one switch is necessary. The converter's principle is proven by simulation and experimental results. The complete principle and operation along with the design, calculation, simulation results and hardware results are presented in the below sections.

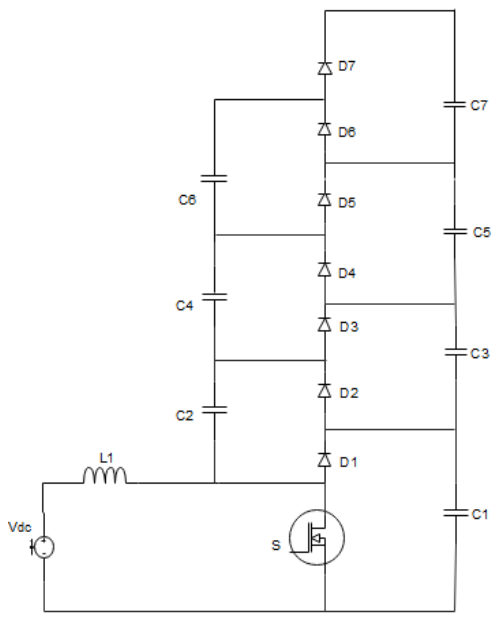
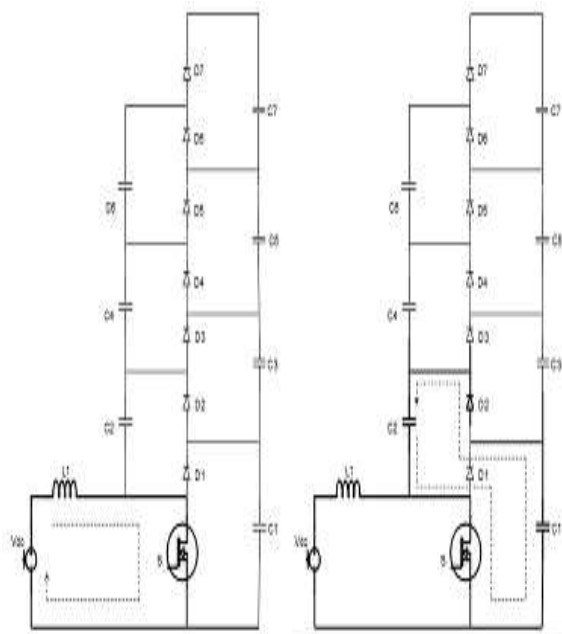


Fig. 1 power circuit diagram

II.DC-DC MULTI-LEVEL BOOST CONVERTER

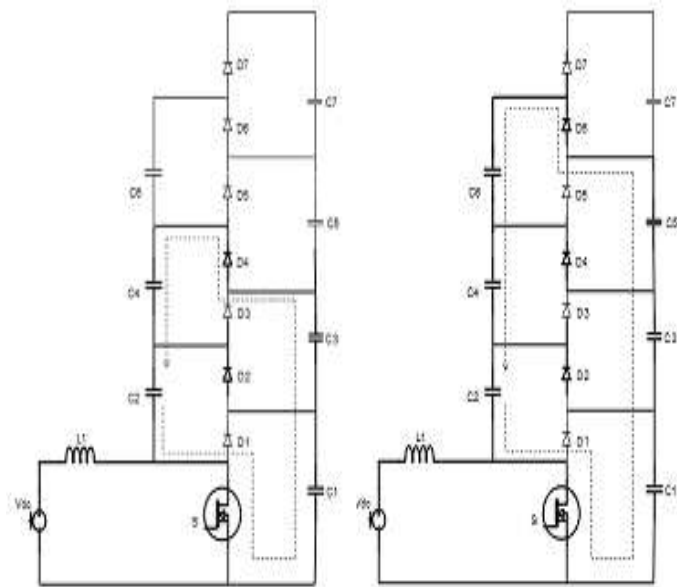
During the switch-on state, the inductor is connected to V_{in} voltage. If C_2 's voltage is smaller than C_1 's voltage then C_1 clamps C_2 's voltage through D_2 and the switch. Simultaneously, if the voltage across $C_2 + C_4$ is smaller than the voltage across $C_1 + C_3$, then C_1 and C_3 clamp the voltage across C_2 and C_4 through D_4 and in a similar way C_3 , C_5 and C_7 clamp the voltage across C_2 , C_4 and C_6 .

When switch is in on state



a

b



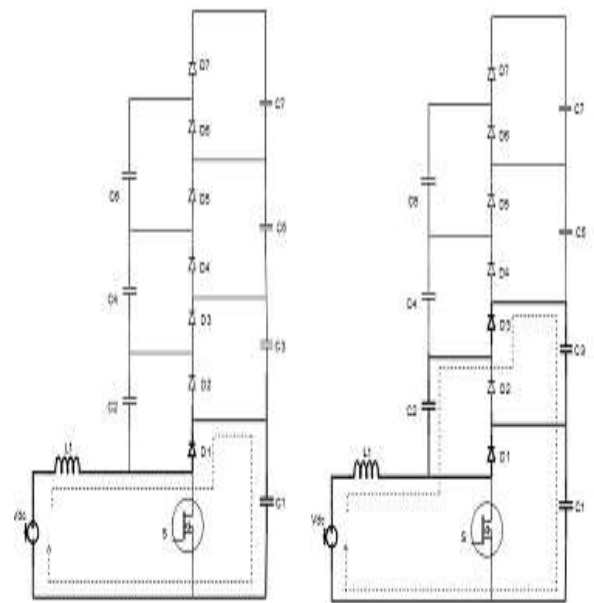
c

d

Fig. 2 Mode 1.power circuit in ON state

During the switch off state, the inductor current closes D_1 charging C_1 . When D_1 closes, C_2 and the voltage in V_{in} plus the inductor's voltage clamp the voltage across C_1 and C_3 through D_3 . Similarly, the voltage across the inductor plus V_{in} , C_2 and C_4 clamp the voltage across C_1 , C_3 and C_5 through D_5 . Finally the voltage across C_1 , C_3 , C_5 and C_7 is clamp by C_2 , C_4 , C_6 , V_{in} and the inductor voltage.

When switch is in off state



a

b

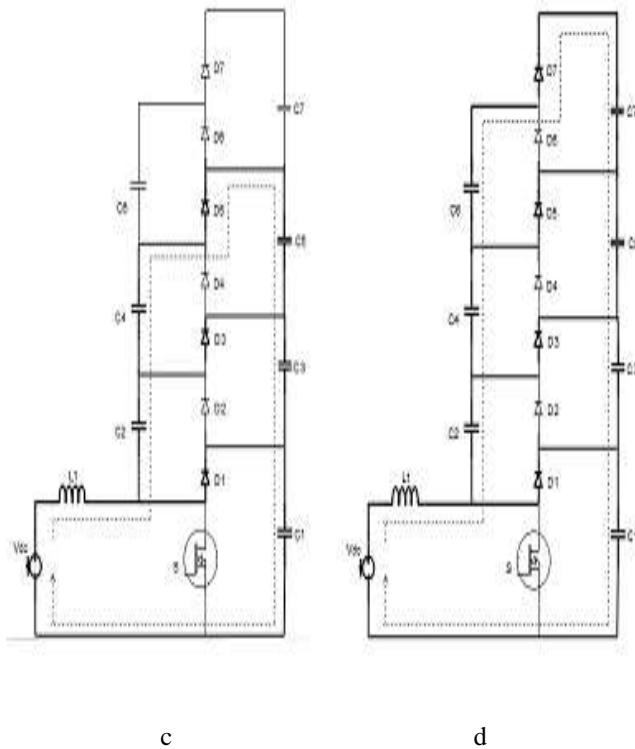


Fig. 3 Mode 2.power circuit in OFF state

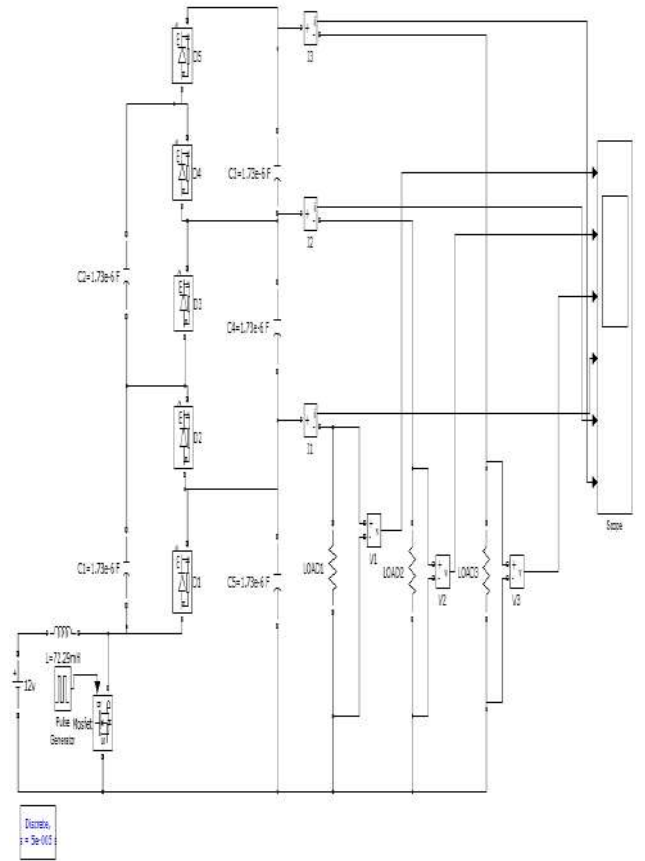


Fig. 4 MATLAB Simulation

III.DESIGN DETAILS

In this converter, the design of elements conventional boost converter.

The voltage gain, for an N-level multilevel boost converter

$$M = \frac{N}{1 - D}$$

The design specifications are input voltage $V_{dc}=12v$, Output voltage $V_o=24v$, output power=2W, switching frequency=10KHz, the number of levels used here is 4.

The value of inductance,

$$L = \frac{V_{in} * (V_{out} - V_{in})}{\Delta I * f_s * V_{out}}$$

The value of capacitance,

$$C = \frac{I_{out(max)} * D}{f_s * \Delta V_{out}}$$

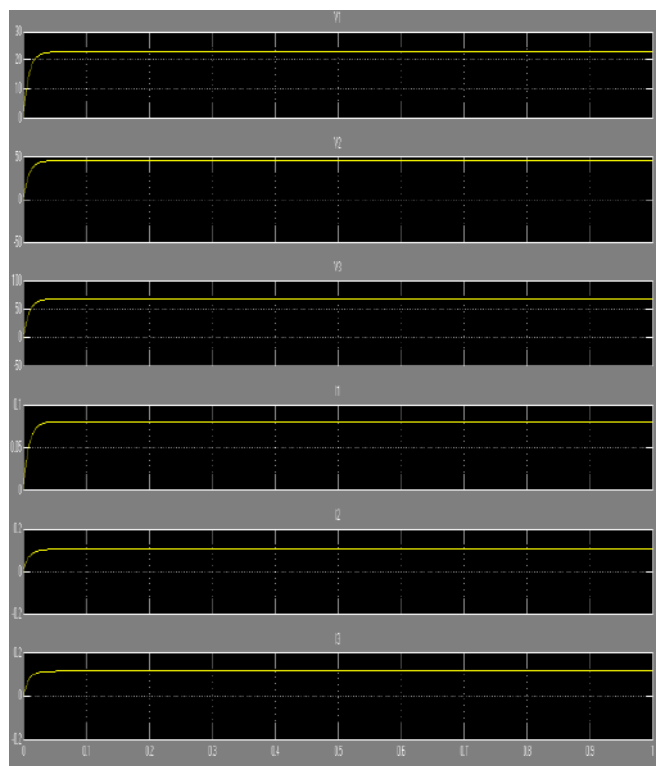


Fig. 5 Simulation Result for Multiple Output

IV. CONCLUSIONS

This paper proposes a DC–DC converter topology. The DC–DC MBC is based on only one driven switch, one inductor, $2N - 1$ diodes and $2N-1$ capacitors for an MBC. It is proposed to be used as DC link in applications where several controlled voltage levels are needed with self balancing and unidirectional current flow, such as PV or fuel cell generation systems with multilevel inverters.

V. REFERENCES

- [1] Prajof P and Vivek Agarwal, Novel boost-SEPIC type interleaved DC-DC converter for low-voltage bipolar DC microgrid-tied solar PV applications., IEEE-2015.
- [2] Niloofar Ghanbari, M.Mobarrez and S.Bhattacharya, Modeling and stability analysis of a DC microgrid employing distributed control algorithm., IEEE-2018.
- [3] Amjad Ali, Yunjie Gu, Chi Xu Wuhua Li, Xiangning He, Comparing the performance of different control techniques for DC-DC boost converter with variable solar PV generation in DC microgrid., IEEE-2014.
- [4] Johannes Hofer, Bratislav Svetozarevic, Arno Schlueter, Hybrid AC/DC building microgrid for solar PV and battery storage integration., IEEE-2017.
- [5] Mateja Car, Mario Vasak, Vinko Lesic, Control of a buck boost DC-DC power converter for microgrid energy storage., IEEE-2017.
- [6] Fengyan Zhang, Chao Meng, Yun Yang, Ying Che, Wen Wei, Advantages and challenges of DC microgrid for commercial building., IEEE-2015.
- [7] Girish Ganesan R, M. Prabhakar, Multi-level DC-DC converter for high gain applications., International Journal of Power Electronics and Drive System(IJPEDS)-2013.

HIGH FREQUENCY DIRECTION FINDING MILITARY ELECTRONIC VEST

Ramanathan.AL¹, R.Sridhar², Prithivirajan.E³, Poovarasan.R⁴, Naveenkumar⁵,
^{1,3,4,5}Student, ²Assistant Professor, EEE, Saranathan college of Engineering
¹alagappanramu12@gmail.com, ³prithivi.cud@gmail.com

ABSTRACT

The scope of this paper is on the development of electronics that can be inserted into military clothing for protection cum rescuing using GPS module. The manufacturing survey was conducted to determine the best performing and most durable materials, to withstand the rigors of textile manufacturing and potential military use. In our proposal, the physical status of a soldier in the battle field is sensed by sensors and it will be messaged to the nearest base station automatically. By this technique, one can monitor the status of a soldier in the battlefield, and can send the rescue team when needed and the soldiers life can be saved at the earliest.

Introduction

During sudden border attacks, large number of soldiers lose their life due to absence of fast rescuing and lack of monitoring soldiers health state in the war zone. By our proposal, one can measure the necessary physiological parameters of the soldiers and can alert the base camp during abnormal condition and can send extra forces or rescue team to the war zone and can save the life of many soldiers.

It enhances the mobility and survivability of soldiers in the war zone. The integration of sensors and other electronic devices in the vest can improve the functionality of soldiers. The proposal functionalities includes soldiers body condition (heart beat rate, body temperature) monitoring, detecting chemical threats, bullet striking. It also provides combat identity. If a soldier is in abnormal state one can rescue him sooner or when a soldier is dead, his corpse can be found easily. By using the air quality sensor in the vest we can also alert the soldiers to take precautions, thus preventing them in losing their life in chemical bombs. The main idea

of the proposal is to provide fast communication using ESP module where the officials can monitor individual soldiers in the base station itself and provide necessary help for the soldiers.

Operation

The abnormal condition of a soldier is sensed by the various sensors like heart beat sensor, temperature sensor, vibration sensor, air quality sensor. When heart beat exceeds the normal rate the analog signal from the sensor is send to the Arduino board. The temperature sensor measures the body temperature, vibration sensor detects heavy vibration and air quality sensor measures toxicity of air in the surrounding environments and give the corresponding analog signal to the micro controller. The microcontroller produce corresponding digital signal to the LCD display and ESP module. The data are collected in a server through cloud computing process using ESP8266. The data are viewed through the webserver.

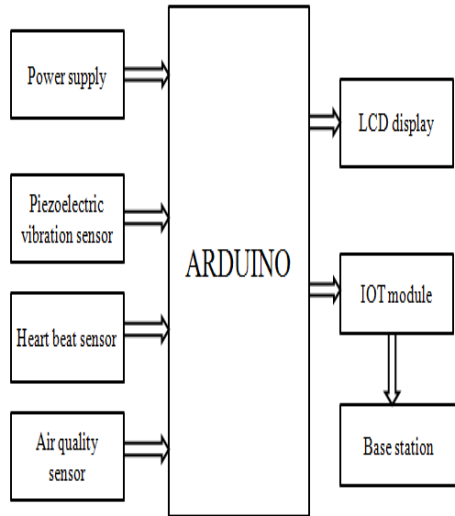


Fig.1. Block diagram of proposed System

Piezoelectric vibration sensor

Many Applications can be created by measuring vibration level, but sensing vibration accurately is a difficult job. This proposal describes about vibration sensor SW-420 and Arduino interface which provides easiest design for vibration measurement. The vibration sensor⁽⁷⁾ SW-420 comes with breakout board that includes comparator LM 393 and adjustable on board potentiometer for sensitivity threshold selection, and signal indication LED.



Fig.2. SW-420-Vibration Sensor

This sensor module produce logic states depends on vibration and external force applied on it. When there is no vibration this module gives logic LOW output. When it feels vibration then output of this module goes to logic HIGH. The working bias of this circuit is

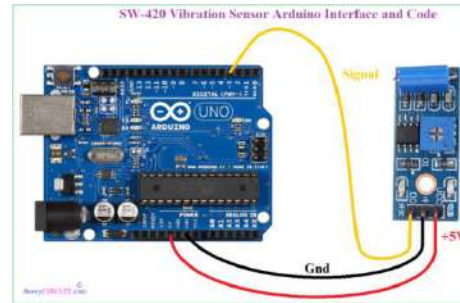


Fig 3. Interfacing vibration sensor with Arduino

Interfacing vibration sensor with Arduino

Connect Vcc pin of sensor board to 5V pin of Arduino board, connect Ground pin to Ground pin of Arduino, Connect DO output signal pin of sensor board to Arduino digital pin D3. Do some calibration and adjust the sensitivity threshold, then upload the following sketch to Arduino board. The vibration of the bullet striking in the military e-vest can be found out by using vibration sensor. The threshold value of the sensor can be varied by using the potentiometer for only detecting hard vibration.

Heart beat sensor

When the finger tissue or the earlobe tissue is illuminated using a light source, the light is transmitted after getting modulated a part getting absorbed by the blood and the rest being transmitted. This modulated light is received by the light detector^[5].

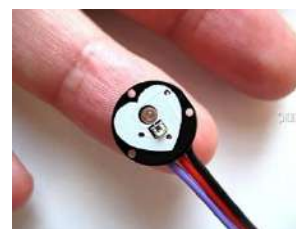


Fig 4. Heart Beat Sensor

Here a Light Dependant Resistor (LDR) is used as a light detector. It works on the principle that when light falls on the resistor, its resistance changes. As the light intensity

increases, the resistance decreases. Thus the voltage drop across the resistor decreases. Here a comparator is used which compares the output voltage from the LDR to that of the threshold voltage. The threshold voltage is the voltage drop across the LDR when the light with fixed intensity, from the light source falls directly on it. The inverting terminal of the comparator LM358 is connected to the potential divider arrangement which is set to the threshold voltage and the non inverting terminal is connected to the LDR. When a human tissue is illuminated using the light source, the intensity of the light reduces. As this reduced light intensity falls on the LDR, the resistance increases and as a result the voltage drop increases. When the voltage drop across the LDR or the non inverting input exceeds that of the inverting input, a logic high signal is developed at the output of the comparator and in case voltage drop being lesser a logic low output is developed. Thus the output is a series of pulses. These pulses can be fed to the Microcontroller which accordingly processes the information to get the heart beat rate and this is displayed on the Display interfaced to the microcontroller.

Temperature Sensor

Usually, a temperature sensor^[8] is a thermocouple or a resistance temperature detector (RTD) that gathers the temperature from a specific source and alters the collected information into understandable type for an apparatus or an observer. Temperature sensors are used in several applications namely HV system and AC system environmental controls, medical devices, food processing units, chemical handling, controlling systems, automotive under the hood monitoring. Then $(-55^{\circ}\text{C} \leq T_J \leq 150^{\circ}\text{C})$ is the operating range of lm35. The most frequent type of temperature

sensor is a thermometer, used to determine the temperature of solids, liquids, and gases. It is also mostly used for non-scientific purposes as it is not so accurate. The different kinds of sensors are categorized by the sensing capacity of the sensor as well as the range of applications.

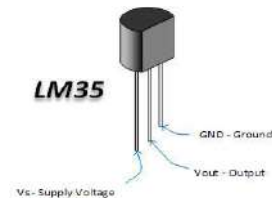


Fig 5. Temperature sensor

Air quality sensor

Air pollution sensors^[5] are devices that detect and monitor the presence of air pollution in the surrounding area. They can be used for both indoor and outdoor environments. These sensors can be built at home, or bought from certain manufactures. Although there are various types of air pollution sensors, and some are specialized in certain aspects, the majority focuses on five components: ozone, particulate matter, carbon monoxide, sulfur dioxide, and nitrous oxide. The sensors were very expensive in the past, but with technological advancements these sensors are becoming more affordable and more widespread throughout the population.



Fig 6. Air Quality Sensor^[5] (MQ135)

The MQ series of gas sensors utilizes a small heater inside with an electro chemical sensor these sensors are sensitive to a range of gasses are used at room temperature.

MQ135 alcohol sensor is a SnO₂ with a lower conductivity of clean air. When the explosive gas exists, then the sensor's conductivity increases more as per the concentration of gas level. By using simple electronic circuits, it convert the change of conductivity to correspond output signal of gas concentration. The MQ135 gas sensor has high sensitivity in ammonia, sulfide, steam, smoke and in other harm full gas. It is low cost and suitable for different applications.

It also suits for detecting venomous gases that are present in the air in homes and offices. The layers of the sensor unit is made up of tin dioxide SnO₂, which has lower conductivity compare to clean air and due to air pollution its conductivity gets increases. It also detects ammonia, nitrogen oxide, smoke, CO₂ and other harmful gases. The air quality sensor has a small potentiometer that permits the adjustment of the load resistance of the sensor circuit. The 5V power supply is used for air quality sensor.

MQ – 135 Air quality sensor

The air quality sensor⁽⁵⁾ is a signal output indicator instruction. It has two outputs: analog output and TTL output. The TTL output is low signal light which can be accessed through the IO ports on the Microcontroller. The analog output is an concentration, i.e. increasing voltage is directly proportional to increasing concentration. This sensor has a long life and reliable stability as well.

Some of the application includes

- Air quality monitor
- Detection of harmful gases
- Domestic air pollution detection
- Industrial pollution detection

ESP Module

The ESP8266 WiFi Module is a self contained SOC with integrated TCP/IP protocol stack that can give any microcontroller access to WiFi network. The ESP8266 is capable of either hosting an application or offloading all Wi-Fi networking functions from another application processor. Each ESP8266 module comes pre-programmed with an AT command set firmware, meaning, you can simply hook this up to your Arduino device and get about as much WiFi-ability as a WiFi Shield offers. The ESP8266 module is an extremely cost effective board with a huge, and ever growing, community.

This module has a powerful enough on-board processing and storage capability that allows it to be integrated with the sensors and other application specific devices through its GPIOs with minimal development up-front and minimal loading during runtime. Its high degree of on-chip integration allows for minimal external circuitry, including the front-end module, is designed to occupy minimal PCB area. The ESP8266 supports APSD for VoIP applications and Bluetooth co-existence interfaces, it contains a self-calibrated RF allowing it to work under all operating conditions, and requires no external RF parts.

There is an almost limitless fountain of information available for the ESP8266, all of which has been provided by amazing community support. The ESP8266 Module is not capable of 5-3V logic shifting and will require an external Logic Level Converter. Please do not power it directly from your 5V dev board.

Air quality detection

The air quality sensor MQ135 which is available in the library is used as a simulation for air quality sensor.

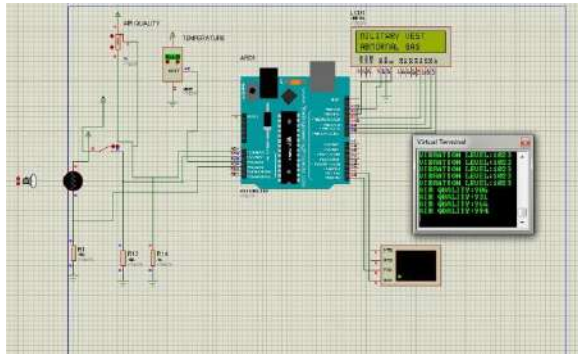


Fig 10. Simulation result of Air Measurement

Conclusion

This proposal provides fast rescuing of soldiers in the war zone by monitoring their physical health condition to the base station through fast communication network using EPS module. Temperature sensor LM35, Vibration sensor, Air quality sensor MQ135 are used to ensure the fast rescuing of the soldiers.

Reference

- [1] Sahin.O, Kayacan.O and YazganBulgun.O (2015) ‘Smart Textiles for Soldier of the Future’- Defence Science Journal, Vol. 55, pp. 195-205.
- [2] SaddamhusenJamadar ‘Applications of Smart and Interactive Textiles. Textile learner’
- [3] Winterhalter C and Teverovsky J. (2004) ‘Development of electronic textiles for U.S.military protective clothing systems’
- [4] R.Nayak, L.Wang andR.Padhye ‘Electronic textiles for military personnel’ School of fashion and textiles, RMIT University, Australia.

- [5] Windmiller.J.R, Wang.J (2013) ‘Wearable Electrochemical sensor and Biosensors. A Review’.
- [6] MatteoStoppa and Alessandro Chiolerio (2014) ‘Wearable Electronics and Smart Textiles’ – Journal of Sensors, pp.58
- [7] Unsal.M, Niezrecki.C and Crane.C ‘Two semi active approaches for Vibration Isolation’ University of Florida, pp. 1-6.
- [8] Tilak Dias (2015) ‘Electronic Textiles’ first edition, Smart fabrics and wearable technology, Vol.2, pp.73-131.
- [9] Dr.MerihSarışik (2016) ‘International Journal of Clothing Science and Technology’, Vol. 28, pp. 108-128.
- [10] Abraham Carrillo, Luis Molina and IsaiOnofre (2014) ‘Homebrew Piezoelectric Crystal’, pp. 1-19.

A Broad Survey on Air Pollution Monitoring and Traffic Management System

Muthu Karuppan N¹, Leo Aldrinraj A S², Madhanraj S³, Manoranjan G⁴,
Ms Gayathri N⁵

U.G. Student, Department Of Electrical and Electronics Engineering, Saranathan College of Engineering, Trichy, India^{1,2,3,4}

Assistant Professor, Department Of Electrical and Electronics Engineering, Saranathan College of Engineering, Nagpur, India⁵

Abstract: Air pollution monitoring is one of the most important issues in day to day life. Air pollution monitoring start from conventional way to the most sophisticated computer has been used to monitor the air quality, however the fresh air is necessary for all human being, for that various advanced technology has been used and some of this technology is really useful in order to provide a real time air quality data. Aim of this paper is to highlight some technology which is used for air pollution monitoring in traffic congestion and how effective of these technologies are for creating awareness to the public and securing their lives.

Keywords: Air quality, pollution, Real-Time Monitoring, Traffic Management, Smart City.

I. INTRODUCTION

Environmental monitoring is a systematic approach for observing, studying and analyzing the conditions of the environment. For the healthy human being require to breathe in clean air but due to increasing the transportation system fresh air gets polluted. Transport system makes a huge impact on the environment in which we live. Increase in the vehicle gives rise to increasing traffic-related pollutant emission. Therefore, to track the effect of this pollution on the environment and health of individual it is necessary to track the level of pollution in urban and suburban areas. Many health-related issues are arising from air pollution due to traffic. The major source of air pollution is road traffic emission which emits various gases such as CO(Carbon Monoxide), NOx(Nitrogen Oxides), SOx(Sulphur Oxides). Therefore, air quality monitoring in traffic congested areas is needed in order to provide useful information about pollution and can take appropriate measures to mitigate the negative impact whenever it is necessary. The purpose of monitoring the air quality is to collect the data and also to provide the information which is required by the scientist, planners, policymakers to make a decision on improving and managing the environment [1]. The main mission of the air quality monitoring network is to record the concentration of pollution and other parameter related to

the pollution and deliver this information or data to the public through government to warn against any danger.

II. NEED FOR MONITORING

Clean air is a vital need for every organism. Contaminated air causes many health problems such as respiratory diseases, lung cancer, stress, blood pressure, etc. Therefore to make any step ahead of controlling the pollution rate it is necessary to monitor the air quality which may help us to reduce the air pollution and to maintain the quality of air. There are various causes of increasing pollution such as gases emitted by the vehicle, chemical discharge from industries, radioactive substance etc. these are the main reasons for polluting the air. The main gases which directly affect the human health are carbon monoxide (CO), hydrogen sulfide, sulfur oxides (SOX), Nitrogen oxides (NOX) and the main contribution of these gases are traffic-related pollutant emission. Tremendous efforts are required to improve the quality of air in both outdoor and indoor environment. Monitoring of the environment has been controlled from the manual to the automatic control in the past decade. There is various improvement in the instrument of environment monitoring but still cannot meet the polluted environment [2].

III. POLLUTANTS FROM TRAFFIC

Combustion of fuels such as natural gas, gasoline, petrol, diesel fuel, fuel oil, or coal is emitted from the exhausts of the vehicles. According to the type of vehicle, it is discharged into the atmosphere through an exhaust pipe. Motor vehicle emissions are a major ingredient which contributes to air pollution.

Some of the pollutants emitted from traffic:

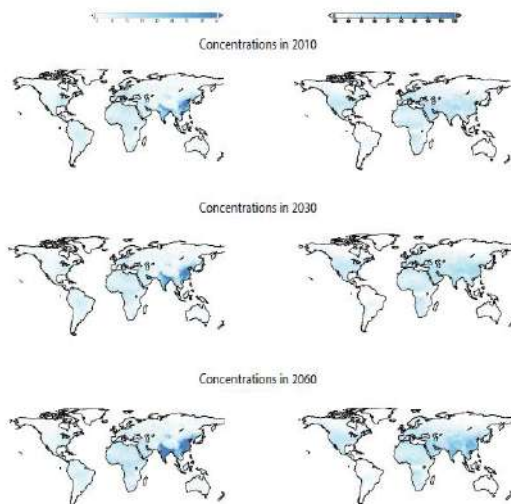
1) **Carbon monoxide (CO)** – Carbon monoxide is the most common type of fatal air pollutant in many countries. CO is colorless, odorless and tasteless, but highly toxic. The largest anthropogenic source of CO is from vehicle emissions. WHO states that breathing more than 35ppm leads to health issues. Breathing the high

concentration of CO typical of the polluted environment leads to reduced oxygen. It combines with hemoglobin to produce carboxyhemoglobin, which is ineffective for delivering oxygen to bodily tissues which cause health effects that include headache, lung cancer, and heart diseases

2) **Ozone (O3)** – Ozone is beneficial in the upper atmosphere but at ground level ozone irritated the respiratory system, causing coughing, choking, and reduced lung capacity. It also has many negative effects throughout the ecosystem.

3) **Particulate Matter (PM10 and PM2.5)** – Inhaling airborne particulate matter mostly affects the health of humans and animals which causes asthma, lung cancer, cardiovascular issues, premature death. Because of the size of the particles, they can penetrate the deepest part of the lungs and damage the respiratory system.

Figure 1: Particulate matter and ozone concentrations - Projected annual average anthropogenic PM2.5 on left panels ($\mu\text{g}/\text{m}^3$) and maximal 6-month mean of daily maximal hourly ozone on right panels (ppb).



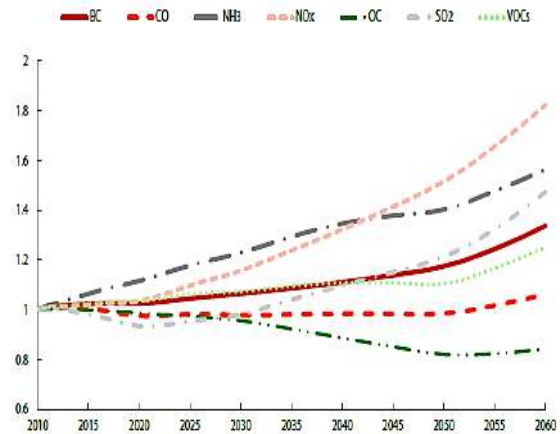
Source: TM5-FASST model, based on projections of emissions from the ENV-Linkages model.

4) **Nitrogen Oxides (NOx)** – Nitrogen oxides NO and NO₂ (NOx) can penetrate deeply into sensitive lung tissue and damage it, causing premature death in extreme cases. Inhalation of NO species increases the risk of lung cancer and colorectal cancer and inhalation of such particles may cause or worsen respiratory diseases. In urban outdoor air, the presence of NOx mainly due to traffic.

5) **Volatile Organic Compounds (VOC)** – When oxides of nitrogen (NOx) and VOC reacts in the presence of sunlight, ground-level ozone is formed, a

primary ingredient in smog.

Figure 2: Emission projections over time Index with respect to 2010

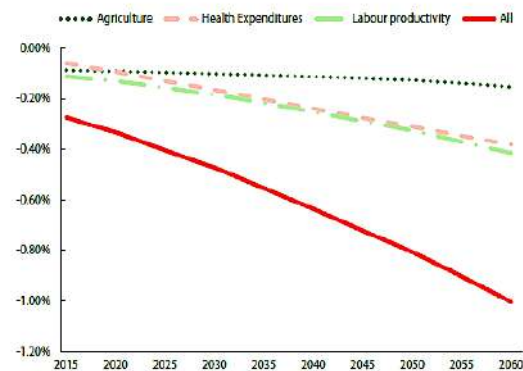


Source: ENV-Linkages model, based on projections of emission factors from the GAINS model.

IV. Impacts on Global Market

The three different market impacts of air pollution are: reduced labor productivity; increased health expenditures; and crop yield losses. They all contribute to a projection of GDP that is below the projection that excludes the pollution feedbacks on the economy (Figure 3). At the global level, the consequences of labor productivity and health expenditure impacts continue to increase significantly relative to GDP. In contrast, agricultural impacts are relatively stable over time in the percentage of GDP, i.e. in absolute terms, these impacts grow at the same speed as GDP. The total annual market costs of outdoor air pollution are projected to rise from 0.3% in 2015 to 1.0% by 2060.

Figure 3: Attribution of macroeconomic consequences to selected climate change impacts, Central projection Percentage change, central projection w.r.t. no-feedback projection.



Source: ENV-Linkages model.

V. COMPARING WITH OTHER METHODS

A. *Technique used for pollution monitoring*

Earlier the air pollution monitoring is done via computerized tomography technique which generates a two-dimensional map of pollutant concentration. It provides many advantages over the differential absorption method. In this system, there is a single laser source located at the center of the area. This laser beam is rotated and directed towards the circumference of the circle. There is a cylindrical mirror so that the incident laser beam is reflected in a fan beam over angle across the circle. The beam from the mirrors is the circular region and strikes a set of detectors lie in the same plane which is parallel to the ground. This technique focuses on lower transmitted laser energy increasing the range and ability to monitor the area that contains several pollutant sources [3].

Another way of monitoring the air pollution is via the online GPRS sensors array which has been designed, implemented and tested. This system unit that consists at a single chip of microcontroller and a pollution server which is a high-end personal application server with internet connectivity where the mobile data acquisition unit that collects the pollution level & packs it into a frame with GPS location, date and time. This frame is uploaded to the GPRS modem and transmitted to the pollution server via the public mobile network. A database server which is attached to the pollution level which is used by the various client. Pollution server for storing the pollution level which is used by the various clients. Pollution server having an interfaced with the Google map to provide a real-time pollutants level as well as the location in a large metropolitan area [4].

B. *Real time Monitoring*

A distributed infrastructure consists of a wireless sensor network and grid computing technology for air pollution monitoring [5]. Wireless sensor network is the great achievement in this field.

An effective solution for the pollution monitoring using a wireless sensor network to provide a real time pollution data. The various gases like CO₂, NO₂ are calibrated by using and these pre-calibrated sensors are integrated with the wireless sensor using a multi hop data aggregation algorithm. A light weight middleware and web interface in order to view the one pollution data in the form of charts and number and also available on the internet. The other parameters like temperature and humidity are also sensed along with the gas concentrations which enable the data analysis through the data fusion techniques this system provide accurate pollutant data [6].

The air quality monitoring system combines with the virtual instrument technology & frequency hopping communication technology to achieve the wireless data transmission. By using a spectrum hole detection specimens that adjust a carrier frequency according to the result & made a full use of available radio spectrum with this specimen there is no signal interference during

the wireless transmission process & the system can receive the real time information effectively and the gas concentration can show clearly and easy to read by the non-professional staff also [7]

The air quality monitoring station are used to monitor the quality of air but most of this method are expensive and provide a low resolution sensing data and these stations are less densely deployed therefore the system consist of sensor mode gateway and back end platform controlled by the lab view program through which the data can be stored in the database the system deployed to the main road in the city to monitor the carbon monoxide concentration caused by the vehicle emission the advantages of these wireless sensor network is that it is easy to set up, inexpensive and also provide a real time data [8].

The system in which several monitoring station communicate wirelessly with the backend server using machine to machine communication & each station equipped with the metro logical sensor and gaseous sensor for data logging and wireless communication capabilities. The backend server collects the real time data from station and converts it in to the information which is used by the user through the web portals and mobile application [9].

The small scale of wireless sensor station to communicate with the backend server and provide their real time data however the collected data are process and analyse in order to provide these data in different format to the end user [10].

C. *Centralized monitoring*

Different sensors are deploying to the different region and each sensor must send their collected information to the server so that the end user can easily see the pollution information in the different area. Centralize monitoring ensure the quality, improve the ability and integrity of data. Collected data are uploaded to the cloud dataset so that it can be analyzed or viewed for future use. All these uploaded data are managed in the database management system over the centralized database with this available information the user can search the record as per their requirement.

D. *Pollution level monitor over the Google map*

The main objective of monitoring is to display the collected information in user friendly format. The mobile application and websites are developing in order to display the real-time data that contains previous history and recent measurement of pollution level. Only the authorized user can access the website which is easily available to the public when the permission is granted. Website allows displaying the different level of pollution in different area over the Google map with the help of internet connectivity, it is possible to display the different level of pollution at a different area on the Google map [11].

E. Types of sensor

There are different types of sensors are available for collecting the atmospherically data. Such as Temperature sensor, Humidity sensor, Rain sensor, Gas Sensor etc...different types of gas sensors are available to collect the different gases from the road traffic emission such as CO₂ sensor, NO₂ sensor, SO₂ sensor etc. Wireless sensor network built a node where each node is connected to one sensor. With the additional sensors may help to enhance the network and monitoring the additional pollutants. With the help of sensors, it may possible to collect the environment-related information. It is deployed in several cities to monitor the concentration of dangerous gases for the citizens. Air quality measurement can process and presented in real time to the end user in a friendly format to spread environmental awareness among the population and allow taking appropriate precaution when it is needed.

VI. CONCLUSION

To monitor air pollution with the wireless sensor network has several benefits over the traditional environment. Wireless sensor network has its own advantage such as low cost, easy to set up and provide real-time pollutant data. Monitoring stations which are used to analyze and collect the real-time pollutant data from the road traffic emission. To monitor the pollution level from a different area of glance is a difficult task and it requires a large infrastructure setup and proper management but if the system can segment the pollution level as per the area so it can be better monitored and a better solution can be provided. In the future, the system can also implement the web-based monitoring of air pollution level and Google map which is used for a live map view of pollution level. An accurate reading of pollution level is important in order to provide guidance for the people who suffer from the asthmatic problem with this information they may help to choose the alternate healthy route.

REFERENCE

- [1] Abdullah kadri, Elias Yaacoub Mohammed Mushthaha And Adnan Abu-Dayya "Wireless Sensor Network For Real-Time Air Pollution Monitoring"IEEE Forum On Strategic Technology-2013.
- [2] Haibao Wang, Tingting Wu, And Guangjie Wu "Air Quality Monitoring System Based On Frequency Hopping System" 2010 IEEE.
- [3] Robert L.Byer Lawrence, A Shepp, "Two-Dimensional Remote Air-Pollution Monitoring Viatomography".Vol.4/March 1979/OPTICS LETTERS.
- [4] Yajie Ma,Mark Richards,Moustafa Ghanem YikeGuo,And John Hassard "Air Pollution Monitoring And Mining Based On Sensor Grid in London"Sensor 2008.
- [5] Al-Ali,A.R;Zualkernan,I;Aloul,F., "A Mobile GPRS

Sensors Array For Air Pollution Monitoring" Sensors Journal,IEEE,Vol.10,No.10,pp.1666,1671,Oct.2010.

[6] Raja Vara Prasad Y1, Mizra Sami Baig2,Rahul K. Mishra3,P.Rajalakshmi4,U.B.Desai5 And S.N. Merchant6, "Real Time Wireless Air Pollution Monitoring System" Ictact Journal on Communication Technology: Special Issue On Next Generation Wireless Networks and Applications, June 2011, Volume – 2, Issue –

[7] Haibao Wang, Tingting Wu, And Guangjie Wu "Air Quality Monitoring System Based On Frequency Hopping System" International Conference On Intelligent Control And Information Processing August 2010.

[8] Jen-Hao Lru, Yu-Fan Chen, Tzu-Shiang Lin, And Da-Wei Lai, Tzai-Hung Wen, Chih-Hong Sun, And Jehn-Yih Juang, Joe-Air Jiang developed Urban Air Quality Monitoring System Based On Wireless Sensor Networks 2011 IEEE.

[9] Srinivas Devarakonda, Parveen Sevusu, Hongz Hang Liu, Ruilin Liu, Liviu Iftode, Badri Nath "Real-Time Air Quality Monitoring Through Mobile Sensing In Metropolitan Areas" August 2013.

[10] Fouzi Harrou, Mohamed Nounou, Hazem Nounou, "Detecting Abnormal Ozone Levels Using Pca Based Glr Hypothesis Testing" 2013 IEEE Symposium On Computational Intelligence And Data Mining.

[11] Elias Yaacoub, Abdullah Kadri, Mohammed Mushtaha, And Adnan Abu-Dayya, "Air Quality Monitoring And Analysis In Qatar Using A Wireless Sensor Network Deployment"596-601, 2013 IEEE.

SIGN LANGUAGE CONVERTER

Mr R.Satheesh

Ms R.Ramya Prabha , Ms L.Rekha , Ms S.Sajitha Nilofer , Ms S.Srimathi

Department of Electrical and Electronics

Saranathan College of Engineering

Tiruchirappalli, India

Abstract—According to a survey of WHO, about 15-20% of the total world's population are mute people. The idea proposed in this paper tries to bridge the gap between voiced and unvoiced community. The artificial mouth is an embedded hardware setup comprised of hand glove, flex sensor, microcontroller and a voice module. The data glove attached with the flex sensors and microcontroller detects all the movements of the hand and compares it with the pre-defined data. The desired output from the controller is transferred to the voice module via Bluetooth transceiver and the voice module has TTS technique that provides the relevant voice (speech) output for the input gesture. The sign language is regional and we have opted Indian Sign Language (ISL).

Keywords— Data glove, flex sensor, hand gesture, sign language.

I.INTRODUCTION

The sign language is generally used by deaf and mute people to communicate with normal people. But these languages vary for different regions and are not same to all people. The blind people can speak easily with the normal people but the dumb people can't speak so they using the language known as sign language. Sometime language is also be an non verbal form and it can be mostly used in deaf and dumb communities. Generally deaf and dumb people are more prone to be left unhelped in emergency situations because of their lack of interaction with others.

And most importantly India is a vast lingually diversified country and so a common mode of communication was needed for speech-hearing impaired people. The advantage of blind people over the deaf and dumb community is that they can freely speak any language and communicate with others. But the deaf and mute people cannot do so and they are in need of their own manual-visual language called as Sign language. Every Sign language is unique with its own signs, letters, numbers, grammar, etc. Certain movements of hands, fingers, wrist and elbows are considered as gestures with certain meaning. Hand gestures made by using the Indian Sign Language symbols are an effective way to bridge the communication gap between the voiced and unvoiced community. This in turn will pave a way for them to express their ideas to the world.

Gesture recognition in certain cases includes facial expressions. The posture on the hand is static. Gesture recognition is majorly grouped into a pair of categories namely *vision-based* and *detector-based*. In this the Vision Based technique include advance algorithm for processing which make it complex. On the other hand, the technique of image and video processing is mostly preferred, but it has varied lighting conditions, backgrounds, occlusion, etc are some of its major constrains. This detector based technique having high quality but less accuracy. The preliminary objective of this paper is to introduce a method that efficiently translates every hand posture to text and voice. Here two aspects are being governed as one with only finger position without changing hand position and orientation and the other one is change in both finger and hand position and orientations. The main need arises when these sign language symbols are not understood by normal people, as most of them would not have studied ISL. As in real time image processing methods, only a single individual can be benefited by capturing his or her image and processing it into text or speech. But in this paper, the flex sensors are used to capture the hand gesture movements of any speech impaired people and produced through the voice module as a voice output as the interpreter uses glove-based technique entirely. Different digital signals are formed for the different hand gestures created in the sensors and the controller which is predominantly programmed matches the pre-stored input with the gesture.

Various researches on sign language interpretation system showed that it is possible to convert single gesture into an alphabet and then be concatenated to word, thereby forming a meaningful sentence. As mentioned in paper [1], the sign language conversion for alphabets [A-Z] and numbers [0-9] is done through a mobile computing device. This device provides the technology for automatic translation of ISL system into speech in English language. An intrinsic mobile camera recognizes the hand gestures and is processed using *HSV algorithm*. The language used in a paper [2] is American Sign Language. The accurate results from flex sensor is processed and controlled by Atmega328. Only limited numbers of outputs were generated due to availability of lesser number of ports.

The bend in the flex sensor is converted into character set by implementing an algorithm called *minimum mean square error machine learning algorithm* [3]. The recognized character is sent to Bluetooth, to an Android phone which does text to speech conversion process. In another system [4], images of a defined set of 32 signs each representing the UP&DOWN position of five fingers are loaded dynamically and then it converts the desired text to speech output. In the research paper [5], flex sensors and accelerometer has been used to detect the finger movements. A particular word is formed by concatenating all the letters formed by the combined action of all fingers. It is obvious from the researches that there are equal limitations in this domain.

Among the various works done so far in gesture to voice conversion, some of them were found to rely on image processing. The major drawback in this technology of image processing is it can be used only for only one individual. So, there is a need for capturing images for each person and calculating them individually. Also, the gap between the camera and the person is an important factor to be considered here as it can disturb the accuracy. The flex sensor is a piezo-resistive sensor that captures the movement depending on hand orientations. Therefore, ISL with eight voice outputs are obtained in this paper. Compared to vision-based technology, sensor-based technology could be opted since it produces 99% recognition rate.

II.MATERIALS AND METHODOLOGY

The hand gesture recognition consist of material like gloves, flex sensor, PIC Microcontroller, voice module (apr33a3), *speaker*.

A. *Data glove*

A data glove can used to support the sensor for sensing and capturing the shape of the finger. It is especially used to capture the shape in effective manner. Each and every finger is fitted with a flex sensor by using a tape or glue. The data glove is worn by the speech impaired person and they can do the action so that the sensor can sense the output.

B. *Sensory part*

The sensory part is nothing but the flex sensors which can able to sense the finger arrangement. For various angle of bending of the flex sensor, its output is varied. The output of the sensor is a resistive value and it can be converted into a corresponding voltage through a voltage-dividing circuit. Here an 82k ohms resistance can be used for the voltage divider circuit.

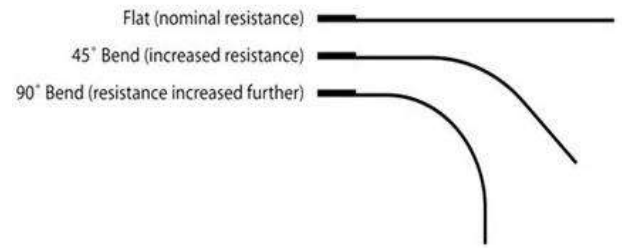


Fig 1: Variation of resistance with respect to the variation in bending of flex sensor.

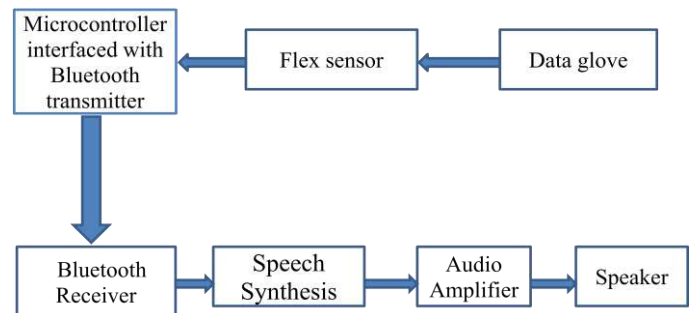


Fig 2: Block Diagram of Indian Sign Language Recognition system (ISL)

C. *PIC Microcontroller*

PIC16F877A Microcontroller consists of 5 ports (A, B, C, D and E) with 8 pin each. It can be used to govern the output of the flex sensor. The output voltage of the flex sensors are fed to the controller for further processing. The other end is connected to the common ground of all the sensory part. These analog signal values are converted to digital by the use of the inbuilt ADC in the microcontroller.

D. *Voice Module*

The voice module receives the input from the microcontroller through a Bluetooth transceiver. It consists of eight channels, in which eight words can be recorded. The voice module can be operated in both parallel and serial mode. The voices were recorded when the both signals CE (reset sound track) and RE (record) are low till the rising edge of the trigger. Then the same voice can be played back when only RE is high and a high to low edge is applied as trigger. The voice module has TTS technique that provides the relevant voice (speech) output for the input gesture. Then with the help of speaker the voice can be received clearly. The voice module itself consists of various allophones, sounds and touch tones.

III. EXPERIMENTAL RESULTS

All sensors were first tested on the data glove. With variation in position, rotation and bending, the flex sensor readings were observed.

The bending in hand is being determined at three bends of the bones of the hand known as distal, middle and proximal phalanges of the flex sensor readings. For the flex sensor, when the sensor is straight, the voltage across the finger is between 2.35 and 3.5V for a 5V power supply. At the middle phalanges bend, the voltage drop across the flex sensor was maximum and minimal when bending at the proximal phalanges. The test readings were taken and the final readings were derived from those readings and given as mean ± standard deviation. Once all the flex sensors with their good reputable readings have been tested, the data glove fitted with sensors after testing was connected to a PIC microcontroller, then to a voice module and speaker to hear the voice signals.

After setting the complete system plan, both sensors were subsequently tested for their repeatable values. After that, the data glove over each finger with flex sensors.

Simultaneously the voltage signal equal to the bend and rotation will be fed to the microcontroller once they get ready with their gestures and start expressing in hands. Depending on the bend in each word, the flex sensor voltage of each finger motion was noted down according to each word gesticulation. Simultaneously the voltage signal equal to the bend and rotation will be fed to the microcontroller once they get ready with their gestures and start expressing in hands. Depending on the bend in each word, the flex sensor voltage of each finger motion was noted down according to each word gesticulation.

The average values of the sensor readings were calculated from these measurements. The eight sets of words most commonly used were listed and their respective fingers and their corresponding values were noted.

The Indian sign language symbols for these words are the gesture movements obtained from people with speech impairments after wearing the sensor - fitted glove

FLOW CHART

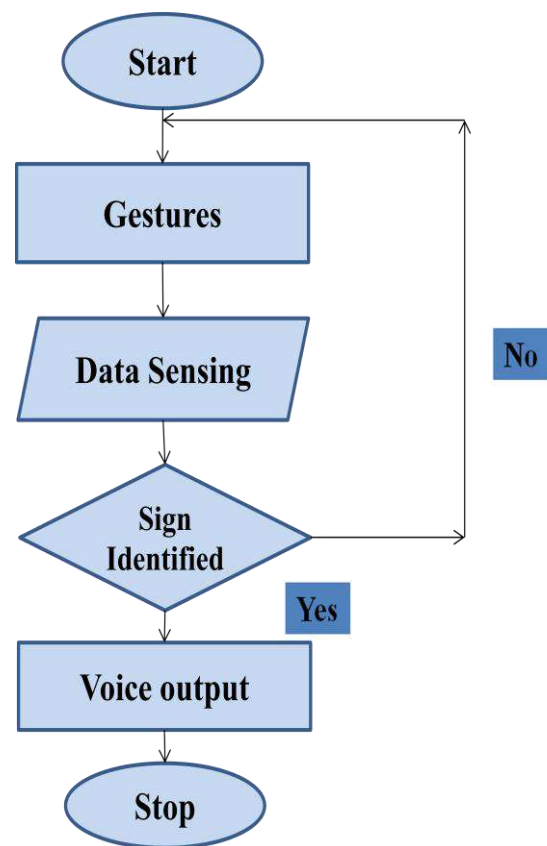


Fig 3: System flow sign language conversion

Similarly, for all other words the same procedure was repeated by calculating their minimum and maximum voltages for their corresponding ISL gestures made by people with speech impairment. These values will be given to the voice module after processed by the PIC microcontroller. The voltages received from the sensors and microcontroller selects their suitable word as sound output in the voice module. If the matches between word and voltage readings are equivalent, the speaker can hear the voice of the words. The same custom of steps will apply to all the voltages of the other word and can be heard as output

IV. CONCLUSIONS

Sign language converter can be a useful gizmo for facilitating communication between deaf-mute community and ordinary people. This methodology of the project interprets the language of sign for speech. Here the sign language is converted into voice output which can be easily perceived by the normal people. The foremost characteristic of this project is that the gesture recognizer may be a standalone system, which can be applied in the common place of living. It is in addition can also be useful even to paralyzed patients who cannot speak properly. Thus this project aims to lower the communication gap between the voiced and unvoiced community.

V. ACKNOWLEDGMENT

We would like to thank the Principal, Teachers and Students of the Saranathan College of Engineering, Trichy who gave us permission to trail this hand gesture system in the college. We would also convey our regards to Mr R.Satheesh, AP, Saranathan College of Engineering who assisted us in the technique of learning Indian Sign Language and guided us throughout our project.

VI. FUTURE ENHANCEMENT

- a. Designing of a whole jacket- Capable of vocalising the gestures and movement of animals.
- b. Virtual reality application- Replacing the conventional devices with data gloves.

VII. REFERENCES

- [1] Sunny Patel, UjjayanDhar, SurajGangwani, Rohit Lad, PallaviAhire, "Hand-Gesture recognition for Automated Speech Generation", IEEE International Conference on Recent Trends in Electronics Information Communication Technology, May 20-21, 2016, India.
- [2] Aarthi M, Vijayalakshmi P, "Sign Language To Speech Conversion", Fifth International Conference on Recent Trends in Information Technology, 2016.
- [3] Ramakrishnan G, Kumar S, Tamse A, Krishnapura N and PreethamC, "Hand and Talk-Implementation of a Gesture Recognizing Glove" , Texas Instruments Conference on Indian Educators on 4-6 April 2013, Bangalore NIMHANS convention centre.
- [4] Balakrishnan G and Rajam P S, "Real time Indian Sign Language Recognition System to aid deaf-dumb people" , IEEE 13th International Conference on Communication Technology on 25-28 September 2011, pp 737-742, Australia.
- [5] Mrs NeelaHarish, DrPoonguzhali S, "Design and developmet of hand gesture recognition system for speech impaired people" , International Conference on Industrial Instrumentation and control (ICIC) College of Engineering, May 28-30, 2015, Pune, India.

AGRIBOT- FARMER'S FRIEND

Pradeep Raaj.K¹, Prasanth.P², Soorya.B³, Hari Prakash.R⁴

Dept. of Electrical & Electronics Engineering, Saranathan College of Engineering,
Tiruchirapalli, Tamilnadu, India

pradeepraja041297@gmail.com¹, prasanthkumar24.pk@gmail.com²,
bsoorya1997@gmail.com³, mymailhari16@gmail.com⁴

ABSTRACT:

In early days farmers used traditional methods for agricultural practices. They had faced many problems in this method. To reduce the farmers struggle in the field with the help of a robot, by helping the farmer by performing various activities like ploughing, watering, seeding and a physical assistant in the field. To reduce the usage of non-renewable resources, like petrol and diesel for the tractor by using renewable resources, like solar power. Today, it is not an efficient way to use agricultural machines that run by petrol or diesel, so in order to stay in safe-zone and provide some fairness to environment. It would be helpful with the help of a rover. The designed robot can perform various jobs. The agribot is designed to be versatile such that the tools can be easily changed. The cost of ploughing a land with robot would

be less than that of tractor. It is incorporated with GPS system, so that we can track the movement of the robot from anywhere.

I.INTRODUCTION:

Most of the countries in the world depend on agriculture. The livelihood for rural people depends on agriculture. Traditionally agricultural practices like ploughing and seed sowing involved a considerable amount of manpower which depends upon the size of the land. Also the required people should be skilled. Cows were used to pull the plough tool for ploughing. In the recent past, inventions of tractors and many advanced technologies in agriculture reduced the manpower required. The productivity increased and the work was completed faster than the traditional method. But the usage of tractors increased the investment and maintenance cost. Initial investment

comprises purchasing of tractors and equipments required for the because of the increasing cost of the fuel for these machines. The modern day machines run on fuel like diesel which are non-renewable sources of energy and are expensive. So autonomous robots, which run on renewable sources like electricity are developed in the agricultural field. Agribot will help in solving these issues faced by the farmer.

II. PROPOSED SYSTEM:

Our agribot was aimed at increasing the productivity and reducing the labor involved. The bot can perform various agricultural practices like ploughing, sowing of seeds and soil leveling. Ploughing tool has sharp edges at the bottom which will turn up the soil. Seed sowing is done by using a container with perforated bottom through which the seed is sowed. Leveling is done by using a metal sheet. All these tools can be attached at the rear of the agribot depending on the purpose. Our bot can be operated in various modes which are fully automated and manually operated. The agribot performs the mentioned functions by using dc motors, CC3200 controller,

agricultural practices like ploughing. The maintenance cost is high ultrasonic sensors, magnetometer and RF transceiver.

HARDWARE:

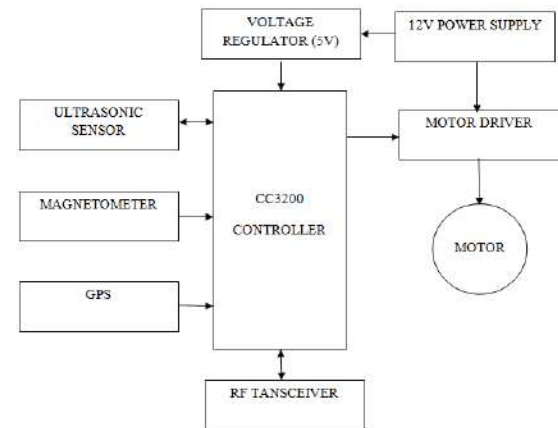


Fig 1: Overall Block Diagram

1) CC3200-LAUNCHXL:

The CC3200 is a high performance microcontroller. It was the industry's first single chip microcontroller (MCU) with built-in Wi-Fi connectivity for the LaunchPad ecosystems. Customers can develop an entire application with a single chip as the SimpleLink Wi-Fi CC3200 device is a wireless MCU that integrates a high-performance ARM Cortex-M4 MCU. Prior Wi-Fi experience is not needed for faster development as there is on-chip Wi-Fi, internet and robust security protocols.



Fig 2: CC3200 Launchpad

2) Magnetometer Sensor:

Magnetometer sensor is a device which is capable of detecting the direction and strength of magnetic field of a particular location. It measures magnetic flux. As the magnetic flux density is proportional to the magnetic field strength, the output directly gives the intensity or strength of the magnetic lines. When any object disturbs the magnetic field lines will be detected by magnetometer.

TYPES:

- Vector Magnetometer
- Scalar Magnetometer

Vector Magnetometer:

Vector Magnetometer is used for the high sensitive applications. Vector sensor drive has an alternating drive

current that runs on a permeable core material.

Scalar Magnetometer:

Scalar Magnetometer uses the Nuclear Magnetic Resonance (NMR) to measure the resonance frequency of the protons in a magnetic field.

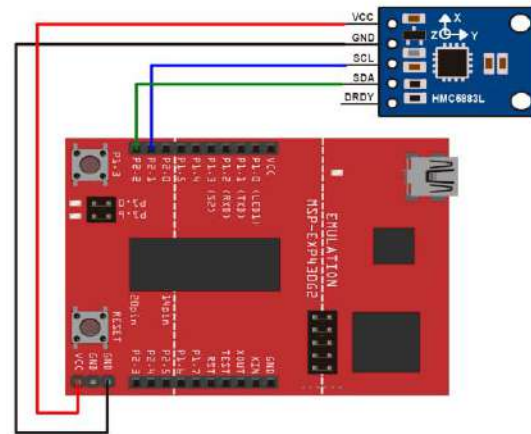


Fig 3: Interfacing of magnetometer

3) Ultrasonic Sensor:



Fig 4: Ultrasonic Sensor

Ultrasonic sensors measure distance by using ultrasonic waves. Sensor head emits an ultrasonic wave and receives the waves which are

reflected back from the target. Sensor measures the distance of the target by measuring the time between the emission and reception. An optical sensor has separate transmitter and receiver, but ultrasonic sensor uses a single ultrasonic element for both emission and reception. In a reflective model ultrasonic sensor, a single oscillator emits and receives ultrasonic waves alternately.

Distance calculation:

The distance can be calculated by using the following formula:

$$\text{Distance } L = 1/2 \times T \times C$$

where; L is the distance,

T is the time between the emission and reception of ultrasonic waves,

C is the sonic speed.

The value is multiplied by 1/2 as T is the time for go-and-return distance.

4) RF Transceiver:

A Radio frequency sensor is an electronic device used to transmit and receive radio signals between devices. It is often used to communicate with another device wirelessly. This wireless communication may be

accomplished through radio frequency (RF) waves.

III.CONSTRUCTION:



Fig 5: Setup of AGRIBOT

The chassis of our bot has been designed and manufactured in a way to keep all the components above the chassis. Four wheels are connected to the chassis for the movement of the agribot. Four wheels are driven using dc motors with one motor for each wheel so totally four dc motors are used. The motors are give power supply using a 12v Lead-acid battery. A motor controller is used to control the dc motors. The CC3200 controller, magnetometer sensor, motor controller and battery are placed above the chassis. Ultrasonic sensors are placed in the front of the chassis. In addition, we have provided a suspension system because the terrain in agricultural fields will require one.

IV. METHODOLOGY:

The working of our agribot can be done in 2 ways, one is fully automated and other way is manually operated using RF sensor. Fully automated is done using a CC3200 in which we have programmed the functions to be performed by the bot. The mode of operation can be selected by the operator. The bot operates in fully automated mode in the following method. Movement of the bot is done by connecting dc motors to wheels of the chassis. Totally four dc motors are used for four wheels. First the bot will move forward till it senses the ridges. The ridges are sensed using an ultrasonic sensor and when it senses a ridge the signal is sent to the CC3200. The CC3200 based on the program turns the agribot. The zigzag path is achieved using the CC3200 and magnetometer sensor. The tool attached to the rear of the chassis will perform its function.

The agribot will operate in the manual mode in the following manner. The bot can be controlled through an application in mobile phone. The signals are sent and received using an RF transmitter and receiver. The movement of the bot is

controlled using the mobile phone or a remote.

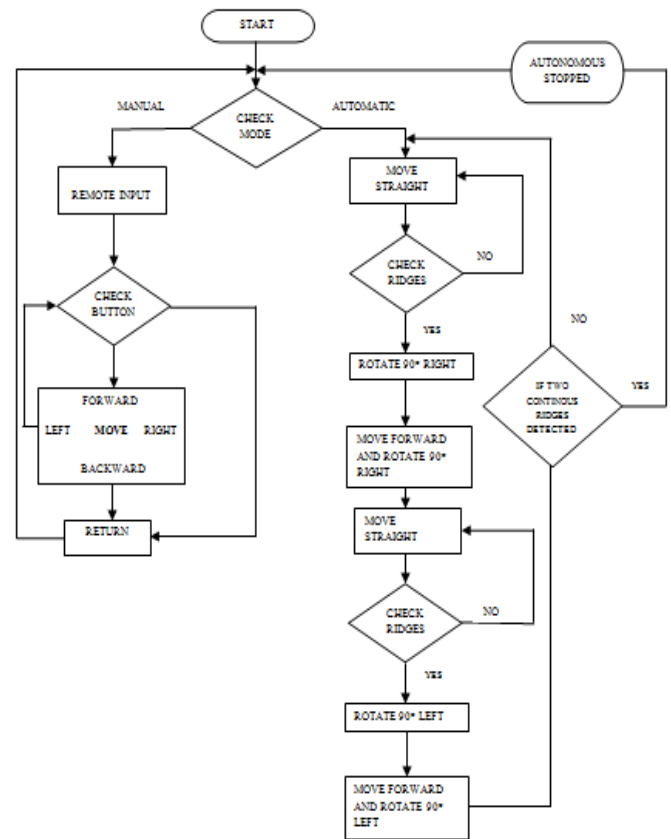


Fig 6: Flowchart of operation

V. TEST RESULT:



Fig 7: AGRIBOT

The above picture shows the agribot in ON condition the GPS

location can be seen in the mobile phone. Also the manual mode of operation using an application in mobile phone is shown. Thus the system has been designed, fabricated and tested and found working successfully.

VI.CONCLUSION:

Hence we have designed, developed and tested a robot named AGRIBOT which will do ploughing automatically in the agricultural field. It is expected that our project agribot will assist farmers in increasing the productivity and reduce the labor involved, hence improving the efficiency of farming and will be the friend of farmer.

REFERENCES

[1] K Durga Sowjanya, R Sindhu, M Parijatham, K Srikanth, P Bhargav, "Multipurpose Autonomous Agricultural Robot", International Conference on Electronics, Communication and Aerospace Technology, ICECA 2017.

[2] Amrita Sneha.A, Abirami.E, Ankita.A, Mrs.R.Praveena, Mrs.R.Srimeena, "Agricultural Robot for Automatic Ploughing and Seeding", 2015 IEEE International Conference on Technological Innovations in ICT for Agriculture and Rural Development (TIAR 2015)

[3] Neha S. Naik, Virendra. V. Shete, Shruti. R. Danve, "Precision Agriculture Robot for Seeding Function", 2016 International Conference on Inventive Computation Technologies (ICICT).

[4] Edwin Prajwal,B.Sujeshkumar,Bonu Mahesh,Balapanuri Vamseedhar Reddy, "GPS based Autonomous Agricultural Robot, 2018 International Conference on Design Innovations for 3Cs Compute Communicate Control.

[5] Akhila Gollakota, M.B. Srinivas, Birla Institute of Technology and Science, Hyderabad, "AGRIBOT - A Multipurpose Agricultural Robot", 2011 Annual IEEE India Conference.

[6] Gulam Amer, S.M.M.Mudassir, M.A Malik, "Design and Operation of Wi-Fi Agribot Integrated System", 2015 International Conference on Industrial Instrumentation and Control (ICIC), College of Engineering Pune, India. May 28-30, 2015.

[7] Palepu V. Santhi, Nellore Kapileswar, Vijay K. R. Chenchela, Venkata Siva Prasad.CH, "Sensor and Vision based Autonomous AGRIBOT for Sowing seeds", International Conference on Energy, Communication, Data Analytics and Soft Computing (ICECDS-2017).

[8] Tanupriya Choudhury, Arashdeep Kaur, Utsav Singh Verma, "Agricultural Aid to Seed Cultivation: An Agribot", International Conference on Computing, Communication and Automation (ICCCA2016).

BIO-BOT FOR SELF SUSTAINING CULTIVATION IN GREENHOUSE FARMING

Raghavan.S.S,Vishal.N,Swaminathan.S

Department of Electrical and Electronics Engineering

Saranathan College of Engineering,Panjappur,Trichy-620012

Email:raghavan.kishore@gmail.com,vishalnrayanan10@gmail.com

ABSTRACT:A global competition is pressing farmers on many fronts, mechanized agriculture has become one of the important modern agricultural methods .With the global population is expected to reach more than 8 billion by 2050, the need for agricultural production to be increased double to meet out the demand. With the limited space, the agriculture production has to be increased. This gives pressure to the Government, Private sectors and Farmers to improve the production in a positive manner. Hence all the developed countries come forth to implement robotic platform for agricultural applications such as monitoring, weed removal and pesticide spraying. Introducing robots in agriculture has been started since 1985.In recent decades, technology as a result of latest scientific research have been widely applied in agriculture to improve quality and productivity Though the latest technologies are

accepted and implemented, it is noticeable that agriculture is still labor intensive. Present day solutions densely depend upon heavy application of chemicals that are sprayed at defined time intervals making the environment toxic. Studies confirm that spraying shows harmful effect on human labours and consumers(Yaghoubi et al., 2013). Hence in order to limit application towards site specific, automation has to be implemented for agriculture operations like monitoring, control environment and inspection

Index---leaf disease,color sensor,background clipping,image segmentation,autonomous movement,

I.INTRODUCTION

The main motive of this proposal is to increase the efficiency of production in horticulture field in a positive direction. It is planned to implement the BIO-BOT for monitoring, and controlling of the infected

horticultural crop in the green house. The biggest challenges faced by agricultural robots are durability and reliability. Apart from this, in real field conditions the unit cost of robot for higher volume production of the mobile platform is very high. Hence, ***the design target is achieved by using domestic resources for developing the platform with commercially available inexpensive control boards (Arduino MEGA, Raspberry PI) and webcams, thereby integrating natively available parts.*** This proposal is about designing a **BOT** that can move through the field autonomously using four individual driving and steering. Factors like dimension of the robot (with respect to height and area of the monitoring plant), land condition (controlled environment) are considered for the design of this BOT. The robot is equipped with color sensors and it is proposed to use an image processing technique for detection of drip irrigation tube as a guide to navigate through the field. Various color code for halting and turning operation has been represented on the tubes which direct the robot accordingly within the field. The BOT is equipped with a sprayer tank (filled with required pesticides) to reduce the spread of the disease from the infected plant. It will spray pesticide only to the affected plant when the disease is curable and does not affect the productivity by affecting the other plants. ***Hence this robot will ultimately monitor and***

prevent further spreading of the disease in the plant at early stage and helps in improving the profit in green house cultivation.

III. Significance of the proposed project:

The proposed Bio-Bot ,

Can move through the field autonomously using four individual driving and steering system

- Can identify the leaves of the Plant and based on algorithm detect and segregate between affected and non-affected plants.
- It is designed in such a way that further addition in Bio-Bot can be performed like weed removal, data collection and manipulation using IoT.

This BOT is designed and used in a controlled laboratory environment with drip tube as guide for movement of the platform. Thereby, it reduces the cost and improves the flexibility. This is more efficient as it uses the drip tubes on the field are selected at target of navigation that guides the platform through the environment by the color representations embedded at the tube instructs the robot to turn accordingly on the field.

Why Tomato plants?

Solanum lycopersicum L. which is commonly known as the Tomato plant is one of the major edible crop in the world which is grown above the

surface of the ground. Tomato grows in the tropical regions of India where minimum soil temperature is 13°C and the air temperature ranges from 10°C to 50°C. They will grow upto 1-3 meters(3-10ft)in height.Tomatoes hybrid varieties are grown all over India in greenhouses. The hybrid varieties highly preferred in India include **Pusa hybrid1, Pusa hybrid 2 and Pusa hybrid 4**(as followed in ICAR, New Delhi).The required pH level for the proper growth of Tomato crop ranges between 6 to 7.Tomato crops mostly prefer acidic soil with essential nutrients provided. Tomato crops are harvested in 3 months time and on a yearly basis 8 to 9 months of harvest is done. Tomato crop is grown in 3 cycles in the southern India. They are

- December to January
- June to July
- September to October

India is the third major producer of Tomato all over the world (18.4 millions of Tonnes per year).

Diseases in Tomato crop:

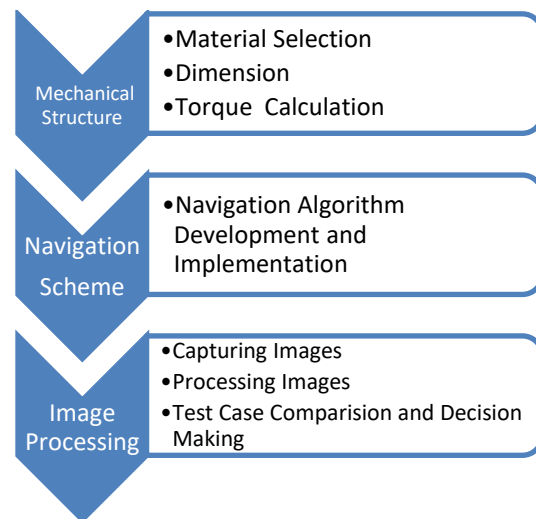
Major diseases in tomato crops grown in green house include early leaf blight, late leaf blight, powdery mildew.

Fungicides used for crop recovery:

1. Copper Oxy Chloride 50% WP (Cu₂(OH)₃Cl)
2. Sulphur 80% WP (S)

3. UPL SAAF fungicide (Carbendazim 12% + Mancozeb 63% WP)
4. Streptocycline (streptomycine sulphate + tetracycline hydrochloride)

IV. METHODOLOGY AND APPROACH:

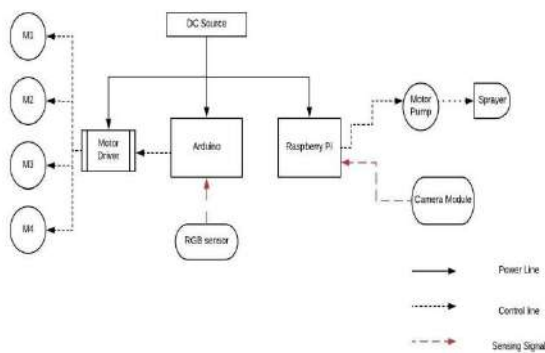


- The mechanical structure of the robot is to be design and prototypal robot has to be fabricated.
- Further the fabricated robot has to get tested on real time environment.
- Suited algorithms for image processing has to be developed and to be incorporated in the processor(Raspberry Pi)
- Various test cases on different conditions of environment has to be collected
- Based on the comparison between collected sample

images by VGA camera and various test cases result will be generated

- Based on the results required corrective measure will be taken

V.BLOCK



TCS3200

With help of the wavelength TCS3200 Color sensor can detect a wide variety of colors. Color matching, Color sorting, Test strip reading are done by this Sensor. TAOS TCS3200 RGB sensor chip is used here to detect color. It also contains four white LED's that light up the object in front of it.

SPECIFICATIONS

- Power-2.7V to 5.5V
- Size-28.4* 28.4mm(1.12*1.12")
- Interface: Digital TTL
- High-Resolution Conversion of light intensity to frequency
- Programmable Color and Full scale output frequency

Communicates directly to microcontroller

WORKING

TCS3200 throws a white light to the color strip that is pasted in the drip irrigation tube. The light ray is bounced back from the color strip which in turn is sensed by the color sensor.



Fig(1):TCS3200 Color Sensor

ARDUINO UNO

Arduino UNO is a microcontroller board that has a set of digital and analog pins precisely 14 digital pins and 6 analog pins. It is powered by either USB or battery. Arduino uses Atmega328P programmed as a USB-to-serial converter.

- Microcontroller: Microchip ATmega328P [7]
- Operating Voltage: 5 Volt
- Input Voltage: 7 to 20 Volts
- Digital I/O Pins: 14 (of which 6 provide PWM output)
- Analog Input Pins: 6
- DC Current per I/O Pin: 20 mA
- DC Current for 3.3V Pin: 50 mA

- Flash Memory: 32 KB of which 0.5 KB used by boot loader
- SRAM: 2 KB
- EEPROM: 1 KB
- Clock Speed: 16 MHz

We are using Arduino UNO to control motor operations with the help of color sensor.

BRUSHED DC ELECTRIC MOTOR

Brushed DC motor is internally commutated and runs on direct current. They were the first commercially important application of electric power to drive Mechanical energy. They can be varied in speed by changing the operating voltage and also by changing strength of magnetic field. Depending on the power supply, the speed and torque characteristics can be altered to provide steady speed or speed inversely proportional to the mechanical load. These Motors continue to be used for electric propulsion, cranes and paper machines and steel rolling mills. Since brushes wear down and require replacement brushless dc motors using power electronics devices have displaced brushed motors from many applications.



Fig(2):DC Motor

MOTOR DRIVER CONTROL

A motor controller is a device or group of devices that serves to govern in predetermined manner the performance of electric motor. Every motor have some sort of controller. Depending on the task the motor performing, motoring control have differing features and complexity. By using a small appliances or power tools, “Switch” (The Simplest case) to connect motor to a power source. The switch may be manually operated or may be relay or contactor, which is connected to some form of sensor to automatically start and stop the motor.

RASPBERRY PI

Raspberry Pi is a series of small single board computers. It may be operated with any generic USB computer keyboard and mouse. It may be also used with USB storage, USB to MIDI converters, and virtually any other device with USB capabilities. Other peripherals can be attached through the various pins and connectors on the surface of the Raspberry Pi. Though Raspberry Pi models have built-in real-time clock, so they are unable to keep track of the time of day independently. As a workaround, a program running on the Pi can retrieve the time from a network time server, thus knowing the time while powered on. To provide consistency of time for the file system, the Pi automatically saves the current system on shut down, and

reloads that time at boot. A real time hardware clock with battery backup may be added.

SPECIFICATIONS:

Instruction Set:-

ARMv8-A(64/32-bit)

SOC:-Broadcom BCM2837B0

CPU:-4*Cortex-A53 1.2GHz

FPU:-VFPv4 + NEON

Weight:-45g(1.6 oz)

The Raspberry Pi Foundation provides Raspbian a Debian-based Linux distribution for download, as well as third-party Ubuntu, Windows 10 , and specialized media centre distributions. It promotes Python and Scratch as the main programming languages, with support for many other languages. The default firmware is closed source, while an unofficial open source is available Many other operating systems can also run on the Raspberry Pi, including the formally verified microkernel.



Fig(3).Raspberry Pi 2 module
OPEN CV

OpenCV is a library of programming functions mainly aimed at real-time computer vision. It was originally developed by Intel and later supported by Willow Garage. The

library is cross-platform and free for use under the open-source BSD license.

APPLICATIONS:

Gesture recognition

Human-computer interaction

Mobile Robotics

Coming to programming language, OpenCv is written in c++, but it still retain a less comprehensive though extensive older C interface. There are bindings in Python, Java and Matlab.The API for these interfaces can be found in the online documentation. Wrapper in other languages such as C#, Perl and Ruby have been developed to encourage adoption by a wider audience.

VI. METHODOLOGY AND RESULT

Movement of Bot:

The bottom portion of the bot is fixed with a TCS3200 color sensor which senses the different colors like Red,Green,Blue,Black.Based upon the threshold value the color is detected.Depending up the color detected suitable command will be given to the motor through the motor driver from Arduino controller.

- Black-Move forward
- Red-Stop
- Blue-Turn left
- Green-Turn Right

Preprocessing

Base of the entire framework of our model is techniques of Image processing and classification. The

digital camera is used to capture the digital image of the leaves. Every sample image was then perfectly analyzed and processed with the use of our proposed approach. Suitable extraction of features has been done to further classification of the image. The major difficulty in pre-processing of digital image is the noise which is present in the image due to the background which will affect the classification. So the background has been removed by masking the major color portion (green in this case).

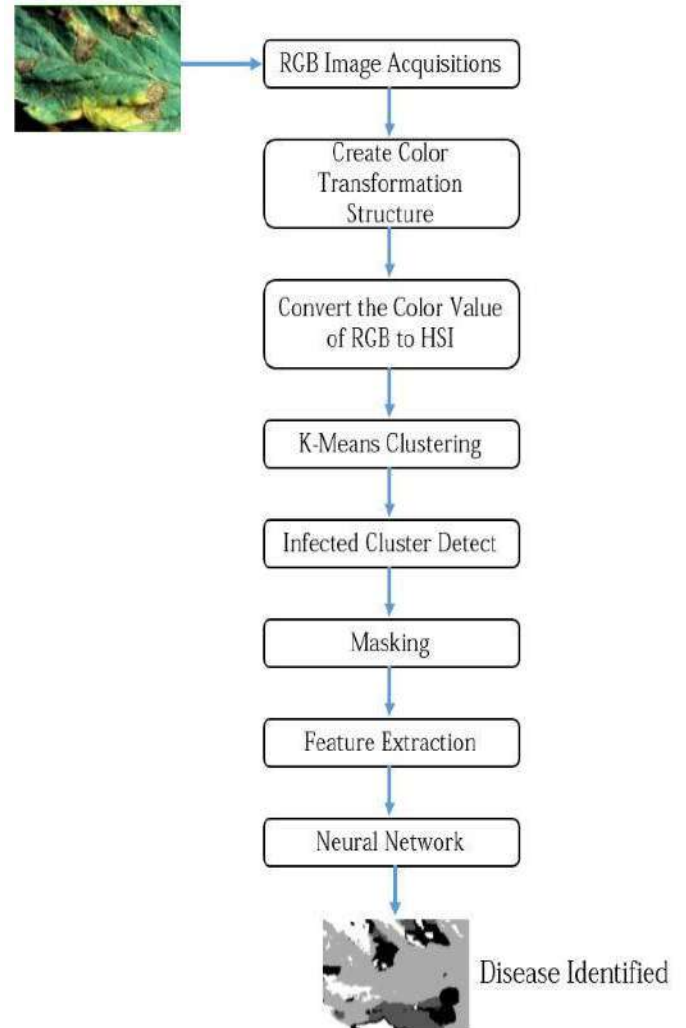


(a)



(b)

Fig 4:(a) Healthy leaf (b) Infected leaf



Fig(5) Image processing algorithm work flow

Histogram equalisation

As the preprocessing is done, before we segment and classify the leaf into faulty and faultless regions, we enhanced contrast and color depth using the well-known histogram equalization technique. This technique widens the available range of intensities and is mapped to a more uniform distribution implemented with a remapping cumulative distribution function. For a histogram $H(i)$ its remapping function will be

$$H'(i) = \sum_{0 \leq j < i} H(j)$$

After equalization, the new intensity values are given by,

$$\text{Equalized}(x, y) = H(\text{src}(x, y))$$

Segmentation

The RGB images of all the leaf samples were studied in the initial time. The samples can be divided into two subclasses: faultless and faulty. After that, the digital image has been converted to a binary image. This conversion is followed by the conversion to an RGB image. These are the part of the color transformation. Image transformation is very important at this stage as it is the input by which K-means clustering is to be done for classification.

Clustering

In computer intelligence data clustering is used for pattern recognition. Clustering means to join objects of similar characteristics in one cluster such that they are different from other clusters. Clustering of image can be done in several ways, K-means Clustering, Fuzzy K-means Clustering. K-means is a centroid based algorithm, where k represents the number of clusters.

The main advantage of K-Means clustering is that if more

number of characteristics are to be considered it is fast.

- Using k-means++ algorithm at first random two centers or pixels are chosen from the infected leaf. The centers represent the faulty and faultless regions of the leaf.
- Now for all the pixels the nearest center is calculated and assigned to the corresponding centers
- At this stage the new two centers are calculated using the assigned pixels and the algorithm goes back to the previous step. This iterative process is followed till the centers stabilize.

Next step is done in two steps, the green and approximate green pixels are identified.

At the second step, after removing all the green or apparently green pixels the first step is repeated until optimized image is acquired..

Histogram Matching and Determination of result:

By far we have identified diseased portion from the healthy portion of the leaf. This can be verified by plotting histogram graph for healthy and faulty leaf.

Actuation of Pesticide pump:

As we have detected the defected part of the plant ,the pump inside the fungicide tank is given a signal from Raspberry pi with help of GPIO command and the sprayer is positioned near the leaf .The fungicide of specified amount is sprayed in the detected portion.

VII.CONCLUSION:

In this paper we have discussed about a automated robot with which

the quality of the agricultural product can be used by reducing the use of pesticide. This bot will automatically identify the infected portion and sprys the pesticide on the specified part and thus reduces the use of fungicide for other affected areas.This project can further improved by adding weed remover, IOT for monitoring crops from remote places and it can be installed with moisture sensor to water the plants autonomously

REFFERENCES

- [1] Arti N. Rathod, Bhavesh Tanawal, Vatsal Shah “Image Processing Techniques for Detection of Leaf Disease” Computer Engineering, Gujarat Technical University, BVM, V.V.nagar, dist.Anand, Gujarat, India.
- [2] Jon Traunfeld, “Late Blight of Potato and Tomato ,home & garden information center”.
- [3] Jayamala K. Patil¹ , Raj Kumar² “ADVANCES IN IMAGE PROCESSING FOR DETECTION OF PLANT DISEASES”.
- [4] Santanu Phadikar & Jaya Sil[2008] “Rice Disease Identification Using Pattern Recognition Techniques”, Proceedings Of 11th International Conference On Computer And Information Technology,25-27
- [5] Amar Kumar Dey, Manisha Sharma, M.R.Meshram Image Processing Based Leaf Rot Disease, Detection of Betel vine ,published in the year of 2015 in Research gate
- [6] Amar Kumar Dey, Manisha Sharma, M.R.Meshram Image Processing Based Leaf Rot Disease, Detection of Betel vine ,published in the year of 2015 in Research gate
- [7] Nursuriati Jamil, Nuril Aslina Che Hussin, Sharifalillah Nordin, Khalil Awang Automatic Plant Identification,published in the year of 2015 in IEEE
- [8] Jin-lin XUE, An agricultural robot for multipurpose operations

in a greenhouse, Published in
research gate in the year of 2017

UNMANNED RAILWAY GATE CONTROL SYSTEM

Ranjith Kumar.A, Sathish Kumar.S, Mahendran.S, Aravinthan.M

Department of Electrical and Electronics Engineering

Saranathan college of engineering, Trichy

Email: 99sathishkumar@gmail.com, abisheikashok@gmail.com

1.ABSTRACT

The main aim of our project is to operate and control the unmanned railway gate in proper manner in order to avoid accidents in unmanned railway crossing. Automatic railway gate system is the innovative circuit which automatically controls the operation of gate. This system uses ATmega328p to control arrival and departure of train. This system uses three various sensors IR sensor, Vibration, Sound sensor. ATmega328p controls the various sensors IR sensor, Sound sensor, Vibration sensor. IR sensor, Sound sensor, Vibration sensor are used as a input components. Servo motor is used to drive the railway gate for opening and closing. This system includes LCD display (Timing device) and buzzer to indicate the people for gate closing. These are components of the controller system. The ATmega328p is used to receive input from the sensor and give output to the gate motor drive for opening and closing the gate. The first set of various sensors is fixed certain distance from the gate and second set of various sensors is fixed same certain distance after the gate. When train crosses the first set of sensors the gate closes and second set of sensors the gate opens. This is one of the efficient systems to avoid accidents.

I.INTRODUCTION:

Railways provide the cheapest and most convenient mode of passenger transport both for long distance and suburban traffic. Also, most of transport in India is being carried out by railway network. Still accidents are the major concern in terms of railway track crossing in Indian railway. About 60% accidents are occurring at railway track crossing in railway tracks resulting in loss of precious life and loss of economy. Therefore there is need to think about new technology which is robust, efficient and stable for both automatic gate closure system in railway track. A level cross, an intersection of a road and a railway line, requires human coordination, the lack of which leads to accidents. If this problem are not controlled at early stages they might lead to a number of derailment resulting in heavy loss of life and property. In traditional system level crossings are managed by the gatekeeper and the gatekeeper is instructed by the means of telephone at most of the level cross from the control room. But the rate of manual error that could occur at these level crosses are high because they are unsafe to perform without actual knowledge about the train time table. Delay in the opening and closing of the gate could lead to railway

accidents. In order to avoid the human errors that could occur during the operation of gates and derailment due to crack , the proposed paper introduces the concept of railway gate automation.

This system is designed using ATmega328p to avoid railway accidents happening at railway gates at the level crossings. ATmega328p helps in sensing, gate closing and opening. As a train approaches the railway crossing from either side, the sensors placed at a certain distance from the gate detects the approaching train and controls the operation of the gate. This system is operated after signal is received from the sensors. This signal is used to trigger the ATmega328p for operating the gate closing and opening using motor. We have also attached alarm system and signal system for indicating the opening and closing of gate.

II.LITERATURE SURVEY

Security in the unmanned railway crossings has always been a matter of uncertainty. Many various systems have been proposed and some implemented but they have some shortcomings. Some systems have poor stability and performance while others utilize active sensors which defects like instability and short reliable life cycle, hence requiring replacement every few years and thereby making the system expensive. This project idea already exists wherein they have used only one sensor to track the movement of train and there is no timing devices used. In our project we have used 3 sensors (IR sensor, Vibration sensor, Sound sensor) . Also we have incorporated

timing devices and alarm for proper opening and closing of gates with perfect time delays.

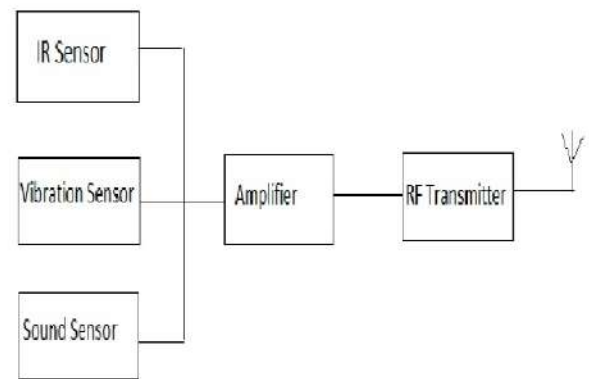
III.METHODOLGY

The principle behind the working of this project lies in the functioning of Sensors. A Reflective type IR Sensor, vibration sensor and sound sensor is used in this project. when there is no crossing of train ATmega328p will not operated.

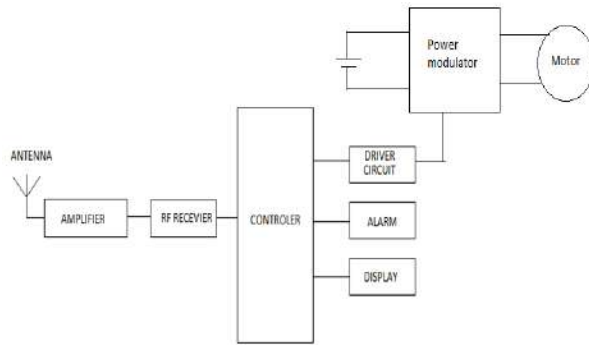
If crossing of train occurs at the sensors ,a signal is transmitted through transmitter and signal is receiver in the receiver ATmega328p closes the gate by using servomotor.similarly the gate opens when the train crosses the sensors.

BLOCK DIAGRAM:

TRANSMITTER CIRCUIT



RECEIVER AND CONTROLER CIRCUIT



IV. PROPOSED SYSTEM WORKING

There are six sensors used in the circuit and it is split into two groups of three sensors. Three sensors (IR sensor, sound sensor, vibration sensor) have been placed in order to close the gate. The gate remains closed as the train passes the crossing. When the train crosses the gate and reaches the right side sensors (IR sensor, sound sensor, vibration sensor), it detects the departure of the train and ATmega328p opens the gate by similar process.

V. CONCLUSION

This system proposed has been a very reliable one. We can prevent heavy loss of life using IR sensor based system. The proposed unmanned railway gate crossing

a position so the sensors will detect only the train and leave other obstacles such as animals which try to cross the track. Both the group of sensors are placed in certain distance away from railway gate on the railway track. First, three IR sensors (IR sensor, sound sensor, vibration sensor) are placed at left side and the other three IR sensors (IR sensor, sound sensor, vibration sensor) are placed at the right side of the railway gate. When the train is arriving on the left side of the gate, the left side sensors detect the arrival of the train and send the signal to the RF transmitter. The signal is received from the receiver using RF receiver. The input is sent to the ATmega328p. The ATmega328p operates the motor by using the motor driver in system perform automatic opening and closing gate function without help of human participation. Provide an automatic railway gate at a level crossing replacing the gates operated by the gatekeeper for

- Reduction of time for closing and opening the gate.
- Higher reliability as it is not subjected to manual errors.
- It provides safety to the road users by reducing the accidents.

Hence our Unmanned Railway Gate Control System provides the above mentioned purposes.

References:

- [1] Atul Kr.Dewangan ,Meenu Gupta and Pratibha patel ,
“Automation of railway gate control Using Frequency Modulation Technique,” International journal of Electrical ,Electronics communication Engineering,vol 2(9),pp-288- 298,2012. [2]
- Theodore L.Beach and Paul M.Kinter ,
“Devlopment and use of GPS Ionospheric Scintillation Monitor,” IEEE Transaction of Geoscience and Remote sensing,vol.39 .NO.5, May-2001
- [3] Arun P,Sabarinath G ,Madhukumar S,
“Implementation of Zig-bee based train Anti- Coliision and Level crossing protection system for Indian Railway ,”International Journal of latest trends in Engineering and Technoloy vol 2 .issue 1 ,January 2013
- [4] ACYM.Kottalil,AbhijithS2,Ajmal MM3,Abhilash L J .4 ,Ajith Bab ,
“Automatic Railway Gate Control System,”International Journal of Advanced Research in Electrical and InstrumentationEngineering,Vol.3,Issue 2,February 2014 5]
- M.kornaszewski , “programmable logic controllers [12] Qiao Jian-hua; Li Lin-Sheng; Zhang Jing -g for Automatic of the Level Crossing ,”Advance in ang ;
“Design of Rail surface Crack Detecting system Electrical and Electronic Engineering , system Based on Linear CCD Sensor ,”IEEE pp-143- 146,2010
Conf.on Networking ,Sensing and Control , vol.14.no.4,pp. 961-970,April 2008
- [6] Khandaker Marsus, P M Ilius,Mamun Hossen,P [13]
K. Vijayakumar ,S.R.Wylie ,J.D.Cullen ,C.C . M Rakibul, “ Programmable Logic Controller Wright,A.I .Shamma , “Non invasive rail track Based Automatic Railway gate control and track detection system using Microwave sen- Remote Monitoring System,” Canadian Journal sor ,”
Journal of App. Phy,vol .9 iss 11,pg on Electrical and Electronics Engineering, Vol. 4, - 1743-1749,June 2009
- [7] H. Tsunashima, T. Kojima, Y. Mastumoto and [14]
Richard J. Greene ,John R.Yates and Eann A. T.Mizuma “Condition Monitoring of Railway Patterson , “Crack Detection in rail

using in- Track and Driver Using In-service Vehicle,” IET frared methods,” Opt.Eng .46,051013 ,May International conference on Railway condition Monitoring, June 2008.

Crack DetectionScheme(RRCDS)Using LED-LDR Assembly ,” IEEE Int.Conf .on Networking sensing and control,, vol 6,issue 3,pg-453-460,May 2012

[8] Takashi Kunifuji, Jun Nishiyam ,Hiroyuki Sugagara, Tetsuya Okada ,Yamato Fukuta and Masayuki Mastsumoto, “A Railway Signal Control System by Optical LAN and Networks, Vol. 3, No. 7, July 200

[9] Burra.Raju ,B.Sreenivas , “Alarm system of Railway Gate Crossing based on GPS and GSM,”International Journal of scientific Engineering and Research,vol 1,issue 1,September 2013

[10] Subrata Biswas ,Rafiul Hoque Bhuiyan ,Samiul Hoque ,Robiul Hasan ,Tanzila Nusrat khan“Pressure sensed Fast Response Anti- Collision sytem for Automated Railway Gate control ,”American Journal of Engineering Research ,vol-02,issue-11,pp-163-173,2013

[11] Selvamraju Somalraju ,Vigneshwar mrunali , Gourav saha ,Dr. Vaidehi , “Robust Railway

OPTIMAL STRUCTURES FOR CROSSED SWITCHED MULTI LEVEL INVERTER

S.NANDA

J.PRINCE THOMSON

M.R.SIVA SHANKAR

S.THAMIZHARASAN

DEPARTMENT OF ELECTRICAL AND ELECTRONICS ENGINEERING
SARANATHAN COLLEGE OF ENGINEERING
TRICHY-620012

Abstract- The general objective of a multi-level converter is used to synthesize the desired level of output voltage acquired through several dc sources. This paper unbinds a new idea for casting a reduced switch count topology for conventional Cascaded Multi Level Inverter. The theory orients to reduce the switch count involved in conduction path which in turn reduced electromagnetic interference and switching losses. The focus enlarges to minimize the amount of power devices required for acquiring different levels of output voltage from the same architecture. The investigation pertains to carry out MATLAB based simulation to illustrate the creditability of the proposed concept.

Keywords- multilevel inverter, harmonic content, reduced count topology, H-bridge.

I.INTRODUCTION

In recent years, multilevel inverters have accorded a significant development to gain higher power with increasing voltage levels. The research relevant to multilevel inverters has been gaining wide attention mainly, and becoming a hot point in the research on electrical and electronics[1]. Multilevel inverter yields an appropriate solution for high [5] and medium power systems to amalgamate an output voltage which allows a scaling down of harmonic content in current waveform and voltage waveform. In order to refine the efficiency and convert low voltage DC source into utilizable AC source, the power electronics converters are used to change DC into AC. The result from simulations shown in this paper upholds the working of proposed MMC topology. This paper presents a novel equal area modulation strategy that has lesser total harmonic distortion of output voltage or current base on analysis of topological

structures and operative principles of the conventional cascade multilevel inverter. Multilevel inverters (MLIs) expose a different incarnation of synthesizing the output voltage to suit specific application details. Their capabilities owe to cater the high power high voltage attributes without in a way harming the voltage limit capability of power devices. The benefits corner to support superior power quality, lesser electro-magnetic interference, low power loss and high voltage blocking capability. Several asymmetrical topologies have been brought out along with a requirement for high frequency switching devices and ability to withstand overall voltage, which restricts their use for high voltage applications. Through a deep insight into the topological structures brought out by several researchers which leave a lead to develop further modifications in traditional MLI converters. In this paper, a new topology is developed with a view to reduce switch count and operating in asymmetrical configuration. The operating sequence is verified by fundamental switching using equal area criteria.

II.PROPOSED MULTILEVEL INVERTER:

The proposed multilevel inverter shown in Fig.1 constituted using a dual reverse connected voltage sources with six switches. The proposed topology looks like a ladder structure which has flexibility in extending for higher number of levels. The dc sources can be obtained from rectified dc-link or from any other renewable energy sources. The Table. I formulates the proposed MLI operate in various configurations. The operating sequence to reach different levels of output voltage for nine level is tabulated in table. II. Table. III represents switching modes to acquire 25 level in the output voltage. In both the

operating modes, the proposed topology needs lesser number of multilevel inverters. Due to this peculiar advantage, the proposed topology can be used in renewable energy and UPS applications. The schematic diagram is represented in Fig.1. The proposed algorithms were simulated using mat lab and the corresponding waveforms for 9-level MLI are listed below. The voltage waveforms is given in Fig 2 and the current waveform is given in Fig 3 and the spectral analysis for the proposed MLI is given in Fig4

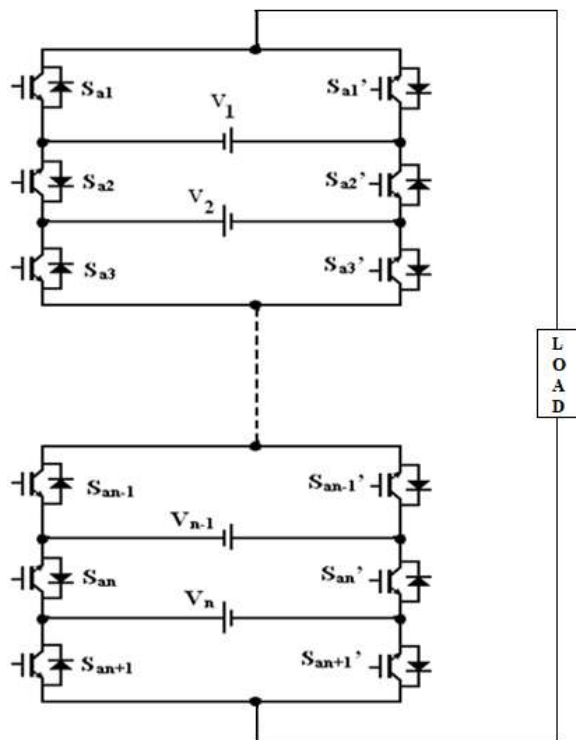


FIG.1 Schematic Diagram of MLI

TABLE-I Proposed Topologies

ALGORITHM	NO.OF DC VOLTAGE SOURCES	NO. OF VOLTAGE LEVELS	MAGNITUDE OF VOLTAGE SOURCES IN MODULE-1	MAGNITUDE OF VOLTAGE SOURCES IN MODULE-2
SYMMETRICAL	4	9	V1 =1Vdc V2 =1Vdc	V1= 1Vdc V2=1Vdc
ASYMMETRICAL 1	4	25	V1 =1Vdc V2 =1Vdc	V1= 5Vdc V2=5Vdc
ASYMMETRICAL 2	4	49	V1 =1Vdc V2 =2Vdc	V1= 7Vdc V2= 14Vdc

TABLE-II Switching sequence for symmetrical configuration (9-level)

VOLTGE LEVELS / SWITCHES	S1	S2	S3	S4	S5	S6	S7	S8	S9	S10	S11	S12
1		✓	✓	✓	✓	✓	✓					
2		✓					✓		✓	✓	✓	✓
3		✓			✓	✓	✓		✓	✓		✓
4		✓			✓		✓		✓	✓		✓
0	✓	✓	✓	✓	✓	✓						
-1	✓							✓	✓	✓	✓	✓
-2	✓		✓	✓	✓	✓		✓				
-3	✓		✓	✓				✓			✓	✓
-4	✓		✓	✓		✓		✓			✓	

TABLE-III Switching sequence for

VOLTAGE LEVELS	CONDUCTING DEVICES
1	S2 S3 S4 S5 S6 S7
2	S2 S7 S9 S10 S11 S12
3	S1 S3 S5 S6 S8 S10
4	S1 S5 S6 S8 S9 S10
5	S5 S6 S7 S8 S9 S10
6	S1 S2 S5 S6 S9 S10
7	S2 S5 S6 S7 S9 S10
8	S1 S3 S5 S8 S10 S12
9	S3 S5 S7 S8 S10 S12
10	S5 S7 S8 S9 S10 S12
11	S1 S2 S5 S9 S10 S12
12	S2 S5 S7 S9 S10 S12
0	S1 S2 S3 S4 S5 S6
-1	S1 S8 S9 S10 S11 S12
-2	S1 S3 S4 S5 S6 S8
-3	S1 S3 S5 S6 S8 S10
-4	S1 S2 S6 S9 S10 S11
-5	S1 S2 S3 S4 S11 S12
-6	S3 S4 S7 S8 S9 S10
-7	S1 S3 S4 S8 S11 S12
-8	S2 S4 S6 S7 S9 S11
-9	S2 S3 S4 S6 S7 S11
-10	S1 S2 S3 S4 S6 S11
-11	S3 S4 S6 S7 S8 S11
-12	S1 S3 S4 S6 S8 S11

Asymmetrical configuration(25-levels)

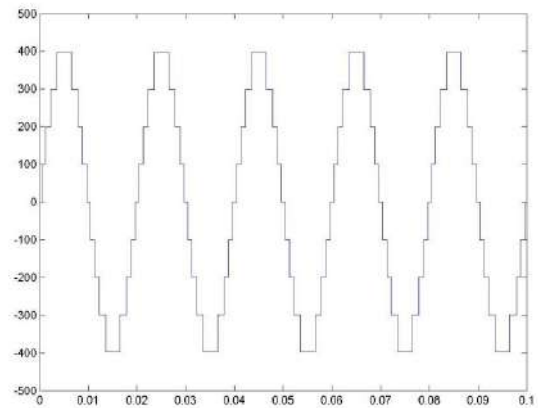


Fig.2 Voltage waveform for 9-level MLI

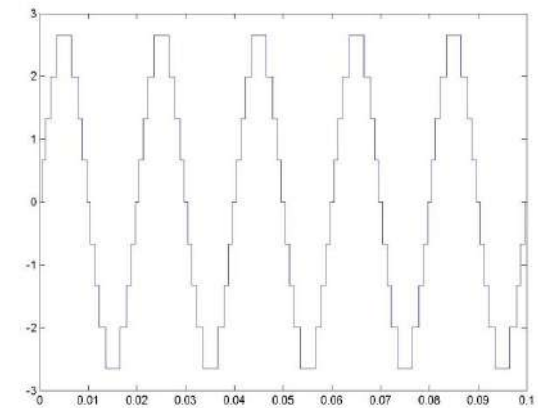


Fig.3 Current waveform for 9-level MLI

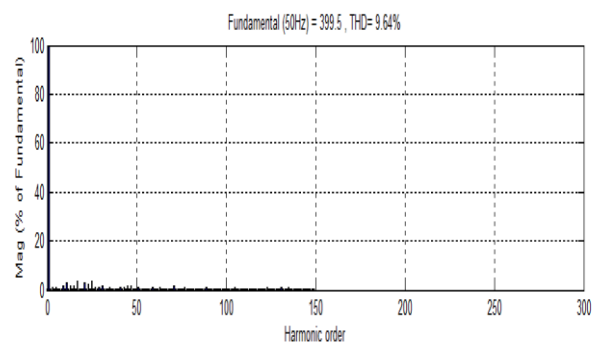


Fig.4 Spectral analysis for 9-level MLI

The mat lab diagram is given for 9level cascaded bridge circuit with all switching and the output waveform is also provided for calculation and verification.

The repeating sequence is obtained from a separate program and by using the equal area modulation method the switching sequence has been generated. The hardware is done and the

trigger pulse is given using this logic by using FPGA algorithm.

The expected output for a 9-level cascaded multi-level inverter is as given in Fig.5

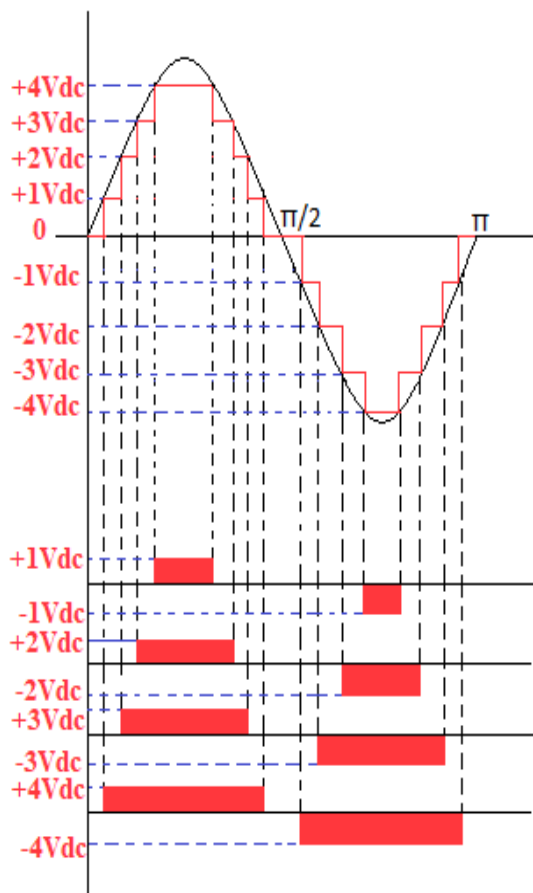


Fig.5 Expected output levels

III. EQUAL AREA MODULATION METHOD

Many modulation strategies have been developed to eliminate harmonic components in the stepped output waveform due to the rich odd harmonics in square waveform. This paper will present a novel equal area modulation strategy for the cascade multilevel inverter. The 9-level single-phase cascade inverters will be studied by using the proposed method. When a stepped waveform is synthesized to approximate a sinusoidal wave, one can let the unfilled area in the sinusoidal waveform equal to the extra area in the stepped waveform. In another word, the area that the sinusoidal waveform covers should

have the same value as that the stepped waveform contains.

$$V_{mt} \sin \alpha_j = \frac{-2j}{m-1}$$

$$\alpha_j = \sin^{-1} \left[\frac{2j}{V_{mt}(m-1)} \right] \left\{ j = 1, 2, \dots \dots \left(\frac{m-1}{2} - i \right) \right.$$

$$\left. \alpha \frac{m-1}{2} = \frac{\pi}{2} \right.$$

$$A_j = \int_{\alpha_{j-1}}^{\alpha_j} V_{mt} \sin \omega t d\omega t - \frac{2i}{m-1} (\alpha_i + 1 - \alpha_i) \left\{ \begin{array}{l} j = 1, 2, \dots \dots \frac{m-1}{2} \\ i = j - 1 \end{array} \right.$$

$$B_j = \frac{2}{m-1} (\alpha_j - \theta_j) j = 1, 2, \dots \dots \frac{m-1}{2}$$

$$\Theta_j = \alpha_j - \frac{V_{mt}(m-1)}{2} [(\cos \alpha_j - 1) - (\cos \alpha_j) + i(\alpha_i + 1 - \alpha_i)] \left\{ \begin{array}{l} j = 1, 2, \dots \dots \frac{m-1}{2} \\ i = j - 1 \\ \alpha_0 = 0 \end{array} \right.$$

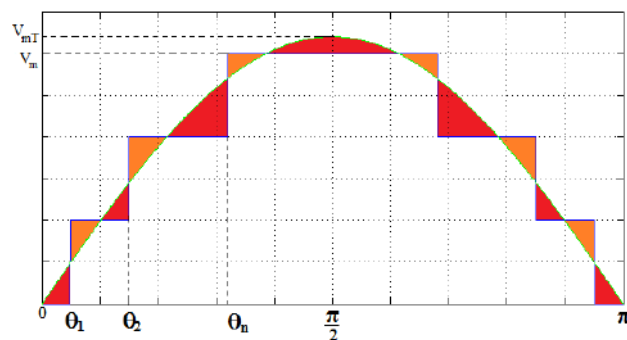


Fig. 6 Conceptual diagram for equal area criteria

From the above equations the value of θ for all the instants have been calculated and the programming is dumped in Xilinx and the desired output is obtained.

IV. CONCLUSIONS:

A multilevel inverter with isolated dc sources has been put forward to use in heavy electric drives. Simulation and Hardware results have guided that with a control strategy operates the switches at the fundamental frequency; these converters have low output voltage THD and high efficiency and it can be used in power conversion for photovoltaic application [7]. In summary, the main advantages of using

multilevel converters for heavy electric drives include the following,

1. They are apt for high volt-ampere rated and /or high voltage motor drives.
2. These multilevel converters system have higher efficiency as the devices switches at lower frequency.
3. EMI problem and common mode voltage/current problem does not exist.
4. Charge unbalance problem are eliminated when the converters are in higher charge or drive mode.

7. V. Fernão Pires, J. F. Martins, Chen Hao“ A Modular Multilevel Power Converter System for Photo Voltaic Application” 2011 international conference on power Engineering ,Energy, Electrical Drive

V.REFERENCE

1. Ehsan Najafi, A.H.M. Yatim, “Design and implementation of new multilevel inverter topology”,IEEE Transactions on Industrial Electronics, Vol.59, No.11, Nov. 2012.
2. Alireza Nami, “A hybrid cascaded converter topology with series connected symmetrical and asymmetrical diode Clamped H- bridge cells”, IEEE Transaction on power Electronics,Vol.26, No.1, Jan 2011.
3. Jinh Zhao, Yunlong Han, “Multilevel circuit topologies based on the switched capacitor converter and diode clamped converter”, IEEE Transactions on Power Electronics, Vol.26, No. 8, Aug. 2011.
4. Youhei Hinago, Hirotaka Koizumi, “A single phase multilevel inverter using switched series/parallel dc voltage sources”, IEEE Transaction on Industrial Electronics,Vol.57, No.8, Aug 2010.
5. Madav.D. Manjrekar “Hybrid multilevel power conversion system: A competitive solution for high power applications”, IEEE Transactions on Industrial applications, Vol.36, No.3, May/June 2000.
6. Amol K Koshti , M.N Rao “A brief review on multilevel inverter topologies” 2017 International conference on Data Management,Analytics Zeal Education Society Feb 24-26,2017

FPGA implementation of phase angle control for AC voltage controllers

S. THAMIZHARASAN, C.KRISHNA KUMAR

PARVATHI.K, PRATHEEBA.R, UDHAYANIRANJANA.V

Electrical and Electronics Engineering

Saranathan College of Engineering

ABSTRACT: This paper encompasses a Universal control algorithm for PWM generation for power converters using Field Programmable Gate Array (FPGA). A Phase angle Control (PAC) is developed using proposed control algorithm in such a way that it controls on-time of the switches in AC voltage controller. The PAC method is implemented in FPGA using two counters. The Algorithm is written using VHDL and the timing analysis is verified using cross compiler Modelsim SE 6.3f. The practicability of the proposed FPGA controller is tested using low cost Xilinx FPGA Spartan 3E-fg320-5 controller with a laboratory prototype of 1kW single phase AC voltage controller. The experimental results project the feasibility of the FPGA controller for real time applications.

INDEX TERMS- FPGA, Phase angle control, VHDL, pulse.

I. INTRODUCTION

In last few decades the use of Power Electronic converters is common in every industry around the world [8] [10]. Even though power electronic devices are of low cost, controlling these devices is a complicated task. Disposing the E-waste is one of the current problems faced by our World [7] [8]. The high usage of more electric and electronic components and not disposing them in an appropriate manner leads to more harmful effects [7] [8]. Power Electronic Converters will work only when gate pulses are provided. Mostly these pulses are generated using Power Electronic and Electrical devices, this leads to the generation of E-Waste. In order to reduce this problem it is wise to find an alternative solution like using software. Many software techniques are available for controlling the

power converters but a notable disadvantage is the requirement of employing individual control techniques for different converters. The hasty advancements made in the field of controlling of Power Converters are done by various controlling techniques which include sinusoidal and symmetrical waveforms. One such control techniques is phase angle control. It is the method of off-putting the power applied for AC. This control is implemented by modulating switching devices [5]. It is developed for fetching an average value of supply and it has been done in many of the digital circuits like Field programmable gate array (FPGA), Digital Signal Processor (DSP), Application Specific Integrated circuits (ASIC) [6]. Although above said devices had their own improvements, FPGA is one of the finest device which is budding currently. FPGA is a programmable device (or) chip which is the promising device that actual design could be done completely through programming. This allows design and implements any virtual digital function within one universal chip which is pretty flexible. Main difference between FPGA and other processor is that has no any intended functions in it [3]. It is fully configurable by the user only. FPGA can be turned into a microcontroller or DSP by programming and they are incredibly flexible. FPGA contains thousands of individual logic elements or configurable logic blocks or they can be called any other depending upon the user. Individual logic blocks can do any basic function or can be built up in any way to perform the desired function that is complex or even simple digital function. While considering various controlling equipments like DSP, Application Specific Integrated Circuits (ASIC). A microprocessor chip consisting of brief architecture

that chains complex algorithm processing with a good rated speed is known as DSP [1] [6]. Although DSP is a high speed software based model, it may face some unfavorable conditions like complex circuitry and learning about DSP is one of the challenging process as different DSP's have different architecture [1]. Major disadvantage that can be faced while using DSP is that it is of high cost. The above said disadvantages of DSP can be overcome by using FPGA as it low cost device.

Most of the microcontroller contains constant hardware structure [2]. Actually most of the application of inverter needs low harmonic content of AC voltages and this can be attained by applying PWM techniques which contain high harmonics, which can be easily filtered by adopting filtering techniques. High harmonic spectra can be accomplished only by using number of controllers [2].

FPGA got a great improvement in their controlling topology [9] [4]. Every device has its own pros and cons, among these FPGA is one of the best device which gives high efficiency, high execution speed, high memory application and so on. It is one of the applications of Control Engineering which gives rise to Hardware Descriptive Language (HDL) like VHDL, Verilog etc [3]. Due to mass availability of hardware and software devices it is made easy. Hardware components of FPGA consist of number of logic gates which are interconnected through metal plates and they can be assigned to perform any function by the user. In the period of development of controllers, generation of source or pseudo code is one of the complex processes that have been faced by the learning candidates. After the revolution, code development process is bit easier and they can be developed easily by knowing the syntax just like C programming [3].

FPGA can be programmed by using any of the software languages like Verilog, VHDL etc. Fundamentally a HDL is used for realization of

digital circuits with the help of simulator [3]. FPGA technology is mainly used in core industries where the people will find ease with hardware languages such as VHDL [3].

II. AC VOLTAGE REGULATOR

An AC voltage controller is a device which converts constant AC voltage to variable output voltage. These devices are used in the application of magnetic amplifiers, industrial heating, speed control of induction motors, saturable reactors etc. These devices provide high efficiency, high flexibility in controlling pulses and desired size. Generally power electronics converters can be controlled in two ways namely phase angle control and extinction angle control. An attempt has been made in this work to develop PAC method using FPGA to control AC voltage controller.

III. DEVELOPMENT OF ALGORITHM

Phase angle control is simply a square wave which depicts the ON instant of the switches used in AC voltage controller. Two counters are assigned for ON/OFF time of the switches. The ON-time counter is turned on when the switch is ON, while OFF counter is switched ON when switch is required to be turned OFF. The generated pulse is required to be phase synchronized with the input voltage. For this, a Zero Crossing Detector (ZCD) is used to turn ON/OFF the counters. The algorithm for generation of the pulses is represented by means of flow chart shown in Fig.1. The flowchart avails three variables, one for input sensing and the remaining two for output declaration. The first temporary variable (int1) is used to load the condition of ZCD. The temporary variable (int1) responses a square wave of frequency equal to input frequency and in phase with ZCD. The other two variables (int2 and int3) toggles in accordance with status of counters.

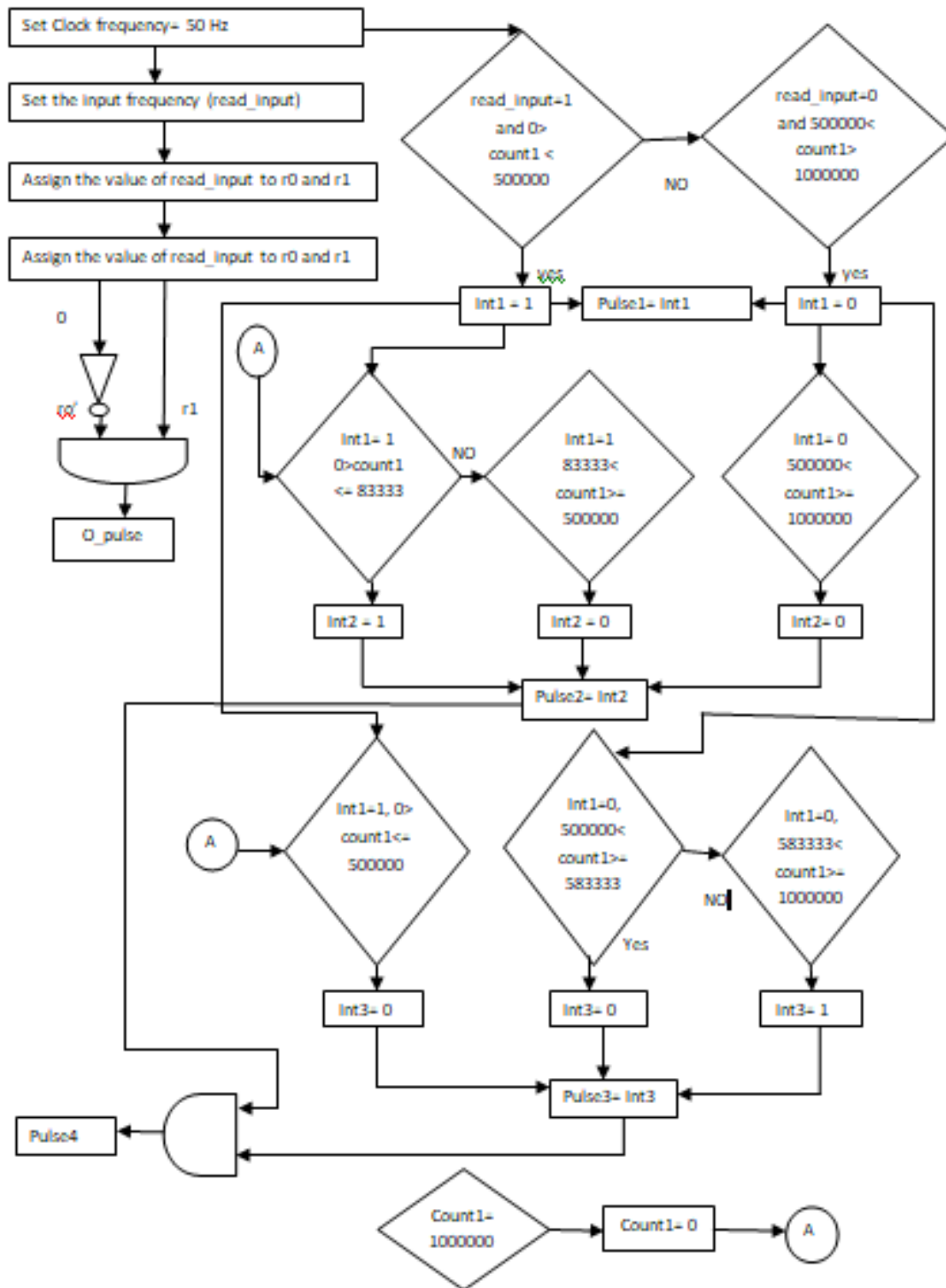


FIG1. SCHEMATIC FLOW OF PHASE ANGLE CONTROL OF AC VOLTAGE REGULATOR

IV. SIMULATION AND EXPERIMENTAL RESULTS

The simulation parameters used to study the operation of ac voltage controller with PAC methods are: $V_s = 24V$, $\alpha = 30^\circ$ and $R = 100\Omega$. The output voltage is represented in Fig.6. The hardware is fabricated with similar simulation specifications. Fig.3 illustrates FPGA controller with inboard clock frequency is 50MHz required to generate PWM pulses to switch the ac voltage controller switches. Fig 4 represents simulated SPWM pulses using Modelsim SE 6.3f and corresponding experimental pulses depicted in Fig.5. The experimental output matches with the simulated response depicted in Fig.2.

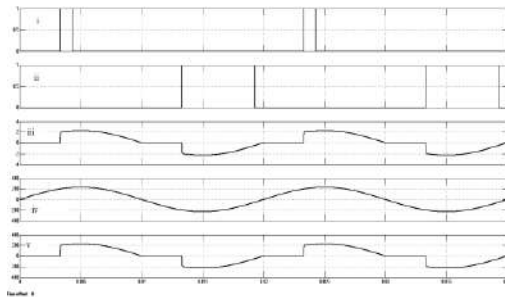


FIG2. OUTPUT WAVEFORMS FROM MATLAB

- i. Pulse for the first device
- ii. Pulse for the second device
- iii. Output voltage of 312V is obtained across the load
- iv. Input AC voltage of 24V is given to the system
- v. Output current through the load



FIG3. DIGILENT NEXYS 2-500 BOARD

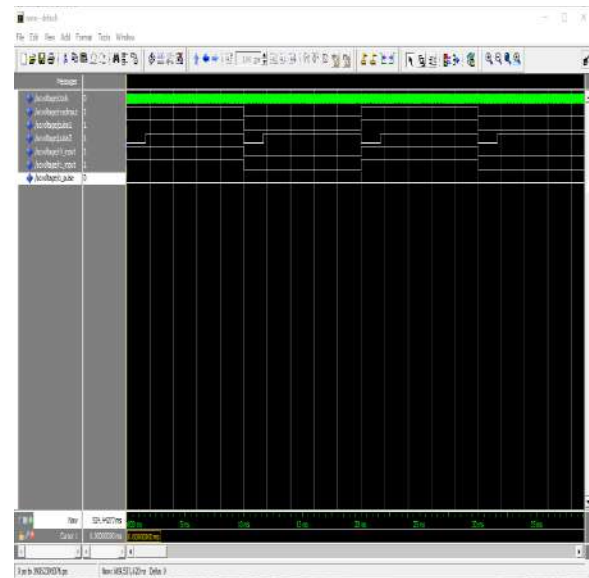


FIG4. PULSE GENERATED USING FPGA

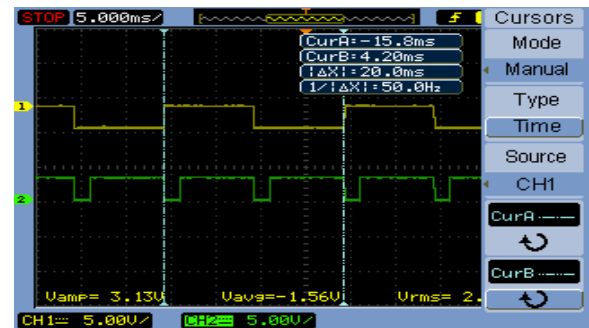


FIG5. RESULT OF PULSE WHILE INTERFACING DIGILENT WITH HARDWARE

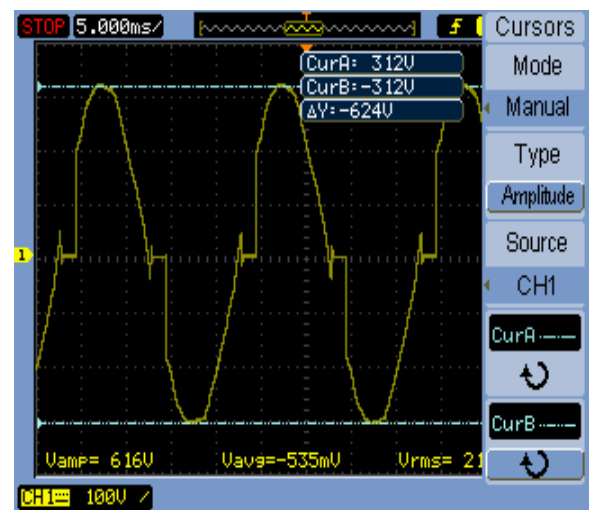


FIG6 OUTPUT VOLTAGE OF AC VOLTAGE REGULATOR

V. SUMMARY

An universal Algorithm for generating pulses required for AC- Voltage Regulator has been devised Xilinx ISE Design Suit 14.7 and the pulses are verified in Modelsim SE 6.3f cross compiler. The results of hardware are compared with that of the simulation and the developed algorithm can be extended for PWM generation required for ac voltage controller.

VI. REFERENCE PAPERS

- [1] Laurentiu Dimitriu & MihaiLucanu, "Control with Microcontroller for PWM Single-Phase Inverter", IEEE journal of research, 2003.
- [2] Abdelrahman Yousif Eshag Lesan & Mamadou Lamain Doumbia, "DSP Based Sinusoidal PWM Signal Generation Algorithm for Three Phase Inverters", IEEE Electrical power and Energy Conference, 2009.
- [3] Rohan Srivatsa & Yogesh K. Chauhan, "Generation of PWM Using Verilog In FPGA", International Conference on Electrical, Electronics and Optimization Techniques, 2016.
- [4] R.K. Pongiannan, S. Paramasivam and N. Yadaiah, "Dynamically Reconfigurable PWM Controller for Three phase Voltage Source Inverters". [5] T.W. Martin and S.S. Ang "Digital Control for Switching Converters"
- [6] T.S. Radwan and M.A. Rahman "Digital Current Control Techniques for Voltage Source Inverter" IEEE, 1995
- [7] Stefanos Th.Tsitomeneas, Apostolos I. Kokkosis, Angelos G. Charitopoulos "Legislation, Design and Management of the electrical and electronics waste producers" MedPower 2014.
- [8] Nikhita Mangaonkar, Pooja Sabhani, Sudarshan Sirsat "Green Technology for avoiding E-Waste with the help of GIS" International Conference on Advances in

Communication and Computing Technologies 2014.

[9] H. Guldner, S. Mohan, J. Losansky, M. Rentzsch "Hybrid Digital Control for Three Phase Rectifier- Inverter System" IEEE Compel Workshop

[10] Ramzy Kahhat, Junbeum Kim and Ming Xu "E-Market for E-Waste"

DUAL OUTPUT DC BOOST CONVERTER FOR ELECTRIC VEHICLE

SRINIVASAN SB
sbs.venkat@gmail.com

SHAHID HASSAN T
tshassan97@gmail.com

SURESH KUMAR M
mvs10000sureshkumar@gmail.com

VINOTH RAJ R T
skrvinoth22@gmail.com

N.VIJAYA SARATHI

vijayasarathi-eee@saranathan.ac.in
Electrical And Electronics Engineering
Saranathan College of Engineering

Abstract— This paper presents the design of DC to DC Boost converter with dual output for e-Vehicles. The Boost Converter with single inductor is designed and simulated. The input side DC voltage is boosted into different voltage levels (12v to 36v and 24v) for e-Vehicle applications. These applications may include headlights, tractive system, etc. In this paper the Dual output DC Boost converter is designed and implemented.

Keywords—Boost Converter, dual output, single inductor, e-Vehicle

I. INTRODUCTION

In recent years, there is a growing need for the development of pollution free vehicle and therefore e-vehicles becomes the opt option. In e-vehicles there arises a need where various levels of voltages are required in order to drive various applications. Therefore, the need for dc voltage converters become prominent, thus under such circumstances a DC to DC boost converts can be employed which converts single source dc voltage (12v dc) into multiple outputs at different voltage levels say 36v and 25v in order to drive the dc motor and to power the lighting systems of the e-vehicle respectively. Conventionally, the transformer-based multi-output DC -DC converters [2] are widely employed in providing multiple output voltages. But however there arises a drawback that these transformer-type converts include the amount as well as the cost of electronic components and circuit volume.

Thus, a single-inductor multiple output two terminal configuration DC-DC converter[7] is developed so as to efficiently reduce the vast requirement of electronic components for providing multiple output voltage is shown in FIG-1.

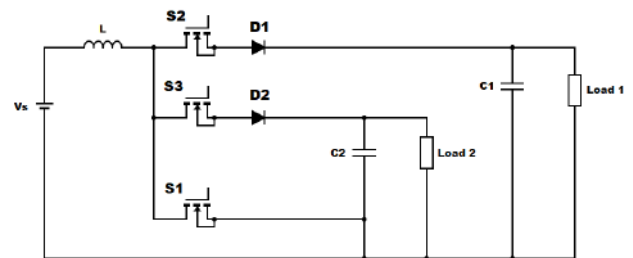


FIG-1. DC to DC Dual Output Boost Converter

Here MOSFET is used as switching device to improve efficiency, as MOSFET is suitable for higher switching frequency. The MOSFET triggering is done by providing a pulse to the gate and a delay time is programmed into the controller so that each MOSFET starts conducting at different time period and at different duty cycle and thus overlapping is avoided.

II. OPERATIONAL PRINCIPLE

The operation of the boost-type single-inductor dual-output DC to DC converter can be classified into three operating stages at steady state. Considering FIG-2, at stage 1 the switch s1 is closed and the inductor L is charged by the input DC source and inductor current increases till the maximum voltage of the input source voltage (12V).

Stage 2 (considering FIG 3): At this stage the switch s1 is open and simultaneously the switch s2 is closed and hence the current stored in the inductor discharges to the low-voltage side with output capacitor C1 and load resistance R1 through diode D1 and thus the inductor current decreases and at this stage a voltage of 36 v can be obtained across the resistor that can be used to drive the DC motor of the E-Vehicle.

Stage 3(considering FIG 4) : At this stage the switch s1 remains closed and here the switch s2 is open by simultaneously closing the switch s3 forming a path for the inductor current to flow , here the remaining current that is stored in the inductor further discharges to the low voltage side with output capacitor C2 and load resistance R2 through diode D2 and at this stage a voltage of 25v can be obtained across the resistor that can be used to power the lighting system of the E-Vehicle and again the process starts over from stage 1 charging the inductor and further on.

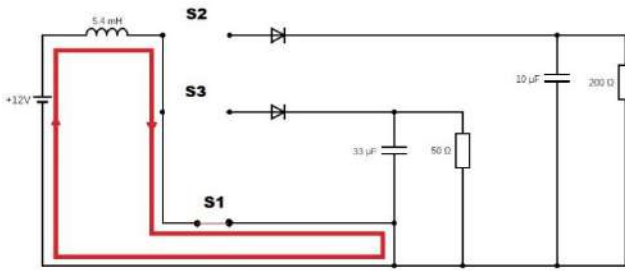


FIG-2. Stage 1 – S₁ closed; S₂, S₃-open

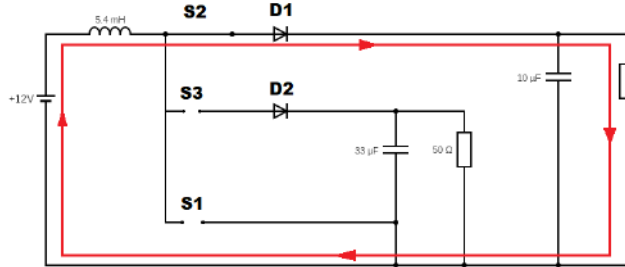


FIG-3. Stage 2– S₂ closed; S₁, S₃-open

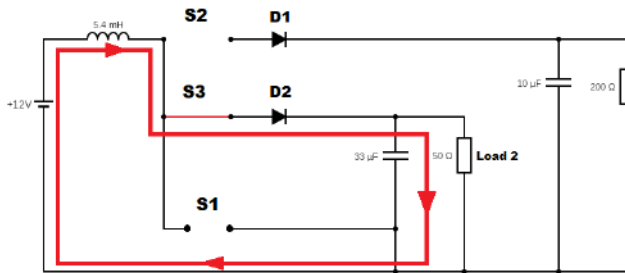


FIG-4. Stage 3– S₃ closed; S₁, S₂-open

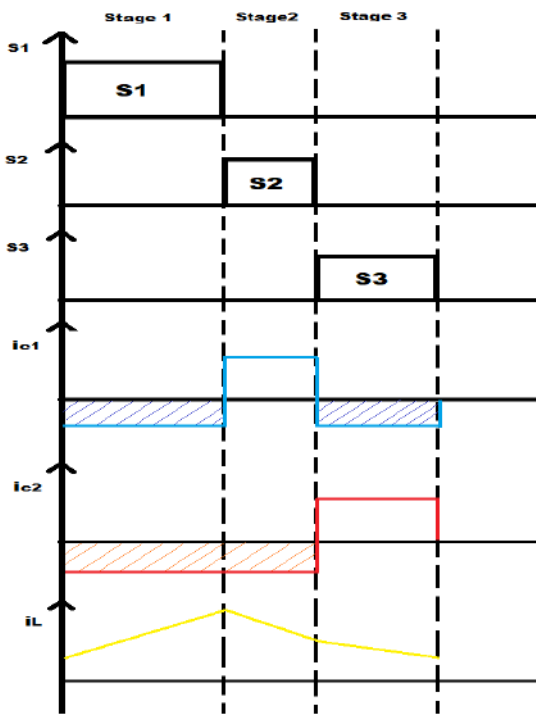


FIG-5. Key waveform of DC boost converter

III. DESIGN OF BOOST CONVERTER

During stage 1, the inductor current is charging and thus incremental (ΔI_1) is,

$$T_1 = \frac{\Delta I_1 L}{V_s} \tag{1}$$

Where, T_1 is the switching time period during stage 1
 V_s is the source voltage.

During stage 2, the inductor will discharge through the switch S_2 and can be calculated by,

$$T_2 = \frac{\Delta I_2 L}{(V_{o2} - V_s)} \tag{2}$$

Where, T_2 is the switching time period of S_2
 Similarly, inductor current can be calculated for stage 3 as,

$$T_3 = \frac{\Delta I_3 L}{(V_{o2} - V_s)} \tag{3}$$

Where, T_3 is the switching time period of S_3
 The currents ΔI_1 , ΔI_2 , ΔI_3 can be obtained from the equations (1), (2), and (3) respectively.
 Therefore, the total time period T ,

$$T = T_1 + T_2 + T_3$$

By substituting and simplifying the equations (1), (2), and (3) we get,

$$T = \frac{\Delta I L [(V_{o1} - V_s)(V_{o2} - V_s) + V_s(V_{o2} - V_s) + V_s(V_{o1} - V_s)]}{[V_s(V_{o1} - V_s)(V_{o2} - V_s)]}$$

Design of Duty Cycle:

$$V_s T = \frac{V_{o2}(1 - D_1 - D_2) - V_{o1} D_2}{(1 - 2D_2)} \tag{4}$$

During the steady state, the charging current ΔI_1 is equal to the sum of discharging currents ($\Delta I_2 + \Delta I_3$). Therefore, the voltage ratio relationship between V_s , V_{o1} , and V_{o2} can be obtained as,

$$V_{in} = V_{o1} D_2 + V_{o2} (1 - D_1 - D_2) \tag{5}$$

Where, D_1 , D_2 , D_3 are the duty cycle of switches S_1 , S_2 , and S_3 respectively. Using the above equation, we can design the duty cycle of each switches for the given input and output levels.

Design of L and C values:

To operate the converter under continuous conduction mode the inductance value must be greater than the min value of

the below inductance. This threshold value can be derived from the energy conservation principle, $P_s = V_s I_L = P_o$

$$L = \frac{D1T}{\Delta I} V_s \tag{6}$$

And the capacitance value is determined by the duty cycle associated and the load,

$$C1 = \frac{V_{o1}}{\Delta V_{o1}} \frac{[1-D2]}{f \times R1} \tag{7}$$

$$C2 = \frac{V_{o2}}{R2 \Delta V_{o2}} \frac{(D1+D2)}{f} \tag{8}$$

IV. IMPLEMENTAION AND EXPERIMENTAL RESULTS FOR DUAL OUTPUT DC-DC BOOST CONVERTER.

The specification of the prototype circuit for dual output dc to dc boost converter with single inductor design is tabulated below. The experimental results are shown as follows.

Parameter	Values
Input DC (Vs)	12v
Output DC (Vo)	Vo1 = 36v Vo2 = 24v
Duty Cycle(D)	D1= 60% D2=10% D3=30%
Inductor(L)	5.4mH
Capacitor	C1=10µF C2=33µF
Switching Frequency(f)	10kHz

Here the n-channel MOSFET and Schottky diode are used for switching devices. The above design values were simulated using MATLAB Simulink and the results are shown below.

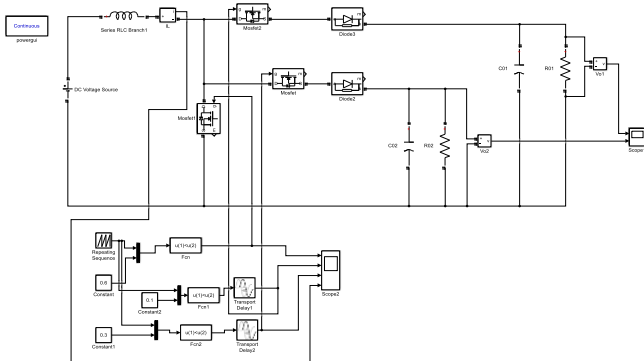


FIG-6. MATLAB Simulink model for DC to DC Boost Converter with dual output

The simulated and measured waveforms of V_{o1} , V_{o2} for boost type single inductor dual output DC to DC converters are shown in the FIG-7 and FIG-8. The resultant boosted

output voltage V_{o1} and V_{o2} are 36v DC and 26v DC respectively, where the duty cycle of switch s1 equals to 60% and the duty cycles of switches s2 and s3 equals to 10% and 30% at steady state respectively.

FIG-7. Dual output Voltage of Boost Converter

$D_1=60\%$, $D_2=10\%$, $D_3=30\%$, $R_{o1}=200$, $R_{o2}=50$, $f=10$ kHz, $V_{o1}=36V$, $V_{o2}=26V$



FIG-8. V_{g1} , V_{g2} , V_{g3} and Inductor Current Waveform

V.CONCLUSION.

With increase in pollution being caused by the emission of IC engines in recent years the need for pollution free e-vehicles becomes a solid option and in order to efficiently operate the e-vehicle, there arises a need for efficient converters and thus the use of DC-DC boost converter with multiple output becomes an ideal option under such circumstances.

In this paper a DC-DC boost converter with multiple output has been simulated ad implemented using MOSFET as power switch. The mathematical model and the experimental verifications are presented. The control algorithm of experimental prototype is implemented using Arduino controller in which the software codes are coded. This paper also represents the design calculations and the simulated output waveforms which represent the output voltage and current along with the inductor current charging and discharging along with the duty cycle waveform of the three switches used.

REFERENCE.

1. A.P.Dancy, R.Amirtharajah, and A.P. Chandrakasan, "Highefficiency Multiple-Output DC-DC Conversion For Low-Voltagesystems," IEEE Trans. VLSI Systems, Vol. 8, No. 3, Pp. 252-263, Jun2000.

2. A.Sharma, and Y.S.Pavan, "A Single Inductor Multiple Output converter With Adaptive Delta Current Mode Control," In Proceedings Of IEEE International Symposium On Circuits And Systems, Pp.5643-3646, 2006.
3. H.Matsuo, and K.Harada, "New Energy-Storage Dc-Dc Converterwith Multiple Outputs," IEEE Trans. Magn., Vol. 14, No. 5, Pp. 1005-1007 Sept 1978.
4. K.Y.Lin, C.-S.Huang, D.Chen, and K.H.Liu, "Modelling Anddesign Of Feedback Loops For A Voltage-Mode Single-Inductor Dual Output Buck Converter," IEEE Power Electronics Specialistconference, Rhodes, Greece, Pp. 3389-3395, Jun. 2008.
5. Lakshmi Krishnan, Sharna S, Sajini Susan Mathayi, "Single Input Dual Output Converter", International Journal Of Emerging Trends In Engineering Research Volume 3, No.12 December 2015.
6. Ming Shang, Haoyu Wang, "A ZVS Integrated Single-Input-Dual-Output DC/DC Converter For High Step-Up Applications", IEEE 2016.
7. Rong-Jong Wai, And Kun-Huaijheng, "High-Efficiency Single-Input Multiple-Output DC-DC Converter", IEEE TRANSACTIONS On Power Electronics, Vol. 28, No. 2, February 2013.

Design and operation of Double Frequency Boost Converter

N.Karthika¹, U.Saranya², G.Selvarani³, M.Nivetha⁴

Assistant Professor/ Department of EEE¹, UG Scholar/ Department of EEE^{2,3,4}

Saranathan College of Engineering, Trichy

¹karthika-eee@saranathan.ac.in, ²n.udhayakumarsdv.12@gmail.com

Abstract—Improving the efficiency and dynamics of the power converter is a concerned exchange in power electronics. In the high frequency switch the current will be operated and it is diverted through the low frequency switch. A double frequency Boost converter has two Boost cells: one works at high frequency, and another works at low frequency. To operate at high frequency, converter performance is improved and at low frequency, efficiency is improved. So both converter performance and efficiency is improved by a double frequency Boost converter. Thus the converter can operate at very high frequency without adding the switching loss of the converter remains small. Simulation results demonstrate that the proposed converter greatly improves the efficiency and exhibits nearly the same dynamics as the conventional high frequency Boost converter.

Key words – DF Boost converter

1. Introduction

Switching losses are more in DC-DC converter. To reduce the Switching losses, Switching techniques are used. There are two types of switching techniques 1.Hard Switching 2.Soft Switching. Soft switching namely Zero Voltage Switching and Zero Current Switching [1]. The major disadvantage of ZVS and ZCS is that they require variable-frequency control to regulate the output. This is undesirable since it complicates the control circuit and generates unwanted EMI harmonics, especially under wide load variations.

Interleaved Converter is only option to reduce the harmonics, and to achieve higher efficiency. The major disadvantage of interleaving technique is Circulating current problem. To overcome the Circulating current problem, a newly proposed converter namely Double frequency Boost Converter is introduced.

In this paper proposes a novel converter topology to achieve high dynamics response and high efficiency of Boost converter. This topology consists of a high frequency Boost cell and a low frequency Boost cell; and call it as “Double Frequency Boost converter” (DF Boost). Double frequency Boost converter consists of two Boost cells: one works at high frequency, and another works at low frequency. To operate at high frequency, converter performance can be

improved and at low frequency efficiency can be improved. Both efficiency and converter performance can be improved by Double Frequency Boost converter .It operates in a way that current in the high-frequency switch is diverted through the low-frequency switch. On the other hand, high frequency

Switching converter in parallel with low frequency converter enhances the output voltage response. The interleaved operation employs N converters to operate in parallel with interleaved clocks, so the total dynamics can reach higher performance [1-2].

3. PROPOSED DOUBLE FREQUENCY BOOST CONVERTER

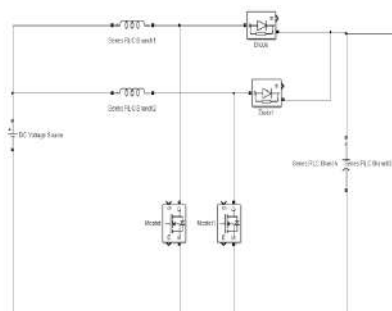


Fig.1: Schematic diagram of double frequency Boost converter

In the steady state, the input (V_s) and the output (V_o) of the converter are carried out by

$$V_o = \frac{V_s}{1-d} \tag{1}$$

Where, d is the duty ratio,

From the above equation (1) we can find that the output voltage of the double frequency boost converter and also it can be same for the boost converter. If the boost converter can be works in the continuous conduction mode, then the inductor current I_l can be regarded as a current source. In each switching cycle, both the current flowing through the switch and the voltage across the diode is averaged [1-3].

In this paper, the proposed converter is called the DF Boost converter, because these Boost cells work at two different frequencies. The cell containing L1, S1 and D1 works at higher frequency, and is called the high-frequency Boost cell. Another cell containing L2, S2 and D2 works at lower frequency, and is called the low frequency Boost cell.

The high frequency Boost cell is used to enhance the output performance, and the low frequency Boost cell to improve the converter efficiency. An active switch, instead of a diode as in the conventional unidirectional Boost converter, is employed to realize D1 in the high-frequency Boost cell. It works complementarily with high-frequency cell switch S1, and improves the transient response. The switch S1 is controlled to operate at the high frequency f_h , and the corresponding switching period is T_{sh} . On the other hand, the switch S2 is controlled to work at a low frequency f_1 , and the corresponding switching period is T_{s1} . Assume that the high frequency is an integer multiples of the low frequency,

$$F_h = M f_1 \tag{2}$$

At each low-frequency cycle, four switching states exist. Table I lists the switching states according to the status of switches S1 and S2 [1, 2].

TABLE 1: SWITCHING STATES

MODE	S1	S2	D1	D2
1	ON	ON	OFF	OFF
2	ON	OFF	OFF	ON
3	OFF	ON	ON	OFF

3.1 MODES OF OPERATION

MODE 1 S1: ON, S2: ON

In mode 1 operation, both the switches S1 and S2 are in ON state and diodes D1 and D2 are in OFF state. The voltage and current equations are given below,

$$v_s = v_{l1} \tag{3}$$

$$v_s = v_{l2} \tag{4}$$

$$i_c = i_o \tag{5}$$

In this state, the voltage V_{L1} across the inductor L_1 is positive, hence the current I_{L1} flowing through L_1 rises, and the current I_{L2} flowing through does not change.

MODE2 S1: ON, S2: OFF

In mode 2 operation, the voltage and current equations are given below,

$$V_s = V_{l2} \tag{6}$$

$$V_{l2} = V_s - V_o \tag{7}$$

$$I_c = I_{l2} - I_o \tag{8}$$

The voltage across the inductor L_1 will be equal to the supply voltage. The voltage across the inductor L_2 is equal to the supply voltage difference the load voltage. The voltage V_{L1} across L_1 is positive, so the current I_{L2} rises. Since the voltage V_{L2} across L_2 is negative, the current I_{L2} through L_2 decreases. The current across the capacitor is equal to the current across the inductor L_2 difference the load current.

MODE3 S1: OFF, S2: ON

For mode3 operation, the voltage and current equations are given below,

$$V_s = V_{L2} \tag{9}$$

$$V_{L1} = V_s - V_o \tag{10}$$

$$I_c = I_{L1} - I_o \tag{11}$$

The voltage across the inductor L_1 is equal to the supply voltage minus the load voltage. The voltage across the inductor L_2 is equal to the supply voltage. The current across the capacitor is equal to the current across the inductor L_2 difference the load current.

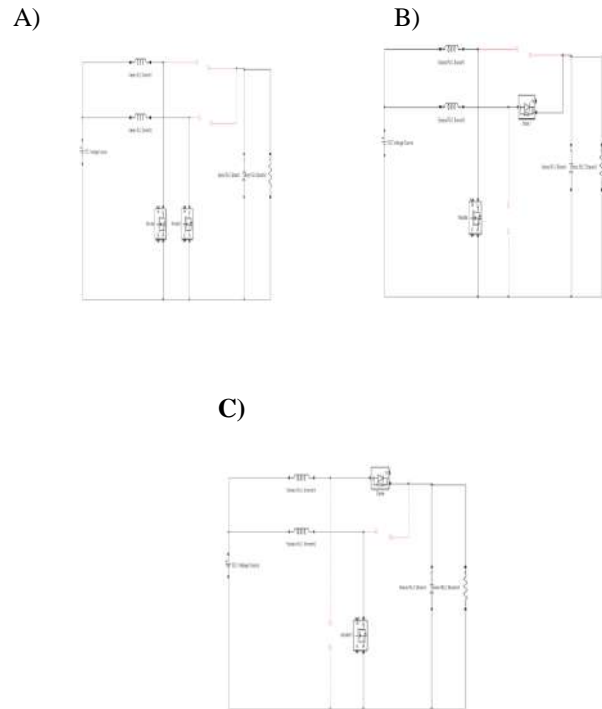


Fig. 2 Switching States of the double frequency boost converter (a) mode 1(b) mode 2(c) mode3

4. DESIGN OF DOUBLE FREQUENCY BOOST CONVERTER

4.1 OPEN LOOP

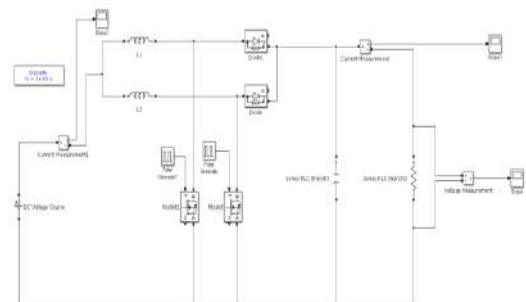


Fig: 2: Simulink diagram for open loop DF boost converter

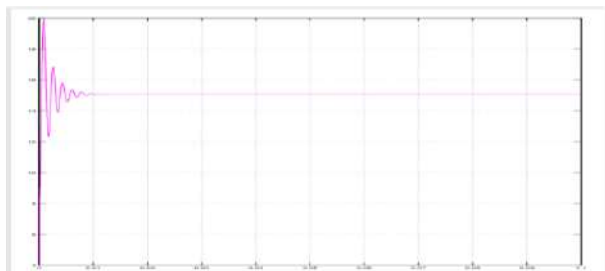


Fig. 3: Output voltage waveform of open loop DF Boost converters

4.2 CLOSED LOOP

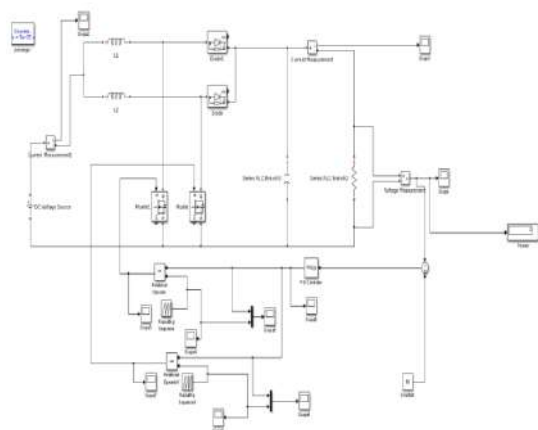


Fig. 4: Simulink diagram for closed loop DF boost converter

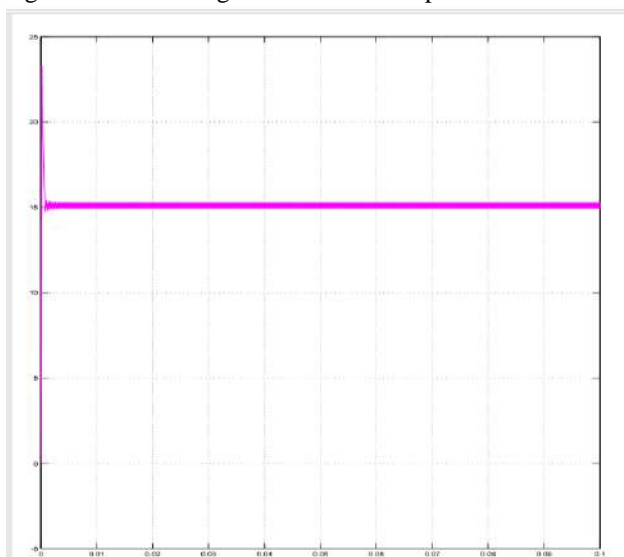


Fig. 5: output voltage waveform for closed loop DF Boost converters

In closed-loop control systems the difference between the actual output and the desired output is fed back to the controller to get the desired system output. This difference can be known as the error signal is amplified and fed into the controller.

4.2.1 PI Controller

A proportional integral derivative controller (PI controller) is a control loop feedback mechanism widely used in industrial control systems. A PI controller can calculate an error value as the difference between a measured variable and a desired set point. PI Controllers are also known as three term controllers Proportional, Integral and Derivative. Proportional action can responds quickly to changes in error deviation. Integral action: is slower but removes offsets between the plant’s output and the reference. Derivative action can Speeds up the system response by adding in control action proportional to the rate of change of the feedback error.

The proportional, integral and derivative term is given by:

$$U(t) = K_p e(t) + k_d \frac{d}{dt} e(t) + k_i \int_0^t e(t) dt$$

By using PI Controller, overshoot of the system is reduced and it improves the stability of the system

6. Conclusion

In this paper, has presented a novel topology of Double Frequency Boost converter. Analytical results have demonstrated that the DF Boost converter not only exhibits the same steady state and transient performance but also improves the efficiency of conventional Boost converters. The proposed converter does not need the load transient change information for accurate current control and does not have the current circulating problem and it is used for high power applications. Future work will investigate whether the proposed Boost converter is applicable for Electric Vehicle and PV cell applications .

7. References

[1]G.Shanmugapriya,E.Arthika, Design and Implementation of Double Frequency Boost Converter ,Students Journal of Electrical and Electronics Engineering issue no.1 ,vol.1,2015

[2]W. Chen and X. Ruan, “Zero-voltageswitching PWM hybrid full-bridge three-level converter with secondary-voltage clamping scheme,” IEEE Trans. Ind. Electron., vol. 55, no. 2, pp. 644–654, Feb. 2008.

[3]Yao-Ching Hsieh, Te-Chin Hsueh, and HauChen Yen, ”An Interleaved Boost Converter With Zero-Voltage Transition” IEEE Trans. Power Electron.,vol. 24, no. 4, Apr 2009.

[4] Z. Ye, P. K. Jain, and P. C. Sen, “Circulating current minimization in high-frequency AC power distribution architecture with multiple inverter modules operated in parallel,” IEEE Trans. Ind. Electron., vol. 54, no. 5,pp. 2673– 2687, Oct. 2007.

[5] C.-T. Pan and Y.-H. Liao, “Modeling and coordinate control of circulating currents in parallel three-phase boost rectifiers,” IEEE Trans. Ind.Electron., vol. 54, no. 2, pp. 825– 838, Apr. 2007.

[6] J. Marcos Alonso, Juan Viña, David Gacio Vaquero, Gilberto Martínez, and René Osorio“Analysis and Design of the Integrated Double Buck–Boost Converter as a HighPower-Factor Driver for Power-LED Lamps”, IEEE Trans. power electron., vol. 59, no. 4, Apr 2012.

[7] Jingquan Chen, Dragan, Maksimovic,and Robert W. Erickson, ”Analysis and Design of a Low-Stress Buck-Boost Converter in Universal-Input PFC Applications” IEEE Trans. power electron., vol. 21, no. 2, Mar 2006

[8] Xiong Du, Luwei Zhou, and Heng-Ming Tai, "Double Frequency BuckConverter" IEEE Trans. power electron., vol. 56, no. 5, May 2009

[9] H. Mao, F. C. Lee, D. Boroyevich, and S. Hiti, "Review of high performance three-phase power-factor correction

circuit," IEEE Trans. Ind. Appl., vol. 44, no. 4, pp. 437-446, Aug. 1997.

[10] U. Borup, F. Blaabjerg, and P. Enjeti, "Sharing of nonlinear load in parallelconnected three-phase converters," IEEE Trans. Ind. Appl., vol. 37, no. 6, pp. 1817-1823, Nov./Dec 2001.

DC-DC Step up Converter using Coupled Inductor with Cockroft Walton Multiplier

K. Gaayathry¹, B. Pooja Sri², K. Priyadharshini³, R. Sindhu Roshni⁴
¹ Assistant Professor, ^{2,3,4} Final Year B.E

Department of Electrical and Electronics Engineering, Saranathan College of Engineering, Trichy.

Abstract— This paper analyses the new scheme of a high step-up dc-dc converter with very high gain based on the Cockcroft-Walton (CW) voltage multiplier with Coupled Inductor. The paper proposes the circuit based on the combination of switched-Coupled Inductor and Cockroft Walton multiplier. This system uses sustainable energy as the first stage for the low voltage source. The employment of Coupled Inductor in Boost Converter makes high voltage attainable with a 50% duty cycle resulting in reduced voltage stress on switch. Incorporating the cockroft Walton-voltage multiplier with Coupled Inductor eliminates the problems related to the conventional Voltage Fed-type such as voltage ripple & low voltage gain.

Keywords— *High gain, Coupled Inductor, Cockroft Walton-Voltage Multiplier, Boost Converter, Sustainable Energy*

I. INTRODUCTION

Many industries use step-up converters with a large voltage gain. A new approach in increasing the DC voltage gain of the converters was incorporated by the use of coupled-inductor, which substituted the inductor in the boost structure [1-4]. The use of Coupled-Inductor can increase the voltage ratio in the other structures such as Buck-Boost, Cuk. [5,6]. The voltage gain can also be increased by the use of voltage multipliers. There are various configurations of voltage multipliers in Direct Current (DC). They are diode-capacitor Cockroft-Walton and Dickson cells, have been projected and analysed in several publications [7-9]. A number of topologies based on Cockroft-Walton and Dickson multipliers with their specific features have been reflected in [12]. The need for additional voltage gain can be met by the combination of the Coupled Inductor Boost Converter with any one of the Voltage Multiplier configuration. Detailed analysis of The Coupled-Inductor Boost Converter with Dickson Voltage Multiplier is given in [15]. This paper proposes the use of Cockroft-Walton Voltage multiplier along with the Switched-Coupled Inductor DC-DC Converter. Due to the advantages of Solar energy (Photovoltaic (PV) panels) and fuel cell stacks, such as availability, cost, and reliability, they have become one of the most popular sustainable energy sources. However, due to the low DC output voltage of these types of sustainable energy sources, incorporating a high voltage boosting stage in the Power Electronics Interface is necessary in order to produce the required DC bus voltage for grid/utility.

Conventional non-isolated converters are not practically applicable, as the voltage gain is maximum only at extremely high duty cycles due to the losses in the switching components and the problem of diode reverse recovery. Several high step-up DC-DC converter topologies have been proposed in the literature with three distinct configurations:

- Impedance-Source Networks Converter
- Transformer isolated (and Inductor Coupled) DC-DC Converter.
- Switched Capacitor Converters.

Impedance networks [2], features some advantages, such as eliminating semiconductor switches that are usually required in the boosting stage, and enhanced reliability because of insensitivity to momentary shoot-through [2]. However, these topologies generally require switches with higher voltage rating. Moreover, traditional snubber circuits are not applicable to the output stage. Isolated DC-DC converters with high turns ratio transformer have been widely investigated in the literature [3]. Although they provide galvanic isolation which is crucial for many applications, their main drawback is their large parasitic capacitances and their leakage inductance of the high turns-ratio transformer, which causes high voltage and current spikes on the power semiconductor devices. There are several ZVS converters presented in [7], [8], [9] and [10]. In a high voltage step up DC-DC converters, voltage stress on various semiconductor switches are one of the main concern. If the voltage stress on switches is low, this helps to choose MOSFETs with low on-state resistance and this improves the efficiency by reducing the conduction loss. However this issue is more applicable in the isolated converter with multiplier cells. In [9], the resonance between the leakage inductance and the parasitic capacitance of the diodes causes large voltage spike on the diodes. However, soft switching helps to eliminate this voltage spike. Hence snubber circuits are not required to protect the output diodes from the voltage stress. Converter in [11] is a hard switched passive clamp converter. MOSFET turn on losses are lower in [1] compared to the conventional Coupled Inductor converters. In soft switched converter of [7], [8] and [9], ZVS of the main MOSFET switch depends purely on the stored

energy of the leakage inductance. Hence to achieve higher efficiency in ZVS with MOSFET switches, large leakage inductance or an external inductor is required. Usage of Inductance reduces the voltage gain of the converter due to the increased duty cycle losses. In order to compensate the duty cycle loss, converter in [8] needs to operate at higher duty cycle which results into high current and thus conduction losses are increased. Moreover utilizing a large external Inductor to maintain ZVS at lighter loads is found to be less effective. To overcome these issues, at light loads, a complex light load frequency modulated control must be applied. Power density of a DC/DC converter mainly depends on the size of magnetic components. To improve the power density of a converter, size of the magnetic components is needed to be reduced. In conventional high voltage gain Coupled Inductor Converters [12], [13], Coupled Inductor transfers its energy to output during only one switching state (either on or off state). Hence to obtain high voltage gain, Coupled Inductor needs to store high amount of energy which leads to the selection of large magnetic core. Hence in ZVS converters, the core size should be optimized to construct the Coupled Inductor. Switched Capacitor Converter has attracted attentions due to its important property: no contribution of magnetic components [14], [15]. This characteristics qualifies it to target a Dual Inductor High Step-up DC/DC Converter Based on the Cockcroft-Walton Multiplier.

II. CONVENTIONAL SYSTEM

In earlier days, the transformer provides the input supply to the Cockcroft Walton voltage multiplier. Now the Boost Converter that acts as the input supply has been replaced. The low input dc provides the Boost Converter and the battery is used for this purpose. The Boost Converter consists of the four switches and the boost inductor. The boost inductor is used to increase the voltage of the input supply. The two switches are made to operate the alternating frequency at a lower frequency. The other two switches, at the modulating frequency, are made to operate at higher frequency. In complimentary mode, these switches work. The advantage of these two frequencies is that it helps coordinate the system's output ripple with its efficiency. The higher frequency helps keep the energy flow through the inductor. The lower frequency is used to supply alternating or pulsating alternating current flow to the multiplier circuit of voltage. The boost voltage of the Boost Converter as the terminal voltage is available through a converter. The charging current of the output capacitor is discontinuous which results in larger capacitor size and Electromagnetic Interference (EMI) issues. As similar to the Buck-Boost Converter, the efficiency is poor for high gain i.e. very large duty cycle. Therefore, high gain operation cannot be

achieved with this converter. Efficiency can be as poor as 60% for a duty cycle of 0.7. This converter cannot step-down the voltage which is crucial for many applications like PV. To extract the maximum power from a PV panel there can be sometimes where you may need to step-down. Hence, this converter cannot provide you a large limit of maximum power point tracking. There is no isolation from input to output which is very critical in many applications like the power supply of gate driver of power semiconductors. This converter is difficult to control similar to the buck-Boost Converter. The transfer function of this converter contains a right half plane zero which introduces the control complexity. In order to overcome these difficulties, Coupled Inductor is used in the Proposed System.

III. PROPOSED SYSTEM

The conventional multiplier for Cockcroft Walton Voltage consists of normal inductor and the output voltage is obtained throughout the load. The Boost Converter's circuit diagram with the Cockcroft Walton voltage multiplier involving Coupled Inductor reduces the ripples. The V_{in} provides the boost inductor with the low input dc supply, which boosts the voltage input. The switches turns on as soon as the switches receive the pulses of the gate from the controller. The terminal voltage obtained from the converter is step up voltage due to the operation of switches with independent frequencies. The current obtained from the Boost Converter is to pulsate a.c form, which is then fed by the multiplier of Cockcroft Walton voltage. Therefore, the Cockcroft Walton voltage multiplier multiplies the voltage to achieve high DC voltage. The boost structure is expressed in two modes, with switches in on (closed) & off (open) modes. The Switch1 is on during positive conducting interval and switch is on during negative conducting interval. A large inductor value is preferable for best system efficiency, as it leads to a small ripple of current. On the other hand, due to the fact that it can achieve fast energy transfer, a small inductor is desirable for good transient response. This conflict inherently limits converter performance using traditional inductors. It would be better if, during the transients, the inductors could have a nonlinear behaviour with large values at a stable state and small values. To overcome these disadvantages, Coupled Inductor is used.

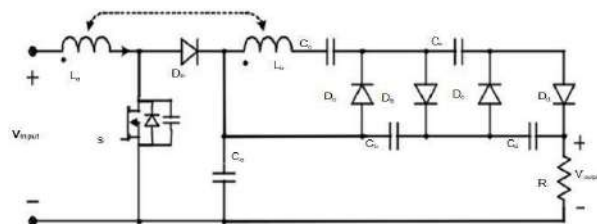


Figure 1: Circuit Diagram for the Proposed System

A. OPERATING PRINCIPLE

The Circuit Diagram of the proposed converter is drawn in figure 1. The Boost Converter is supplied by the low input dc and here the battery is used for this purpose. The Boost Converter consists of boost inductor and the four switches. The boost inductor is used to boost the input supply voltage. The two switches are made to operate at lower frequency known as the alternating frequency. The other two switches are made to operate at higher frequency known as the modulating frequency. These switches work in complimentary mode. The advantage of these two frequencies is that it helps to provide the coordination between the output ripple of the system and its efficiency. The higher frequency helps to maintain the flow of the energy through the inductor. The lower frequency is used to provide the flow of the alternating or the pulsating alternating current to the voltage multiplier circuit. The boost voltage of the Boost Converter is available across a converter as the terminal voltage. The circuit shows the arrangement of the boost inductor, switch, ladder network of diode and capacitor with the voltage being obtained across the load. The working condition depends mainly on Negative conductive interval: The current is less than zero in this interval and only one of the odd diodes conducts at a time with the sequence of odd condensers being charged and even the condensers being discharged through the conductive diodes. The condition for the current polarity of the switch depends on the switching condition. Accordingly, depending on the current polarity, the circuit operation is divided mainly into two major operating states. They are Positive conducting interval: the current is greater than zero in this interval and only one of the even diodes conducts at a time starting with the right most diodes in a sequence of even condensers and the odd condensers are charged through the conducting diodes.

B. CONTROL STRATEGY

The controller used in this paper follows the average current mode control to design the PWM process to obtain the proposed Continuous Conduction Mode (CCM) converter and PI(Proportional –Integrator) Controller will obtain the modulated voltage. Compared to the actual obtained (V_0) from the proposed system, the V_{ref} which is the desired output. The difference is called the V_{error} between the desired output and the actual output. If V_{error} is present, the output is regulated by the PI Controller. This controlled output is then multiplied by the $[Rs(V_0)]$ resistance. This product is then divided by the modulated voltage (V_m) given between the reference value and the actual output voltage by the error command here. So with this the objective is obtained to regulate the average current

of the inductor so that it is proportional to the voltage of the input. Now compared to the ramp generator, the average waveform. The Pulse Width Modulation (PWM) is performed by a ramp signal intersection with the average inductor current, thus generating the signal for Switch. The signal is obtained through the use of the PWM signal OR operator as their inputs The PWM signal is given by the pulse generator as the input for and the other input, with these two inputs the logic operator provides the switch's triggering pulse.

C. SWITCHING TOPOLOGIES OF ANALYSED CIRCUIT

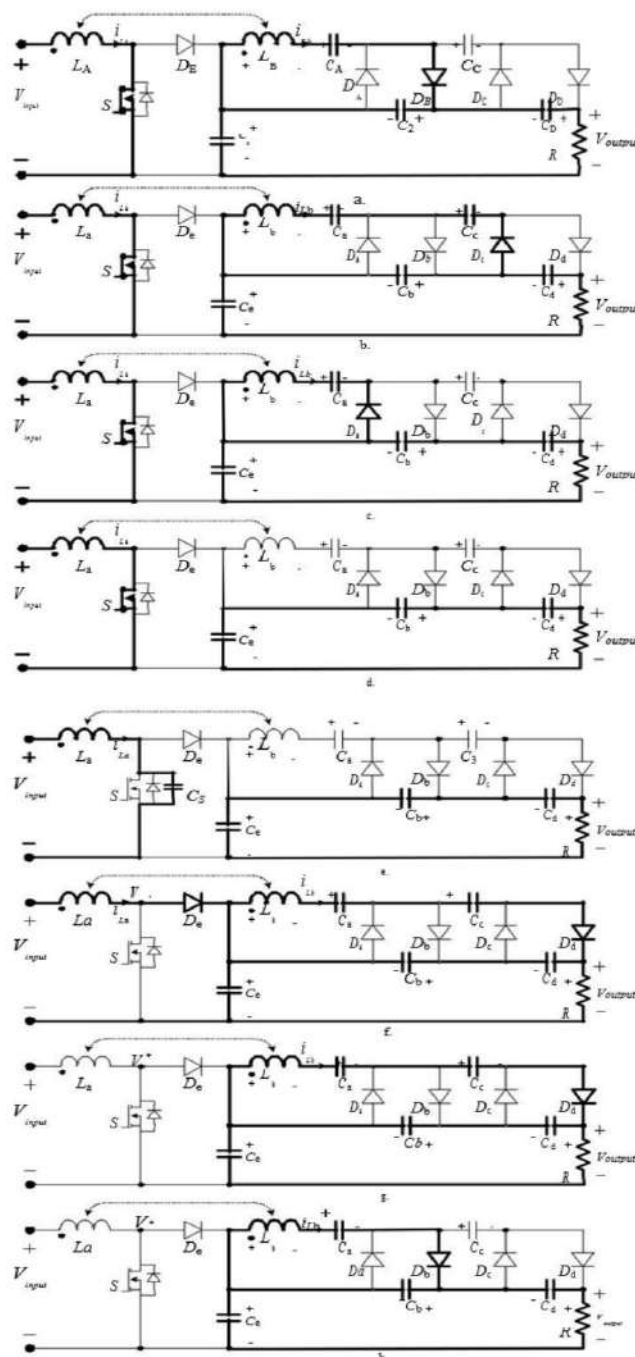


Figure 2: Switching Topology of the proposed system

D. DC ANALYSIS

The operating conditions under various pulsating DC are shown in fig 2.

We took the following hypothesis:

Magnetic coupling ratio, $K=1$

and in all system $V_{Lb} = nV_{La}$

Voltages are constant in the steady state regime (actually there are small ripples of these voltages)

As in case of conventional Boost Converter the voltage value on the C_e (capacitor)

$$V_{C_e} = V_{input} / (1 - D)$$

In advance analysis we are using the subsequent relations: The voltages on the main (primary) inductance: $V_{La.on} = V_{input}$;

$$V_{La.off} = V_{input} - V_{ce} = V_{input} - V_{input} / (1 - D)$$

$$(i.e.), = - V_{input} * D / (1 - D)$$

Here the term D refers to the duty cycle.

The voltages on the subordinate (secondary) inductance:

$$V_{Lb.on} = V_{input};$$

$$V_{Lb.off} = -n V_{input} * D / (1 - D)$$

The voltage V_{ca} can be found using Kirchoff's equation at

the respective interval:

$$V_{Lb.on} + V_{ca} = 0$$

So:

$$V_{ca} = -V_{Lb.on} = -n * V_{input};$$

The voltage V_{cb} can be found conferring to the respective interval:

$$V_{Lb.off} + V_{ca} + V_{cb} = 0$$

So:

$$V_{cb} = -V_{Lb.off} - V_{ca} = n V_{input} * D / (1 - D) + V_{input}$$

$$= n * V_{input} / (1 - D)$$

The voltage V_{cc} can be found with the help of Kirchoff's equation for the interval:

$$V_{Lb.on} + V_{ca} + V_{cb} + V_{cc} = 0$$

So:

$$V_{cc} = -V_{Lb.on} - V_{ca} - V_{cb} = -n * V_{input} + n * V_{input} - n * V_{input} / (1 - D) = -n * V_{input} / (1 - D)$$

The voltage V_{cd} can be found according to the time interval :

$$V_{Lb.off} + V_{ca} + V_{cb} + V_{cc} + V_{cd} = 0,$$

so:

$$V_{cd} = -V_{Lb.off} - V_{ca} - V_{cb} - V_{cc} = n * V_{input} * D / (1 - D) + n * V_{input} - n * V_{input} / (1 - D) + n * V_{input} / (1 - D) = n * V_{input} / (1 - D)$$

And finally the output of the voltage multiplier;

$$V_{output} = V_{cb} + V_{cd} + V_{cc} = n * V_{input} / (1 - D) + n * V_{input} / (1 - D) + V_{input} / (1 - D) = V_{input} * ((1 + 2n) / (1 - D)).$$

In general case for number of diode-capacitors cells

$$N = 6, 8, 10, \dots \text{ One can easily obtain..}$$

$$\text{Gain} = V_{output} / V_{input} = (1 + (N/2)n) / (1 - D).$$

IV. SIMULATION RESULTS

A prototype with 160 Volts rating was built to verify the validity of the proposed converter. The system specifications and components of the prototype are summarized below. Moreover, Matlab/Simulink is applied to simulate. Some selected waveforms for simulation using the proposed mathematical model at full-load gives $V_{out} = 160V$ at $V_{in} = 12V$. The mathematic model and control strategy of the proposed converter have been proposed. Some selected waveforms of the proposed converter at $V_o = 128V$, $V_{in} = 12V$, for both simulation and experiment are shown in Figs. Respectively.

V. CIRCUIT DIAGRAM:

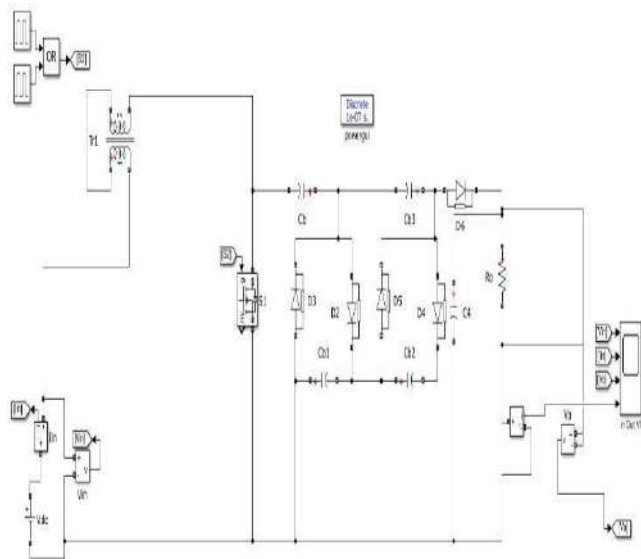


FIGURE 3: Simulink Model of the proposed system

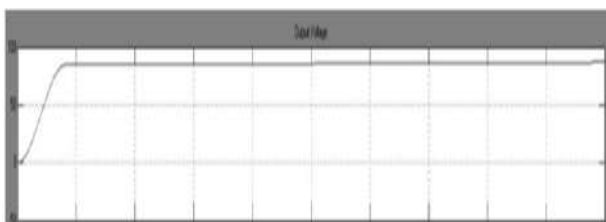


Figure 4: Simulink output for the proposed system.

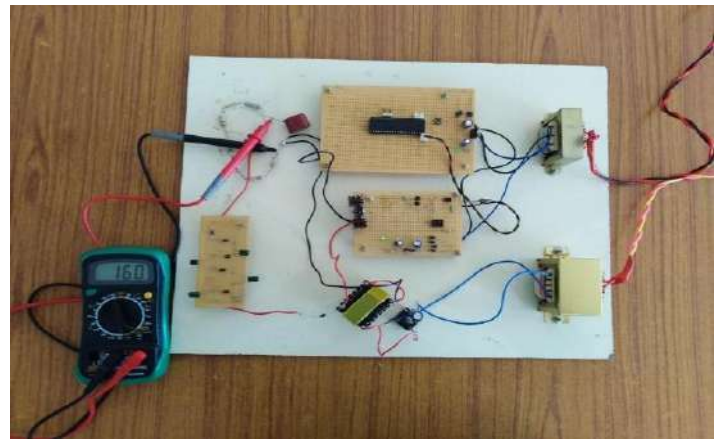


Figure 5 Hardware Prototype of the proposed converter

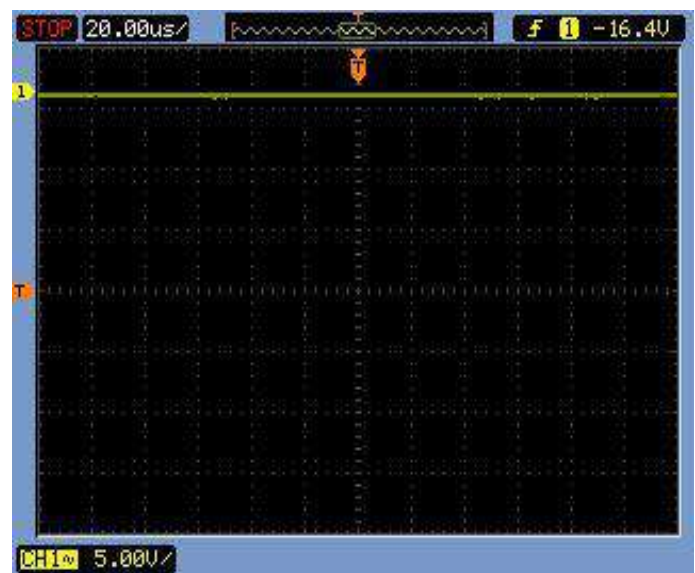


Figure 6 Experimental Result of the system.

VI. EXPERIMENTAL RESULTS:

The hardware setup was implemented by having the input voltage 12V was boosted upto 160V .the hardware set up is shown in figure.5 and the experimental result in figure 6.The Tables 1&2 explained the parameters and the components list used in the proposed system.

Table 1. MAIN PARAMETERS OF PROPOSED CONVERTER

PARAMETER	DEFINITION	VALUES
V_{IN}	INPUT VOLTAGE	12V
V_{OUT}	OUTPUT VOLTAGE	160V
f_s	SWITCHING FREQUENCY	10MHz
D	DUTY CYCLE	0.85
R_o	RESISTIVE LOAD	55MΩ
K	URNS RATIO	1

Table 2.MAIN COMPONENTS OF PROPOSED CONVERTER:

COMPONENT	SPECIFICATIONS	
	TYPE	CHARACTERISTICS
DIODE	1N4007S	V _{RRM} : 1000V I _{FSM} : 30A I _o : 1A
VOLTAGE REGULATOR	KA7805, 7812CV	POSITIVE 5V AND 12V 1A
TRANSISTOR(NPN)	SPS42	V _{CBO} =300 V V _{CEO} =300 V V _{EBO} =6 V
TRANSISTOR(PNP)	SPS92	V _{CBO} =300 V V _{CEO} =300 V V _{EBO} =6 V
OPTOCOUPLER	FL817C	4 PIN DIP (CTR: 50~600% at I _F = 5mA, V _{CE} = 5V)
MOSFET	IRF630FP	V _{DS} -200V R _{DS} - 0.40 Ω I _D - 9 A
MICROCONTROLLER	PIC16F877 A	40 pin dip 5v
BRIDGE RECTIFIER	MICBR1010	V _{rms} =700V V _{rm} =1000V V _{dc} =1000V
CRYSTAL OSCILLATOR	YXC 200SD	20Mhz

VII. CONCLUSION

By using a switched-Coupled Inductor in combination with a Cockroft-Walton voltage multiplier effect, also very high voltage gain was accomplished. The scheme provides a soft switch and diode switches automatically. The circuit structure is simple and rational variety of the coupling coil turns ratio and the number of multiplier cells provides a very high voltage gain at the Boost Converter's duty cycle of 0.75. The Very high gain is obtained by cascading diodes and capacitors which is robust and simple.

VIII.REFERENCES

[1]R.-J. Wai, R.-Y. Duan, "High step-up converter with coupledinductor," IEEE Trans. Power Electron., vol.20, no.5, pp.1025-1035, Sept. 2005.

[2]Q. Zhao, F.C Lee, "High performance coupled-inductor DC-DC converters," in Proc. 2003 IEEE Applied Power Electronics Conference, vol. 1, pp. 109- 113.

[3]D.M. Van de Sype, K. De Gusseme, B. Renders, A.R. Van den Bossche, J.A. Melkebeek, "A single switch boost converter with a high conversion ratio," in Proc. 2005 IEEE Applied Power Electronics Conference , vol. 3,1581- 1587.

[4]K.C. Tseng, T.J. Liang, "Novel high-efficiency step-up converter," in Electric Power Applications, IEE Proceedings - , vol.151, no.2, pp.182-190, Mar 2004

[5]B. Axelrod, Y. Berkovich, A. Ioinovici, "Switched coupled-inductor cell for DC–DC converters with very large conversion ratio," in Proc. 2006 IEEE Industrial Electronics Conf. , pp. 2366–2371.

[6]Y. Berkovich, B. Axelrod, "Switched-Coupled Inductor cell for DC-DC converters with very large conversion ratio,"Power Electronics, IET , vol.4, no.3,pp.309-315, March 2011.

[7]J.C. Rosas-Caro, J.M. Ramirez, F.Z. Peng, A.Valderrabano, "A DC– DC multilevel boost converter," Power Electronics, IET , vol.3, no.1, pp.129-137, January 2010.

[8]S.V.Araujo, R.P.T Bascope, G.V.T. Bascope, L. Menezes, "Step-up converter with high voltage gain employing three-state switching cell and voltage multiplier," in Proc. 2008 IEEE Power Electronics Specialists Conference, pp.2271-2277.

- [9]M. Prudente, L.L. Pfitscher, G. Emmendoerfer, E.F. Romaneli, R. Gules, "Voltage Multiplier Cells Applied to Non-Isolated DC–DC Converters," IEEE Trans. Power Electronics, vol.23, no.2, pp.871887, March 2008
- [10] B. Axelrod, Y. Berkovich, A. Shenkman, G. Golan, "Diode-capacitor voltage multipliers combined with boost-converters: topologies and characteristics," Power Electronics, IET, vol.5, no.6, pp.873-884, July 2012
- [11] B. Axelrod, Y. Beck, Y. Berkovich, "High step-up DC– DC converter based on the switched-coupled-inductor boostconverter and diodecapacitor multiplier: steady state and dynamics," Power Electronics, IET, vol.8, no.8, pp.1420-1428, 2015.
- [12] Kjaer, S.B.; Pedersen, J.K.; Blaabjerg, F.; "A review of singlephase grid-connected inverters for photovoltaic modules", IEEE Trans. on Ind. Appicat., vol.41, no.5, pp. 1292- 1306, Sept.Oct.2005.
- [13]S. Sathyan, H. M. Suryawanshi, M. S. Ballal, and A. B. Shitole, "Softswitching dc-dc converter for distributed energy sources with high stepup voltage capability,"IEEETrans. Ind. Electron., vol. 62, no. 11,pp7039–7050, Nov. 2015.
- [14]H.-W. Seong, H.-S. Kim, K.-B. Park, G.-W. Moon, and M.-J. Youn, "High step-up dc-dc converters using zero-voltage switching boost integration technique and light-load frequency modulation control," IEEE Trans. Power Electron., vol. 27, no. 3, pp. 1383–1400, Mar. 2012.
- [15] Zhao, W. Li, and X. He, "Single-phase improved active clamp coupled-inductor-based converter with extended voltage doubler cell," IEEE Trans. Power Electron., vol. 27, no. 6, pp. 2869– 2878, Jun. 2012.
- [16]M. Das and V. Agarwal, "Design and analysis of a highefficiency dc-dc converter with soft switching capability for renewable energy applications requiring high voltage gain," IEEE Trans. Ind. Electron., vol. 63, no. 5, pp. 2936–2944, May. 2016.
- [17]T.-F. Wu, Y.-S. Lai, J.-C. Hung, and Y.-M. Chen, "Boost Converter with Coupled Inductors and buck–boost type of active clamp," IEEE Trans. Ind. Electron., vol. 55no. 1, pp. 154–162, Jan. 2008.
- [18]S. Dwari and L. Parsa, "An efficient high-step-up interleaved dc–dc converter with a common active clamp," IEEE Trans. Power Electron., vol. 26, no. 1, pp. 66–78, Jan.2011.
- [19]T.-F. Wu, Y.-S. Lai, J.-C. Hung, and Y.-M. Chen, "Boost Converter with Coupled Inductors and buck–boost type of active clamp," IEEE Trans. Ind. Electron., vol. 55, no. 1, pp. 154–162, Jan. 2008.

DESIGN for 1KVA 1 ϕ SOLAR HYBRID INVERTER for DOMESTIC LOADS

G.KIRUTHIKA

Department of Electrical and Electronics Engineering,
Saranathan College of Engineering,
Panjapur, Trichy, Tamil Nadu, India.
kiruthikagreets@gmail.com

Dr.C.KRISHNAKUMAR

Department of Electrical and Electronics Engineering,
Saranathan College of Engineering,
Panjapur, Trichy, Tamil Nadu, India.
krishnakumar-eee@saranathan.ac.in

Abstract - This paper proposes about the solar PV off-grid inverter that employs two or more source other than PV which senses the presence of solar power, grid power and has dual functionality to manage the inputs from both solar panels and battery bank. Accordingly, it gives the selection and orientation for charging batteries with either solar PV panels or electricity grid based on energy storage consumption. The main idea of the topology is to utilize single conversion which improves the efficiency, feasibility and reducing loss.

Key words - Pure sinewave output, Solar Priority Charge Controller(SPCC), Digital display, Battery, Solar photovoltaic (PV), inverter.

I.INTRODUCTION

There is an increase in the energy demand due to world's population growth and techno-economic growth, particularly in developing countries which has become a significant part of our daily life. There is either lack for sufficient infrastructure to supply energy or insufficient of fuel at reasonable cost. There is a huge shortage for energy requirement and it can be consumed in the form of coal, hydro, nuclear and other renewable energy sources to fulfill our demands. Among the non-renewable energy resources, the fossil fuels are virtually inexhaustible and take millions of years to form naturally, although their rate of replenishment is not known. There exists scarcity of fossil fuels which cause environmental pollution and threaten irreversible change to the global climate. The conversion of nuclear energy doesn't pollute the environment but it is highly hazardous to plant and wildlife if not properly disposed and it is associated with potentially dangerous radioactive contamination which is harmful for human beings. In case of renewable energy resources, the hydroelectric power plant and wind turbines significantly take longer time for installation and disturb the ecology of the area by way of uprooting people.

For instance, the solar radiation energy is infinite and reaches the earth in the form of electromagnetic radiation. A solar cell in the PV module converts radiation energy into electrical energy. It doesn't need any several steps for converting the solar irradiation. The electricity generated by PV module can be used in a decentralized manner in small quantities which is an obvious path to flow, when compared to the fossil fuels. In order to make solar PV electricity affordable, the cost of solar PV systems is decreasing rapidly.

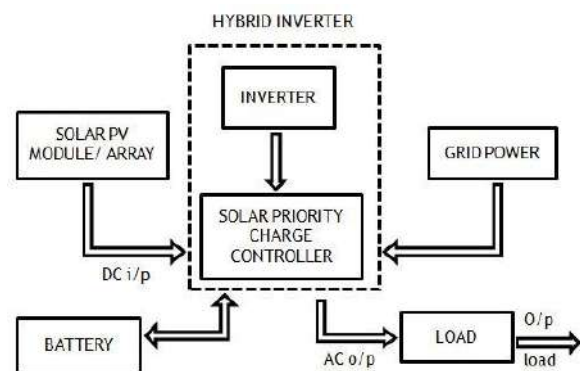


Fig. 1 Block Diagram of Solar Hybrid Inverter

During the non-sunshine hours, PV module output is zero and the PV panels are connected in parallel. The Tubular electrode batteries are used which is necessary to balance the power demand that varies with function of time. To ensure good performance, Solar Priority Charge Controller controls the charging and discharging level of the battery. In hybrid mode, the inverter has dual functionality which can simultaneously manage the dc input either through solar radiation or grid power. The PWM pulses are generated through the microcontroller and the four drives output are fed to the driver section. The LCD displays the indications for grid on, inverter on, solar on, backup mode, etc.

II. DESCRIPTION OF THE TECHNOLOGY

A. Solar PV module:

More than 80 percent of solar PV modules are currently provoked from crystalline silicon solar cells (c-Si) while the rest are made up of thin-film and multi-junction technologies. In contrast, the solar radiation energy is dependent on location where the system is to be installed. The increase in need of electricity depends on the physical size of the module.

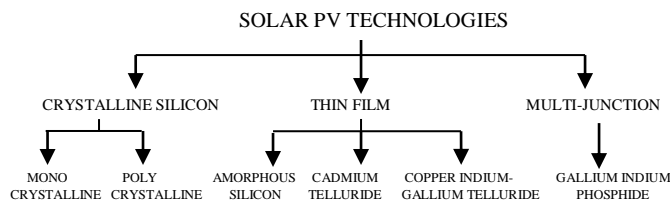


Fig. 2 Types of Solar PV Technologies

Module electrical connections are connected in series then their voltage get added up to achieve a desired output voltage and currents in parallel get added up to provide a required current capability. Both series and parallel combination of solar PV module is known as solar PV array.

B. Battery:

The selection of a battery is done depending on the battery parameters. The batteries for photovoltaic systems must be rechargeable, easily serviced and allow deep discharge with low-self discharge. Either, batteries used for PV systems are frequently charged and discharged or it should meet the high number of charging - discharging cycles. Hence, Lead-acid deep cycle batteries are used for PV system applications. In Lead-acid batteries, Flat-plate electrode designs are used for car battery applications where as the Tubular electrode batteries are used for PV applications. It ranges from 1-12000 Ah, 500 to 800 charge-discharge cycles with voltage ratings of 6 V, 12 V, 24 V. When the required PV system voltage is higher than the terminal voltage, batteries are connected in series and in parallel when required PV system capacity is higher than the individual battery capacity. Batteries obtain both high voltage and high capacity in mixed-type connection. For example, the life cycle of battery is 3 years; if it is discharged continuously below its DoD (Depth of Discharge) then it will stop functioning within 6months.

C. Solar Priority Charge Controller:

Though surplus, solar irradiation is an unpredictable source of energy. It varies with function of time and a backup energy source such as batteries are necessary to balance the power

demand. By measuring the voltage level of the batteries, over-charge and over-discharge status is spotted. In charge controllers, SPCC converts the existing normal inverter into a solar inverter and control the charging and discharging level of the battery. To ensure good performance, it continuously tracks the solar voltage, battery voltage, grid voltage and prefers to run the load without affecting the battery status. Hence, during night applications, an automatic mains change over take place when necessary.

D. Microcontroller

The 40/44-pin devices have five I/O ports, fifteen interrupts and eight A/D input channels where as the high and low pulses are generated using the PIC microcontroller at high frequency. The DC operating speed is 20MHz with DC clock input 200ns instruction cycle. Not only it has In-Circuit Serial Programming with 5V single supply but also have wide operating voltage range (2.0 to 5.5V). It has programmable code protection with selectable oscillator options and inbuilt A/D converter.

E. Inverter

The device which converts dc power to form a desired ac output voltage and frequency. The dc power input to the inverter is obtained from solar PV array or electricity grid. The hybrid inverters can manage solar irradiation, electrical grid and battery, which are coupled directly to the unit. Therefore in hybrid mode, the inverter has dual functionality which can simultaneously manage the dc input either through solar radiation or grid power.

F. LCD Display

A Liquid Crystal Display (LCD) is a flat-panel display which is the most enduring technologies and has become affordable. Due to low power consumption, small amount of heat emitted during the operation. The LCD is powered by 5V power supply and 16 characters with 2 lines alphanumeric display is used. Indications for grid on, inverter on, low battery, charging/discharging, overload and backup mode is displayed.

III.METHODOLOGY

When the photons in the sunlight fall on a solar PV module, it converts the solar radiation to electrical energy. Around mid – day, solar radiation is at peak generation. Unfortunately, the availability of solar irradiation throughout the day is not constant. Under cloudy conditions, the solar insolation intensity of PV array varies continuously even if sun is

available. In such a scenario, partial shading pattern decreases the power output and also changes the electrical characteristics of the PV array. A modified configuration is essential when the electricity demand is more than the electricity generation. Under such conditions, batteries are required in hybrid PV systems other than the solar radiation and electricity grid. Over-charge and over-discharge condition of the battery is checked by measuring the battery voltage level whereas the Solar Priority Charge Controller continuously tracks the solar voltage, battery voltage, grid voltage and the load run without affecting the battery status . In case of hybrid PV system, both PV and other sources operate simultaneously.

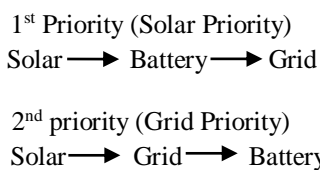


Fig. 3 Solar Priority Logic

Solar Priority Charge Controller (SPCC) plays a major role on hybrid part. It is mainly built with two priorities. One of them is grid priority - used in homes, hostels and the other is solar priority- used in colleges. Depending on the customer needs, the solar priority logic is used. The jumper J9 is given to the 22nd pin of microcontroller which acts as a switch in priority

setting. During day time or mid-day, the jumper J9 will be in open condition then 1st priority is selected. Here, the battery is fully charged by solar radiation energy and SPCC will obstruct the grid power. If the solar radiation and battery charge is insufficient to meet the load requirement, the jumper J9 is closed and 2nd priority is selected. Hence, the energy demand of the load is met by grid power and the Solar Priority Charge Controller will permit the grid connectivity to charge the battery. Once the battery is fully charged, SPCC cuts-off the electrical grid for protecting the batteries from overcharge and over-discharge conditions which help to preserve their life span and performance. For the above two priority conditions, the 9th pin and 3rd pin of the microcontroller is verified simultaneously for solar radiation and battery sensing. Under grid condition, practically, the 2nd pin senses the grid voltage which is to be read and displayed, followed by 34th pin that ensures the presence of grid. The microcontroller accepts the grid power, when both the 2nd and 34th pin is present. The microcontroller program is usually fed through MCLR (1st pin) but involves the combination of MCLR (1st pin), power supply (32nd pin) and ground (31st pin). Through solar irradiation, solar PV generates direct current electricity from solar radiation with the help of DC to AC converter. Not only an inverter converts the battery voltage to 220V ac signal but also charges the battery in the grid condition. These inverters have predominant interface between the solar PV module and the load.

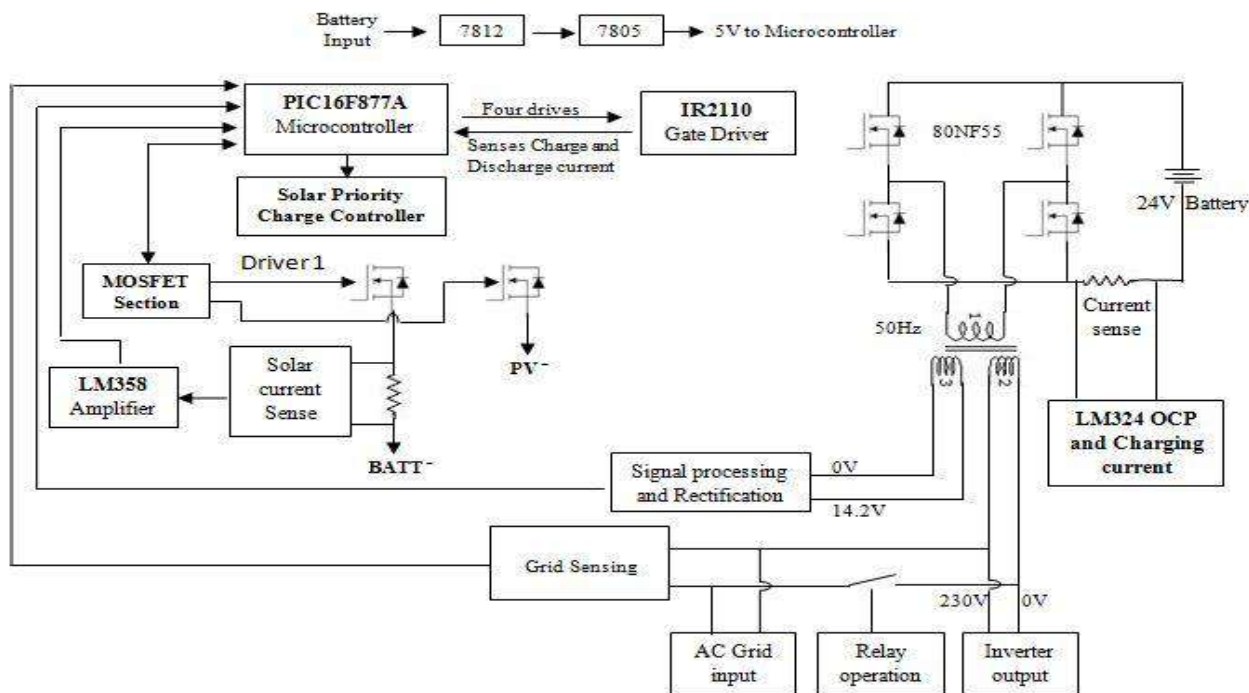


Fig.4 Pure Sine wave Inverter Design

In inverter mode, the relay between AC input and the inverter output will remain open when the AC input is not in an appropriate range or AC fails. The PWM pulses are generated through the microcontroller and the four drives output are fed to the driver section (IR2110) as High1- Low1 and High2 - Low2 pulses. In full-bridge topology, the MOSFET driver/ gate driver receives the low-power inputs from the microcontroller and provokes appropriate high-current gate drive for power MOSFETs. Now, the H-bridge circuit fed 50Hz to the transformer which boost the 14.2V (primary) to 230V (secondary) and the output of secondary side transformer contains 200µF capacitor that filters the distortion to form pure sinewave output. The bridge output voltage is sensed through the auxiliary secondary winding of (0-14)V is used for feedback mode. Using LM324 comparators, the amplified voltage output is compared with predetermined value, if either over current discharge (ODC) or over current charge(OCC) limit is crossed then PWM is immediately shutdown or short circuited.

In the grid mode, the relay between grid AC input and the inverter output is closed when the AC input is within valid range. When the input AC is given to the transformer, the full bridge topology consisting of MOSFETs (80NF55) are driven with the help of microcontroller to charge the battery where both the high-side MOSFETs is switched off and both lower side MOSFETs is grounded in the H-bridge are switched at same time. Once the lower MOSFETs are turned on at same time and generated voltage is boosted across the leakage inductance (primary) connected to H-bridge and the energy stored in the primary inductance flows through high-side MOSFETs body diode whereas each body diode of high-side MOSFETs conducts on AC half cycle. Therefore, charging current is proportional to the duty cycle of the PWM switching on lower side MOSFETs.

IV.DESIGN CALCULATION

A. Parameters of Solar Cells

A solar cell performance depends on the parameters of solar cells which determine the effectiveness of sunlight, particularly the amount of power it will produce in a given condition for electricity conversion.

- 1) *Short circuit current (I_{sc})*: It is the maximum current produced by the solar cell where J_{sc} - short circuit current density and A - solar cell area.

$$I_{sc} = J_{sc} * A$$
- 2) *Open circuit voltage (V_{oc})*: It is the maximum voltage produced by the solar cell. The terminal voltage is less than the open circuit voltage.
- 3) *Current at maximum power point (I_m) and Voltage at maximum power point (V_m)*: Both can be attained through current – voltage curve

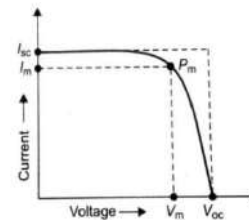


Fig.5 Typical I-V Curve of Solar PV cell

- 4) *Maximum power point (P_m)*: Higher the P_m , the better is the cell and it is also referred as W_p or W_{peak} .

$$P_m \text{ or } P_{max} = I_m * V_m$$
- 5) *Fill Factor (FF)*:

$$FF = \frac{I_m * V_m}{I_{sc} * V_{oc}} = \frac{P_m}{I_{sc} * V_{oc}}$$
- 6) *Efficiency (η)*: According to Standard test conditions (STC), the input power for solar radiation (P_{in}) is considered as 1000 W/m².

$$\eta = \frac{P_m}{P_{in}} = \frac{I_{sc} * V_{oc} * FF}{P_{in} * A}$$

B. Parameters of a Solar Module

A solar PV module comprises of same set of parameters similar to solar cell parameters and the electrical parameters of solar PV module can be obtained with the help of I – V curve.

C. Parameters of Batteries

The battery parameters are very important for identifying and knowing the design, installation, maintenance and performance of the battery.

- 1) *Battery terminal voltage (V)*: 6 v and 12 v battery ratings are available in solar PV system applications.
- 2) *Battery storage capacity (C)*: Capacity of the battery is given in terms of ampere-hour (Ah).

$$\text{Capacity (C)} = \text{Current (A)} * \text{Hour (h)}$$

3) *Energy stored (Wh) :*

$$\text{Energy} = \text{Capacity (Ah)} * \text{Voltage (v)}$$

Battery power (W):

$$\text{Power} = \text{Terminal voltage (v)} * \text{Current drawn (A)}$$

4) *Charge or Discharge Rate:*

One cycle of battery = One charging cycle + One discharging cycle.

$$\text{C-rating (A)} = \frac{\text{Battery capacity (Ah)}}{\text{Full charge or discharge duration (h)}}$$

5) *Battery Efficiency (η):* The battery efficiency can be expressed in Ampere-hour (or) Watt-hour efficiency. The ampere-hour efficiency is used to calculate the panel array for solar power requirement calculations.

$$\text{Ah efficiency} = \frac{\text{Discharged energy (Ah)} * 100\%}{\text{Charging energy (Ah)}}$$

V.HARDWARE IMPLEMENTATION

A. Working on Hardware

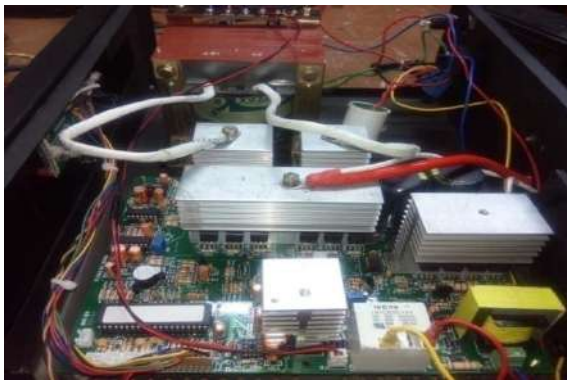


Fig. 6 Hardware model for Solar Hybrid Inverter

Boards without components are usually bare-board tested for shorts and opens. In order to reduce the chance of failure, the PCB is tested to avoid the errors and problems that have been overlooked during production stage. The components may include capacitors, resistors, diodes, transistors, connectors and fuses need to be tested for any signs of irregularities and malfunctions. The components are selected using bill of materials and soldered onto the PCB board.

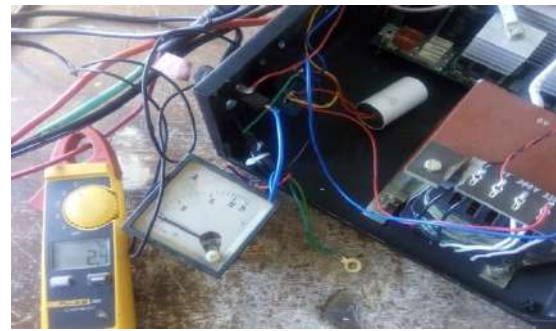


Fig. 7 current obtained on 1st priority



Fig.8 current obtained on 2nd priority

B. Switching waveform



Fig. 9 Positive half cycle on High-side MOSFETs

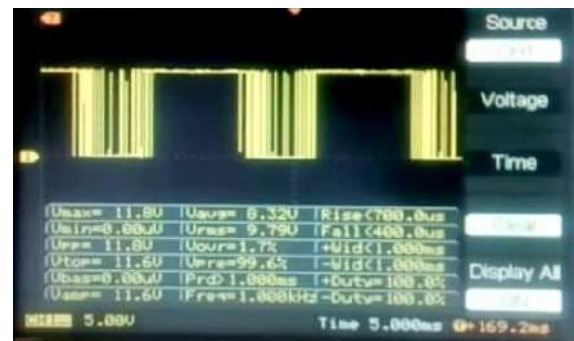


Fig. 10 Negative half cycle on Low-side MOSFETs

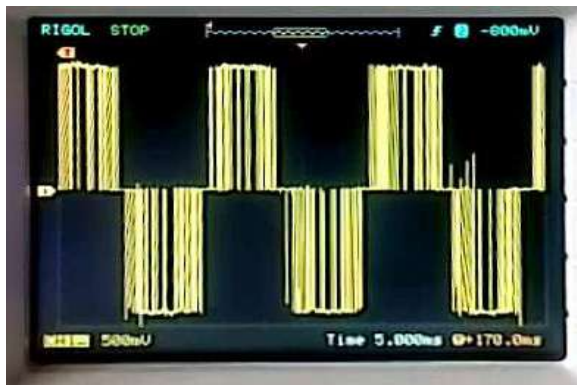


Fig. 11 The Full-Bridge output after switching

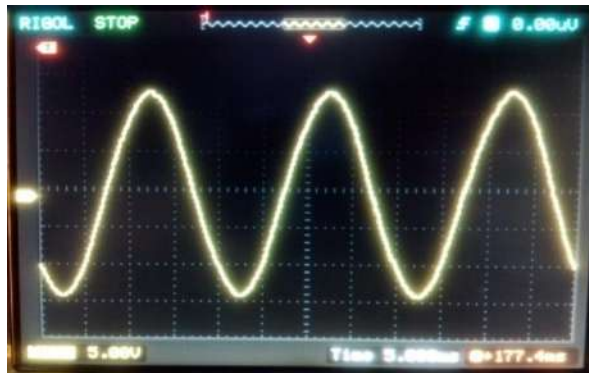


Fig. 12 Inverter's Output at load with 24V battery input

C. LCD display



Fig.13 Hybrid mode of an inverter when solar radiation is present



Fig.14 Solar current obtained in solar priority



Fig.15 Grid voltage obtained in grid priority



Fig.16 Output load when backup mode is On

VI.CONCLUSION

As there is a huge shortage for energy requirement where the energy can be consumed in the form of renewable energy sources. The proposed control strategy is designed to give maximum benefit from solar radiation and the intelligent battery charging which ensures more battery life. It enables pure sinewave output with low TDH and has user – friendly LCD display mode of operation. Depending upon the load requirement, an individual can generate one’s own energy in a sustainable manner which is eco-friendly and had future scope. As it has no potential damage and poised to grow strongly in upcoming years.

REFERENCES

- [1] Chetan Singh Solanki, *Solar Photovoltaic Systems and Technology*. 2013.
- [2] Monisha, M.Jyothi, SD Sundar Singh Jebaseelan and G.Natarajan, “**Hybrid solar inverter for grid synchronization.**” *Circuit Power and computing Technologies (ICCPCT),2015 International Conference on IEE,2015.*
- [3] S.Z.Mohammed Noor,A.M.Omar,N.N.Mahzan,and I.R.Ibrahim,“A review of single-phase single stage inverter topologies for photovoltaic system,”in *4th IEEE Control Syst.Graduate Res. Colloq.,Aug, 19-20,2013,pp.69-74.*
- [4] Neupane,Krishna,Tore Marvin Undeland,and Amit Rouniyar.”**Smart controller design for solar-grid hybrid system:Microcontroller based automatic adjustable discretized solar-grid integration system.**”*Intelligent Green Building and Smart Grid(IGBSG),2014 International Conference on. IEEE,2014*

A SMART SELF DEFENSE MECHANISM for WOMEN'S SECURITY USING SOS

Priyaa Darshini R S¹, Ragavi S², Sangeetha N²,
Swetha Gayathri S², Vijaya Lakshmi K²

[1]Assistant Professor ,Department of Electrical and Electronics Engineering,Saranathan College of Engineering, Trichy,India.
[2]]UG Scholar ,Department of Electrical and Electronics Engineering,Saranathan College of Engineering, Trichy,India.

Abstract—Women now-a-days have become independent and are confident. They have reached heights. But still safety is a major concern outside. Every country has its own laws against domestic violence, sexual assault and other forms of violence to protect their female citizens, yet these laws are not complete in its action. Thus the society has become unjust and insecure for women. Self defense is the need for the hour. They must fight for their own cause .Modern technology plays a vital role here. A protective device employing modern trends in technology is the answer to all women who wants to be safer outside.

Keywords—self designed circuitry, protective device, practical application, compact circuit.

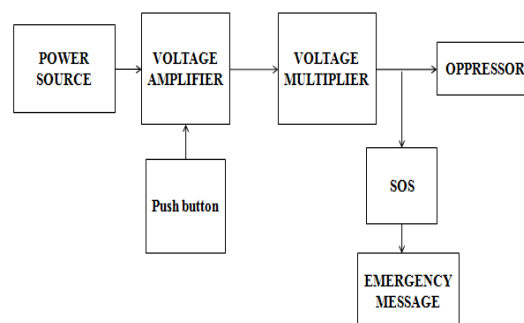
I.INTRODUCTION

Women from past are prone to physical and mental violence. We are still not completely free from these violences. Its now the time to adopt strategies to overcome these pressures from the society.

The device has been made in the form of footwear and is completely electronic. The person with the footwear only has to trigger the circuitry attached with the footwear to attack the oppressor and protect herself from the danger. The circuitry is mounted beneath the footwear .The circuit is properly insulated so that it does not cause any danger to the wearer. A panic button is provided on the footwear straps and can be activated by the wearer on encounter of any violent activity. The surface beneath the footwear gives a daunting

shock to the oppressor and parallelly sends an alert message to the saved contacts. The device is designed such that the oppessor do not collapse with the amount of shock generated, but is rendered weak with muscular contraction in the body .Thus, the wearer can easily overpower any aggressor and can escape from the danger with complete ease. Constant efforts and analysis are made to further include innovations making it an ideal tool for women's safety.

II. BLOCK DAIGRAM



III.MECHANICAL DESIGN

This device is attached to the bottom of the footwear. The electronic circuitry is completely below the footwear. A panic button is provided on the footwear strap. The sole is insulated from the lower part while the bottom surface constitutes of a conducting layer which will transfer the electric shock to the attacker and parallelly sends an SOS message along with the current location to the saved contacts.

IV.ELECTRONICS INVOLVED

The circuit design involves a self designed circuitry. It is designed keeping in mind the effectiveness, safety, size and weight of the circuitry.

A. Transistor

The metal-oxide-semiconductor field-effect transistor (MOSFET) used in our device is BD880, which is a p-n-p silicon transistor. The MOSFET is used for amplifying the electronic signals. This MOSFET's V_{ce} is 60V, V_{cb} is 60V and V_{be} is 7V. It is used as a switch and has a high collector current, which is required by the fly-back transformer.

B. Fly-back Transformer

In our device fly-back transformer is used for amplifying low amplitude oscillating voltage into high amplitude voltage. This device has a small and very light weighted fly-back transformer. It is used because the ratio of turns of the winding is very high and hence use in the applications which requires high voltage and low current. The transformer generates fluctuating high voltages and simultaneously decreases the current.

C. Fly-back driver circuit

The fly-back driver circuit are inbuilt in fly-back transformers and use DC as input, driver circuit provides saw-tooth waves on the coil of the transformer and the output received is in the form of pulsating DC and charges the capacitor. The capacitors are responsible for input as well as output frequencies; hence the frequency can be controlled by altering the values and arrangements of capacitors. The voltage transformer through capacitors combination is low; it needs appropriate proportion of power.

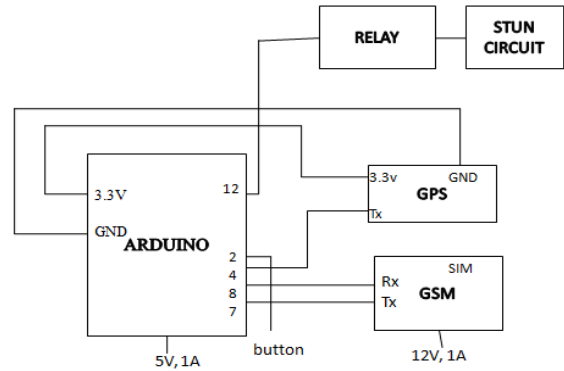
D. Cockcroft Walton Ladder Network

The pulsating DC produced by the transformer is fed into a combinational circuit of capacitors and diode called as Cockcroft Walton ladder network. This is a voltage multiplier network ladder. This circuit is an electric circuit that generates a high DC voltage from a low-voltage AC or pulsing DC input (output of the transformer). The combination of diodes and capacitors is use to generate high voltages. The value of power generated from the circuit will be solely

dependent upon the size of the Cockcroft Walton ladder.

E. SOS Circuit

The SOS circuit comprises of three blocks, which are the arduino control unit, the GPS unit and the GSM unit.



I. The arduino control unit

- The circuitry is controlled by the arduino controller. The Arduino was chosen as it is relatively inexpensive compared to other microcontroller platforms. The Arduino software runs on Windows, Macintosh OSX, and Linux operating systems acting as a cross-platform. Most microcontroller systems are limited to Windows. It is an opensource and extensible hardware and is a simple, clear programming environment. It is programmed to function in such a way that when triggered through the push of a button it commands the GPS unit to send the current coordinates to the GSM unit. Simultaenously it triggers the stun circuit through a relay to simulate a high voltage signal.

II. The GPS unit

The time, position and velocity of any GPS receiver can be found with the help of GPS. The constellations of 27 earth orbiting satellites enable the Global Position System. These 27 earth orbiting satellite includes 24 in operation and 3 extras, in case one fails.

This satellite network was invented by the U.S. military for the purpose of the military navigation system. The unit will be continuously reading the coordinates of the user. Once it receives a signal from the controller it sends the instant to the GSM.

III. The GSM unit

The location points that are received will be sent to presaved numbers with an alert message through the GSM unit. The unit requires a standard sim card for sending the message. The most used her is GSM800A.

Features of GSM800A

- Improved spectrum efficiency
- International roaming
- Compatibility with integrated services digital network (ISDN)
- Support for new services.
- SIM phonebook management
- Fixed dialing number (FDN)
- Real time clock with alarm management
- High-quality speech
- Uses encryption to make phone calls more secure
- Short message service (SMS)

V.RESULT

Under this section the result analysis is discussed. GPS receiver is used to get information of the current position of the object. It is connected to the microcontroller through it's transmit pin through a relay used to control the operation of GPS receiver. When latch is enabled, GPS receiver continuously sends data to the receiver pin of the microcontroller and the required information of longitude and latitude is extracted by the program. The Arduino signals the relay and the relay at the same instant activates the stun gun and the SOS circuitry.

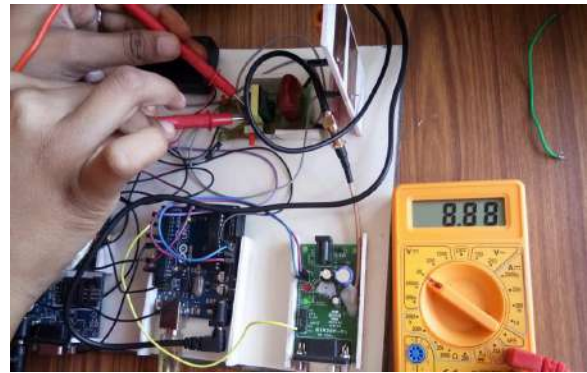


Figure 1: input voltage to the transformer

The voltage builds up as it passes through the fly-back transformer. A high output voltage is obtained at the output terminal. The output voltage is non-lethal but still high enough to immobilize and paralyze a person.

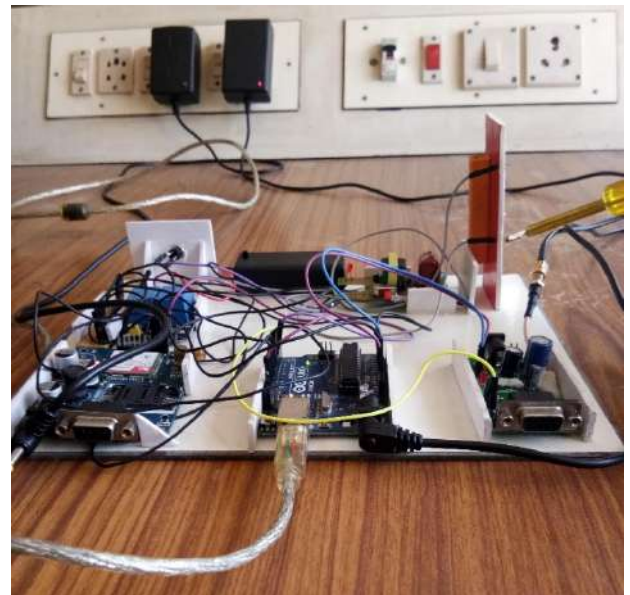


Figure 2: high voltage output

The following figure shows the text message received by the registered contact number. It gives the location of the victim. The location is shared as a link. It gives the exact location with the use of Google Maps application. The number of contacts that receive the message can be customized.

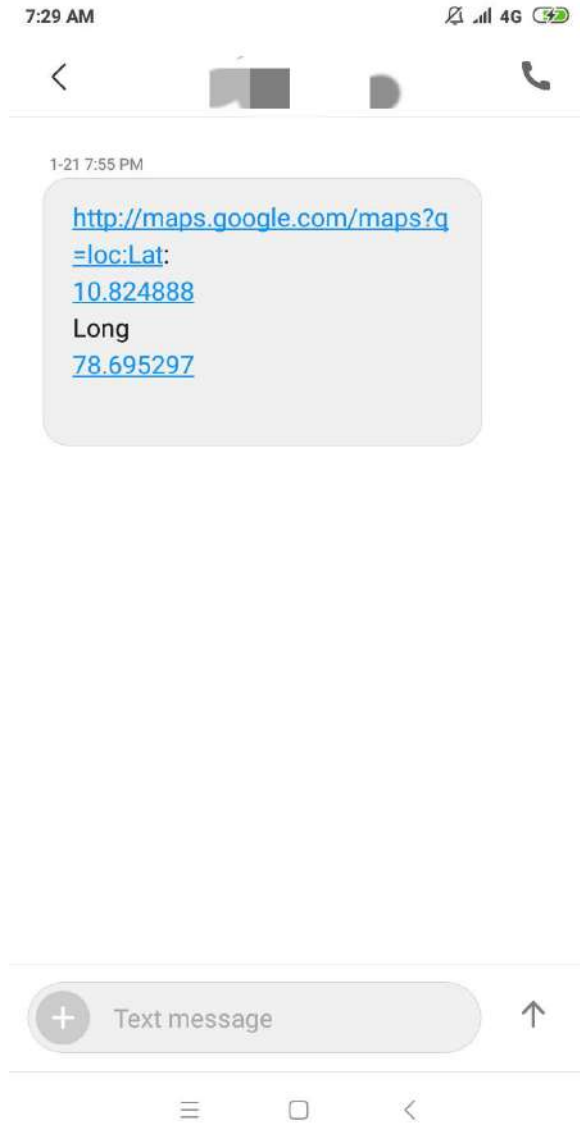


Figure 3: SMS received by registered contact

VI.CONCLUSION

This device simulates shock to paralyse the oppressor non-lethally and simultaneously send an alert message along with the current location. This device is aimed to have minimum network interference.

ACKNOWLEDGEMENT

We sincerely thank our college SARANATHAN COLLEGE OF ENGINEERING,,TRICHY for its extended support and our faculties for their guidelines. We also thank our colleagues who laid a helping hand in our research.

REFERENCES

- [1] Design of a women safety device 2016, Divya Chitkara, Nipun sachdev, Yash Dev Vashisht, IEEE Region 10 Humanitarian Technology Conference (R10-HTC).
- [2] Smart foot device for women safety, Nandita Viswanath, Naga Vaishnavi Pakyala, G. Muneeswari, 2016 IEEE Region 10 Symposium (TENSYP).
- [3] iBrella: A smart parasol Zeeshan Saquib, ECE Dept., BNMIT, Sana Anaum, ECE Dept., BNMIT, Ujwal SS, ECE Dept., BNMIT.
- [4] Nishant Bhardwaj, Nitish Aggarwal, "Design and Development of "Suraksha"-A Women Safety Device", International Journal of Information & Computational Technology, vol. 4, no. 8, pp. 787-792, 2014.
- [5] Premkumar P, Cibi Chakkaravarthy R, Keerthana M, Ravivarman, Sharmila T "One Touch Alarm System for Women's Safety using GSM" International Journal of Science, Technology and management, Volume No 7, Special Issue No 1, March 2015.

PWM RECTIFIERS: STATE OF ART FOR ACTIVE POWER FACTOR CORRECTION

S. SIVASUBRAMANIAN SURENDRAN.K. R M. PAVINTHAN A. AJITH KUMAR
sssmanian97@gmail.com surendranram98@gmail.com pavinthanpapu07@gmail.com thalaasa1999@gmail.com

S. RAMPRASATH

ramprasath-eee@saranathan.ac.in

ELECTRICAL AND ELECTRONICS DEPARTMENT
 SARANATHAN COLLEGE OF ENGINEERING

Abstract— Rectifiers are almost inevitable in all electronic circuits. This paper contains simulation and implementation of a single-phase PWM boost rectifier operating at a unity power factor. The power circuit used is a single-phase full bridge converter made of MOSFET switches. The algorithm used for control provides the regulation of the output DC voltage as well as the control of supply current harmonics. The experimental framework offers several advantages such as: simplified control system, sinusoidal ac line current that satisfies the harmonic current standard IEC 1000-3-2 Class D [2].

Keywords—PWM AC-DC convertors, C2000 based PWM switching, Active power factor correction, Regulated DC voltage.

I. INTRODUCTION

Conventional rectifiers used diode bridge rectifier circuits which has the following demerits,

- i) They produce a lagging displacement factor with respect to the distributed system voltage.
- ii) Increased total harmonic distortion (THD) of ac supply current.

These aspects have a dismissive influence on both power factor and power quality. So, they were replaced with thyristor-controlled rectifiers having good rectification efficiency while it created high level of current harmonics in input current. Harmonic current limits are recommended by the IEC standards (IEC 1000-3-2). The IEC 1000-3-2 International Standard [1] establishes limits to all low power single-phase equipment having an input current with a ‘special wave shape’ and an active input power $P \leq 600W$. Diode rectifier fails to comply with the standard, because the input current is highly distorted, and has a very low power factor due to its large harmonic content. In order to meet these requirements, power-factor correction techniques are essential. Additionally, it is desirable to have minimal size, high efficiency, and low electromagnetic interference Hence, we move on to Pulse width modulated rectifiers made of 4 MOSFET switches triggered by pulse width modulation pulses from C2000 microcontroller. By use of pulse width modulated rectifiers active power factor correction can be

implemented and also nearly sinusoidal input current waveform can be achieved.

II. POWER FACTOR CORRECTION

A. NEED FOR POWER FACTOR CORRECTION

Poor power factor signifies insufficient use of power and increase in the operating cost hence leading to poor performance. By use of power factor correction techniques input current waveform can be shaped into a perfect sinusoidal waveform. This in turn reduces the eddy current loss (I^2R losses), maximizes the real power, saves power bill and decreases the voltage drop.

B. ACTIVE POWER FACTOR CORRECTION

The active power factor correction is used for nonlinear loads. In this technique switching pre regulator is placed in the input side. This pre regulator maintains the dc voltage and checks whether input current is in phase with supply voltage. Hence power factor can be corrected to near unity. This method of power factor correction is of high efficiency with values of power factor varying from 0.9 to 0.95. The conventional method which uses passive filters for power factor correction only results in power factor range of 0.7 to 0.75.

III. PULSE WIDTH MODULATION RECTIFIERS

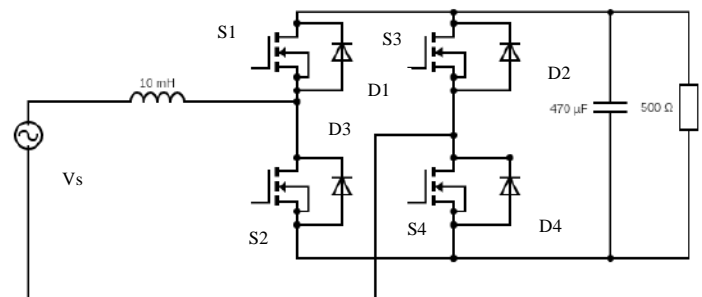


Figure 1: Single phase PWM boost rectifier using MOSFET

Pulse width Modulation (PWM) rectifier is an AC to DC power converter, that is implemented using forced commutated power electronic semiconductor switches. This paper uses MOSFET switches because of its higher

commutation speed and greater efficiency during operation at low voltages. I can also sustain a high blocking voltage and maintain a high current.

PWM rectifiers can be grouped into two types according to power circuit configurations – the current and the voltage type [6]. For current type rectifier, the supply voltage must be higher than the value of the rectified voltage (BUCK CONVERTORS). For voltage type rectifiers voltage on the DC side is greater than the value of the supply voltage (BOOST CONVERTORS). The rectified voltage on the output of voltage type rectifiers is smoother than the output voltage of the current type rectifier. they also require a more powerful microprocessor for their control. Output voltage lower than the voltage on input side can be obtained only with increased reactive power consumption. In this paper a single phase PWM boost type rectifier is designed, simulated and implemented.

A. WORKING

During positive half cycle, S2 operates and D1 D4 conducts. Firstly, the inductor stores energy when S2 is ON. The following circuit diagram depicts the charging of inductor wherein the switch S2 conducts,

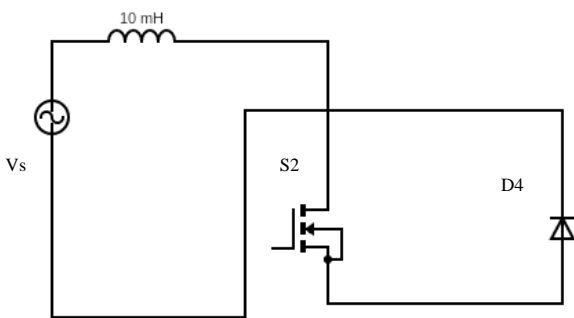


Figure 2: Single phase PWM boost rectifier-inductor charging during positive half cycle

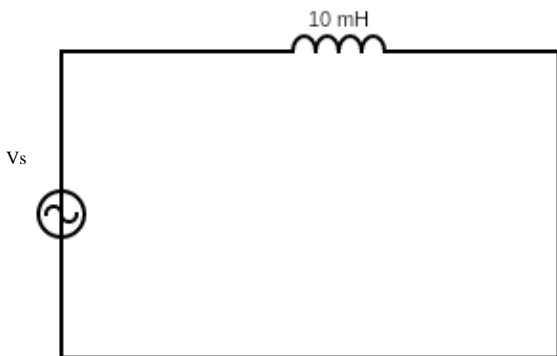
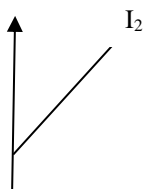


Figure 3: Equivalent circuit for inductor charging in PWM boost rectifier

By using Kirchoff's voltage law,

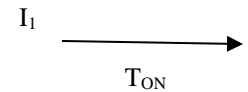
$$V_c = 0$$

$$V_s = L_s (di_s/dt)$$



$$V_s = L_s (I_2 - I_1)/T_{ON}$$

$$I_2 - I_1 = V_s T_{ON}/L_s \quad (1)$$



Then the stored energy gets discharged to the opposite side through diode D1 and D4. This is given by,

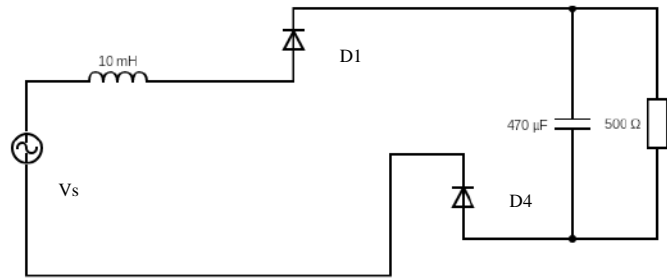


Figure 4: Single phase PWM boost rectifier-inductor discharging during positive half cycle

By using Kirchoff's voltage law,

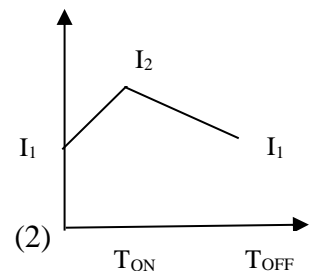
$$V_c = V_{dc}$$

$$V_s = V_L + V_{dc}$$

$$V_s - V_{dc} = L_s di_s/dt$$

$$V_s - V_{dc} = L_s (I_2 - I_1)$$

$$I_2 - I_1 = (V_s - V_{dc}) T_{OFF} / L_s \quad (2)$$



Similarly, for negative half cycle S4 operates, D3 D2 conducts. S4 – D2 – ON for charging the inductor. D3 - D2 – ON while discharging energy to the load.

B. DESIGN EQUATIONS

Inductor and capacitor play an important role in the PWM boost rectifier. Inductor is used for bi-directional power flow and boost operation, while the capacitor is used to maintain the constant DC output for a given period of time and also reduce the output DC ripples. Hence designing of inductance and capacitance have a significant role in the operation. [5]

1) VOLTAGE OUTPUT:

The boosted output DC voltage can be calculated by using (1) and (2) as follows:

By equating (1) and (2),

$$V_s T_{ON}/L_s = (V_s - V_{dc}) T_{OFF} / L_s$$

$$V_s [T_{ON} + T_{OFF}] = V_{dc} T_{OFF}$$

$$V_s T = V_{dc} T_{OFF}$$

$$V_{dc} = V_s T / T_{OFF}$$

$$V_{dc} = V_s T / [T - T_{ON}]$$

$$V_{dc} = V_s(1/(1-D))$$

Where,

D is the duty cycle

2) INDUCTOR DESIGN:

(i) Finding duty cycle,

$$V_{dc} = V_s(1/(1-D))$$

$$1 - D = V_s/V_{dc}$$

$$D = 1 - V_s/V_{dc}$$

(ii) Calculate inductor current,

$$I_L = V_s / ((1 - D)^2 * 100)$$

(iii) Calculate change in inductor current,

$$\Delta I_L = 40\% \text{ of } I_L$$

(iv) Calculate Inductance,

$$L = V_s D / (f * \Delta I_L)$$

3) CAPACITOR DESIGN:

The load current contains both DC current and ripples. Capacitor smoothens DC current with a ripple of maximum 5%.

(i) Finding output voltage ripple,

$$\Delta V_{dc} = 4\% \text{ of } V_{dc}$$

(ii) Finding capacitance,

$$C = D / (100 * (\Delta V_{dc} / V_{dc}) * f)$$

4) SWITCHING FREQUENCY:

In this implementation 10KHz is chosen as switching frequency.

C. DESIGN RESULTS

By using the design equations, the Inductance and Capacitance can be obtained. Using these results the system parameters for simulation can be determined.

PARAMETER	VALUE
OUTPUT VOLTAGE	380V
INPUT VOLTAGE	230V (RMS)
INDUCTOR	2.5mH
CAPACITOR	3.5μF
LOAD RESISTANCE	100 Ω
SWITCHING FREQUENCY	10KHz

Table 1: System parameters for simulation

IV. SIMULATION RESULTS

A simulation platform using Simulink and Power System Block Set under MATLAB was built to evaluate the performance of proposed single-phase boost PWM rectifiers. The system parameters are shown in Table 1. The step time of solution was 100μsec, which is equivalent to 10KHz sampling rate.

A thyristor-based rectifier was taken into consideration and simulated to analyze the input side current. It was found to be non-sinusoidal due to harmonics injection in the source side due to use of thyristor switches.

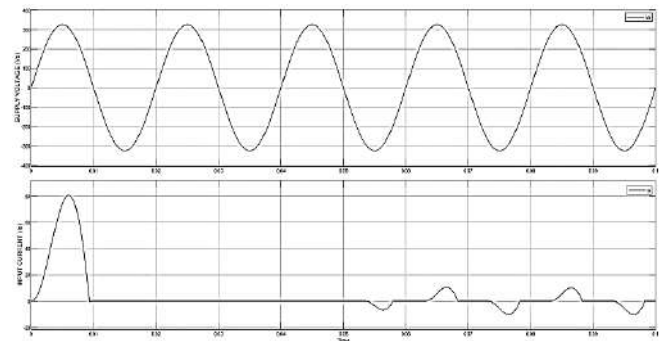


Figure 5: Input current waveform for thyristor rectifier

The proposed single phase PWM boost rectifier was then simulated and the input current was analyzed. The source side current waveform of the proposed rectifier was found to be sinusoidal with comparatively low level of harmonics.

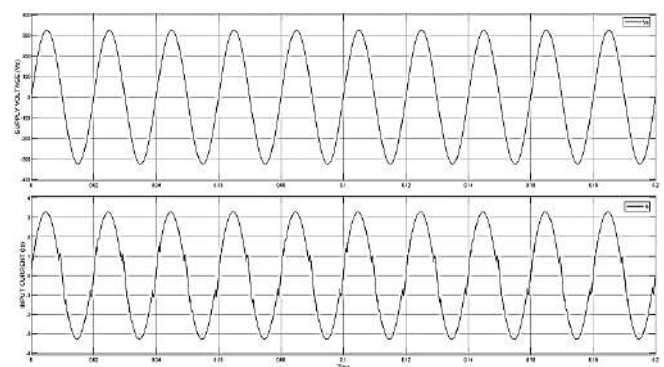


Figure 6: Input current waveform for PWM boost rectifier

In addition to sinusoidal shaping of input current, the current waveform was also found to be in phase with supply voltage waveform. Hence a power factor nearing to unity can be achieved. So PWM rectifiers operated in boost mode can be used for active power factor correction.

V. EXPERIMENTAL IMPLEMENTATION

Figure 7 represents the functional block diagram of the implemented system. Primary connections between the different elements in the complete system are indicated. The software algorithm was implemented using an C2000 embedded microprocessor.

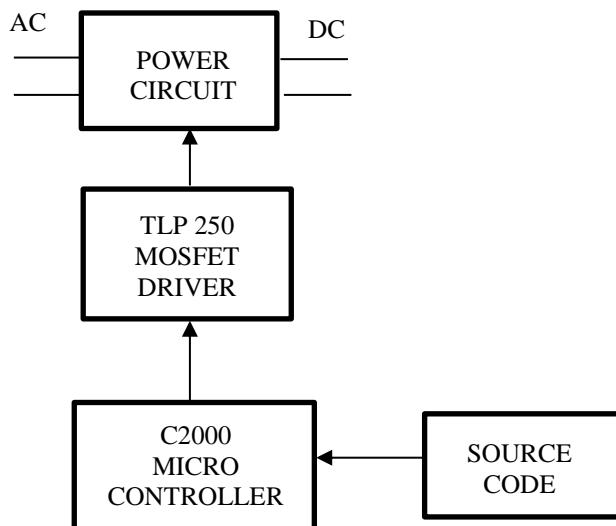


Figure 7: Block diagram for experimentation

The source code for triggering the gate pulses was uploaded to the C2000 microcontroller. The PWM signals from the microcontroller was then fed into the TLP250 isolated gate driver. TLP250 MOSFET DRIVER was designed to operate at 12V DC with switching frequency of 10KHz. The gate and source output coming out of driver was given to the MOSFET switches of the power circuit. The power circuit was powered with AC Voltage Source and the given AC supply was rectified to DC with a boosted level of voltage at the output.

VI. CONCLUSION

In this paper an optimum performance single phase PWM boost rectifier has been implemented using MOSFET transistors as a power switching device. The mathematical model and the experimental verification are presented. The switching algorithm of experimental prototype is implemented using C2000 microcontroller. The experimental results prove that the converter draws a near sinusoidal current waveform with low level of total harmonic distortion. The converter can operate at unity power factor. The ac line current is regulated against load harmonics and fluctuations. This method of power factor correction can be highly effective and can be applied in may industrial applications.

REFERENCES

Standards, Texts, and Review Articles

- [1] *IEEE Recommended Practices and Requirements for Harmonics Control in Electric Power Systems*, IEEE Std. 519, 1992.
- [2] *Electromagnetic Compatibility (EMC)—Part 3: Limits—Section 2: Limits for Harmonic Current Emissions (Equipment Input Current < 16A per Phase)*, IEC1000-3-2 Doc, 1995.
- [3] M. Shen and Z. Qian, "A novel high efficiency single stage PFC converter with reduced voltage stress," *in Proc. IEEEAPEC'01*, 2001, pp.363-367.
- [4] J. Sebastian, A. Fernandez, P. Hernando, and M. J. Prieto, "New topologies of active input current shaper to allow AC-to-DC converters to comply with the IEC-1000-3-2," *in Proc. IEEE PESC'00*, 2000, pp.565-570.
- [5] V. R. Kanetkar and G. K. Dubey, "Economical single phase current controlled unipolar and bi-directional voltage source converters," *in Proc. IEEE PESC'93*, 1993, pp. 862-867
- [6] M. H. Rashid, *Power Electronics: Circuits, Devices, and Applications*, 2nd ed. Englewood Cliffs, NJ: Prentice-Hall, 1993
- [7] R. Martinez and P. N. Enjeti, "A high-performance single-phase rectifier with input power factor correction," *IEEE Trans. Power Electron.*, vol.11, pp. 311-317, July 1996.

Low Cost Smart Cane for Visually Impaired person

Mythili S, Prasanthini S, Shanthi L, Vijithra N

EEE, Saranathan College of Engineering, Tiruchirapalli, India,

Abstract: To enlighten the darkened life of visually impaired people we proudly introduce our innovation-THIRD EYE, smart cane which is to support the life of visually challenged people. Our proposed third eye project is to convert an alternate for a conventional blind stick for visually impaired persons to detect and navigate from place to place without relying on others. We use Microcontroller ARDUINO UNO +Bluetooth module for data collection and to communicate with the user. To detect obstacles of different sizes, we plan to place 3 pairs of ultrasonic sensors at different places in the cane for object recognition. An adjustable mechanism is included to vary the height of the smart cane so that it can be used for all age groups of different heights. The sensor unit and controller unit are placed inside the smart cane. For powering controller and sensor 6F229 volt battery is used

Keywords: Ultrasonic sensor, Bluetooth module, MIT App Inventor, Arduino microcontroller

I. INTRODUCTION

Visual impairment, also known as vision impairment or vision loss, is a decreased ability to see to a degree that causes problems not fixable by usual means, such as glasses^[1]. Some also include those who have a decreased ability to see because they do not have access to glasses or contact lenses^[1]. The term **blindness** is used for complete or nearly complete vision loss^[2]. Visual impairment may cause people difficulties with normal daily activities such as driving, reading, socializing, and walking

The World Health Organization (WHO) estimates that 80% of visual impairment is either preventable or curable with treatment^[1]. This includes cataracts, the infections river blindness and trachoma, glaucoma, diabetic retinopathy, uncorrected refractive errors, and some cases of childhood blindness. Many people with significant visual impairment benefit from vision rehabilitation, changes in their environment, and assistive devices^[2]. Physical movement is a challenge for visually impaired persons, because it can become tricky to distinguish where he is, and how to get where he wants to go from one place to another. To navigate unknown places he will bring a sighted family member or his friend for support. Over half of the legally blind people in the world are unemployed. Because limited on the types of jobs they can do. They have a less percentage of employment.

There are many guidance systems for visually impaired travellers to navigate quickly and safely against obstacles and other hazards faced. Generally, a blind user carries white cane or a guidance dog as their mobility aid. With the advances of modern technologies many different types of devices are available to support the mobility of blind^[3]. Blindness can occur in combination with such conditions as intellectual disability, autism spectrum disorders, cerebral palsy, hearing impairments, and epilepsy. Blindness in combination with hearing loss is known as deaf blindness.

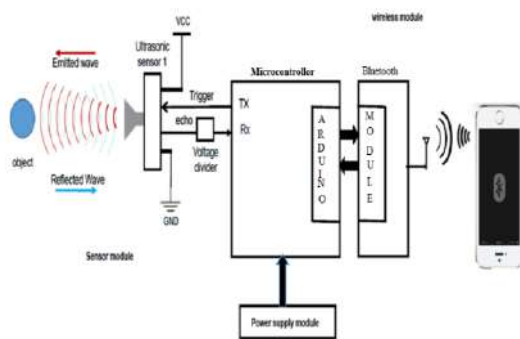
Our proposed idea of helping a visually impaired person is to provide them the highly technological walking cane called smart cane. Cane basically plays an important role in visually impaired people's life.

In order to enhance their life to the next level our proposed design consists of a sensor called ultrasonic sensor (HC-SR04) connected to a microcontroller called ARDUINO UNO.

The stick is made by our own in the material called CPVC (chlorinated poly vinyl chloride) which is stronger and cheaper when compared to PVC pipes, as our project title is low cost smart cane. Ultrasonic (US) and infrared (IR) sensors are

frequently used for mid-range distance measurements [6]. The reason behind choosing Ultrasonic sensor for our project is that it can even be used in sunlight environment, while IR sensor cannot be used so. The fundamental difference between them is that, IR sensors are detecting electromagnetic radiation while ultra sound sensors are detecting mechanical or acoustical energy [7].

The smart cane detects the obstacle using the ultrasonic sensor and send the signals to the Microcontroller ARDUINO UNO [8] for calculating the distance from the cane and size. HC-05 module which is integrated with antenna to transfer the information from microcontroller to the mobile application, where the user can receive the information about the obstacles in the form of voice alert using wireless Bluetooth technology. HC-05 module has to configure to be powered from the UNO microcontroller. The obstacles are differentiated based on the heights because the sensors are place at three different heights in the cane. The cane has an adjustable mechanism which helps different people belonging to different age group can use. It is highly supportive and acts as a third eye to them.



PROPOSED SOLUTION:

Many blind people use cane in order to avoid obstacles. Therefore, we embedded the face recognition system in the cane. Several studies tried to apply to engineering and technology to cane for helping blind people.

A) Sensor module:

Third eye consists of three HC-SR04 Ultrasonic Range Finder. The module has two eyes like projects in the front which forms the Ultrasonic transmitter and receiver. The HC-SR04 ultrasonic sensor uses sonar to determine the distance to an object. The Trigger and the Echo pins are the two I/O pins, they can be connected to the I/O pins of the microcontroller. When the receiver detects return wave the Echo pin goes high for a particular amount of time which will be equal to the time taken for the wave to return back to the sensor. The Echo pin give 5V when goes high, but the controller voltage level is maximum 3.3V, so it's essential to have a voltage divider between sensor and the controller.

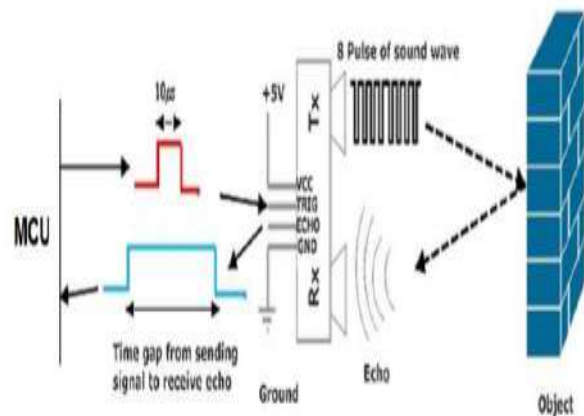


Figure 3 Sensor Module

figure(3):Sensor module.

B) Power supply module: We need to provide 3.7V dc power supply for Launch Pad Bundle and 5V supply for sensors. A separate charging unit is placed to charge the battery from ac supply by ac adopter and a voltage regulator is provided to power the launch pad from the battery.

Fig 2.Overall block diagram

C) Wireless Bluetooth module:

Hardware setup required to set up Bluetooth data transfer

- i) Arduino microcontroller
- ii)Bluetooth Module called HC-05.

Software requirement:

- i. Code Composer Studio™ integrated development environment (CCS 6.1.1.00022).
- ii. IAR Embedded Workbench® v7.3

The system is designed to transform the signal from ultrasonic sensor’s echo pin to the trigger pin of the sensor. The output of the ultrasonic sensor is given to the Bluetooth module HC-05 and that has been given to the application developed by us using MIT app inventor in which the time and the conference location has been displayed whenever the visually challenged one need that information into tactile information to help the blind recognizing obstacles detection in any form. We used object detection and recognition algorithms and layer sensors in order not to allow any object exceed out of the sensor detection range.

The proposed system consists of a sensor, mobile and cane that equip Microcontroller and Bluetooth module and recognized result is sent to

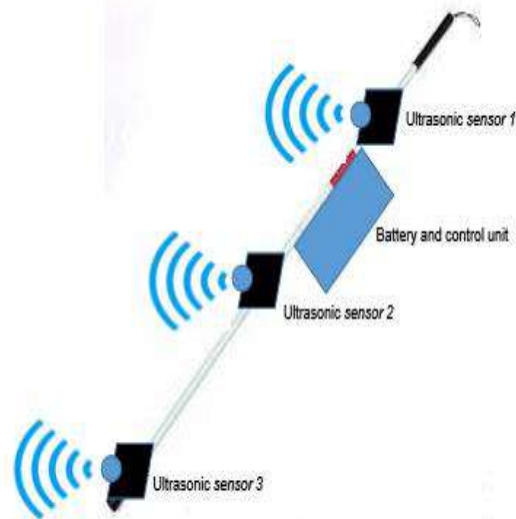


Figure 7 Proposed model THIRD EYE

Figure 1. This figure shows the structure of proposed third eye smart cane

microcontroller of the cane using Bluetooth communication. The result of object recognition is given in a form of number. The cane consists of a microcontroller and Bluetooth module as shown. Microcontroller generates signal using according to result of object recognition. The above two figures says the initialisation and the display of the distance from cane to the object.

II. CONCLUSION

In this paper, we proposed object recognition application system in form of cane and wireless communication. This system is designed to help blind people. The experimental results show that our system can help blind people when they recognize person who is around themselves. For future works, we will solve the way to use navigation system in our application

ACKNOWLEDGMENT

This work was funded by the TEXAS INSTRUMENTS

REFERENCES

- [1]- https://en.wikipedia.org/wiki/Visual_impairment#Associated_problems

- [2]- <https://simple.wikipedia.org/wiki/Blindness>
- [3]-
https://www.researchgate.net/publication/282686024_An_electronic_walking_stick_for_blinds
- [4]-
<https://pdfs.semanticscholar.org/df35/9ab8b894f5180e844a1ff24f186c7ed75a67.pdf>
- [5]-
<https://soe.rutgers.edu/sites/default/files/imce/pdfs/gset-2014/Smart+Cane+Final.pdf>
- [6]- <http://ijssst.info/Vol-15/No-2/data/3251a439.pdf>
- [7]- <https://www.quora.com/What-is-difference-between-IR-sensor-and-ultrasonic-sensor>
- [8]-
<https://www.google.com/search?q=Arduino+uno&oq=Arduino+uno&aqs=chrome..69i57j69i61j69i65j35i39j0l2.6734j0j7&sourceid=chrome&ie=UTF-8>

A Single-phase Half Bridge DC to AC Inverter

Gaayathry.K¹, Nivetha.R², Swarna Gowri.M³, Swetha.S⁴, Vishali.G⁵,

¹ Assistant Professor, Department of Electrical and Electronics Engineering,
Saranathan College Of Engineering, Tiruchirapalli-12.

^{2,3,4,5} Final year B.E, Department of Electrical and Electronics Engineering,
Saranathan College Of Engineering, Tiruchirapalli-12.

Abstract - In this paper, two Switched Capacitor Boost Inverters are proposed. Switched capacitor cells may operate as a gain multiplier in Inverter. The integration of switched capacitance and different boost Inverter may offer an attractive solution to provide high static gain. Thus the boost Inverter with switched capacitor is intended to be used in applications wherever high output Alternating Current (AC) voltage is needed as Uninterrupted Power Supply (UPS). The Inverter as a combination of Boost Inverter and Switched Capacitor is proposed in this paper which is designated as Switched Capacitor Boost Inverter. In this topology, power loss is reduced by avoiding unnecessary double stages of power conversion. Amount of harmonics is reduced as much as possible. In this paper, Simulation is done using MATLAB – Simulink Software. The Simulation results is correlated with hardware prototype and the hardware results are obtained.

Keywords—Boost Inverter, Switched Capacitor, Reduced harmonics.

I. INTRODUCTION

Generally, the DC-AC Inverters are necessary in residential grid connected system. Many Researchers have worked on the topologies and control schemes of Inverter circuits. In order to step up voltage, an additional step up converter is required. Due to this, circuit complexity and cost becomes high. The main issue is lower efficiency caused by multistage power conversion. To overcome these challenges, High efficiency Inverters are proposed by using Direct Current (DC) to AC Inverter with switched capacitor. The

output voltage waveform is almost a sinewave with minimum harmonic value, thereby improving the performance. Additionally, the output voltage is boosted by switching the load currents through capacitors. The use of lower power rated devices and lower Inductor values results in minimized total power losses and thus, the proposed system gives improved efficiency when compared to the conventional hybrid converters.

II. EXISTING SYSTEM

The main contribution of this paper is to implement a Single - Phase Single - Stage solar converter called Reconfigurable Solar Converter (RSC) in the solar powered hybrid AC/DC residential building with Energy storage devices. The basic concept of the RSC is to use a Single power conversion system to perform different operational modes such as solar Photo Voltaic (PV) to Grid (Inverter operation, DC-AC), Solar PV to battery/DC loads (DC-DC operation), battery to Grid (DC-AC), battery/PV to grid (DC-AC) and Grid to battery (AC-DC) for solar PV systems with Energy storage. This Inverter is used in a solar powered hybrid AC/DC home, which contains both AC and DC household loads.

Individual appliances are selected according to the harmonic contributions they are injecting to the distribution grid from a typical modern house. Apart from the aforementioned, other additional contributions are the electrical components and sensors are different and a normal Inductor alone is used for DC/DC operation. The variation in solar radiation is also considered and solar PV -battery operation is verified. The circulation current is mitigated due to operation of the switches in the topology for DC/DC operation.

III. PROPOSED SYSTEM: CIRCUIT CONFIGURATION AND - OPERATION

This section explains the operating principle and the topological stages or modes of the proposed switched capacitor based boost Inverter. The circuit diagram of the proposed system is shown in figure (1). The DC-AC Inverter consists of power MOSFETs, Switched capacitors, Boost Inductor and Filters.

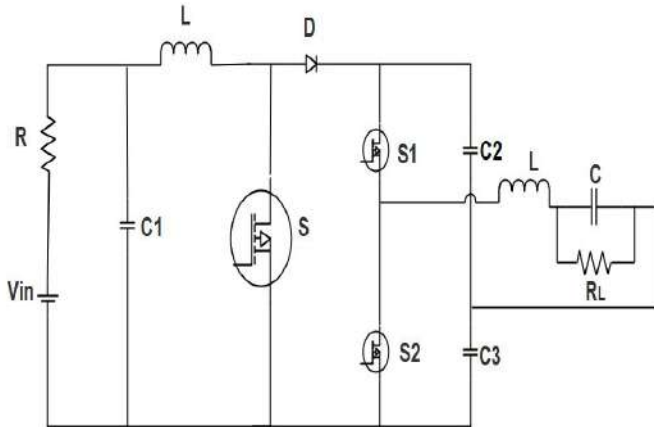


Fig.1 Circuit Diagram of the proposed system

MODE 1:

When switch (S) is turned ON, the current into the boost inductor increases linearly so that electric energy is accumulated in Inductor (L). After the switch (S) is turned OFF, the mode 1 is transferred to mode 2.

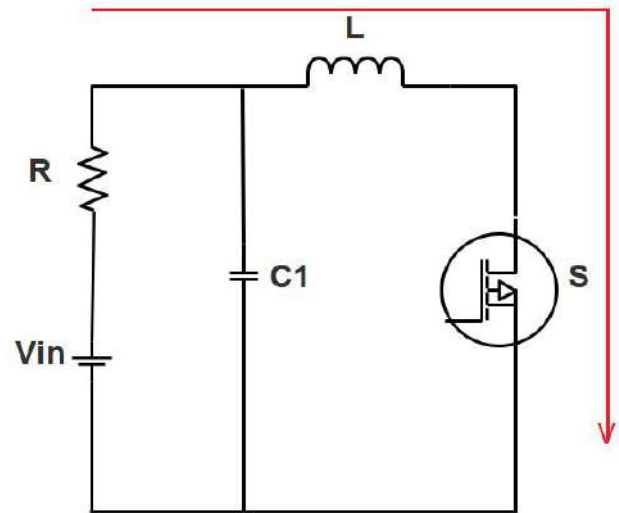


Fig.2 Operation during switch (S)-Turn ON

MODE 2:

Now the switches S and S2 are open and switch (S1) is closed, the current flows through the capacitor (C3) thus C3 gets charged, when switch (S) is open, then Inductor (L) starts to discharge thus giving increment to output voltage.

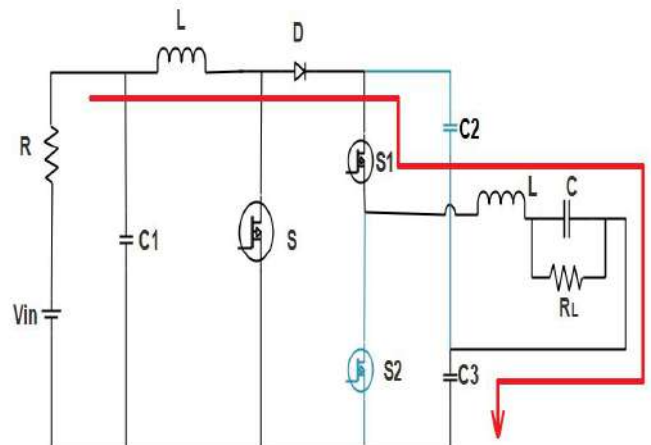


Fig.3 Operation during switch (S1)-Turn ON

MODE 3:

Now the switches S1 and S are open, and switch (S2) is closed, the current flows through capacitor (C2), now the capacitor (C3) and C2 discharges simultaneously.

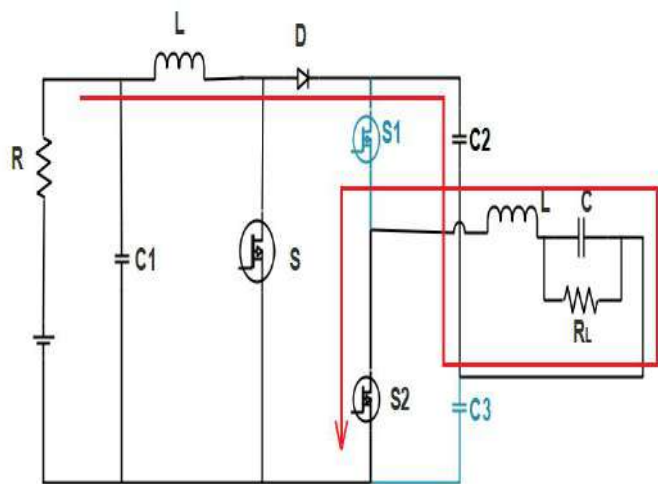


Fig.4 Operation during switch (S2)-Turn ON

IV.THEORETICAL ANALYSIS

This section presents a theoretical analysis of the proposed Single-phase Boost Inverter with Switched Capacitor. The duty cycle for the Single-phase Boost Inverter with Switched Capacitor is calculated based on the desired output voltage.

$$D = 1 - [V_{in} / V_{out}]$$

The duty cycle is basically denoted by D. Through this analysis, the dc amount shall be assumed to be 50%.

where, V_{IN} (min) is the minimum input voltage and V_{OUT} is the desired output voltage.

The next step to calculate the maximum switch current is to determine the inductor ripple current.

$$\Delta I_L = \frac{V_{IN(min)} \times D}{f_s \times L}$$

where f_s is minimum switching frequency of the Boost Inverter and L is Inductor value.

Now the maximum output current is calculated by

$$I_{MAXOUT} = \left(I_{LIM(min)} - \frac{\Delta I_L}{2} \right) \times (1-D)$$

Where I_{LIM} (min) is minimum value of the current limit of the integrated switch, ΔI_L is inductor ripple current and D is duty cycle. The lower the Inductor value, the smaller is the solution size. Note that the Inductor must always have a higher current rating than the maximum current, because the current increases with decreasing inductance.

$$L = \frac{V_{IN} \times (V_{OUT} - V_{IN})}{\Delta I_L \times f_s \times V_{OUT}}$$

$$C_{OUT(min)} = \frac{I_{OUT(max)} \times D}{f_s \times \Delta V_{OUT}}$$

where C_{OUT} (min) is the minimum output capacitance, I_{OUT} (max) is the maximum output current and ΔV_{OUT} is the desired output voltage ripple.

V.SIMULATION RESULTS

In order to verify the proposed boost Inverter operation, Switched capacitor boost Inverter has been verified by numerical simulation. Thus, the Simulation Circuit Diagram and results are obtained and shown in figure 5 and 6 (a,b,c,d).

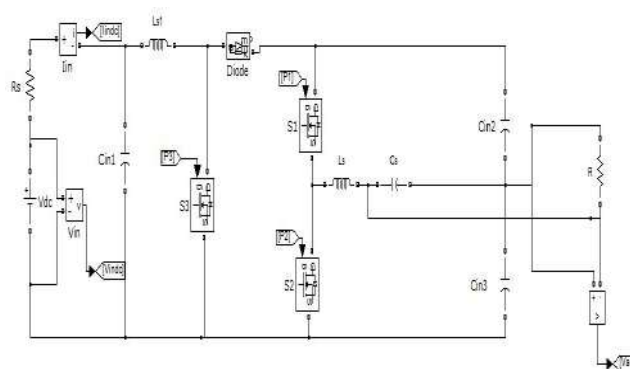
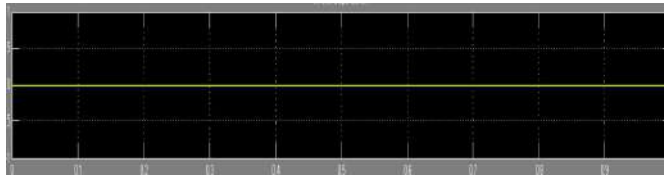
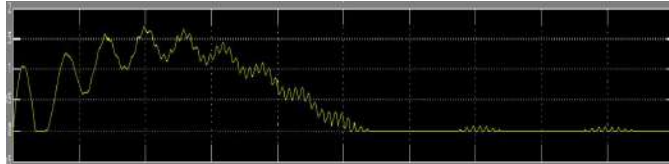


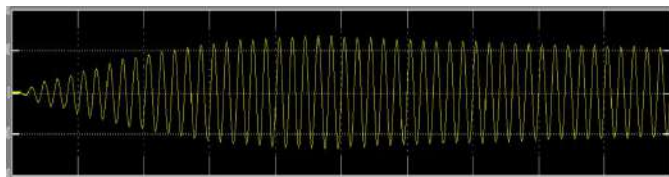
Fig.5 Simulation - Circuit Diagram



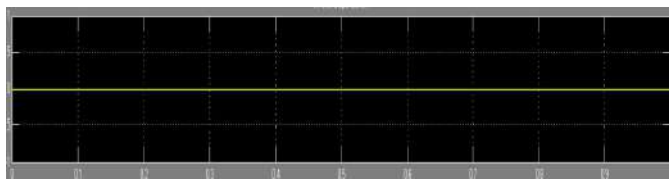
a) Inverter input voltage



b) Inverter input current



c) Inverter output voltage



d) Inverter output current

Fig.6 Simulation Results

VI.EXPERIMENTAL RESULTS

The hardware prototype was made using power MOSFETs, Switched capacitors, Boost Inductor and Filters. The Inverter input voltage is 12V and it is boosted to 100 V as output. The hardware prototype is shown in figure(7). Finally, the hardware output is obtained.

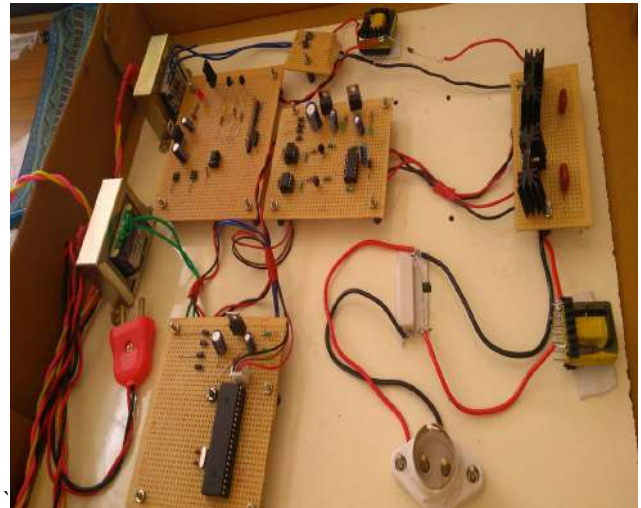


Fig.7 Hardware prototype

VII.CONCLUSION

This paper proposes a developed DC-AC Inverter, with switched capacitor. In this, the switches operates with duty cycle around 50%. The switched capacitor used here ensures the voltage multiplication capacity, resulting in the possibility to achieve a greater gain at the output of the Inverter. This Inverter is applicable in UPS design and Renewable energy supplies, whenever an AC voltage larger than DC input voltage is required. And there is no need of a second power conversion stage.

VIII.REFERENCES

- [1] GSR (2014) - Renewables 2014 Global Status Report.
- [2] J. Von Appen, T. Stetz, M. Braun, A. Schmiegel, "Local Voltage Control Strategies for PV Storage Systems in Distribution Grids,"IEEE Trans. Smart Grid, Vol. 5, No. 2, pp.1002-1009, March 2014.
- [3] A. Arancibia, K. Strunz, F. Mancilla-David, "A Unified Single- and Three-Phase Control for Grid Connected Electric Vehicles,"IEEE Trans. Grid, Vol. 4, No. 4, pp.1780-1790, Dec. 2013.

[4] B. T. Patterson, "DC, Come Home: DC Microgrids and the Birth of the Enernet,"IEEE Power and Energy Magazine, Vol. 10, No. 6, pp.60-69, Nov.-Dec. 2012.

[5] Vagelis Vossos, Karina Garbesi, Hongxia Shen, "Energy savings from direct-DC in U.S. residential buildings," Energy and Buildings, Vol. 68, Part A, January 2014.

[6] Nikhil Sasidharan, Nimal Madhu M., Jai Govind Singh, Weerakorn Ongsakul, "An approach for an efficient hybrid AC/DC solar powered Homegrid system based on the load characteristics of home appliances," Energy and Buildings, Vol. 108, 1 December 2015.

[7] B. Mariappan, B. G. Fernandes, M. Ramamoorthy, "A novel single-stage solar Inverter using hybrid active filter with power quality improvement,"40th Annual Conference of the IEEE in Industrial Electronics Society, pp. 5443-5449, Oct. 29 2014-Nov. 1 2014.

[8] Chien-Ming Wang; Chia-Hao Yang, "A novel high input power factor soft-switching single-stage single-phase AC/DC converter,"2005 IEEE Conference in Vehicle Power and Propulsion, 7-9 Sept. 2005.

[9] K. M. Shafeeque, P. R. Subadhra, "A Novel Single-Phase Single-Stage Inverter for Solar Applications,"2013 Third International Conference on Advances in Computing and Communications (ICACC), pp. 343-346, 29-31 Aug. 2013.

LC FILTER BASED POWER FACTOR IMPROVEMENT FOR BOOST CONVERTER

K. ABINAYA, J. JANE MIRIAM, K. KALAISELVI, R. KIRTHIKA

DEPARTMENT OF EEE

SARANATHAN COLLEGE OF ENGINEERING

ABSTRACT

This paper consists of two loops of an AC-DC boost converter in order to improve the input power factor. Inter control loop and Outer control loop. Single-phase high-power factor rectification is frequently established using a boost converter. The purpose of this rectification is to restore the current waveform to sinusoidal waveform which is in phase with the input voltage. The sinusoidal current with low distortion is obtained using several control techniques. Hence to improve the power factor, LC filter is used whereas to regulate the output voltage PID controller is used. Single phase AC-DC boost converter is achieved in continuous mode and both LC filter and PID controller are simulated in MATLAB SIMULINK.

KEYWORDS:

Power factor Improvement, Boost converter, LC filter, PID controller

I. INTRODUCTION:

AC-DC converter finds a wide range of application in our day to day life in the form of chargers, LED lighting etc. Convectional AC-DC converter use a diode rectifier followed by a DC link capacitor which draws a non-sinusoidal AC current from the supply by injecting higher order harmonics

into the supply which results in power factor reduction.

From IEEE standards the harmonic content of line current of mains is below certain limits. The widely used structure of a power system consist of a rectifier and DC-DC converter which is used to shape the input current to sinusoidal form under DC-DC converter for output regulation. Such configuration has corresponding control circuits.

The main aim of this paper is to regulate the output voltage and to improve the input power factor. Therefore, it combines two stages (Rectifier, AC-DC) into one. This combination is used to improve the power factor at constant duty cycle D and constant switching frequency F_s . To achieve the object inductor current mode and capacitor voltage mode are used. Buck-Boost converter is very good in inductor current mode and improves the power factor whereas Boost-Buck converter are having good improvement under certain condition. In combination of these two stages 1st stage Inductor current mode is used to improve the power factor and for 2nd stage-Capacitor voltage mode is used to regulate the output voltage. However, in inductor current mode operation there are some disadvantages in improving the input power factor of a boost converter, hence we are in need of an input filter which makes the inductor current from discontinuous to continuous.

Boost converter with LC input filter operating in discontinuous capacitor voltage mode provides continuous input current and improves the power factor. The aim of this paper is to provide a wide comprehensive analysis of the boost converter with LC input filter operating in capacitor voltage mode. The design criteria of rectifier with input voltage is 230V which is discussed below.

II. MODES OF OPERATION

Mode 1: (switch is ON)

Continuous conduction mode in which the current through inductor never goes to zero i.e. inductor partially discharges before the start of the switching cycle.

MODE 1: ($0 < t < t_{on}$)

1. This Mode 1 begins when the switch S is turned ON by applying control signal at $t=0$. At that time, diode becomes reverse biased. Due to this load is isolated from input.

2. The input current rises, flows through inductor L1 and through the switch.

3. The inductor voltage V_L is equal to the supply voltage V_s .

Mode 2: (switch is OFF)

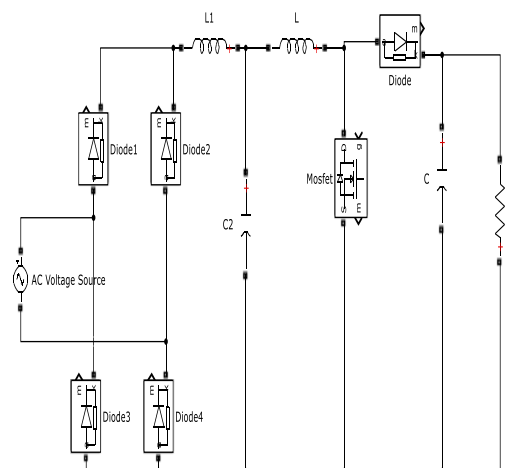
Discontinuous conduction mode in which the current through inductor goes to zero i.e. inductor is completely discharged at the end of switching cycle.

MODE 2: ($t_1 < t < T$):

1. This mode begins when the switch (SW1) is switched OFF at $t=1$.

2. The current that was flowing through the switch would now flow through L, C, load and the diode. The direction of current flow in Mode 2. The inductor current falls until the switch is turned ON again in the next cycle. The energy stored in inductor L is

transformed to the load. Inductor current mode and capacitor voltage mode are two operating modes in which current through the inductor and voltage across the capacitor is zero during a part of switching cycle. It can be obtained in fourth order converter topology which consists of two inductors and emulate current sources, which is used to charge or discharge the capacitor operating in capacitor voltage mode. For large enough inductance the current through the inductors can be considered constant during one switching cycle. If the capacitance is small then the capacitor cannot operate as a storage element and voltage across this is discontinuous.



FILTER DESIGN

230V AC supply is given as input to AC-DC converter

Hence LC filter is calculated using the formula,

$$C = \frac{10}{2w\sqrt{R^2 + (2wL)^2}}$$

$$VRF = \frac{\sqrt{2}}{3} \left[\frac{1}{(2w)^2 LC - 1} \right]$$

Therefore, by knowing the values of VRF and C the value of L can be calculated.

CONVERTER DESIGN

Assuming Duty cycle (D) = 50% and Switching Frequency (Fs)=10K

Consider R load as 100Ω

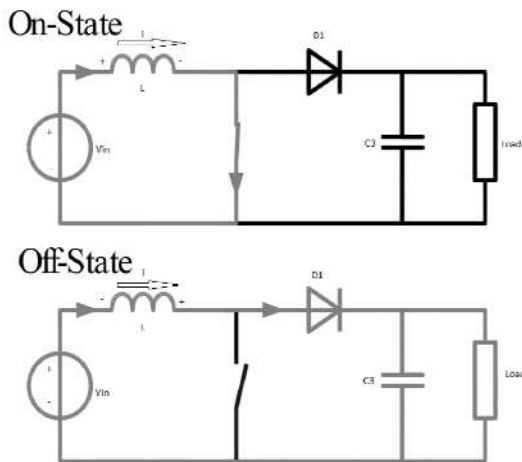
Hence the L and C values of the Boost converter is calculated using the formula,

$$L = \frac{D(1-D)^2R}{2f}$$

$$C = \frac{D}{R(\frac{\Delta V_o}{V_o})f}$$

III. SYSTEM CONFIGURATION OF BOOST CONVERTER

Different topologies are used in power factor improvement converter. This conversion is performed by means of LC filter and a rectifier. Capacitor (C1) has low value and operates in capacitor voltage mode and the output capacitor (C2) is large enough so that the voltage across it is said to be constant



ON STATE:

When S=1; Switch in On-state

$$V_{in} = L \frac{di}{dt} \tag{1}$$

$$\frac{di_L}{dt} = \frac{V_{in}}{L} \tag{2}$$

$$\frac{di_L}{dt} = \frac{-V_o}{R} = \frac{-V_c}{R} \tag{3}$$

$$\begin{bmatrix} i_L^0 \\ V_c^0 \end{bmatrix} = \begin{bmatrix} 0 & 0 \\ 0 & \frac{-1}{R} \end{bmatrix} \begin{bmatrix} i_L \\ V_c \end{bmatrix} + \begin{bmatrix} \frac{1}{L} \\ 0 \end{bmatrix}$$

$$[V_o] = [0 \quad 1] \begin{bmatrix} i_L \\ V_c \end{bmatrix} \tag{4}$$

OFF STATE:

When S=0; Switch in Off-state

$$\frac{di_L}{dt} = \frac{V_c}{L} - \frac{V_{in}}{L}$$

$$\frac{dV_c}{dt} = \frac{i_L}{C} - \frac{V_c}{RC}$$

$$V_o = V_c$$

$$[V_o] = [0 \quad 1] \begin{bmatrix} i_L \\ V_c \end{bmatrix} \tag{5}$$

$$\begin{bmatrix} i_L^0 \\ V_c^0 \end{bmatrix} = \begin{bmatrix} 0 & \frac{1}{L} \\ \frac{1}{C} & \frac{-1}{RC} \end{bmatrix} \begin{bmatrix} i_L \\ V_c \end{bmatrix} + \begin{bmatrix} \frac{-1}{L} \\ 0 \end{bmatrix} V_{in}$$

$$A = \begin{bmatrix} 0 & \frac{(1-D)}{L} \\ \frac{-(1-D)}{C} & \frac{D(1-D)-1}{RC} \end{bmatrix}$$

$$B = \begin{bmatrix} \frac{2D-1}{L} \\ 0 \end{bmatrix}$$

$$C = [0 \quad 1] \tag{6}$$

$$\begin{bmatrix} i_L \\ V_c \end{bmatrix} = \begin{bmatrix} 0 & \frac{1}{L} - \frac{V_{in}}{V_c L} \\ \frac{-1}{C} & \frac{-1}{RC} \end{bmatrix} \begin{bmatrix} i_L \\ V_c \end{bmatrix} +$$

$$\begin{bmatrix} 2 \frac{V_{in}-V_o}{L} \\ \frac{i_L}{C} + V_o \left(\frac{R-RC}{R^2 C} \right) \end{bmatrix} [D] \tag{7}$$

$$V_o = [0 \quad 1] \begin{bmatrix} i_L \\ V_c \end{bmatrix} \tag{8}$$

IV. CONTROL TECHNIQUES- CURRENT AND VOLTAGE

Different current control techniques are usually used for controlling the power factor improvement.

The parameters used in the controllers for the generation of gate signals of the switches are the input voltage, input current and the output voltage. There are two loops the inner loop and the outer loop. The inner loop is responsible for controlling the shape of the inductor current. The error obtained from this comparison makes the input of the PID controller. In inner loop the inductor current is compared with the reference current

V. VOLTAGE CONTROL TECHNIQUE

As there are two loops available. The outer loop controls the output voltage and keeps it constant at predefined set point. In the outer loop, the output voltage level is scaled and compared with the given set point. The output of this controller is used to obtain the current reference

VI. SIMULATION RESULTS

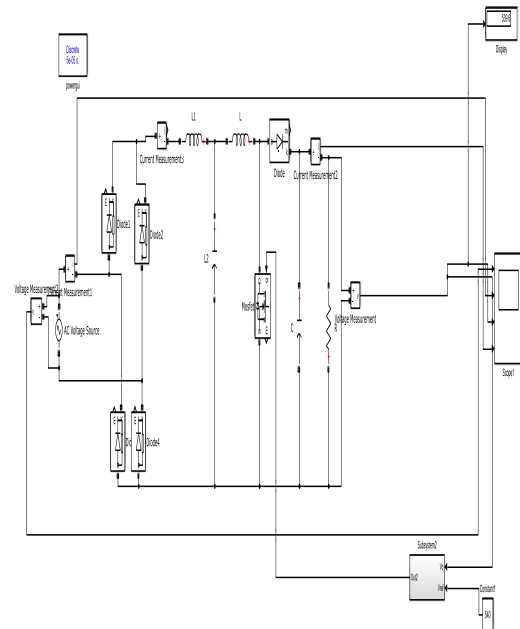
Single phase boost power factor improvement converter is simulated using voltage and current control loop

TABLE-1

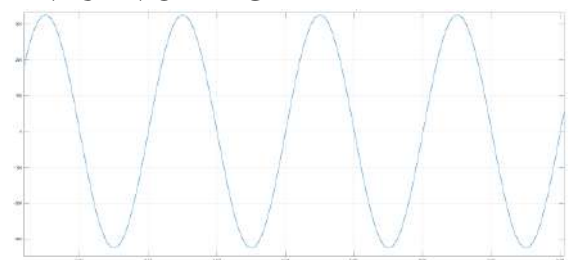
SIMULATION PARAMETERS

V_{in}	230V
V_0	540V
F_s (Switching Frequency)	10K
C (Capacitor Output)	$7.21e^{-4}$
L (Inductor Output)	$7.96e^{-7}$
C_2	$7.957e^{-7}$
L_2	$1.955e^{-3}$

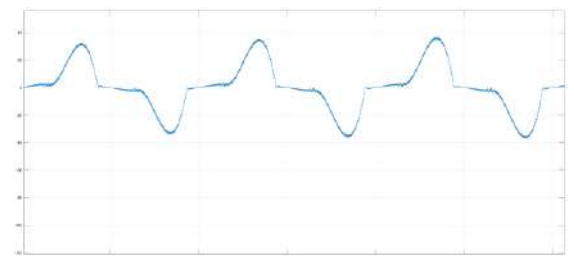
VOLTAGE CONTROL LOOP SIMULATED BLOCK



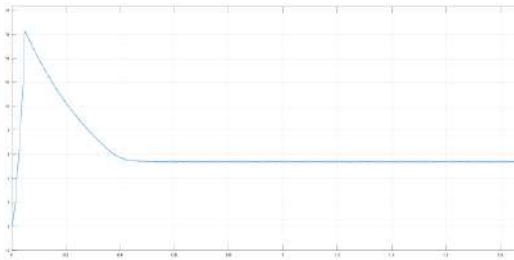
INPUT VOLTAGE



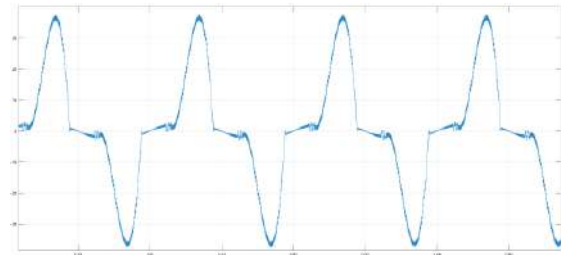
INPUT CURRENT



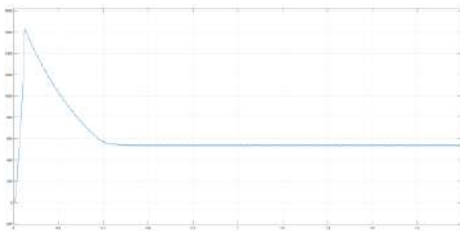
OUTPUT CURENT



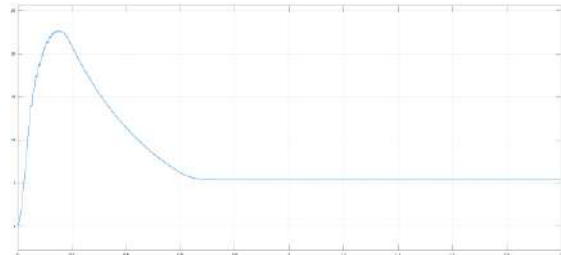
INPUT CURRENT



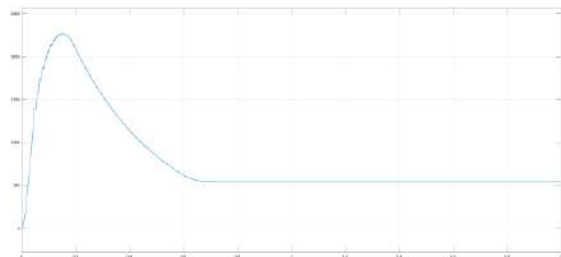
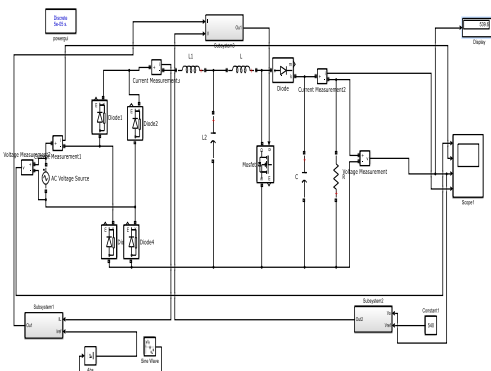
OUTPUT VOLTAGE



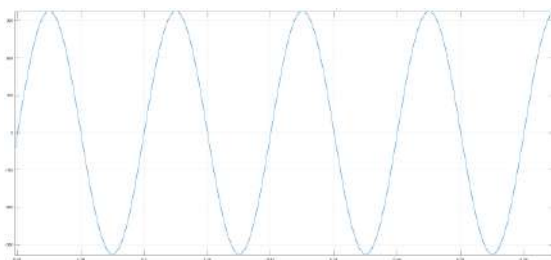
OUTPUT CURRENT AND VOLTAGE



CURRENT CONTROL LOOP



INPUT VOLTAGE AND CURRENT



VII. CONCLUSION

The boost converter with LC input filter operating in capacitor voltage mode offers good power factor improvement properties, continuous input current and to obtain output voltage higher than the peak input voltage . Simulation study of the converter was carried out using MATLAB/SIMULINK program. Hence the aim of this paper is achieved by regulating the output voltage and improving the input power factor.

VIII. REFERNCES

- 1) Grigore, Vlad, and Jorma Kyra. "High power factor rectifier based on buck converter operating in discontinuous capacitor voltage

mode." *IEEE Transactions on power electronics* 15.6 (2000): 1241-1249.

2) Sudalaimani, M., L. V. Revathi, and N. Senthilkumar. "Direct Power based Sliding Mode Control of AC-DC Converter with Reduced THD." *Tehnički vjesnik* 25.1 (2018): 72-79.

3) Chandra, Ambrish, et al. "An improved control algorithm of shunt active filter for voltage regulation, harmonic elimination, power-factor correction, and balancing of nonlinear loads." *IEEE transactions on Power electronics* 15.3 (2000): 495-507.

4) Lu, Dylan Dah-Chuan, Herbert Ho-Ching Iu, and Velibor Pjevalica. "A single-stage AC/DC converter with high power factor, regulated bus voltage, and output voltage." *IEEE Transactions on Power Electronics* 23.1 (2008): 218-228.

5) Redl, Richard, Laszlo Balogh, and Nathan O. Sokal. "A new family of single-stage isolated power-factor correctors with fast regulation of the output voltage." *Proceedings of 1994 Power Electronics Specialist Conference-PESC'94*. Vol. 2. IEEE, 1994.

Simulation Study of pwm strategy for single phase five level MLI using equal area criterion

C.Krishnakumar¹, S.Thamizharasan², G. Srimati³

¹Professor, ²Associate Professor, ³UG Scholar

Departement of Electrical and Electronics Engineering

Saranathan college of Engineering

Panjapur, Trichy

Abstract— This paper presents an equal area criterion modulation strategy for single phase five level multilevel inverter. The main aim of this strategy is to achieve a minimum lower order harmonics for any preferred level. This method excludes the need for the carrier in the generation of PWM pulses by matching the output level with the sectionalized dc levels and the switching instants are calculated using mathematical relations. It includes simulation results from MATLAB platform for a single phase five level MLI.

1.INTRODUCTION

A multilevel inverter is a power electronic device which is capable of producing desired alternating voltage at the output using multiple lower level dc voltages as input. In many industrial applications, multilevel inverters have been used as an alternative in medium voltage and high-power situations [3].

Many multilevel inverter topologies are in practice. The main difference lies in the switching mechanism and the source of input voltage. Among various topologies used, there are three commonly used topologies namely diode clamped or neutral clamped multilevel inverter, flying capacitor multilevel inverter, and cascaded H-bridge multilevel inverter [2].

A diode clamped multilevel inverter uses clamping diodes to limit the voltage stress on the power devices. The major disadvantage of this type of inverter is that the maximum output voltage is only half of the input dc voltage [2]. So, in order to increase the output voltage level, the number of switches, capacitors and diodes have to be increased which makes the circuit very complex.

Using capacitors to limit the voltage stress on the power devices, instead of diodes leads to a new topology named flying capacitor multilevel inverter topology, which has its own advantages and disadvantages [2]. Particularly, Capacitors incorporated in this topology are incapable of blocking the reverse voltage which becomes the major drawback for this type of topology.

A cascaded H-bridge multilevel inverter uses several H-bridge cells connected in series in order to produce a

sinusoidal output. The output voltage generated by the multilevel inverter is the sum of the voltages generated by each cell [9]. Each cell can provide three voltages which are zero, negative dc and positive dc. This topology uses lesser number of components which is a major advantage [1].

Different modulation strategies are available to control the output voltage of multilevel inverter. Some of the commonly used strategies are sinusoidal PWM [SPWM], space vector PWM [SVPWM], multicarrier PWM [MCPWM], and selective harmonic elimination [SHE] techniques.

Sinusoidal Pulse Width Modulation [SPWM] is a popular method used in inverters. Different SPWM methods are Phase disposition PWM [PDPWM], Phase opposition disposition PWM [PODPWM], Alternative opposition and disposition PWM [AODPWM], Phase shift PWM [PSPWM], Carrier overlapping PWM [COPWM] and Multicarrier Sinusoidal Pulse Width Modulation with Variable Frequency [MCSPWMVF]. All the above-mentioned methods use many levels shifted or phase shifted triangular waves and compare with a single sine wave. The intersection of single sine wave with many triangular waves produce the gating signal for the switches [4]. This technique is applicable only for unsymmetrical topology and cannot be applied for symmetrical topology.

A classical Space Vector Pulse Width Modulation [SVPWM] involves calculation of sector and estimation of regions. A simplified algorithm developed adds a common mode voltage to the reference phase voltage [5]. The implementation of this technique is difficult as the complexity and computational cost increases as the number of levels increases.

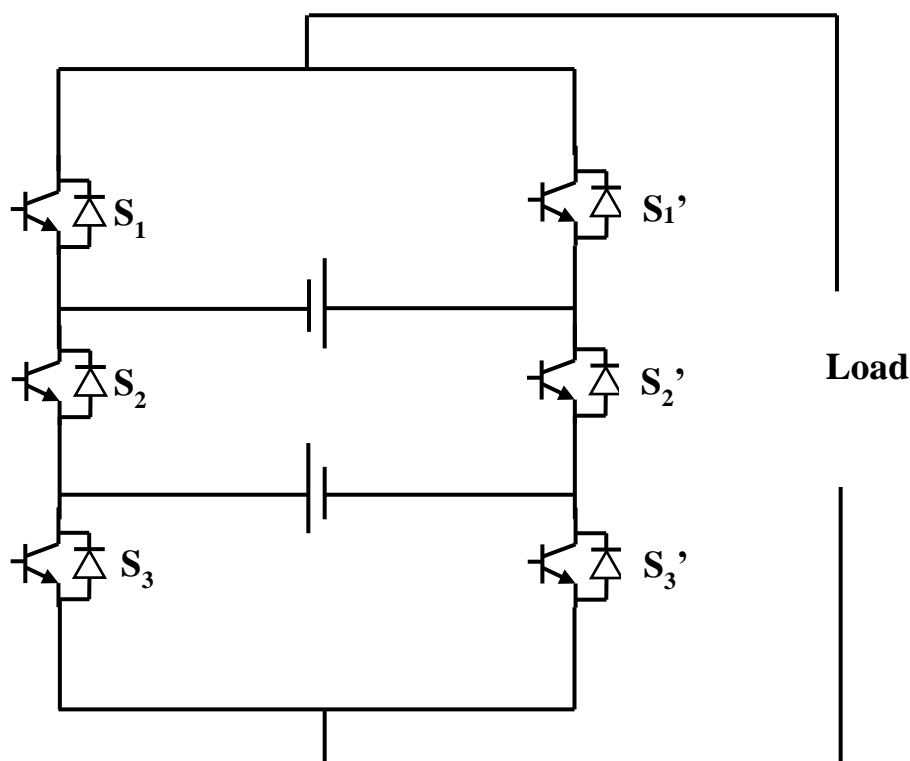
In Multicarrier Pulse Width Modulation [MCPWM], a sinusoidal wave is compared with each carrier to generate the switched output voltage for the multilevel inverter. Generally, phase shifted MCPWM and level shifted MCPWM are used. Phase shifted strategy is the most commonly used strategy for multilevel inverters. In this method each carrier is linked with the individual cell by suitable phase shift. Level shifted strategy has more types to name a few: In phase disposition [IPD], where all the carriers

are in phase; Alternative phase opposite disposition [APOD], where all carriers are alternatively in opposite disposition and Phase opposite disposition [POD], where all carriers above the zero reference are in phase and those below the zero reference are in opposition [6]. Though the output voltage waveform is obtained with low current distortions, it results in high switching losses.

Selective harmonic elimination [SHE] technique has been introduced to eliminate the lower order harmonics through the entire voltage profile and yield superior output quality among all the PWM methods [7]. In this method transcendental equations are solved to compute the switching angles. It is difficult to solve these SHE equations as they are highly non-linear in nature. A mammoth task in this method is to get all possible solution sets. Once these solution sets are obtained, the solution with least THD is chosen [8,10]. A difficulty in this approach is that for several H-bridge cells which are connected in series, the order of the polynomial becomes high

which makes the computation very complex. This method achieves high efficiency but it is not feasible for higher level inverters.

All the above-mentioned techniques are used for some particular topologies only. And as the number of level increases, the complexity of the circuit increases and the switching losses are also increased. The developed modulation strategy is suitable for all multilevel inverter topologies irrespective of the level for which they are connected. This paper presents a modified cascaded h-bridge multilevel inverter topology, in which only six switches are used for five level MLI instead of eight switches (Fig.1). For a m level MLI, the number of dc sources is (m-1)/2. So, for a five level MLI, two dc sources are used. The principle idea revolves around area equalization to produce the target fundamental from the available dc levels.



2.PROPOSED METHODOLOGY

The basic idea of the proposed modulation technique relies on equal area criterion which involves equalizing the area under the target sinusoidal waveform and the actual pulses. The width of the PWM pulse is calculated by making the area under the PWM signal equal to that under the sampled section of the reference waveform for the desired target fundamental load voltage.

The conceptual diagram shown below has the target output voltage and actual output voltage waveforms. The diagram is common for any number of voltage levels in which the target output voltage waveform is vertically divided into ‘n’ number

of levels for a target half cycle. The source voltage of each cell desire to acquire the maximum value for the desired target fundamental output voltage (v_{mT}) and $((n-1)E, \theta_n)$ which represents the cross over point between any horizontal line and the target sine wave. The solid base pattern area is subtracted directly from the target for every level without changing the position because both are equal in magnitude/time product as pictured in the below figure. The remaining portion of the target voltage waveform is sub-divided into time base samples and individually equalised to the PWM pulses patterns for computing the pulse width.

The actual output voltage waveform consists of (p-1)/2 pulses in every cross over and spreads between the limits

$(\theta_j + ((k - 1)(\theta_{j+1} - \theta_j)/p)), (\theta_j + (k(\theta_{j+1} - \theta_j)/p))$
 and the pulse width during the kth pulse interval is ' δ_k ' where 'p' is the total number of odd pulses in each level and 'j' is the crossing instant as mentioned in Fig.2. The pulse width of the actual output voltage waveform is directly proportional to the corresponding instantaneous magnitude of the target fundamental output voltage waveform.

The PWM pulse width is determined by equating the area under the actual output voltage waveform and the area under the target output voltage waveform for every sampling interval between the cross over points [2]. Therefore, the pulse widths are directly proportional to the output voltage and inversely proportional to the output frequency.

The value of the cross over instants can be obtained as

$$\theta_{j+1} = \sin^{-1} \left(\frac{jv_{dc}}{v_m} \right)$$

The value of θ_1 can be assumed to be zero.

The area containing kth pulse in the nth level of the actual output waveform is given by

$$A_k' = E\delta_k$$

$$K = 1, 2 \dots p$$

If $\theta_j < 90^\circ$, then $\theta_{j+1} = \theta_j + \theta_j, j = 0, 1 \dots (n-1)$

If $\theta = 90^\circ$, then $\theta_{j+1} = 180^\circ - \theta_i$, where 'i' is the position of solid base in the target output voltage. The pulse width δ_k of each kth pulse can be found by the following equation:

For R phase,

$$\delta_k = 2 \left(\frac{v_m}{v_{dc}} \right) \left[\sin \left\{ \theta_j + \frac{(k - 0.5)(\theta_{j+1} - \theta_j)}{p} \right\} \sin \left\{ \frac{\theta_{j+1} - \theta_j}{2p} \right\} - i \left\{ \frac{\theta_{j+1} - \theta_j}{p} \right\} \right]$$

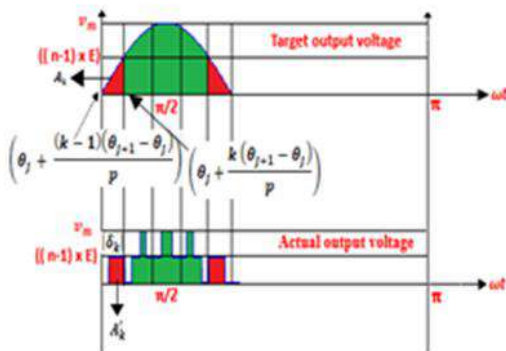


Fig.2 Conceptual diagram

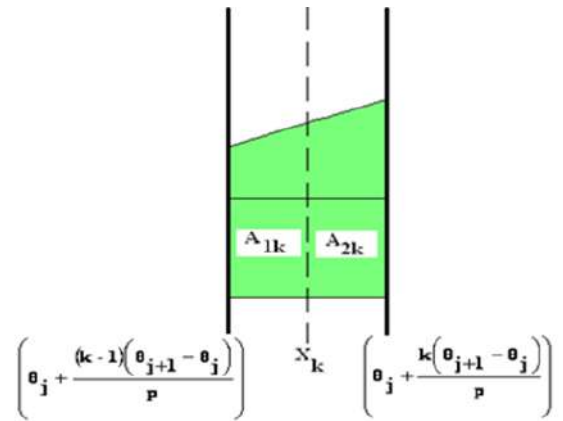


Fig.3. Centre Of Area

The pulses are positioned in the centroid of the sampled waveform after determining the pulse interval by equating the area A1 and A2 in the sampled pulse interval as indicated in the fig.3.

The value of X_k can be obtained as follows:

For R phase,

$$X_k = \cos^{-1} \left[\frac{\cos \left\{ \theta_j + \frac{(k-1)(\theta_{j+1} - \theta_j)}{p} \right\} + \cos \left\{ \theta_j + \frac{k(\theta_{j+1} - \theta_j)}{p} \right\}}{2} \right]$$

Pulse width of each kth pulse is directly proportional to the target output voltage and inversely proportional to the total number of pulses. Based on the calculated value of δ_k , the switching pulses are given to the power devices for any target fundamental voltage.

3. SIMULATION RESULTS

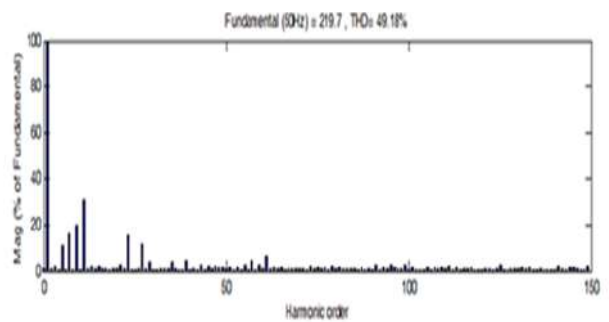


Fig.5. Simulated Output Voltage Spectrum for 225 V

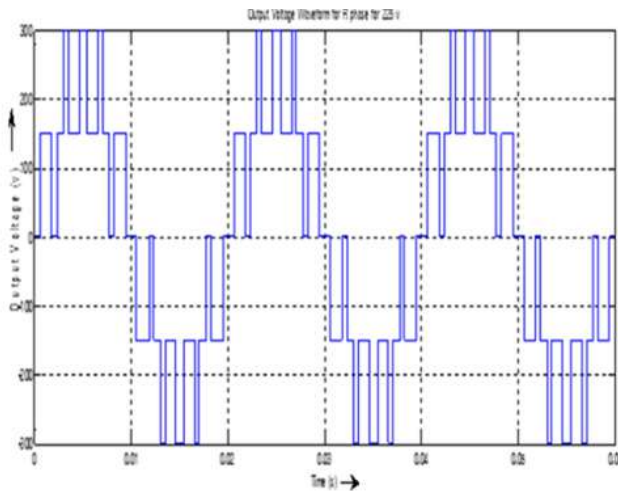


Fig4. Output Voltage Waveform for 225 V

4. CONCLUSION

A digital PWM technique suitable for different level MLIs has been developed mathematically to reduce the switching losses and to improve the output harmonic performance. The PWM method used has extensively reduced the number of switching devices and the lifetime of the switching devices has been increased. The simulation has resulted with reduced lower order harmonics.

5. REFERENCES

1. A. Gaikwad and P. A. Arbune, "Study of cascaded H-Bridge multilevel inverter," *2016 International Conference on Automatic Control and Dynamic Optimization Techniques (ICACDOT)*, Pune, 2016, pp. 179-182.
2. Jih-Sheng Lai and Fang Zheng Peng, "Multilevel converters-a new breed of power converters," in *IEEE Transactions on Industry Applications*, vol. 32, no. 3, pp. 509-517, May-June 1996.
3. S. Laali, K. Abbaszadeh and H. Lesani, "Development of multi-carrier PWM technique for multilevel inverters," *2010 International Conference on Electrical Machines and Systems*, Incheon, 2010, pp. 77-81
4. S. Vaddiraj, K. N. Swamy and B. P. Divakar, "Generic SPWM technique for multilevel inverter," *2013 IEEE PES Asia-Pacific Power and Energy Engineering Conference (APPEEC)*, Kowloon, 2013, pp. 1-5.
5. V. S. Sabah *et al.*, "A simplified space vector pulse width modulation technique for multilevel inverter fed induction motor drive," *2015 International Conference on Circuits, Power and Computing Technologies [ICCPCT-2015]*, Nagercoil, 2015, pp. 1-5.
6. H. Gupta, A. Yadav and S. Maurya, "Multi carrier PWM and selective harmonic elimination technique for cascade multilevel inverter," *2016 2nd International Conference on Advances in Electrical, Electronics, Information, Communication and Bio-Informatics (AEEICB)*, Chennai, 2016, pp. 98-102.
7. S. Thamizharasan, L. U. Sudha, J. Baskaran, S. Ramkumar and S. Jeevananthan, "Carrierless pulse width modulation strategy for multilevel inverters," in *IET Power Electronics*, vol. 8, no. 10, pp. 2034-2043, 10 2015.
8. Jagdish Kumar & Das, B & Agarwal, Pramod. (2008) "Selective harmonic elimination technique for a multilevel inverter" Fifteenth National Power Systems Conference (NPSC). 608-613.
9. Y. Zhang, Y. Zou, C. Wang, J. Zhang and Z. Wu, "A Novel Modulation Technology for Multilevel Inverter Based on Equivalent Area," *IECON 2007 - 33rd Annual Conference of the IEEE Industrial Electronics Society*, Taipei, 2007, pp. 2115-2118.
10. J. Rodriguez, Jih-Sheng Lai and Fang Zheng Peng, "Multilevel inverters: a survey of topologies, controls, and applications," in *IEEE Transactions on Industrial Electronics*, vol. 49, no. 4, pp. 724-738, Aug. 2002.

DC POWERED RESISTIVE HEATING STOVE USING SOLAR ENERGY

M.Marimuthu , Assistant professor

G.Princy smitha ,A.Swathi, R.Tharani, G.Yamuna

Department of Electrical and Electronic Engineering

Saranathan College Of Engineering , Tiruchirapalli

Email id: princysmitha810@gmail.com,rvtharani98@gmail.com

Abstract-- This paper proposes a electric stove is heated by using solar power with cascaded boost converter. Solar energy is use to solar heating and solar electricity. In the last few years there is a shortage for supplying a domestic gas for cooking purpose and the cost of the gas also increasing nowadays. In order to solve this problem an solar powered DC electric stove was used instead of normal stove. The solar power is superabundant, free of cost, pollution free and environment friendly and distributed all over the world therefore this paper preferred a solar energy for cooking purpose. In a solar electric heating system, it is difficulty to heat a stove at a required temperature continuously due to the variation in solar radiation over a day or even in the different seasons of the year, so the plan is to design a MPPT algorithm for the efficient heating of resistive electric stove and to design a cascaded boost converter for effective heating of stove.

INDEX TERMS: Electric stove, solar panel, controller, cascaded boost converter.

I. INTRODUCTION:

The plan was to design an effectual cascaded boost converter and Maximum power point tracking algorithm for the solar powered DC electric stove. There is a shortage for cooking gas, considering this circumstance we have come up with a project of a new technique of cooking which could take a full advantage of renewable energy that is solar

photovoltaic energy .Our aim is to create a solar operated DC electric stove. Nowadays there is a increasing demand for DC supply. so we plan to use a DC electric stove. This stove was designed in such a way so that it will consume less power from the

power sources and it is more suitable against the cylinder gas stove and induction stove.

II. LITERATURE REVIEW:

Cooking with sunlight is not a new idea .It was started in the early period in 1767.In this year, Horace de Saussure, a French-Swiss scientist design a miniature greenhouse with glass boxes with one inside the other set on a black tabletop. Some fruits are kept in the innermost portion of the box which was perfectly cooked and this was the beginning of the new technology .From this he is named as a “FATHER OF SOLAR COOKING” .In 1980 Barbara Kerr ,with her other colleagues ,proceed to make a solar cooking prototype .In July 1987,solar cooker was designed and used internationally.

In order to overcome the above mentioned problem we designed a “SOLAR POWERED DC ELECTRIC HEATING STOVE” in which we used a DC electric stove for that we get a power from solar panel and for efficient heating, the maximum power from the PV module is extracted well by using Incremental algorithm which is one of

the most advantageous algorithm in MPPT. The cascaded boost converter is used to quadruple the voltage from the PV panel to the load which is a DC electric stove.

III. DESIGN OF PROPOSED SYSTEM

750W panels were used where 3 panels of 250W are connected in series. Each panel has 250W and 12V. when we connected a three panel in series, then the voltage gets added as 36V. Thus the system input voltage is 36V and the required output voltage is 220V for that, a cascaded boost converter is used which will boost the voltage four or five times from the input voltage. we made a switching frequency as 8KHZ. We used a TLP250 IC for making a triggering circuit which will generate a pulse to the cascaded boost converter.

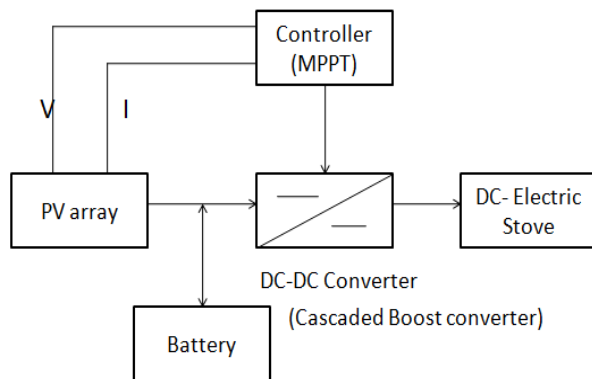


Fig 1: Block Diagram of the System

IV.DC-DC CASCADED BOOST CONVERTER:

Nowadays there is an increased demand in the portable devices and this leads to an increased demand for converters such as the DC-DC cascaded boost converter. Such converter have a ability to generate high voltage in single battery in each devices. Cascaded boost converter will boost the voltage four or five times but the normal boost converter will boost two or three times. In our project the input voltage is 36V but the output voltage as 220V where our load rating is 220V so we preferred a cascaded boost converter.

The circuit diagram consists of diode D1, D2, D3, Capacitors C1 and C2, inductor L1 and L2 and MOSFET switch.

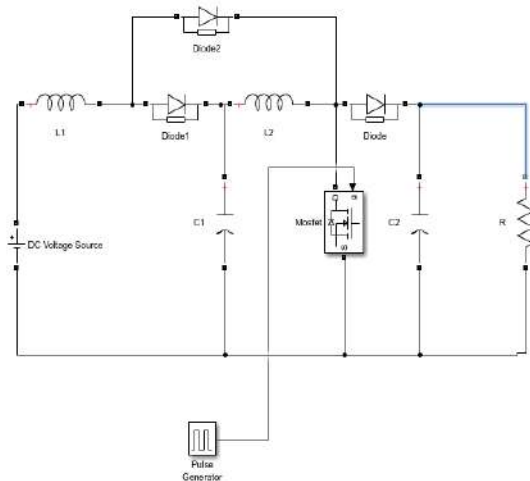


Fig 2: The Circuit diagram of cascaded boost converter

V.PRINCIPLES OF OPERATION:

MODE 1:

In this transition interval, MOSFET is turned ON at $t=0$ and it terminates at $t=ton$. Diode D2 is conducted but diode D1 and D3 are turned OFF. The energy of the dc source V_{in} is transferred to the input inductor L1 through the diode D2, and the voltage across the input inductor L1 is V_{in} ; the input current i_{L1} is equal to i_{D2} and is increased the capacitor C1 delivers its energy to the magnetizing inductor L2.

The current flow through the inductor L2 increases with voltage V_1 during the switching ON period dT , and decreases with voltage (V_0-V_1) during the switching OFF period $(1-d)T$.As the result of voltage across the capacitor C2 charge to V_0 .

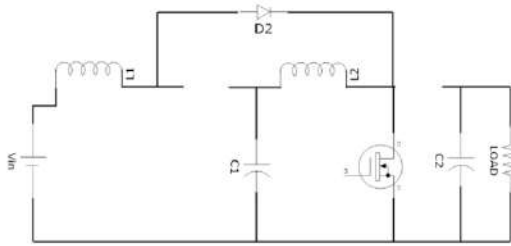


Fig 3:Mode 1 operation of cascaded boost converter

MODE 2:

When the MOSFET is turned OFF at $t=t_{off}$ the diode D1 and D3 are conducted but diode D2 gets turned OFF. The current in the inductor cannot change instantaneously, the voltage in the inductor reverses its polarity in an attempt to maintain a constant current. The current, which was flowing through the MOSFET would now flow through L1, L2, C1, C2 and Load. The inductor current falls until the MOSFET is turned ON again in a next cycle. The voltage across the inductor is $(V_{in}-V_{c1})$ and its current falls linearly from I_2 to I_1 in time T_{off} .

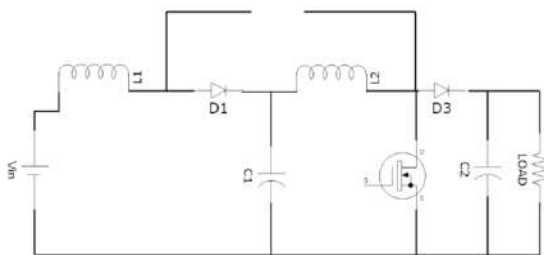


Fig 4:Mode 2 operation of cascaded boost converter

VI.CIRCUIT DESIGN:

Choosing a sample frequency of 8KHZ and a duty cycle of 0.6 the following equation were used to design of converter.

OUTPUT VOLTAGE:

$$V_0 = \frac{v_{in}}{(1-D)^2}$$

The load will equal to

$$R = \frac{V^2}{P}$$

OUTPUT CURRENT:

$$I_0 = \frac{v_0}{R}$$

Current in the first inductor L1,

$$I_{L1} = \frac{I_0}{(1-D)^2}$$

Current in the second inductor L2,

$$I_{L2} = \frac{I_0}{(1-D)}$$

INDUCTOR:

$$L1 = \frac{V_{in} * D}{\Delta I_{L1} * f}$$

$$L2 = \frac{V_{in} * D}{(1-D) \Delta I_{L1} * f}$$

S.NO	CASCADED BOOST CONVERTER PARAMETERS	VALUES
1	L1(mH)	1
2	L2(mH)	5
3	C1(μF)	100
4	C2(μF)	22
5	R(Ω)	100
6	f(Hz)	8000
7	Vin(V)	36
8	Vout(V)	220

Table 1: Cascaded boost converter calculator parameter

VII. CIRCUIT SIMULATION:

To perform a simulation of the designed cascaded boost converter, MATLAB SIMULINK is used to validate the proposed design.

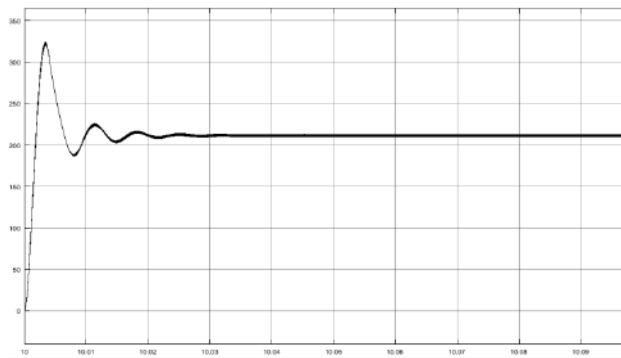


Fig 5: Output Current waveform of cascaded boost converter

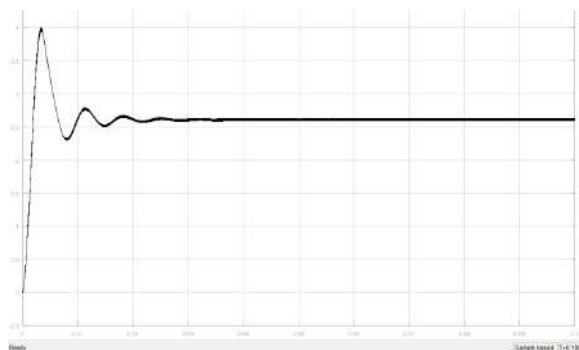


Fig 6: Output voltage waveform of cascaded boost converter

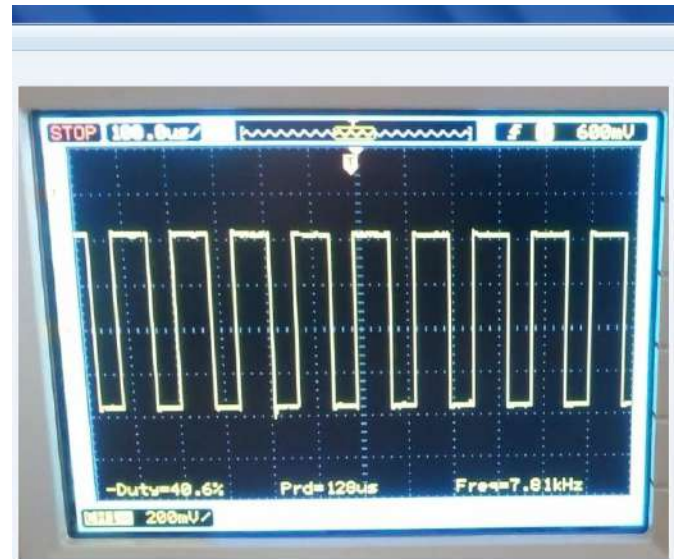


Fig 7: Triggering pluses for cascaded boost converter

The pulses which was produced by the triggering circuit is given to the cascaded boost converter to switch ON the MOSFET .This triggering circuit consists of a TLP250IC which has a eight pins , three resistors of R1, R2, and R3 as 330Ω, 1KΩ , 100Ω , Arduino.

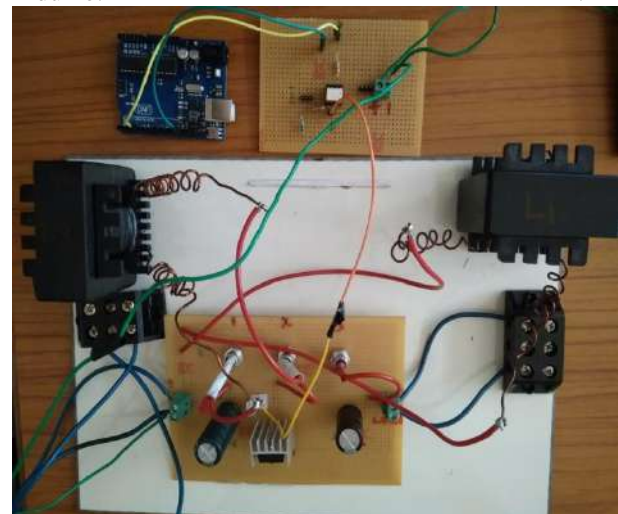


Fig 8: Hardware design of cascaded boost converter

VIII. MAXIMUM POWER POINT TRACKING (MPPT):

The PV curve of a solar cell is nonlinear. Due to its nonlinear nature the output power of the cell will not be always increasing with the increase in voltage. In order to track the maximum power of the PV cells certain methods are used and these methods are generally called MPPT. To obtain the maximum power output under certain a temperature and irradiation.

The MPPT is algorithm that include in charge controller used for extracting maximum available power from PV module under certain conditions. Since the tracking of maximum power will increases the efficiency of heating .So the MPPT algorithm is used. In MPPT many types of algorithm is used in that perturb & observe (P&O) algorithm which does not produce oscillation.

IX. RESISTIVE ELECTRIC STOVE:

In Electric stove, electricity runs to a wire inside the coils on the cook top. The electric stoves have coiled heating elements just the right size to heat cooking pots and pans. The heating elements are mostly used as a nichrome which consists of 80% of nickel and 20% of chromium. The main reasons why nichrome is used as a popular heating elements is that it has a high melting point ,it doesn't oxidize (even at high temperatures), doesn't expand too much when it heats up. Smooth top stoves have an internal coil that sits underneath the cooking surface. when supply gives to the stove ,the electricity flows to the coil and heats up the metal. This stove can operate both in AC and DC supply. The cost is also so efficient when compared to normal gas stove and induction stove so the middle class people can also use this electric stove in suitable manner. This electric stove cooking time is faster when compared to the normal gas stove. So this stove is considered as a cheap and best when compared to normal gas stove.



Fig 9: Electric heating stove

Comparison of cooking time is also a big part of duty in this project .We compared the time duration for cooking with our stove and to the ordinary cooking gas. Results are also given below.

S N O	NAME OF THE ITEM	DURATION OF ELECTRIC STOVE IN MINUTES (500 watts)	DURATION OF INDUCTION STOVE IN MINUTES (500 watts)	DURATION OF GAS STOVE IN MINUTES
1	Milk (250 ml)	5	3	7
2	Water (250 ml)	4	3	5

Table 2: Time duration comparison



Fig 10: Hardware design of solar powered DC electric heating stove

X.CONCLUSION:

The project is based on the solution of real life problem and can open a new era for cooking environment. It highlights on reducing the gas and electricity shortage of our country and at same time making the best use of solar energy. This electric stove is portable, cheap and is easy to operate at both AC as well as on DC supply. The coils are designed to produce a maximum heat and the controller is used to control the heat if needed. Batteries are used as a backup of the solar power. In this paper, a cascaded boost converter is designed and developed and implemented for a solar energy system. The designed circuit is simulated using MATLAB. Finally the result was verified successfully by building the circuit. The INC MPPT method are also implemented. This method is used to improve the dynamic and steady state performance of the PV system. This can track the maximum power point quickly when the external environment changes suddenly. Thus our aim is to provide people with a good product which is easy to use, pollution free and make proper use of renewable energy resources.

XI.REFERENCE:

- [1]S.Islam,S.B.Azad,H.Fakir and R.Rahman A.Azad,(2014, August 6-9) "Development Of electric stove for the smart use of solar photovoltaic Energy."
- [2]S.Gomathy,S.Saravanan,Dr.S.Thangavel, "Design and Implementation of Maximum Power Point Tracking(MPPT) Algorithm For A Standalone PV System."
- [3]Ahmad Al Nabulsi,Muneer Al Sabbagh,Rached Dhaouadi,Habib-ur Rehman,"A 300W Cascaded Boost Converter Design For Solar Energy System."
- [4]Using gas to cook food is waste of energy: Muhith [Online].Available: [gas_cook-food-waste-energy-muhith-1269166](#)[Last modified:13 August 2016]
- [5]A.Pandey,N.Dasgupta,and A.K.Mukerjee,"Design issues in implementing MPPT for improved tracking and dynamic performance,"in proc.IEEE IECON,2006,pp.4387-4391(Conference proceedings)

[6]Q. Zhao and F. C. Lee, "High-efficiency, high step-up dc-dc converters," IEEE Trans. Power Electron., vol. 18, no. 1, pp. 65–73, Jan. 2003.